



AD-A199 161

Proceedings of the Antiproton Science and Technology Workshop, 6-9 October 1987

July 1988

Editors:
B. W. Augenstein
F. E. Mills
B. E. Bonner
M. M. Nieto

RAND Corporation
1700 Main Street
P. O. Box 2138
Santa Monica, CA 90406-2138

Approved for Public Release

Distribution is unlimited. The AFAL Technical Services Office has reviewed this report, and it is releasable to the National Technical Information Service, where it will be available to the general public, including foreign nationals.

Prepared for the:

**Air Force
Astronautics
Laboratory**

Air Force Space Technology Center
Space Division, Air Force Systems Command
Edwards Air Force Base,
California 93523-5000

DISTRIBUTION STATEMENT A

Approved for public release;
distribution is unlimited

DTIC
ELECTE

SEP 08 1988

H

88 9 6 07 T

NOTICE

When U.S. Government drawings, specifications, or other data are used for any purpose other than a definitely related government procurement operation, the government thereby incurs no responsibility nor any obligation whatsoever, and the fact that the government may have formulated, furnished, or in any way supplied the said drawings, specifications, or other data, is not to be regarded by implication or otherwise, or conveying any rights or permission to manufacture, use, or sell any patented invention that may in any way be related thereto.

FOREWORD

This is the conference proceedings of the Antiproton Science and Technology Workshop held 6-9 October 1987 at the RAND Corporation in Santa Monica, CA. Project Manager for the Air Force Astronautics Laboratory is Lt Steve Thompson.

This conference proceedings has been reviewed and is approved for distribution in accordance with the the distribution statement on the cover and on the DD Form 1473.


STEVEN D. THOMPSON, 1LT, USAF
Project Manager

FOR THE COMMANDER


STEPHEN L. RODGERS
Chief, ARIES Office

REPORT DOCUMENTATION PAGE

Form Approved
OMB No. 0704-0188

1. REPORT SECURITY CLASSIFICATION UNCLASSIFIED		1b. RESTRICTIVE MARKINGS	
2a. SECURITY CLASSIFICATION AUTHORITY		3. DISTRIBUTION/AVAILABILITY OF REPORT Approved for public release; distribution is unlimited.	
2b. DECLASSIFICATION/DOWNGRADING SCHEDULE		5. MONITORING ORGANIZATION REPORT NUMBER(S) AFAL-CP-88-002	
4. PERFORMING ORGANIZATION REPORT NUMBER(S)		7a. NAME OF MONITORING ORGANIZATION Air Force Astronautics Laboratory	
6a. NAME OF PERFORMING ORGANIZATION RAND Corporation	6b. OFFICE SYMBOL (if applicable)	7b. ADDRESS (City, State, and ZIP Code) LSX Edwards Air Force Base, CA 93523-5000	
6c. ADDRESS (City, State, and ZIP Code) 1700 Main Street P. O. Box 2138 Santa Monica, CA 90406-2138		9. PROCUREMENT INSTRUMENT IDENTIFICATION NUMBER	
8a. NAME OF FUNDING/SPONSORING ORGANIZATION	8b. OFFICE SYMBOL (if applicable)	10. SOURCE OF FUNDING NUMBERS	
8c. ADDRESS (City, State, and ZIP Code)		PROGRAM ELEMENT NO. 61101F	PROJECT NO. 5730
		TASK NO. 00	WORK UNIT ACCESSION NO. 2J
11. TITLE (Include Security Classification) Proceedings of the Antiproton Science and Technology Workshop (U)			
PERSONAL AUTHOR(S) Augenstein, B. W., Mills, F. E., Bonner, B. E., and Nieto, M.M., eds			
13a. TYPE OF REPORT Conference Proceedings	13b. TIME COVERED FROM 87/10/6 TO 87/10/9	14. DATE OF REPORT (Year, Month, Day) 88/7	15. PAGE COUNT 753
16. SUPPLEMENTARY NOTATION			
17. COSATI CODES		18. SUBJECT TERMS (Continue on reverse if necessary and identify by block number)	
FIELD	GROUP	SUB-GROUP	
20	08		
		Antimatter, Propulsion, Annihilation, Antihydrogen, Antiprotons, Portable Traps, Hadron Production.	
19. ABSTRACT (Continue on reverse if necessary and identify by block number) The Antiproton Science and Technology Workshop was held at the RAND Corporation in Santa Monica, CA from 6-9 October 1987. The conference was held to provide the U.S. Air Force with independent advice on the development of a near term antiproton experimental and analytical program through a detailed technical assessment. Genesis, cooling, storage, transport, and utility of antiprotons were all addressed.			
20. DISTRIBUTION/AVAILABILITY OF ABSTRACT <input checked="" type="checkbox"/> UNCLASSIFIED/UNLIMITED <input type="checkbox"/> SAME AS RPT. <input type="checkbox"/> DTIC USERS		21. ABSTRACT SECURITY CLASSIFICATION UNCLASSIFIED	
22a. NAME OF RESPONSIBLE INDIVIDUAL STEVEN D. THOMPSON, 1LT, USAF		22b. TELEPHONE (Include Area Code) (805) 275-5671	22c. OFFICE SYMBOL LSX

TABLE OF CONTENTS

	Page
Preface	viii
Introduction	1
Group I Papers - Machines	
Précis of Group I Activities	
1. Potential Low Energy Antiproton Sources in the United States D.C. Peaslee (University of Maryland)	15
2. Low Energy Antiproton Possibilities at BNL Y.Y. Lee, D.I. Lowenstein (Brookhaven National Laboratory)	25
3. The AGS Complex as an Antiproton Filling Station Y.Y. Lee, D.I. Lowenstein (Brookhaven National Laboratory)	39
4. A Storage Ring for Antimatter Transport D. Cline (University of California at Los Angeles)	45
5. An Advanced Hadron Facility: Prospects and Applicability to Antiproton Production T. Goldman (Los Alamos National Laboratory)	117
6. The TRIUMF Kaon Facility E. Blackmore (TRIUMF-Canada)	151
7. Scaleup of Antiproton Production Facilities to 1 milligram per year F.E. Mills (Fermi National Accelerator Laboratory)	165
8. Scaleup of Antiproton Production and Collection D.J. Larson (University of California at Los Angeles)	179



By	
Distribution/	
Availability Codes	
Dist	Avail and/or Special
A-1	

Group II Papers - Basic Science

	Page
Précis of Group II Activities	217
1. Antimatter: Its History and its Properties	223
M.M. Nieto, R.J. Hughes (Los Alamos National Laboratory)	
2. Basic Physics Program for a Low Energy Antiproton Source in North America	245
B.E. Bonner (Rice University)	
M.M. Nieto (Los Alamos National Laboratory)	
3. Antiproton Annihilation in Nuclei	279
G.A. Smith (Pennsylvania State University)	
4. Particle Emission from Antiproton Annihilation at Rest in Uranium	293
G.A. Smith (Pennsylvania State University)	
5. Using $\bar{p}p$ Annihilation to find Exotic Mesons	301
S.R. Sharpe (Stanford Linear Accelerator Center)	
6. Tests of CP Violation at LEAR	321
J. Miller (Boston University)	
7. Looking for New Gravitational Forces with Antiprotons	329
M.M. Nieto (Los Alamos National Laboratory)	
B.E. Bonner (Rice University)	
8. Normal Matter Storage of Antiprotons	343
L.J. Campbell (Los Alamos National Laboratory)	
9. Antihydrogen Production Schemes	361
J.B.A. Mitchell (University of Western Ontario)	
10. The Synthesis of Large Cluster Ions from Elementary Constituents: A Possible Route to Bulk Antimatter	375
W.C. Stwalley (University of Iowa)	
11. Bibliography of Hydrogen Cluster Ions	395
W.C. Stwalley (University of Iowa)	
12. Production of Heavy Antinuclei: Review of Experimental Results	437
R.L. Forward (Hughes Research Laboratories)	

	Page
13. The Standard Model and its Problems: The Physics Background for an Advanced Hadron Facility	449
T. Goldman (Los Alamos National Laboratory)	
Group III Papers - Applied Science and Technology	
Précis of Group III Activities	479
1. Portable Pbars, Traps that Travel	483
S.D. Howe, M. Hynes, A. Picklesimer (Los Alamos National Laboratory)	
2. Extreme States of Matter: Could Antiprotons be used to Power Table-top Equation of state or Opacity Experiments?	505
J.C. Solem (University of Illinois at Chicago)	
3. Initial Laboratory Propulsion Testing	533
D.L. Morgan, Jr. (Livermore, California)	
4. Antimatter Spacecraft Propulsion Experiments with Current Antiproton Production Rates	569
J.L. Callas (Jet Propulsion Laboratory)	
5. Energy Transfer in Antiproton Annihilation Rockets	577
B.N. Cassenti (United Technologies Research Center)	
6. Some Thoughts on the Muon - Catalyzed Fusion Process for Antimatter Propulsion and for the Production of High A Mass Numbers Antinuclei	605
H. Takahashi (Brookhaven National Laboratory)	
7. Multiple Collision Effects on the Antiproton Production by High Energy Protons (100-1000 GeV)	623
H. Takahashi, J. Powell (Brookhaven National Laboratory)	
8. Biomedical Potential of Antiprotons	645
T. Kalogeropoulos, L. Gray, R. Muratore (Syracuse University)	
J. Archambeau (Loma Linda Medical Center)	
D. Bassano (SUNY Health Science Center)	
G. Bennett (Brookhaven National Laboratory)	
B. Gottchalk, A. Koehler (Harvard Cyclotron Facility)	
M. Urie (Massachusetts General Hospital)	

	Page
9. Potential Applications of Antiprotons for Inspection and Processing of Composites	685
L.B. Greszczuk (McDonnell Douglas Astronautics Company)	
10. Antimatter Science and Technology Bibliography	693
R.L. Forward (Hughes Research Laboratories)	
Includes: Production and Collection of Antiprotons	
Production of Heavy Antinuclei	
Production of Low Energy Antiprotons	
Production of Antihydrogen Atoms, Molecules, and Clusters	
Slowing, Cooling, and Trapping of Atoms, Ions, and Molecules	
Low Energy Antiproton Annihilation Processes	
Non-Propulsion Applications of Antimatter	
Antimatter Propulsion	
Conference Proceedings	
Antimatter News and Popular Articles	
List of Workshop Attendees	761

PREFACE

The United States Air Force in its Project Forecast II - which was conducted to help the Air Force make longer-term investment decisions - identified antiproton science and technology as a promising area supportive of new technologies and a broad technical base. The RAND Corporation, through Project Air Force and in conjunction with the USAF Astronautics Laboratory, was charged with providing a technical evaluation of antiproton science and technology.

As part of this effort, RAND organized and structured two conferences to review what was known, and what needed to be investigated, in the field of low energy antiproton research. The April 1987 Conference identified critical issues. The October 1987 Workshop - the subject of these Proceedings - reviewed these critical issues to help define needed tools and to formulate goals and research objectives for a sound, comprehensive U.S. antiproton research program. Three major areas were addressed - machine issues; basic science; and applied science and technology. Large multidisciplinary groups of scientists and technologists participated in these reviews. The findings of these groups present compelling and well-documented arguments for undertaking in North America a substantial, fast-paced program of low energy antiproton research. Such a program would expand, in major ways, the research accessible via LEAR.

The RAND Corporation wishes to acknowledge the invaluable scientific contributions to and participation in the conferences, and assistance in preparation of these Proceedings, of the co-editors - Professor B. Bonner, Rice University; Dr. F. Mills, FNAL; and Dr. M. Nieto, LANL. Special thanks are also given to Captain W. Sowell, AFAL, and to Dr. H. Mayer, Mr. J. Dewar, Dr. E. Harris, Dr. P. Rehms, Mr. S. Pace, of RAND, for their essential aid and advice on technical and planning issues. Ms. O. Stauber, conference secretary, provided indispensable help in the conduct of the conferences.

INTRODUCTION

There were four major incentives for this Workshop on Antiproton Science and Technology. First, the realization that an enormous array of fundamental science experiments is possible using low energy antiprotons. Second, the U.S. is in a position to provide an intense low energy antiproton source, via relatively modest facilities additions at Fermilab (FNAL) or Brookhaven (BNL). LEAR could thus be complemented, allowing a very substantial broadening of the physics which can be addressed. Third, portable storage devices (rings and ion traps) appear feasible, whereby antiprotons can be transported to experiment locations removed from FNAL or BNL. Fourth, provision of enabling tools (an antiproton source, and portability of antiprotons) and experiment technologies necessary to conduct fundamental science experiments permit very interesting applied science and technology research, using numbers of antiprotons available from the contemplated intense low energy antiproton source.

The goal of the Workshop was to discuss these possibilities at a level of detail appropriate to inform and to stimulate many others in the physics community to begin planning for experiments using antiprotons. In this process one hopes that the case for an intense U.S. low energy antiproton source and portable antiprotons will become accepted, and that these basic tools as a consequence become speedily available.

For the purposes of concurrent reviews in the Workshop, discussions were organized into three groups - Group I, machines (production, collection and cooling of antiprotons); Group II, basic science (classes of experiments and numbers of antiprotons necessary); Group III, applied science and technology employing antiprotons. These proceedings are arranged the same way, with 8 papers in Group I, 13 papers in Group II, and 10 papers in Group III.

It is appropriate in this Introduction to highlight just a few of the Workshop reviews, to support our belief that a persuasive case for major expansions of antiproton physics is documented here. The potential audience interested in and contributory to experiments in this field seems to us to be very great. The papers of this Workshop Proceedings provide much greater detail and full additional references supportive of this case, and expand these highlights.

During the past few years there have been numerous workshops and conferences devoted to the science under discussion here. In particular one should mention the series of LEAR workshops, the Madison workshop on the Design of a Low Energy Antimatter Facility, and the Fermilab workshop on Antimatter Physics at Low Energy (AMPLE). The present Proceedings assembles what appear to be the most compelling examples of the wide variety of physics investigations that would become accessible. These examples are developed to a depth adequate to allow one to judge the basic physics case for a North American intense source of antiprotons.

Guidelines for the present Workshop postulated a somewhat arbitrary 200 MeV antiproton maximum energy for the source under discussion. The limitations thus imposed on the diversity of physics by such a ceiling, while considerable, are far from devastating. In any case, such limitations may be alleviated, as noted later. Missing from the agenda would be the very interesting higher energy topics such as the $\Delta S = 1$ CP violation experiment, $\bar{p}p \rightarrow \bar{\Lambda}\Lambda$; the new measurements that could be done in charmonium spectroscopy; and the puzzle of the enormous deviation from QCD predictions of the ratios for the branching fractions of the J/ψ and the ψ' to exclusive final states. These topics are discussed in papers of this Proceedings.

As emphasized previously by Bob Jaffe in the 1986 Fermilab Proceedings, there are two broad areas of concern in particle physics today. These can be described as the "Origins of the Standard Model" and the "Dynamics of Confinement in QCD". A low energy antiproton facility such as the one under consideration here can address both these questions in a vital and straightforward manner.

The standard model has enjoyed considerable success, but there are many parameters and phenomena that are arbitrary and not understood. Examples are i) the sources of weak symmetry breakdown, ii) the origin of CP violation, iii) the origin of quark and lepton masses and angles, and iv) even why $SU(3) \times SU(2) \times U(1)$ should be the fundamental gauge groups chosen by nature. The absence of proton decay at the 10^{32} year lifetime has cast serious doubt on this simplest version of the standard model. A low energy antiproton machine will contribute to our understanding in this area most directly through precision tests of various invariance principles such as CP, CPT, and T. Therefore, this topic forms one of the cornerstones of the basic physics program for the facility.

The theory of Quantum Chromodynamics has also had its many successes. However, after more than a decade, many fundamental questions are still unanswered. The nature and origin of confinement is still mysterious; that the rich spectrum of particles can be reproduced by naive bag models is astonishing. The absence (so far) of definitive evidence for states of gluons and/or gluons and quarks may turn out to be fundamental; and yet the large number of particles that have been reported which do not fit into the accepted scheme portends excitement ahead. In the field of meson spectroscopy, a low energy antiproton machine can be used to provide high statistics measurements of exclusive final states resulting from $\bar{p}p$ and $\bar{p}n$ annihilations, to enable definitive determinations of possible new states.

The various processes which occur when antiprotons annihilate in nuclei offer a rich milieu for uncovering unanticipated phenomena. There have been many speculations and even some calculations concerning the energy densities to be expected when \bar{p} 's are absorbed in nuclei. Using a reasonable model for the hadronization process, estimates have been made that energy densities in the very interesting range of 2 GeV/fm^3 for periods of about 2 fm/c should be attainable. Under such conditions we would expect to observe the change of state of nuclear matter to that which is often referred to as "quark-gluon plasma".

Fundamental experiments await in measurements of the gravitational force on antimatter - the determination of $g(\bar{p})$. Modern theories of gravity predict that the acceleration of protons and antiprotons in the earth's gravitational field will be different. The difference arises in quantum theories of gravity which have massive partners of the tensor graviton as carriers of the force of gravity. This prediction remains regardless of the results from current experiments searching for anomalous gravitational attraction between matter and matter. A program of experiments with antiprotons to determine the strengths and ranges of these additional components to the gravitational force will be an important activity at a low energy antiproton facility.

A variety of precision tests of CPT could be done given a source of antihydrogen atoms. One can for instance envision a measurement of the Lamb shift in \bar{H}^0 . In addition, precision measurements of the gravitational properties of antimatter may well become feasible if sources of \bar{H}^0 were to become available. Estimates of what is achievable in antihydrogen production using reasonable extensions of presently existing positron sources are available.

Other areas of great fundamental interest include experiments on antiproton interactions with condensed normal matter, and on formation and phenomenology of very large cluster ions of antimatter. Such research will intersect with many fields currently under intensive investigation, and can in many cases exploit normal matter simulations. These areas are also of direct potential importance in the technologies for storing larger amounts of antimatter.

Participants in Group II discussions of the Workshop summarized the experimental requirements for these topics, the degree of difficulty for the range of experiments treated, and the number of antiprotons required to perform the experiments. The range of numbers is very large - from just a few antiprotons to more than 10^{14} . As a reference point, we note that LEAR has provided fewer than 10^{13} \bar{p} 's in any year of operation up to the present time. In the opinion of the attendees at the workshop, the physics case for proceeding with a low energy antiproton source in North America is most alluring, having great potential for new and

unexpected discoveries. The time is right for a push for speedy construction of such a facility.

A major issue is thus the provision, in the near term - within a very few years - of a low energy antiproton source in the U.S. A collection of papers in Group I activities is devoted to this issue.

These papers include a general review of how FNAL and BNL could serve as a source of low energy antiprotons, comparing these sources with the European CERN facility (LEAR) as a model. Both antiproton production and delivery of these antiprotons at low energy are treated. The improved antiproton source at CERN (ACOL) is suggested to give up to 10^{12} antiprotons per day, but the LEAR duty cycle is such as to result in $\sim 10^{13}$ low energy antiprotons per year. For FNAL several machine options are possible, giving a range of $\sim 10^{13}$ to several times 10^{14} antiprotons per year available at 9 GeV/c and suitable for delivery to lower energies (≤ 50 KeV). Delivery at ≤ 50 KeV would be possible via several schemes at no significant loss of antiprotons, so that $\sim 10^{13}$ - 10^{14} antiprotons per year might be delivered at ≤ 50 KeV. BNL currently has no dedicated antiproton source, but one can evolve from the ongoing Booster project in the near term. The BNL source possibilities are described in some substantial detail. Using realistic duty cycles, about 10^{14} antiprotons per year become available; however, at BNL one can also purchase additional accelerator time. With dedicated time a several fold improvement in antiprotons per year is plausible at momenta of 4 GeV/c. A further ACOL-type enhancement at BNL might in the future get production up to \sim several $\times 10^{16}$ antiprotons per year. For delivery at BNL, one could take a no-cooling approach, but accept large losses in the beam. Provision of substantial cooling would give little loss of antiprotons to 20 KeV.

Thus the U.S. has several alternative routes to a near term low energy antiproton facility. Papers in Groups II and III suggest some powerful motivations for aiming at the high end of the accessible near term U.S. low energy antiproton delivery rates (i.e., $\sim 10^{14}$ rather than $\sim 10^{11}$ antiprotons per year).

A number of additional important topics were treated by Group I participants. An advanced hadron/kaon facility has a very compelling physics motivation, discussed in the Proceedings, and world-wide is the subject of four separate proposals. Such a facility might permit a potential factor of $\sim 10^3 - 10^5$ scaleup in antiproton delivery over the yields from a first U.S. low energy antiproton facility, by cleverly adapting the basic machinery such a facility would possess for its primary physics missions.

Issues inherent in additional large scaleups of production and collection of antiprotons were also assessed. The consensus was: the necessary accelerators can be built, selecting from several options; targetry can be scaled up, with appropriate R&D; cooling is the most serious problem, needing intensive study and innovation.

These observations are the subject of several review papers. One comprehensive paper treats, in a fundamental way, accelerator and collector options; candidate accelerators; antiproton cooling methods; and, very importantly, a menu of R&D topics to pursue to support large advances in production and collection of antiprotons. The papers treat these issues in the context of the serious and challenging goals of producing and collecting milligrams per year of antiprotons.

There was much discussion at the Workshop about the very important topic of portable sources of antiprotons. Here one would use the U.S. low energy source as a filling station to deliver antiprotons to portable sources. The portable sources would then be transported to any competent laboratory (in North America, say), where the actual antiproton experiments would be run. This approach would open up antiproton research to a quite large new community, drawn from university, industry, and national laboratory personnel, and would take advantage of the circumstances that many very skilled experiment teams could best at their home locations use their personnel and experimental facilities in antiproton research. Additionally, there could result a much broader student involvement in antiproton research.

The Workshop Proceedings include two major review papers, each of which discusses a major option for antiproton portability. One option considers small portable storage rings. The other option is use of ion traps. Either option would provide a remote antiproton source, and would, with additional local acceleration capabilities, also provide the possibility for antiprotons at higher energies than the storage energy. Such possibilities would be one means to make accessible antiprotons at energies suitable for the "higher energy" topics mentioned earlier in this Introduction.

The portable storage ring is used as an antiproton source generally, with no experiments normally carried out in the ring. At a weight of ≤ 10 tons, and with dimensions of $\sim 4.4 \times 2.4$ meters, a ring immediately storing $\sim 10^{10} - 10^{11}$ (possibly up to $\sim 10^{12}$) antiprotons seems feasible, with particle lifetimes of ≥ 3500 hours with cooling, and capable of a kinetic energy range of ~ 100 MeV - 200 KeV, using superconducting technology. Work is needed on the superconducting magnet. An emergency beam dump into the magnet structure as one safety measure looks feasible. The proposed design is based on a design base of a number of low energy storage rings, particularly the LEAR-ELENA proposal, and hence is called SELENA (Superconducting ELENA). The experiments using such a ring are any requiring significant momenta. A partial list would include medical applications; annihilation phenomenology; nuclear physics tests; tabletop tools; and a variety of other applications. All such uses are treated in various papers in these Proceedings.

Another paper discusses the principles of and a point design for a large portable ion trap storing 10^{12} to 10^{13} antiprotons at 25-50 KeV. The design is conservative, with particle densities a large factor down from the Brillouin limit. The particles are confined in a cylindrical plasma volume about 100 cm. long, 4 cm. in diameter; the vacuum is $\leq 10^{-12}$ Torr, giving a storage time of ~ 30 to 100 days or better; the magnetic field is 10T. A complete installation, including all support equipment, can easily fit into a large truck. Replicating the trap design might cost ~ 250 K\$, once the design has been validated.

Shielding requirements were assessed. R&D topics identified include vacuum requirements, need for confinement data, whether feedback can nullify slow radial losses, etc. The point design can be scaled to smaller storage levels and more compact storage assemblies, in several alternative ways. Assessment of ion trap feasibility is based on two levels: what could be done with present day technology and what future technology could achieve. The paper concludes with a radiation safety study indicating that shows that about 10^{11} antiprotons can easily be transported safely. However, federal guidelines for this transport must be reviewed in detail. Transporting more antiprotons than this would require additional transportation arrangements.

The combination of an intense source and portable storage devices filled by that source would provide unique research capabilities. Both on-site research - co-located with the source - and off-site research - at any competent laboratory, the home institution of the researcher - could be conducted. The latter possibility alleviates much of the potentially troublesome impact of on-site low energy antiproton research on the high energy physics program of the laboratory where the intense source is located. The off-site research program is an appealing mode of operation to involve the capabilities of the many excellent laboratories which today do not have access to antiprotons. A broad and multidisciplinary research community could get hands-on experience with antiproton physics and applied science. The consensus of the participants was that the sheer number of appealing physics opportunities provides plenty of work for a facility additional to LEAR at CERN. Provision of an intense low energy antiproton source in North America, and capabilities for both on-site and off-site research, would open up many more of these opportunities for U.S. and foreign scientists and experiment teams.

A collection of papers from Group III discusses a range of applied science uses of low energy antiprotons, generally employing numbers of antiprotons deliverable from the intense low energy antiproton source postulated for basic physics uses - i.e., a source capable of delivering about 10^{14} antiprotons/year. For most of these applied science uses, the off-site capabilities provided by portable storage devices will be important to exploit.

One example of the compelling near term applied science use for low energy antiprotons is biomedical applications. An encompassing review paper treats antiproton uses for imaging; for simulation and monitoring of conventional proton and heavy ion therapies; for actual therapeutic treatments; and for mesic chemistry, using x-ray emissions or nuclear gammas, whereby one could monitor all elements in the living body. The paper, coauthored by a multidisciplinary team of physicists and medical practitioners, discusses in detail what could be done with $\leq 10^9$ antiprotons. Biomedical applications of antiprotons offer the promise of fundamentally new capabilities.

Properties of antimatter of compelling physics interest also provide attractive new technological possibilities in other applied science fields. One very important example is the physics of antiproton annihilation in nuclei and the particle emission from antiproton annihilation. The manifold physics interests involved here cover a very broad range, from production of very high nuclear temperatures to exploiting fission as a new tool for studying strangeness of heavy nuclei. Several papers from Group II treat these interests in detail. The same phenomenology, including questions of energy deposition and energy partition into heavy charged particles, is critical for issues in applied science uses detailed in a number of papers from Group III. These applied science uses again can be experimentally investigated using numbers of antiprotons not exceeding those needed for fundamental physics. Such investigations are therefore accessible via the very near term intense low energy antiproton source postulated.

In the longer term, much larger amounts of antimatter may become available. A number of technological possibilities derived substantially from the bulk energy release of such larger amounts can become of increasing interest. While such possibilities are considered speculative by many, several papers from Group III review questions inherent in the availability and applications of much larger amounts of antimatter. The view of the Workshop participants on such questions can likely be summarized in this way: understanding such possibilities - informed determination with adequate information of whether, how, and

when it can be sensible to pursue them - depends critically on accomplishments of the basic science, enabling technology, and applied science programs outlined, including exploration of fundamental issues of machine scaleup to produce and collect much larger number of antiprotons.

Participants in this Workshop were able to convey the excitement and promise of near term programs using low energy antiprotons. By near term we typically mean the approximate 5-7 year period following availability of a North American intense low energy antiproton source. The extensive Workshop representation of diverse groups - from universities, national laboratories, governmental organizations, major hospitals, U.S. industry, and from scientists already collaborating in international physics programs - is evidence of the rapidly growing U.S. interest in low energy antiproton research. Possibilities for a consortium of sponsors/users of such research thus appear attractive.

Given appropriate support, very significant near term research results are within our grasp, at what is likely to be a surprisingly rapid pace. We believe the findings of this Workshop, summarized in these Proceedings, provide an initial basis for planning a comprehensive near-term program of antiproton research in North America. That research, in our view, promises to result in very compelling basic and applied science rewards. The science case for low energy antiproton research is excellent. We should get on urgently with providing the intense North American source and other enabling tools, such as portable storage, to spur this research.

PRÉCIS OF GROUP I ACTIVITIES

Paper (1) - Peaslee - is a general review of how FNAL and BNL could serve as a source of low energy antiprotons, and compares these sources with the European CERN facility (LEAR) as a model. For FNAL several machine options are possible, giving a range of $\sim 10^{13}$ to several times 10^{14} antiprotons per year available at 9 GeV/c and suitable for delivery to lower energies (≤ 50 KeV). Delivery at ≤ 50 KeV would be possible via several schemes at no significant loss of antiprotons, so that $\sim 10^{13}$ - 10^{14} antiprotons per year might be delivered at ≤ 50 KeV. BNL currently has no dedicated antiproton source, but one can evolve from the ongoing Booster project. The BNL source possibilities, schedules, and costs are described in some substantial detail in paper (2) - Lowenstein and Lee - and in paper (3) - Lee and Lowenstein. Using realistic duty cycles, about 10^{14} antiprotons per year become available; however, at BNL one can also purchase additional accelerator time, and with dedicated time get up to $\sim 5 \times 10^{14}$ antiprotons per year at momenta of 4 GeV/c. For delivery at BNL, one could take a no-cooling approach, but accept a very large loss factor in the beam. Provision of substantial cooling would give a small loss factor to 20 KeV. In this way, BNL might get $\geq 5 \times 10^{13}$ antiprotons per year at 20 KeV, in 3-4 years.

Paper (4) - Cline - discusses a portable storage ring. The ring is used as an antiproton source generally, with no experiments normally carried out in the ring. At a weight of ≤ 10 tons, and with dimensions of $\sim 4.4 \times 2.4$ meters, a ring storing $\sim 10^{10} - 10^{11}$ (possibly to $\sim 10^{12}$) antiprotons seems feasible, with particle lifetimes of ≥ 3500 hours with cooling (≥ 100 hours sans cooling), and capable of a kinetic energy range of ~ 100 MeV - 200 KeV, using superconducting technology. The experiments using such a ring are any requiring significant momenta. A transportable storage ring is one of the key enabling tools permitting use of antiprotons in industry, university, and national laboratories: uses include filling existing rings, etc.

Paper (5) - Goldman - and paper (6) - Blackmore - discuss the potential scaleup for antiproton production and collection provided by an advanced hadron or kaon facility. The physics case for such a facility is very compelling, and is described here and in paper (III13) - Goldman. The physics uses include hadron spectroscopy, kaon decays, hypernuclei, neutrino physics, special proton physics, and other physics of electroweak and strong interactions. Four proposals exist for such a facility: Canada (TRIUMF); U.S. (LAMPF AHF); European HF; and Japanese HF. These are machines in the 30-60 GeV energy, ~50-100 μ A current range. It seems probable that at least one such machine may be built. Used as an antiproton source to reach higher production and collection rates, current technology would need extensions in target design, collection, and cooling. The papers suggest a factor of $\sim 10^3 - 10^5$ scaleup over the yields "immediately" available from FNAL or BNL. The earliest such a machine might be available is in the mid 1990s.

Paper (7) - Mills - takes up fundamental general issues of machine scaleups to produce and collect of the order of $\sim 10^{14}$ antiprotons per second, giving annual yields in the few milligram range. Paper (7) is a comprehensive review paper covering general topics of production issues; collector and accelerator types; candidate accelerators; antiproton cooling methods; and, most importantly, some 18 potential research and development areas to support serious consideration of large scale production and collection of antiprotons. Ultimate embodiments for scaled-up production and collection could accordingly differ significantly from current concepts. In each of the topics noted, a number of critical discrete issues is treated. For example, in the section on antiproton cooling methods, the discussion covers stochastic cooling, electron cooling, resistive cooling, dE/dx cooling, and radiative cooling (important for electrons and positrons in plasma type collectors). Power estimates for production are assessed.

Paper (8) - Larson takes up the pragmatic engineering involved in large scaleup issues, and discusses use of electron cooling as one possible special way to cool $\sim 10^{14}$ antiprotons per second in real time. The proposal suggests use of a very large dedicated cooling ring and

very intense (~100 KA) electron cooling beams. The paper discusses the theory of electron cooling; cooling time constants; scaling issues; technological issues; plasma cooling; and topics for additional consideration. Engineering issues for this cooling effort are reviewed.

Some Major Observations from Group I Activities

- There are several alternative routes to a U.S. low energy antiproton facility, at BNL or FNAL, capable of delivering $\sim 10^{14}$ antiprotons per year at ≤ 50 KeV.
- The time is ripe to prepare a formal proposal for such a facility and to push for its speedy construction, in view of the great potential for new and unexpected physics discoveries, and insights into applied science, suggested by Groups II and III.
- The notion of portable storage rings is alluring, and construction should be sought. Their uses would be manifold, and such rings would be one enabling tool to bring antiprotons for experimentation to any competent laboratory in North America.
- Issues inherent in production scaleup to milligrams per year levels were assessed; the consensus was:
 - The necessary accelerators can be built, selecting from several options.
 - Targetry can be scaled up, with appropriate R&D.
 - Cooling is the most serious problem, needing intensive study and innovation.
- One possible solution to the cooling problem at milligrams per year delivery levels lies in electron cooling, and one such specific cooling embodiment was discussed.
- A comprehensive RDT&E program treating issues to achieve milligrams per year of antiproton delivery levels can be formulated. Some outputs of this program could benefit improved designs of advanced hadron/kaon facilities.

POTENTIAL LOW ENERGY \bar{p} SOURCES IN THE U.S.

D. C. Peaslee
Department of Physics and Astronomy
University of Maryland
College Park, Maryland 20742

There are two possibilities for major sources ($\sim 10^{14}$ /yr) of low energy (~ 20 -50 KeV) antiprotons in the United States: Brookhaven National Laboratory (BNL) and Fermilab (FNAL). In the following report they are compared in two aspects: (I) \bar{p} production and (II) delivery at low energies. It turns out, given present and developing facilities, that (II) may require more supplemental funding than (I). The European facility (LEAR) at CERN serves as a model for comparison.

I.1 - Production at CERN

Typical operation at LEAR consisted [1] of stacking 3×10^9 antiprotons every 75 minutes, corresponding to 6×10^{10} \bar{p} /day. This beam was provided to experiment [2] about 30 days/yr during the 3 years that LEAR has operated: i.e., a \bar{p} yield of

$$Y = 2 \times 10^{12} \bar{p}/\text{yr} \quad @ 1 \text{ GeV}/c \quad (1)$$

An improved antiproton source (ACOL) is now commencing to operate at LEAR with an expected order of magnitude increase [3] in intensity to 10^{12} \bar{p} /day, but at an anticipated decrease [3] in duty cycle to 10 days/year; thus,

$$Y' = 10^{13} \bar{p}/\text{yr} \quad @ 1 \text{ GeV}/c \quad (2)$$

I.2 - Production at FNAL [4]

At Fermilab antiprotons are produced by directing a 120 GeV proton beam at a tungsten target. Production seems to peak at a \bar{p} momentum around 5 GeV/c, but the accumulator system is designed to operate around 9 GeV/c. Under these conditions the production cross section at forward lab angles appears to be

$$d\sigma = 2.4 \times 10^{-5} |\mathcal{F}| d\Omega \text{ (msr)} \quad (3)$$

where $|\mathcal{F}|$ is 1/2 the width of the relative momentum bite (units of 10^{-2}).

For the Fermilab accumulator system with $|\mathcal{F}| = 1.5$ for the momentum bite the \bar{p} collection rate is [5]

$$R = 1.3 \pm 0.4 \times 10^{10} \bar{p}/\text{hr} \quad (4)$$

The main ring at FNAL delivers about 1.3×10^{12} p/pulse at a repetition rate of $(2.5 \text{ sec})^{-1}$; through Eq. (4) this represents a \bar{p} yield of

$$Y = 0.7 \times 10^{-5} \bar{p}/p \quad (5)$$

During collider runs no antiprotons will be available for other purposes; but during fixed target (FT) running, \bar{p} can still be manufactured most of the time while the Tevatron is operating to supply the external targets. There are 3 factors of reduction:

- i) Some dead time in the acceleration cycle after ramping up to the maximum - 800 GeV. This has to do with resonances in the power grid and may be corrected; it represents a minor reduction by some 20%.
- ii) Other demands for \bar{p} during FT runs: E760 and its successors; improvements to the p system; test runs of the collider. This is a substantial reduction of order 50%.
- iii) Finally, the overall fraction of FT running, fixed at 50% for the immediate future at Fermilab.

Taking these factors all together suggests an availability of about 10 weeks/yr. for low energy \bar{p} production at FNAL. Assuming the canonical operating rate of - 100 hrs/week, we have an annualized yield of

$$Y = 10^{13} \bar{p}/\text{yr} \quad @ 9 \text{ GeV}/c \quad (6)$$

Corresponding to ACOL an upgrading program for FNAL has been proposed [6], to increase the ultimate collider luminosity by a factor of - 50. Most of this is in stages up to and including the accumulator - say a factor 20, which Eq. (6) would then acquire:

$$Y' = 2 \times 10^{14} \bar{p}/\text{yr} \quad @ 9 \text{ GeV}/c \quad (7)$$

This proposal has an estimated cost of - \$250M, however, and there is at present no foreseeable date for its initiation.

I.3 - Production at BNL [7]

Currently at Brookhaven there is no dedicated \bar{p} source; but one could evolve from the Booster project, which has started construction. The yield of \bar{p} from proton bombardment of a target is about 25 times less at 28 GeV/c than at 120 GeV/c:

$$d\sigma = 0.9 \times 10^{-6} |\eta| d\Omega \text{ (msr)} \quad (8)$$

for \bar{p} at the peak momentum of 4 GeV/c. The Booster acceptance is 50 m^3 , and with a spot diameter of 1 mm, the corresponding solid angle is 31 msr. Insertion in Eq. (8) with $|\eta| = 1$ yields

$$d\sigma = 2.8 \times 10^{-5} L \bar{p}/p = 2.5 \times 10^{-6} \bar{p}/p \quad (9)$$

where $L = 9\%$ allows for target losses due to depth of focus and absorption. This is a factor 3 less than Eq. (5) for FNAL.

According to Ref. [7] the post-booster AGS will accelerate in every cycle 12 buckets of 0.5×10^{13} protons each, of which 3 can be extracted to produce antiprotons while the other 9 buckets are available for the rest of the program. The result is about $3 \times 10^7 \bar{p}/\text{pulse}$, which must be ejected from the booster each cycle of about 2.5 seconds. Typical AGS performance is some 1.5×10^3 pulses/hr for about $10^2/\text{hr}$ week when the SEB program is running, which lasts for 10 weeks or more in a normal year. Thus the potential antiproton yield in this mode is of order $0.5 \times 10^{14} \bar{p}/\text{yr}$.

A flexibility in the Brookhaven situation is the option of obtaining more accelerator time by paying the expenses of operation, of order \$100 K/week.

Dedicated \bar{p} running using all 12 buckets for 3 months at double cycling rate would increase the previous estimate by a factor of order 10 to

$$Y = 5 \times 10^{14} \bar{p}/\text{yr} \quad @ 4 \text{ GeV}/c \quad (10)$$

Some further discussion of adding \bar{p} capability to the Booster and a comprehensive cost estimate are presented in the paper submitted by Y. Y. Lee and D. I. Lowenstein to this conference. Their cost estimate is \$8.6M, including development and contingency; if started within a year, this modification would proceed concurrently with the Booster construction and should be operational in 3 to 4 years.

An ACOL - type enhancement is also feasible at BNL. The parameters work out more favorably than at LEAR to suggest a theoretical increase of order 50 in yield: namely, a factor $(4)^2$ from angular aperture and 3 from momentum bite. If only a factor 20 can be realized, this still scales up Eq. (10) to

$$Y' = 10^{16} \bar{p}/\text{yr}. \quad @ 4 \text{ GeV}/c \quad (11)$$

No detailed cost estimates exist for such development, but an allowance of order \$20M seems appropriate. Design and construction would require a couple of years each.

II.1 - Delivery at CERN

In principle, delivery of \bar{p} at 20-50 KeV kinetic energy is relatively easy at CERN. The LEAR yield in Eq. (2) is already at $\sim 1 \text{ GeV}/c$ momentum; extraction, slowing to 2 MeV kinetic energy in a small linac designed to

introduce negligible beam loss, plus a final RFQ (radio frequency quadrupole) stage could be accomplished at relatively low cost - say, \$5 M.

Such a development would be useful mainly as a proof of some principle. The input of 10^{13} \bar{p} /yr. is unlikely to increase because of the pressure of high energy collider experiments, and that input must also satisfy all the other users of LEAR. Realistically, the consumable yield of very low energy \bar{p} would be 1-2 order of magnitude lower:

$$Y = 10^{11} - 10^{12} \bar{p}/\text{yr} \quad @ T = 20-50 \text{ KeV} \quad (12)$$

II.2 - Delivery at FNAL

The \bar{p} system at Fermilab was not designed with low energies in mind, so additional construction will be required for that purpose.

The \bar{p} are available at 8.9 GeV/c, and it is not feasible to reduce their momentum substantially in the accumulator. Tests have been made, and the beam was essentially lost somewhere below 3 GeV/c; preferably the reduction should be only to about 5.5 GeV/c, above the transition energy. At this stage it would be necessary to transfer the \bar{p} to a specially designed and constructed ring that would decelerate them to ~ 200 MeV kinetic energy, then transfer to a specifically designed linac plus RFQ combination to yield the final energy of 20-50 KeV. This system, with appropriate cooling, would be a substantial project, comparable to the accumulator itself, costing at a guess around \$50M and requiring 3-5 years to complete. There is no present indication that Fermilab would be willing to finance such a project.

An alternative scheme was suggested by F. Mills at the 1st Antiproton Conference at RAND (April, 1987). The \bar{p} in the accumulator are already

sufficiently cooled to decelerate in the booster without exceeding its emittance at 200 MeV. At this point there would be substantial loss from injection into the linac because of acceptance mismatch. Therefore a separate ring at 200 MeV would be built, with cooling and rf necessary to decelerate the beam without loss to about 2 MeV, when it can be decelerated by an RFQ to its final energy. The model for this system is the Indiana University Cyclotron Facility Cooler, which has a budget of about \$8M, excluding many salaries, and a time scale of 4 years. At Fermilab it seems prudent to allow a cost factor of 2 to 3 : say about \$20M. Barring changes in the present situation, these costs would fall primarily on the low energy \bar{p} users.

In either scheme there would be no significant loss of \bar{p} , so that from Eqs. (6,7)

$$Y = 10^{13} - 10^{14} \bar{p}/\text{yr} \quad @ T = 20-50 \text{ KeV} \quad (13)$$

III.3 - Delivery at BNL

The principal limitation of the Booster scheme is the loss of beam intensity during deceleration because of emittance growth: the loss factor could be as great as 10^{-4} , assuming no loss in the final RFQ stage. To overcome this limitation, cooling facilities could be inserted into the Booster. With cooling both at $\sim 1 \text{ GeV}/c$ and at a lower momentum the \bar{p} beam can be brought down to $\sim 2 \text{ MeV}$ kinetic energy with only one factor of 10 loss from optimal intensity. It can then be extracted to a new RFQ that will span the range from 2 MeV to 20 KeV without appreciable loss. The thumbnail cost estimate for this modification is \$5-6M, the time estimate ~ 3 years. If funded promptly, this development could be concurrent with

the Booster. Otherwise, it can be added later without incurring major extra costs by the delay.

Based on the simple Booster yield in Eq. (10), we have for this alternative

$$Y = 5 \times 10^{13} \bar{p}/\text{yr} \quad @ T = 20-50 \text{ KeV} \quad (14)$$

If one goes directly to the ACOL mode, such cooling in the Booster can be bypassed. The accumulator that yields Eq. (11) can also be designed to match the acceptance down to any point in the Booster chain, thus allowing a design figure of

$$Y' = 10^{16} \bar{p}/\text{yr} \quad @ T = 20-50 \text{ KeV} \quad (15)$$

This of course is a more substantial project than Eq. (14) envisions.

III. Summary

Table 1 collects the rough estimates in the text above.

Acknowledgements

This report was prepared in consultation with Dr. D. I. Lowenstein (BNL) and Dr. F. Mills (FNAL).

The author wishes also to express his thanks for discussions to Drs. Y. Y. Lee, R. Orr and J. Peoples.

Table 1. Antiproton

Yield(\bar{p} /yr.)
 Cost (\$M)
 Construct(yrs.)

@ T = 20-50 MeV

	<u>LEAR</u>	<u>FNAL</u>	<u>BNL</u>
		$10^{13}-10^{14}$	5×10^{13}
(Simple)		20-50	10-15
		4-5	3-4
	$10^{11}-10^{12}$	$10^{14}-10^{15}$	10^{16}
(ACOL)	20-25	250	20-25
	2-3	(10?)	5

References

1. P. Lefevre, D. Mohl, and D. J. Simon, Proc. Workshop on Antimatter Physics at Low Energy, FNAL (1986), p. 69.
2. R. E. Bonner and L. S. Pinsky, Ref. 1, p. 457.
3. R. Landua, Ref. 1, p. 36.
4. Interviews with F. Mills, R. Orr and J. Peoples.
5. J. L. Crawford and D. A. Finley, Fermilab Report (May/June, 1987), p. 4.
6. H. Edwards, Fermilab DOE Labwide Review (May, 1987), p. 167.
7. Proc. 1986 Workshop on Antiproton Beams, BNL 52082 (1987).

LOW ENERGY ANTIPROTON POSSIBILITIES AT BNL *

Y.Y. Lee and D.I. Lowenstein
Brookhaven National Laboratory
Upton, NY 11973

Antinuclear physics in the energy range of 0-20 GeV has long been a mainstay of the high energy physics program at BNL. The emphasis of the experimental program in the last couple of years has however moved to other areas as new facilities in the world have come on line. The initiatives stimulated by the USAF has caused a renewed interest in the low energy capabilities at BNL, which are still very competitive and considerable for the production of low energy antiprotons. In the following, we present a synopsis of the present BNL accelerator plans and the near term possibilities for a high yield antiproton production experiment. In this paper we will not address the longer term facility possibilities of producing "large" amounts of antimatter. Parenthetically, even though several aspects of the program are of little interest for this audience, such as the Relativistic Heavy Ion Collider (RHIC) and the Stretcher, it is important to understand their parameters and impact upon various possible antinucleon initiatives at BNL.

Accelerator Complex

The future BNL high-energy and heavy ion physics programs are centered about the 30 GeV Alternating Gradient Synchrotron (AGS) and the proposed 100-250 GeV/amu (gold-protons) Relativistic Heavy Ion Collider. The complex of accelerators is shown in Fig. 1. The high-energy physics complex consists of two 750 keV preinjectors (Cockcroft Walton for protons, RFQ linac for polarized protons, a second RFQ for protons is under construction) followed by a 200 MeV linac. Presently the 200 MeV protons are directly injected into the AGS and accelerated to 30 GeV. Under construction is a Booster Synchrotron that will boost the proton energy to 1.5 GeV prior to injection into the AGS. This will allow for an increase in delivered proton intensity by a factor of 4, to the 5×10^{13} protons/second level, and an increase in the delivered polarized proton intensity level by a factor of 20, to 4×10^{11} protons/pulse. The major machine parameters are listed in Table I. The heavy-ion physics complex consists of two 15 MV MP Tandems that inject several MeV/amu ions into the AGS. For the present, only fully stripped light ions ($< {}^{32}\text{S}$) can be accelerated in the AGS. With the completion of the Booster Synchrotron, all ion species will be accelerated in the AGS to 10-15 GeV/amu (final energy is dependent on the ion species Z/A). The AGS will then have the option to either slowly extract these ions for fixed target operations or inject them into RHIC. RHIC will be capable of accelerating all ion species with storage lifetimes of 10 hours at top energy and highest mass ion, e.g., 100 GeV/amu ${}^{197}\text{Au}$. Figure 2 describes as a function of collider energy, for various ion species, the design luminosity and central collision event rate for RHIC.

The AGS is now being required to provide, for experiments, a vast variety of particle species in several types of extraction modes that were never contemplated thirty years ago when it was being designed. From a

*Work performed under the auspices of the U.S. Department of Energy and the U.S. Air Force Rocket Propulsion Laboratory.

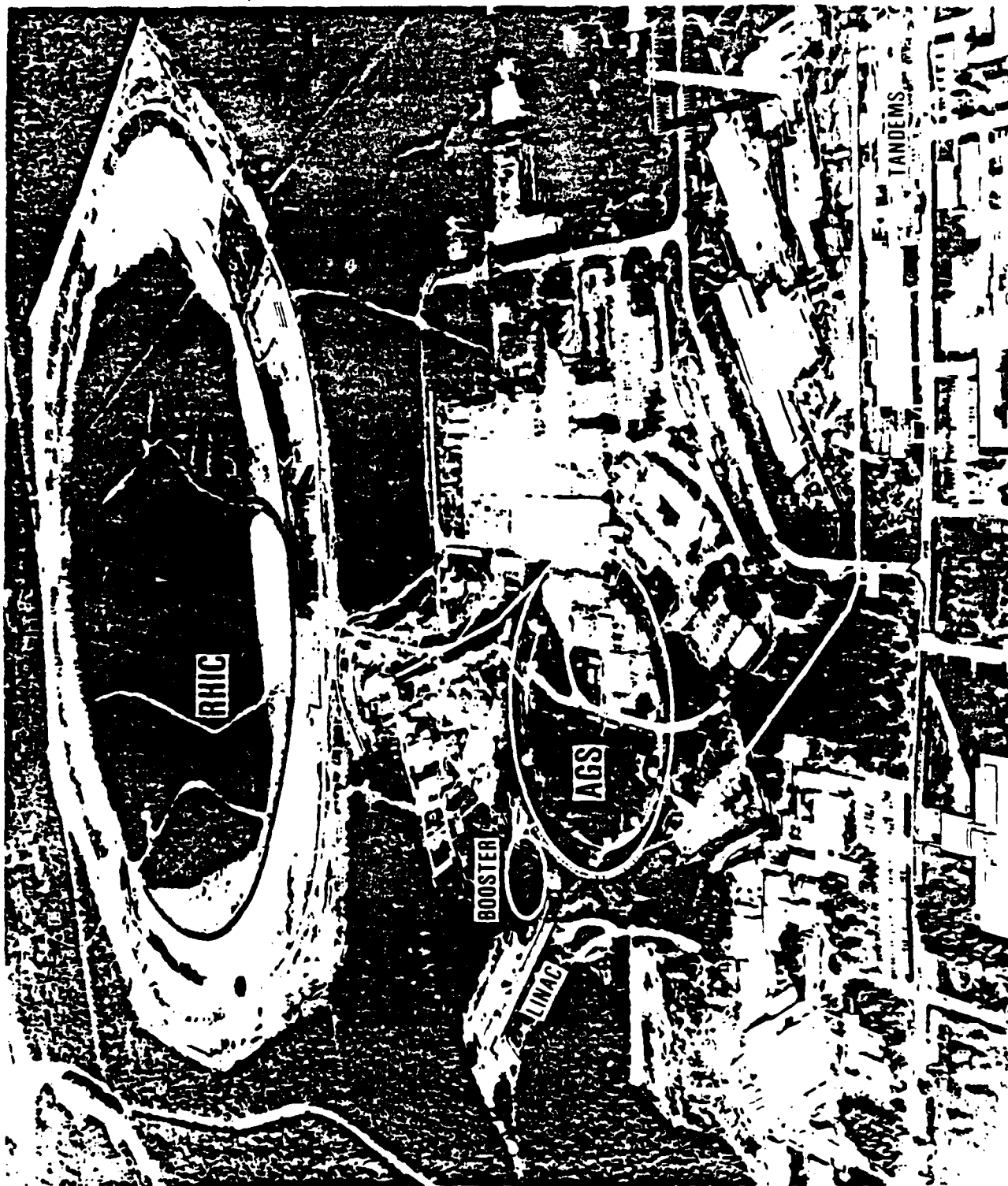


Figure 1. BNL accelerator site.

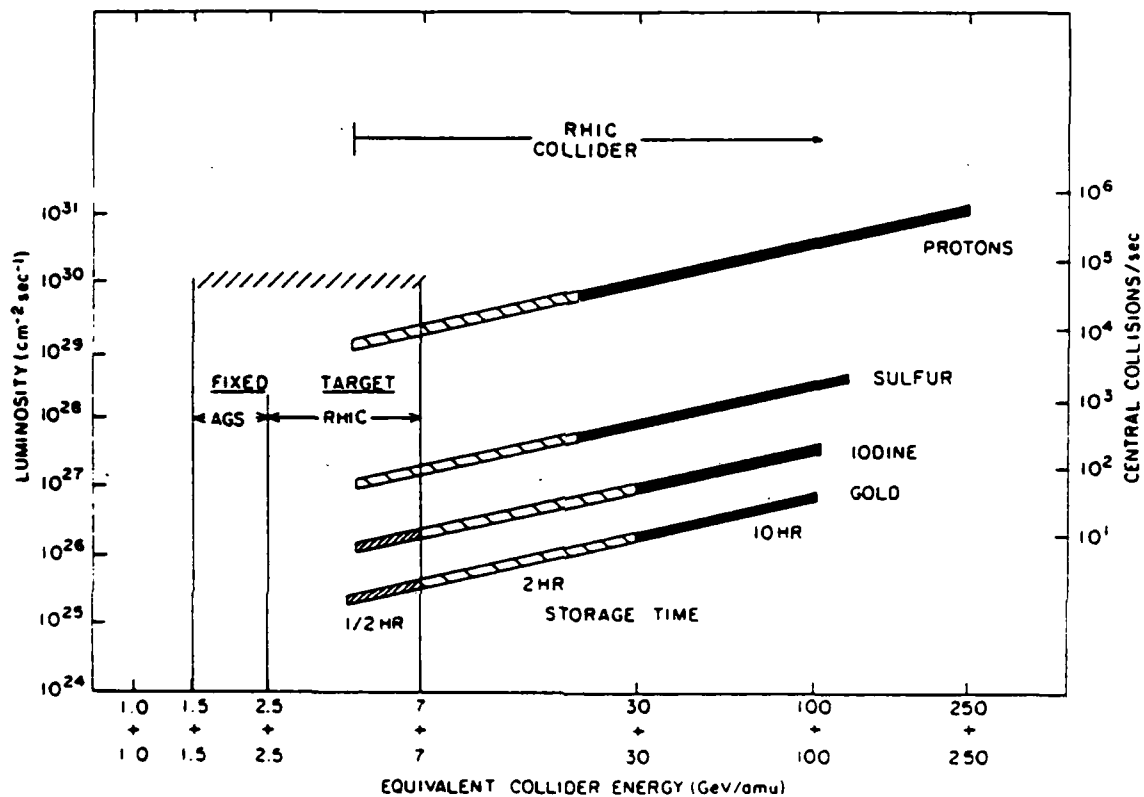


Figure 2 The design luminosity, for various ion masses, as a function of collision energy over the full range accessible with AGS and RHIC. On the left-hand scale, central collisions correspond to impact parameter less than 1 Fermi.

machine that was initially designed to accelerate 10^{10} protons/pulse with internal target operation, the AGS now has accelerated 1.9×10^{13} protons/pulse, 2.0×10^{10} polarized protons/pulse (46% polarization @ 22 GeV/c and 2×10^8 ^{28}Si ions to 15 GeV/amu). The internal targets have now been replaced with various slow and fast extraction modes of operation. With the completion of the Booster Synchrotron, the AGS operating modes will reach levels of 5×10^{13} protons/sec, 4×10^{11} polarized protons/pulse using the accumulator features of the Booster and the 5×10^{12} polarized protons/pulse level with significant improvements in ongoing ion source development, and the acceleration of $10^9 - 10^{10}$ heavy ions (all species). In addition to the Booster construction, a Stretcher is under initial design to improve the slow extracted beam duty factor from 40% to $\approx 100\%$ and

Table I. Booster Synchrotron Parameters

	Protons	Heavy Ions
Injection		
Energy	200 MeV	$> 0.75 \text{ MeV/amu}$
Ejection		
Energy/ Momentum	1.5 GeV	$p=5.27 \frac{Q}{A} \text{ GeV/c/amu}$
Circumference		
(1/4 AGS)	201.78 m	
# Focusing Cells	24 FODO	
Cell Length	8.4 m	
Periodicity	6	
# Straight		
Section/Length	12/3.7 m	
Phase Advance/ Cell	72.3 °	
$\nu_x \sim \nu_y$	4.82	
$B_{\text{max}}/B_{\text{min}}$	14/3.7 m	
η_{max}	2.9 m	
Transition γ	4.86	
rf harmonics	3	3
# dipoles/length	36/2.4 m	
Field Injection	1.56 kG	$> 0.105 \frac{A}{Q}$
Field Ejection	5.46 kG	12.78
# Quadrupole/ length	48/0.5 m	
Repetition Rate	7.5 Hz	1

increase the delivered slow extracted beam intensity by a factor of two to 2.5 to 5.0×10^{13} protons/sec. The fast extracted proton intensity of 5×10^{13} protons/sec would not be affected by the Stretcher. At this level of operation ($8 \mu\text{A}$ current), the AGS could be classified as a mini-hadron factory. With additional alterations, such as, increasing the Booster energy to its maximum design energy of 2.5 GeV and several major AGS system modifications, e.g., main power supply, rf, shielding, etc., the AGS could provide 2×10^{14} protons/sec ($32 \mu\text{A}$). Figure 3 summarizes the available proton intensity for each major enhancement for both fast extraction (FEB) and slow extraction (SEB). The AGS is presently the world's major hadron factory, and with the modest inclusion of a Stretcher, it could also serve as a very cost effective next step in the progression up the intensity frontier to the $100 \mu\text{A}$ domain as proposed by at least four different laboratories around the world.

The mainstream future at BNL is directed, however, to the exploitation of a unique heavy ion collider, RHIC. RHIC consists of two independent rings of superconducting magnets in the former CBA tunnel, operating at a top field of 3.5 Tesla and 4.5° K . Tables II and III list the general parameters for RHIC. Prototype magnets have been constructed at both BNL and in industry and meet the required specifications. In addition to the injector system (AGS), four of six experimental areas are complete, the liquid helium refrigeration system is complete and operational, the collider tunnel is complete, and the prototype control system is being implemented on the AGS. With this collider, one can accelerate all ion species from protons (polarized with the introduction of Siberian snakes) to gold and uranium. For proton-on-proton collisions, one could achieve a center-of-mass energy of 500 GeV with an average luminosity of $8.4 \times 10^{30} \text{ cm}^{-2} \text{ sec}^{-1}$. For gold-on-gold collisions, one could achieve a center-of-mass energy of 40 TeV (100 GeV/amu) with an average luminosity of $4.4 \times 10^{26} \text{ cm}^{-2} \text{ sec}^{-1}$. The maximum performance specifications for RHIC are defined by the beam physics of 100 GeV/amu gold ions. The major limiting condition is the intrabeam scattering process at the highest energy and the highest mass ion. At the lowest energies of RHIC, where beam lifetimes are less than one hour, one would operate RHIC in a fixed target mode by use of a gas jet target in one ring. RHIC will also allow for asymmetric operations, such as, protons in one ring and gold in the other. RHIC is expected to take four years to complete, with a requested start date of construction of October 1988.

Antiproton Production Experiment

The possibility of obtaining very low energy antiprotons of the order of 20 keV kinetic energy from the AGS was first described by Lee.¹ In this paper we would like to outline the requirements for such a facility (or experiment) to accomplish the very low energy antiproton source.

The basic magnetic cycle of the AGS and the Booster is given in Figure 4. After injecting 1.5 GeV protons into the AGS, the magnetic field of the Booster is ramped up to 8.5 kG in order to receive 3.5 GeV/c antiprotons produced by the AGS. The antiprotons are decelerated by the Booster and then extracted to the 200 MeV linac while the AGS delivers the rest of the

1. Y.Y. Lee, 59-61. Proc. 1986 Summer Workshop on Antiproton Beams in the 2-10 GeV/c Range, Brookhaven National Laboratory, August 18-22, 1986, Formal Report, BNL 52082 (1987).

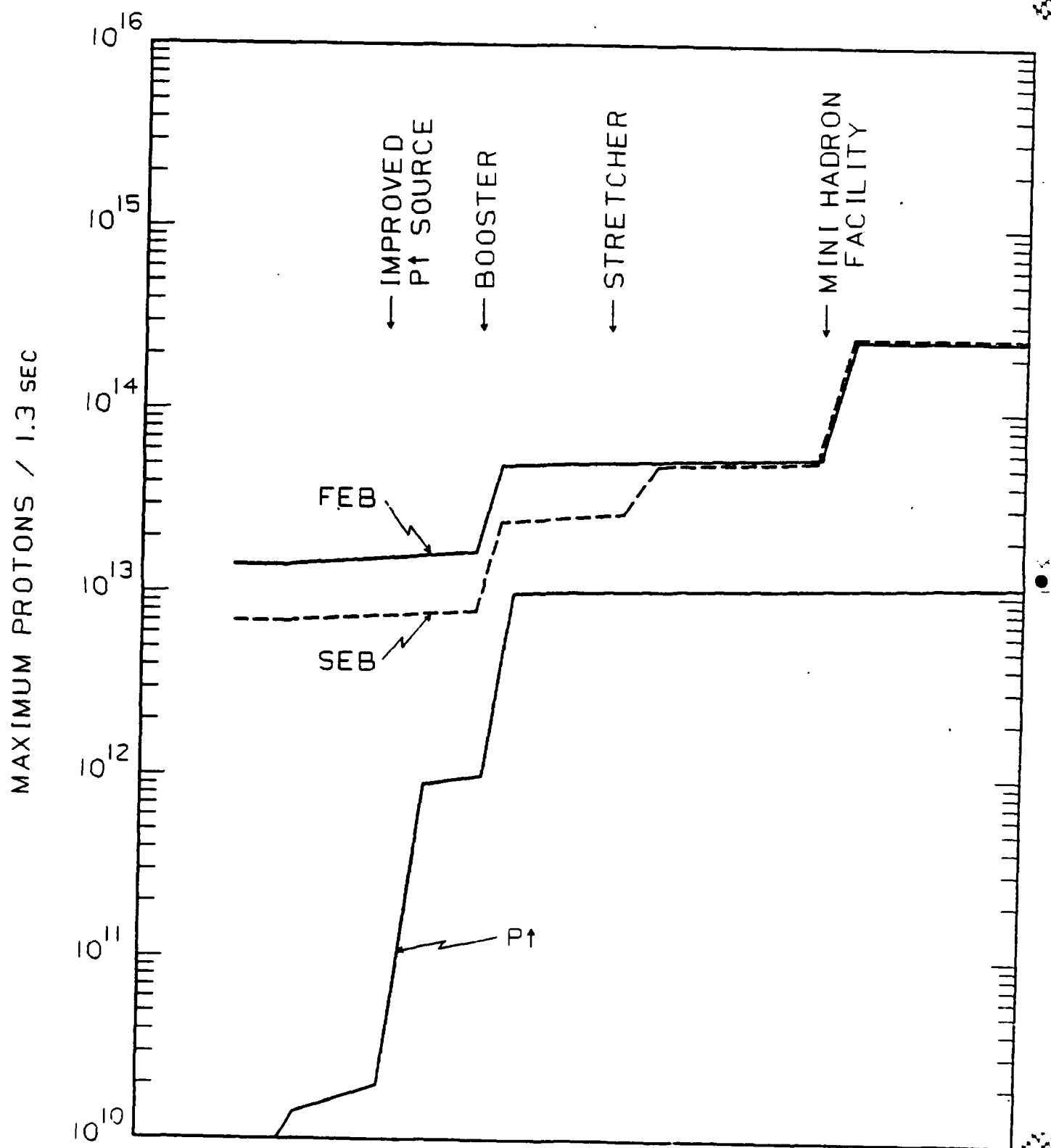


Figure 3

PROTON AND POLARIZED PROTON (P↑) INTENSITY

Table II RHIC General Parameters

Energy Range (each beam),	
Au	7-100 GeV/amu
protons	28.5-250 GeV
Luminosity, Au-Au @	
100 GeV/amu &	
10 H av.	$4.4 \times 10^{26} \text{ cm}^{-2} \text{ sec}^{-1}$
Operational lifetime	
Au @ $\gamma > 30$	> 10 h
Diamond length @	
100 GeV/amu	$\pm 27 \text{ cm rms}$
Circumference,	
4-3/4 C _{AGS}	3833.87 m
Number of crossing	
points	6
Free space at	
crossing point	$\pm 9 \text{ m}$
Beta @ crossing,	
horizontal/vertical	6 m
low-beta/insertion	3 m
Betatron tune,	
horizontal/vertical	28.82
Transition energy, γ_T	25.0
Filling mode	Box-car
No. of bunches/ring	57
No. of Au-ions/bunch	1.1×10^9
Filling time (ea. ring)	$\sim 1 \text{ min}$
Magnetic rigidity, B ρ	
@ injection	96.5 T·m
@ top energy	839.5 T·m
No. of dipoles	
(180/ring+12 common)	372
No. of quadrupoles	
(276/ring+216 insertion)	492
Dipole field @	
100 GeV/amu, Au	3.488 T
Dipole magnetic length	9.46 m
Coil i.d. arc magnets	8 cm
Beam separation in arcs	90 cm
rf frequency	26.7 MHz
rf voltage	1.2 MV
Acceleration time	1 min

Table III. RHIC Beam Parameters

Element	Proton	Deuterium	Carbon	Sulfur	Copper	Iodine	Gold
Atomic No. Z	1	1	6	16	29	53	79
Mass No. A	1	2	12	32	63	127	197
Rest energy (GeV/amu)	0.9383	0.9376	0.9310	0.9302	0.9299	0.9303	0.9308
<u>Injection:</u>							
Kinetic energy (GeV/amu)	28.5	13.6	13.6	13.6	12.4	11.2	10.7
β	0.99947	0.99947	0.99793	0.99794	0.99757	0.99704	0.99680
Norm. emittance (mm.mrad)	20	10	10	10	10	10	10
Bunch area (eV.sec/amu)	0.3	0.3	0.3	0.3	0.3	0.3	0.3
Bunch length (nsec)	± 8.6	± 8.6	± 8.6	± 8.6	± 8.6	± 8.6	± 8.6
Energy spread ($\times 10^{-4}$)	± 3.8	± 7.6	± 7.6	± 7.6	± 8.3	± 9.2	± 9.6
No. ions/bunch ($\times 10^9$)	100	100	22	6.4	4.5	2.6	1.1
<u>Top Energy:</u>							
Kinetic energy (GeV/amu)	250.7	124.9	124.9	124.9	114.9	104.1	100.0
$\beta\gamma$	268.2	134.2	135.2	135.3	124.6	112.9	108.4

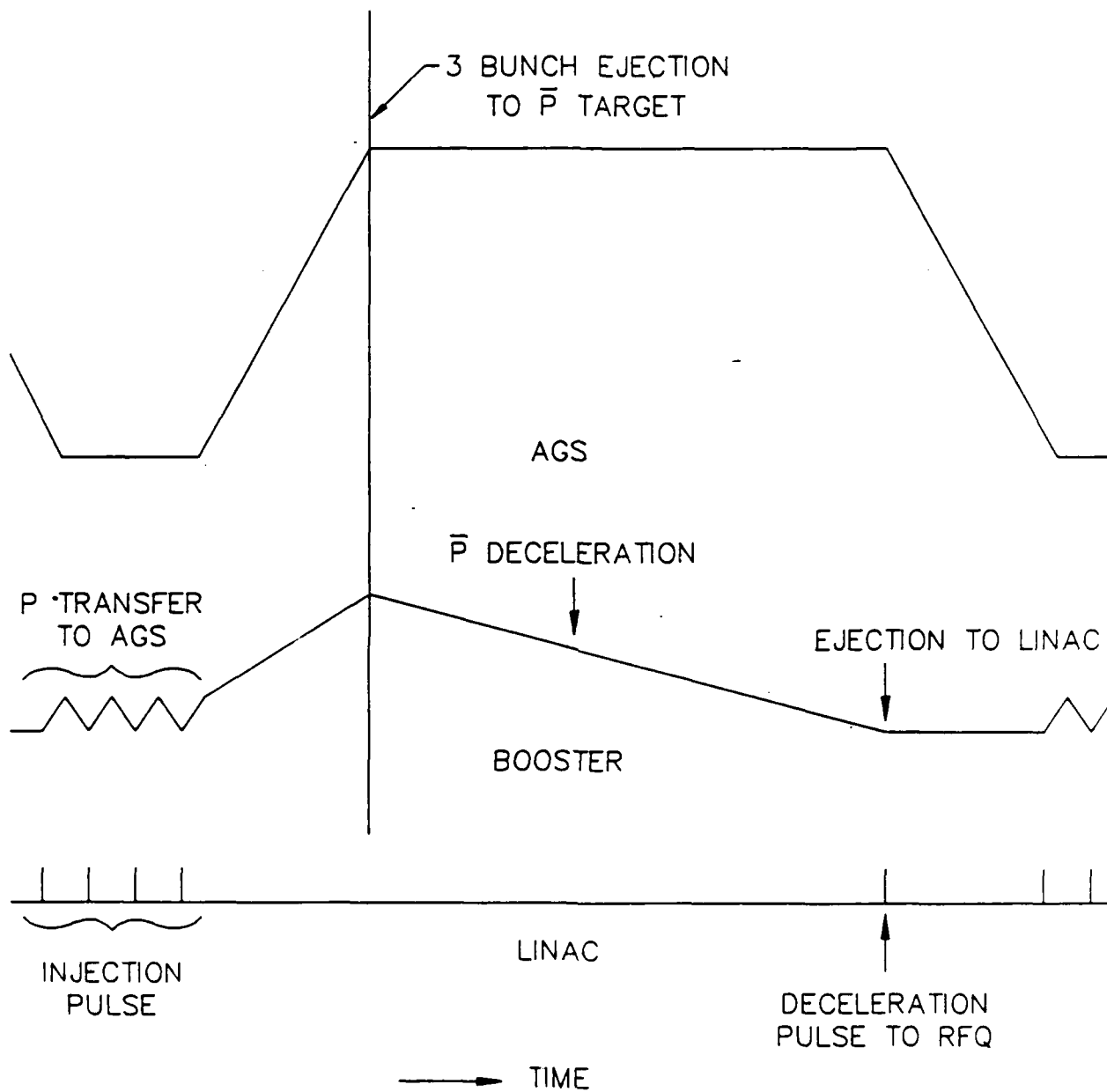


Figure 4
Booster and AGS magnetic cycle

available protons for other experiments. The antiprotons are then decelerated in the linac to 750 keV and then to 20 keV in the RFO linac. Figure 5 is a description of the accelerator complex.

At the end of the AGS acceleration cycle, the AGS rf voltage is raised to shorten the bunch length to a few nanoseconds before extracting three of the twelve bunches through the H10 extraction channel. This will increase the proton beam momentum spread and provide for a short antiproton bunch. The extraction channel and the beam transport should be able to accommodate the proton momentum spread. The additional equipment needed for the extraction is a ferrite kicker and power supply similar to the ones installed at H5 or E5, an extraction septum and power supply similar to the one at H10, and an AGS orbit bump and power supply.

The beam transport consists of six quadrupoles, a triplet in the AGS tunnel for beam shaping and another triplet upstream of the target for focusing the beam on to the target. A special target station similar to the ones at the CERN and Fermilab antiproton facilities must be constructed because of the high intensity beams involved. A focusing element such as a lithium lens is required in order to focus the produced antiprotons into the apertures of the transport quadrupoles. The antiprotons produced by the AGS are then transported to the Booster. The length of the line is approximately 150 meters and requires about 30 degrees of total bend. It requires the order of 10 quadrupoles and six 5 degree bending magnets. Injection into the booster is accomplished by duplicating the Booster extraction septum and kickers.

The antiprotons transported to the Booster will have a 50 pi-mm-mr emittance in both planes and a momentum bite of 2%. The length of the antiproton bunch is the same as the AGS proton bunch which was tailored to a few nanoseconds. By allowing the bunch to rotate in longitudinal phase space one can lengthen it to 50 nanoseconds and the antiproton momentum spread can then be reduced to about a tenth of a percent. No special equipment is needed to decelerate the beam to 200 MeV kinetic energy. One may have to install special instrumentation to detect the low intensity beam.

Decelerated antiprotons can be extracted at the Booster straight section C6. A fast ferrite kicker of strength 6 kG-meter can extract 200 MeV antiprotons from the Booster. A transport system identical to the injection line but of opposite polarity can transport the antiprotons to the HEBT line of the linac. A fast kicker can inject the beam into the upstream end of the linac.

At present we do not foresee any additional equipment required to decelerate the antiprotons through the linac and RFO except increased sophistication in phase and amplitude controls. At the exit of the RFO a kicker is required to deflect the decelerated antiprotons away from the regular proton channel and direct it to the detector region.

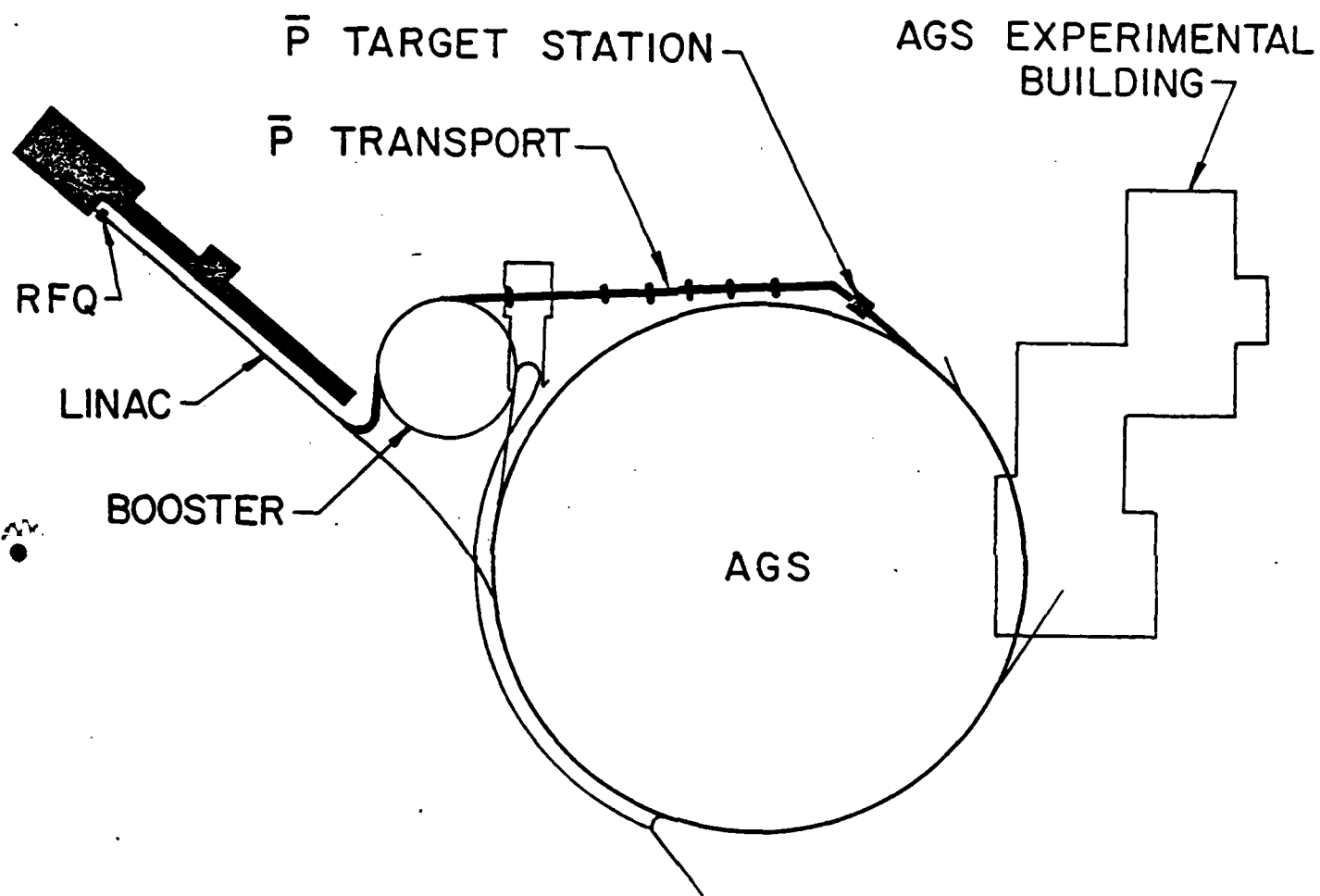


Figure 5
AGS accelerator complex

Additional sophistication is needed in the control system of the AGS, Booster and linac. Pulse-to-pulse modulation of the system is required, not only for the magnetic cycle of the machines, but also to all other systems such as rf and extraction systems.

At present there are two modes of Booster operation, namely fast cycling proton operation and slower cycling heavy ion operation. The proton operation needs higher voltage and lower current while heavy ion operation needs lower voltage but higher current. Power supply modules are rearranged for each of the operations. For the proposed antiproton option, the range of antiproton deceleration current requirements forces one to use the arrangement of the heavy ion option which results in the Booster cycle period to be lengthened by a factor of two. If faster cycling of the Booster is important, one would add a set of modules to the present power supply to increase the repetition rate. It is inefficient to bunch and decelerate in the linac unless the antiproton beam is prebunched to the linac frequency. One would add a 200 MHz rf cavity to bunch the antiprotons in the Booster. This will bring the efficiency to about 80% compared to 50% for decelerating through the linac and RFQ.

It has been demonstrated that one can reduce the six dimensional emittance of the beam in a synchrotron either by stochastic or electron cooling. As a proof of principle experiment the option of cooling is not compelling. It has been calculated¹ that there is a factor of 900 decrease in the available antiproton flux at 20 keV without cooling versus with cooling because of the reduction in the 6-dimensional phase space. We have not estimated the additional costs of introducing stochastic cooling but refer the reader to the copious literature from both CERN and Fermilab.

We estimate the order of magnitude costs to carry out a test of the scheme. The estimate is scaled from either existing AGS equipment costs or scaled from the Booster proposal. We used a rule of thumb number of about \$150/kilowatt for the power supply estimates. We summarize them in Table IV.

Conclusion

BNL's future high-energy and heavy ion physics plans consist of three major components. The first is to exploit the present and near-term upgraded AGS complex for 30 GeV physics, such as, the study of the TeV domain via flavor changing rare kaon decays, neutrino physics, glueball and exotics, spectroscopy, etc. The second is the primary BNL long-term goal of constructing RHIC to study the fundamental properties of matter in a state in which the primordial quarks and gluons are no longer confined as constituents of ordinary particles. The third component, which is now beginning to be considered are the possibilities of a mini-hadron factory with the AGS. Should the physics results of the next years justify the effort and cost, this would be a natural extension of the present and near-term AGS high-energy program.

TABLE IV
(cost in thousands)

I. EXTRACTION FROM AGS-----	360.
FERRITE KICKER	50.
POWER SUPPLY	50.
EXTRACTION SEPTUM	100.
POWER SUPPLY	100.
ORBIT BUMP	10.
POWER SUPPLY	50.
II. TARGET STATION AND PROTON TRANSPORT-----	1070.
QUADRUPOLES (6)	240.
POWER SUPPLIES	180.
TARGET STATION AND LI LENS	650.
III. P-BAR TRANSPORT AND BOOSTER INJECTION-----	1750.
TRANSPORT TUNNEL(450 FT)	450.
QUADRUPOLES (10)	400.
POWER SUPPLIES	300.
DIPOLES (5)	200.
POWER SUPPLIES	100.
INJECTION SEPTUM	100.
POWER SUPPLY	100.
FAST KICKER	50.
POWER SUPPLY	50.
IV. BOOSTER EXTRACTION AND TRANSPORT TO LINAC-----	1010.
EXTRACTION KICKER	100.
POWER SUPPLY	100.
QUADRUPOLES (15)	150.
POWER SUPPLIES	250.
DIPOLES (8)	160.
POWER SUPPLY	150.
KICKER	50.
POWER SUPPLY	50.
V. INSTRUMENTATION AND CONTROLS-----	500.
VI. CHANGES IN BOOSTER TUNNEL AND BUILDING 914-----	100.
VII. BOOSTER POWER SUPPLY ADDITION-----	1000.
VIII. 200 MHz CAVITY SYSTEM-----	450.
SUBTOTAL-----	6240.
EDIA(@15%)	940.
CONTINGENCY(@20%)	1440.
TOTAL	<u>8620.</u>

THE AGS COMPLEX AS AN ANTIPROTON FILLING STATION*

Y.Y. Lee and D.I. Lowenstein
AGS Department, Brookhaven National Laboratory
Associated Universities, Inc.
Upton, New York 11973

A transportable antiproton storage device to store and transport low energy antiprotons for use away from the production facility has been proposed.¹ In this note we examine the AGS complex as a filling station for such a device.

In previous notes² we explored the possibility of using the AGS as a very low energy antiproton source and its implication to the AGS complex. The scheme was to decelerate antiprotons in the AGS Booster to a kinetic energy of 200 MeV, reinject these antiprotons into the linear accelerator backward at the high energy end. The structure of the Linac would decelerate the antiprotons to the normal proton injection kinetic energy of 750 keV. The further deceleration would be accomplished with the RFQ linac to a final energy of 30 keV. The scheme allows the antiprotons to be extracted from the system at any point during deceleration inside the Booster; however, once the particles are injected into the linac, it only can be extracted at the low energy end, i.e., 750 keV or 30 keV at the end of the RFQ.

The production and collection rate of antiprotons can be estimated in the following way. We show in Figure 1 the AGS antiproton production rate for collection solid angles of 5 and 40 milliradians.³ We then apply several correction factors to these rates. The fraction of surviving antiprotons corrected for the focal depth of the lithium lens and the finite length of the target can be approximately expressed as⁴

$$\frac{2}{L} \beta_0 \tan^{-1}\left(\frac{L}{2\beta_0}\right) \quad (1)$$

where L = length of the target,

$\beta_0 = r_0 / \Delta\theta$ at target center,

r_0 = incident beam radius,

$\Delta\theta$ = angular acceptance.

*Work performed under the auspices of the U.S. Department of Energy.

The fraction of incident beam interacting in the target segment can be expressed

$$df = 1/\lambda \cdot e^{-z/\lambda} \cdot dz \quad (2)$$

where λ = nuclear absorption length.

The fraction of the produced antiprotons that survive to the end of the target is

$$e^{-(L - z)/\lambda} \quad (3)$$

By combining (2) and (3), and integrating

$$L/\lambda \cdot e^{-L/\lambda} \quad (4)$$

Combining (1) and (4), one obtains the total production and collection efficiency

$$E = \frac{2\beta_0}{\lambda} e^{-L/\lambda} \tan^{-1} \left(\frac{L}{2\beta_0} \right)$$

For example, taking $\lambda = 10$ cm, $r_0 = 0.5$ mm, $\Delta\theta = 100$ mr, one gets a broad maximum around $L = 2.7$ cm where $E = 0.093$. We will assume this efficiency for estimating the intensity of antiprotons.

The intensity of the extracted antiproton beam depends on several factors. Since transverse emittances of the beam changes inversely proportional to the momentum of the particle, one expects to lose antiproton intensities by a factor of the momentum squared while decelerating inside the Booster. Since the normalized admittance of the AGS linac is about 90π mm-mr, which is larger than that of the Booster at 200 MeV, one does not expect to lose antiprotons due to the transverse aperture of the drift tube structure. However, the longitudinal acceptance (rf bucket size) of the linac is estimated to be 3.5×10^{-4} eV-sec at 200 MHz, which is about a factor of 30 smaller than expected longitudinal emittance of the antiprotons inside the Booster.⁵ Table I summarizes the expected intensity at various points assuming the antiprotons are produced at 2.5 GeV/c by three rf bunches of a post-Booster AGS and are not cooled in the Booster.

Table I
Expected Intensity Without Cooling

ENERGY	INTENSITY (per 1.5×10^{13} protons)
2.5 GeV	7.2×10^7
200 MeV	4.8×10^6
750 keV	1.6×10^5
30 keV	1.6×10^5

An obvious solution to losing intensity in six dimensional phase space is to cool the beam inside the Booster. Adequate cooling can be achieved by means of stochastic cooling. Figure 2 shows the antiproton yield and relative time constant for ideal stochastic cooling in the Booster versus antiproton momentum. Since the whole production and deceleration cycle should be within the AGS cycle, certain compromises must be made as to the momentum which antiprotons are collected at for maximum intensity and the cooling time required.

The following is one possible scenario for the antiproton collection and deceleration cycle. We chose 2.5 GeV/c as the production momentum as a compromise between production and coolability. The antiprotons are then pre-cooled transversely for 200 milliseconds before decelerating to 200 MeV. At this point, the antiprotons are cooled both transversely and longitudinally before bunching to the linac frequency. The cooling time required is estimated to be 20 milliseconds.

In order to be a filling station, antiprotons should be available at all reasonable energies. The scheme mentioned above lacks availability between 200 MeV and 750 keV. One solution is to decelerate the beam further in the Booster. First, we examine the lowest energy one can reasonably decelerate to in the Booster. One of the many functions of the Booster is to pre-accelerate heavy ions of initial kinetic energy as low as 1 MeV per nucleon. The radio frequency system for this mode is capable of tuning to antiproton kinetic energy of as low as 1 MeV. For an iron dominated accelerator ring magnet, one may assume good magnetic field for pole tip fields of above 100 Gauss.

This would correspond to an antiproton momentum of 65 MeV/c or kinetic energy of 2.3 MeV. For this scheme, the cooling of the transverse emittance of the beam is essential to avoid losses of over a factor of 100 in transverse emittance blowup. Longitudinal cooling is not required because the rf bucket size is big enough to contain the bunches. At this point, one could extract and inject into a suitably designed RFQ linac to decelerate to 30 keV. Table II summarizes the available fluxes at various energies.

TABLE II
Available Antiproton Intensity with
Cooling per 1.5×10^{13} AGS Protons

ENERGY	LINAC	BOOSTER
	----- cooling -----	
2.5 GeV/c - 0.644 GeV/c (1.75 GeV - 200 MeV)	7.2×10^7	7.2×10^7
	----- cooling -----	
< 644 MeV/c - 66 MeV/c (200 MeV - 2.3 MeV)	N/A	7.2×10^7
37.5 MeV/c* (750 keV)	6.9×10^7	N/A
7.5 MeV/c (30 keV)	6.9×10^7	$6.9 \times 10^{7**}$
*Bunching efficiency assumed at 95%.		
**New RFQ required.		

References

1. T. Kalogeropoulos, private communication.
2. Y.Y. Lee and D.I. Lowenstein, Proceedings of the Rand Antimatter Workshop, 1987.
3. BNL 52082, Proceedings of the 1986 Workshop on Antiproton Beams, 1986.
4. F.E. Mills, Proceedings of the Rand Antimatter, Workshop, 1987.
5. We would like to thank Dr. F. Mills for pointing this out.

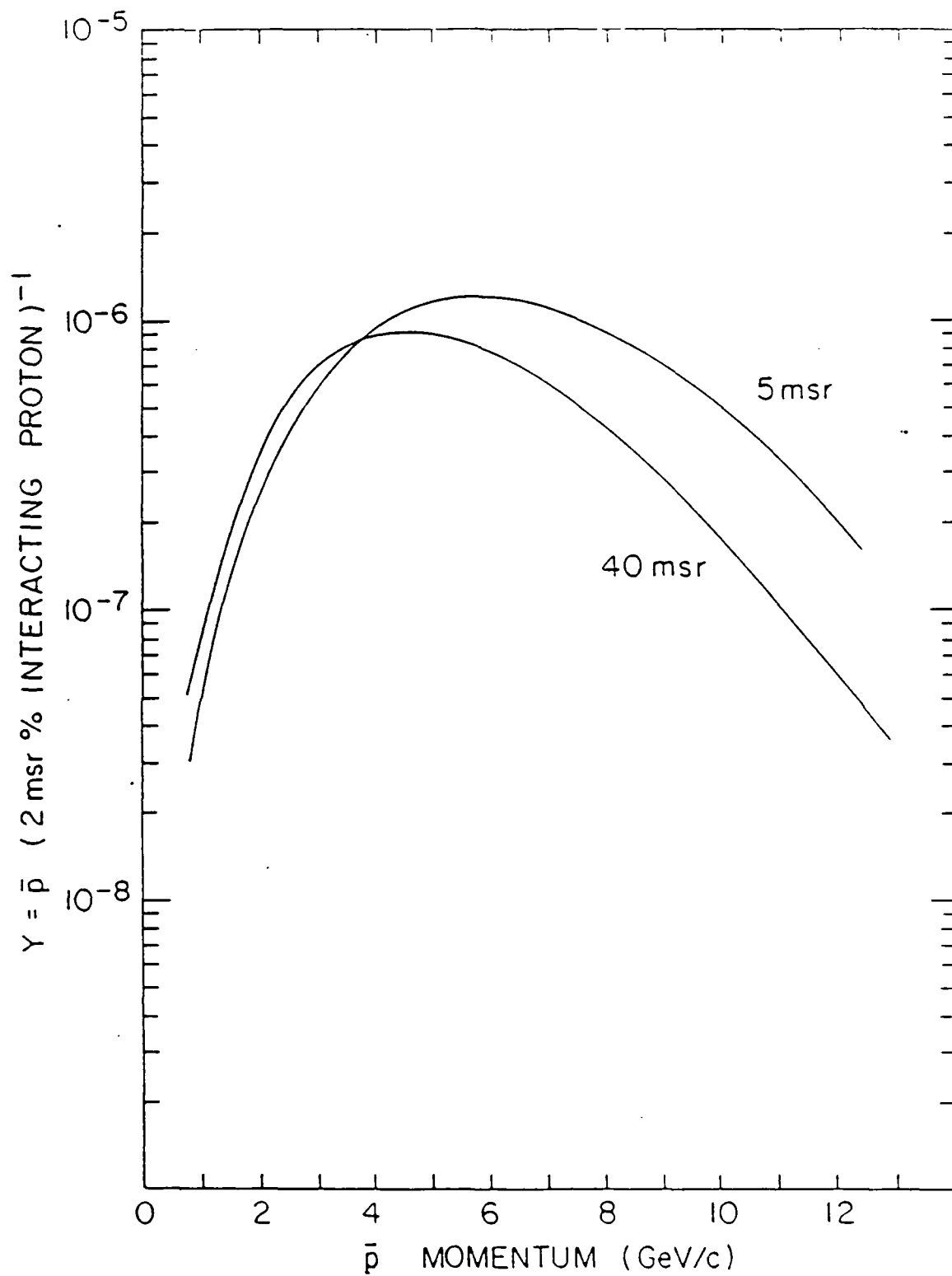


Figure 1

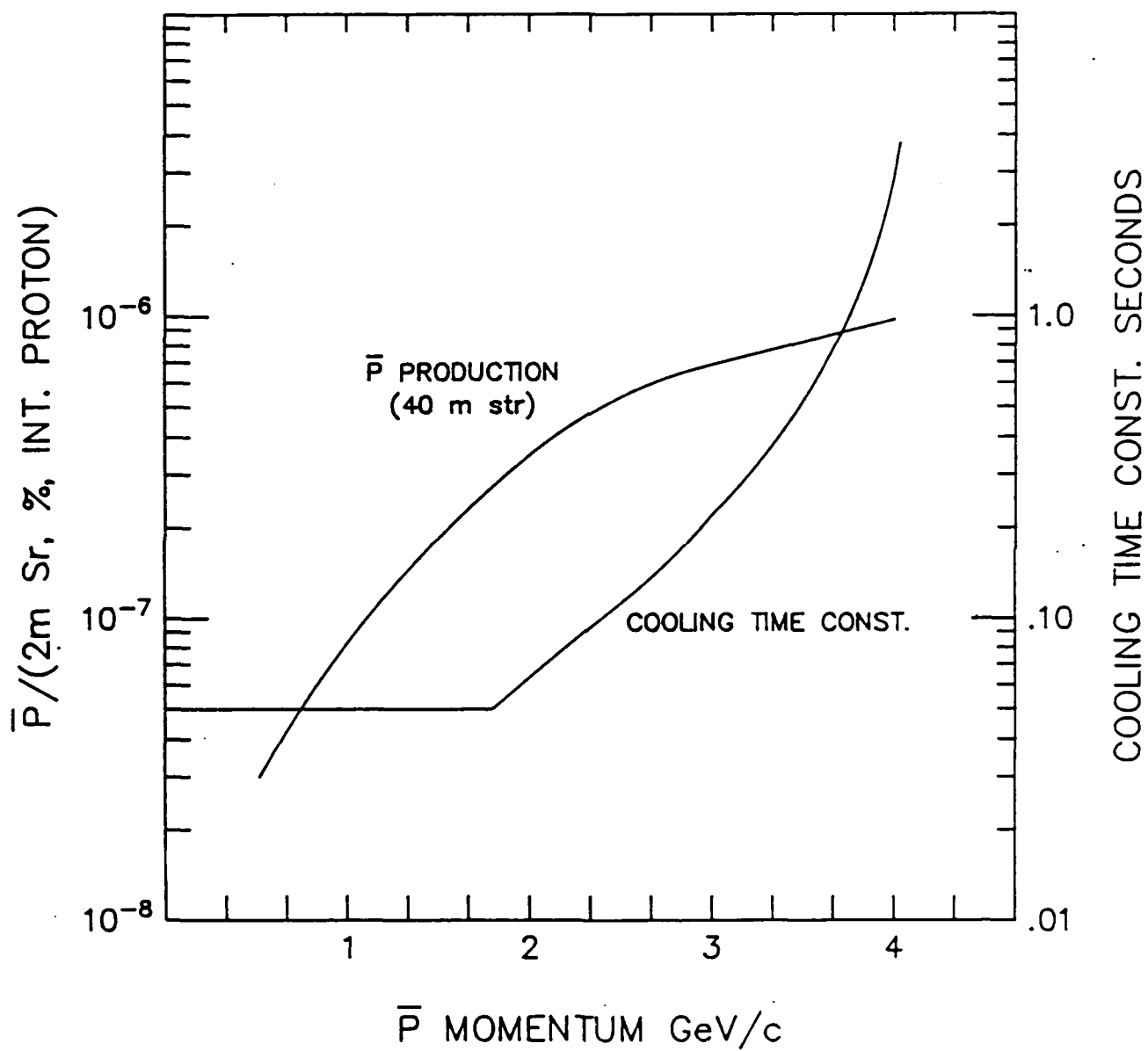


Figure 2

A Storage Ring for Antimatter Transport*

David B. Cline**

Department of Physics
UNIVERSITY OF CALIFORNIA
Los Angeles
California

1. Introduction

The future studies of antimatter/matter interactions and applications require additional facilities for study. Currently no dedicated facility exists in the USA. We outline a scheme here to produce antiprotons at BNL and store them in a modest superconducting storage ring that is designed along the lines of the ELENA storage ring that was designed for the CERN LEAR application. It is envisioned that this storage ring will constitute a transportable antimatter facility that can be carried to various locations in the USA to carry out studies of antimatter/matter interactions and applications. The transport of antimatter will also demonstrate the possibility of applications of antimatter energy sources that are removed from the site of the antimatter production, a key development in the eventual use for space applications.

* Prepared for the RAND meeting, 6-9 October 1987

** In conjunction with H. Herr (CERN), C.J. Wang (UCLA), Y.Y. Lee (BNL) and T. Kalogeropoulos (Syracuse)

The storage ring outlined here is designed to be stable for transport and to store 10^{10} – 10^{12} antiprotons for periods of several months. The ring will use superconducting magnets for the purpose of low energy consumption and transport. Many other aspects of the storage ring are similar to the parameters of the ELENA ring that was designed for CERN. In particular, the ring is designed to decelerate the antiproton on the site to ~ 200 KeV kinetic energy. It is assumed that a suitable source of antiprotons will exist to "fill" the ring, however the construction and testing and transport of the storage ring can be carried out with protons to demonstrate the feasibility of this approach. In this report we first describe the possible source of antiprotons at the BNL site, and then give a brief survey of the state of the art in low energy storage rings and electron cooling techniques that are needed for the accumulation and long-time storage of the antiprotons. We then describe the ring and its parameters and the expected properties under the transportable conditions. Finally the possibility of decelerating in the ring is described. We expect this work to be followed by a detailed proposal for the design and construction of the storage ring by the CERN-BNL-UCLA-Syracuse group. In addition a special workshop on the conceptual design will be held at UCLA, 16–21 November 1987. After that period a Conceptual Design Proposal will be produced.

2. Antiproton Source at BNL as an Example

The possibility of obtaining antiprotons of the order of 200 MeV kinetic energy from the AGS was recently described by A. Carroll et al elsewhere (Appendix B). In this paper we would like to outline the requirements for such a facility (or experiment) to accomplish the very low energy antiproton

source. A similar scheme was first worked out at FNAL in 1977 (D. Cline, F. Mills, P. McIntyre, C. Rubbia — see Appendix A for details of this scheme).

The basic magnetic cycle of the AGS and the Booster is given in Figure 1. After injecting 1.5 GeV protons into the AGS, the magnetic field of the Booster is ramped up to 8.5 kG in order to receive 3.5 GeV/c antiprotons produced by the AGS. The Booster must be ramped down to 100 MeV (or 444 MeV/c) compared to 640 MeV/c for the present design. This requires a modest change in the lowest magnetic field in the Booster. The antiprotons are decelerated by the Booster and then extracted to the 200 MeV linac while the AGS delivers the rest of the available protons for other experiments. The antiprotons are then decelerated in the linac to 750 keV and then to 20 keV in the RFQ linac. Figure 2 is a description of the accelerator complex.

At the end of the AGS acceleration cycle, the AGS rf voltage is raised to shorten the bunch length to a few nanoseconds before extracting three of the twelve bunches through the I10 extraction channel. This will increase the proton beam momentum spread and provide for a short antiproton bunch. The extraction channel and the beam transport should be able to accommodate the proton momentum spread. The additional equipment needed for the extraction is a ferrite kicker and power supply similar to the ones installed at H5 or E5, an extraction septum and power supply similar to the one at H10, and an AGS orbit bump and power supply.

The beam transport consists of six quadrupoles, a triplet in the AGS tunnel for beam shaping and another triplet upstream of the target for focusing the beam on to the target. A special target station similar to the ones at the CERN and Fermilab antiproton facilities must be constructed because of the high intensity beams involved. A focusing element such as a lithium lens is required in order to focus the produced antiprotons into the apertures of the transport quadrupoles. The antiprotons produced by the AGS are

then transported to the Booster. The length of the line is approximately 150 meters and requires about 30 degrees of total bend. It requires the order of 10 quadrupoles and six 5-degree bending magnets. Injection into the booster is accomplished by duplicating the Booster extraction septum and kickers.

The antiprotons transported to the Booster will have a 50π -mm-mr emittance in both planes and a momentum bit of 2% (see AGS Booster Parameter List — Table 1). The length of the antiproton bunch is the same as the AGS proton bunch which was tailored to a few nanoseconds. By allowing the bunch to rotate in longitudinal phase-space one can lengthen it to 50 nanoseconds and the antiproton momentum spread can then be reduced to about a tenth of a percent. No special equipment is needed to decelerate the beam to 200 MeV kinetic energy. One may have to install special instrumentation to detect the low intensity beam.

Decelerated antiprotons can be extracted at the Booster straight section C6. A fast ferrite kicker of strength 6 kG-meter can extract 200 MeV antiprotons from the Booster. A transport system identical to the injection line but of opposite polarity can transport the antiprotons to the HEBT line of the linac. A fast kicker can inject the beam into the upstream end of the linac.

At present we do not foresee any additional equipment required to decelerate the antiprotons through the linac and RFQ except increased sophistication in phase and amplitude controls. At the exit of the RFQ a kicker is required to deflect the decelerated antiprotons away from the regular proton channel and direct it to the detector region.

Additional sophistication is needed in the control system of the AGS, Booster and linac. Pulse-to-pulse modulation of the system is required, not only for the magnetic cycle of the machines, but also to all other systems such as rf and extraction systems.

At present there are two modes of Booster operation, namely fast cycling proton operation and slower cycling heavy ion operation. The proton operation needs higher voltage and lower current while heavy ion operation needs lower voltage but higher current. Power supply modules are rearranged for each of the operations. For the proposed antiproton option, the range of antiproton deceleration current requirements forces one to use the arrangement of the heavy ion option which results in the Booster cycle period to be lengthened by a factor of two. If faster cycling of the Booster is important, one would add a set of modules to the present power supply to increase the repetition rate. It is inefficient to bunch and decelerate in the linac unless the antiproton beam is prebunched to the linac frequency. One would add a 200 MHz rf cavity to bunch the antiprotons in the Booster. This will bring the efficiency to about 80% compared to 50% for decelerating through the linac and RFQ.

It has been demonstrated that one can reduce the six dimensional emittance of the beam in a synchrotron either by stochastic or electron cooling. As a proof of principle experiment the option of cooling is not compelling. It has been calculated that there is a factor of 900 decrease in the available antiproton flux at 20 keV without cooling versus with cooling because of the reduction in the 6-dimensional phase-space. We have not estimated the additional costs of introducing stochastic cooling but refer the reader to the copious literature from both CERN and Fermilab.

We estimate the order of magnitude costs to carry out a test of the scheme. The estimate is scaled from either existing AGS equipment costs or scaled from the Booster proposal. We used a rule of thumb number of about \$150/kilowatt for the power supply estimates.

Table 1
AGS
Booster Parameter Summary

type of machine	synchrotron for protons and heavy ions, polarized proton accumulator						
beam energy, max							
	p	d	C	S	Cu	I	Au
	1.50	1.93	11.60	30.95	53.81	74.62	68.95 GeV
	1.500	0.963	0.967	0.967	0.854	0.588	0.350 GeV/nucleon
circumference	201.78 m ($1/4$ AGS)						
straight-section use	RF, h=3, A6 and E6 RF, h=1, B3 and B6 proton inj. kickers, C3 and C6 heavy ion inj. kicker, A3 heavy ion elec. septum, A3 ejection kicker, F3 ejection septum, F6 absorber blocks, D3						
bunch separation, number of bunches							
number of particles/pulse*	protons, $1 - 3 \times 10^{13}$ polarized protons, $\sim 10^{12}$						

* These values are based on the assumptions specified in BST/TN 55, "Expected Heavy Ion Intensity in the Booster," by Y.Y. Lee.

AGS

Booster Parameter Summary (continued)

C	S	Cu	I	Au	
54	~15	~10	~6.6	~3.2	$\times 10^9$ ions

beam current

p	p↑	d	C	S	Cu	I	Au
---	----	---	---	---	----	---	----

mA pk

mA avg

beam energy, max

p	p↑	d	C	S	Cu	I	Au
---	----	---	---	---	----	---	----

kJ

transverse emittance, inj., (90% area/ π)

50 mm-mrad

rms fractional energy spread, inj-ejec

bunched to 1.5 eV-s, protons

bunched to 0.05 eV-s/nucleon, heavy ions

longitudinal emittance, inj-ejec (rms area/ π)

lattice, total number of cells FODO, 8.4075-m cells, 24

betatron tune, x y 4.82, 4.83

natural chromaticity

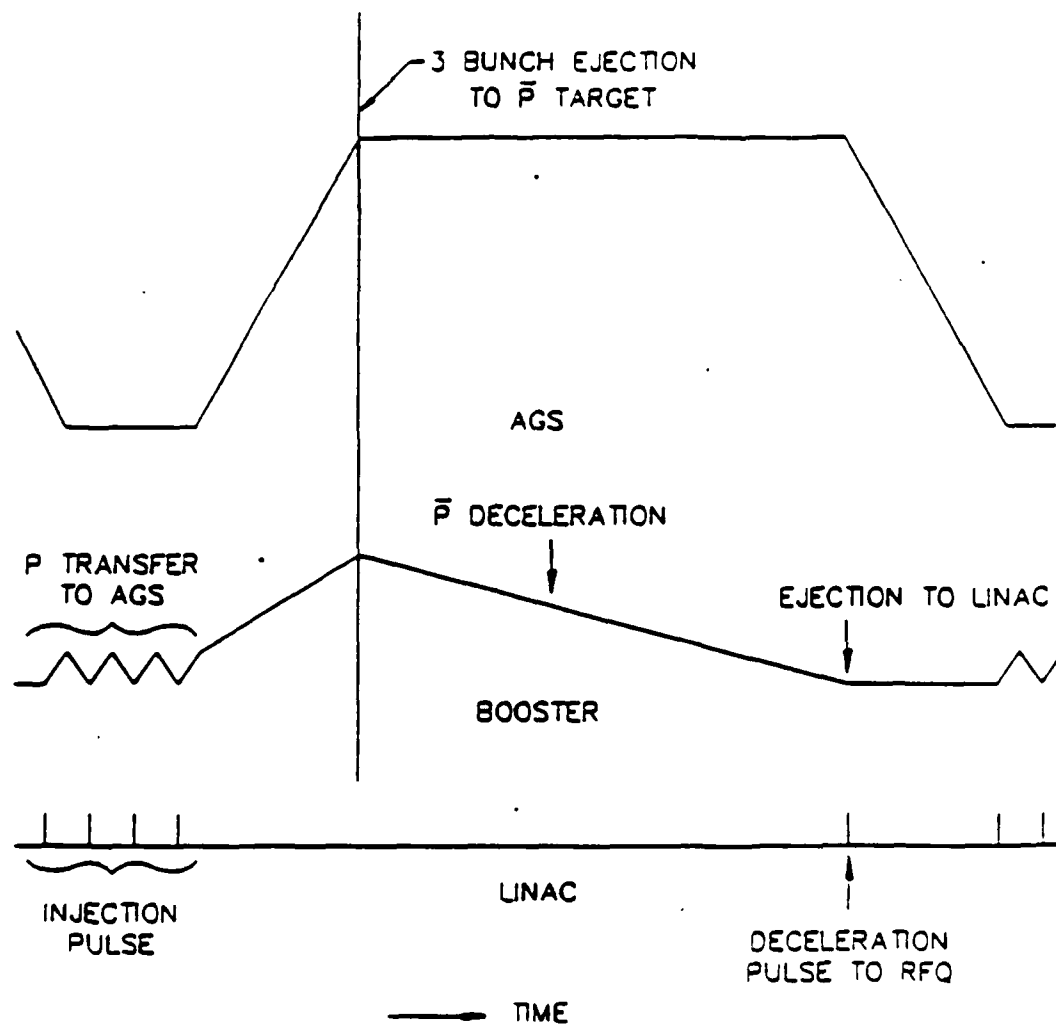


Figure 1. Booster and AGS magnetic cycle

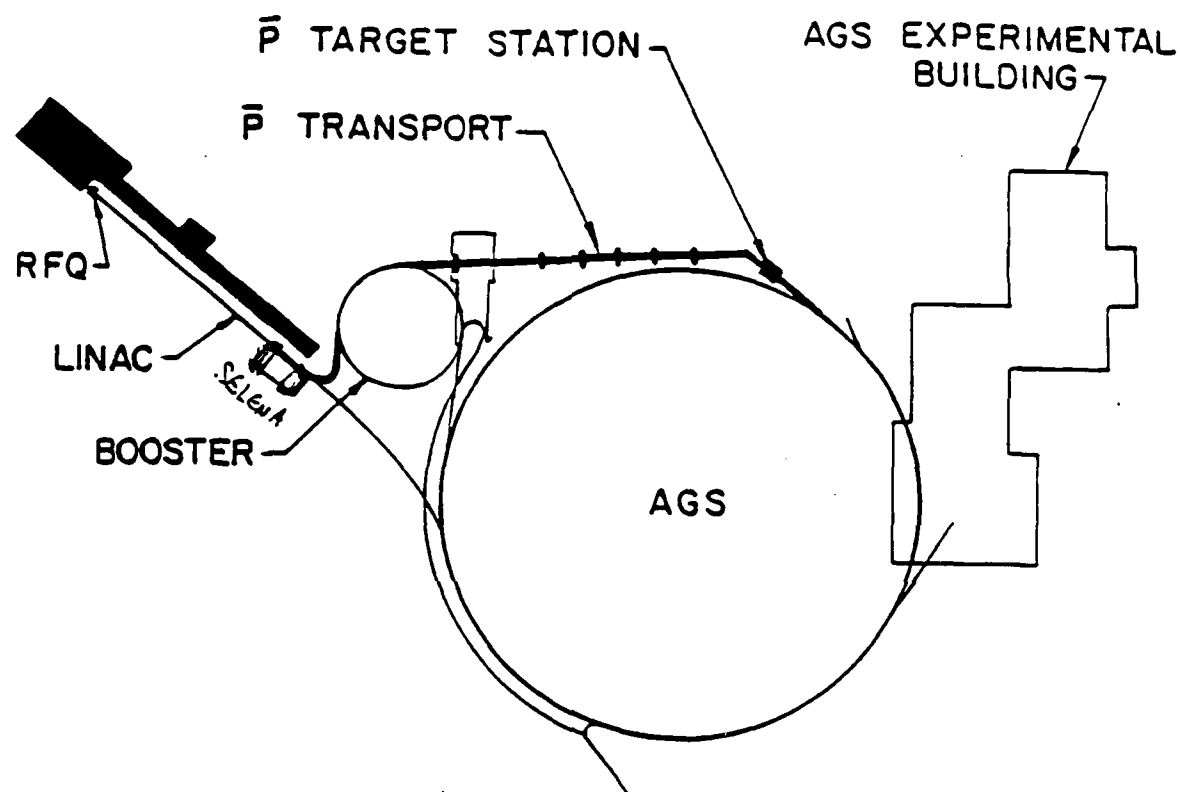


Figure 2. AGS accelerator complex

Table 2
Low Energy Storage Rings
Around the World

	Machine	Location	Particles	Energy M_{az}	Cooling
1.	LEAR	CERN	Antiprotons	5 MeV to 2 GeV/c	s - e ⁺
2.	CELSIUS	Uppsala, Sweden	Ions	1.3 GeV	e
3.	COSY	Jülich	p - Li	1.5 GeV	s - e
4.	TARN I	Japan	p	7 MeV	s
	TARN II	(INS) Tokyo	p - Ne	1.3 GeV	s - e
5.	INDIANA COOLER	Indiana	p - Li	0.5 GeV	e
6.	AARHUS RING	Sweden	p - u	125 MeV/A	e-Laser
7.	CRY-RING	Stockholm Sweden	p - u	125 MeV/A	e-Laser
8.	TSR	Heidelberg	p - u	150 MeV/A	e

S=stochastic cooling, e=electron cooling

Table 3
Basic Lear Parameter

Momentum (kinetic energy) range	0.1-2 GeV/c (5.3 MeV - 1.3 GeV)
Injection momentum (kinetic energy)	0.6 GeV/c (175.4 MeV)
Circumference	78.54 m
Typical cycle	10^9 \bar{p} injected every 10^3 s
Typical extracted beam	10^6 \bar{p} 's per second
Typical spill length	900 s
Long straight sections	4 of 8 m length each
Short straight sections	8 of 1 m length each
Bending magnets:	
Number, arc length, field at 2 GeV/c	4, 6.55 m, 1.6 T
Quadrupoles:	
Number, magnetic length, max gradient	16, 0.5 m, 12 T/m
Focusing structure	4 superperiods, BoDFOFDoB
Betatron wave number	$Q_H \sim 2.3$, $Q_V \sim 2.7$
Momentum compaction	$\alpha = \gamma_{tr}^{-2} = 4.8 \times 10^{-3}$
Aperture limitations	$a_H = \pm 70\text{mm}$, $a_V = \pm 29\text{mm}$
Acceptances	$\epsilon_H = 240\pi\text{-mm-mr}$ $\epsilon_V = 48\pi\text{-mm-mr}$ $\Delta p/p = \pm 1.1\%$
Vacuum system design pressure	10^{-11} - 10^{-12}
Bake-out temperature	300° C
Pump down time	40 h
RF system frequency range ($h = 1$)	0.4 - 3.5 MHz
Peak voltage per turn	12 kV

Circumference	: 11.4 m = $\frac{1}{7}$ of LEAR
Length of straight sections	: 2.0 m
Bending radius	: 0.54 m
Gradient of D-magnet	: -1.6 m^{-2}
Kinetic energy range	: 5 MeV ... 200 keV
Magnetic field	: 0.62 T ... 0.124 T
Revolution time	: 360 ns ... 1.8 μ s
Tune Q_H/Q_V	: 1.63/1.43
Size of vacuum chamber	: $\sim 10 \times 5 \text{ cm}$
Vacuum	: $\sim 10^{-11}$ Torr

Table 4. Some Parameters of ELENA

3. Low Energy Storage Rings Around the World

There are more than 10 low energy storage rings around the world that are either in a state of construction or being designed. Table 2 lists some of these rings.

These storage rings are constructed for a number of purposes including antiproton collection, atomic physics, et cetera. This widespread construction of such machines indicates that low energy storage rings are rather common and increases the possibility that the transportable superconduct-

POS	S	UX	UY	UX	UY	UX	UY	UX	UY
0	0.0000	0.00000	0.00000	.44450	.59913	-.00000	-.00000	1.00364	.00000
1	.1000	.33922	.32261	.46700	.71343	-.22497	-.14304	1.00364	.00000
2	.2000	.06729	.34435	.53449	.75434	-.44984	-.28607	1.00364	.00000
3	.3000	.09449	.06491	.54697	.82756	-.67492	-.42911	1.00364	.00000
4	.4000	.11062	.08271	.50449	.92709	-.89989	-.57214	1.00364	.00000
5	.5000	.13434	.09881	1.00693	1.05672	-1.12486	-.71918	1.00364	.00000
6	.6000	.14892	.11288	1.25440	1.21406	-1.34983	-.89821	1.00364	.00000
7	.7000	.15996	.12510	1.54686	1.40000	-1.57481	-1.00125	1.00364	.00000
8	.8000	.16828	.13549	1.88412	1.61455	-1.79978	-1.14428	1.00364	.00000
9	.9000	.17499	.14489	2.26677	1.85771	-2.02475	-1.28732	1.00364	.00000
10	1.0000	.18343	.15289	2.69422	2.12948	-2.24972	-1.43035	1.00364	.00000
11	1.1000	.18920	.16030	3.13264	2.40609	-2.47192	-1.57253	1.00364	.00000
12	1.2000	.19428	.16698	3.47434	2.61904	-2.61904	-.83131	1.00364	.00000
13	1.3000	.19896	.17322	3.69126	2.75318	-.69891	-.43098	1.00364	.00000
14	1.4000	.20349	.17926	3.76560	2.79898	-.00000	-.00000	1.00364	.00000
15	1.5000	.20799	.18530	3.69126	2.75318	.69891	.43098	1.00364	.00000
16	1.6000	.21263	.19155	3.47434	2.61904	1.34043	.83131	1.00364	.00000
17	1.7000	.21771	.19823	3.13264	2.40609	1.87192	1.17253	1.00364	.00000
18	1.8000	.22347	.20564	2.69422	2.12948	2.24972	1.43035	1.00364	.00000
19	1.9000	.22992	.21364	2.26677	1.85771	2.02475	1.28732	1.00364	.00000
20	2.0000	.23762	.22284	1.88412	1.61455	1.79978	1.14428	1.00364	.00000
21	2.1000	.24695	.23343	1.54686	1.40000	1.57481	1.00125	1.00364	.00000
22	2.2000	.25838	.24565	1.25440	1.21406	1.34983	.89821	1.00364	.00000
23	2.3000	.27256	.25972	1.00693	1.05672	1.12486	.71918	1.00364	.00000
24	2.4000	.28928	.27582	.50449	.92709	.89989	.57214	1.00364	.00000
25	2.5000	.31241	.29402	.54697	.82756	.67492	.42911	1.00364	.00000
26	2.6000	.33981	.31418	.53449	.75434	.44984	.28607	1.00364	.00000
27	2.7000	.37168	.33592	.46700	.71343	.22497	.14304	1.00364	.00000
28	2.8000	.40690	.35893	.44450	.69913	.00000	-.00000	1.00364	.00000
29	2.9000	.44450	.38418	.46700	.71343	.22497	.14304	1.00364	.00000
30	3.0000	.48450	.41163	.53449	.75434	.44984	.28607	1.00364	.00000
31	3.1000	.52697	.44135	.54697	.82756	.67492	.42911	1.00364	.00000
32	3.2000	.57186	.47346	.50449	.92709	.89989	.57214	1.00364	.00000
33	3.3000	.61918	.50897	.46700	.99913	.99913	.99913	1.00364	.00000
34	3.4000	.66889	.54697	.44450	1.00000	1.00000	1.00000	1.00364	.00000
35	3.5000	.72098	.58732	.44450	1.00000	1.00000	1.00000	1.00364	.00000
36	3.6000	.77543	.63035	.46700	1.00000	1.00000	1.00000	1.00364	.00000
37	3.7000	.83131	.67607	.53449	1.00000	1.00000	1.00000	1.00364	.00000
38	3.8000	.88821	.72481	.54697	1.00000	1.00000	1.00000	1.00364	.00000
39	3.9000	.94607	.77656	.50449	1.00000	1.00000	1.00000	1.00364	.00000
40	4.0000	1.00486	.83131	.46700	1.00000	1.00000	1.00000	1.00364	.00000
41	4.1000	1.06455	.88821	.44450	1.00000	1.00000	1.00000	1.00364	.00000
42	4.2000	1.12486	.94607	.46700	1.00000	1.00000	1.00000	1.00364	.00000
43	4.3000	1.18571	1.00486	.53449	1.00000	1.00000	1.00000	1.00364	.00000
44	4.4000	1.24709	1.06455	.54697	1.00000	1.00000	1.00000	1.00364	.00000
45	4.5000	1.30898	1.12486	.50449	1.00000	1.00000	1.00000	1.00364	.00000
46	4.6000	1.37135	1.18571	.46700	1.00000	1.00000	1.00000	1.00364	.00000
47	4.7000	1.43418	1.24709	.44450	1.00000	1.00000	1.00000	1.00364	.00000
48	4.8000	1.49746	1.30898	.46700	1.00000	1.00000	1.00000	1.00364	.00000
49	4.9000	1.56118	1.37135	.53449	1.00000	1.00000	1.00000	1.00364	.00000
50	5.0000	1.62535	1.43418	.54697	1.00000	1.00000	1.00000	1.00364	.00000
51	5.1000	1.69000	1.49746	.50449	1.00000	1.00000	1.00000	1.00364	.00000
52	5.2000	1.75513	1.56118	.46700	1.00000	1.00000	1.00000	1.00364	.00000
53	5.3000	1.82074	1.62535	.44450	1.00000	1.00000	1.00000	1.00364	.00000
54	5.4000	1.88683	1.69000	.46700	1.00000	1.00000	1.00000	1.00364	.00000
55	5.5000	1.95340	1.75513	.53449	1.00000	1.00000	1.00000	1.00364	.00000
56	5.6000	2.02046	1.82074	.54697	1.00000	1.00000	1.00000	1.00364	.00000
57	5.7000	2.08800	1.88683	.50449	1.00000	1.00000	1.00000	1.00364	.00000
58	5.8000	2.15603	1.95340	.46700	1.00000	1.00000	1.00000	1.00364	.00000
59	5.9000	2.22456	2.02046	.44450	1.00000	1.00000	1.00000	1.00364	.00000
60	6.0000	2.29359	2.08800	.46700	1.00000	1.00000	1.00000	1.00364	.00000
61	6.1000	2.36312	2.15603	.53449	1.00000	1.00000	1.00000	1.00364	.00000
62	6.2000	2.43315	2.22456	.54697	1.00000	1.00000	1.00000	1.00364	.00000
63	6.3000	2.50368	2.29359	.50449	1.00000	1.00000	1.00000	1.00364	.00000
64	6.4000	2.57471	2.36312	.46700	1.00000	1.00000	1.00000	1.00364	.00000
65	6.5000	2.64624	2.43315	.44450	1.00000	1.00000	1.00000	1.00364	.00000
66	6.6000	2.71827	2.50368	.46700	1.00000	1.00000	1.00000	1.00364	.00000
67	6.7000	2.79080	2.57471	.53449	1.00000	1.00000	1.00000	1.00364	.00000
68	6.8000	2.86383	2.64624	.54697	1.00000	1.00000	1.00000	1.00364	.00000
69	6.9000	2.93736	2.71827	.50449	1.00000	1.00000	1.00000	1.00364	.00000
70	7.0000	3.01139	2.79080	.46700	1.00000	1.00000	1.00000	1.00364	.00000
71	7.1000	3.08592	2.86383	.44450	1.00000	1.00000	1.00000	1.00364	.00000
72	7.2000	3.16095	2.93736	.46700	1.00000	1.00000	1.00000	1.00364	.00000
73	7.3000	3.23648	3.01139	.53449	1.00000	1.00000	1.00000	1.00364	.00000
74	7.4000	3.31251	3.08592	.54697	1.00000	1.00000	1.00000	1.00364	.00000
75	7.5000	3.38904	3.16095	.50449	1.00000	1.00000	1.00000	1.00364	.00000
76	7.6000	3.46607	3.23648	.46700	1.00000	1.00000	1.00000	1.00364	.00000
77	7.7000	3.54360	3.31251	.44450	1.00000	1.00000	1.00000	1.00364	.00000
78	7.8000	3.62163	3.38904	.46700	1.00000	1.00000	1.00000	1.00364	.00000
79	7.9000	3.69966	3.46607	.53449	1.00000	1.00000	1.00000	1.00364	.00000
80	8.0000	3.77769	3.54360	.54697	1.00000	1.00000	1.00000	1.00364	.00000
81	8.1000	3.85572	3.62163	.50449	1.00000	1.00000	1.00000	1.00364	.00000
82	8.2000	3.93375	3.69966	.46700	1.00000	1.00000	1.00000	1.00364	.00000
83	8.3000	4.01178	3.77769	.44450	1.00000	1.00000	1.00000	1.00364	.00000
84	8.4000	4.08981	3.85572	.46700	1.00000	1.00000	1.00000	1.00364	.00000
85	8.5000	4.16784	3.93375	.53449	1.00000	1.00000	1.00000	1.00364	.00000
86	8.6000	4.24587	4.01178	.54697	1.00000	1.00000	1.00000	1.00364	.00000
87	8.7000	4.32390	4.08981	.50449	1.00000	1.00000	1.00000	1.00364	.00000
88	8.8000	4.40193	4.16784	.46700	1.00000	1.00000	1.00000	1.00364	.00000
89	8.9000	4.47996	4.24587	.44450	1.00000	1.00000	1.00000	1.00364	.00000
90	9.0000	4.55799	4.32390	.46700	1.00000	1.00000	1.00000	1.00364	.00000
91	9.1000	4.63602	4.40193	.53449	1.00000	1.00000	1.00000	1.00364	.00000
92	9.2000	4.71405	4.47996	.54697	1.00000	1.00000	1.00000	1.00364	.00000
93	9.3000	4.79208	4.55799	.50449	1.00000	1.00000	1.00000	1.00364	.00000
94	9.4000	4.86961	4.63602	.46700	1.00000	1.00000	1.00000	1.00364	.00000
95	9.5000	4.94764	4.71405	.44450	1.00000	1.00000	1.00000	1.00364	.00000
96	9.6000	5.02567	4.79208	.46700	1.00000	1.00000	1.00000	1.00364	.00000
97	9.7000	5.10370	4.86961	.53449	1.00000	1.00000	1.00000	1.00364	.00000
98	9.8000	5.18173	4.94764	.54697	1.00000	1.00000	1.00000	1.00364	.00000
99	9.9000	5.25976	5.02567	.50449	1.00000	1.00000	1.00000	1.00364	.00000
100	10.0000	5.33779	5.10370	.46700	1.00000	1.00000	1.00000	1.00364	.00000

Table 5. Lattice Functions

ing storage ring described here can be constructed. We will describe only two rings here.

1. Lear — The properties of this storage ring are given in Table 3 and a drawing of the ring is Figure 3.
2. ELENA — This storage ring was proposed to decelerate antiprotons from LEAR to 200 KeV. The basic parameters are given in Table 4 and 5.

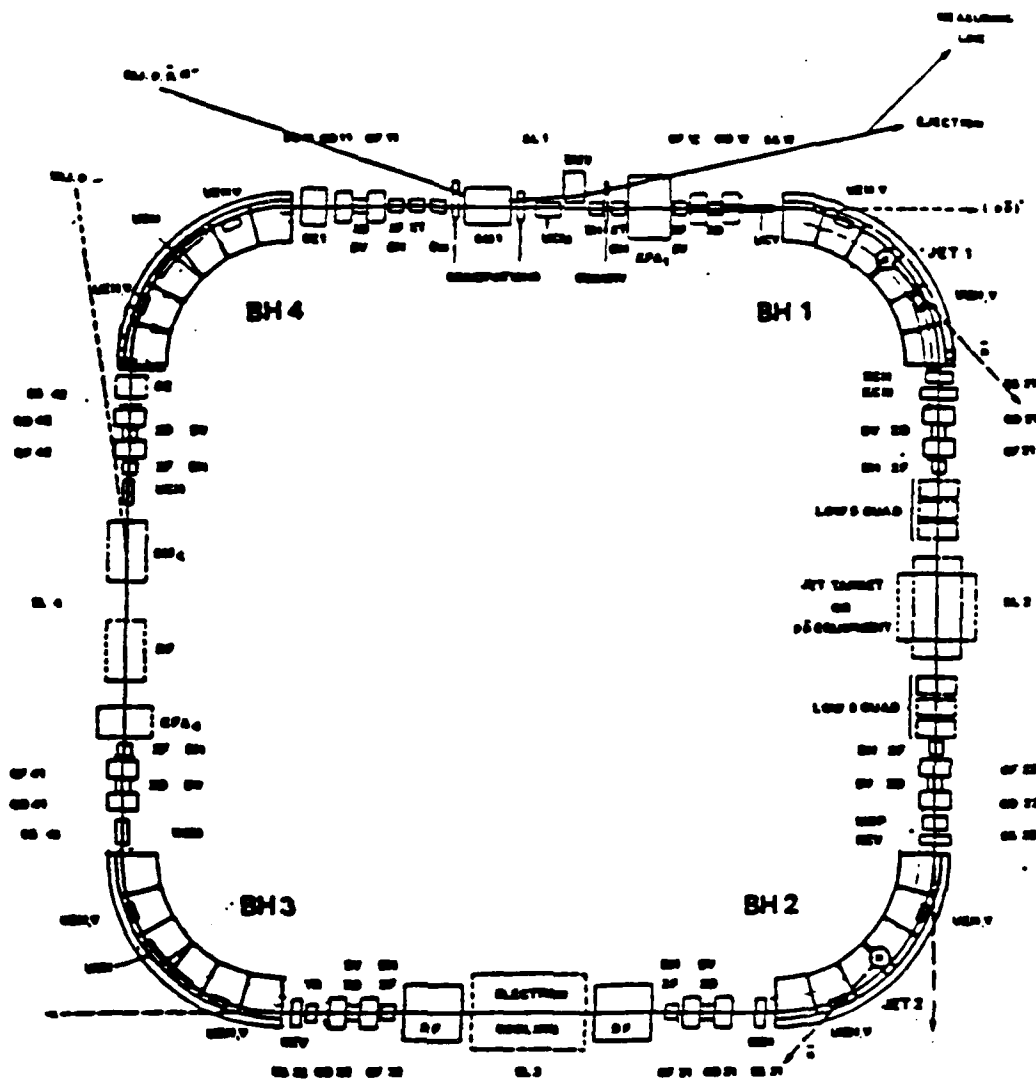


Figure 3. The Lear antiproton storage ring at CERN

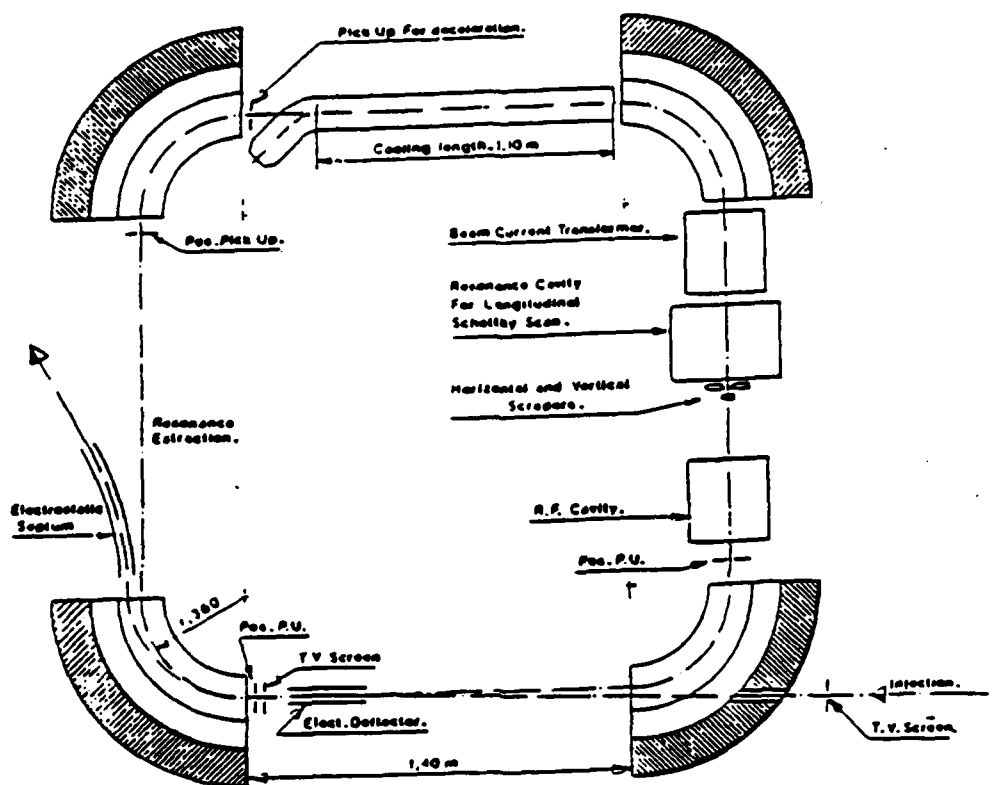


Figure 4. ELENA

The Deceleration Ring

Figure 5 shows the layout of the ring hereafter called ELENA (Extra Low ENergy Antiproton ring). It consists of four 90° bending D-magnets and four straight sections of 2 m length each. The circumference of the ring is 11.4 m, which corresponds to $\sim 1/7$ of that of LEAR. To allow a fine-tuning of the machine all magnets will be equipped with pole-facing windings. A summary of the ring parameters is given in Table 4. The corresponding lattice functions are shown in Table 5.

The fast extracted beam from LEAR at 5 MeV will have an emittance between 10 and 20 π mm·mrad and a momentum spread of $\pm 2 \times 10^{-3}$. Up to 10^8 antiprotons in a 200 ns long bunch will be injected into ELENA with the help of a magnetic septum in straight section 1 and a fast magnetic kicker displaced by $1/4$ of a betatron wavelength at the beginning of straight section 2. As the revolution time in ELENA is about 360 ns, injection can be made in 1 turn and a pulse fall-time of the kicker of ~ 150 ns can be accepted.

To decelerate the antiproton beam a small RF cavity is mounted in straight section 3. The cavity works on the first harmonic of the revolution frequency with a maximum RF voltage of 200 V. After deceleration the antiprotons will be ejected by means of a slow resonance extraction. The orbit is shifted by 2 bumpers nearer to an electric septum in straight section 1, which deflects the particles into the magnetic septum already used for injection.

A rough estimate of the beam properties of the extracted beam shows that with 10^8 antiprotons a horizontal emittance of $\sim 3 \pi$ mm·mrad, a vertical emittance of 6π mm·mrad, and a momentum spread of $\pm 5 \times 10^{-4}$ seems to be possible. An adjustable spill length of ~ 1 –200 ms can be expected.

A vacuum of $\sim 10^{-11}$ Torr in the deceleration ring is desirable to restrict particle losses at 200 keV.

4. *Electron Cooling at Low Energies*

Electron cooling is now being used extensively around the world. This type of cooling will be essential in the initial collection of antiprotons at BNL as well as to maintain a very long lifetime after the antiprotons have been transported to the final location. In addition slow deceleration of the antiprotons can be carried out using the energy ramped electron beam with very little loss of particles in the cycle.

The strong velocity dependence of electron cooling seems to favor the application at low energies as the cooling time is given by:

$$\tau = 0.16 \frac{\beta^4 \gamma^5 e (\theta_e^2 + \theta_i^2)^{3/2}}{r_p r_e \eta L_c j} \cdot \frac{A}{Z^2}$$

with β and γ being the usual kinematical factors, e the electron charge [Cb], $\theta_{e,i}$ the divergence of the electron resp. ion beam, r_e, r_p [m] the "classical particle radius" of the electron resp. proton, η the ratio between the length of the cooling straight section and the circumference of the storage ring, L_c the Coulomb logarithm, j [A/m²] the current density of the electron beam and, in the case of ions, A the atomic number and Z the charge state.

While the divergence of the ion beam can be adjusted by the focusing properties of the storage ring, the divergence of the electrons is given by the temperature of the cathode and the gun construction.

As it seems to be quite reasonable to have a cooling time for 200 MeV protons in the order of 1 sec⁹ one could deduce from the above formula a cooling time of $\sim 10^{-4}$ sec for 2 MeV protons! Unfortunately however, this is not realistic. The reason is the minimum transverse divergence of the electron beam which is given by the cathode temperature. This temperature is for example for a Ba-Sr-Oxide cathode in the order of 0.1 eV ($\sim 800^\circ\text{C}$). As the temperature of the beam is given for one plane by

$$T = \frac{1}{2}mc^2\beta^2\gamma^2\theta^2$$

the beam divergence increases while the velocity βc is decreasing.

In contrast to the longitudinal plane the divergence in the transverse directions stays unchanged by the electrostatic acceleration of the electron beam, which means that:

The β^4 dependence of cooling is counteracted by a $1/\beta^3$ dependence due to the transverse divergence of the electron beam.

If the electron gun has a constant perveance another velocity dependence is given by the relation between beam current I and acceleration voltage U ; as $I \sim U^{3/2}$ and $U \sim \beta^2$ one finds:

The β^4 dependence of cooling is counteracted in a gun with constant perveance by $1/\beta^3$ due to the dependence on the current.

Both effects give an overall dependence of the cooling time of

$$\tau \sim 1/\beta^2!$$

Table 6
Electron Cooling Parameters — ELENA

\bar{p} kinetic energy	5 MeV	200 keV
e^- gun voltage	2870 V	113 V
Cathode ϕ		1 cm
\bar{p} beam size in straight section		~ 0.8 cm
e^- current	20 mA	0.16 mA
Cooling length		1.1 m
Magnetic guiding field	380 Gauss	76 Gauss
Potential depression in the e^- beam	5.7 V	0.23 V
Tune shift to \bar{p} beam	3.8×10^{-3}	3.8×10^{-3}
Cooling times	0.13 sec	3.25 sec

5. The Design of a Transportable Storage Ring

As was shown in Section 3 there are many low energy storage rings in the world. Some of these use superconducting technology. In addition cryopumping of the vacuum is expected to give the lowest possible pressure and is suitable for long-time storage.

Finally, in the actual transport of a storage ring, superconducting-cryogenic systems require the least power. It will be necessary to carry along a Dewar of liquid He to refill the system at need. In the conceptual design reported here we have started with the parameter of the ELENA ring (designed by H. Herr) and extended them to the superconducting option. We therefore call this SELENA (Superconducting ELENA). H. Herr and C.J. Wang have provided the calculations reported here.

Table 7 gives some preliminary parameters for SELENA. A sketch of the machine is shown in Figures 5a and 5b.

The number of particles that can be stored in a very low pressure storage ring for a long period depends on the intrabeam scattering which in turn depends on momentum spread^{*}. Figure 6a shows this effect for two storage rings CELSIUS and the CERN ICE Ring. Approximate scaling laws and the effect of various instabilities are shown in Figure 6b. It is clear that the key technique to increase the number of stored particles is to increase the momentum spread. In turn this means that electron or stochastic cooling techniques must have a long time constant in order to keep the momentum spread large. In the case of SELENA we take 2.7×10^{-3} for the momentum spread and an electron cooling time of 1000 seconds.

* The Kiel-Schnell criteria is usually given as $l|_{L_{\text{limit}}} = 1.9\eta \frac{p^3}{(z/n)} (\Delta p/p)$

The parameters of the proposed electron cooling device for ELENA are summarized in Table 6. The voltages and currents needed can be supplied by a standard photomultiplier supply which fulfills all requirements for a low ripple and stability. It should be pointed out that owing to the small power of a maximum of 57 W in the electron beam, it is not necessary to recuperate this energy in a collector.

The simple 4 dipole design of SELENA is shown in Figure 5b. The Superferric magnets will be D-type in the horizontal plane. The desired horizontal good field should be ~ 20 cm. A detailed preliminary calculation of the lattice functions for this storage ring are given in Table 8 using the MAD computer program. This simple system is idea for a cryogenic storage ring that uses liquid He temperature for cryopumping.

Some additional properties of the machine are given in Table 9. The limiting current is found to be 0.65 Amps of antiprotons (this corresponds to $\sim 6 \times 10^{11}$ \bar{p} in the ring).

The most crucial parameter is the lifetime of the stored beam due to interbeam scattering. This process converts the internal momentum spread of the beam into an increased beam size due to the particle scattering. The lifetime due to IBS goes like $\beta^3 \gamma^4$ and therefore forces the storage of the particles to the energy of 100 MeV adequate lifetimes for transport are to be achieved. For SELENA it is estimated that the beam will blow up to 45π mm mr after 3×10^5 sec. This corresponds to a beam size of 6 cm which should be well within the aperture of the machine. It is also possible to increase this lifetime by using a very modest (very low power with the amplifiers in liquid He cryostat). Such a system would have a modest band width of ~ 1 GHz giving a cooling time of ~ 100 sec. This system could increase the IBS lifetime to $\sim 5 \times 10^6$ sec at least.

The other important properties of the first design of SELENA include

the small dispersion (which also decreases the effects of IBS). A stronger focusing version of SELENA is also being studied for comparison where the tunes are $Q_x = 1.22$, $Q_y = 1.88$. This machine has a larger dispersion and has so far indicated a shorter IBS lifetime.

In summary the current parameters of SELENA are listed in tables 7, 8 and 9. This machine, provided the magnets can be constructed has all the required properties of antiproton collection, storage, long lifetime for transport and deceleration required for antimatter transport from the production source to a location where the antimatter studies can take place.

SELENA ANTIMATTER TRANSPORT

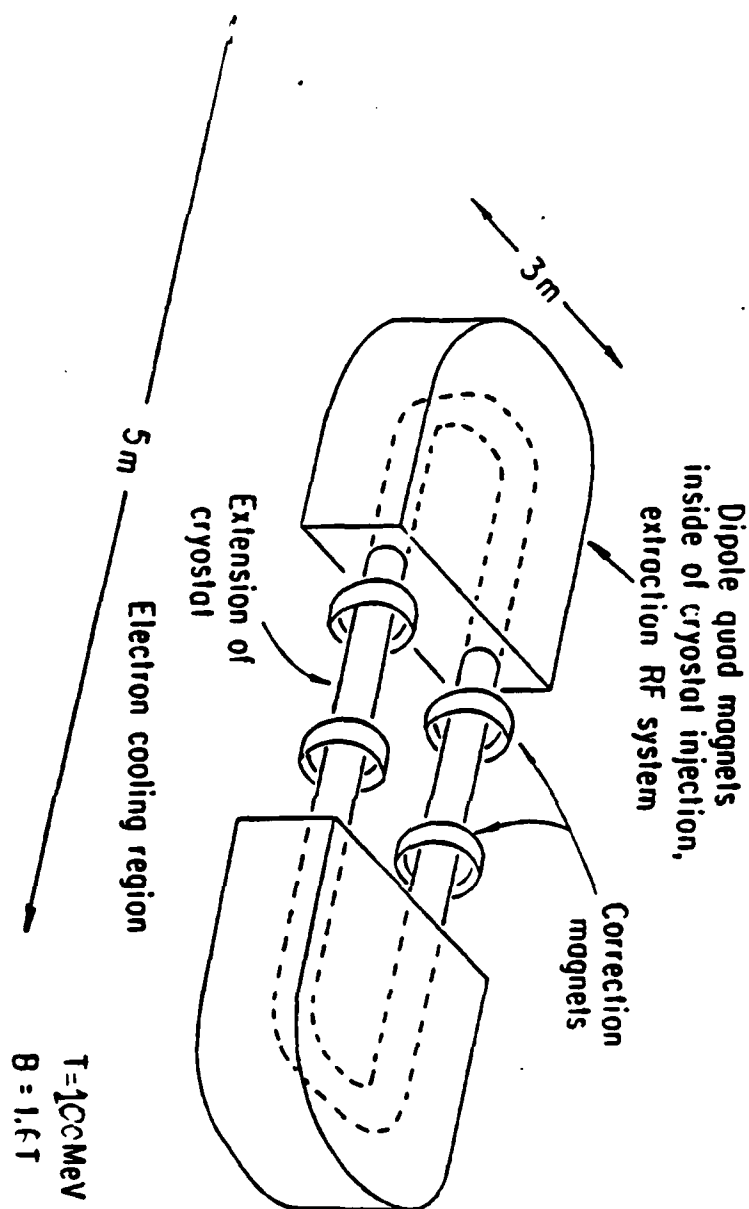
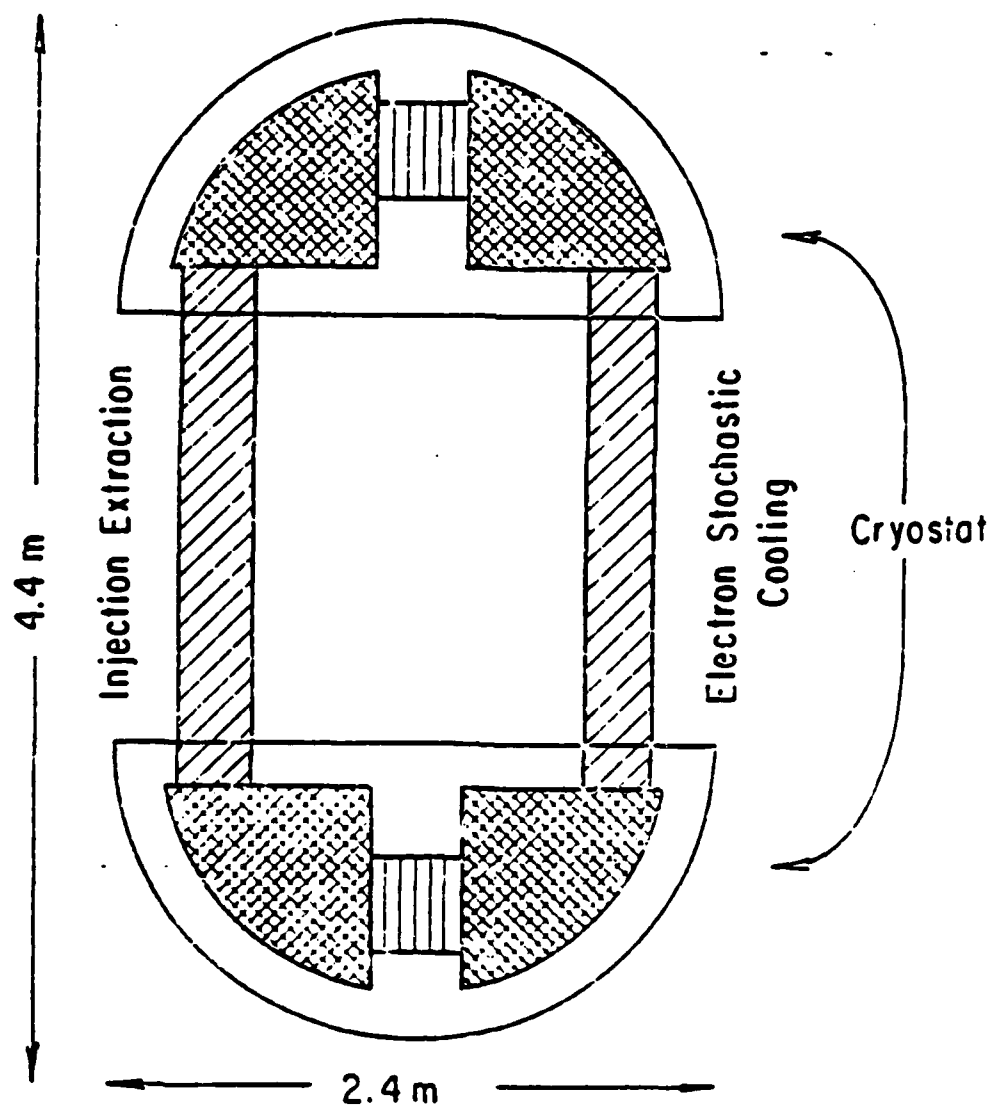


Figure 5a. A sketch of the SELENA storage ring

SELENA



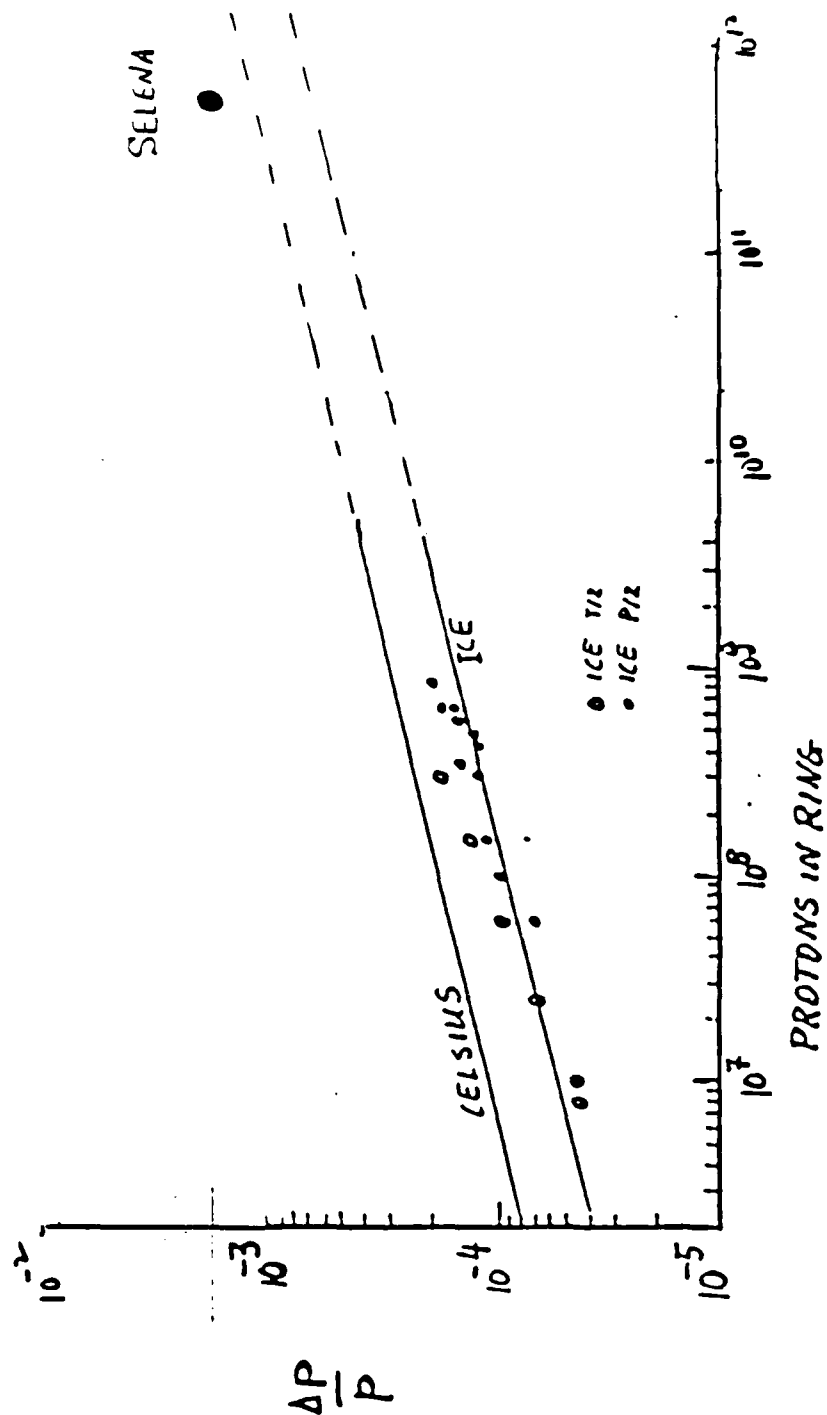


Figure 6a. Limiting momentum spread for proton or antiprotons in a storage ring

Table 7
Properties of SELINA

Circumference	11.6 m
Length of Straight Sections	2 m
Bending Radius	0.92 m
Kinetic Energy Range	100 MeV - 200 KeV
Momentum Range	444 MeV/c - 20 MeV/c
Magnetic Field	1.62 T
— Combined Function —	
Revolution Time	180 ns - 1.8 μ s
Size of Vacuum Chamber	$\sim 20 \times 10$ cm
Vacuum (Cryopumping)	$\lesssim 10^{-12}$ Torr
Lifetime (440 MeV/c)	
Without Cooling	$\gtrsim 100$ hours
With Cooling	$\gtrsim 3500$ hours
($\Delta P/P \sim 10^{-3}$)	
N_p Stored	$\sim 10^{10} - 10^{11}$
Emittance (200 MeV/c)	$\epsilon_H \sim 20\pi$ mm-mn
($\Delta p/p$)	$\epsilon_V \sim 40\pi$ mm-mn
	(2×10^{-3})
Emittance (30 MeV/c)	$\epsilon_H \sim 7\pi$
($\Delta p/p$)	$\epsilon_V \sim 7\pi$
	($\pm 2 \times 10^{-3}$)

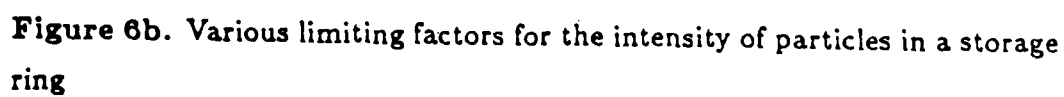


Table 8

ELSA 3-WHEEL LINEAR LATTICE PARAMETERS FOR SEAN LINE: INSERT " RANGE = 25 / 25" DELTA1/P = 0.000000 0.000000															"HAD" VERSION: 6.6.0/00 RUN: 87/07/11 11:11:11														
ELEMENT SEQUENCE															ELEM. DATA														
POS. NO.	ELEMENT NAME	SEQUENCE NO.	UNIT (M)	BETAX (M)	ALFAX (1)	NUA (1/P)	NUB (1/P)	NUC (1/P)	NUD (1/P)	NUV (1/P)	BETAY (M)	ALFAY (1)	NUY (1/P)	NUZ (1/P)	NUW (1/P)	NUX (1/P)													
BEGIN INSERT																													
1	DRIFT	1	0.000	3.444	0.000	0.000	0.000	0.000	0.000	0.000	2.135	0.000	0.000	0.000	0.000	0.000													
2	DRIFT	1	0.000	3.444	0.000	0.000	0.000	0.000	0.000	0.000	2.135	0.000	0.000	0.000	0.000	0.000													
3	DRIFT	1	0.000	3.444	0.000	0.000	0.000	0.000	0.000	0.000	2.135	0.000	0.000	0.000	0.000	0.000													
4	DRIFT	1	0.000	3.444	0.000	0.000	0.000	0.000	0.000	0.000	2.135	0.000	0.000	0.000	0.000	0.000													
5	DRIFT	1	0.000	3.444	0.000	0.000	0.000	0.000	0.000	0.000	2.135	0.000	0.000	0.000	0.000	0.000													
END INSERT																													
TOTAL LENGTH =			11.623240	2X		1.198099		0.000000		0.000000		0.000000		0.000000		0.000000													
ALFA			0.019021E+00	BETAX(MAX)		-0.990723		BETAY(MAX)		0.000000		0.000000		0.000000		0.000000													
GAMMA(1R)			1.271522	ORINAXI		1.000000		OYIPAXI		0.000000		0.000000		0.000000		0.000000													
				XCOI(MAX)		0.000000		YCOI(MAX)		0.000000		0.000000		0.000000		0.000000													
				XCOI(P-MAX)		0.000000		YCOI(P-MAX)		0.000000		0.000000		0.000000		0.000000													

Table 9
Summary of SELINA Properties

Machine Parameters — $E_p = 100 \text{ MeV}$; $p_p = 444 \text{ MeV}/c$

$$Q_H = 1.186$$

$$\epsilon_H^{\text{BEAM}} = 15.8\pi \text{ mm mr}$$

$$Q_V = 0.636$$

$$\epsilon_V^{\text{BEAM}} = 12.4\text{-mm-mr}$$

$$\eta = 0.2$$

$$\frac{\Delta p}{p} = 2.7 \times 10^{-3}$$

$$\epsilon_H^{\text{MACHINE}} \approx 200\pi$$

$$\epsilon_V^{\text{MACHINE}} \approx 100\pi$$

Beam Size (for 6π , 95%)

1 cm

Lasslet Tune Shift

$$\Delta Q = 7 \times 10^{-3}$$

$$N_p = 5 \times 10^{11}; I = 0.65 \text{ Amps}$$

Lifetime — Multiple Scattering

$$= 5.4 \times 10^5 \text{ sec}$$

$$(p = 10^{-12} \text{ Torr})$$

$$(p = 10^{-13} \text{ Torr})$$

$$= 5.4 \times 10^6 \text{ sec}$$

Single Scattering

$$= 5 \times 10^7 \text{ sec}$$

$$(p = 10^{-12} \text{ Torr})$$

IBS Lifetime = $5 \times 10^5 \text{ sec}$ without cooling

> 10^7 sec with modest stochastic cooling

Deceleration lowest energy

200 KeV

Electron cooling parameters

$$E_e = 54 \text{ keV}$$

$$\tau_{\text{cool}} = 1000 \text{ sec}$$

6. *Expected Properties of the Storage Ring under Transport conditions*

We now discuss the transport of the antimatter from the \bar{p} source (say BNL) to the location where studies of antimatter/matter interactions are to take place. The various uncertainties and potential problems are only briefly addressed here but will be presented in detail in the conceptual design proposal.

We now discuss the possible sequence for the filling and transport of the antiprotons in SELENA. We assume that $10^7 \bar{p}$ at 100 MeV can be injected into SELENA every second (an average) from the BNL Booster source. The cooling time of the stochastic and electron cooling system can be made 1 sec or so. After 10^4 – 10^5 pulses the storage ring will be filled with cold antiprotons (the \bar{p} stack).

During preparation for transport it is important that a large momentum spread be created in the stack to reduce the effects of IBS (as discussed previously). Before transport the cryogenic magnets are taken off their power supply to test for stability of the system.

The expected weight of SELENA is about 10 tons. This can be easily transported by rail or truck. It may also be possible to transport it in a very large cargo airplane.

During transport there is the chance of losing the antiproton store. We now discuss the technique to reduce the hazards from this spill. The basic idea is to use one or more of the dipole magnets to act as a beam dump for a single turn deviation of the beam.

10^{11} antiprotons annihilation correspond to about 100 Rads and if this beam was all deposited in one place it would be dangerous. However it will be very easy to shield against this possibility since SELENA has 4 large dipole

magnets each of about 2.5 tons of material. A natural loss of the beam would occur over several turns and the amount that is lost that does not hit the dipoles is likely small. Detailed calculations of the beam loss under several possible source should be carried out. It is also possible to provide a fast kicker (driven by a capacitor bank) to have a rapid abort system.

7. Deceleration in the Storage Ring: Applications to Remote Energy Sources

The key advantage of using a storage ring to transport antiprotons is the possibility of storing the \bar{p} 's at high enough energy to maintain stability and then decelerating the antiprotons to the desired energy at the site of the studies. We note again that the ELENA ring was designed to decelerate \bar{p} 's to 200 keV. In addition it should be noted that deceleration can be carried out on the DC \bar{p} beam by using electron cooling and decreasing the electron energy. This avoids the necessity of bunching the beam in the storage ring and reduces the complexity of the system. The possibility of "electron drag deceleration" was also considered for ELENA.

The deceleration technique is to ramp down the voltage of the electron beam (starting at 54 kilovolts) to the desired value according to the final \bar{p} energy. Electron cooling at very low energy has yet to be studied but will require a very cold electron gun (see Appendix C for a discussion of this point by H. Herr). For ELENA the emittance and average β function in the straight section are

$$\theta_p^H \simeq 1.2 \times 10^{-3}, \quad \theta_p^V = 2.5 \times 10^{-3}, \quad \text{and} \quad \theta_p^L = 2 \times 10^{-3}$$

At 200 keV \bar{p} energy the required to be

$$T_L = 2.2 \times 10^{-5} \text{ eV}$$

The divergence of the electron beam will be larger than that of the antiproton beam and the cooling time will be independent of the amplitude of the antiproton oscillations. Under these conditions the cooling time has the functional dependence

$$\tau \alpha \beta^4 \gamma^5 (\theta_e^T)^3 / \alpha_e$$

For example at $E_p = 5$ MeV the cooling time for a 1 meter cooler with 20 ma of electron current is 0.13 sec. At 200 KeV the cooling time is 3.2 sec. Thus if the electron beam is ramped down in energy slowly the \bar{p} beam will stay in equilibrium and the beam will be decelerated and cooled at the same time. The effect of IBS is hard to determine and this is one of the important calculations still to be carried out on SELENA.

Under the above conditions the beam can be decelerated at the rate of 1 MeV/sec down to about 5 MeV and then it will take ~ 60 sec to go to 200 KeV. The total deceleration time would be less than 3 minutes.

The advantage of this scheme is that the DC electron beam is decelerated and therefore the beam does not have to be rebunched.

8. *Extraction of the Antiprotons at the Lowest Deceleration Energy*

We assume that the major use of SELENA is to transport $> 10^{11}$ and 100 MeV antiprotons to a location where they can be used to study the properties and interactions of low energy (few keV – 200 keV) antimatter. In this case the extraction system may be quite different from the injection system that was used for the initial collection of the antiprotons.

The extraction system for SELENA will be similar to that of ELENA shown in Figure 4. Since electron cooling will be used for the deceleration process the beam will remain cooled at the lowest energy of 200 keV. The emittance of the beam will be about 7π -mm-mr and the momentum spread $\pm 2 \times 10^{-3}$. However at the lowest energy the space charge beam blow up can be severe and this must be studied for the extremely intense \bar{p} beam in SELENA.

After deceleration the antiprotons will be ejected by means of a slow resonance extraction and an electrostatic septum. This technique is used at the CERN ps and would lead to a spill length of (1-100) ms. Detailed calculations of this extraction technique must be carried out before the system can be designed.

The cryopumped vacuum is crucial to restrict particle losses at 200 keV.

9. *Summary and Future R&D Effort*

In this report we have shown that it is feasible to transport antiprotons in a special storage ring that has been designed along the lines of the ELENA ring proposed at CERN. We have not specifically discussed the initial collection of antiprotons other than to indicate that a deceleration system such as that possible at BNL could provide a source of \bar{p} 's. The collection system would be similar to that used for the ACOL \bar{p} collector at CERN. It may use electron cooling and stochastic cooling to bring the cooled \bar{p} 's into a small good field region of the storage ring. We believe this system is feasible.

The storage ring would use superconducting magnets to operate at very small power for the transport condition. In addition the use of liquid He temperatures will be useful for

1. Low Power-Low Noise amplifiers for the stochastic cooling
2. Cryopumping for a very low pressure vacuum thus giving a long lifetime for the transport and long term storage of the antiprotons

The most serious problem in the transport (when the normal electron and stochastic cooling is turned off) is the beam blow up due to IBS. While it seems possible that the lifetime could be several days, the addition of a low power stochastic cooling system could give a protection from this problem.

The remaining questions concerning the storage ring are technical concerning the superconducting magnets. To our knowledge such magnets have not been built but operate at relatively low fields and currents compared to superconducting magnets used in colliders. An R&D program leading to the construction of a magnet would be very important for this project. We estimate that the first phase of this program would need funding at the level of about \$300K. SELENA could then be constructed and tested with protons.

10. *Acknowledgements*

This brief report has been written for RAND. It follows from many discussions and earlier reports such as those for ELENA and LEAR as well as notes at FNAL, BNL and CERN. We have benefitted from discussions with D. Lowenstein, F. Mills, H. Poth, A. Wolfe and many others. I wish to thank H. Herr and C.J. Wang for help with the calculations reported here.

Appendix A

1. INTRODUCTION

It is an old dream of particle physicists to construct a proton-antiproton colliding beam machine. High energy accelerator beams produce copious numbers of antiprotons. Recently we¹ have pointed out that the existing high energy rings at CERN and Fermilab can be transformed into $\bar{p}p$ storage rings of about 800 GeV in the center of mass. Furthermore the forthcoming Energy Doubler/Saver at Fermilab could give access to the fantastic energy of 2 TeV in the center of mass and would be quite suitable for a high performance storage ring.² In order to transform existing machines into $\bar{p}p$ colliding beams a method must be devised to collect and cool the antiproton phase space followed by reinjection of the \bar{p} beam into the storage ring. Several methods have been devised to carry out this repetitive accumulation and cooling.^{3,4,5}

A fundamental progress in this direction has been accomplished by the Novosibirsk group, which has recently demonstrated the possibility of damping betatron motions and momentum spread of 80 MeV protons with the help of collinear electrons traveling at the same speed³ (electron cooling). In these beautiful experiments the proton beam size collapses to sub millimetric dimensions and $\Delta p/p \sim 10^{-5}$ in about 80 milliseconds.⁶

In order to adapt this technique to antiproton cooling, one faces the problem that phase space compression with electrons works efficiently only at non-relativistic energies ($\gamma \sim 1.5$), while the greatest majority of \bar{p} 's are produced fast in the laboratory system, i.e. $\langle \gamma \rangle = \sqrt{s}/2m$. For instance for $E = 100$ GeV $\langle \gamma \rangle = 7$ and the cooling time will then increase

by the factor $2^4 \cdot 7^5 = 260,000$! Furthermore the technological problems associated with an electron cooler operating at $\gamma = 7$ are formidable⁶, (e.g. the electron accelerating voltage must be 3.5 million volts) and they have not been satisfactorily solved to date.

It has occurred to us that one could bridge the gap between optimum production and cooling energies for antiprotons by introducing an additional stage of deceleration between the production of \bar{p} 's and the subsequent electron cooling.⁷ We elaborate a realistic scheme making use of the rapid cycles of the Fermilab booster to decelerate \bar{p} 's to 200 MeV where we could perform Budker-type cooling and stacking in a modest ring (housed in the same tunnel).

We believe this scheme has several attractive features among which are the availability of the major components, their inherent reliability, and the modest nature of the required 200 MeV storage ring. It could be carried out at modest cost and with very little need for new technological innovations. Thus within a few years the Fermilab accelerator can be transformed into a high energy $\bar{p}p$ storage ring device.

The scheme consists of three separate phases:

1. Antiproton production, deceleration and accumulation.
- Secondary particles at about 6.5 GeV/c are produced by 100 GeV/c protons from the main ring impinging on a small tungsten target. Particles are injected into the booster ring and decelerated to 200 MeV. Only \bar{p} 's survive at the end of the production.

TM-689
2000.000

TM-689
2000.000

The beam is transferred to the storage ring where it is cooled and added to the stack of previous accumulations.

One expects to accumulate 4×10^7 \bar{p} /pulse leading to $\sim 10^{11}$ particles in 2×10^3 pulses (3 hours).

ii. Injection of p and \bar{p} in the main ring, and experimentation in $p\bar{p}$ collisions. The \bar{p} beam is transferred from the Freezer to the Booster, accelerated to 8 GeV, and reverse injected in the main ring (MR). A standard proton Booster pulse is then injected in the main ring, with appropriate phasing in order to give collisions at the desired point of the main ring. There are then 84 proton and 84 antiproton bunches counter-rotating. With 10^{11} \bar{p} 's and 4×10^{12} p's with standard emittances, we expect a luminosity of $\sim 10^{29} \text{ sec}^{-1} \text{ cm}^{-2}$ in the low-beta section designed by T. Collins. The scheme is shown in Fig. 1.

iii. Antiproton beam regeneration. After some time, beam-gas scattering, R.F. noise and higher order resonances could lead to an appreciable blow-up of the beams with consequent loss of luminosity. In order to restore beam quality, we propose to dump the proton beam, decelerate \bar{p} 's first in the MR to 8 GeV then in the Booster to 200 MeV, then cool again in the Freezer. The cooling process should take only seconds. After this, \bar{p} 's are accelerated again by the Booster, injected in the MR with a new companion proton beam and accelerated to high energies.

The main open question is how well electron cooling works.

The recent results of Budker's group at Novosibirsk have shown that it is possible to cool a modest proton beam of 50-80 MeV in less than 100 msec. This impressive result allows one to attempt extrapolations to our conditions. However it is clearly imperative to perform additional experimentation at Fermilab on cooling techniques (see Appendix I, III).

11. MAIN PHYSICS MOTIVATIONS

The past ten years have seen remarkable progress in the understanding of elementary particles. First there is the experimental discovery of $\Delta S = 0$ weak neutral currents,⁸ which when contrasted with the previous limits on $\Delta S = 1$ neutral current decay processes⁹ leads to the suggestion of additional hadronic quantum numbers in nature.¹⁰ Evidence now exists for new hadronic quantum numbers that are manifested either directly^{11,12} or indirectly.¹³ The experimental discoveries are complemented by the theoretical progress of unified gauge theories.¹⁴ These developments lead to the expectation that very massive intermediate vector bosons ($50 - 100 \text{ GeV}/c^2$) may exist in nature.¹⁴ The search for these massive bosons and other new phenomena require three separate elements to be successful: a reliable physical mechanism for production, very high center of mass energies, and an unambiguous experimental signature to observe them. In addition to the high center-of-mass energy available in \bar{p} - p collisions, several considerations suggest that they may present a much better opportunity of discovering new phenomena than p - p collisions.¹⁵

First we consider production process. There is now very strong support for the notion of pointlike constituents in the hadron obtained from lepton-hadron scattering and very high energy neutrino experiments. The experimental detection of weak interaction processes in hadronic collisions almost certainly involve quark-antiquark (or proton-antiproton) annihilation.

lution processes very much like e^+e^- collisions. (For example, the processes $u + \bar{u} \rightarrow \mu^+ + \bar{\mu}$ or $u + \bar{d} \rightarrow \mu^+ + \nu$.) There are clearly more antiquarks in an antiproton, then in a proton, and furthermore the antiquarks in an antiproton, being valence quarks, carry a much larger fraction of the total energy than do the (sea) antiquarks in a proton. The exact size of these effects at high energy are uncertain, but qualitatively cross sections probably differ by a factor up to $10 - 100$ in favor of the \bar{p} - p system.

The \bar{p} - p system is an eigenstate of charge conjugation (C) invariance whereas the pp system is not. Thus there are many simple experimental tests of C violation in the \bar{p} - p system. The observation of C violation may be an important technique to observe the effects of weak interactions in very high energy collisions. In the case of the pp system the "equivalent" way to observe weak interaction effects is through parity violation. This very likely involves polarization measurements which are considerably more difficult than tests of C violation. Thus proton-antiproton collisions at the highest energy offer distinct advantages in the search for new phenomena in nature, especially those associated with the weak interaction.

We now turn to the specific case of the production and detection of the weakly interacting intermediate vector bosons. Present neutrino data indicate a mass limit of $>20 \text{ GeV}$ for the charged intermediate vector boson.¹⁶ The center-of-mass energy available in a proton-antiproton storage ring is $> 2.0 \text{ TeV}$, sufficient to produce very large mass intermediate vector

this suggests $S > 2 \times 10^5 \text{ GeV}^2$ or $\sqrt{S} \geq 450 \text{ GeV}$. In the case of pp scattering the $\langle \alpha_{q p} \rangle$ is expected to be much less and the $\alpha_{q p}$ distribution probably falls very rapidly.

Detailed estimates have been given by several authors^{1,15} and give

$$\sigma(\bar{p}p \rightarrow W^+ + \text{hadrons} + e^+ + e^- + \text{hadrons}) = 10^{-32} \text{ cm}^2$$

More optimistic cross section estimates also exist in the literature.¹⁸

The cross section estimated above leads to 1.6 events/hour given a luminosity of $10^{29} \text{ cm}^{-2} \text{ sec}^{-1}$ and 100% detection efficiency. The $\mu^+ \mu^-$ is expected to be very small compared to the W^0 signal. Furthermore if the W^0 decay into hadronic states is detected the corresponding event rate will increase. We note that since the q and \bar{q} have comparable x distributions in pp collisions, a large fraction of the W 's produced will have low x_W and hence decay symmetrically in the lab. In pp collisions, the widely different q and \bar{q} x distribution can produce sizeable x_W . Finally the charged vector bosons may well have lower mass and thus larger cross sections, with a somewhat weaker experimental signature.

Another challenging possibility is a search for fractionally charged quarks. Overwhelming evidence favors the existence of light, fractionally charged constituents inside the hadrons. Absence of direct production of free quarks suggests the existence of confinement mechanisms (bag). It is not known, but it appears likely that at very high energies the "bag" could be broken, thus liberating the elementary constituents. A search for quarks in very high energy hadron-hadron collisions is mandatory.

bosons. In the Weinberg-Salam model the W^0 the W^\pm 1,14,16 masses are now estimated to be $80 \pm 6 \text{ GeV}$ and $64 \pm 11 \text{ GeV}$, respectively. This mass is outside the reach of the presently planned new generation of e^+e^- storage rings.

The derivation of the W^0 cross section exposes the basic simplicity of the assumptions for the case of $\bar{p}p$ collisions.^{1,15} By analogy the $q\bar{q}$ annihilation behaves like e^+e^- scattering.

In the e^+e^- case a sharp resonance peak would be expected in the cross section for the process

$$\begin{aligned} e^+ + e^- &\rightarrow W^0 \rightarrow e^+ + e^- \\ &\rightarrow \mu^+ + \mu^- \\ &\rightarrow u + \bar{u} \quad (\text{hadron}) + (\text{antihadrons}) \\ &\quad d + \bar{d} \quad \text{jet} \end{aligned}$$

In order to estimate the cross section for $\bar{p}p$ collisions the structure functions of partons must be known. Neutrino and charged lepton scattering experiments provide the necessary structure functions and have set limits ($>20 \text{ GeV}$) on any non-locality in the parton form factor.¹⁷ The main difference with respect to e^+e^- is that now the kinematics is largely smeared out by the internal motion of the q's and \bar{q} 's. The average center of mass energy squared of the $q\bar{q}$ collision is roughly

$$\langle S_{q\bar{q}} \rangle \sim S \langle \alpha_{q p} \rangle \langle \alpha_{\bar{q} p} \rangle$$

where S is the center of mass energy squared of the $\bar{p}p$ system and $\langle \alpha_{q p} \rangle = \langle \alpha_{\bar{q} p} \rangle$, we find $\langle S_{q\bar{q}} \rangle \sim 0.04 S$. For $M = 100 \text{ GeV}/c^2$

Finally there is one additional possibility for interesting and unique physics with the low energy antiproton storage ring itself. It appears that the present universe has a net positive baryon number for unknown reasons. A simple, but seemingly unlikely possibility is that the antiproton is unstable and has a lifetime much shorter than 10^{10} years. The present limit on the antiproton lifetime is likely no better than milliseconds. Using a small antiproton storage ring with $10^{10} - 10^{12}$ antiprotons stored for periods of days it appears possible to detect an unstable antiproton if the lifetime is less than 10^7 years. This must be considered a long shot but we know of no other way to discover antiproton disintegration.

The observation of an unstable antiproton, coupled with the observed stability of the proton ($>10^{29}$ years); would violate the CPT theorem.

III. ANTIPROTON PRODUCTION AND DECELERATION

III-1. Introduction

In this phase, the Booster is alternately accelerating 12 proton pulses and decelerating 12 antiproton pulses (see Fig. 2). The settings of the magnetic cyclotron are unchanged. However, the rf is turned on alternately on the rising and falling sides of the magnet ramp and the phase sequence among cavities is inverted. Since the p and \bar{p} currents are vastly different (4×10^{12} p vs. 1×10^7 \bar{p}) two separate beam control systems will be necessary. In order to ease the extraction of the 100 GeV primary protons, 12 Booster pulses are injected in the Main Ring, leaving a time gap between pulses to allow for the rise and fall times of the kicker magnet. We propose to eject the beam from the medium straight section F17 and to transport it along the newly-planned line from there to the Booster (Fig. 1 and Fig. 3). Targeting and the beam dump occur along this line, and \bar{p} 's can be reverse injected in the Booster through the new 8-GeV proton extraction channel. We have taken the "good field" Booster ring acceptance at 200 MeV and adiabatic extrapolation to other energies. We understand that these goals have not been reached as yet and that more work is necessary.

III-2. Gymnastics on Proton Beam, Ejection and Targeting.

The largest possible beam current is accelerated to 100 GeV/c, then the main ring is flat-topped with rf at maximum voltage. With $V_{rf} = 3.4 \times 10^6$ Volt, $h = 1113$, $f = 53.4$ kHz and $\eta = 3.3 \times 10^{-3}$ we calculate

$$v_s = \left[\frac{h \text{ eV}}{2\pi} \right]^{1/2} = 3.65 \times 10^{-3}$$

The bunching factor B (bunch length/bunch separation) is then

$$B = \left(\frac{h}{2\pi} \right) \left(\frac{8\pi n}{p} v_s \right)^{1/2} \lambda_b^{1/2} = 0.27 \lambda_b^{1/2}$$

where λ_b is the invariant bunch area, expressed in eV - sec.

Taking $\lambda_b = 0.1$ eV sec, which is about four times the injection area in the booster, we get

$$B = 0.085$$

$$\frac{\Delta p}{p} \left(\frac{1}{\lambda_b} \right)^{1/2} = \frac{1}{B} \left[\frac{8\pi n}{p} v_s \right]^{1/2} = 1.67 \times 10^{-3}$$

We eject 84 bunches of the main ring at a time and focus the beam on a very small tungsten target. The extraction of 100-GeV protons is shown in Fig. 3. At position E48 in the Main Ring, there is a missing magnet position giving a straight section of 7m available length. A pulsed magnetic kicker S_1 at that position produces a horizontal bump of 3cm at the medium straight section F17 ($\Delta v = 0.81$). There exists there an available length of 14m. Two Lambertson septa S_2 will deflect the beam vertically by 25 mrad, producing a deflection of 18 cm at the face of the next dipole.

Taking an invariant transverse beam emittance of

$\epsilon_{xy} = 30 \times 10^{-6}$ rad m and $\theta_y = \theta_H = 2.5$ m at the target which can still be realized with standard gradient quadrupoles, we calculate a spot of 0.30 mm radius (two standard deviations in the gaussian approximation). The focus has to be made a chromatic in order to avoid additional contributions from the relatively large momentum spread.

It has been calculated that $5 \times 10^{13}/12 = 4.16 \times 10^{12}$ particles is about the maximum beam intensity which can be concentrated on a tungsten target of special construction. Substantially higher beam intensities would lead to destruction. Heat propagates in tungsten with a speed about 1 m/ms. Since successive pulses are ejected at 66 ms in time, we can cool the target between pulses by simple conduction.

After the target, the residual proton beam must be separated from the low-energy particles by bending and absorbed in a suitable beam dump.

III-3. Bunch Synchronization

The antiproton bunches have the same time structure as the protons in the Main Ring and they must also fit precisely within the buckets of the Booster. This is not an entirely trivial operation. Frequencies are quantized by the requirement of integer harmonic numbers in the Main Ring and the Booster. The two frequencies are automatically

matched for particles of equal energies. However, antiprotons have an energy which is substantially lower than that of the parent protons while retaining the same time structure, and frequency shift cannot be neglected.

We propose to overcome this difficulty by increasing by one unit the harmonic number in the Booster for antiproton capture and deceleration, i.e., instead of $h = 84$ which is the nominal value for protons, we propose to operate at $h = 85$. In order to make this possible, the proton and antiproton relativistic factors γ_p and $\gamma_{\bar{p}}$ have to satisfy the relation:

$$\frac{1}{2\gamma_p^2} - \frac{1}{2\gamma_{\bar{p}}^2} = \frac{1}{85}$$

giving $\gamma_{\bar{p}} = 6.518$, corresponding to $T_{\bar{p}} = 5.177$ GeV. This is sufficiently away from the transition energy $\gamma_t = 5.446$ to present no complications. The area of the antiproton bunches is determined by the bucket area at 200 MeV, which is 0.0352 eV sec. At the magic energy $T_{\bar{p}} = 5.177$ GeV, we have $\eta = \frac{1}{\gamma_t^2} - \frac{1}{\gamma_{\bar{p}}^2} = 6.43 \times 10^{-3}$, $f = 0.637 \times 10^6$ Hz. For the maximum rf voltage $eV = 700$ KeV/turn and $\cos \phi_s = 1/2$ we calculate

$$v_s = [hnev \cos \phi_s / 2\pi E]^{1/2} = 2.16 \times 10^{-3}$$

$$B = (h/2\pi) [0A(n/\nu_s)]^{1/2} = 0.122$$

$$\Delta p/p_{full} = \frac{1}{B} [8A(\nu_s/\nu_n)]^{1/2} = 3.0 \times 10^{-3}$$

341

In order to match bunches, we must increase the proton bunching factor from 0.085 to 0.122. This can be easily done by reducing the MR voltage from 3.4×10^6 V to 8.0×10^5 V during extraction.

III-4. Production and Collection of Antiprotons

The booster acceptances, after allowance for alignment errors, are taken to be

$$\Lambda_V(200 \text{ MeV}) = 40\pi \cdot 10^{-6} \text{ m rad}$$

$$\Lambda_H(200 \text{ MeV}) = 40\pi \cdot 10^{-6} \text{ m rad}$$

Acceptances must match the beam emittances at 200 MeV.

Assuming adiabatic damping during deceleration the emittances scaled to 5.2 GeV injection energy are

$$\Lambda_V(inj) = \Lambda_H(inj) = 4.0\pi \cdot 10^{-6} \text{ m rad}$$

The value of the β function for the antiprotons at the production target is taken to be $\beta_V = \beta_H = 0.25$ m. The \bar{p} angular divergence is then $\theta_V = \theta_H = 13$ mrad, and the solid angle accepted is $\Omega = \pi \theta_V \theta_H = 5.3 \times 10^{-4}$ sterad.

Inclusive \bar{p} and π^- production has been parametrized for the existing data in Ref. 21:

$$E \frac{d^3\sigma}{dp^3}(p) = 0.26N [p_x^2 + 1.04]^{-4.5} (1-x_R)^7$$

$$E \frac{d^3\sigma}{dp^3}(\pi^-) = N [p_x^2 + 0.86]^{-4.5} (1-x_R)^4$$

We establish the normalization N from the data of Ref. 22

In the region $s > 1000$ GeV² where scaling holds, $N = 10.2 \text{ mb GeV}^{-2}$

Also in Ref. 22 is a plot of the production ratio

$$f(s) = \bar{p}/s \quad (x=0.35, p_L=0.5 \text{ GeV}/c) \text{ in the range } 25 < s < 2830 \text{ GeV}^2$$

Using the cross section parametrizations we extrapolate

to obtain $f_0(s) = \bar{p}/s \quad (x=0, p_L=0)$. By normalizing to the

saturation value $f_0(\infty)$ in the region of scaling, we obtain

the scaling parameter $\alpha(s) = f_0(s)/f_0(\infty)$ which is plotted

in Fig. 4. We then have

$$\Sigma \frac{d^3\sigma}{dp}(\bar{p}) = 2.65 \alpha(s) [p_L^2 + 1.04]^{-4.5} (1-x_F)^7 \text{ (mb GeV}^{-2}\text{)}$$

This invariant cross section, expressed in convenient

lab frame variables, is just $(1/p^2) \frac{d^2\sigma}{d\Omega(d\bar{p}/p)}$. This cross

section is plotted in Fig. 5 as a function of \bar{p} momentum,

for various primary proton energies. For $p_p=6.5 \text{ GeV}/c$,

the optimum primary proton energy is 100 GeV, and the

cross section is 57 mb/sterad. The 5 cm tungsten target

has an efficiency of $\epsilon=1/3$. The momentum acceptance of

the Booster from Sect. III-3 is $\Delta p/p = 3.0 \times 10^{-3}$. The \bar{p}

yield is then

$$Y = \frac{N_p}{N_p} = \epsilon \frac{d^2\sigma}{d\Omega(d\bar{p}/p)} \frac{\Delta p/p}{\sigma_{\text{tot}}} = 7.5 \times 10^{-7}$$

This result agrees within 30% with the Monte Carlo cascade

calculation of Ref. 23. With 4.6×10^{13} protons in 12

Booster pulses in the MR, this corresponds to $N_p = 3.5 \times 10^7$.

We have designed with some detail the critical parts

of the \bar{p} collection channel. It consists of three distinct

parts:

i) The collecting lens system.

It is a 6-quadrupole system consisting of an initial doublet (Q_1, Q_2), two field-lenses (Q_3, Q_4) and a final matching doublet. The quadrupole dimensions and gradients are

listed in Table II. We show in Fig. 6 trajectories of off-momentum particles and several limiting rays.

ii) A momentum matching section. This section separates

the antiprotons from the main proton beam and matches

dispersion of the beam to the requirements of the Booster.

iii) Injection into the Booster. Here we can use the new extraction system to be installed in straight section 3

(see Fig. 7). Although the detailed design is only now

in progress, it is well within present technology and we

anticipate no major problems.

IV. ANTIPROTON STORAGE AND COOLING

4-1. Design Criteria

Antiprotons are transferred to a 200 MeV storage ring (Freezer Ring) where cooling and repetitive accumulation takes place.

We suggest a very simple lattice and reduced periodicity. The central requirement of the lattice is a good acceptance and adequate long straight sections for electron cooling. The major goal is to design a lattice with a minimum number of dipoles and quadrupoles that gives the longest good quality straight sections. We present here one example of a lattice which approximately satisfies these criteria. The basic lattice has 12 cells, 24 dipoles, and 36 quadrupoles. Figure 8 shows a unit cell and the resulting betatron functions. The machine parameters and performance are given in Table III. A large acceptance is obtained that is well matched to the booster or to the Fermilab linac should the Freezer be used as a proton cooler or for multiturn linac injection (see Appendix III).

We would like to preserve the possibility of transferring synchronously to the Freezer. This places a constraint on the circumference of the Freezer, since in order to match harmonics with the Booster we have

$$\frac{h_F}{85} = \frac{C \times 13.25}{2\pi \times 10^7 \text{ m.}}$$

The choice $h_F = 86$ yields $C = 479.78 \text{ m}$, which fits comfortably in the Booster tunnel (see Figure 9 and 10).

When we return the cooled and stacked anti-protons to the

Booster for reacceleration and injection in the MR, it is necessary to do so with $h = 86$ in the Booster. This dictates $h_F = 85$. This corresponds to a circumference $C = 479.85 \text{ m}$, negligibly different from that for injection to the Freezer.

The transfer of the \bar{p} beam from the Booster to the Freezer has to have sufficient aperture to accommodate the full Booster beam acceptance. This can be achieved using a fast kicker B_1 in long straight 7, followed by a pulsed current septum B_2 in long straight 6. These elements are described in Table II. A second, identical pair of elements are then used in reverse sequence in the Freezer ring for injection.

The transfer from the Freezer into the Booster is accomplished at straight 5 with a more modest version of B_1 , B_2 , since the aperture requirement is now minimal.

We find that because of the rise and decay times of the full aperture kickers which are necessary to extract and inject the relatively large beam, as many as 3 bunches corresponding to 100 msec may be lost in the transfer process.

IV-2. Magnetic Structure

There are several possible designs for the bending and quadrupole magnets that form the building blocks of the Freezer lattice. The bend can be either a window-frame or H design; the quadrupole can be either a standard design with iron pole tips, or a Panofsky quad formed by a box of 4 alternating current sheets. We are presently evaluating each design in regard to the required field quality and cost.

For the bending magnet, we have examined a number of existing

designs (Fermilab 10' EPB dipole, SLAC 180722, ANL BM105, 107, 109, 110, 114). It seems in general that the fraction c of horizontal "good field" aperture to physical aperture is $c = (0.2a)^{-1}$ in a good design of either an M or window frame, where a is the ratio of vertical/horizontal aperture in the desired good field region. For the case discussed here $c = 0.5$. The field quality in the window frame is, however, sensitive to coil placement, and places rather stringent demand on the fabrication process. This also potentially produces significant variations in multipole moments from one magnet to another. For the design case presented here, we use a scaled replica of the 10' EPB M dipole, shown in Fig. 11.

One question that arises in the context of the bending magnets is what guide field should be used. Three considerations arise in this connection. First, the field quality of a dipole below a few kG suffers from the variation of Fe magnetization at low field. Second, the sagitta for a magnet of given bending angle decreases as guide field increases. The sagitta δ [m] of particles of momentum p [GeV] in a magnet of field B [T], bend angle ϕ [rad] is

$$\delta = \frac{p\phi^2}{2.48}$$

Thus for a fixed number of bends (fixed ϕ), sagitta is minimized for maximum B . Third, as will be discussed in the next section it seems desirable to locate a distributed ion pump system in the fringe field of the dipoles. An optimized design of such a system improves in pumping speed up to a field of 4kG. We have tentatively chosen for this design a guide field of 5kG, corresponding to 24 lm dipoles.

For the quadrupoles, there exist 21 quadrupoles that previously

formed the muon channel of the Chicago synchrocyclotron. The design is shown in Fig. 12. We are examining their suitability for the Freezer ring. Several Panofsky quads have been built at Cornell.²⁵ The Panofsky design is problematic for a storage ring for the same reasons as a window frame dipole. Additionally, its power requirements are greater for a given gradient than for a standard quad.

The parameters of both magnets are given in Table IV.

IV-3. Long Straight Sections for Electron Cooling

In order to obtain rapid cooling of the beam it is desirable that the \bar{p} beam have a small divergence in the straight section. This requirement can be met by having β_H , β_V large in the straight section. We have achieved one simple design of such a straight section using two quadrupole triplets that match well the basic cell described before. The horizontal acceptance remains 100 π m and 8" bore quadrupoles are adequate for the triplets. The β_V , β_H are in the range of 15-40 m leading to an angular divergence of $\sim (1-2)$ mrad. The p function (off momentum function) goes to 1.2m in the same straight section. We suggest that the cooling straight sections be instrumented in this way whereas the other straight sections need fewer quads (1-2 doublets, incorporating the D quads of the regular cells).

IV-4. Vacuum System

The Freezer ring must be capable of storing an antiproton beam for a time of the order of a day without serious losses due to beam gas scattering. We will examine the vacuum requirements implied and discuss one attractive approach to meeting them.

Beam growth occurs by Coulomb scattering from gas molecules, and beam loss occurs each time an antiproton collides with a gas nucleus. The rate of increase in the mean square of the projected angle of Coulomb scattering is:²⁶

$$\frac{d\langle\theta^2\rangle}{dt} = \frac{4\pi r_p^2 c}{\beta^2 \gamma^2} \frac{1}{i} n_i z_i^2 \ln \frac{38360}{\sqrt{\Lambda_i^2}}$$

where $r_p = 1.54 \times 10^{-16}$ cm the proton radius, n_i is the density and z_i and Λ_i are the atomic number and atomic weight of atoms of type i . Snowden²⁷ has analyzed the residual gas composition in the MR at a pressure of 0.21 μ Torr. We will assume the same composition in the freezer, and follow here his calculation of beam growth. The angular growth is

$$\frac{1}{p} \frac{d\langle\theta^2\rangle}{dt} = 0.25 \text{ rad}^2 \text{ sec}^{-1} \text{ Torr}^{-1}$$

The diffusion rate of the quantity $W = (dy/d\theta)^2 + v^2 \gamma^2$ is $D = R^2 d\langle\theta^2\rangle/dt$ where y is the amplitude of betatron motion, $v=4$ is the tune, and $R = 75$ m is the average radius. The beam lifetime is²⁸

$$\tau = \frac{1}{D} \left(\frac{2va}{2.4} \right)^2$$

where $a = 1$ cm is the tolerable aperture growth. The lifetime against Coulomb scattering is then τ [sec] = $9.0 \times 10^{-7} / p$ [Torr]. A lifetime of one hour requires a mean pressure of 2×10^{-10} Torr. Clearly we must rely on electron cooling to damp the growth of the stack.

The fraction f of beam removed by nuclear collisions with gas is

$$df/dt = \beta c n_{pp} \frac{1}{i} n_i \Lambda_i$$

where $\sigma_{pp} = 170$ mb is the $p\bar{p}$ total cross-section at 650 MeV/c.

$$\frac{1}{p} \ln \frac{\Lambda_i^2}{\Lambda_1^2} = 1.5 \times 10^{13} \text{ cm}^{-3} \text{ Torr}^{-1}$$

$$\tau \text{ [sec]} = 2.3 \times 10^{-3} / p \text{ [Torr]}$$

A lifetime of one day requires a mean pressure of 2.5×10^{-6} Torr.

The vacuum in the Freezer should thus be 5×10^{-10} Torr. One appealing approach to achieving this in the bending lattice is to locate a distributed ion pump system in the fringe field of the dipoles.²⁴ Rowe and Winter²⁹ estimate a pumping speed of 1600 l/sec from each 1 m dipole so equipped. The cost is about 1/2 that of a standard ion pump of capacity 500 l/sec. Standard ion pumps would still be required in the straight sections. The conductance of a 5 m section of the Freezer vacuum pipe is approximately 22 l/sec.

IV-5. Electron Cooling

The Novosibirsk group has demonstrated that low-momentum proton beams can be "cooled" to very small transverse dimensions and very small momentum spread.³ The basic idea is that the transverse and longitudinal oscillations of the proton beam are transferred by Coulomb scattering to an electron beam that is injected in one of the straight sections of the storage ring. For maximum cooling efficiency the velocity of the \bar{p} and of the e^- should be the same ($\beta_{\bar{p}} = \beta_e$), since the Coulomb scattering cross section will be a maximum. Their results will be used to extrapolate the cooling rates expected in our case.

We assume the entire Booster beam is transferred in one turn at 200 MeV into the Freezer Ring. The emittances of the beam

at this stage are $\lambda_V = \lambda_H = 40 \times 10^{-6}$ m. $\Delta p = 1.3$ MeV/c. The beam is assumed to be adiabatically debunched either in the Booster or in the Freezer. In the cooling points ($\theta_V = \theta_H = 15$ m) the half-beam sizes are as follows:

$$W_H = \sqrt{\lambda_H \delta / \pi} = 2.5 \text{ cm} \quad W_{\Delta p} = \lambda \cdot \frac{\Delta p}{p} = 0.4 \text{ cm}$$

$$h = \sqrt{\lambda_V \delta / \pi} = 2.5 \text{ cm}$$

The total area is then $A = \pi(W_H + W_{\Delta p}) \cdot h = 23 \text{ cm}^2$.

Angular divergencies are also of interest. They are

$$\theta_H = \sqrt{\lambda_H / \delta \pi} = 1.6 \text{ mrad}$$

$$\theta_V = \sqrt{\lambda_V / \delta \pi} = 1.6 \text{ mrad}$$

which are, as we shall see, quite comparable to the angles of the electron beam.

An approximate formula for the cooling time for a parallel e^- and p (or \bar{p}) beam is given by ($\theta_e \ll \theta_p$)

$$\tau = .05 \left(\frac{M_e}{M_p} \right) \frac{V_e^{-5} \theta_e^{-3}}{n_e r_{CL} \eta \ln(\theta_p / \theta_e)}$$

This formula reduces to

$$\tau = \frac{1.2 \times 10^7 \delta^{5/3} \theta_e^{-3}}{j_e \eta \ln(\theta_p / \theta_e)} = \frac{2.5 \times 10^6 \delta^{5/3}}{j_e \eta}$$

where τ = end-point cooling time [sec]

j_e = electron beam current density [A/cm^2]

r_e = classical electron radius [cm]

n_e = electron beam density [cm^{-3}]

θ_p = \bar{p} beam divergence [rad]

$V = E_e / m_e c^2$, $\theta_p = (p_e / E_e)$

η = cooling length/total circumference of cooling ring

L = Coulomb logarithm = 15

In the approximation $\theta_e \gg \theta_p$, the formula will contain the factor θ_e^3 instead of θ_p^3 .

The latest experimental results from Novosibirsk are as follows:

Proton energy	65 MeV
Electron energy	35 keV
Cathode diameter of the electron gun	20 mm
Electron current I_e	0.1 - 0.8 A
Proton current I_p	20 - 100 μA
Average vacuum	5×10^{-10} Torr
Equilibrium size (diameter) of the proton beam in the middle of the section	0.47 mm
Cooling Time ($I_e = 0.8 A$) τ_e	83 msec
Proton life time in the cooling regime	more than 8 hours
Angular divergence of electrons	0.2 ± 3 mrad
Specific flux of neutral hydrogen atoms $(\frac{dN}{dt} / I_e I_p)$	$80 A^{-1} \mu A^{-1} sec^{-1}$

In order to extrapolate to our situation, we must take into account the following factors:

(i) The kinetic energy is higher, 200 MeV instead of 65 MeV. According to the $\gamma^{5/4}$ scaling law, this increases the cooling time by a factor 10.8.

(ii) The angular divergence of the electron beam which dominates with respect to that of the (anti) proton in both cases is given by the formula discussed in Appendix II:

$$r = \frac{V}{\gamma} = 0.102 \frac{I}{5Vr_0}$$

For our case, $r_0 = 2.5$ cm, $V = 1.1 \times 10^5$ V, $B = 0.2$ T, and $I = 23$ A. Comparing it with Budker's case, we can see that electron temperatures are expected to be comparable. Hence, the factor is the same for both cases.

(iii) The fraction of circumference with electron beams was $\eta = 0.016$ for Budker and it is $\eta = 0.063$ for us. This decreases the cooling time by a factor 4.

A detailed comparison between the Novosibirsk and Fermilab situations is summarized in the following table:

	Novosibirsk	Fermilab
Proton energy	65	200 MeV
Electron energy	35	110 keV
Electron current	0.8	23A
Proton current	100	3 μ A
Electron beam radius	1	2.5 cm
Fraction of circumference cooled	0.016	0.06
Angular electron spread	3.0	3.0 mrad
Proton angular spread	-	1.6 mrad
Cooling time	0.086	0.0466 (*)

(*) Extrapolated using the dependence
 $t \sim \gamma^{5/4} Q^3 / \eta j_e$, where $j_e = I_e / \pi r_0^2$

We remark that the cooling time is expected to be appreciably shorter than necessary.

In the above table, the space charge of the electron beams lead to a tune shift of about .25 in both transverse dimensions. Although this may seem large, it should be noted that the electron density must, in any case, be very uniform so the tune spread will be small and correction, if necessary, can be straightforward. The half integral stopbands caused by the electron beam can be cancelled by proper periodicity of the cooling sections in the cooling ring.

IV-6. Electron Beam and Electron Gun

We propose that a total of at least 30m of cooling length be incorporated into the machine. The electron beam must be maintained parallel over 10m length. Space charge effects will blow up the electron beam unless a solenoidal magnetic field is maintained over the entire length of cooling. Furthermore, as discussed in Appendix II, the magnetic field lines must be shaped and carried all the way back into the electron gun cathode.

The electrons, after exiting the cooling section, are to be decelerated to regain the large energy in the beam. The system is shown schematically in Fig. 13.

The accelerating voltage must be 110 kV, equivalent to a beam power of 2.5 MW. Assuming a 98% efficiency of recovery, we have a dissipation of 50kW/beam or a total of 200kW, which is acceptable.

The electron current requirement is about 1 A/cm^2 over approximately 10 cm^2 at 110 KeV energy. CW electron guns have been constructed that give this performance. For example, one such gun is shown in Fig. 14, that is to be used in PEP. This gun gives $\sim 23 \text{ A}$ of current for a voltage of 110 keV over an area of approximately 10 cm^2 .

IV-7. Stacking in the Freezer

Two techniques are used for stacking in the Freezer.

Electron cooling can be used to move the beam and therefore to remove the antiprotons from the injection area after the previous Booster capture has been cooled. This motion is slow, and a more efficient technique will be needed to move each booster capture into a preliminary stack that will contain all 12 captures. For this purpose, rf stacking is to be used. During the time that the Booster is being filled with protons and the protons accelerated in the Main Ring, a modest rf will be used to adiabatically capture the newly-cooled beam. This can be done without disturbing the cool beam already present at the inner edge of the aperture. The new beam is then moved over to the stack and stacked next to it. This procedure is shown schematically in Fig. 15.

ACKNOWLEDGEMENTS

We gratefully acknowledge the contributions of A. Ruggiero to the evolution of this project. We also thank M. Barton, T. Collins, E. Courant, C. Curtis, D. Edwards, H. Edwards, R. Muson, D. Johnson, R. Johnson, J. Laslett, M. Lebacqzue, P. Livdahl, J. LoSucco, S. Snowden, L. Teng, K.R. Wilson, D. Winn, and W. Winter for helpful discussion. Special thanks are due to E. Rowe and W. Tizack for lattice design.

References

1. C. Rubbia, P. McIntyre and D. Cline, "Producing the Massive Intermediate Vector Meson with Existing Accelerators, submitted to Phys. Rev. Letters, March 1976.
2. D. Cline and C. Rubbia, "Energy Doubler at FNAL as a High Luminosity pp Storage Ring Facility," Report in preparation.
3. G. I. Budker, Atomic Energy 22,346 (1967); G. I. Budker, et al.: "Experimental Facility for Electron Cooling," BNL-TR-588 (1974); "Preliminary Experiments on Electron Cooling," BNL-TR-593 (1974); "Experimental Study of Electron Cooling," BNL-TR-635 (1976).
4. S. Van der Meer, CERN-ISR-PS/72-31, August, 1972 (unpublished).
5. D. Cline, P. McIntyre, and C. Rubbia, "Proposal to Construct an Antiproton Source for the Fermilab Accelerator," Fermilab Proposal Number 492 (1976).
6. G. I. Budker, et al., "New Results of Electron Cooling Studies," preprint submitted to Nat. USSR Conf. on High Energy Accelerators (Dubna) Oct. 2, 1976.
7. The possibility of using the Booster accelerator for phase-space cooling has been remarked at informal meeting by ourselves, D. Berley, and R. Johnson.
8. F. J. Hasert, et al., and A. Benvenuti et al., papers submitted to the Sixth International Symposium, Bonn (1973); F. J. Hasert et al., Phys. Letters 46B, 138 (1973); A. Benvenuti et al., Phys. Rev. Letters 32, 800 (1974).
9. U. Camerini, D. Cline, W. Fry and W. Powell, Phys. Rev. Letters 33, 318 (1964); M. Bott-Bodenhausen et al., Phys. Letters 2:8, 194 (1967).
10. S. L. Glashow, J. Iliopoulos and L. Maiani, Phys. Rev. D2,1285, 1970.
11. B. Aubert et al., "Experimental Observation of $\mu^+\mu^-$ Pairs Produced by Very High Energy Neutrinos," in Proceedings of the Seventeenth International Conference on High Energy Physics, London, 1974 and in Neutrinos - 1974, AIP Conference Proceedings No. 22, edited by C. Baltay (American Institute of Physics, New York, 1974), p. 201. A. Benvenuti et al., Phys. Rev. Letters 34, 419 (1975), *ibid.* 34, 597 (1975), J. J. Aubert et al., Phys. Rev. Letters 23, 1404 (1974), and J. E. Augustin et al., Phys. Rev. Letters 23, 1406 (1974).
12. J. von Krogh et al., Phys. Rev. Letters 36, 710 (1976); J. Blietschau et al., Phys Letters 60B, 207 (1976).
13. J. J. Aubert et al., Phys. Rev. Letters 33, 1404 (1974); J. E. Augustin et al., Phys. Rev. Letters 33, 1406 (1974).

References (Continued)

14. S. Weinberg, Phys. Rev. Letters 19, 1264 (1967), and A. Salam in Elementary Particle Physics (edited by N. Svortholm. Almqvist and Wiksells, Stockholm, 1968), p. 367.
15. L. Okun and M. Voloshin, "Production of Intermediate Bosons in pp and pp Collisions," Preprint ITP-III, 1976. Many informal calculations have been made by several authors.
16. J. D. Bjorken, Report at the 1976 SLAC Summer School.
17. A. Benvenuti et al., "Test of Locality of the Weak Interaction in High Energy Neutrino Collisions," submitted to Phys. Rev. Letters (March, 1976).
18. T. K. Gaisser, F. Halzen and E. A. Paschos, "Hadronic Production of Narrow Vector Mesons," BNL preprint 21489.
19. Booster Synchrotron, Fermilab TM-405, edited by E.L. Hubbard (1973).
20. F. Mills, private communication.
21. D. Carey et al., "Unified Description of Single-Particle Production in p-p Collisions," NAL-Pub-74/49-TUV/EXP.
22. M. G. Albrow et al., "Negative Particle Production in the Fragmentation Region at the CERN ISR," Nucl. Phys. (1973).
23. B. Chirikov, V. Tayursky, H. Nohring, J. Ranft and V. S. Shirmester, "Optimization of Antiproton Fluxes from Targets Using Hadron Cascade Calculations," KMU-HEP 7606 (preprint), March 1976.
24. Cummings et al., "Vacuum Systems for SPEAR," SLAC-Pub-797.
25. M. Tigner, private communication.
26. B. Rossi, "High Energy Particles," Prentice-Hall, New Jersey, 1952.
27. S. Snowdon, "Residual Gas Analysis in Main Ring to Obtain Round Square Scattering Angle and Beam Lifetime," Fermilab TM-341.
28. L. C. Teng, Accelerator Experiment Note (1/11/72) Fermilab.
29. E. Rowe and W. Winter, private communication.
30. T. Collins, "Easy Low β for the Main Ring," TM-649, March 11, 1976.

Table I. Parameters of \bar{p} injection
and deceleration in the Booster.

Antiproton injection energy (kinetic)	$\gamma_{\bar{p}}$	5.717 GeV
Target length and material	L_t	5cm, tungsten
Target efficiency		0.3
Proton beam size at target		≈ 0.5 mm
Betatron function of \bar{p} 's at target center		
- vertical betatron	β_y^*	0.025 m
- horizontal betatron	β_x^*	0.025 m
- momentum dispersion	η_x^*	~ 0
Acceptances of the Booster ring at 200 MeV		
- vertical	A_y	$40\pi \cdot 10^{-6}$ r.m.
- horizontal	A_x	$40\pi \cdot 10^{-6}$ r.m.
- longitudinal	A_0	3 eV sec
Acceptances from the target		
- production angle	θ_{pvt}	0°
- solid angle	$\Delta\Omega$	5.3×10^{-4} sterad
- momentum acceptance ($\theta = -.12$)	Δp	2.0 MeV/c
Antiproton yield for incident proton	\bar{p}/p	0.83×10^{-6}

Table II. Major Beam Transfer Elements

<u>Element</u>	<u>Description</u>	<u>Length</u>	<u>Field</u>	<u>Deflection Angle</u>
S1	Fast Magnetic Kicker	7m	0.05 T	1.0 mrad
S2	Lambertson Septum(2)	7m	0.9T	20 mrad
B1	Fast Magnetic Kicker(2)	2.5m	0.06T	7 mrad
B2	Pulsed Current Sheet Septum	5m	0.3T	70 mrad
<u>Quadrupole</u>	<u>Length(m)</u>	<u>Half Aperture (cm)</u>	<u>Gradient (Tm⁻¹)</u>	
Q1	1.0	7.0	+1.560	
Q2	1.0	9.0	-1.365	
Q3	1.0	3.0	-1.950	
Q4	1.0	2.0	-2.925	
Q5	1.0	2.0	+0.780	
Q6	1.0	2.0	-0.975	

Table III Tentative parameters of the Freezer Ring

Nominal momentum	P_0	644 MeV/c
Guide field	B_0	0.5T
Magnetic radius	ρ	4.3 m
Orbit radius	R	75 m
focussing type	separated function	
Number of cells	12	
Length of each cell	39.3 m	
Rotation functions:		
- maximum value	β_{max}	27 m
- of the cooling sections	$\beta_{st: straight}$	15 m
Momentum compaction	$x_{p, max}$	6 m
Transition - energy	$x_{p, straight}$	~2 m
	$y_{t=9}$	7.5 m
Length of cooling straight sections		
Betatron acceptance	E_H	96×10^{-6} m
	E_V	75×10^{-6} m
Momentum acceptance	$\Delta p/p$	$\pm 5 \times 10^{-3}$
Phase advance per cell	ϕ_x	0.27
	ϕ_y	0.26

Table IVa. Freezer Ring Dipole

Field Strength	0.5T
Magnet Length	1.0m
Magnet Gap	3"
Pole Aperture	12"
Field Aperture	6"
Field Quality	± 0.11
Coil Turns(Top + Bottom)	140
Copper Conductor Cross Section	.325" x .325"
Water Cooling Hole Diameter	.181"
Conductor Corner Radius	.063"
Conductor Current	220 A
Magnet Inductance	.006 H
Coil Resistance	.12 Ω
Voltage Drop	26 V
Power	5.7 kW
Cooling Water Pressure	150 psi
Number of Water Paths	4
Water Flow	1.4 GPM
Temperature Rise	20°C
Outside Dimensions	25" x 15"
Iron Weight	3000 lb.
Copper Weight	300lb.

TM-689
2000,000

Table IVb. Freezer Ring Quadrupole

Field Gradient	10 T/m
Magnet Length	10"
Aperture	9" dia.
Width of Good Field Gradient	±5"
Gradient Quality ($\Delta B/B$ at 1.5" Rad.)	±.1%
Coil Turns per Pole	30
Copper Conductor Cross Section	.325" x .650"
Water Cooling Hole Diameter	.128"
Conductor Corner Radius	.981"
Conductor Current	300A
Magnet Inductance	.010H
Coil Resistance	.011Ω
Voltage Drop	3.3 V
Power	1.0kW
Cooling Water Pressure	150 psi
Number of Water Paths	1
Water Flow	0.6 GPM
Temperature Rise	8 °C
Outside Dimensions	27" dia.
Iron Weight	1300 lb.
Copper Weight	200 lb.

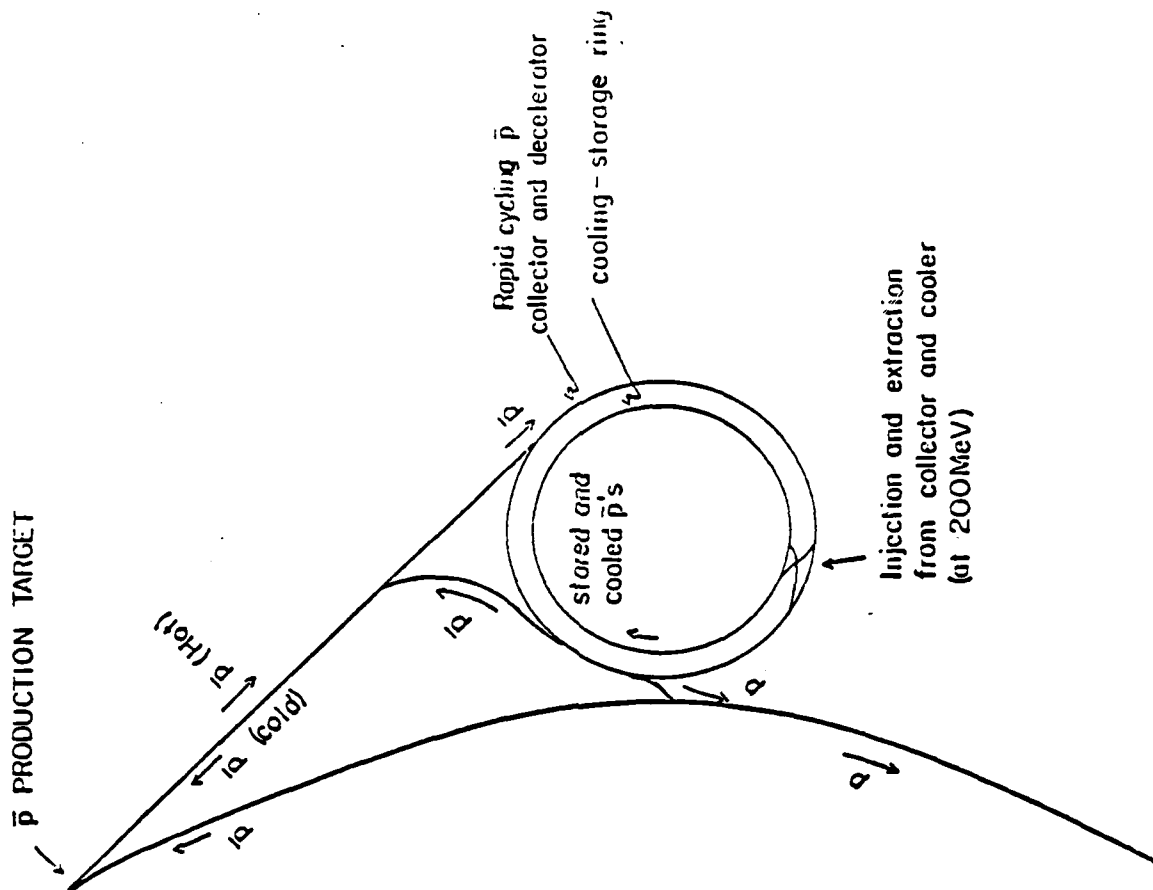


FIG - 1

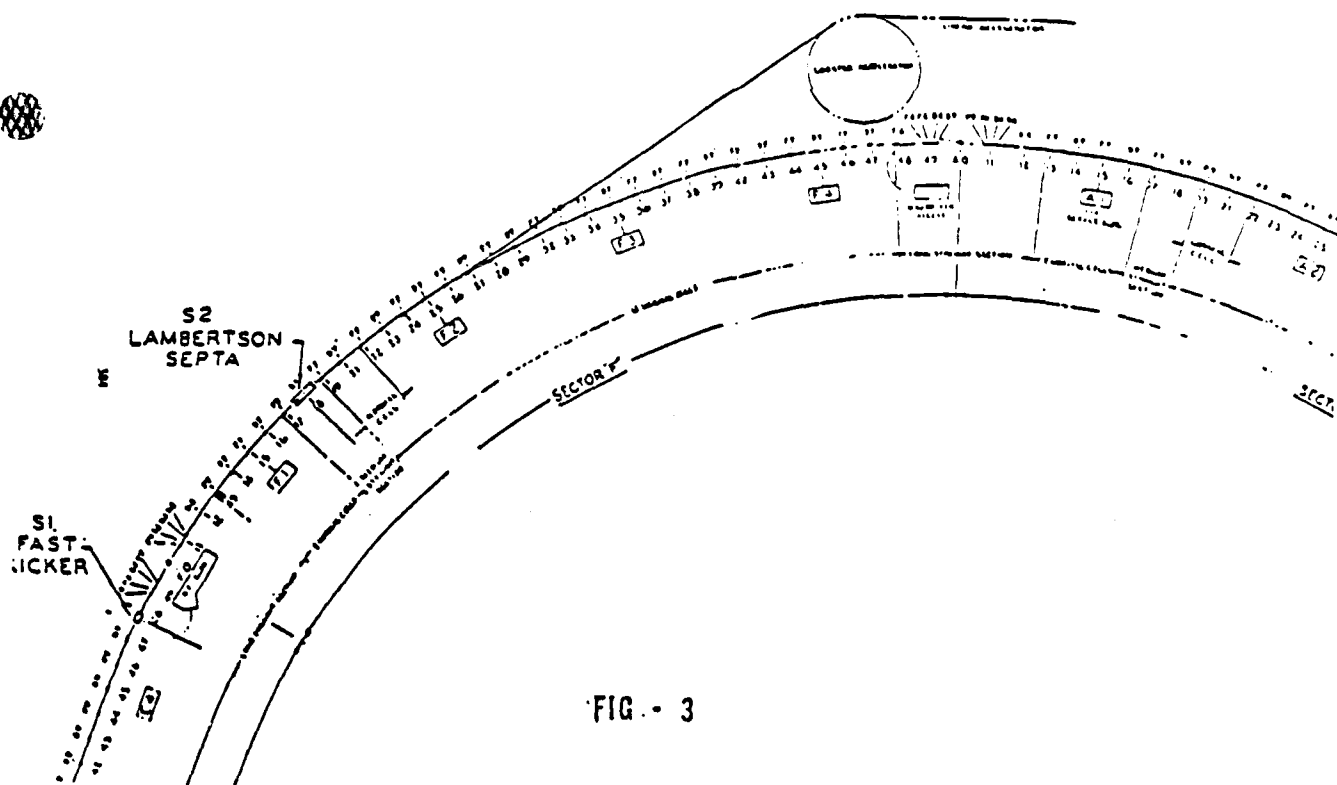


FIG - 3

MAIN RING CYCLE DURING \bar{P} PRODUCTION

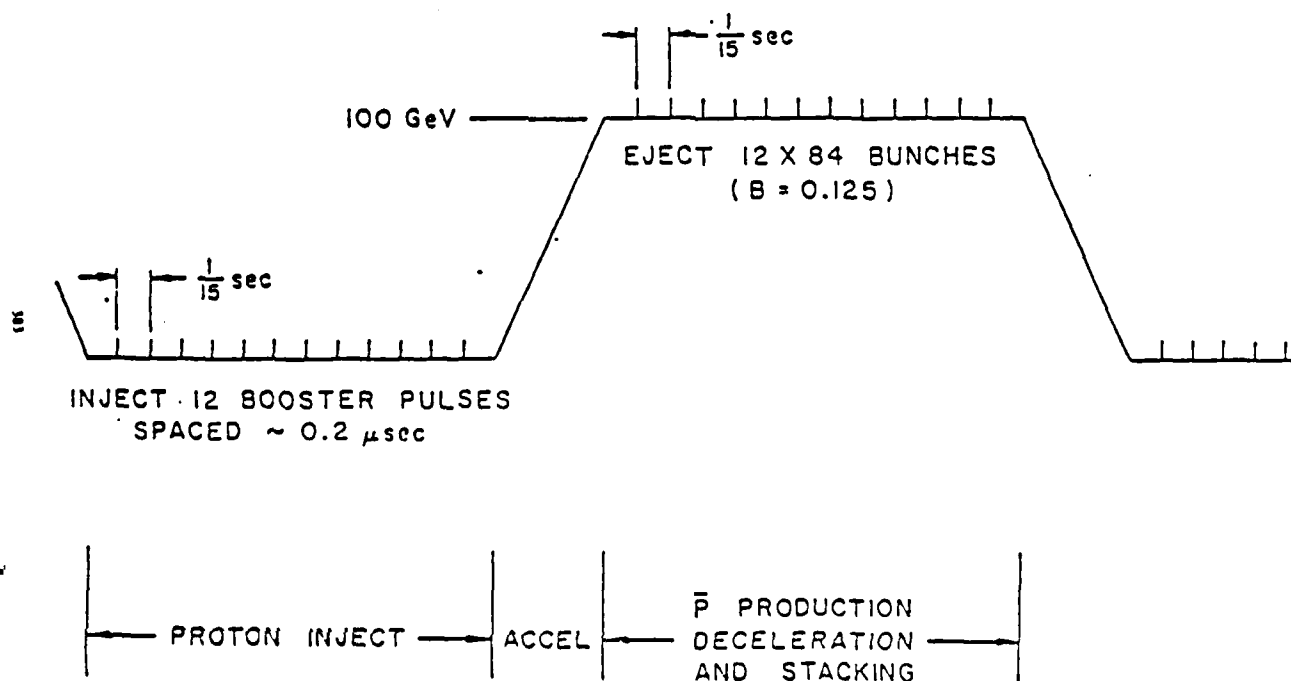
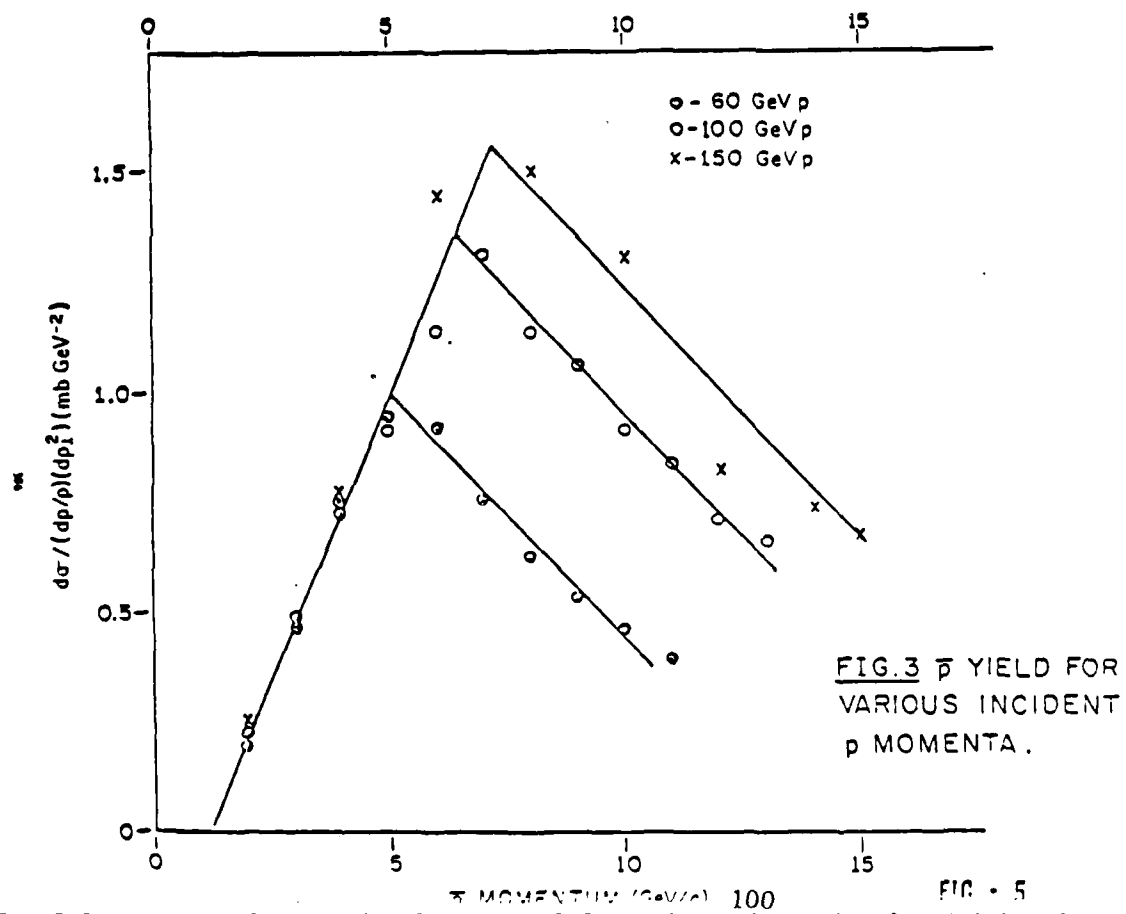
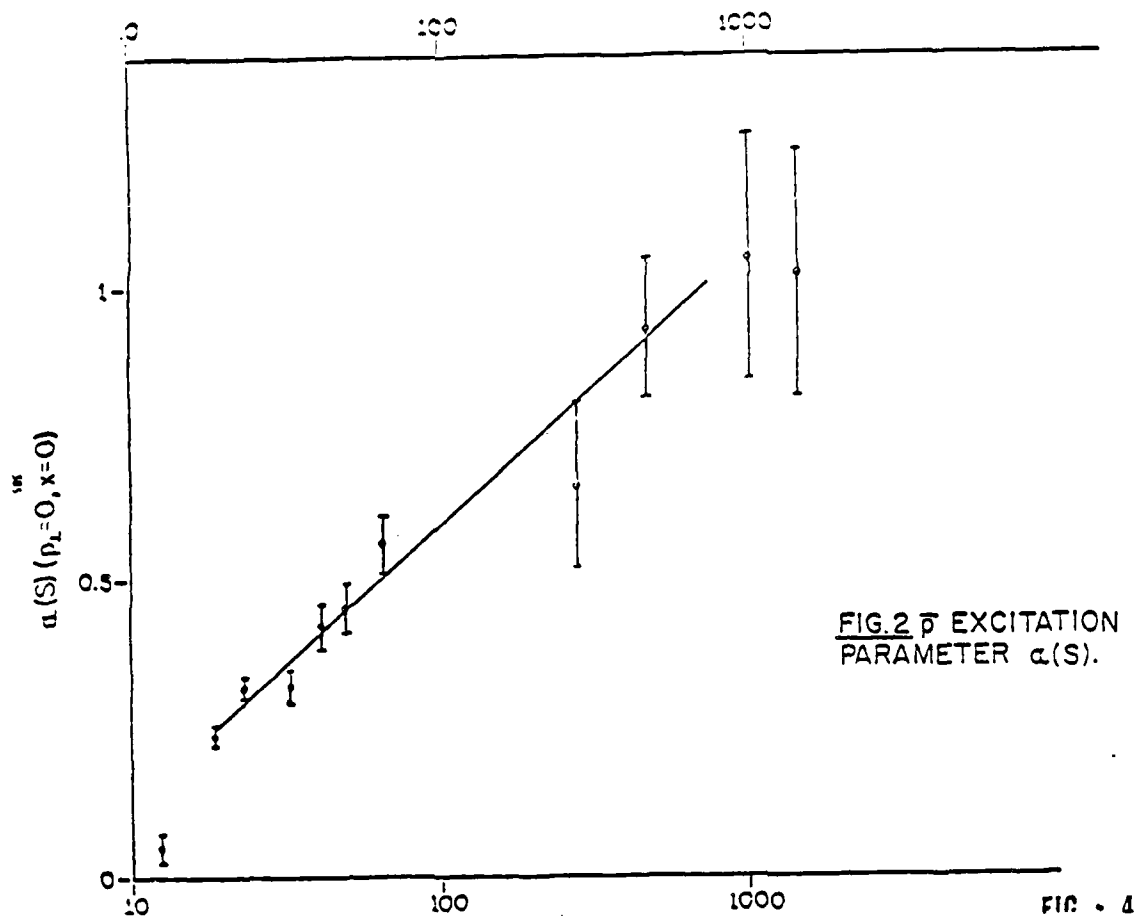


FIG - 2



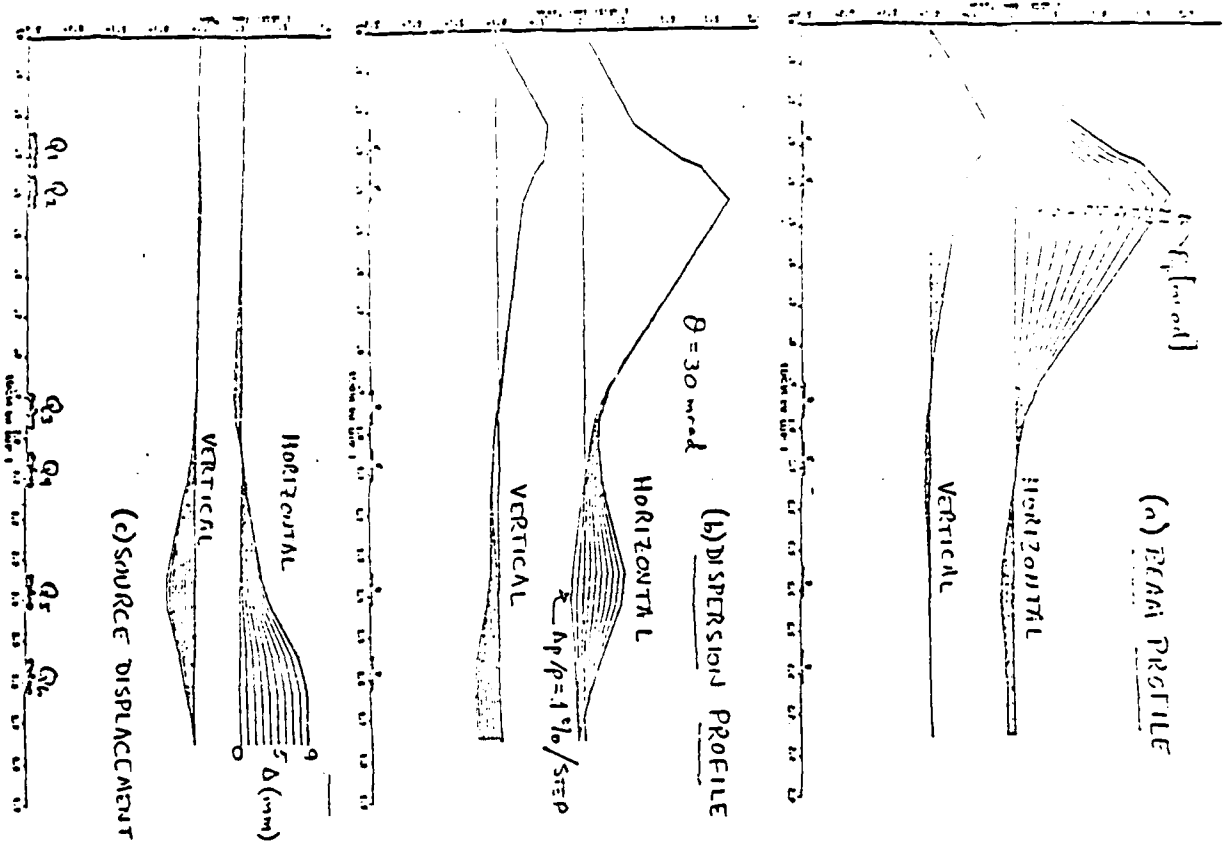
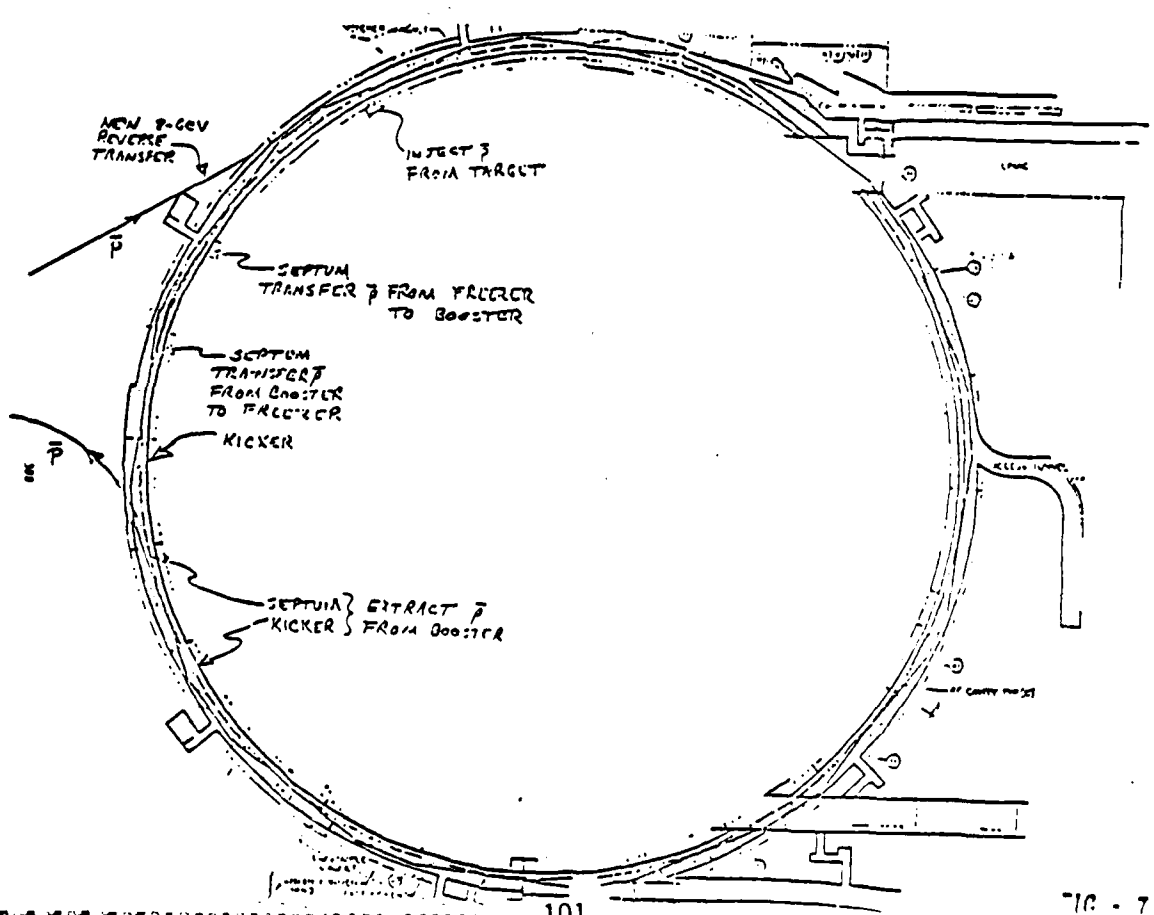


FIG - 6



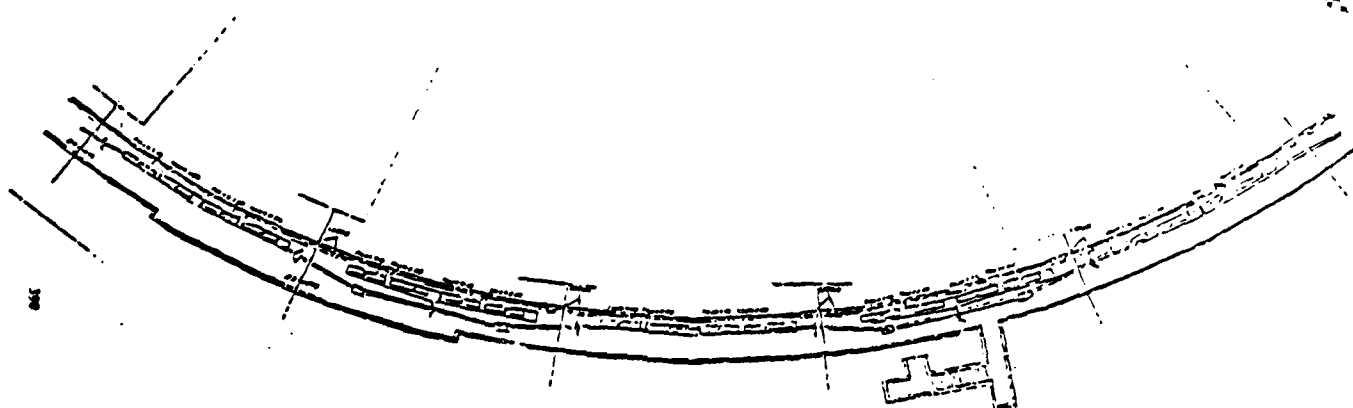
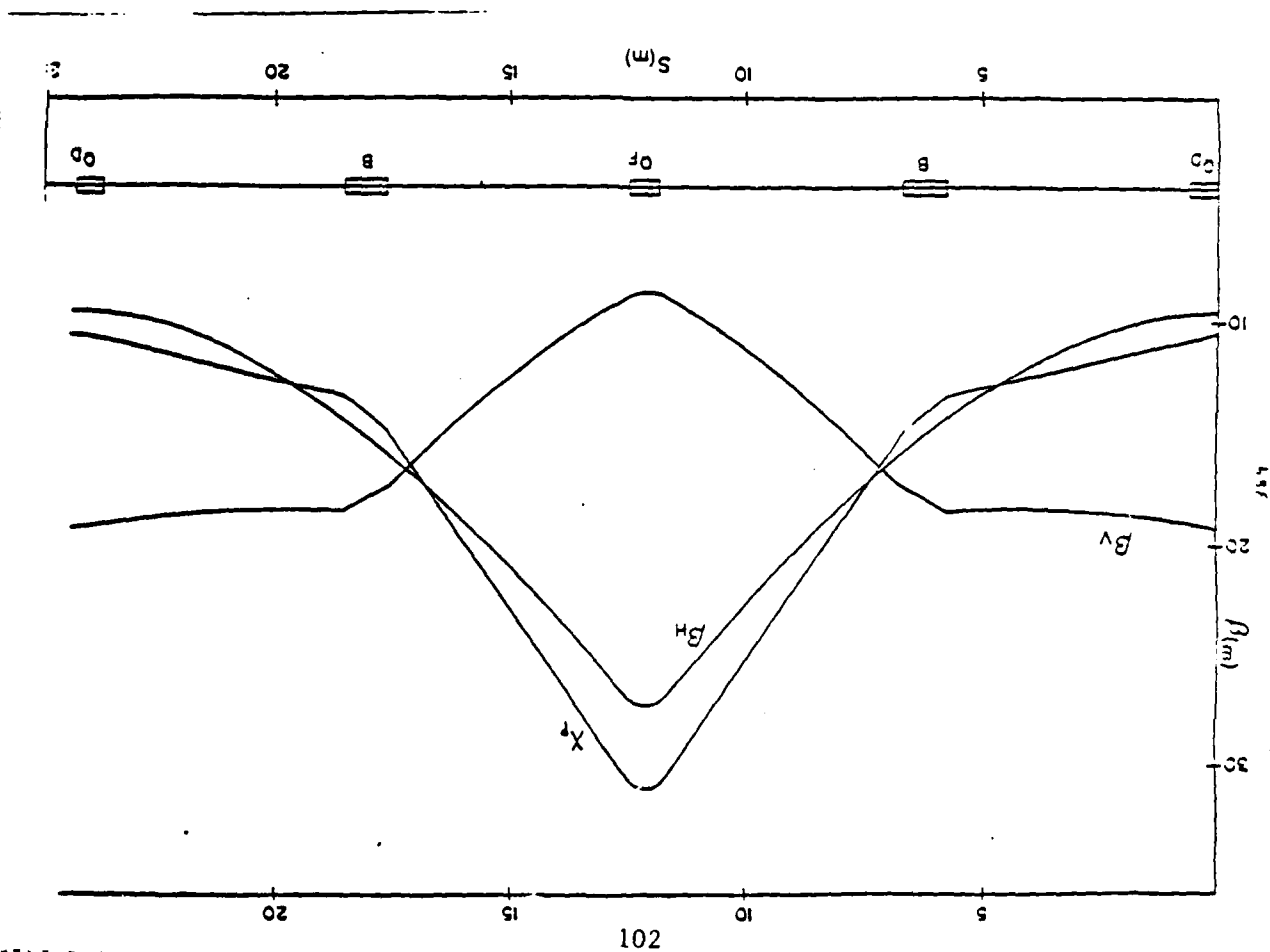


FIG - 9



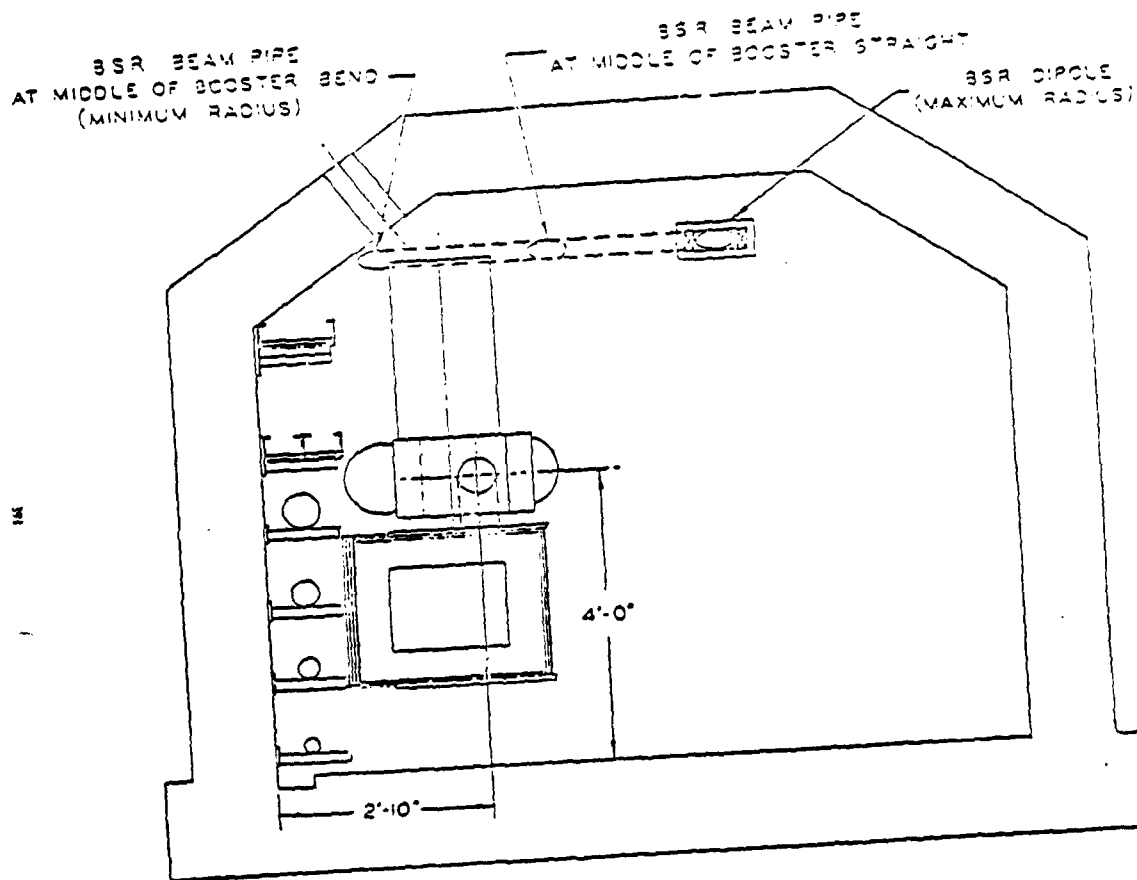
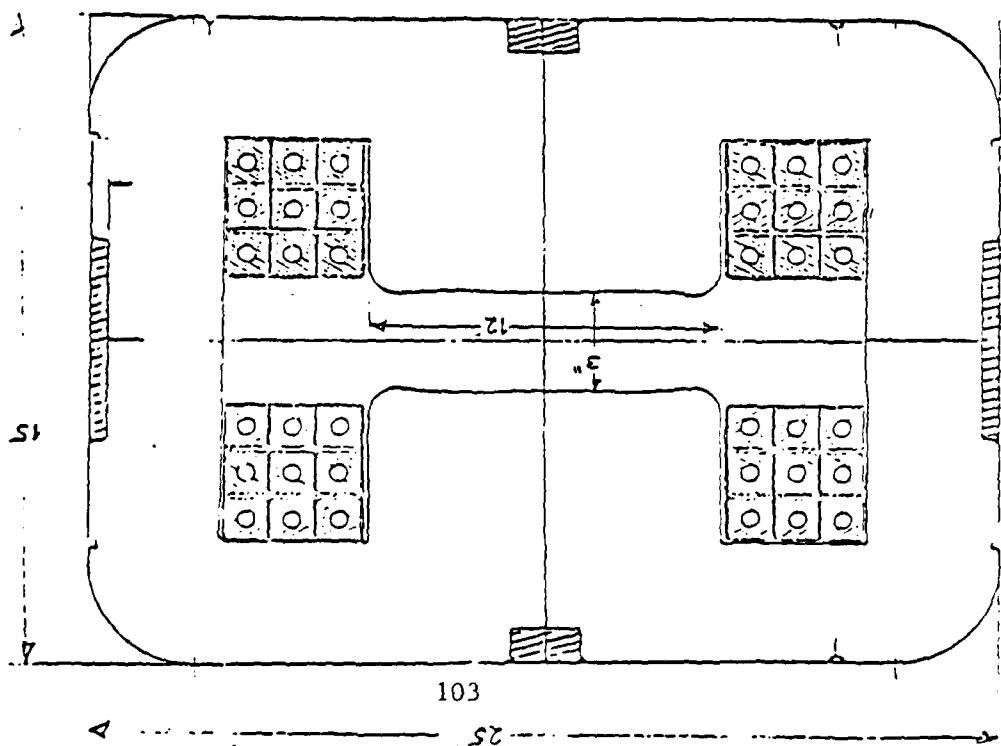


FIG - 10

FIG



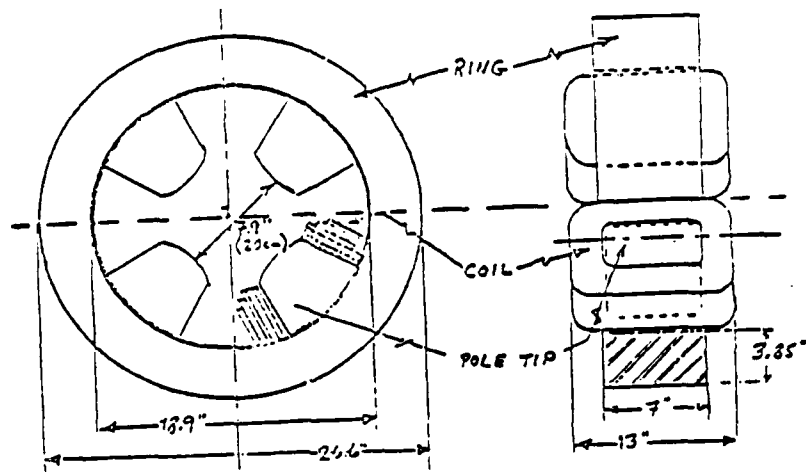


FIG - 12

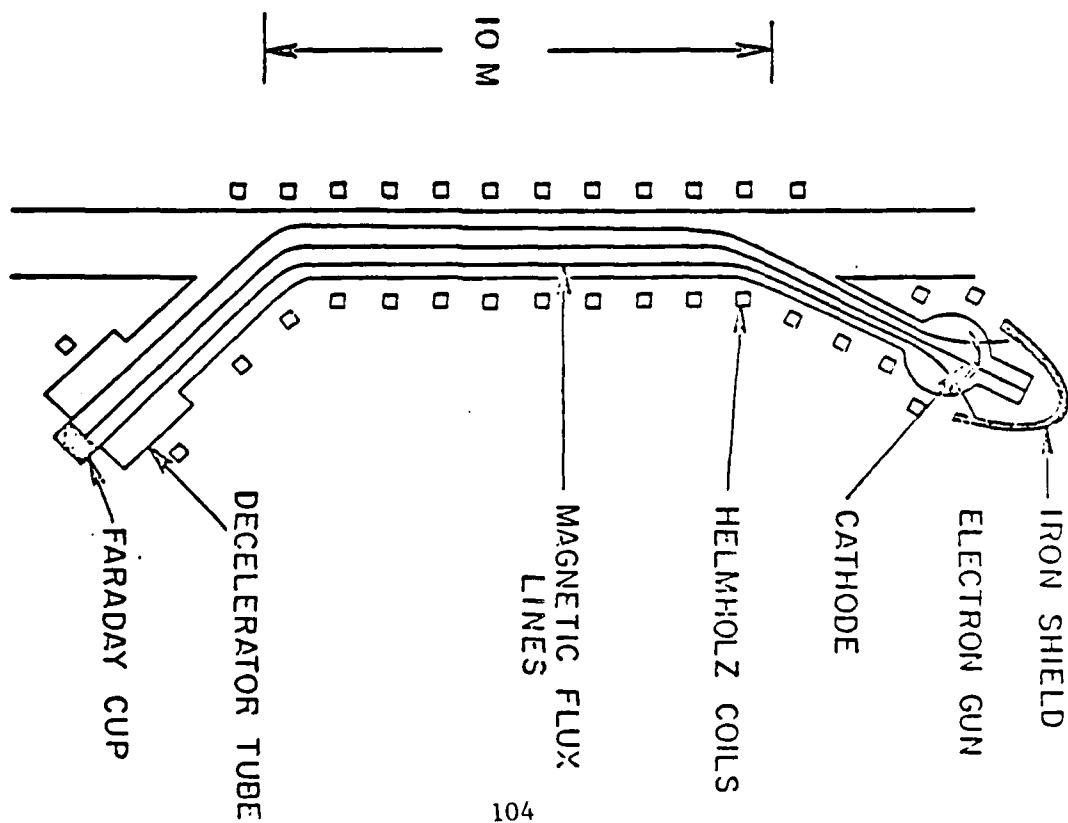


FIG - 13

Cooling straight section
(Schematic)

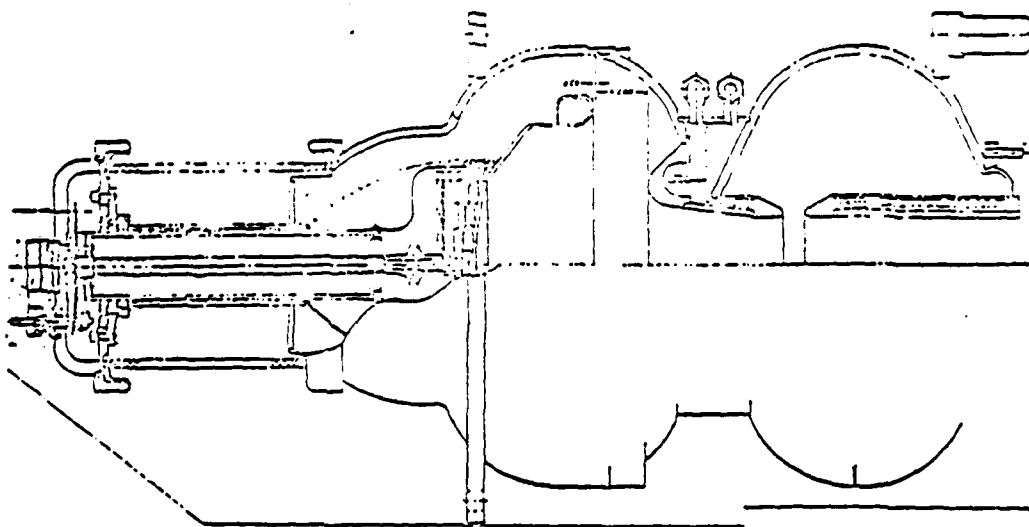


FIG - 14

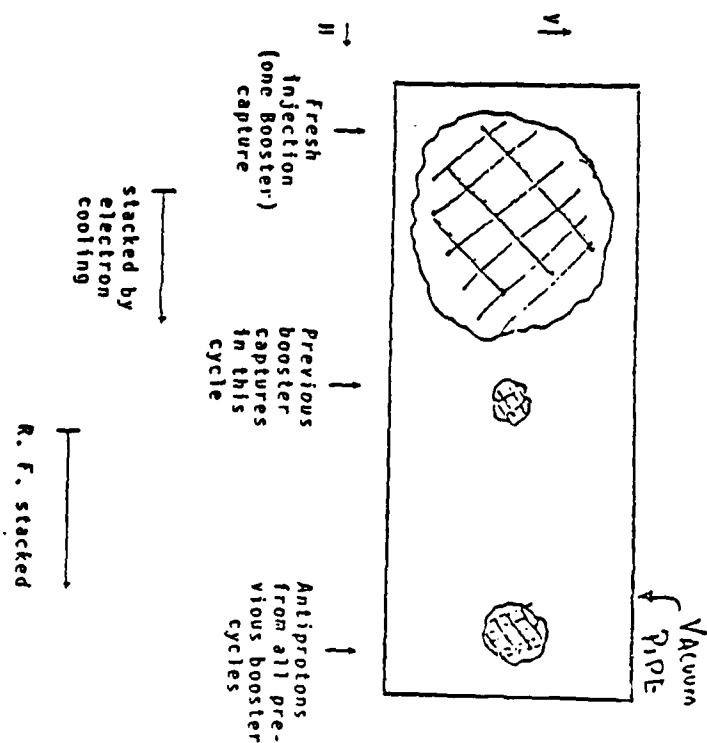


FIG - 15

7.4m

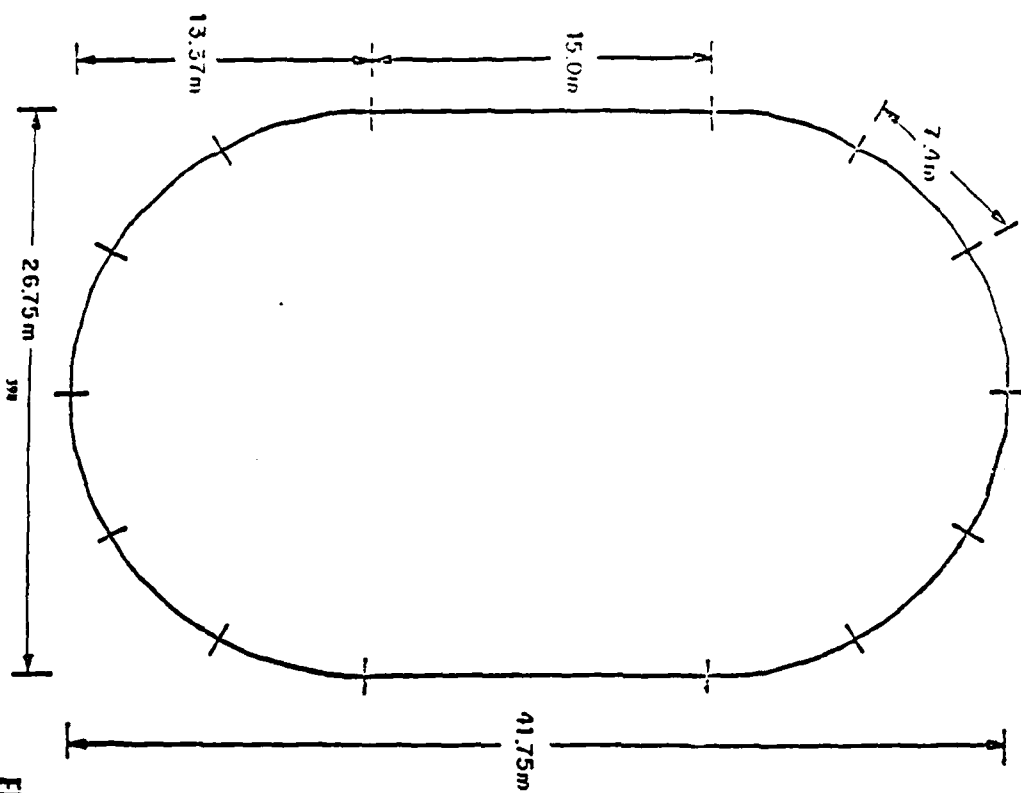
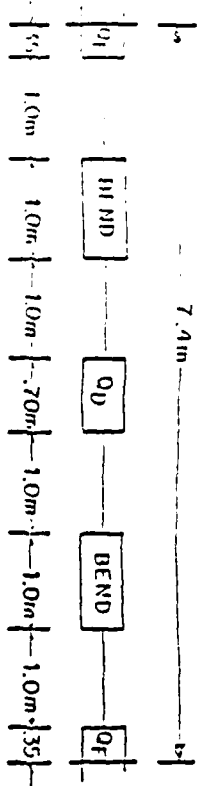


FIG - 17

Motion of Antiprotons in the Electron Rest System

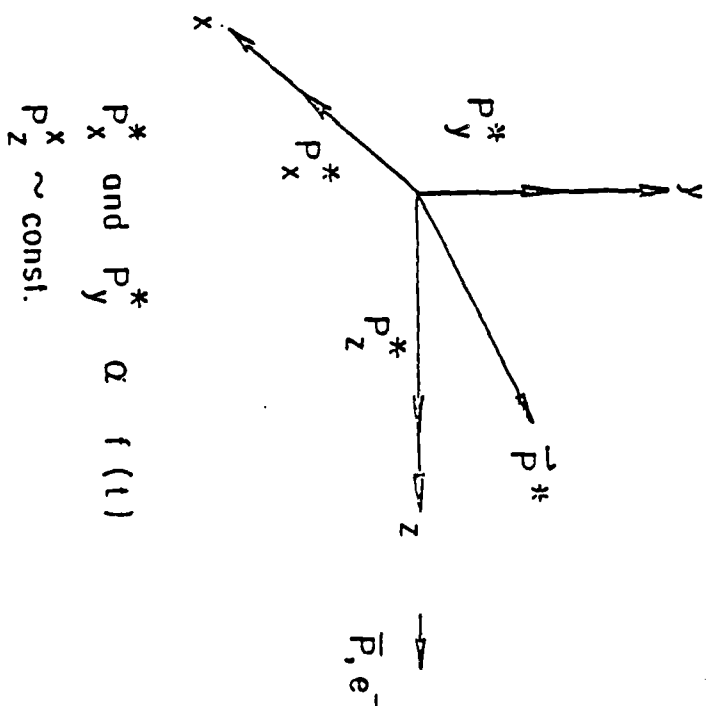


FIG - 16

Appendix B

APPENDIX B

15.

4. ANTI-PROTON BEAMS FROM THE BOOSTER

A.S. Carroll, Group Leader
Y.Y. Lee
D.C. Peaslee
A.L. Pendzick
L.S. Pinsky

I. Introduction

The concept is outlined in Fig. 4-1. In each AGS cycle the booster is filled with protons and operates normally, ejecting into the AGS. After acceleration in the AGS, fast extraction of 3 rf beam bunches occurs at H10 into the U-line where they are focused on an antiproton production target. The remaining 9 AGS bunches are available for other purposes. The antiprotons are collected by a lithium lens and transported at 4 GeV/c, near peak production, to the booster where they are injected through the proton extraction channel, running in reverse direction around the booster. They are then extracted in one straight section with a moderately thick septum tangent to the AGS and transported directly to the 80-inch bubble chamber complex, which serves as an experimental area.* The extraction and transport occurs during the AGS spill. The booster is then ready to accept the next charge of protons at the usual repetition rate.

II. Beam Characteristics

Table 4-1 summarizes the beam characteristics which are further explained in the following paragraphs.

The booster magnet system as presently designed can reach an antiproton momentum of 5.2 GeV/c at 12.7 kg corresponding to a center-of-mass energy in $\bar{p}p$ collisions of $s^{1/2} = 3.42$ GeV. This would allow formation of $n_c(2980)$, $J/\psi(3100)$, and $x_0(3415)$ but nothing higher in the hidden charm sequence. A more desirable limit physically is $s^{1/2} = 3.70$ GeV, corresponding to a \bar{p} momentum of 6.3 GeV/c, which would allow production of $\psi'(3685)$, $n_c'(3590)$ and all the x states. More detailed studies in Appendix 5 address the feasibility of such an extension in momentum range.

* The 80-inch bubble chamber building has been chosen as the Experimental Hall for the muon g-2 experiment since the time of the workshop.

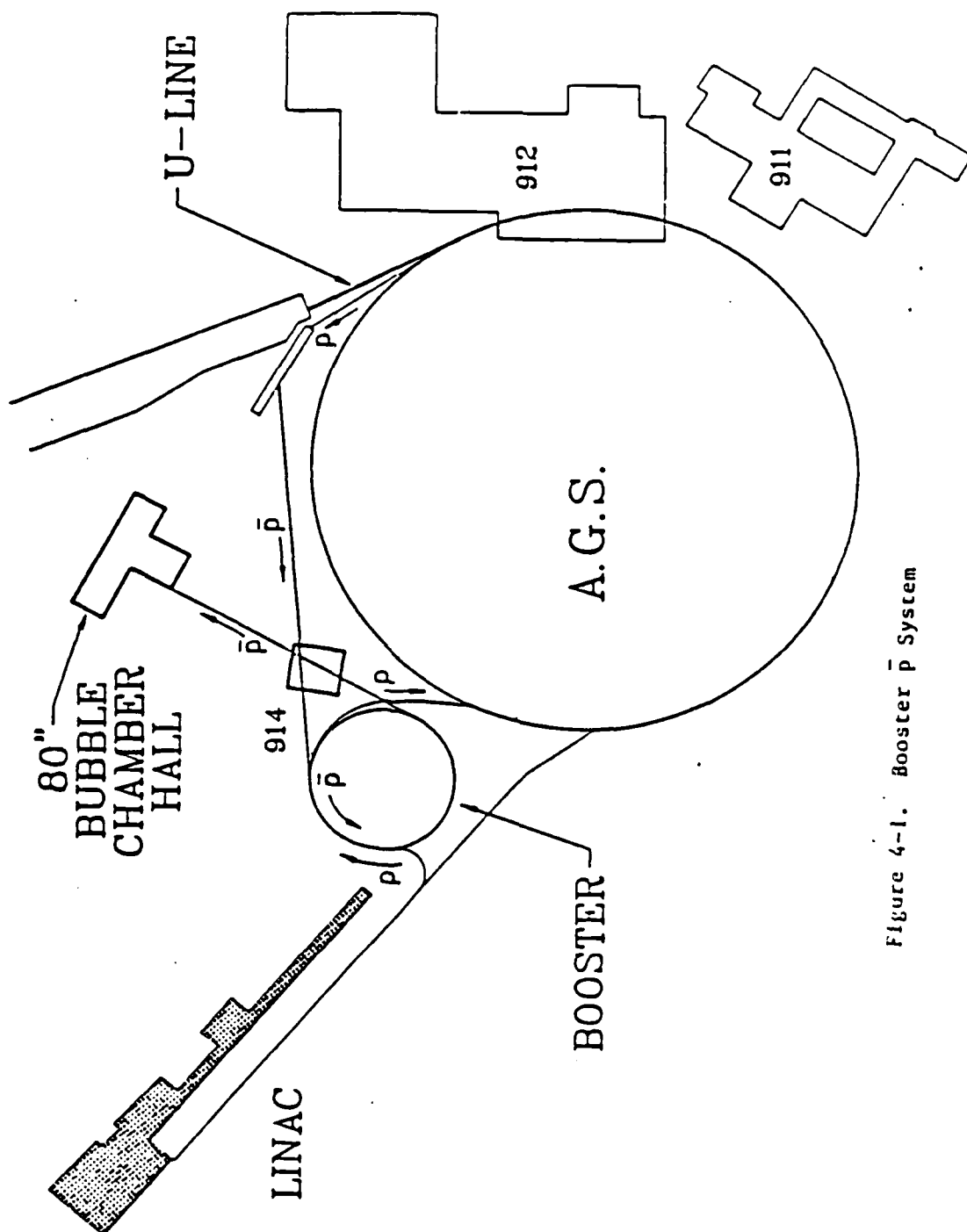


Figure 4-1. Booster \bar{p} System

Table 4-1. BOOSTER ANTIPROTON BEAM CHARACTERISTICS

Momentum range:	0.65 - 5.2 GeV/c
Momentum acceptance $\Delta p/p$:	.02
Angular acceptance:	40 msr
Maximum \bar{p} flux (10^{13} beam prot.) ⁻¹ :	4×10^7
Purity π^-/\bar{p} (all momenta):	0:1
Length (meters):	(not relevant)
\bar{p} production target location:	U-line target
Experimental Area:	80" bubble chamber bldg. *

The momentum spread of $\pm 1\%$ delivered from the \bar{p} production target can be reduced to $\sim 10^{-4}$ by debunching, and further by phase displacement acceleration during extraction. It is important to note that this procedure compresses the Δp of the total \bar{p} flux without loss of particles; a double advantage results--wide Δp for search and scan, narrow Δp for study of a resonance already located.

The purity of the extracted \bar{p} beam is essentially perfect, since the booster ring functions as an extremely long beam line with very large dispersion.

The muon g-2 experiment can use the same target and experimental area. Since both \bar{p} 's in the booster and g-2 require fast extraction and there are no slow extraction requirements in the U-line, the compatibility may be better than in other lines such as C' and D where experiments requiring slow extraction are also mounted.

The availability of antiprotons from this system must wait on completion and commissioning of the booster. Under ideal conditions this could occur as early as 1990, but it seems more realistic to allow early 1991 as the initial date likely for antiproton experiments. Of course the target and direct beam line to the experimental area can be built at once and used for antiproton and muon g-2 studies.

The cost estimate for 5.2 GeV/c antiprotons is detailed in Table 4-2 and includes all necessary modifications to the booster itself, as well as the extra costs of going to 6.3 GeV/c.

* The 80" Bubble Chamber building has been chosen for the muon g-2 experimental area since the conclusion of the Workshop. An extension to this building would provide an ideal experimental area at low cost by utilizing existing services.

III. Discussion

1. Advantages

The specifications above already display some of the advantages of this concept, but it may be worthwhile to recount a more complete list:

- i. Pure \bar{p} beam with no muon halo.
- ii. High flux, \bar{p} 's always taken at production maximum.
- iii. High resolution (10^{-4}) without additional means such as HRSS.
- iv. Momentum compression with existing booster rf.
- v. Continuously tunable momentum.
- vi. Well equipped experimental hall immediately available.*
- vii. Compatible with AGS slowly extracted beam (SEB) operation.
- viii. Nearly ideal compatibility with muon g-2 experiment.
- ix. Very flat spill, booster acts as \bar{p} stretcher.
- x. \bar{d} beams available without modification.
- xi. Very low momentum antiprotons also possible (cf. Appendix 6).

2. Disadvantages

The principal drawbacks of this scheme are as follows:

- i. The time before availability is approximately 4 years.
- ii. The maximum momentum $\bar{p} \leq 5.2$ GeV/c with the present booster design.

If the present concept appears viable, it will be necessary to make immediate plans for adapting the booster as described, in order to incorporate the needed changes in construction.

IV. Cost Summary

The cost summary in Table 4-2 assumes the use of the present HHO extraction system and of all shielding in the proton target area already provided for the muon g-2 experiment, as well as the same target. If it should not prove possible to use the same target, the booster option must

* The 80-inch bubble chamber building has been chosen as the Experimental Hall for the muon g-2 experiment since the time of the workshop.

include the cost of a primary target station, which is included as a contingency. If, however, the preferred extraction for g-2 is at I-10 then locating there would effect savings in the \bar{p} transport line and bending magnets.* A more detailed breakdown is presented in Appendix 8.

The preliminary cost estimate of \$3.6M is on the same order as any other scheme that produces \bar{p} beams of comparable flux, purity, resolution and controllability.

Table 4-2. COST SUMMARY - BOOSTER OPTION

	Cost (KS)	Labor (MW)
Target region	945	123
50° bend and \bar{p} transport to booster	1016	378
Booster magnet modifications to reach 6.3 GeV/c	990	284
Transport to 80" bubble chamber**	626	175
Experimental area	430	25
TOTAL	<u>4107</u>	<u>985</u>

* I-10 has been chosen for extraction to a target for the muon g-2 experiment since the conclusion of the workshop.

** The 80" Bubble Chamber building has been chosen for the muon g-2 experimental area since the conclusion of the Workshop. An extension to this building would provide an experimental area at low cost by utilizing existing services.

5. CONCLUSIONS

The highest performance option for a purified intense antiproton beam at the AGS would clearly be the booster option if not for the limited momentum range. The ability to vary the momentum spread is a unique and powerful tool for formation spectroscopy. Once a given state has been located in a scan with a relatively large momentum bite e.g. $\frac{\Delta p}{p} = .02$, the bite could then be reduced to scan an object of width less than 1 MeV. This amounts to an increase in effective luminosity by the same two orders of magnitude. This would not be possible in the long beam options. Unfortunately the top momentum of 6.3 GeV/c would not permit formation of the 1D_2 and 3D_2 states. The economic and political aspects of further modifying the booster design at this stage would weigh heavily on this option.

The long flight path beams are in general not terribly different from one another in performance or cost. The most attractive is the beam from the C' target area to a new area adjacent to the RHIC Open Experimental Area. It is the longest beam and would deliver antiprotons to a "bargain" experimental hall, which would obtain power and water from the Open Area Hall. The other long beam options suffer somewhat in their shorter lengths and compromises with other installations such as the neutrino area and RHIC injection and experimental areas.

The high resolution spectrometer would be necessary for any of these beam line options to be competitive in the measurement of widths of charmonium states. At best, time-of-flight can yield resolutions approaching 2 MeV in the center-of-mass, even if one ignores the very high rates in the beam counter hodoscopes due to more than 10^8 beam pions per spill.

The momentum resolution is plotted as a function of momentum, for each of the beams under consideration, in Fig. 5-1. A similar plot for the center-of-mass resolution is given in Fig. 5-2.

Table 5-1 compares costs of all the schemes considered here.

Table 5-1. OVERALL COST SUMMARY

	Cost (M\$)	Labor (MW)
C' Option (with inexpensive hall)	2.90 (2.58)	1099 (1099)
U-line Option	3.16	771
D/U-line Option	2.60	757
D/(g-2) Option	1.64	515
D/(g-2)' Option	1.81	667
High Resolution Beam Spectrometer for above	1.07	300
Booster Option	4.11	985

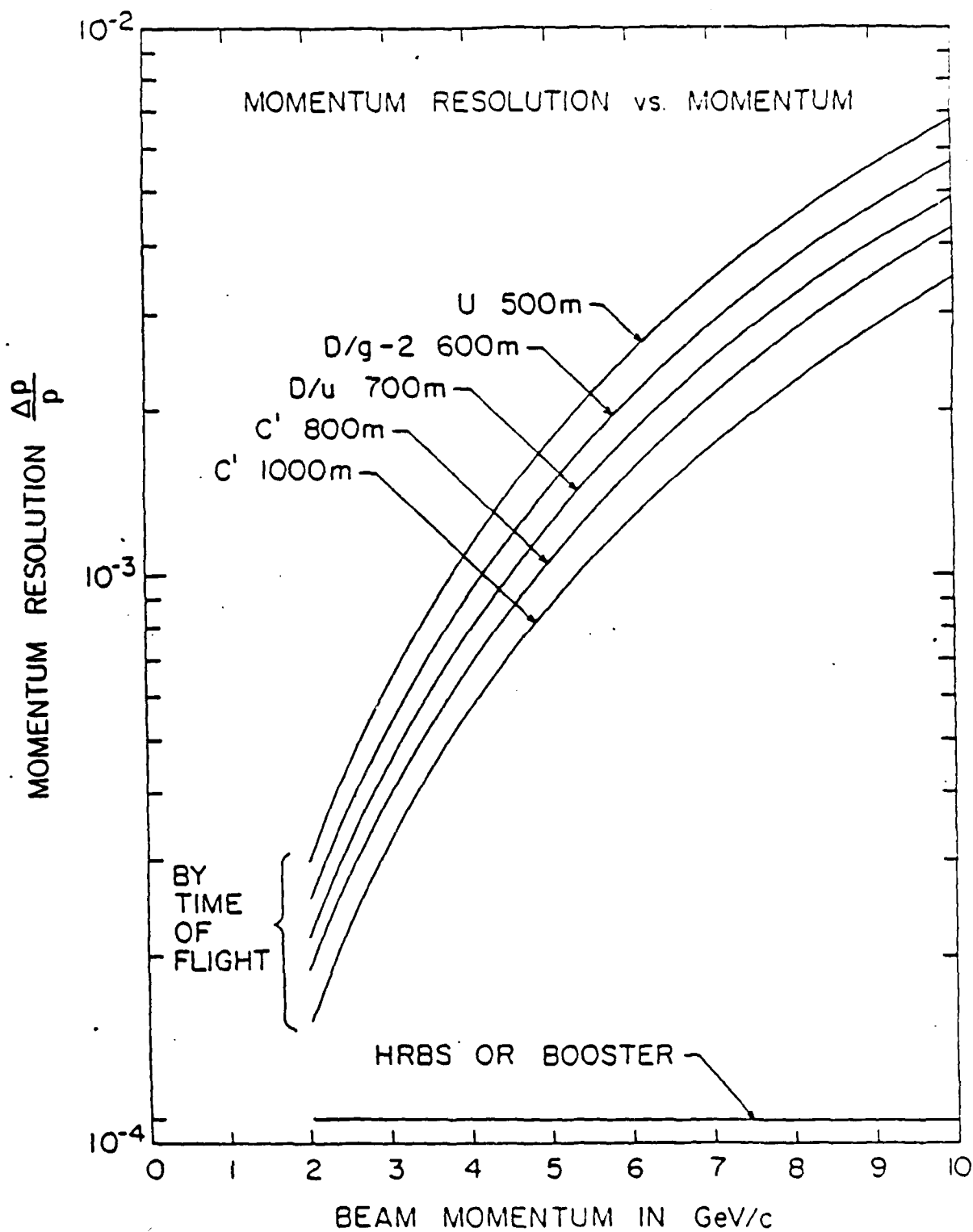


Fig. 5-1. Momentum resolution for the various beam options.

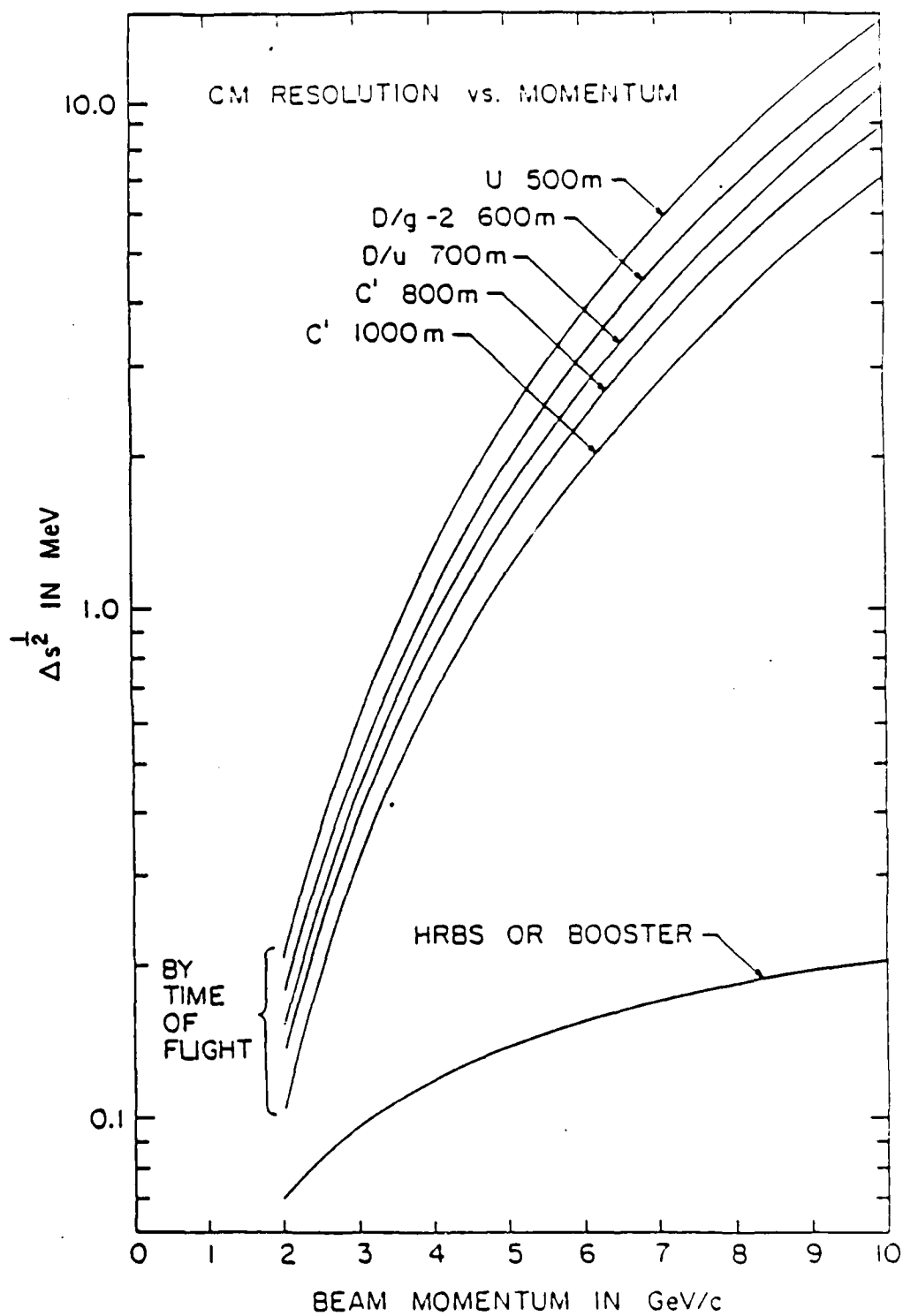


Fig. 5-2. Center-of-mass resolution for the various options.

Appendix C

AN ADVANCED HADRON FACILITY:
PROSPECTS AND APPLICABILITY
TO ANTIPROTON PRODUCTION

by
T. Goldman

Theoretical Division, Los Alamos National Laboratory
Los Alamos, New Mexico, 87545

ABSTRACT

An Advanced Hadron Facility is designed to address physics problems within and beyond the Standard Model. High fluxes of secondary beams are needed for the requisite precision tests and searches for very rare decay modes of mesons and baryons. Such high fluxes at useful secondary energies are readily obtained from high intensity, intermediate energy proton beams, which are also well suited to antiproton production. If the AHF primary proton beam were merely dumped into a beam stop, it would produce on the order of 10^{19} to 10^{20} antiprotons per operating year. Current collection techniques are not likely to be capable of absorbing more than one part in 10^3 of this production. Thus, an AHF provides both the immediate possibility of collecting quantities of antiprotons substantially beyond those available from the LEF discussed at this meeting, and for significant increases in the available antiproton supply upon the development (at an AHF) of more efficient collection and cooling methods. Of these, the most difficult problems appear to arise for increasing cooling rates, whereas production targetry and improving collection efficiencies have readily viable possibilities. The prospects are presently good for the completion of an AHF in the late 1990's.

I. INTRODUCTION

An Advanced Hadron Facility is needed to further precision tests of the standard model and to address problems both within it, and that go beyond its limitations. Nuclear physicists are primarily interested in the opportunities afforded to extend the study of QCD, the theory of the strong interactions, to longer distance (>1 fm.) regimes and in the nuclear medium. This effort is to be complemented by electron scattering experiments at Bates Laboratory and at the Continuous Electron Beam Accelerator Facility (CEBAF), and by heavy ion collisions to study the quark-gluon plasma using the proposed Relativistic Heavy Ion Collider (RHIC) at Brookhaven. Particle physicists are more concerned with experiments involving the electroweak interactions; these either provide precision tests of the standard model or search for new processes which illuminate questions not addressed within it. An introductory discussion of the standard model and a description of some of its problems and tests may be found in a companion paper available at this meeting. Here, I will only briefly review some of the most outstanding experiments which define the physics requirements for an AHF.

1.1 Electroweak Experiments

The most outstanding particle physics experiment at an AHF is the search for the decay of a neutral kaon into a muon and an electron. This process does not occur in the standard model unless neutrinos have non-zero masses. From the limits on those masses, the branching ratio for this process relative to normal kaon decay would be less than 10^{-30} at best. The present experimental limit is less than 10^{-8} and there is an experiment currently underway at Brookhaven to reduce this by at least one and possibly three more orders of magnitude. This limit may be interpreted as requiring the mass of a "family-changing" boson to be greater than about $30 \text{ TeV}/c^2$ (see Standard Model paper). Note that this is already beyond the range of new physics directly accessible at the

proposed Superconducting Super Collider. At an AHF, the increased kaon flux, and beam quality allow this process to be searched for down to a branching ratio at the 10^{-13} level, which corresponds to a 500 TeV/c² mass. Once again, the value of a precision experiment is apparent. Although this limit is important, it would of course be even more valuable to discover the process and to be able to study it in detail. Thus, discovery of the process at a larger branching ratio would only enhance the value of an AHF which would provide the means for such study.

Within the standard model, the decay of a charged kaon to a charged pion and two neutrinos is not allowed to lowest order in the weak interaction, but does occur to second order by means of a quantum field theory correction. This process is sensitive to the number of light (mass much less than a kaon) neutrinos, and to details of the quantum field theory corrections. Because of uncertainty in these details, this process is only predicted to occur somewhere in the range between 10^{-10} and 10^{-11} in branching ratio. The current limit is at the 10^{-7} level. An AHF allows the observation of this predicted process and, again, detailed study of the new physics implied if the process is discovered at a larger branching ratio.

Studies of neutral kaon decays are also necessary to elucidate the physical basis for the observed violation of CP-invariance (the combination of charge conjugation, or exchanging particles and antiparticles, and of parity, or mirror reflection). Finally, there are neutrino scattering processes of interest with scattering cross sections as small as 10^{-41} cm², or about 15 orders of magnitude smaller than normally found for the strong interactions. As for the high precision or small branching ratio kaon experiments, these require enormous neutrino fluxes to be available if the experimental detectors are to be of reasonable size and cost. (Producing more kaons in the same volume -- higher brightness --

also obviates the need for larger and more expensive detectors for the work with kaons, too.)

Although some of these kaon experiments are best performed with stopping kaon beams (of momentum less than 1 GeV/c), many require high momentum beams (5-20 GeV/c). This is primarily due to the fact that the decay products are then also at high momentum, and are relatively less disturbed by the material in the detectors which analyze them. When the beam must be purified and momentum analyzed, relativistic time dilatation also helps reduce the contamination due to other particles (especially decay products) and minimizes the loss of kaon flux during that process. Studies at Los Alamos suggest that a 45 GeV/c primary proton beam produces sufficient quantities of these high momentum kaons. For most of the nuclear or strong interaction studies described next, lower momentum kaons would be preferable. However, more of those are also produced by a higher energy proton primary, and there is one particular experiment that demands an even higher energy proton beam.

1.2 Hypernuclear and Other Strong Interaction Experiments

Secondary beams of pions and kaons at an AHF would provide for a broader examination of the spectrum of strongly interacting states than has been made so far using only nucleon and pion beams. Despite decades of effort, the full spectrum of three-quark and of quark-antiquark states has not been experimentally observed. And with the advent of QCD, new exotic states containing extra quark-antiquark pairs or gluons, and states composed solely of gluons, have been predicted. Discovery and detailed study of these states is vital to our deepening understanding of QCD. Dibaryons, especially those containing more than one strange quark, and which are most easily and cleanly formed for better study using kaon beams, may be the first examples of new kinds of hadronic matter intermediate between nuclei and the quark-gluon plasma sought in heavy ion collisions.

Hypernuclei, containing one or more strange quarks, provide an extension along these lines which offers further opportunities to understand the relation between a QCD-inspired quark view of nuclear structure and the more traditional meson-baryon picture. Even in purely traditional terms, continuum states in ordinary nuclei can be shifted into the bound state spectrum of corresponding hypernuclei, allowing for more detailed study and verification of our understanding of the forces in non-strange nuclei. Lower momentum (0.5-2.0 GeV/c) kaon beams are very efficient at producing these hypernuclei by strangeness exchange, as the momentum transfer can be minimized with excess energy being carried off by an outgoing pion; this leaves the resulting hypernucleus in a very low excitation (if not the ground) state.

Due to their relatively small cross-section even at low energies, positively charged kaons also make an excellent probe of the matter distribution of ordinary nuclei in elastic and quasi-elastic scattering. The distortion corrections so difficult to apply for pions are significantly reduced, making the connection between theory and experiment more direct and transparent. Through the so-called Drell-Yan process, however, a higher energy proton primary may provide even more significant information on the (nuclear) medium-induced distortion of the nucleon structure itself.

In the Drell-Yan process, a quark and an antiquark from the beam and target annihilate to form a off-shell photon, which immediately "decays" into a muon and antimuon, or into an electron and positron. It is particularly easy to identify these particles and to measure their momenta. From the kinematics of this final state pair (overall mass and momentum), one can infer the momenta of the initial quark and antiquark involved in the (sub-)scattering. For a 60 GeV/c proton beam, it turns out that the kinematic region is large enough to allow a detailed study of the antiquark probability distribution in the (nuclear) target. (The quark distribution in the incident proton is well-known from high energy, deep-inelastic electron scattering on hydrogen targets.) From

electron scattering experiments on nuclei, it is known that this scattering, even at high energy, cannot simply be represented as a sum of incoherent scatterings on the individual nucleons (isolated in space), a result termed the EMC effect after the European Muon Collaboration which made the experimental discovery. This effect can be described as due to a distortion of the nucleon structure by the nuclear medium. However, experiments have not so far resolved whether this is due to a change of the three-quark structure of the bound nucleon, or due to the formation of additional quark-antiquark pairs (perhaps even correlated into pions). This Drell-Yan experiment offers the cleanest possible test of these conjectures. Such an understanding of the nucleon structure within the nuclear medium is crucial to a QCD-based understanding of nuclear structure, and is an extremely interesting and important question for nuclear physics.

2. PRIMARY AND SECONDARY BEAM REQUIREMENTS

This broad range of exciting physics clearly demands a broad range of primary and secondary beams and beam momenta. Low momentum beams are particularly demanded by hypernuclear studies and "stopped" decays. Low to intermediate momenta are required for meson and baryon spectroscopic studies and for in-flight decays. Finally, the highest momenta are required for Drell-Yan studies of the EMC effect. It turns out that these requirements are not mutually conflicting due to general properties of particle production for secondary beams.

As shown schematically in Fig. 1a, the cost of an accelerator complex such as the AHF is roughly proportional to the total beam power. Thus, at constant cost, one may increase the primary energy only by reducing the beam current. Because the phase space constraints on the number of particles per "bucket" of the radiofrequency accelerating voltages are most severe at the lowest (injection) energy for each step, it is somewhat easier to design a system at lower current. One is then naturally driven to higher energy, lower current machines. However, as

shown in Fig. 1b, both the mean momentum and the flux of secondaries in each momentum bin rises with increasing primary energy; the low momentum secondaries are a smaller fraction, but of a larger total. Thus, one can obtain the desired range from low to high momentum secondaries without cost to the lower momentum flux.

This provides a natural benefit for production of antiprotons which are ultimately desired at low energies. Antiproton production has a similar structure to that shown for any secondary. There is a "knee", or decline in the rate of increase of production, which occurs for a proton primary in the region of 40 to 80 GeV, and a continued increase in the mean antiproton momentum produced. Thus, while total production continues to rise, if these antiprotons are to be deaccelerated after being captured, this will become increasingly difficult and expensive. So fortunately, the general physics demands for an AHF place its primary beam energy in an excellent region for efficient production, collection and deacceleration of antiprotons.

3. SURVEY OF AHF PROPOSALS: THE GENERIC AHF

There have been six areas of the world in which there have been discussions relevant to an AHF. The Japanese are embarked on upgrading the current and energy capabilities of the proton synchrotron at KEK. However, even at 12 GeV energy and 10 μ A current, this is insufficient to be a true "kaon factory". In the Soviet Union, there has been some consideration of an AHF near Moscow, and in Western Europe, there has been a conference/workshop regarding a European Hadron Facility. The sponsoring group of the latter, however, is not associated with any particular laboratory, which may prove a significant drawback to realizing their plans. There have been detailed discussions at Brookhaven regarding increasing the 30 GeV machine current there up to 10 μ A. Unfortunately, an AHF is competitive for machine time with RHIC, which is the stated highest priority of that laboratory. The two most serious efforts have been at the Canadian pion factory, TRIUMF, in Vancouver.

and at LAMPF, in Los Alamos. The Canadian KAON (Kaons, Antiprotons, Other hadron and Neutrinos) proposal is for a 30 GeV, 100 μ A machine, which represents an effective, if relatively low energy, AHF.

The Los Alamos AHF proposal has been through a number of variations in response to efforts to maximize the efficacy of the machine for research in several additional areas (including pulsed muon and neutron beams for material science studies) and to minimize costs in response to budgetary constraints. The original proposal included a 6 GeV booster designed to provide maximum current for a neutrino source, and a 45 GeV main ring, capable of up to 68 μ A average current. Since then, various options considered have included LINAC boosters of up to 2 GeV of kinetic energy, and a coupled 15 and 60 GeV booster and main ring with a 50 μ A current. These energy and current trade-offs reflect the design constraints referred to earlier. (See Fig. 2 for a Los Alamos version of an AHF.)

From the panoply of these proposals and designs, a common theme emerges for a generic AHF: It has a low energy injector, most often a LINAC, which drives a maximum amount of current from a few kiloVolt ion source up to relativistic velocities on the order of 85% of the speed of light. Next comes a booster, which bridges the transition to the fully relativistic regime (99% of the speed of light). This requires the widest range of change in radiofrequency of the accelerating fields, and hence is the most difficult to achieve. Typically, this booster cannot make use of all of the current that can be supplied to it. Next comes a final or main ring which again cannot absorb all of the current supplied. It raises the beam to the final energy of 30 to 60 or more GeV, using only a modest swing in the radiofrequency of the voltage applied to the accelerating cavities. In between these stages may be compressor rings to collect pulses from the lower energy device and manipulate them to enhance the current which can be accepted into the higher energy device. At any stage, but especially at the highest energy, a stretcher

ring may be added to smooth out the extracted current and provide a better duty factor for experiments.

4. THE PRODUCTION OF SECONDARY BEAMS AND OF ANTIPROTONS

There is no reason to suppose that any less efficient use of the primary beam can be made for secondary particle production at an AHF than at lower current accelerators. And, in fact, antiprotons are even a significant contaminant in kaon beam designs. (See Fig. 3.) But just to set the overall scale for antiproton production, let us consider what would occur if the proton beam were simply passed to the beam dump, without encountering any production targets. In a dump, the protons all interact, usually more than once although at rapidly declining energies. Interpolation formulae based on some production measurements (see Hojvat and van Ginneken) suggest that at 60 GeV, about one antiproton is created for every 100 proton interactions. Therefore, in the dump, the 3×10^{14} protons per sec of AHF primary produce more than 3×10^{12} antiprotons per sec. As there are typically 10^7 operating seconds per calendar year at such a research facility, we see that the total production exceeds 10^{19} and may approach 10^{20} antiprotons per year.

The formation of secondary beams at an AHF is shown schematically in Fig. 4. Following the example of LAMPF, the extracted beam is transported to a sequence of production targets, each of one interaction length or less. This is a compromise between getting the primary protons to interact, and getting the secondaries out of the target without excessive absorption losses. A short target also reduces optics problems in the secondary beam lines. With appropriate design, both neutral and charged (either sign) secondaries may be derived from any target station. Since a sizeable fraction of the scattering is elastic or quasi-elastic, there is still significant beam power at the dump, although it is relatively diffuse. (See Figs. 5 and 6 for typical target and target station/secondary beam extraction line designs.)

One of the problems of targetry is the power dissipation level in the production targets. LAMPF has considerable experience with targets involving beam powers only a factor of 3 to 5 lower than the ~1 MW total anticipated for an AHF. Thus, while difficulties, even severe ones, are to be expected, insurmountable problems are not. One of the advantages of a higher current machine over one at higher energy shows up here: phase space limitations require that the current be raised by increasing the frequency of accelerating "buckets" with the same number of particles per bucket. (These buckets are 25% full in the conservative designs originating from Los Alamos.) Thus, the thermal shocks to the target are increased in frequency, rather than in magnitude, and the problem can be limited to one more of cooling rate than of structural damage, as has been found in the production targets at Fermilab and at CERN.

The peak instantaneous target loading at the Los Alamos AHF is of order 5×10^{13} protons over 4 μ sec at up to 60 GeV, compared to a similar number at CERN delivered over half the time interval at about half the energy. The Fermilab current is an order of magnitude smaller than at CERN, but at up to six times the proton energy. These currents deposit a great deal of energy "instantaneously" in the beam spot region, and heat this region to within a factor of two of melting temperatures, for the typical W or Cu targets used. Nonetheless, the average target temperature can be well below 1000°C.

The beam-induced shock tends to crack and powder high yield strength materials such as W. (A strong cladding, such as Ti, is provided to maintain structural integrity. Using a lower strength material with a larger region of plastic yield, such as Cu, results in voids (presumably from gas produced in the target) over periods on the order of months. Both of these effects reduce target density and so antiproton yield. Thus, the higher currents at an AHF raise serious questions regarding useful target lifetimes (greater than a day?). At present, target design is inhibited by a lack of knowledge regarding the

equation of state of materials under high stress in the plastic deformation region. Los Alamos is in a position to remedy this, as our Dynamic Testing Division presently pursues just such studies for nuclear materials, among others, using high-explosive driven shocks.

There may be interesting possibilities to study in the area of throwaway targets, such a liquids, or moving wires or ribbons¹, (both of which require containing highly radioactive wastes), as well as beam-on-target management techniques such as "painting" Lissajous patterns, while similarly adjusting the collector acceptance, or focusing the beam into a ribbon structure. (The beam-sweeping techniques are sure to work, but may be very expensive.) As a last resort, target lengths (currently 5-10 cm) can be shortened, and the number increased. This reduces the load faster than the length is reduced as electromagnetic energy can escape more efficiently before the showers are fully developed. (Again, depth-of-field problems in the secondary beam-line optics are also ameliorated.) One is limited in doing this in the transverse direction by the requirement that the difference δ , between target and beam sizes satisfy

$$\delta > \nu t \quad (1)$$

where ν is the speed of sound in the target and t is the pulse length of the incident beam.

The peak power on target at CERN is currently 2-3 times that of Fermilab, and another similar factor of increase can be reasonably foreseen, even without sweeping, etc. techniques. Similarly, the total energy deposition is approaching, (at least with Cu targets), but has not reached the nominal 200 J/gm limit. Thus, it seems quite likely

¹ Krienen and Mills have suggested that there are advantages to moving the target material at greater than the shock velocity.

that targets will not limit antiproton production at an AHF. The biggest question for the long term, however, is whether target design can help improve collection efficiencies. At present, Lithium lenses are used to focus the antiprotons onto the acceptance of a collector. Can these cycle faster? And can their focusing be improved by integration with the target? Unfortunately, their currents will increase the target heating significantly.

5. COLLECTION AND COOLING

What would it take to collect an appreciable fraction of the enormous available production? Note first that the sequential target design of an AHF naturally means that even a target station dedicated to studying this question would not significantly interfere with the main scientific goals of the AHF. At any point, collectors/decelerators followed by coolers and "bottlers" could be added (see Fig. 7), perhaps even at the beam dump itself. The second thing to notice about collecting and cooling the antiprotons produced at an AHF is that the secondary flux is still negligible in beam current. The product of the production and collection efficiencies is such that less than one antiproton appears in the collector for every $10^{5\pm1}$ primary protons. Thus, one does not have to worry about any beam loading type problems -- only the wretched phase space occupied by the antiproton secondaries. The size and scale of current collectors is adequate to accept and handle a significantly larger number of antiprotons.

Thirdly, notice that the antiproton source brightness is about two orders of magnitude greater at an AHF than at Fermilab, one from the number of particles per bucket and one from the increased cycling rate. Thus, whatever lenses/collection efficiencies are available, now or in the future, an AHF would seem to guarantee an immediate factor of 100 improvement in the number collected. Actually, there is only one caveat here. The best Fermilab collector design makes use of a phase space

rotation to accept a large momentum bite of antiprotons and convert it to a small width momentum distribution in the collector. To make use of the increased brightness, this procedure must also be capable of cycling ten times faster.

Of course, in the future, one would also like to increase the collection efficiency. This requires larger acceptances in the transverse and longitudinal antiproton momenta. Fig. 8 shows the longitudinal momentum spectrum of antiprotons produced by 45, 60 and 80 GeV protons on a tungsten target, calculated using formulae fit to actual production data. (See again the work of Hojvat and Van Ginneken.) It is distressingly wide, and the effort at Fermilab has already been very clever about making maximum use of it. However, there is still over an order of magnitude to be had. Will it be by clever lens design? Is it even possible to use this additional flux unimaginatively by directing the rings of incompletely focused higher momentum antiprotons into parallel collectors?

On the other hand, the transverse momentum distribution has a Gaussian fall-off with a 1 GeV/c scale, as might be expected from dimensional arguments in QCD. Thus, there is not a particularly wide angular spread of the antiprotons near the momentum peak. (This feature is worse at a lower energy AHF, such as the TRIUMF proposal.) As a result, increasing the angular aperture of collectors will not be very cost effective, although as much as a factor of five improvement may still be available over current designs. This is also related to the question of lens design since an appropriate angularly dependent chromatic aberration can add at least high momentum particles into the region of acceptance.

Stuffing two to four orders of magnitude more of antiprotons into a collection system will do us no good, however, unless we can cool them at correspondingly higher rates. There does not seem to be much more ($\times 10$) rate available with currently employed stochastic cooling, due to

bandwidth and frequency limitations. Stochastic cooling times (τ) are proportional to the number of particles (N) to be cooled and inversely proportional to the bandwidth (Δf) of the kicker/amplifier system:

$$\tau \propto \frac{N}{\Delta f} \quad (2)$$

The amplifiers/bandwidths currently used are in the several GHz range. Thanks to radioastronomy, amplifiers up to 80 GHz already exist, but large bandwidths have yet to be demonstrated.

Even if tens of GHz bandwidths are achieved soon, this is just enough to make use of one factor of 10 increase in brightness of the antiproton source at an AHF. If the full brightness is realized, or if either of the additional two orders of magnitude of angular and longitudinal momentum collection efficiency available are realized, even higher frequencies will be required. Although such amplifiers appear quite plausible, here we do seem to run into a fundamental limitation, as wavelengths smaller than the beam size can be of no use. For typical mm beams sizes, this means a 1 THz limit or less, unless one can arrange to focus the beam to a smaller size in the pickup and kicker regions. Thus, we must also consider other cooling mechanisms.

Antiprotons are too massive for significant radiation cooling, even at much higher magnetic fields (which may be achievable with the new high temperature superconductors, eventually). This leaves only electron and ionization cooling. The latter involves passing a widely dispersed antiproton beam through a material which absorbs energy by being ionized, and then re-accelerating the antiprotons to recover the longitudinal energy loss. In the EHF proposal, it is argued that this leads to unacceptably high annihilation losses while the antiprotons traverse the material. (This incidentally argues against the otherwise ingenious idea of D. Cline to solve the target, solid angle and cooling problems at one stroke by using colliding beams, a 4π solenoidal magnetic collecting field aligned with the beams, and a gas in the magnetic field volume to collisionally slow the antiprotons. This idea also

faced a question of overall rate, due to the notoriously low luminosity of colliding beams.) This leaves us with the prospect of producing large currents of 3 to 4 MeV electron beams running parallel to the antiprotons, since their cooling effect is best at low relative velocities. Obviously, much innovative research remains to be done.

Lenses, collectors, coolers -- all of these features are clearly very expensive add-ons to the AHF, as it has so far only been envisaged to produce higher-energy antiprotons for research purposes. This has been partly due to the extra cost for collecting/cooling/decelerating, but also partly due to the perception that LEAR (and possibly Fermilab) would provide much of the low-energy antiprotons needed for that research well before turn-on of the AHF. Thus, R&D for increasing the supply of low-energy antiprotons must be viewed as a significant additional cost at an AHF, even though it should cause only minimal interference with the basic research program.

It is difficult to seriously imagine today how to make use of the entirety of the antiproton production available at an AHF, other than by multiplexing targets, collectors and coolers. However, the cooling/collection rates achieved at Fermilab and at CERN are some four orders of magnitude smaller than needed. Given their scale of size and costs, the multiplexing of collectors and coolers is only an existence proof of little comfort and less imagination. On the other hand, this makes the AHF an attractive place to study the problem of increasing the collection: With the antiprotons right there for the taking, there is a powerful incentive for thinking up a good way to get them.

6. PROGRESS TOWARDS AN AHF

There has already been much progress on technical elements of an AHF, around the world. I will mention only two particular items developed at Los Alamos which I find particularly interesting.

The first of these is the beam pipe itself. The high beam current produces eddy current heating in a conducting beam pipe, in addition to the eddy-current magnetic field distortion due to the rapid-cycling magnetic fields. The Los Alamos solution (see Fig. 9) is a ceramic (alumina) beam pipe with transverse and longitudinal strips of metallization separated by insulating layers, and a thin, vapor deposited interior metal coating (≈ 1000 Angstroms of Ni). This reduces the eddy currents, while still providing low impedance paths to avoid the buildup of static charge and to provide for high-frequency image charges needed for beam stability.

The second is the nature of the accelerating cavities in the intermediate booster. These require a wide tuning range because of the significant change in velocity, but also high efficiency to provide the power demanded by the heavy beam loading. These seemingly contradictory demands have been satisfied by changing the cavity tuning design from the standard parallel-biased ferrites (bias magnetic field parallel to the RF magnetic field) to a perpendicular bias design (see Fig. 10). Test cavities have demonstrated Q's in excess of 2000 over a 25% tuning range from 60 to 80 MHz, (see Fig. 11) which is more than sufficient. The cavity was tested to breakdown, which occurred at 140 kV, well above the 80 kV design limit. It is apparent that every "kaon factory" built will use cavities of similar design.

On the political front, an AHF is beginning to get more attention, also. After some consultation with the community, the Nuclear Science Advisory Committee (NSAC) developed a long range plan (in 1983) calling for an intermediate energy high duty factor electron accelerator, which is embodied in CEBAF currently under construction, a high energy heavy ion collider, which is embodied by RHIC which is awaiting construction funds, and finally a kaon factory, or AHF. At a Washington luncheon this spring, D. Allan Bromley of Yale noted that with the first two elements of the plan falling into line, it was becoming time to seriously consider proposals for an AHF to be available in the late

1990's. (A new IUPAP committee has also been formed to consider the building of a kaon factory.) Indeed, the proposal from TRIUMF has already cleared several important hurdles in Canada, including lining up a significant fraction of the required funding. The remaining question seems to be whether Canada, a country which has traditionally funded science at a lower level than in the United States, wishes to undertake science funding at a level in their economy comparable that of the SSC here.

7. BEYOND THE AHF

Without any improvements in target engineering or in cooling rates, an AHF will do no better than Fermilab at producing antiprotons. However, it will be able to do so with a tiny fraction of its total current. If only cooling rates can be improved (as seems possible at least with a combination of stochastic and electron cooling), then with Fermilab collection efficiencies an AHF could provide up to 10^{17} antiprotons per year. And over a ten or twenty year period, up to two orders of magnitude increase in the collection efficiency may be realizable. Thus, an AHF offers the prospect, over its research lifetime, of a total of four orders of magnitude increase in antiproton supply over that envisioned at the LEF. Can we imagine going even further?

I have noted that there is a serious problem in collecting and cooling antiprotons as well as producing them at large rates, but I believe these problems can be solved when large, "hot" supplies are available on which to test out appropriate ideas. So the question becomes one of the intensity limits for intermediate energy accelerators of the primary protons. To go further in this area probably requires that we turn away from synchrotrons and return to linacs. These are intrinsically high current devices (10 mA?, 1A? -- even higher currents have been proposed at lower energies), heretofore limited by the cost of input power. For instance, with further improvements in superconducting

accelerating cavities, a linac only an order of magnitude larger than LAMPF (≈ 1 km) could reach the appropriate energies for efficient antiproton production. With focusing quadrupoles interspersed between accelerating cavities, even higher currents should also be achievable. Thus, again apart from the questions of how to collect and cool them, we can already imagine, before an AHF, that successors to it could be built which would produce fractions of a gram per year of antiprotons.

8. CONCLUSION

An Advanced Hadron Facility has a strong science justification. There are also some scientific reasons for stretching its energy to the higher values more suitable for efficient antiproton production, collection and deceleration to rest. It will produce significantly large quantities of antiprotons per year, but significant expenditures will be required in add-ons to capture only a very small fraction of this production. New collection/cooling ideas are needed to fully utilize the output that will be available.

Nonetheless, the intermediate prospect is for tens of μg of antiprotons per year to become available at an AHF. Lest this strike you as fantastical, let me point out that significant amounts of antiparticles are already being produced and used for engineering convenience! For example, in the March 1987 issue of the CERN Courier, the 7 GeV Advanced Photon Source at Argonne National Lab was described. An earlier stored electron beam light source at Wisconsin (Aladin) had had significant difficulties maintaining long beam lifetimes due to positive ions from residual gas being attracted into the beam. Heroic efforts at cleaning the beam pipe and improving the vacuum were required to solve the problem. The group at Argonne found it more convenient to produce, collect, and store positrons, since in this case residual positive ions would be repelled from the stored beam. In some respects, the difference in problems is simply a matter of scale. And it will take some time to gain the factor of 2000 between electron-positron pair threshold

and that for antiprotons. But perhaps it is indeed only a matter of time.

I am glad to thank R. D. Carlini, D. Grisham, and H. A. Thiessen of Los Alamos, and J. Dugan, J. Griffin, and J. Mariner of Fermilab for valuable conversations.

9. REFERENCES

C. Hojvat and A. Van Ginneken, Nucl. Instr. Meth. 206, 67 (1983).

Proposal for a European Hadron Facility, ed. by J. F. Crawford (SIN, Villigen, Switzerland), EHF-87-18 (May 1987).

Physics and Plan for a 45 GeV Facility, Los Alamos manuscript LA-10720-MS, May 1986.

LAMPF-II Proposal, Los Alamos preprint, LA-UR-84-3982 (Dec. 1984).

A Long-Range Plan for Nuclear Science, DOE/NSF Nuclear Science Advisory Committee, J. P. Schiffer, Chairman (Dec. 1983).

Proceedings of the 3rd LAMPF-II Workshop, Los Alamos, LA-9933-C (2 Vols.), July 1983, ed. by J. C. Allred, T. S. Bhatia, Kit Ruminer and Beverly Talley.

Physics with LAMPF-II, Los Alamos proposal, LA-9798-P, June 1983.

Proceedings of the 2nd LAMPF-II Workshop, Los Alamos LA-9572-C (2 Vols.) July 1982, ed. by H. A. Thiessen, T. S. Bhatia, R. D. Carlini and N. Hintz.

Intense Medium Energy Sources of Strangeness, (UC-Santa Cruz, 1983) AIP Conf. Proc. No. 102, Particles and Fields Subseries No. 31 (AIP, N.Y., 1983), ed. by T. Goldman, H. E. Haber and H.F.-W. Sadrozinski.

Proceedings of the Workshop on Nuclear and Particle Physics at Energies Up to 31 GeV: New and Future Aspects, Los Alamos LA-8775-C (Jan. 1981), ed. by J. D. Bowman, L. S. Kisslinger and R. R. Silbar.

FIGURE CAPTIONS

Figure 1. a) Beam current vs. beam energy at constant beam power. Costs increase with increasing beam power. b) Flux of secondaries at fixed secondary momentum and (same curve) mean momentum of secondaries from a production target vs. beam energy.

Figure 2. A recent Los Alamos design for an Advanced Hadron Facility based on LAMPF as an injector.

Figure 3. Antiproton contamination in kaon beamlines at a 45 GeV AHF. These are rates at the end of the secondary beams for 34 μ A of extracted proton beam, including absorption of both primaries and secondaries in the targets and decay in the secondary beam transport. Targets 1 and 2 are assumed to be 5 and 10 cm of tungsten, respectively. The dashed curves are for the available solid-angle of the channel when separators are used and the solid curves are for the maximum solid angle without separators.

Figure 4. Schematic layout of production targets and secondary beams at a generic AHF. Magnetic separation of charged secondary beams is indicated at each target station, as are beam focusing quadrupoles between stations.

Figure 5. Possible design for rotating production target for an AHF.

Figure 6. Typical target station/secondary beam extraction design at an AHF. Extraction from a) target 1 and b) target 2): Q = quadrupole, HQ = half-quadrupole, Q8 = narrow quadrupole, BH = H-type bending magnet, BWF = window frame-type bending magnet, 6P = sextupole.

Figure 7. Antiproton collector/cooler test designs could be added to an AHF at any production target, or a dedicated target station could be used, both without interfering with other research.

Figure 8. Differential cross section for antiproton production on tungsten vs. produced antiproton momentum at zero degrees per differential unit (DW) of solid angle: a) On log scale at 60 GeV primary proton energy. b) On linear scale at 60 GeV primary proton energy. c) On log scale at 45 GeV primary proton energy. d) On log scale at 80 GeV primary proton energy.

Figure 9. Construction of eddy-current resistant vacuum beam pipe for proposed Los Alamos AHF.

Figure 10. Los Alamos design for perpendicularly biased RF accelerating structures for an AHF. Except for the power tetrode region, the structure is a figure of revolution about the beam axis.

Figure 11. The variation of a test cavity Q with frequency. The upper curve (Q_T) is the calculated Q of the cavity, assuming that the ferrite samples are lossless and that the only loss is due to the resistivity of the metal cavity walls. The two G26 curves were obtained with type G26 Mg-Mn-Al ferrite toroids manufactured by TDK. The upper curve was obtained with perpendicular bias applied to the ferrite, while the lower curve shows the cavity Q when it is tuned in the conventional manner with parallel bias. The Y1 curve was obtained with type Y1 aluminum-doped yttrium-iron-garnet ferrite (also manufactured by TDK Electronics Co., Ltd).

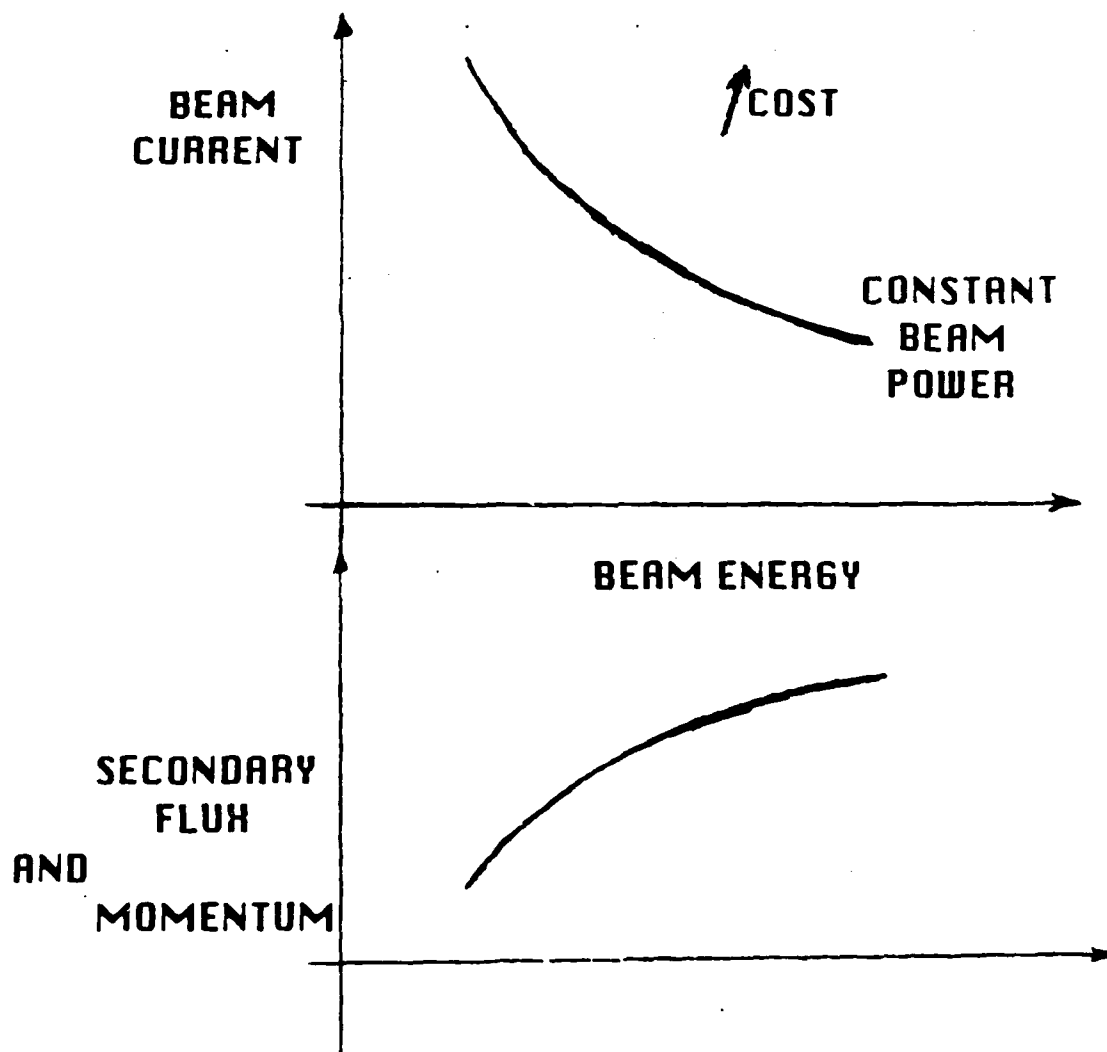


FIGURE 1

60 GeV Main Ring
15 GeV Booster

Area N
Neutrons
& Neutrinos

2 GeV Compressor

1.2 GeV
Superconducting
Linac

ADVANCED
HADRON FACILITY
AUGUST 1986

Area A

FIGURE 2

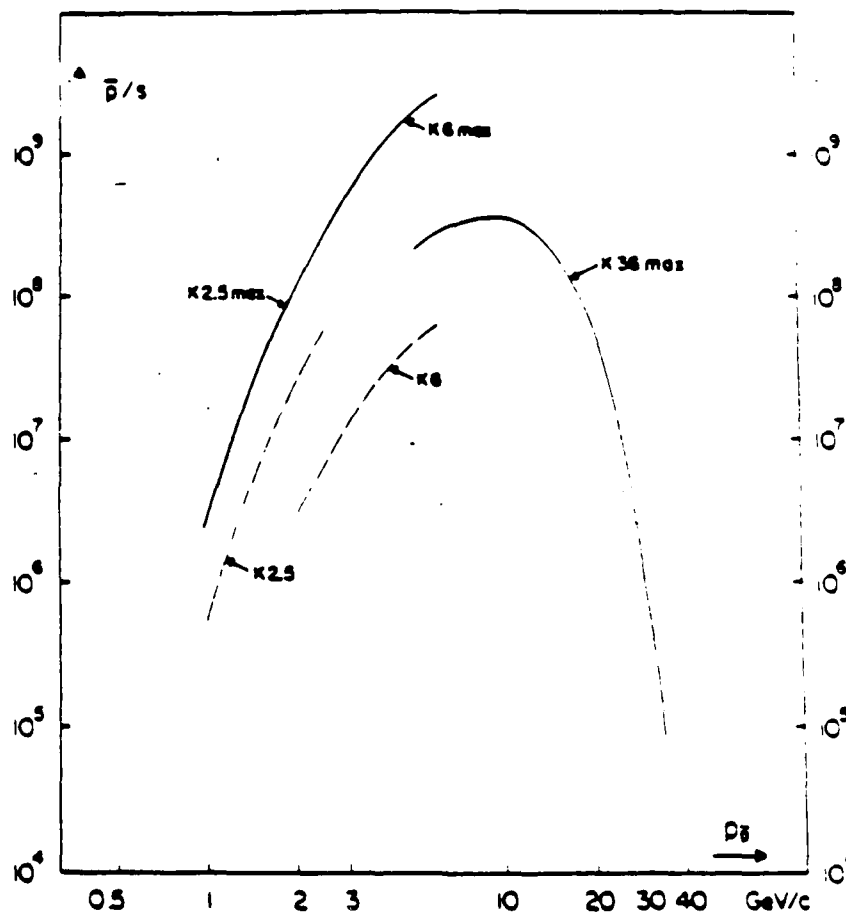


FIGURE 3

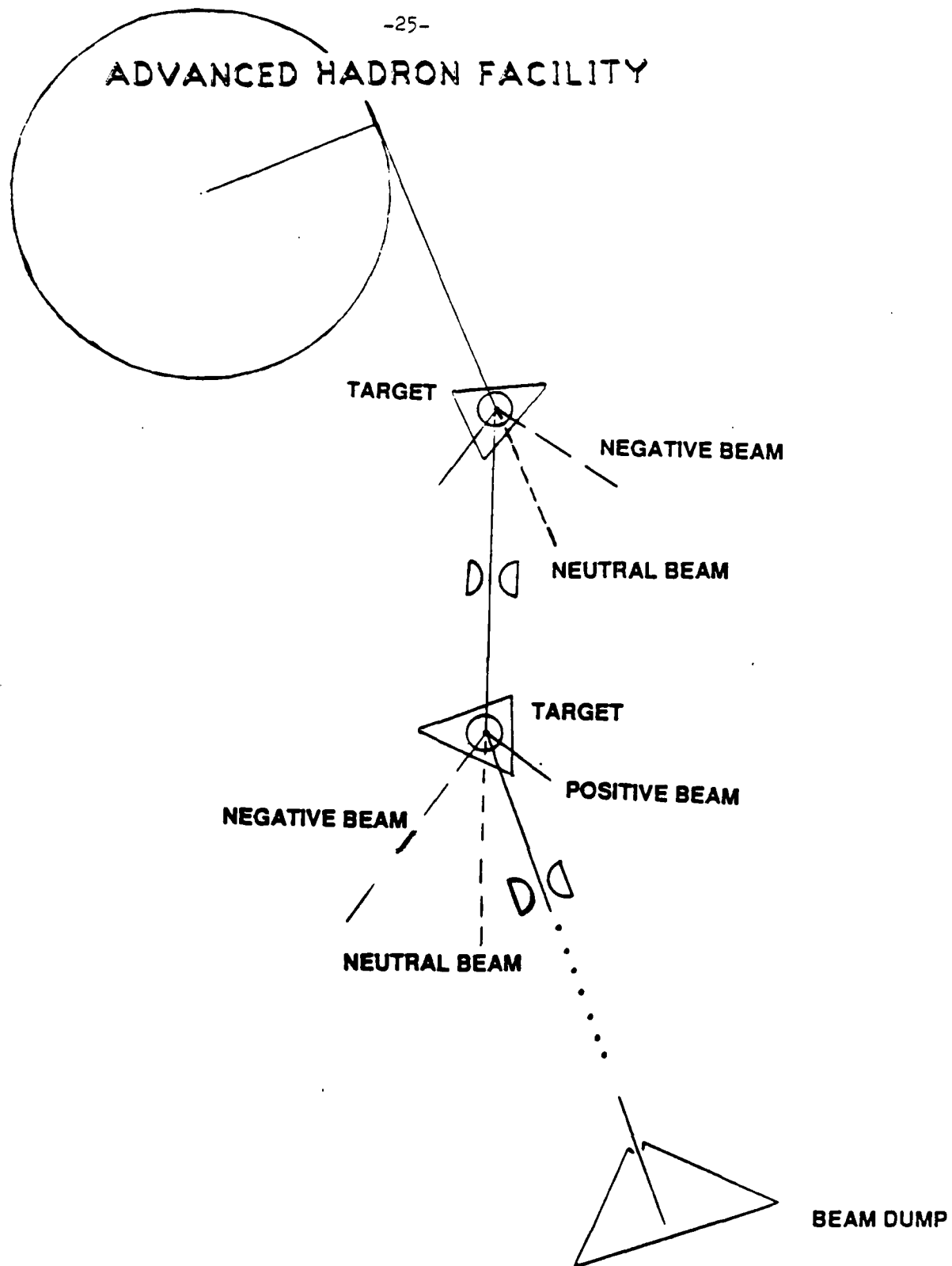


FIGURE 4

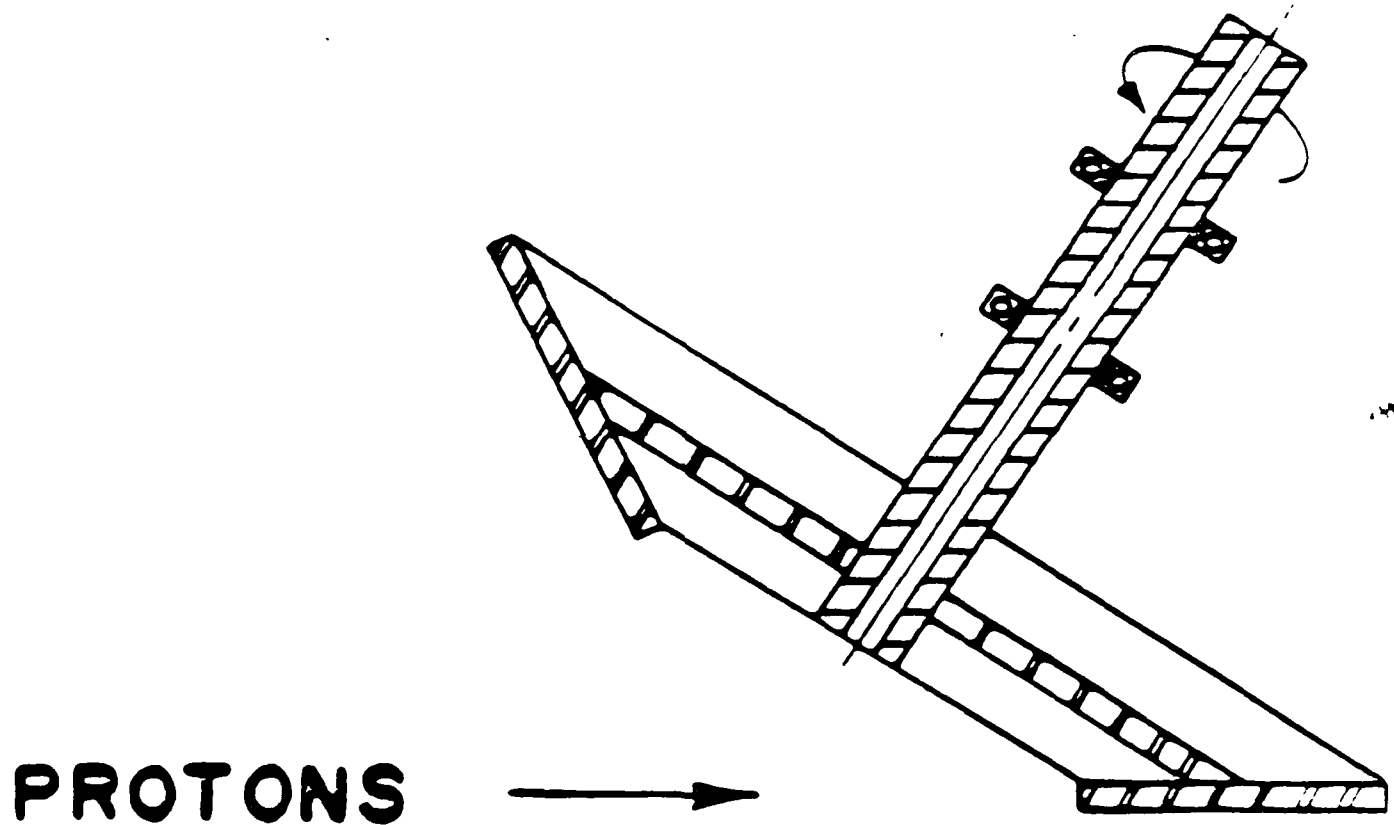
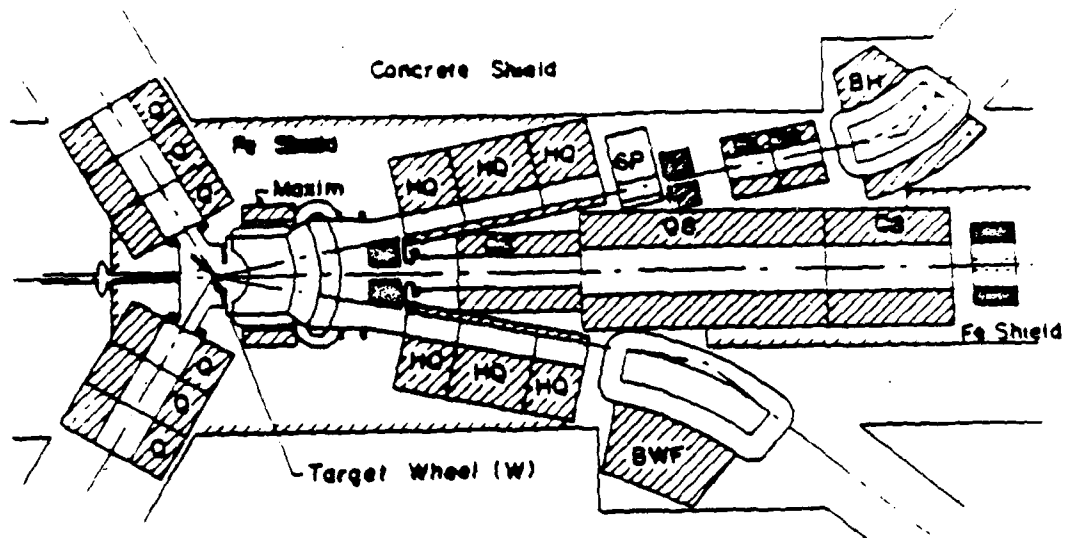
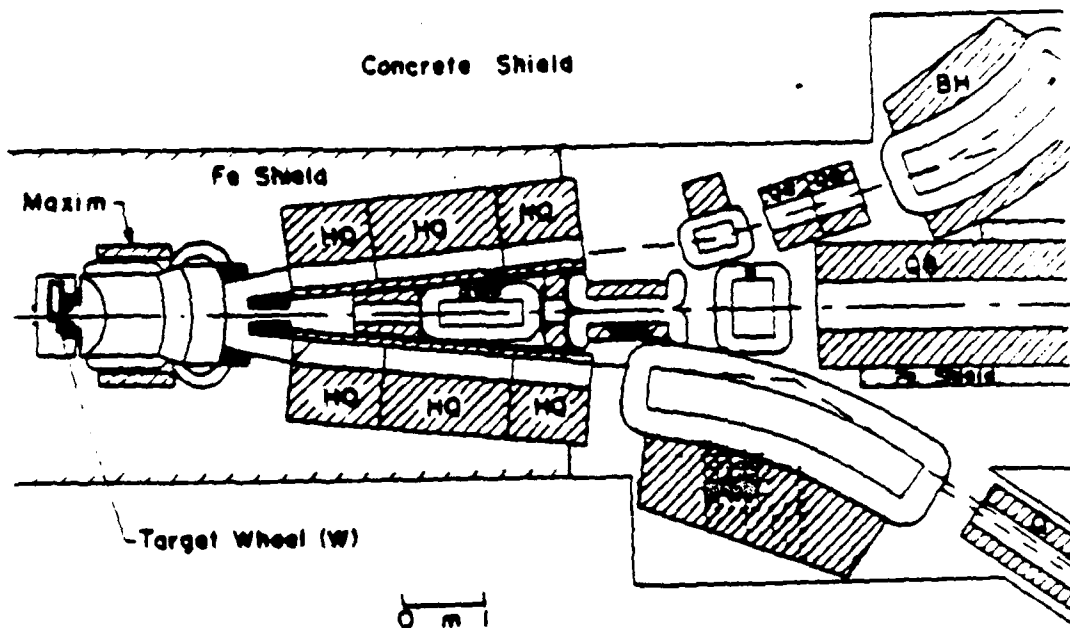


FIGURE 5



(a)



(b)

FIGURE 6

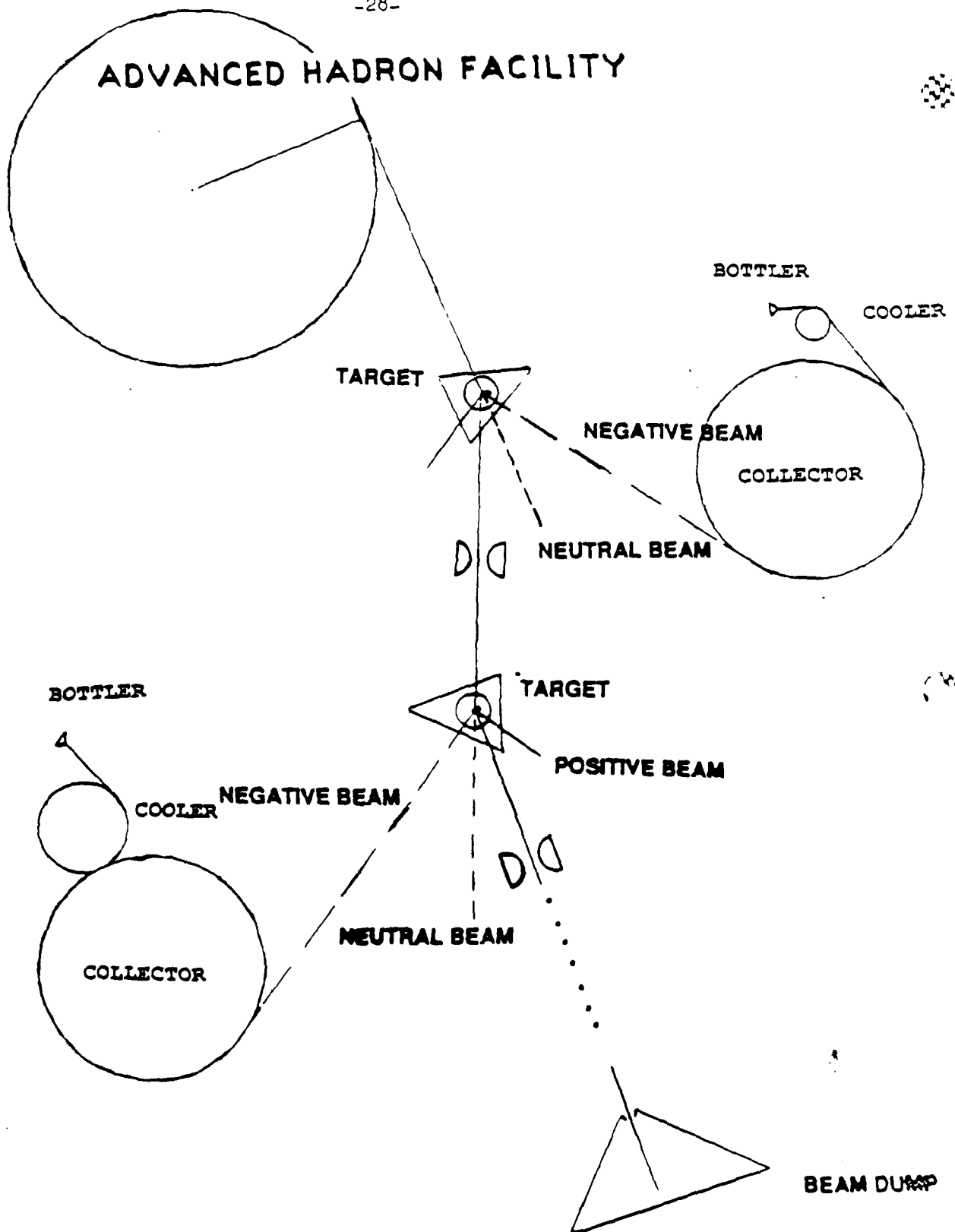


FIGURE 7

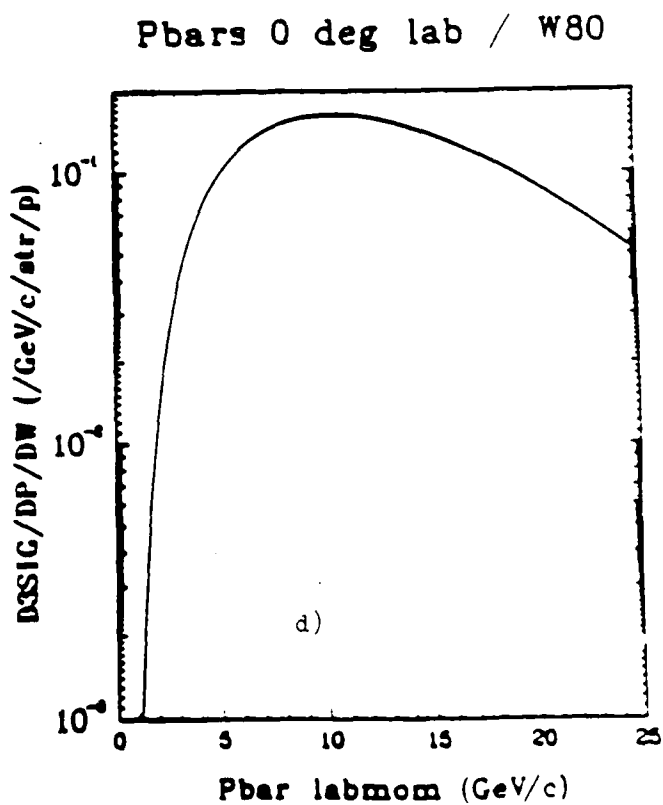
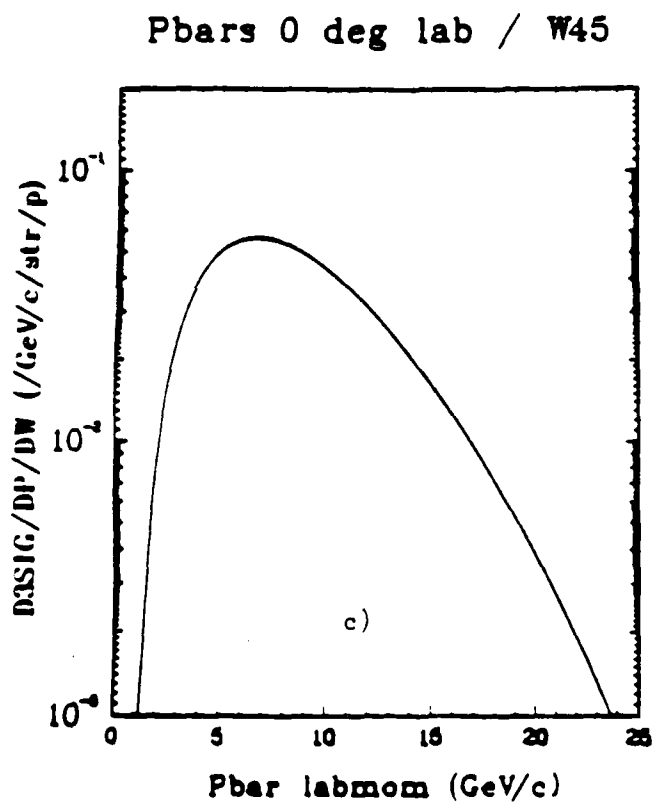
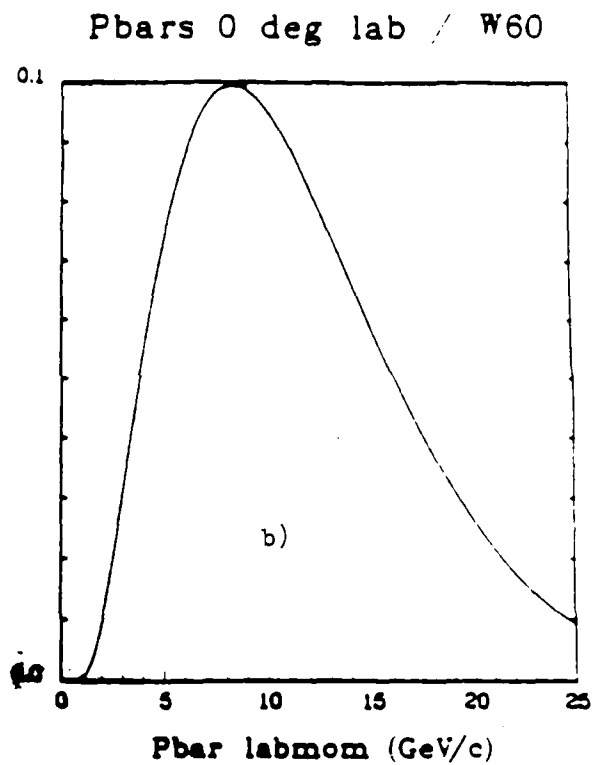
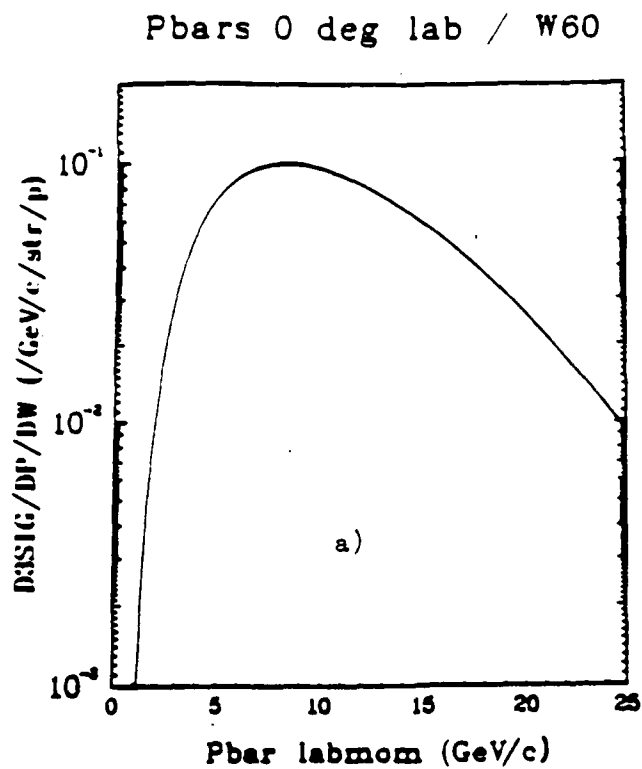
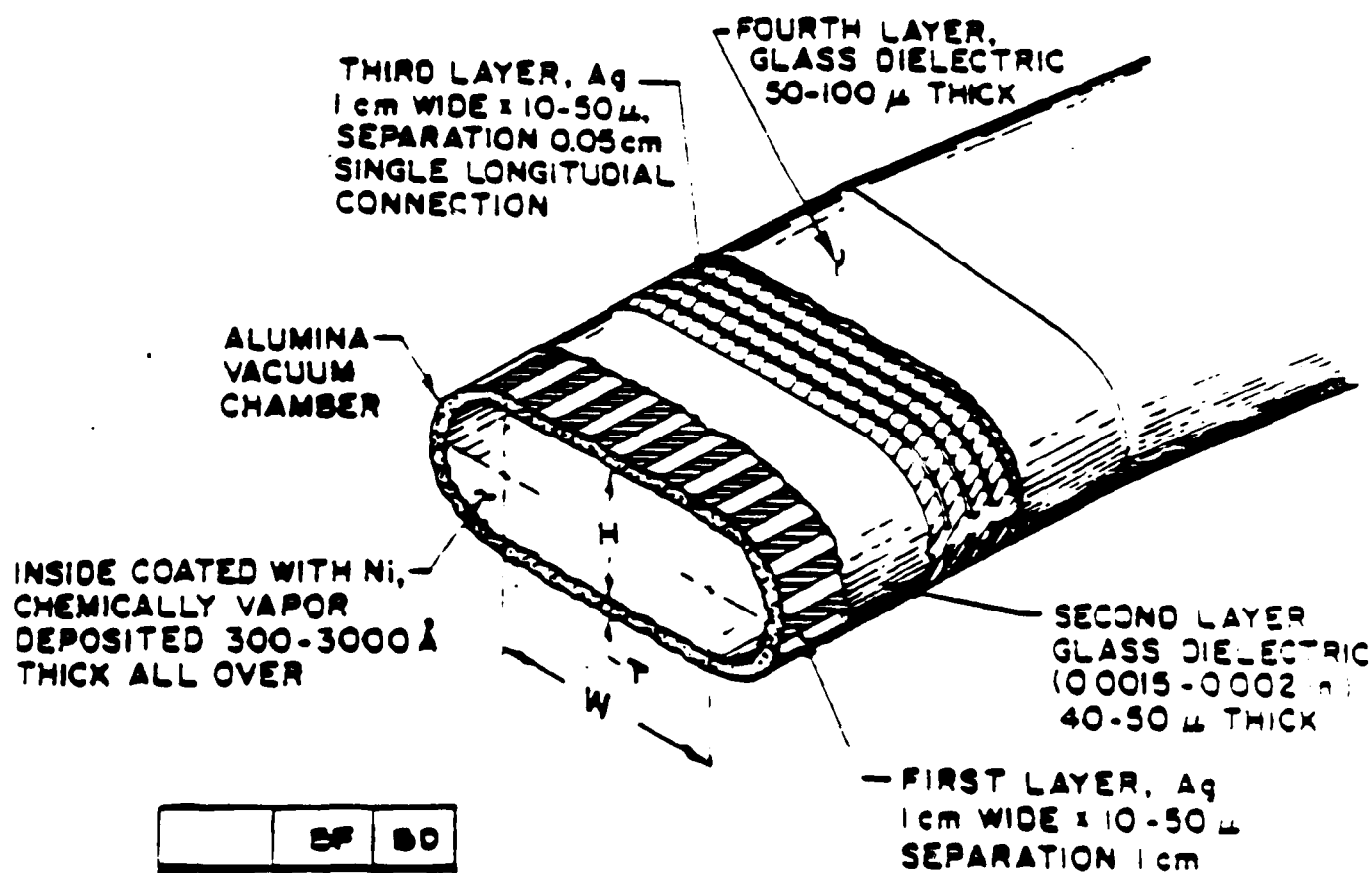


FIGURE 8



	BF	BO
H	4.5	7
W	13	7
T	0.5	0.3

ALL CM.

FIGURE 9

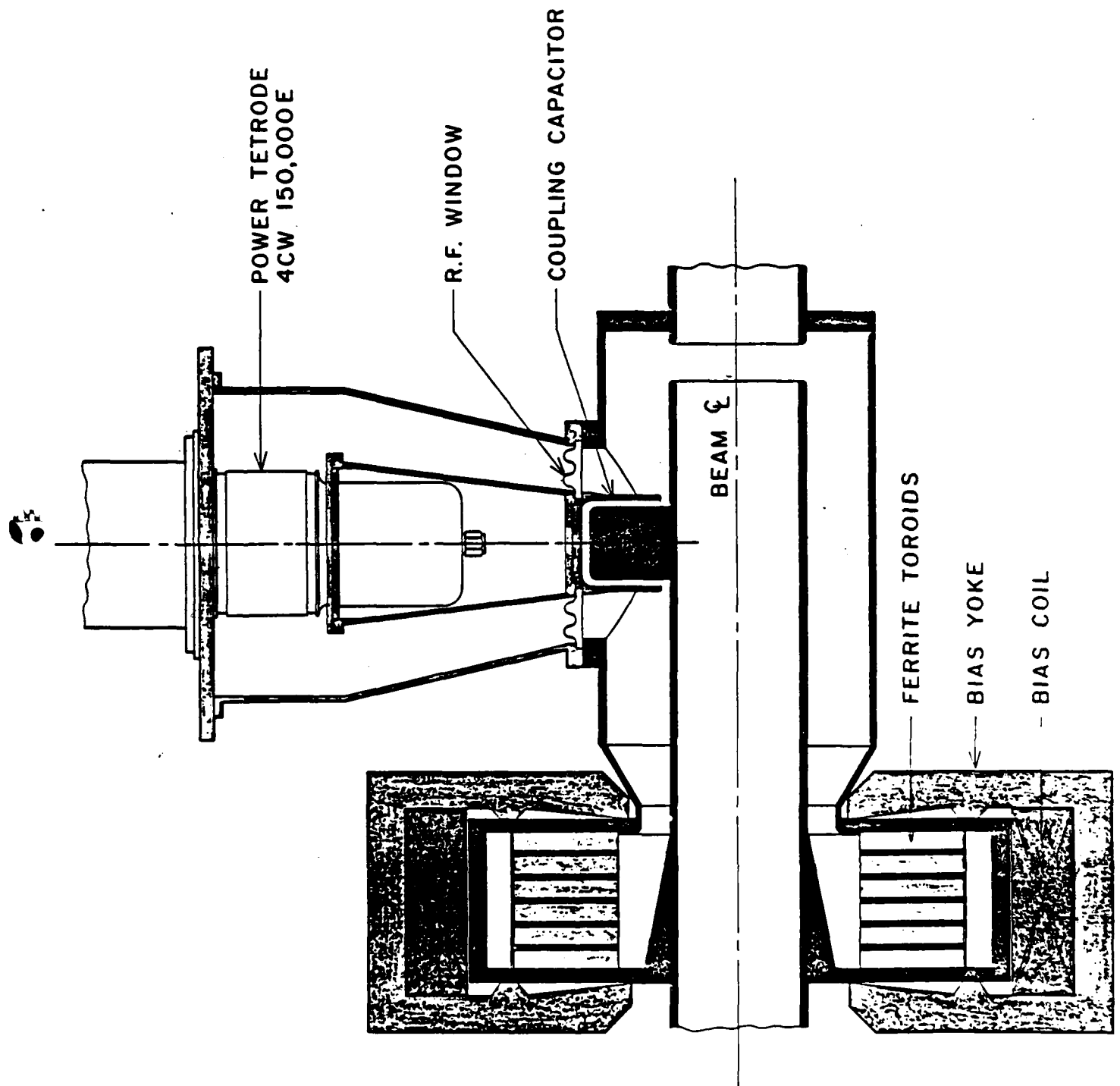


FIGURE 10

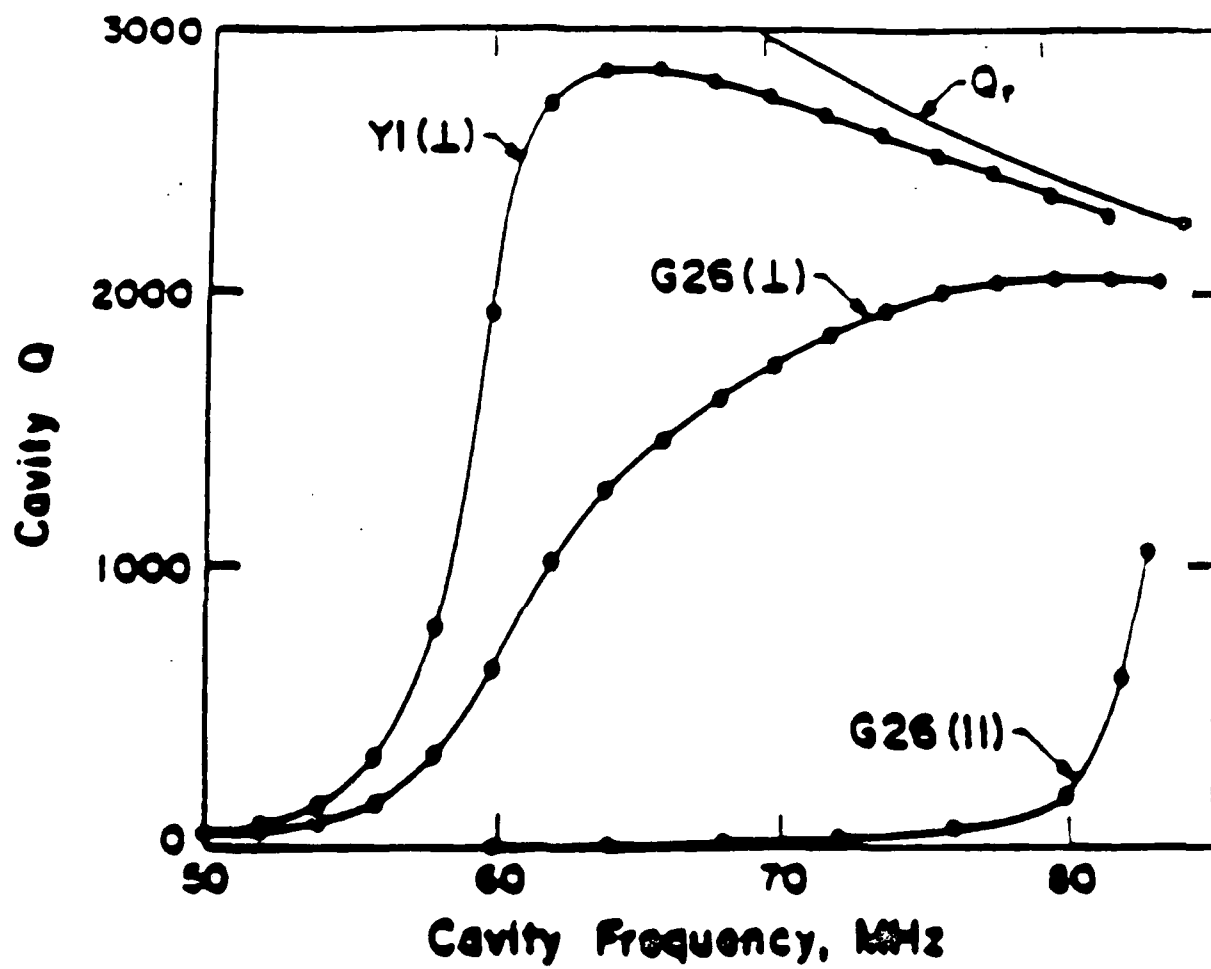


FIGURE 11

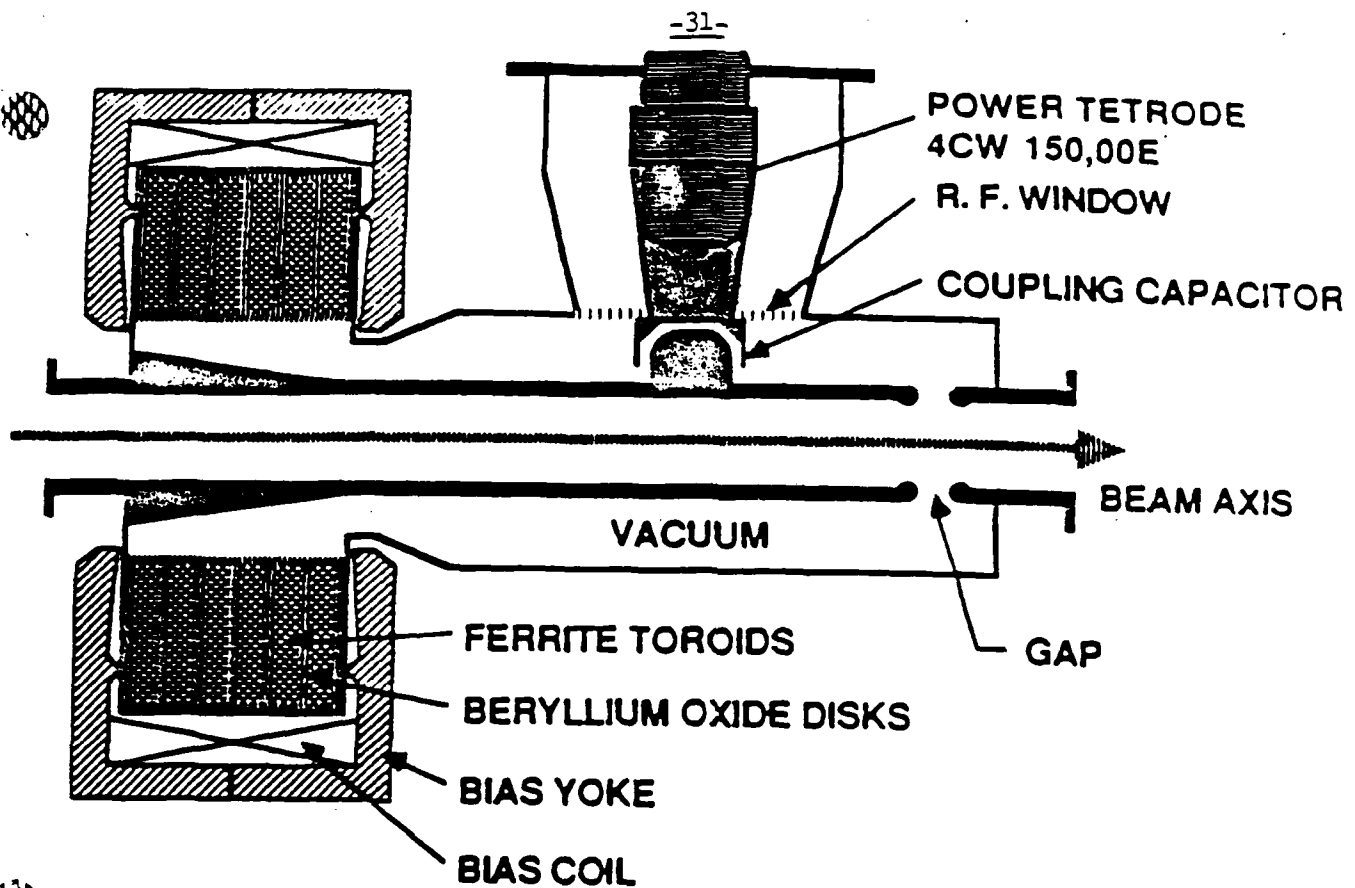


FIGURE 10

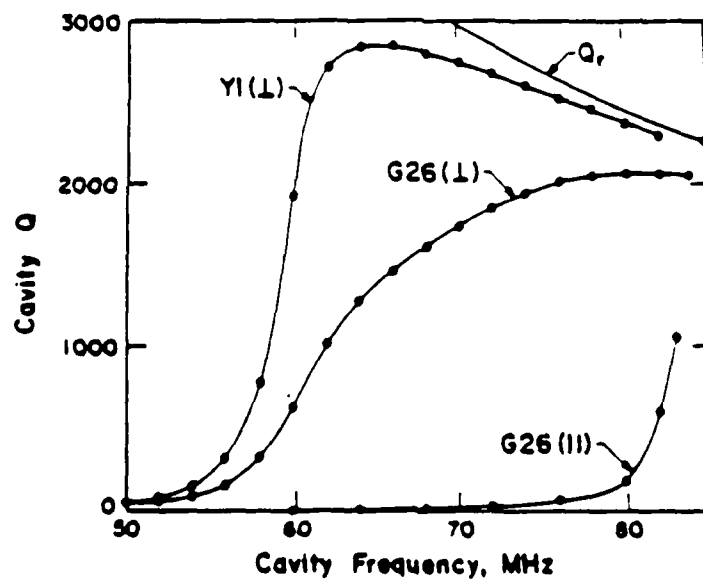


FIGURE 11

Paper presented at the RAND workshop on
Antiproton Science and Technology

THE TRIUMF KAON FACTORY PROPOSAL

E. W. Blackmore

TRIUMF, 4004 Wesbrook Mall, Vancouver, B.C., Canada V6T 2A3

Abstract

The TRIUMF KAON factory will provide 30 GeV protons with an intensity of 100 μ A, more than 80 times greater than that available at present in this energy range, and will be capable of producing correspondingly more intense beams of secondary particles, particularly kaons, antiprotons and neutrinos. The proposed accelerator consists of a chain of two rapid-cycling synchrotrons and three storage rings and uses as the injector the present 500 MeV TRIUMF H⁻ cyclotron. The system of accelerators, the proposed experimental areas and the current status of the proposal are described. Some comments on the use of the KAON factory as an antiproton source are included.

ACCELERATOR SYSTEMS

The KAON factory accelerator is based on a rapid-cycling (10 Hz) 30 GeV proton synchrotron. The fast cycling rate keeps the charge per pulse down to 10 μ C (6×10^{13}) protons and restricts the time available for instabilities to develop. The existing 30 GeV synchrotrons (see Table I), the Brookhaven AGS and CERN PS, are limited in beam intensity both by their low cycling rates (< 1 Hz) and by their low injection energies (< 200 MeV into the first synchrotron stages). The injection energy is crucial because space charge forces near

injection reduce the transverse focusing strength and the charge per pulse which can be accelerated for a given tune shift scales as $\beta^2\gamma^3$. To achieve the 10 μC charge per pulse specified for the KAON factory an injection energy of at least 400 MeV is required. The TRIUMF cyclotron is capable of accelerating H^- beams to energies of 520 MeV and currents in excess of 200 μA . The present extraction by foil stripping provides simultaneously up to three beams of variable energy and intensity to two experimental areas.

The main problem of using the cyclotron as an injector into a synchrotron is how to match this cw machine, which provides a continuous stream of beam bunches at 23 MHz, with a 10 Hz synchrotron accelerating 3 μs long pulses every 100 ms. This is accomplished by first extracting the beam from the cyclotron as H^- ions so that injection into the first synchrotron stage can occur by the stripping process, a standard technique now used in most high current synchrotrons. This process circumvents Liouville's theorem on phase space conservation allowing many thousands of turns to be collected in a reasonable phase space for subsequent accumulation and acceleration. Extraction of a small emittance beam of H^- ions at 440 MeV has already been demonstrated in tests on the TRIUMF cyclotron.¹

The rapid-cycling rate of the synchrotron puts severe demands on the rf system as a high energy gain per turn is required necessitating high rf voltages. In addition the large frequency swing, which amounts to a factor 1.37 from 440 MeV to 30 GeV, poses an additional problem. The solution is to decouple the problems of frequency swing and high rf voltage by providing an intermediate Booster synchrotron of 3 GeV and with a circumference one-fifth that of the main synchro-

tron. The choice of 3 GeV for the Booster energy is based mainly on cost optimization.² There is a further ease in the demands on the rf system by using an asymmetric magnet cycle on each synchrotron with the rise time 3 times longer than the fall. The requirement for a flat-bottom or flat-top on the magnet cycle for multi-turn injection or slow extraction is avoided by using three relatively inexpensive dc storage rings. The proposed arrangement as shown in Fig. 1 has the TRIUMF cyclotron followed by a chain of 5 rings:

- A Accumulator: accumulates cw 440 MeV beam from the cyclotron over
20 ms periods
- B Booster: 50 Hz synchrotron; accelerates beam to 3 GeV
- C Collector: collects 5 booster pulses and manipulates beam
longitudinal emittance
- D Driver: main 10 Hz synchrotron; accelerates beam to 30 GeV
- E Extender: 30 GeV storage ring for slow extraction

An energy-time plot showing the progress of the beam through the 5 rings is given in Fig. 2. The Accumulator is mounted directly above the Booster in the small tunnel, and the Collector and Extender rings above and below the Driver in the main (1072 m circumference) tunnel. The rf frequency of the Accumulator is twice that of the TRIUMF cyclotron, 46.1 MHz, making the frequency at top energy 62.9 MHz. The design parameters of the two synchrotrons are listed in Table II. As is the case with the existing cyclotron the successful operation of a high intensity accelerator requires every effort to be made to minimize beam losses. This design incorporates such features as H^- injection into the accumulator to eliminate injection spill, the use of bucket-to-bucket transfer between the rings, magnet lattices which

have their transition energy above top energy and magnet apertures which can accommodate a 50% growth in the horizontal and 100% growth in the vertical beam emittance. Details of the accumulator injection scheme, the various lattice designs, control of instabilities, operation with polarized beam, slow extraction and some of the present technical developments in dual frequency resonant magnet excitation, ferrite-tuned rf cavity design and the H^- extraction system have been presented elsewhere and are summarized in Ref. 2. A recent study has looked into the feasibility of replacing the Extender with a 100 GeV superconducting magnet ring operating with a 6 s overall cycle time and accepting 15 pulses from the Driver for an average current of 25 μA .³ Such an energy and time structure might be more suitable as a high intensity source of antiprotons for a storage ring.

EXPERIMENTAL AREAS

The layout of the proposed experimental hall is shown in Fig. 3. Both a fast extracted beam directly from the Driver stage and a slow extracted beam from the Stretcher ring are transported to target areas in this hall which is 75 m \times 120 m in area and about 8 m below grade. The science programme at a KAON factory has received a lot of attention over the past five years or so and is well documented in the proceedings of a number of workshops held at TRIUMF, Los Alamos and in Europe. A wide variety of secondary beams and experimental facilities are required to tackle the interesting scientific questions.

To identify these requirements a number of representative proposals were prepared for an initial research programme at a KAON factory and these are summarized in Table III. Table IV lists the parameters of the secondary beam lines which would be initially

installed. The proposed channel designs are aimed at a pion contamination which is an order of magnitude better than present day channels.⁴ This is accomplished by better definition of the channel acceptance with slits and by two-stage electrostatic separation. One consequence of these designs is that the beam lines are relatively long, resulting in a limited useful momentum range. For this reason a number of channels spanning a momentum range of about a factor two are provided. Typically a low momentum channel is combined with a high momentum channel, as shown in Fig. 5.

One of the difficult engineering design problems is the target areas where a significant fraction of the total beam power of 3 MW is lost in the production target, nearby collimators and the front-end magnets of the secondary channels. Power densities range from 60 kW/cm³ in the production target to 1 kW/cm³ in collimators or nearby magnets and up to 1 W/cm³ in the steel shielding surrounding the target⁵ (see Fig. 5). In addition to the thermal loads there are the problems of radiation damage, activation and the provision of adequate biological shielding. Experience at the present meson factories has indicated some solutions to these problems but there will have to be new ideas in magnet and target design, remote handling and servicing for proper optimization of the target areas. These same solutions could be applied to high flux antiproton sources as well.

ANTIPROTON CONSIDERATIONS

Antiproton beams with momenta up to 10 GeV/c and fluxes in excess of 10⁸/s would be available from the proposed secondary channels (see Fig. 6). These beams would be used for a wide range of experimental studies such as high precision measurements on the nucleon-antinucleon

system, \bar{p} nucleus scattering, nuclear dynamics after \bar{p} annihilation in a nucleus and the study of charmonium states. The latter experiments require antiprotons in the 3 to 7 GeV/c range, right at the production peak of a 30 GeV machine. The secondary channels are optimized for the production of clean kaon beams and it would be feasible to produce much higher fluxes of antiprotons in a dedicated facility.

Table V gives a comparison of the present CERN⁶ and Fermilab⁷ antiproton sources with that which could be achieved with a KAON factory. While not part of the initial proposal, a low-energy antiproton facility is being considered at TRIUMF as a natural add-on. To fully utilize the factor of 100 increase in antiproton flux available from a KAON factory, assuming existing technologies, a number of significant design problems have to be overcome or perhaps entirely new solutions will have to be found. These problems include:

Targeting: The antiproton production targets would have to withstand a factor 3-5 higher proton flux per burst and a factor of 50-100 higher average energy loss.

Collection: Pulsed collection devices such as current carrying targets, lithium or plasma lenses or magnetic horns would have to operate at 10 Hz, about 20 times faster than at present.

Debunching the time available for debunching and stochastic cooling
& **Cooling:** of the antiprotons prior to accumulation is less than 100 ms assuming this process is done on a pulse-by-pulse basis.

Some consideration of the problems of storing higher intensity anti-proton beams has already come out of the Hadron facility proposals from LAMPF⁸ and Europe⁹ and for the SSC.¹⁰ Hopefully workshops such as the present one will provide the motivation which will lead to further developments in this field.

STATUS OF THE PROPOSAL

TRIUMF's submission of the KAON factory proposal to our funding agencies in October 1985 led to the commissioning of a number of scientific and economic reviews of the project. During 1986 an international panel of experts in accelerators and subatomic physics gave a strong endorsement for the scientific merit and technical feasibility of the KAON factory. A second, overview panel, consisting of Canadian industrialists and scientists in other disciplines, considered the impact of the KAON factory on other science programs in Canada and the economic and technical benefits for Canada. This panel recommended a number of conditions to be satisfied prior to approval. These included: no rival project funded, a 15% international contribution, a national management structure and no cuts to other areas of scientific and engineering research.

Two economic studies have recently been completed which showed that the KAON factory project would be highly effective in stimulating industrial growth, in providing jobs, both direct and indirect, and would lead to valuable medical and industrial spin-offs. These studies were instrumental in persuading the British Columbia provincial government to give high priority to this project and in addition to approving the necessary funds for the civil construction it is helping TRIUMF to carry forward its case to the federal government.

REFERENCES

1. G.H. Mackenzie, "Efficient Extraction of H^- ions from the TRIUMF Cyclotron", Proceedings of the 1987 Particle Accelerator Conference, Washington (1987).
2. M.K. Craddock, "The TRIUMF KAON Factory Proposal", Proceedings of the Int. Workshop on Hadron Facility Technology, Sante Fe (1987)
3. J.R. Richardson, private communication, and R. Baartman, "Intensity Limitations in TRI-100", TRIUMF internal report TRI-DN-86-38 (1986).
4. J. Doornbos, "Possible Secondary Channels in a KAON Factory Proposal" TRI-DN-83-48 (1983).
5. C. Yamaguchi, "Some Energy Deposition and Absorbed Dose Calculations for a KAON Factory", TRIUMF internal report TRI-DN-85-11 (1985).
6. E. Jones, "Progress on ACOL", Proceedings of Third LEAR Workshop, Tignes, France (1985).
7. G. Dugan, "Tevatron I: Energy Saver and \bar{p} source", IEEE Trans. Nucl. Sci. NS-32, 1582 (1985).
8. F. Mills, "Collecting Antiprotons", Physics with LAMPF II, LA-9798-P, 424 (1983).
9. Proposal for a European Hadron Facility, EHF-87-18, ed. J.F. Crawford, (1987).
10. G.R. Lambertson and C.W. Leemann, "Intense Antiproton Source for a 20 TeV collider", IEEE Trans. Nucl. Sci. NS-30, 2025 (1983).

Table I. High-intensity proton synchrotrons.

	Energy (GeV)	Average current (μ A)	Rep. rate (Hz)	Protons/ pulse N ($\times 10^{13}$)	Circulating current I (A)
Fast Cycling^b					
Argonne IPNS	0.5	14	30	0.3	4.0
Rutherford ISIS	0.55(0.8)	40(200)	50	(2.5)	(6.1)
Fermilab Booster	8	7	15	0.3	0.3
AGS Booster	(1.5)	(20-40)	(7.5)	(1.8-3.5)	(4-8)
Slow Cycling^a					
KEK PS	12	0.32	0.6	0.4	0.6
CERN PS	26	1.2	0.38	2	1.5
Brookhaven AGS	28.5	0.9	0.38	1.6	0.9
- with Booster		(4-8)		(7-14)	(4-8)
Proposed Boosters^b					
TRIUMF	3	100	50	1.2	2.7
European HF	9	100	25	2.5	2.5
LAMPF AHF	12	25	12	1.3	0.5
JHF Booster	2	200	50	2.5	6.7
Kaon Factories^a					
TRIUMF	30	100	10	6	2.8
European HF	30	100	12.5	5	2.5
LAMPF AHF	60	25	12	1.3	0.5
Japanese HF	30				

^aSlow extraction

^bFast extraction

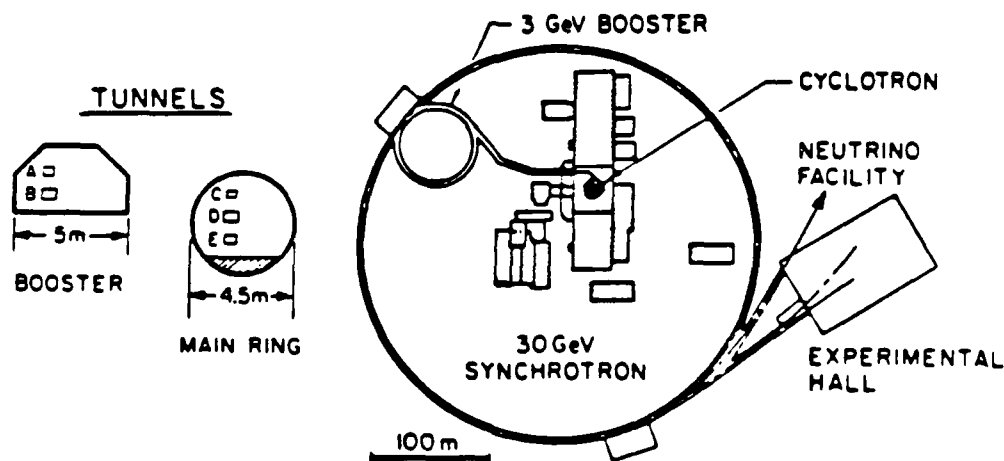


Fig. 1. Proposed layout of the accelerators and cross sections through the tunnels.

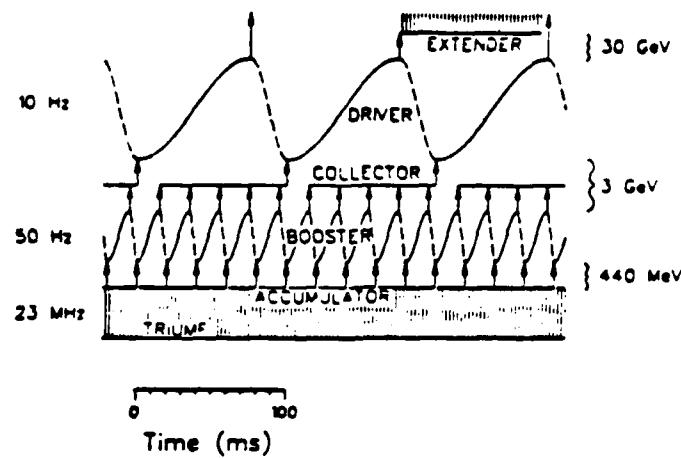


Fig. 2. Energy-time plot showing the progress of the beam through the five rings.

Table II. Synchrotron design parameters

	Booster	Driver
Energy	3 GeV	30 GeV
Radius	$4.5 R_T = 34.11 \text{ m}$	$22.5 R_T = 170.55 \text{ m}$
Current	$100 \text{ } \mu\text{A} = 6 \times 10^{14} / \text{s}$	$100 \text{ } \mu\text{A} = 6 \times 10^{14} / \text{s}$
Repetition rate	50 Hz	10 Hz
Charge/pulse	$2 \text{ } \mu\text{C} = 1.2 \times 10^{13} \text{ ppp}$	$10 \text{ } \mu\text{C} = 6 \times 10^{13} \text{ ppp}$
Number superperiods	6	12
Lattice structure	FODO	FODO
structure	OBOBBOBO	BBBBBOBO
Number focusing cells	24	48
Maximum $\beta_x \times \beta_y$	$15.8 \text{ m} \times 15.2 \text{ m}$	$38.1 \text{ m} \times 37.5 \text{ m}$
Dispersion η_{max}	4.0 m	9.09 m
Transition $\gamma_t = 1/\sqrt{\eta}$	9.2	=
Tunes $\nu_x \times \nu_y$	5.23×7.22	11.22×13.18
Space charge $\Delta \nu_y$	-0.15	-0.09
Emittances at injection	$139\pi \times 62\pi \text{ (}\mu\text{m)}$	$37\pi \times 16\pi \text{ (}\mu\text{m)}$
$\epsilon_x \times \epsilon_y$	0.064 eV-s	0.192 eV-s
ϵ_{long}	45	225
Harmonic	46.1 + 61.1 MHz	61.1 + 62.9 MHz
Radio frequency	210 keV	2000 keV
Peak energy gain/turn	576 kV	2400 kV
Maximum rf voltage	12 x 50 kV	18 x 135 kV
Rf cavities		

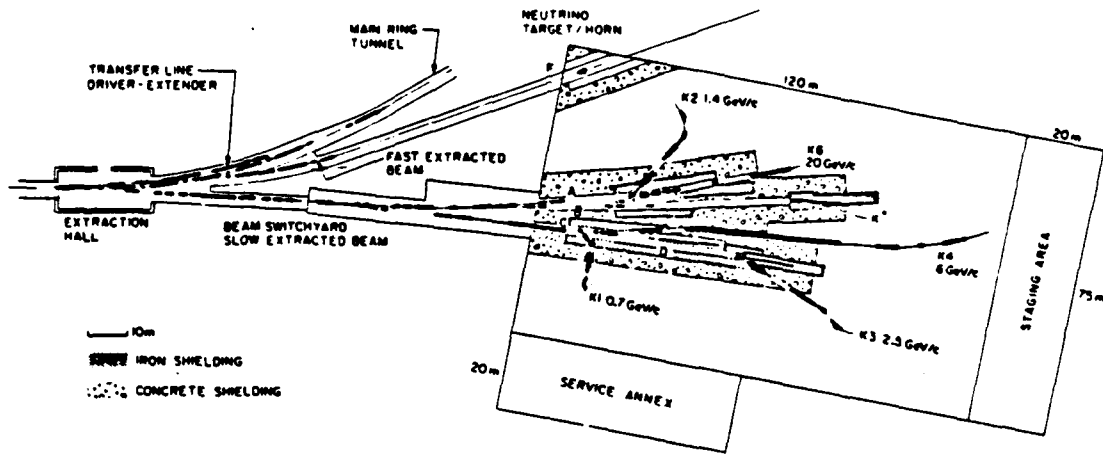


Fig. 3. Layout of the experimental area showing the primary and secondary beam lines.

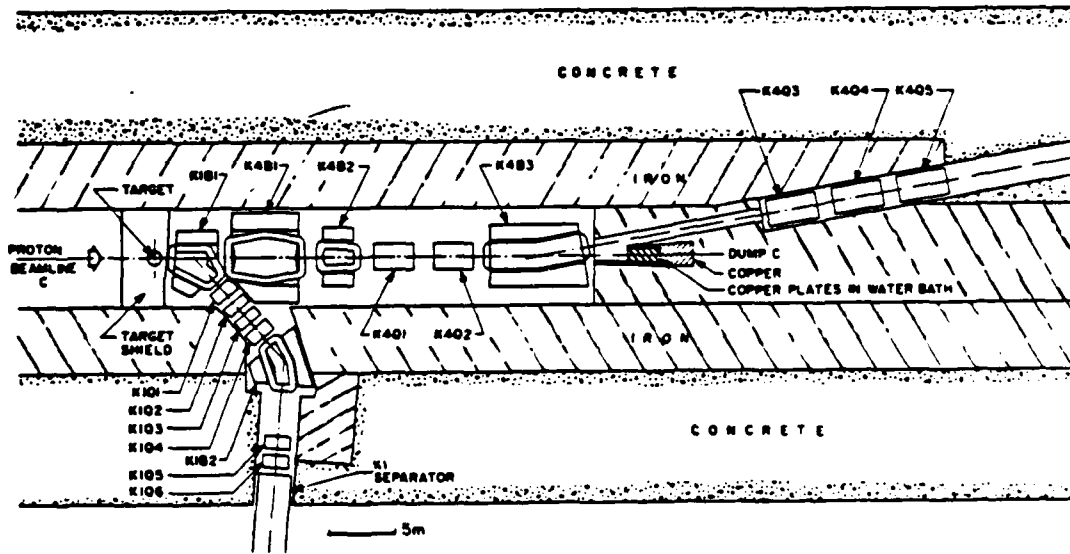


Fig. 4. Combination of a low momentum channel K1 with a high momentum channel K4 using the same production target.

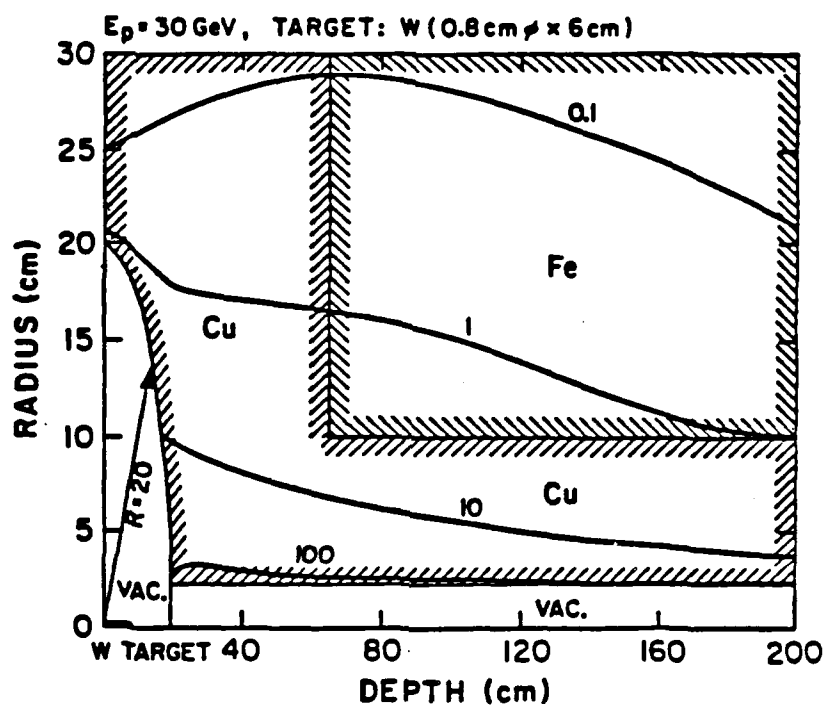


Fig. 5. Contours of equal energy density in W/cm^3 for $100 \mu\text{A}$ on an interaction length target surrounded by copper and steel.

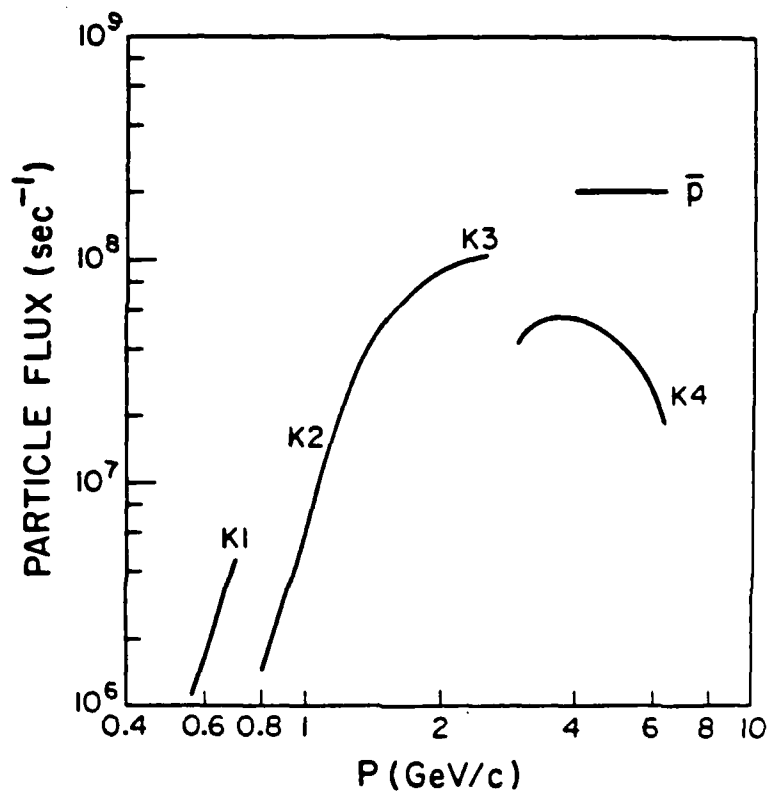


Fig. 6. Calculated antiproton fluxes for the different secondary channels in the proposal.

Table III. Facilities applicable to representative programme.

Proposal	Requirements		Beam Line/Facility
	Momentum Range (GeV)	Particle Flux (per second)	
Hadron Spectroscopy			
Y* resonances	0.4-2.5	K ⁺ 10 ⁸	K1 K2 K3
Light quark spectroscopy	4	K 10 ⁸	K4
Quark structure of hyperons	0.5	K 10 ⁸	K1
Charmonium	3-7	\bar{p} $\sim 10^7$	K4
Kaon Decay			
Measurement of η , η_{12}	4-12	K _L ⁰ 10 ⁷	K0
CP violation in K _L ⁰	4.5	K ⁺ 10 ⁷	K4
K _L ⁰ $\rightarrow \mu e$	1-10	K ⁰ 10 ⁷	K0
RHC in K _L ⁰ decay	0.5	K ⁺ 10 ⁷	K1
K $\rightarrow \pi \mu \bar{\nu}$	0.6	K ⁺ 7.5×10^6	K1
Hypernuclei			
Double hypernuclei	2	K ⁺ 10 ⁷	K3
Gamma ray spectroscopy	0.5-0.7	K 10 ⁸	K1
Charged particle spectrometer	0.3-1.1	K π^+ 10 ⁷	K1, K2
Neutrino Physics			
Neutrino elastic scattering	1-2	$\nu_e \nu_\mu$ 10 ¹¹ μ	ν Facility
Neutrino oscillations		day ⁻¹ cm ⁻²	
Proton Physics			
Polarized proton experiments	30	\bar{p} 10 ¹²	

Table IV. Secondary beam line parameters.

Beam Line	Momentum Range (GeV/c)	Solid Angle (msr)	Takeoff Angle (Deg.)	Momentum Acceptance (%)	Length (m)	Length of Separator
K1	0.4-0.7	6	10	5	17.9	1.30 m
K2	0.7-1.5	1.6	0	3.8	29.7	2.30 m
K4	2.0-6.0	0.8 (6 GeV/c) 0.30 (3 GeV/c)	0	3	11.5	1.30 m
K0	0.5-10.0	0.03	6	Wide	20	
K3	1.25-2.5	5 (2.5 GeV/c) 2.0 (1.5 GeV/c)	0	4	54	2.75 m dc
K6	up to 20 GeV/c	0.16	0	8	46.3	unseparated
Muon	30-200 MeV/c	35	135	10	18	1.15 m rf or 3 m dc

Table V. Comparison of existing antiproton sources with that possible at a KAON factory.

	CERN/ACOL	FERMILAB	KAON FACTORY
Proton Energy(GeV)	26	120	30
Antiproton momentum(GeV/c)	3.5	8.9	3.5
Protons/pulse(10^{10})	2.0	0.3	6.0
Pulse rate (Hz)	0.42	0.5	10.0
0° p production $1/\sigma d\sigma/d\Omega dp$.013	.25	.015
Acceptance (mm-mrad)	100-200	20	?
Collection device	pulsed target lithium/plasma lens	lithium lens	?
p accumulation rate (10^{10} /hr)	6	10	500

Scaleup of Antiproton Production Facilities to 1 mg/yr

F. E. Mills

Fermi National Accelerator Laboratory

September 30, 1987

1. Production of Antiprotons

1.1. Cross sections

We will consider the production of antiprotons in collisions between protons and ions, including protons themselves. In such collisions, the fundamental interaction is between the quarks which are the constituents of the individual nucleons. It is awkward, however, to use the fundamental cross sections, even if known, because the quarks are confined and have large Fermi momentum. We will instead describe the production in the center of mass of the nucleons. In heavy nuclei, interactions with other nucleons may modify the distribution of antiproton momenta.

1.2. P_{cm} , P_{\perp} , P_{\parallel} , σ_{tot} vs E: Total pbar per p

Our current understanding is that the distribution in transverse momenta is independent of bombarding energy or center of mass momentum. The distribution is approximately gaussian with $\sigma_{\perp} = .56$ geV/c for heavy nuclei, and .41 geV/c for proton targets. In all data presented here, the P_{\perp} distribution has been integrated away, leaving only the P_{\parallel} distribution. Collectors which do not collect all the P_{\perp} will need to take account of that fact.

The velocity B of the center of mass for a proton of momentum P_p colliding with another nucleon is given by ($c = 1$, $M =$ nucleon mass))

$$B = P_p / [M + (M^2 + P_p^2)^{1/2}] \quad 1.1$$

and the Lorentz factor Γ is

$$\Gamma = [1 - B^2]^{-1/2} \quad 1.2$$

The momentum of the proton in the nucleon-nucleon center of mass system is

$$P_{pcm} = B\Gamma M \quad 1.3$$

This is the "colliding beam" momentum corresponding to the incident proton momentum.

An antiproton produced with laboratory momentum P_L has momentum in the center of mass

$$P_{cm} = \Gamma [P_L - B (P_L^2 + M^2)^{1/2}] \quad 1.4$$

Given the antiproton momentum spectrum in the laboratory system dN/dP_L , we can transform it to the center of mass by multiplying by

$$dP_L/dP_{cm} = \Gamma [1 + BP_{cm} / (P_{cm}^2 + M^2)^{1/2}] \quad 1.5$$

Production spectra are given for four incident proton momenta, 25, 100, 300 and 1000 GeV/c in figures 1-4 below. These cross sections were fitted to known existing data in 1982 by Hojvat and van Ginneken¹ and required extrapolation of the heavy nucleus data to small center of mass momentum. Since that time, other data² has shown that in heavy nuclei, the cross section is about a factor of 2.5 lower, at least for the Fermilab case³. The reduction, compared to the extrapolation, takes place near zero center of mass antiproton momentum but in fact covers most of the region where significant numbers of antiprotons are produced. Here, when we actually apply these data, we will simply apply the "experience" factor of 2.5. In figures 1-4⁴ the ordinates are the number of antiprotons per GeV/c produced at momentum P_L in the laboratory system. Figures 5-8 are the integrals of these spectra, that is the fraction of antiprotons with momenta less than the abscissa. Figures 8-12 show the same spectra in the center of mass of the nucleon - nucleon system as a function of longitudinal momentum in that system. These are of interest for the case of proton - heavy ion colliders. These data are subject to the corrections mentioned above.

Absorption of the protons and antiprotons is not included in the calculations. In an optimum length target, one interaction length, the yield is reduced by a factor of $e = 2.71...$ The total number N_{pbar} of antiprotons per proton can be gotten by integrating the spectra over momentum. We can characterize the production by calculating the rms antiproton longitudinal momentum $\sigma_{p_{cm}}$ in the center of mass system, and the laboratory momentum P_{cm} of an antiproton at rest in the center of mass system. These parameters are given in Table 1 below.

Table 1. Antiproton production in Tungsten. Momenta in GeV/c

P_p	P_{cm}	σ_{pcm}	$10^3 \cdot N_{pbar/p}$
25	3.36	.488	3.24
100	6.82	.828	54.1
300	11.84	1.227	156
1000	21.65	1.877	314

Several features of the production are apparent. First, considering only the total number of antiprotons produced, it is economical to get at least into the 100 GeV/c range of incident energy. On the other hand the spread of momenta becomes large. Later on we will consider the difficulty of cooling away this momentum spread. Second, The spread σ_{pcm} in the center of mass system goes up fairly slowly, and is of the same order of magnitude as the transverse spread σ_{\perp} . Colliding beam systems, if they can collect large solid angles, will ease the cooling problem, but will pose problems in obtaining adequate rate or luminosity.

Finally, in figures 13 - 16, the cross section per GeV/c for production of antiprotons in p - p collisions in the center of mass is given as a function of longitudinal center of mass momentum. These data are the best known, even at zero center of mass momentum, and are not subject to the correction discussed above. As noted above, the σ_{\perp} is 0.41 GeV/c for p - p collisions. These data are summarized in table 2 below.

Table 2. Antiproton production cross sections and rms center of mass antiproton momenta σ_p in p-p collisions for different collider momenta P_p . Momenta in geV/c, total cross sections in μ barns.

P_p	σ_p	Total Cross section
5	0.69	12.8
10	1.16	59.6
20	1.91	133
100	7.05	329

As a crude beginning to the problem of scaleup, suppose we could collect all the antiprotons made by the Tevatron beam on a one interaction length W target under ideal conditions: that is, 10^{13} protons/pulse, 2 pulses per minute every minute of a year. This is a shortfall of about a factor of 1400. ($4.4 \cdot 10^{17}/\text{yr}$ vs $6 \cdot 10^{20}/\text{yr}$ for one milligram). This includes absorption and the cross section factor of 2.5 mentioned above, and assumes that all P_{\perp} and P_{\parallel} up to 100 geV/c collected.

¹C. Hojvat and A. van Ginneken, NIM, 206, (1983),67-83

²L.M. Barkov, et.al., Preprint 79-92, Institute of High Energy Physics, Serpukhov, 1979 and, N.I.Bozhko, et.al.,Preprint 79-78,Institute of High Energy Physics, Serpukhov, 1979, and F. Binon, et.al.,Phys. Lett. 30B, 506 (1969)

³M. F. Gormley, private communication.

⁴I am indebted to M. F. Gormley for providing this data in a form suitable for plotting.

2. Collector and Accelerator Types

2.1 Beam Type Collector Systems

It is convenient to think of collectors as being of two generic types. The first type is the beam type, of which two have been built, at CERN and at Fermilab. We understand that we employ HEP beam technology, with targets, beam lines, storage rings, and beam cooling. Such collectors are built with existing technology and are subject to detailed cost optimization to perform reasonably well defined experiments. Their general makeup is dictated by already existing accelerators. Since the goal is to perform the experiments, as opposed to accelerator R&D, the technology employed is not very adventurous. It follows that we can describe the beams by emittance, momentum spread, and intensity. The collectors are described by their aperture, that is the acceptance in emittance and momentum spread, and by their focal properties in the three phase space projections. The cooling systems also enter strongly into these descriptions, and these will be discussed separately in section 4. A general discussion of the main parameters affecting the performance of these systems follows.

2.1.1. Target heating; Emittances and Phase space areas

In beam type collectors, and probably plasma type collectors as well, to be discussed in section 2.2 below, there is a great premium in keeping the 6 dimensional phase volume of the antiprotons as low as possible. In the transverse projections of phase space, the transverse momentum spread is governed by the production process, or by the strength of collection lenses. Then it is advantageous to keep the transverse dimension of the incident proton beam as small as possible to minimize the phase space areas, or emittances, of the antiprotons in the transverse projections. As the dimensions are decreased, the temperature excursion of the target volume increases. Presently conventional wisdom states that the temperature excursion in tungsten should be limited to about 1500°C, corresponding to an energy deposition of 200 Joules/gm, else shock waves will destroy the target. For 120 GeV protons, this is predicted to occur with $2 \cdot 10^{12}$ protons with an rms beam radius of 0.4 mm¹. Experience has shown that this estimate was not sufficiently conservative. Both at CERN and at Fermilab, W targets have fractured under these conditions. The tungsten targets have been replaced with Cu, at a small penalty in yield. At

higher energy deposition, when the targets are destroyed in one pulse, the shock waves can cause target density depletion and reduction of yield².

Some care must be taken in scaling energy deposition with beam size. High energy nuclear cascades have finite size. For the case above most of the secondary deposition is outside the proton beam, but it is now speculated that the peak deposition is due largely to the electromagnetic showers from π^0 decays within the beam, underestimated in the earlier calculations. The radiation length is so short in tungsten that most of the energy from these decays falls within the beam. Apparently this effect was underestimated in early calculations at Fermilab. Recent calculations at CERN predict higher energy deposition in W, in general agreement with the experience at CERN and Fermilab. Both calculations agree for lighter metals, for example Cu. For larger beams the secondary deposition is mostly within the proton beam.

The other phase space projection is in energy and time, or in longitudinal momentum and beam length. Strong focussing in this projection has been employed in the Fermilab collector, and will be incorporated in the upgraded CERN collector (ACOL). The proton beam is bunched as tightly as possible, in 82 bunches at Fermilab. In the first ring (Debuncher), under the influence of an RF system, the resulting antiproton bunches are rotated in energy time phase space, and then adiabatically debunched, reducing the energy spread while increasing the time spread. In the Fermilab system, the antiproton momentum spread is reduced from 3% to .25% while the bunch length increases from about one nsec to 19 nsec (completely debunched).

2.1.2. Collection Lenses; Depth of Focus

Efficient collectors will, in addition to collecting the maximum possible longitudinal momentum spread, also collect large transverse momentum spread to obtain the highest yield. In the Fermilab system which collects at 9 geV/c, σ_{\perp} corresponds to an angle of about 60 mrad. In order to transport the beam, a short focal length lens is located near the target to make the beam more "parallel". The lens is composed of a high (500 kA) current flowing in a cylindrical column of lithium about one cm in radius and 15 cm long³. The magnetic field at the periphery is about 10T. The 9 geV/c antiprotons are brought from point to parallel at 1 cm radius for a collection angle of 44.4 mrad with the center of the target 14.5 cm upstream of the entrance to the lens,

corresponding to a focal length of 22.5 cm. There is, therefore, a severe depth of focus problem. The efficiency of the optical system at collecting the antiprotons varies throughout the target. The collection emittance is $20\pi \mu\text{m}$ so that the waist spot size is .45 mm (about 2.5σ); the β function at the waist is about 10 mm. Efficient collection takes place over a length comparable to the β function. In fact, considering this effect alone, the effective target length is

$$L_{\text{eff}} = 2\beta^* \tan^{-1}(L/2\beta^*) \rightarrow \pi\beta^* \text{ as } L \rightarrow \infty \quad 2.1$$

The efficiency, from the point of view of depth of focus, is $(\tan^{-1}x)/x$, where $x=L/2\beta^*$. For the Fermilab target, this is 29%. The fraction of particles accepted depends on the P_{\perp} collected as $[1-\exp(-P_{\perp}^2/2\sigma_{\perp}^2)]$. For the Fermilab case this is 22.5%, where $P_{\perp} = 0.4 \text{ geV}/c$.

Long targets do not add antiprotons, but in fact lose antiprotons, as will be discussed below. The depth of focus limitation has stimulated a desire to use heavy metal targets with short interaction lengths to obtain the maximum number of antiprotons.

Several ideas have been discussed to overcome these limitations, and there is a possibility of gaining a factor of two or more by pursuing them. First, the depth of focus problem can in principle be overcome by passing a high current through the target to focus the antiprotons much in the same way the Li lens does after the target⁴. Then the beta function can be made to stay constant in the target and eq. 2.1 does not apply. Of course the proton beam is defocussed so this cannot go on forever, but some definite gain can be made, typically, provided the target holds together. The current density required to maintain a value β of the beta function for a particle of magnetic rigidity $B\rho$ is given by

$$J = 2B\rho/[2\mu_0\beta^2] \quad 2.2$$

For 9 geV/c particles and $\beta = 10 \text{ mm}$, this is about $1/2 \text{ MA/mm}^2$. For the 0.4 mm radius pbar beam described above, 240 kA must be inside the beam. Even if the current does not penetrate the target, the antiprotons are reflected back into the target and a gain is realized. Further, the proton defocussing can be avoided by using alternating gradients, that is alternating the direction of current in adjacent segments of the target⁵.

Second, the proton beam can be swept across the target, lowering the specific energy deposition⁶. The antiproton collection channel can be swept at

the same time. Then the proton spot size can be reduced, and for the same emittance, the antiproton collection angle can be increased, provided the appropriate collection lens can be built.

The first of these methods has been tried at CERN⁷ and shows some promise, but the target breaks rather soon. It is planned to investigate the second method at Fermilab.

In the longitudinal projection, more antiprotons will be collected the greater the momentum spread captured. This is limited by several considerations. First, it is difficult to transport large momentum spread beams without significant phase space dilution. Second, the circular debunching process, in order to operate with reasonable RF voltage and power, requires that the debunching ring operate near transition energy (in the Fermilab Debuncher $\eta = -.005$). This is in direct conflict with the needs of the stochastic precooling system which needs large η to obtain adequate mixing. Some improvement in the outlook can be gained by the use of a linear debuncher before the first ring. Large, $\sim 10\%$, momentum spread can be reduced to about $.4\%$ spread, with no need for rotation in the ring⁸. Some RF is useful to adiabatically debunch the beam, but η can be large, say $.02$, facilitating the stochastic precooling, perhaps even allowing momentum cooling in addition to transverse cooling. There is concern for the high impedance of the high frequency cavity required in the synchrotron for prebunching the protons, and the peak energy gain in the linac is about half the momentum spread to be debunched (about $2/3$ LAMPF at Fermilab). In order to handle high P_{\perp} in the linac, large bore holes must be used, probably lowering the shunt impedance, requiring large RF power. On the other hand the beam current is low so there is no beam loading. No serious design of a linear debuncher has been undertaken. If the proton accelerator is a linac, then a linear debuncher is a natural addition, and may allow acceptance of more than 10% in momentum.

2.1.3. Absorption and Multiple Scattering

Absorption is an important consideration in the design and optimization of targets. In the Fermilab system, (120 geV/c p , 9 geV/c pbar) the proton collision length is 9.86 cm and the antiproton absorption length is 9.29 cm , about the same. The protons are absorbed in the target so the number available reduces with depth in the target. The antiprotons are also absorbed,

so that the population of antiprotons increases and then decreases, varying as $\lambda \exp(-z/\lambda)$. The optimum target length is λ , and the effective target length is λ/e in this case. Note that this is reasonably matched to the depth of focus. Less than 10% of the antiprotons are absorbed in the Li lens by nuclear interaction.

In the target, multiple scattering is not perceived to be a serious problem. The protons have such a high energy that the scattering does not appreciably increase the beam size in passing through the target. The antiprotons scatter more, about 10 mrad in each plane for a 9.5 cm W target, but this adds in quadrature to the rms production angle of $.56/9 = 60\text{mrad}$, so neither the density in solid angle nor the rms production angle changes very much due to the scattering.

Scattering in the collection lens can be more serious. The acceptance phase space has rotated so that the effective angular width is reduced, and there are no antiprotons to scatter in to replace those scattered out. Then the population of antiprotons is reduced, or equivalently the emittance of the antiproton beam is increased. In the Fermilab system, the angular width of the channel at the lens has reduced to about $\pm 2.2\text{ mrad}$. The scattering in 15 cm of Li is about 0.4 mrad, so the effect is not very important. At CERN, where the antiproton momentum is three times lower, the effect is taken more seriously. Plasma lenses, of the type which were used to focus pion beams to form neutrino beams at BNL, can have fewer radiation lengths in the beam, and provide large field gradients for focussing, comparable to the Li lens. Predictably, these are being developed at CERN, not at Fermilab.

2.1.4 Reconciliation with actual Fermilab source performance

Taking the 100 geV/c data (actually P_p is 120 geV/c at Fermilab), dN/dP as given in section 1 is 0.0036/geV/c, and we can compare to a measurement of $p_{\text{bar}}/p = 14\text{ ppm}$ in the Debuncher for a momentum spread of 3.5%, and an acceptance of $20\pi\text{ }\mu\text{m}^9$. Then ΔP is .315 geV/c, depth of focus correction .287, P_{\perp} factor .225, and absorption factor .368. Combined, these yield 27 ppm. As remarked earlier, measurements made after the design showed that the cross section is a factor of about 2.5 lower than those given by Hojvat and van Ginneken, yielding a final value of 11 ppm, in reasonable agreement with the 14 ppm measured. In the actual system, inefficiencies in rotation, extraction,

transport, injection, RF capture, and stochastic accumulation lead to about another factor of two loss in the accumulation rate.

2.1.5. Performance requirements for beam type collectors

In order to discuss choices to be made, it is instructive to derive some performance requirements based on the cross sections and known physical limitations on the production process. In table 3 below, the required proton currents and beam powers are given assuming that antiprotons from a one interaction length target are collected at the peak of the production curve P_{pbar} in a 10% momentum bite, and that all transverse momenta are collected. The data are from the figures above corrected by the factor of 2.5 discussed above and for absorption.

Table 3. Beam power vs. proton energy, 10% momentum collection at optimum momentum, beam type collector, 1 mg/yr, 1 interaction length target, momenta in geV/c, current in mA, beam power in gW. Absorption included, cross sections scaled by 2.5.

P_p	P_{pbar}	$10^3 dN/dP$	$10^4 pbar/p$	I_p	Power
25	3.1	.795	0.36	84	2.11
100	5.0	5.01	3.69	8.3	0.83
300	6.5	7.95	7.60	4.0	1.21
1000	7.0	9.45	9.70	3.1	3.14

Aside from the unfamiliar beam currents and powers, some features are worth noting. First, there seems to be an optimum proton energy near 100 geV. More investigation might show its location more closely. Second, kinematics is moving the optimum collection momentum to negative values in the center of mass. It is heartening that the collection momentum is no greater than present sources, so we can better visualize what such sources might look like. Third, the beam powers suggest that modularity might be a good tactic. This is in the right direction for considerations of targetry and beam cooling.

2.2. Plasma Type Collector Systems

Another type of collector can be contemplated, one in which the goal is to collect all the antiprotons produced in a target. Perusal of figures 1-8 convinces one that a better strategy would be to collect some fraction, say 50%, of the antiprotons to reduce the maximum momentum, and hence size, of the collector. We can imagine such a collector to be a plasma type containment device, most likely a mirror machine. Mirror machines exhibit many similarities to rudimentary accelerators, at least insofar as orbit properties are concerned. Some of these properties will be discussed in section 2.2.2. Table 4 below shows the performance requirements for the accelerators to power such a source.

Table 4. Beam power vs. proton energy, lower 50% collection in momentum. Plasma type collector, 1 mg/yr, 1 interaction length target, momenta in GeV/c, current in μA , power in MW. Absorption included, cross section scaled by 2.5.

P_p	$P_{pbar}(50\%)$	$10^3 pbar/p$	I_p	Power
25	3.7	0.24	12800	321
100	7.6	3.76	814	81.4
300	13	11.5	267	80.0
1000	22	23.2	132	132

Again there seems to be an optimum energy, now above 100 GeV. The expected reduction in beam power is evident, and does not look as extreme as for the beam type collectors. On the other hand the collection energy is high, and will result in an enormous field volume.

Another type of plasma collector has been proposed employing colliding beams in which the collisions take place on the axis in the center of a mirror machine. Several problems are solved immediately. In the first place, injection is automatic. In the second place, one need only confine the center of mass momentum, which is in the 1 - 2 GeV/c range. There are two difficulties: the first

is obtaining adequate luminosity, the second is dealing with the other particles produced and trapped in the collector.

Using the cross sections given above in section 1, we can derive performance requirements for colliders. For p-p we can use the cross sections directly to derive required luminosities. For p-W we can derive cross sections knowing the production figures above and the interaction length. These are given in tables 5 and 6.

Table 5. Required luminosities to produce 1 mg/yr antiprotons in p - p colliders. Momenta P_p in geV/c, total cross sections σ_T in μbarn , Luminosities L in units of $10^{40}/\text{cm}^2\text{sec}$.

P_p	σ_T	L
5	12.8	149
10	59.6	32
20	133	14.4
100	329	5.8

Table 6. Required luminosities to produce 1 mg/yr antiprotons in p - W colliders. Momenta P_i in geV/c/nucleon, total cross sections σ_T in mbarn, Luminosities L in units of $10^{37}/\text{cm}^2\text{sec}$.

P_i	σ_T	L
3.36	2.15	889
6.82	36.6	52.2
11.84	110	17.3
21.65	232	8.2

Luminosities of colliders are limited by many things, but that which is thought to be fundamental is the beam - beam effect, that is, the electromagnetic interaction between the two beams. In addition to the magnetic effect similar to the Li lens above, there is also an electric interaction. Since the two beams

have opposite velocities, the electric and magnetic forces aid each other, as compared to the single beam effect where they oppose each other. In colliders of opposite sign particles, as in $p - \bar{p}$, or $e^+ - e^-$, the beams have a (nonlinear) focusing effect on each other, and the beam - beam effect can actually enhance the luminosity, at least for linear colliders. For like sign colliders, the type discussed here, the beams defocus each other, so the beam-beam effect can only detract from the achievable luminosity. If the beam - beam effect is not dominant, the attainable luminosity is determined by beam brightness, and focussing strength.

Consider two bunched ion beams 1 and 2, colliding at a rate of F bunches/sec, with N_1 or N_2 particles per bunch, Z_1 or Z_2 charges per ion, A_1 or A_2 AMU mass per ion, and each beam having the same velocity β and Lorentz factor γ so that the center of mass is the laboratory system. Each bunch has radius a and length d . Then we can define a "disruption" parameter D_1 or D_2 which is essentially the number of e -foldings in radius an ion in one beam receives due to the defocussing of the other beam. r_p is the classical proton radius, $1.53 \cdot 10^{-16}$ cm.

$$D_2^2 = [4r_p Z_1 Z_2 N_1 d] / [\gamma A_2 a^2] \quad 2.3$$

Requiring equal disruption in each beam demands

$$N_1 A_1 = N_2 A_2 \quad 2.4$$

Then the luminosity L can be written

$$L = N A \gamma F g(D) / [4\pi r_p Z_1 Z_2 d]$$

$g(D)$ varies as D^2 for $D \ll 1$, is about 1 at $D = 1$, and increases as $D/2$ for $D \gg 1$. In the disruption limited regime, the luminosity depends mainly on the charge state of the ions and the proton beam current $I_p = NF/e$. Heavy ions must collide in low charge states, or their higher cross section will be wasted by a lower luminosity. The tolerable disruption is larger in linear colliders than in circular colliders, which must retain the emittance of the beam to maintain luminosity.

It is interesting to calculate the luminosity in an extreme case. Take $I_p = 1$ A, $D = 1$, $\gamma = 20$, $d = 1$ mm. The luminosity turns out to be about $6.5 \cdot 10^{35}/\text{cm}^2\text{sec}$, too low to be interesting, either for $p - p$ or for $p - \text{heavy ion}$. Further, there is 20 gW of power in each beam. It is not clear that one can get to the disruption limit, so let us calculate the luminosity in a case which is

determined by brightness and focussing limits. Take the bunch frequency to be 400 MHz, the invariant emittance to be $5\pi \mu\text{m}$, and the beta function at the intersection region to be 1 cm. The luminosity for 1 A p - p linear colliders is about $1.2 \cdot 10^{33} / \text{cm}^2 \text{ sec}$.

2.2.1 Fixed target plasma type collectors

Mirror machines can be characterized by the mirror ratio or alternatively by the field index $n = -r dB/Bdr < 1$ at the plane of symmetry. Orbits of all radial sizes are stable up to the diameter of the machine, while there is a limit on axial orbit size caused by the geometry of the coils, where the field lines become parallel and there is no longer a radial component of field to give an axial restoring force. For large radial orbits we describe the motion as a betatron oscillation whose frequencies of oscillations in the radial and axial directions are $\omega_r = \sqrt{1-n}\omega_0$ and $\omega_z = \sqrt{n}\omega_0 = v_z\omega_0$. Consider a particle which initially has no radial velocity and is being deflected inward by the magnetic field. Since $1-n < 1$, its orbit will return to the same radius only after 1 turn. Its orbit is a circle precessing in the direction of its initial velocity with a frequency $\omega_0[1-\sqrt{1-n}] = \omega_0 v_p$. At the same time the circle is oscillating axially with the axial frequency. Orbits of particles with smaller momentum exhibit the same characteristics, only the circle size is smaller, and the frequencies are different, depending on the momentum and the average n value at the orbit. These properties provide a mechanism for injection of a large momentum spread beam into the device. The particles will return to the same radius and azimuth only after $1/v_p$ gyroorbits. If the axial and precession frequencies are not integer multiples of each other, the orbit will not return to the same point in space for $1/[v_p v_z]$ gyroorbits. During this time, a deflector can be turned on to provide the proper initial values for the orbits without subsequently perturbing the orbits. Between injections the particles must be cooled to move them away from the deflector so their orbits will not be perturbed by subsequent injections. As yet, no candidate has emerged for this cooling mechanism. This will be discussed in section 4 below.

Since the proton momentum is much greater than the antiproton momentum, the proton beam can traverse the mirror machine. Then the target can be located in the mirror machine, avoiding the problem of transporting a large momentum spread antiproton beam. The direction of the magnetic field is

chosen to deflect the protons outward at the target and the antiprotons inward. This gives the initial condition for the antiproton orbits described above. This also provides a way to remove positive reaction products, since they will move at a larger mean radius and can be absorbed by baffles or other means. The electrons produced in the target will be captured along with the antiprotons, and will be cooled rapidly by radiation. This has interesting consequences as discussed below in section 4.

2.2.2. Colliding beam plasma type collectors

In this type of collector, proposed by Cline¹⁰, the two beams are transported along the axis of the mirror machine, colliding in the center or possibly at several places along the axis. Injection of the antiprotons is automatic and requires no special provision. The total momenta contained are the center of mass momenta, described by σ_{\perp} and σ_{\parallel} above, 0.56 and about 1 -2 geV/c. Some investigation should be made lest not too many of the antiprotons find themselves in the loss cone of the mirror. Presumably an acceptable mirror geometry can be found.

There is a serious problem with this type of collector. Since all the particles are produced on the axis, they have zero angular momentum and will always return to the axis on each precession. The trapping is independent of sign of charge, so at least, protons will be trapped also. Electrons and positrons will also be trapped from meson decay¹¹. Such plasmas, called Migma's, or LOZCAMP's¹² (large orbit zero canonical angular momentum plasmas) have a high collisionality near the axis, at least for low plasma β . This leads to interaction and annihilation of the antiprotons. Even if the high collisionality can be avoided, there is no known way to separate the matter from the antimatter in bulk form at a later stage. This is called, in Astrophysics, "The Problem of the Symmetrical Early Universe."¹³

¹N. V. Mokhov and A. van Ginneken, Fermilab High Intensity Targeting Workshop, 1980, p64-80

²G. Bohannon, Fermilab High Intensity Targeting Workshop, 1980, p85-102 and J. E. Reaugh, ibid, p81-84

³T. A. Vsevolozhkaya, M. A. Lyubimova, and G. I. Sil'vestrov, Zh. Tekh. Fiz., 45, 2484-2507 (December 1975)

-
- ⁴L. N. Blumberg and A.E.Webster, IEEE Trans. Nuc. Sci. NS-24#3 p1539 June 1977 and
D. Cline and F. Mills, Exploding Wire Lens for Increasing Pbar Yield, Fermilab Pbar Note 7, January
1979
- ⁵J. MacLachlan, Fermilab FN 334, April 1982
- ⁶F. Krienen and F. Mills, Fermilab High Intensity Targeting Workshop, 1980, p61-63
- ⁷T.W. Eaton and C. Carter, CERN PS/AA/Note 85-11, August 1985 and
C. Johnson, private communication
- ⁸F. E. Mills and D. E. Young, Linear Antiproton Debuncher, Pbar Note 145, December 1982
- ⁹M. F. Gormley, private communication.
- ¹⁰D. Cline, Proposal for a Moving Target High Intensity Antiproton Source, UCLA Note ECP-022,
April 20, 1987
- ¹¹B. Maglich, "Speculations on Laboratory Ambiplasma as a Source of Antihydrogen Atoms and
Molecules", International Symposium On Aneutronic Fusion, 1987, Princeton, New Jersey
- ¹²B. Maglich, Panel Discussion, International Symposium On Aneutronic Fusion, 1987,
Princeton, New Jersey
- ¹³Usually attributed to H. Alfven

3. Candidate Accelerators

3.1. Synchrotrons

There have been four recent serious studies¹ of intense proton synchrotrons as particle sources for physics experiments. These studies treat proton synchrotrons in the energy range 30 - 60 GeV, with average beam currents of about 100 μ A. Typically these are rapid cycling synchrotrons, except for the AGS II proposal. There is no reason in principle that similar performance could not be achieved in the 100 - 200 GeV region. Then about 10 of these might be sufficient to feed plasma type collectors, or about 100 to feed 10% beam type collectors. Since this subject will be addressed by other speakers at this conference, no more will be said here about it.

3.2. Linear Accelerators

Linear accelerators can be expected to provide higher average beam currents than synchrotrons. For example, LAMPF has produced 1 mA average beam current at 0.8 GeV. Typically the linac produces 15 mA beam pulses of 1/2 msec duration at a 120 Hz repetition rate. The Fermilab injector linac operated for several years producing 300 mA pulses 5-10 μ sec long at a 15 Hz repetition rate, the pulse length being determined by available RF power. Extension of these parameters in energy seems feasible, though expensive. It now seems feasible to design linacs with gradients of 6 - 7 MeV/m, so a 100 GeV linac would be about 150 km in length, somewhat longer than the SSC tunnel. Of course many problems would need to be solved, for example the problem of deflecting modes in the higher energy region where the beam has little Landau damping.

The conclusion is that accelerators to provide the proton beams of intensity adequate to provide the gross numbers of antiprotons can be built. The real problems will lie in the targetry, containment, and cooling, which, if soluble, will determine which accelerator type to build.

¹Report of the AGS II Task Force, HEDG Document, BNL, February 1984

The Physics and Plan for a 45 GeV Facility.....(LAMPF II), LA-10720-MS, LANL Document, May 1986

Proposal for a European Hadron Facility, EHF-87-18, Univ. Trieste, May 1987

KAON Factory Proposal, TRIUMF Document, September 1985

4. Antiproton Cooling Methods

4.1. Stochastic Cooling

Stochastic cooling systems detect fluctuations in, for example, the current or dipole moment of a short sample of beam in a storage ring, and later apply a correction signal to the sample derived from the measurement¹. A single particle sees its own correction and also a noise signal from the other particles in the sample. The particle's own signal can be arranged to damp degrees of freedom of the particles motion, while the noise signal causes diffusion in the particles motion. There is a competition between the damping and diffusion which limits the cooling rate. The diffusion rate is proportional to the power spectrum of the signal, so large frequency spread leads to less diffusion and faster cooling. In simple systems there exists an optimum cooling time T_{opt} which is given by

$$T_{opt} = 2N M / BW \quad 4.1$$

Where N is the number of particles in the beam, BW is the bandwidth of the system and M is a "mixing factor". For ideal cases $M = 1$ (rarely attained), or for more typical cases,

$$M = [\ln(f_2/f_1)]/[n\eta\Delta p/p] \quad 4.2$$

The frequencies f_1 and f_2 are the upper and lower band edges, $\Delta P/P$ is the fractional momentum spread in the beam, n is the number of Schottky lines in the bandwidth and,

$$\eta = |\chi^2 - \gamma^2| \quad 4.3$$

where χ is the "transition γ " of the storage ring, which can be adjusted somewhat by the design of the lattice. In the unlikely circumstance that we can design a ring so that $M = 1$, the required bandwidth of the system required to cool $6 \cdot 10^{20}$ antiprotons per year, or $2 \cdot 10^{13}/\text{sec}$ is 20,000 GHz. Alternately one could use 2000 systems of 10 GHz bandwidth. There are many other constraints on the design of stochastic cooling systems. For example, the sensitivity of pickup electrodes falls off rapidly as the aperture approaches $\lambda/4$. This conflicts with the need to collect large emittance beams to get the large p_{\perp} antiprotons produced. Yet stochastic precooling is an essential part of any high flux beam type antiproton collection system. Stochastic accumulation systems, in addition to the band width limitations discussed above, heat the radial betatron oscillations, requiring small emittance beams to begin with. Electron

cooling systems in the energy range appropriate to this discussion require extremely small ion emittances to be at all effective in accumulating beams.

4.2. Electron Cooling

Electron Cooling² is another beam type cooling system in which an electron beam is made to travel in spatial coincidence with an ion beam at the same velocity. In the system moving with the mean velocity the view is of an ion gas being cooled by coulomb collisions in an electron gas. Electron beams in this energy range³ can be made which have sufficiently low temperatures, but the ion temperatures, due to the ions P_{\perp} , are so high that cooling is very slow. On the other hand, the cooling rate does not depend on numbers of particles so drastically as stochastic cooling, at least in experiments performed to date. The rate of collecting in momentum in this energy range is inversely proportional to the fourth power of energy and the square of the emittance. For an example, to replace the Fermilab 1 GHz bandwidth stochastic accumulation system, which was designed to accumulate $7 \cdot 10^7$ antiprotons in a 0.3% momentum bite every 2 seconds, would require a 4 A 4 MeV 5 m long electron system and precooling of the antiproton beam to about $0.5\pi \mu\text{m}$ emittance. The system would be capable of higher antiproton accumulation rates, if the antiprotons were available. The technology of electron cooling systems in this energy range is unproved as yet. Another paper at this conference will address this subject more carefully⁴.

4.3. Resistive Cooling

Any energy loss mechanism which can be described by a drag force, or friction force oppositely directed to the motion of a particle, can be shown to lead to reduction of the phase space volume of a collection of the particles. For example image currents induced in neighboring walls by a particle's charge cause energy loss due to the resistivity of the walls. The details of the cooling rates are determined by the dependence of the friction force on the coordinates q_i and canonical momenta p_i describing the motion of the particle. If the friction is described by a generalized force

$$F_i = dp_i/dt \quad R_i = dq_i/dt \quad 4.4$$

then the rate of reduction of the projected phase space area V_i for the i th degree of freedom is

$$\lambda_i = -(dV_i/dt)/V_i = -(\partial F_i/\partial p_i + \partial R_i/\partial q_i) \quad 4.5$$

An example of this is the radiation cooling used in $e^+ - e^-$ storage rings. It also applies to resistive losses suffered by a particle which induces currents in resistive walls. Usually this effect is very small, but it apparently has been used successfully in Penning traps used to capture and measure the properties of individual particles. Such a method was also employed in the Astron plasma device, although the motivation was to damp collective instabilities, not phase space volume.

4.4. dE/dx Cooling

Since the very first extraction systems employed in proton synchrotrons, the "Piccioni" scheme used on the Cosmotron, it has been recognized that transverse phase space could be damped by energy loss in foils. In fact this led to the earliest discussions of methods to collect antiprotons for colliders. It has been shown that the total fractional reduction in phase space volume depends on the total fractional energy lost by a particle⁵. For beams, the energy loss to ionization of the electrons is several MeV/gm/cm² while the absorption length is about 100 gm/cm². Then for GeV beams this type of cooling is ineffective due to the absorption.

For the fixed target plasma type collector discussed above the goal is not so much to cool the phase space of the antiprotons as it is to remove the kinetic energy of the particles. Collisions with electrons, or positrons is an acceptable way to do this. Positrons are the preferable way to do this, since they are needed later in any case to make antihydrogen, and can be used to neutralize the space charge due to the antiprotons and the electrons produced. Hadron targets produce copious quantities of electrons and positrons, many times more than antiprotons, and the unused protons from the internal target can be devoted to this end. As a way of approaching this subject more closely, let us consider a collector for 4.5 GeV/c ($B\rho = 15 \text{ Tm}$) with a field of 5T at the target. Then the maximum radius is 3 m, and the volume of the device is about 10^8 cm^3 . If one month's supply of antiprotons is in the trap, the density is $4 \cdot 10^{11}$. Now suppose there are 10 times as many electrons, and sufficient numbers of positrons to achieve electrical neutrality, or a lepton density of $8 \cdot 10^{12}$. The energy loss of the antiproton is about 80 μeV per cm or about 2.4 MeV per sec. Then in one second the 5 GeV/c orbit shrinks by about 3 mm, which is slow for rapidly repeated injection. It is clear that under the assumptions above the

density, and the cooling rate will be faster at higher magnetic fields, but the injection problems will certainly be more difficult.

4.5 Radiative Cooling

Radiative cooling is too slow to cool hadrons in this energy range, however it will be important for the electrons and positrons in plasma type collectors.

¹S. van der Meer, Stochastic Damping of Betatron Oscillations in the ISR, CERN/ISR-PO/72-31

²Budker, G.I. et.al., Proc. Int. Symp. Electron and Positron Storage Rings, Atomnaya Energiya, 22, 346 (1967)

³D. Larson et.al., IEEE Proc. Nuc. Sci. NS-30, 2370, August 1983

⁴D. Larson, Paper at this Conference.

⁵K.R. Symon, D.B. Lichtenberg and P. Stehle, Bull. Am. Phys. Soc. II 344, 1956. See also MURA Report No.-126, July 1956, Unpublished

5. Potential Research and Development Areas

The following discussion of scaleup accelerator R&D was developed by the working group on accelerator issues at the RAND Workshop held October 6-9, 1987. The working group included E. Blackmore, D. Cline, R. Forward, T. Goldman, D. Larson, Y. Y. Lee, D. Peaslee, and the author.

5.1 Antiproton Production Cross Sections in Heavy Nuclei

There is insufficient data to predict yields of antiprotons from heavy nuclei over the range of proton energies of interest (25-1000 GeV). An analysis similar to that of Hojvat and van Ginneken should be undertaken with all modern data. Experiments to measure the yield in missing parameter ranges should be proposed and supported.

5.2 Energy Deposition in Heavy Metal Targets

A study should be undertaken to update codes that predict energy deposition of protons penetrating heavy targets. An analysis of available experimental data should be made, and experiments proposed to verify the predictions. The results should be incorporated into codes that are made widely available.

5.3 Positron Production in Heavy Metal Targets

Intense cold positron sources will be required for cooling of antiprotons, and for formation of antihydrogen. Production and cooling of positrons should be studied theoretically and experimentally as a component of antiproton production techniques. Existing data at national laboratories should be evaluated in detail.

5.4 Target Materials and Hydrodynamics Studies

A better theoretical understanding of the problems of target behaviour is required and hydrodynamics calculations should investigate the dependence on bulk properties of the materials such as thermal expansion coefficients, densities, Young's modulus, etc. Experimental studies should investigate the practicality of change-of state targets where the temperature rise is reduced by latent heat of fusion.

5.5 Plasma Collection Lenses

Studies should be made of larger and higher current plasma lenses than those now under development at CERN.

5.6 Large Aperture Collector Rings and Beam Transport

Collector rings with acceptances of more than $200\pi \mu\text{m}$ and $\Delta P/P > 15\%$ may be required. The optics of such rings should be studied, particularly chromaticity correction and dynamic aperture. Optics studies of beam transport systems with similar acceptances is required, to learn how to control aberrations. Engineering studies of components for these rings and beams should address fabrication problems.

5.7 Plasma Lenses for Colliders

Recent studies have indicated the potential utility of a laser actuated Bennett pinch as a useful "low β " focusing system for linear colliders. Studies should be made to explore the utility of this concept to enhance antiproton production in collider systems. Theoretical studies of nonlinear plasma effects in the relativistic particle regime are required.

5.8 Intermediate Energy Electron Cooling

Electron cooling in the energy range appropriate to antiproton collection has not yet been demonstrated. Technological demonstration of 1 Mev (magnetized) cooling beams has recently been made at Novosibirsk, and a test of higher energy (2-3 MeV unmagnetized beams) is in progress at the National Electrostatics Corporation. Support for such efforts and for theoretical studies of cold beam processes would help clarify the role electron cooling might play in advanced collectors.

5.9 dE/dx Cooling

New cooling techniques should be investigated if progress is to be made toward a milligram per year antiproton production facility. Studies needed for ionization cooling in plasma type collectors include the effect of multiple scattering on particle trajectories, mixing of various plasma layers used in the cooling process, evaluation of expected cooling times, and an investigation of the difficulties associated with separation of the cold antiprotons from the plasma.

5.10 Combined Electron and Stochastic Cooling

A novel type of cooling has been proposed by Derbenev that combines electron and stochastic cooling using an electron beam as a high gain pickup, large bandwidth amplifier, and kicker. Studies of this cooling technique should be carried out.

5.11 Passive Electronic (Resistive) Cooling

Studies should be carried out to find means to couple particle fields more closely to resistive (lossy) media to enhance energy loss and therefore cooling of particles. the use of plasma or other intermediates may allow improved performance of this cooling method.

5.12 Wideband Electronics for Stochastic Cooling

High frequency electronics and optic-microwave systems (to 100 GHz) are being developed for several uses, particularly communications and military radar. Investigations should be made to determine the utility of these developments to stochastic cooling systems.

5.13 Simulation of Collider Collectors

In order to fully simulate scaleup of antimatter quantities, schemes involving production, collection, and dE/dx cooling in the center of mass should be studied. It is essential that realistic simulation by Monte Carlo techniques be used to determine the potential for this scheme.

5.14 Intense High Repetition Rate Proton Linear Accelerators

Although proton linacs can certainly be expected to provide the necessary beam power to produce the antiproton flux, they may be called upon to do so with non-standard repetition rates and beam currents in order to accommodate to the needs of debunching, targetting, and cooling systems. In all likelihood the demands will be in the direction of high beam currents (1/2 amp), short pulse lengths (microseconds), and high repetition rates (kHz). Design studies of this type of linac should be carried out.

5.15 Intense Rapid Cycling Proton Synchrotrons

Synchrotrons offer the unquestioned advantage of lower cost . The required beam currents are about an order of magnitude above those planned for kaon facilities. Studies should be carried out of such synchrotrons, with particular emphasis on efficient high power high frequency cavities operating with strong beam loading, instabilities and injection/extraction schemes, and rapid magnet pulsing.

5.16 Modularity and Complexity Studies

Each component and each subsystem in the production system may or may not be improved by the "brute force" method of utilising many simpler subunits. Similarly, improved performance may possibly be obtained by making the subunits more complex. Examples of this are the targets, collection lenses, and stochastic cooling systems. Tradeoff studies should be performed to determine which areas are fertile for these approaches, and design studies of the subunits performed.

5.17 Scaleup of Antiproton Transport Storage Rings

The SELENA portable antiproton storage ring is designed to carry up to 10^{12} pbars from one location to another at a storage energy of 100 MeV. Extensive design is necessary to define the parameters of a similar system to carry, say, 10^{15} - 10^{17} pbars.

5.18 Future Workshops

In order to follow through on the design of the scaleup of antiproton production facilities, it is suggested that a number of miniworkshops should be held in the near future.

Figures

Antiproton Spectrum, 25 GeV p on W
1 Interaction Length Target

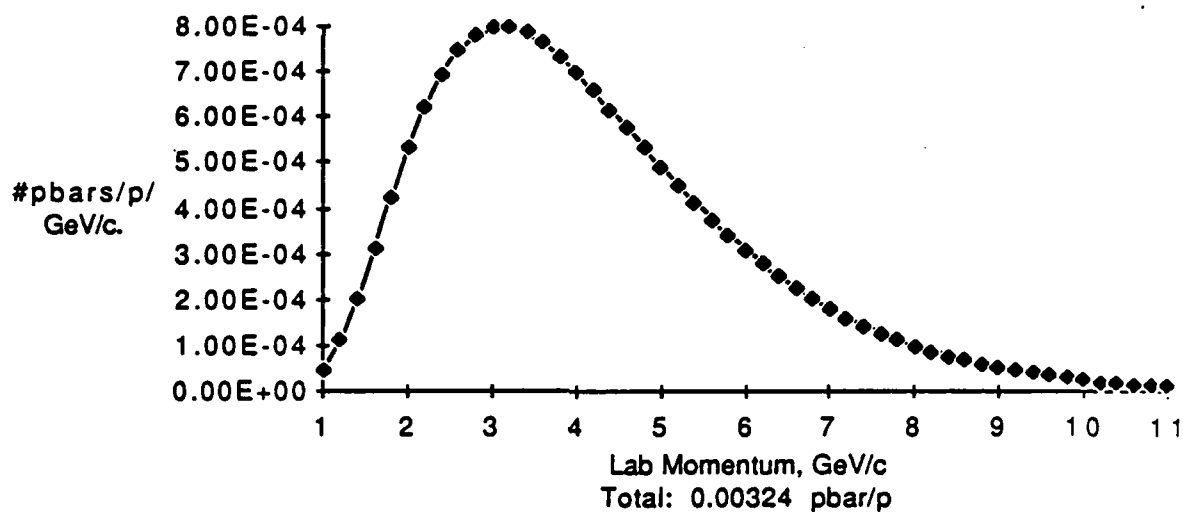


Figure 1. Antiproton Laboratory Momentum Spectrum, 25 geV/c p on W

Antiproton Spectrum, 100 GeV p on W
1 Interaction Length Target

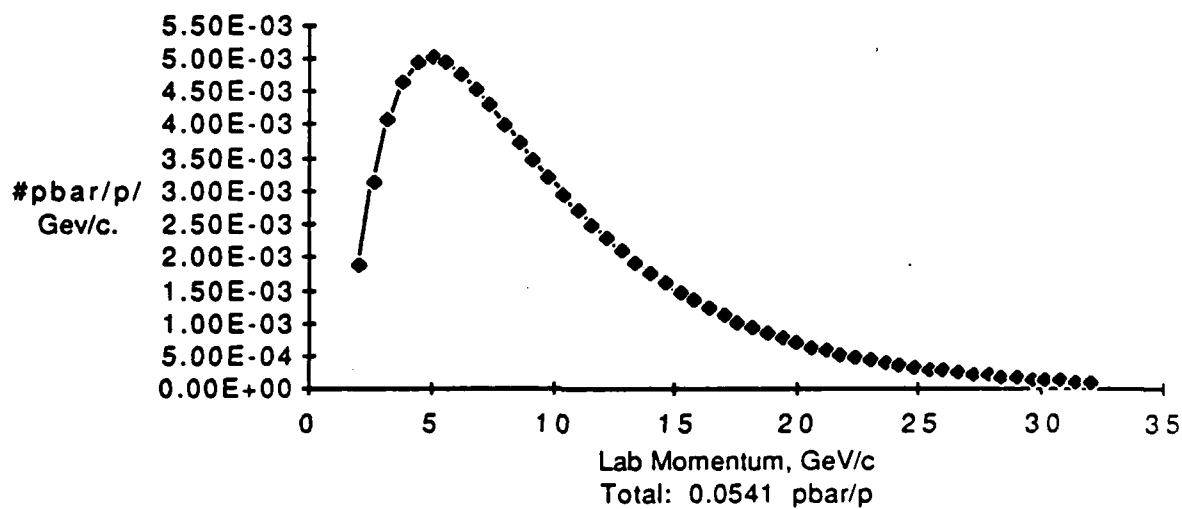


Figure 2. Antiproton Laboratory Momentum Spectrum, 100 geV/c p on W

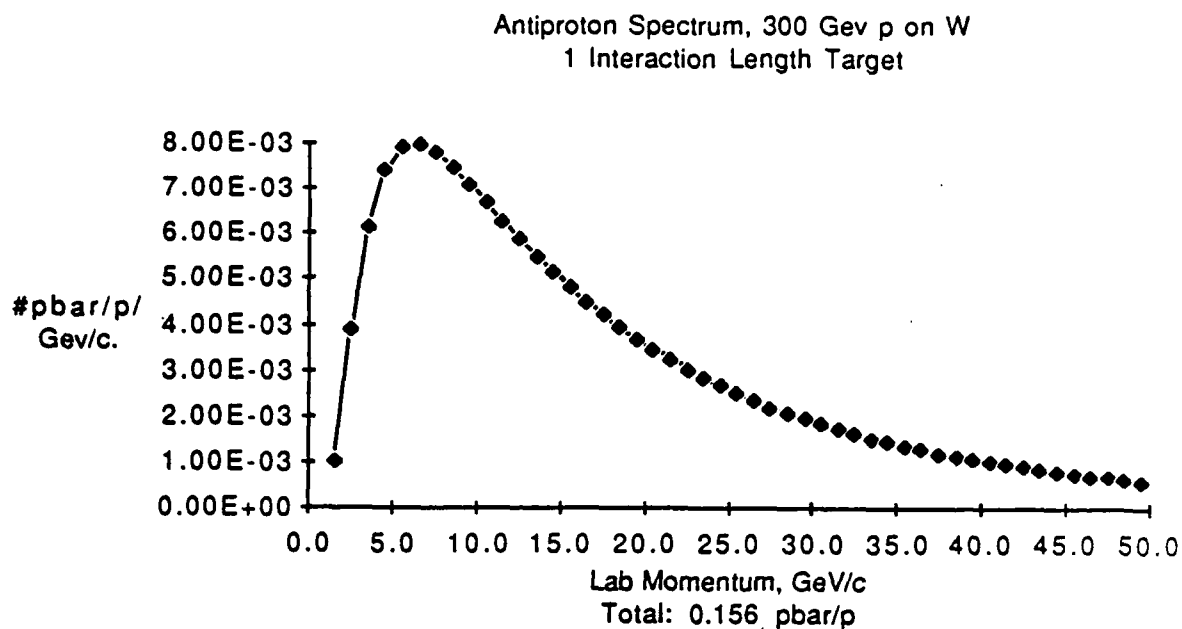


Figure 3. Antiproton Laboratory Momentum Spectrum, 300 geV/c p on W

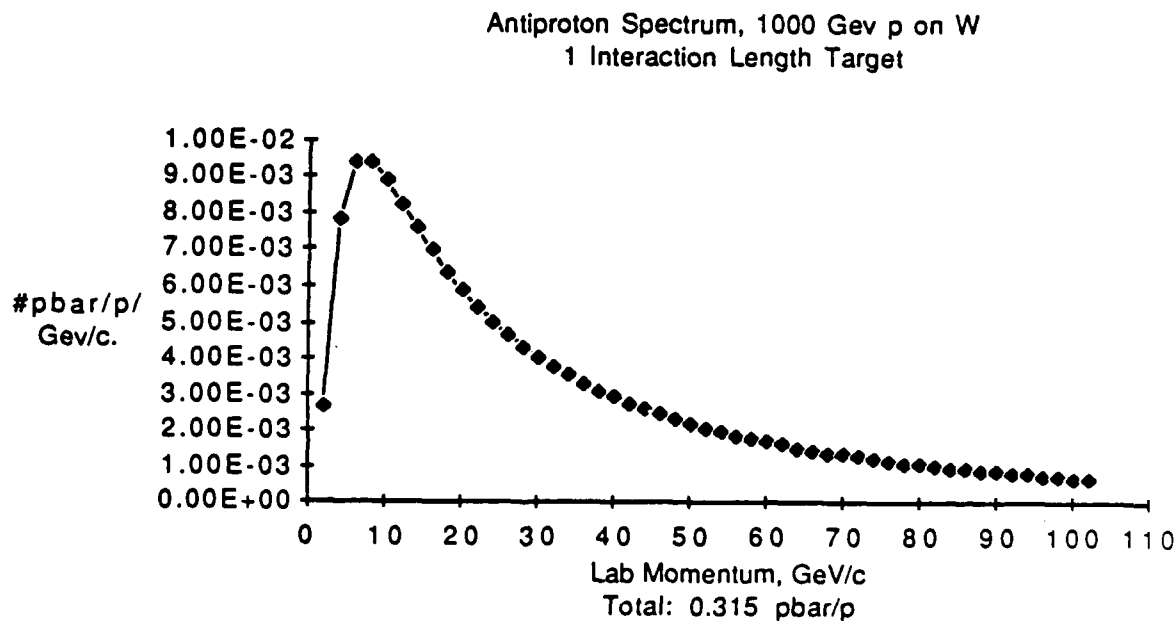


Figure 4. Antiproton Laboratory Momentum Spectrum, 1000 geV/c p on W

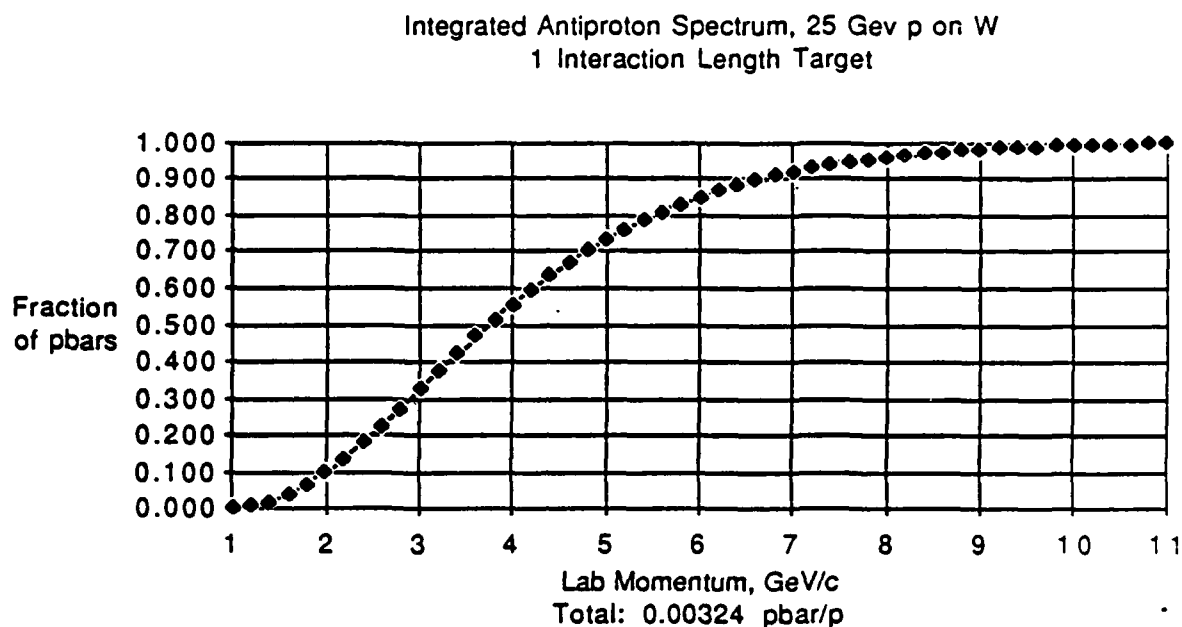


Figure 5. Integrated Antiproton Laboratory Momentum Spectrum, 25 GeV/c p on W

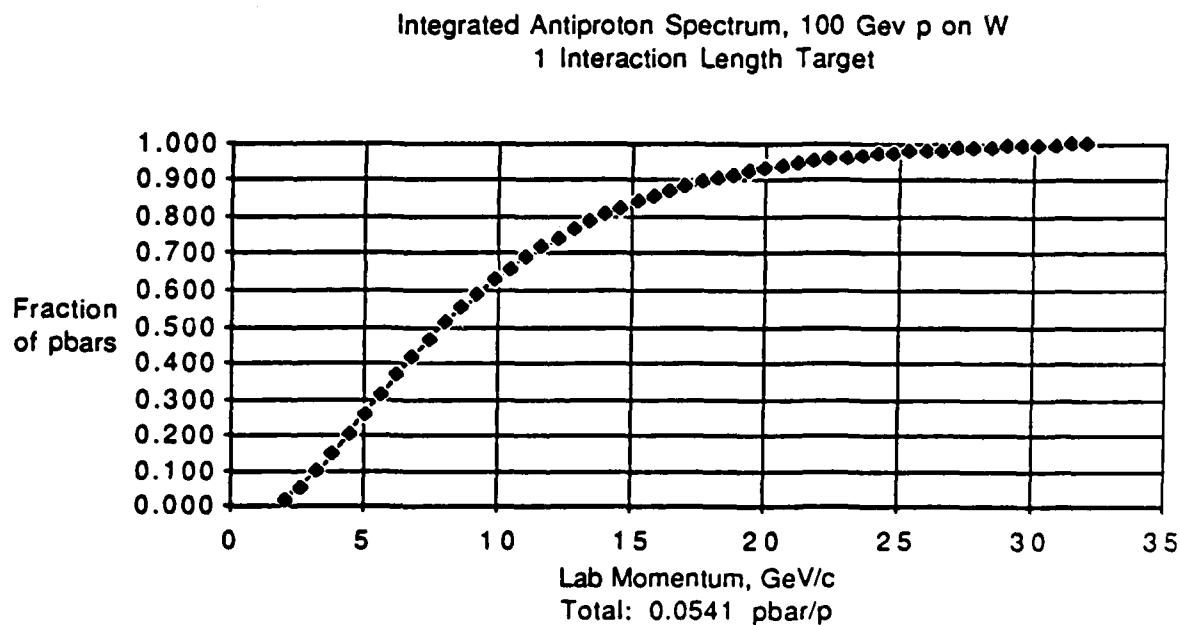


Figure 6. Integrated Antiproton Laboratory Momentum Spectrum, 100 GeV/c p on W

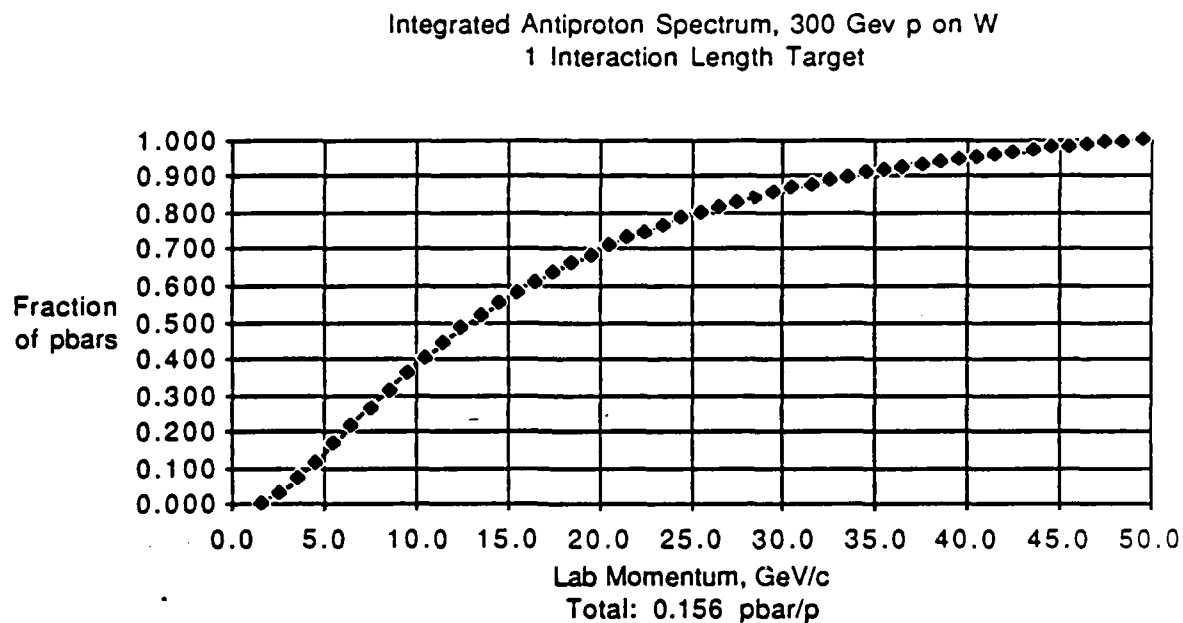


Figure 7. Integrated Antiproton Laboratory Momentum Spectrum, 300 GeV/c p on W

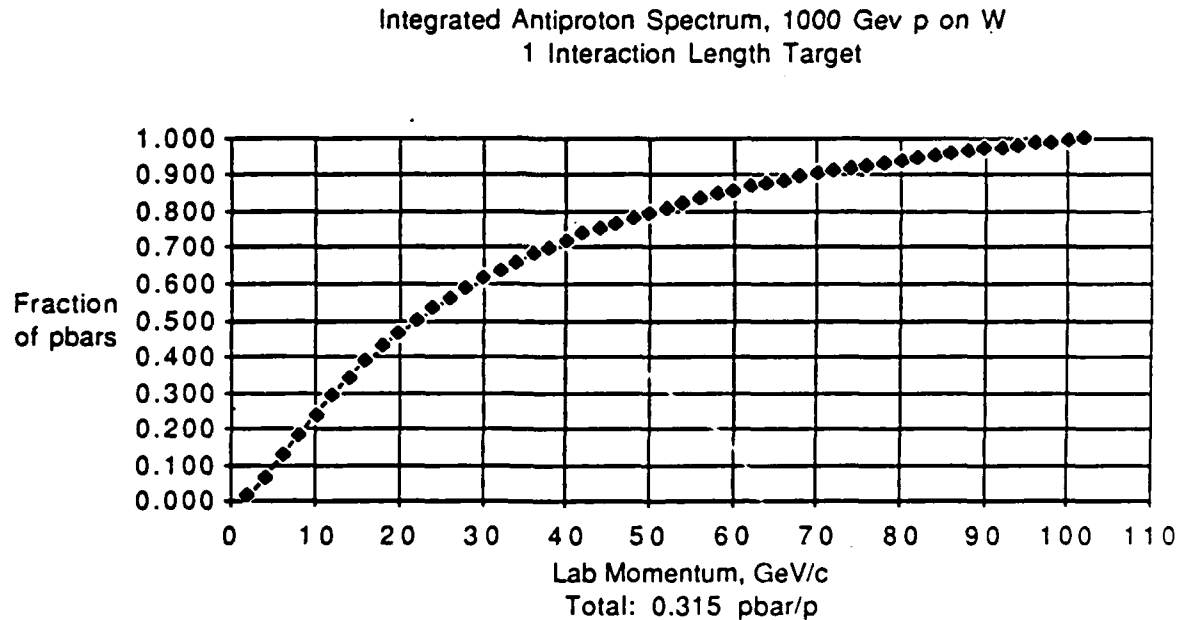


Figure 8. Integrated Antiproton Laboratory Momentum Spectrum, 1000 GeV/c p on W

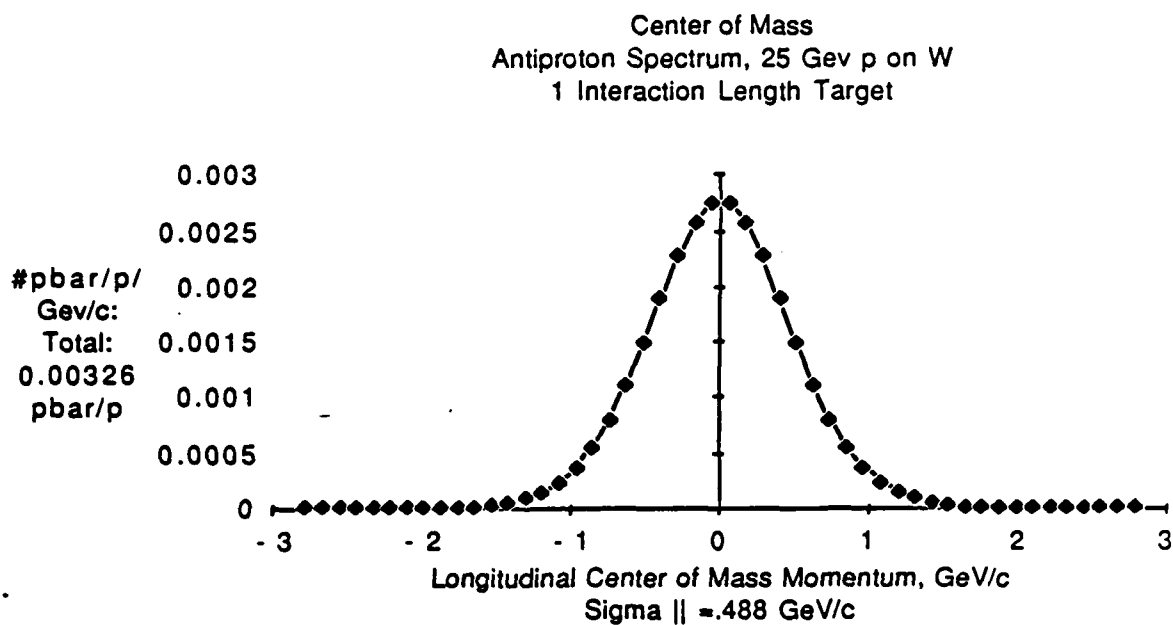


Figure 9. Longitudinal Antiproton Center of Mass Momentum Spectrum, 25 geV/c p - W

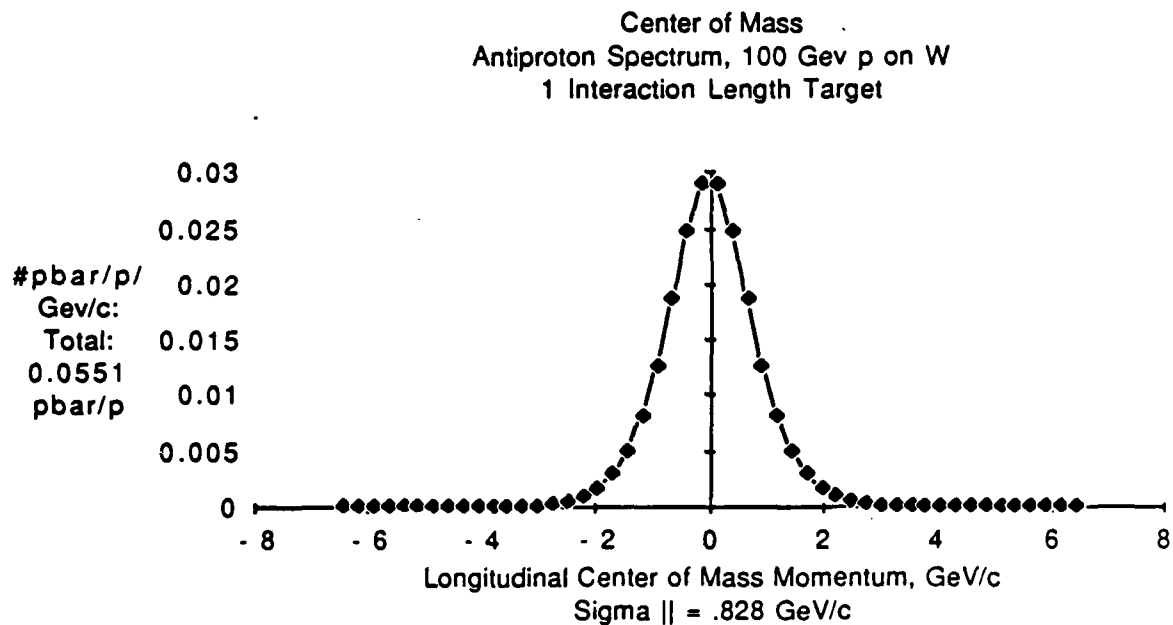


Figure 10. Longitudinal Antiproton Center of Mass Momentum Spectrum, 100 geV/c p-W

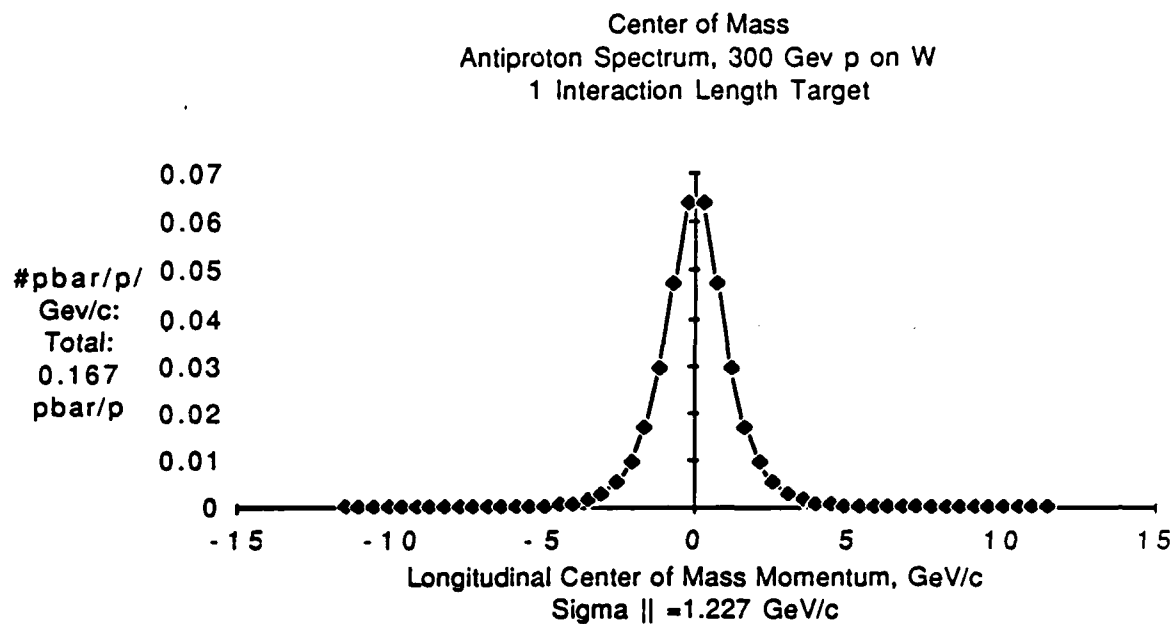


Figure 11. Longitudinal Antiproton Center of Mass Momentum Spectrum, 300 geV/c p-W

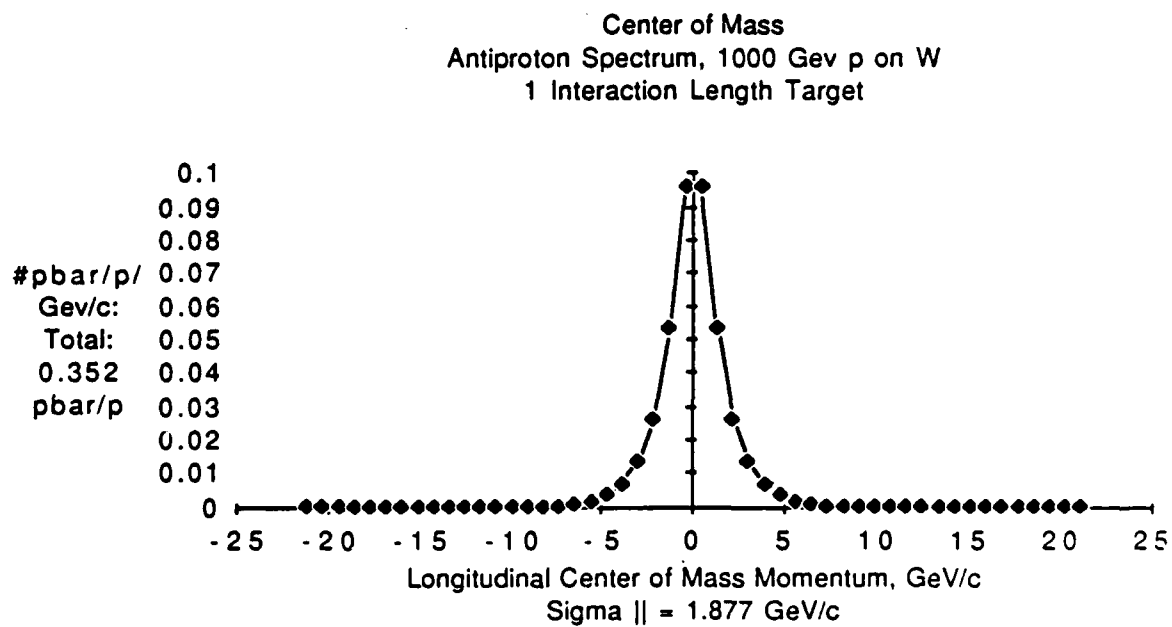


Figure 12. Longitudinal Antiproton Center of Mass Momentum Spectrum, 1000 geV/c p-W

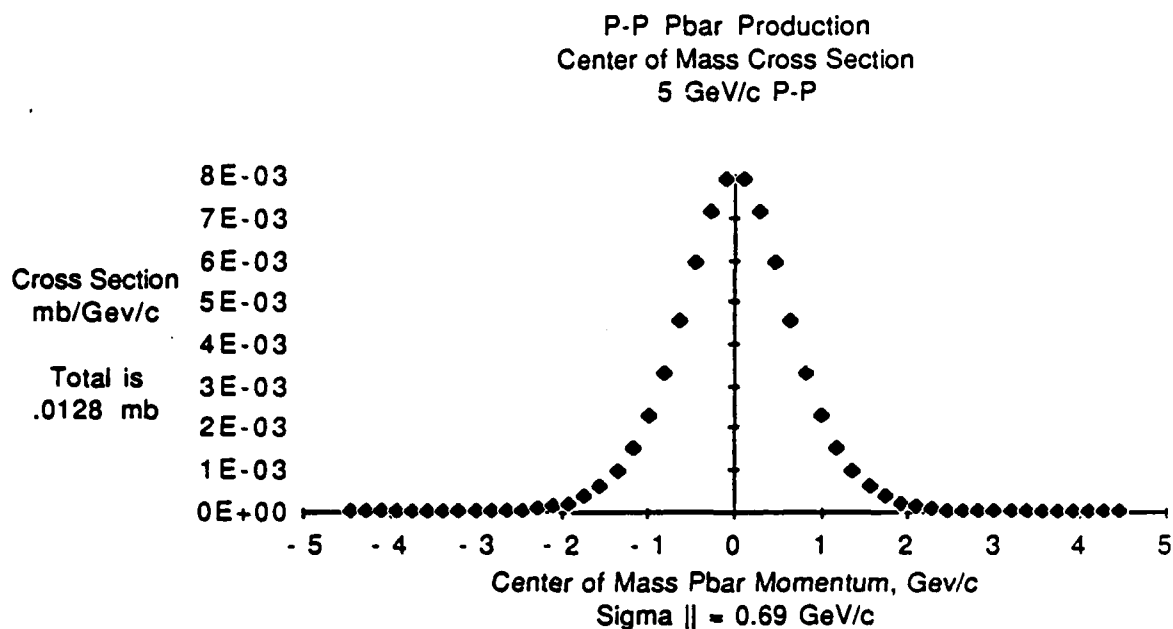


Figure 13. Antiproton Cross Section vs C. M. Longitudinal Momentum, 5 geV/c p on p

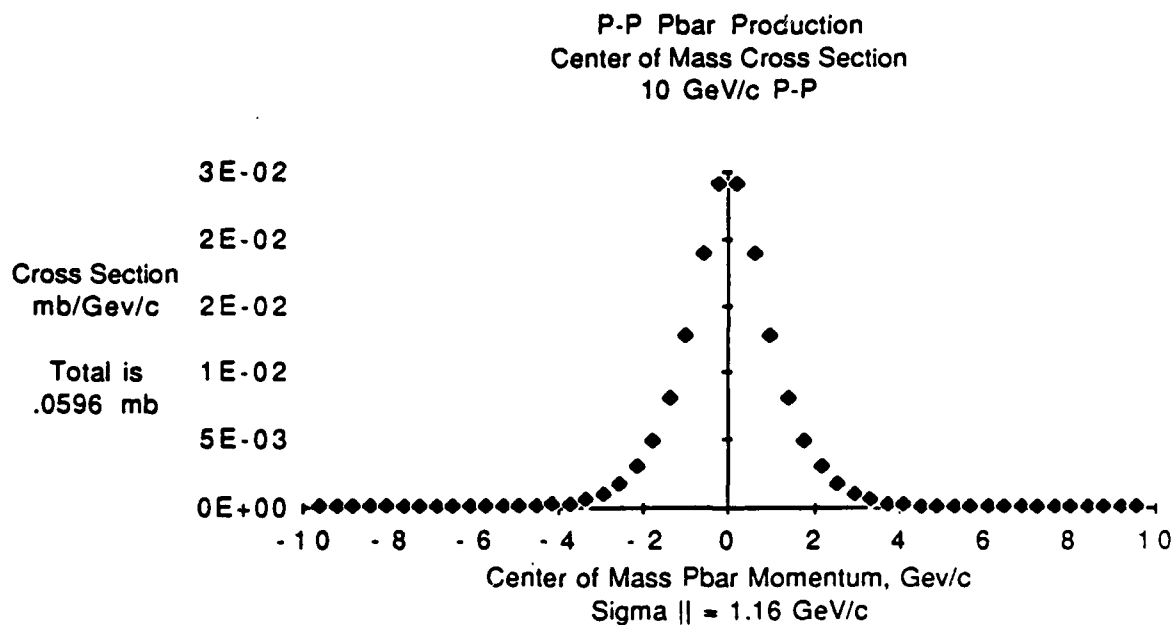


Figure 14. Antiproton Cross Section vs C. M. Longitudinal Momentum, 10 geV/c p on p

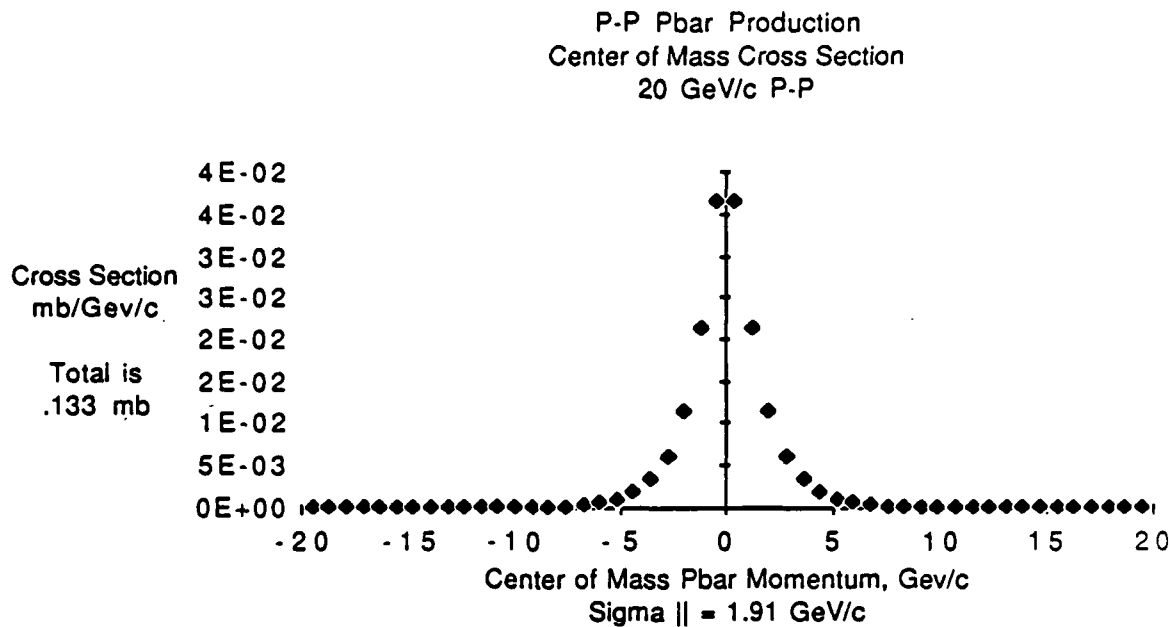


Figure 15. Antiproton Cross Section vs C. M. Longitudinal Momentum, 20 geV/c p on p

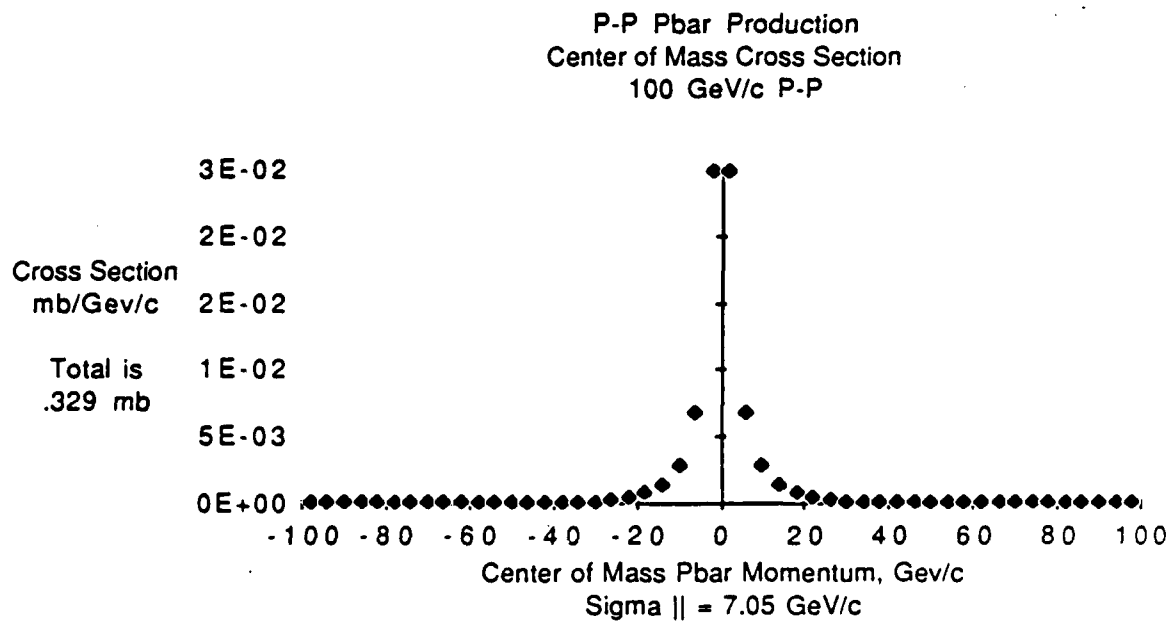


Figure 16. Antiproton Cross Section vs C. M. Longitudinal Momentum, 100 geV/c p on p

Scaleup of Antiproton Production and Collection

D. J. Larson

UCLA - Department of Physics

405 Hilgard Ave., Los Angeles, CA 90024

ABSTRACT

The possibility of increasing antiproton accumulation by several orders of magnitude is discussed. An antiproton accumulator ring is proposed that employs a fixed target for production of the antiprotons, and uses large scale electron cooling for the accumulation process. This system is evaluated in detail, and a set of parameters are given that could accomplish real time accumulation of more than 10^{14} antiprotons per second. Other possible antiproton production and accumulation schemes are discussed briefly.

INTRODUCTION

Background of Electron Cooling

Electron cooling was originally proposed by Budker in 1966¹. The basis for his proposal came from work done by Spitzer² (1956) who showed that warm ions come to equilibrium with cooler electrons in a plasma. Due to the much larger mass of the ion, the final rms speed of the ions is much less than that of the electrons. Budker realized that an electron beam is simply a moving electron plasma. By superimposing an ion beam on a comoving electron beam, warmer ions are cooled by the electron beam. A representation of the electron cooling process is shown in Figure 1.

In the 1970's electron cooling was demonstrated to be an extremely good way of increasing the phase space density of proton beams. Cooling times of between one and five seconds were reported by experiments at Novosibirsk³, CERN⁴, and Fermilab⁵. Present experiments are under way at Indiana University⁶ and in

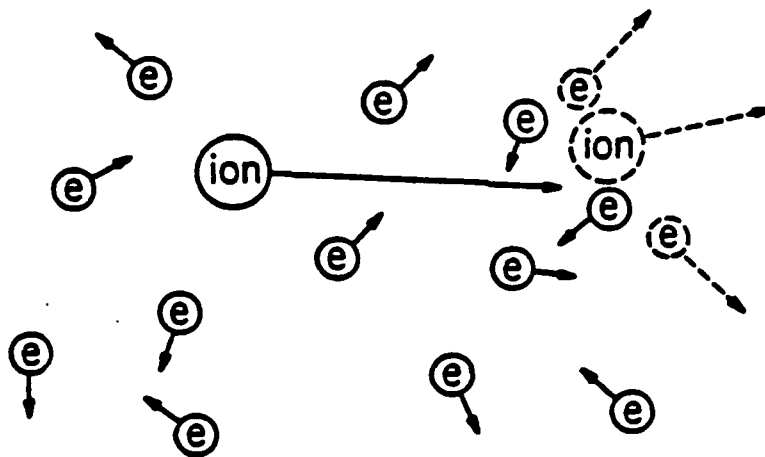
Madison, Wisconsin⁷ that plan on extending the use of electron cooling to ion and antiproton beams, respectively.

Possible Production and Collection Schemes

Antiprotons are typically produced by impinging an energetic proton beam upon a high Z fixed external target. This means of production has the advantage of using the highest density target material possible, and does not require recirculation of any particle beams. In addition to fixed external targets, two other possibilities exist for antiproton production. Fixed internal targets would have the advantage of fully utilizing the proton beam, as those protons that pass through the target without significant interaction could be recycled back to the target on the next pass. This approach has the drawback that the proton beam must be kept in the ring, despite the considerable beam emittance growth experienced as the beam passes through the target. Colliding beams have been proposed as an alternative means of antiproton production. Here, the problem of maintaining beam integrity is even more severe, as both the proton and target beams must be recycled. Also, the large decrease of the target density adversely affects the antiproton production rate. For these reasons, this paper will be devoted to issues involved in the scale up problems associated with fixed external target production and collection of antiprotons.

The present antiproton accumulators at Fermilab and CERN use *stochastic cooling* to obtain the necessary antiproton densities to operate these high energy physics facilities. While this process is sufficient to obtain enough antiprotons to operate the colliders, *stochastic cooling* is best utilized on beams with relatively low numbers of particles. Another means of particle beam cooling, *electron cooling*, is independent of the number of particles being cooled, and may prove to be effective in increasing the collection rate of antiprotons. *Electron cooling*, as described above, relies on coulomb collisions to slow down the antiprotons. A similar effect can be accomplished by using a plasma to slow down the particles. This paper will evaluate the parameters of *electron cooling* techniques for antiproton collection, and discuss some of the difficulties associated with plasma

Spitzer (1956)



Rest Frame – Slowing of an
Ion in a Plasma



Lab Frame – Comoving Beams

γ^{-2} , but no
I-dependence

Budker (1966)

Figure 1 – Schematic Representation of the Electron Cooling Process

cooling techniques.

TIME REQUIRED FOR ELECTRON COOLING OF ANTIPROTONS

Derivation of the Cooling Time Expression

The process of electron cooling will be evaluated in a frame moving along with the electron beam – in this frame the electron beam appears as a stationary electron cloud. The electron density in the moving frame is given by the following expression.

$$n_e = \frac{I}{\gamma \pi r^2 \beta c e} \quad (1)$$

In equation (1) I is the electron current measured in the lab frame, c is the speed of light, e the electron charge, and r the radius of the electron beam. Note that the factor of γ arises from the length contraction experienced in transforming from the lab frame. In the above equations, and for the remainder of this paper, β and γ (unprimed and without subscripts) are the usual relativistic quantities, β is the velocity of the particle divided by the speed of light, and γ is the total energy of the particle divided by the rest mass of the particle.

A rough estimate of the cooling time may be obtained by using the equation for the slowing down of a particle beam in a plasma as found in the NRL Plasma Formulary. (Originally derived by Spitzer.²)

$$\frac{dv}{dt} = -\nu_s v \quad (2)$$

The cooling time is approximately $\tau_s = 1/(\nu_s)$. For the case where the antiprotons have much more energy than the average electron energy in the plasma, ν_s may be approximated by the following equation.

$$\frac{\nu_s}{n_e \lambda_e} = 1.7 \times 10^{-4} E^{-3/2} \quad (3)$$

In equation (3) E is the energy of the antiprotons in eV, n_e is the electron density in cm^{-3} , and λ_e is the Coulomb log. Combining equation (1) with equation (3)

leaves the following expression for the cooling time in the moving system.

$$\tau_e = \frac{\beta\gamma\pi r^2 c e E^{3/2}}{(1.7 \times 10^{-4}) I \lambda_e} \quad (\text{moving frame}) \quad (4)$$

When evaluating the cooling time in the lab system an additional factor of γ appears due to time dilation, as well as a factor of η due to the fact that only a fraction of the cooling ring (η) is occupied by the electron cooler. The cooling time in the lab frame is thus:

$$\tau_e = \frac{\beta\gamma^2\pi r^2 c e E^{3/2}}{(1.7 \times 10^{-4}) I \lambda_e \eta} \quad (\text{lab frame}) . \quad (5)$$

Initial Velocity Distributions in the Electron Cooling Sector

The initial velocity distributions of the electrons and antiprotons will be evaluated in a frame moving along with the electron beam. The equations that make the transformation from the lab to the moving frame are:

$$\beta'_{\parallel} = \beta \frac{\Delta p}{p} \quad \text{and} \quad \beta'_{\perp} = \theta_{\perp} \beta \gamma . \quad (6)$$

$$\text{Now,} \quad \theta_{\perp} = \frac{\epsilon}{\pi r} \quad \text{so} \quad \beta'_{\perp} = \frac{\epsilon \beta \gamma}{\pi r} . \quad (7)$$

The perpendicular velocity of the particles is determined by the beam emittance and space charge beam expansion of the two beams. The parallel velocity is determined by the momentum spread of the beams. For this reason it is necessary to estimate the electron and antiproton beam emittances and momentum spreads in order to determine the initial velocity distributions. For the study conducted here, beam energies corresponding to $\gamma = 10$ will be used. This is the operational energy of the Fermilab antiproton source, a logical starting ground.

The thermal emittance ϵ of a beam is defined to be the area in phase space in which 90% of the beam trajectories lie. The only contribution to the perpendicular velocity of the electrons is assumed to be the perpendicular thermal velocity of the electrons as they are emitted from the cathode. The area of the phase space ellipse is

$$\epsilon = \pi x_{\max} \theta_{90} . \quad (8)$$

In evaluating ϵ , it is assumed that the cathode emits electrons uniformly over its surface. Thus x_{\max} is the radius of the cathode. The quantity θ_{90} is defined to be the angle with respect to the beam axis that contains 90% of the electron trajectory angles.

$$\theta_{90} = p_{\perp}/p_{\parallel} = m_e v_{\perp 90} / \beta \gamma m_e c \quad (9)$$

$v_{\perp 90}$ is evaluated by assuming a one-dimensional Maxwell distribution with a cathode temperature of $kT = 0.1$ eV. For a cathode radius of 10 mm the electron beam emittance is about 1.1π mm-mr. This cathode radius is appropriate for the production of a four amp electron beam.

The electron beam current of four amperes used here corresponds to the electron current of a single Pelletron accelerator. To do electron cooling of antiprotons in real time, many such beams will be required. The emittance of the cooling beams will be larger as more beams are employed. Since the emittance is proportional to the radius of the cathode, and the current proportional to the square of the radius, the emittance will scale as the square root of the electron current. The emittance of the electron beam is given by the following expression:

$$\epsilon_e = 0.57 I^{1/2} \pi \text{ mm} - \text{mr} \text{ (I in amps)} \quad (10)$$

One contribution to the longitudinal velocity of the electron beam comes from the space charge voltage depression of the beam at its center. The space charge depression is evaluated using the simple expression

$$V = \frac{30I}{\beta} \quad (11)$$

and for a four amp beam at 4.5 MV this is about 120 Volts. Voltage ripple in the electron gun power supply may increase the parallel velocity in the moving system, a good estimate is about 150 Volts. An estimate for the momentum spread in the electron beam is thus $(\Delta p)/(p) = 2 \times 10^{-4}$. When many electron beams occupy the cooling region there will also be a space charge voltage depression from one beam to the next. This space charge voltage depression does not produce a momentum spread between beams, since if it did, the voltage of the affected beam could be changed to compensate.

The emittance of the antiproton beam is determined by the emittance of the antiproton source. It is assumed that the antiprotons are produced by the hadronic shower resulting from impinging a proton beam on a high Z material. The Fermilab antiproton source produces about 10^8 antiprotons per pulse in this fashion, with one pulse arriving every two seconds. The transverse emittance of the pulse is 20π mm-mr, and the momentum spread is $\Delta p/p = 3\%$. The debuncher ring reduces the momentum spread to $\Delta p/p = 0.2\%$, accomplished by a phase space rotation of the antiproton bunch. For an antiproton source to operate in real time, the momentum spread must be reduced further, by a factor of five, to $\Delta p/p = .04\%$. For the design goals of this conference, 10^{14} antiprotons per second are desired, representing an increase in production by a factor of 10^6 . Since the emittance of the antiproton beam scales as the radius of the targeted material, and the production scales as the area of the targeted material, two orders of magnitude can be obtained by increasing the initial antiproton emittance to 200π mm-mr. Two more orders of magnitude can be obtained by increasing the size of the accumulating ring from the Fermilab circumference of

500 meters to a circumference of 50 kilometers. The final two orders of magnitude will be assumed to come from advances made in target technology, allowing for more protons to impinge the target, and hence more antiproton production.

Now that the emittances and momentum spreads of the two beams are estimated, the velocity distributions of the two beams may be obtained. The equations that make the relativistic velocity transformation to the moving frame are (6) and (7), which indicate that the longitudinal velocity of the antiprotons in the moving frame is 1.2×10^5 m/s. The perpendicular velocity is inversely proportional to the beam radius. Therefore it makes sense to use a very large beam radius in the cooling region. Assuming a beam radius of 5 meters, the perpendicular velocity of the antiprotons in the moving system is 1.2×10^5 m/s. For this set of parameters the energy of antiprotons in the moving frame is 75 eV.

Required Electron Cooler Parameters For Real Time Cooling

It is necessary to cool the initial antiproton beam in one second so that subsequent antiproton batches can be injected and cooled. By setting τ , equal to one second in equation (5), and evaluating the expression for beam energies corresponding to $\gamma = 10$, the required electron current is 150 kiloamps. (For this example the energy of the antiprotons is 75 eV, the radius of the beams is 5 meters, the coulomb log is estimated to be 15, and the proportion of the ring devoted to electron cooling is 66%.) It has been shown in prior work⁷ that for the Fermilab antiproton source the cooling rate is enhanced by about a factor of 1.5 over that predicted by equation (5). This implies that real time cooling of antiprotons will require an electron cooling current of about 100 kiloamps. (This enhancement comes from the fact that betatron oscillations periodically decrease the antiproton velocity, increasing the cooling effectiveness.)

Scaling Issues of an Electron Cooled Antiproton Source

In the moving frame the energy of the antiprotons is given by the nonrela-

tivistic expression $E = (1/2)mv^2$. If the velocity of the antiprotons in the moving system is primarily transverse, the antiproton energy in the moving system can be given in terms of the initial emittance of the antiproton beam. The equations that make the velocity transformation from the lab frame to the moving frame are equations (6) and (7).

By using the normalized beam emittance, $\epsilon_n = \beta\gamma\epsilon$, in equation (7), and assuming that the perpendicular velocity is the dominant contribution to the antiproton velocity in the moving frame, the following expression is generated for the antiproton energy as evaluated in the moving system:

$$E = \frac{1}{2}mv^2 = \frac{1}{2}mc^2\beta_{\perp}^2 = \frac{1}{2}mc^2\left(\frac{\epsilon_n}{\pi r}\right)^2. \quad (12)$$

This leaves the equation for the cooling time in the following form.

$$\tau_s = \frac{\beta\gamma^2 c^4 m^{3/2} e \epsilon_n^3}{2^{(3/2)} (1.7 \times 10^{-4}) \pi^2 r I \lambda_e \eta} \quad (\text{lab frame}). \quad (13)$$

Equation (13) indicates that the cooling time for electron cooling scales as $\beta\gamma^2$. If the normalized emittance is replaced by the emittance in expression (13) the cooling time scales like $\beta^4\gamma^5$. This scaling law has been often quoted and has led to the conclusion that electron cooling works best at low energy. However, the use of non-normalized emittance in the cooling time expression is not elucidating of the physical process involved. When beams are accelerated it is the normalized emittance that stays constant. Thus the true relativistic scaling of the cooling time is as $\beta\gamma^2$. The additional factors of β and γ only come into play if one is accepting a larger initial normalized emittance to be cooled.

Once the energy of antiproton production is chosen, the following scaling law may be used for the cooling time.

$$\tau_s \propto \frac{\epsilon^3}{r I \eta} \quad (14)$$

Intermediate energy electron cooling has been studied in detail for the case of

the Fermilab antiproton accumulator⁷. In that study the electron cooling is assumed to be done at the completion of the stochastic cooling process. Upon completion of stochastic cooling, the antiproton beam has an emittance of 2π mm-mr, and the beam radius in the cooling region is about five millimeters. In the study it is assumed that 2% of the accumulator ring would be devoted to an electron cooling straight, and that a four ampere electron beam would be used for cooling. The study obtained a predicted cooling time of about 850 seconds.

In order to cool an initial antiproton emittance of 200π mm-mr, equation (14) indicates that cooling will proceed at a rate 10^6 times slower than for the Fermilab case, where $\epsilon = 2 \pi$ mm-mr. This would indicate a cooling time of just under 10^9 seconds. The increase in beam radius by a factor of 1000, in η by a factor of 33, and in beam current by a factor of 25,000 is what allows the cooling time of one second to be obtained.

TECHNOLOGICAL ISSUES

Required Vacuum in the Cooling Ring

As the antiproton beam recirculates in the cooling ring it will undergo emittance growth due to multiple scattering with residual ions present in the system. This beam growth is dependent upon the vacuum attained in the cooling ring. The equation for emittance growth is

$$\frac{d\epsilon}{dt} = \pi \beta_L \frac{d\theta^2}{dt}. \quad (15)$$

The Particle Properties Data Booklet has the following the formula for rms angular beam growth due to multiple scattering.

$$\Delta(\theta^2) = \left(\frac{15 \text{ MeV}}{p \beta c} \right)^2 \frac{L}{L_R} \quad (16)$$

In equation (16) L_R is the radiation length of that material doing the scattering. For a pressure of 3×10^{-10} Torr, $L_R = 10^{15}$ m. For a 5 meter beam radius

and an emittance of 200π mm-mr, the lattice beta function is 125,000 meters. Replacing the length of the trajectory, L , by the velocity of the beam yields an equation for the emittance growth of the antiproton beam as a function of time.

$$\frac{d\epsilon}{dt} = \frac{\pi(1.25 \times 10^5 \text{ m})(3.0 \times 10^8 \text{ m/s})}{10^{15} \text{ m}} \left(\frac{15}{9000}\right)^2 = 1\pi \times 10^{-7} \text{ m/s} \quad (17)$$

The initial electron cooling rate is much larger than the beam growth rate due to multiple scattering. As the cooling proceeds, the cooling force becomes even stronger due to the inverse relationship between the cooling force and the antiproton beam emittance (velocity), therefore beam emittance growth due to multiple scattering should not represent any problem here.

Technological Progress

In order to do electron cooling in the MeV energy range, DC electron beam sources must be obtained that operate with ampere current intensities at an energy of 1 to 10 MeV. Work toward development of such a system has been underway for the past five years. A collaborative effort involving personnel from National Electrostatics Corporation, the University of Wisconsin, and Fermilab has led to the construction of a 3 MeV electrostatic Pelletron accelerator⁸ that has recently shown successful operation with a DC current of 30 milliamps. This system was originally intended as an electron cooler for antiproton sources.⁹ Operation of this system relies upon recirculation of the accelerated electron beam which effectively recovers a large portion of the beam energy. Figure 2 shows a schematic of the electron cooler test set up.

The experimentally obtained current of 30 milliamps should not be viewed as a limit. The machine had only been operated sparingly over a three month period when this result was achieved. Indeed, the optics design¹⁰ and bench test of the critical system components¹¹ both indicate that ampere intensities should be achievable with this technology.

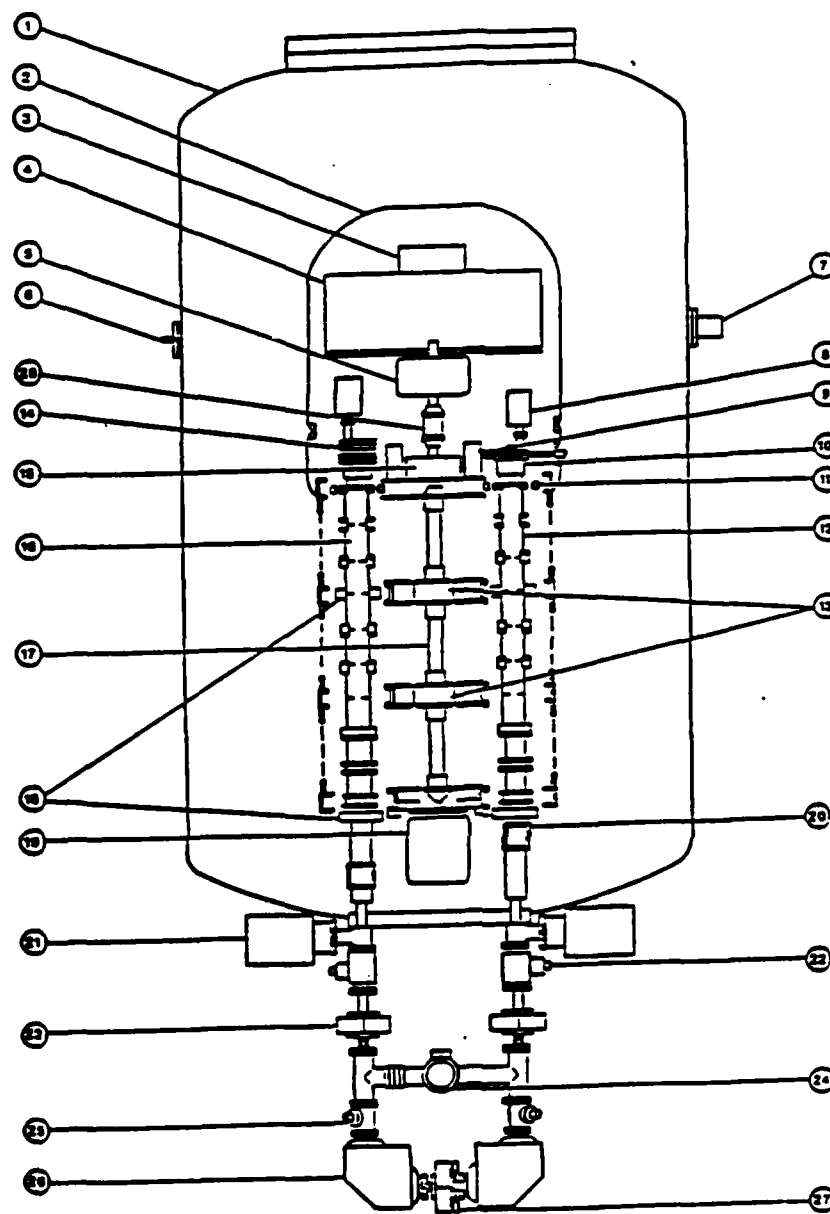


Figure 2 - Schematic of Pelletron Recirculation Test Facility

Electron Beam Requirements

The electron current required to do real time cooling of antiprotons has been stated above to be 100 kiloamps. Since the Pelletron accelerators have design currents of a few amperes, many parallel electron beams must be used in the cooling straight. These beams will enter and exit the cooling straight by passing through a magnetic dipole. (Due to the large mass of the antiprotons, this dipole will not affect the antiproton trajectories.) Since the antiproton cooling ring is estimated to be 50 kilometers in length, each of the electron beams must also propagate this distance. Two problems are associated with such transport, emittance growth and space charge dominated transport optics.

The emittance growth can be calculated by an analysis similar to that done above for the antiproton beam. With the electron beamlets assumed to be one centimeter in radius, and an initial emittance of 1π mm-mr, the expression is now:

$$\frac{d\epsilon}{dt} = \frac{\pi(100 \text{ m}) (3.0 \times 10^8 \text{ m/s}) \left(\frac{15}{5}\right)^2}{10^{15} \text{ m}} = 2.7\pi \times 10^{-4} \text{ m/s} \quad (18)$$

Since the transit time for the electron beam is about 0.2 milliseconds, the emittance growth experienced by the electron beam should not be a problem in the recirculation.

A complete study of the electron beamlet optics is a very complicated issue, and will not be attempted here. Each beamlet will have its centroid steered due to the space charge of the other beamlets, as well as expanding due to its own space charge and emittance. An approximation of the overall situation can be done by assuming the electron cooling to be done by one continuous 100 kiloamp beam. Space charge expansion of such a beam causes the outer edge to expand from a waist. If the beam radius at the waist is five meters, after a twenty meter drift the beam size is 5.37 meters, and the divergence at the beam edge is about 3%. The average divergence of the beam edge over the entire drift is half this,

and the average over the entire electron beam is one third of this, or 1%. Since the antiproton thermal divergence is .004%, the space charge expansion of the electron beam is a very important consideration in the cooling process, as the average antiproton velocity is now less than the electron average velocity. The electron beam must be focused every five meters to keep the divergence small enough to allow cooling to proceed. If the space charge can be neutralized, this would no longer pose a problem. One possibility is to use alternate electron and positron beamlets in the cooling region. Since the positron beams can not be generated by thermionic emission, they too would require electron cooling, and would need regeneration over time. The complicated problem of focusing the cooling beams is left for later study.

PLASMA COOLING OF ANTIPROTONS

Use of a plasma or gas may prove to be useful in precooling the antiprotons prior to the onset of the electron cooling process. Any emittance decrease achieved in this way would help a great deal, as indicated by equation (14). The time scale for the slowing down of the antiprotons in the plasma can no longer be evaluated using the simple expression given by the NRL Plasma Formulary, as the antiprotons are now at relativistic speeds with respect to the plasma electrons. Confinement of 10 GeV antiprotons in the initial trap, as well as the problem of keeping the orbits from reentering the target material seem to be difficult issues in this scheme.

Using a plasma surrounding a beampipe to cool antiprotons in the colliding beam mode has an additional difficulty. If the antiprotons are intended to be confined by a solenoidal field, they will make one circular path and reenter the beampipe. Thus, the slowdown will predominantly occur in the beampipe, and the antiprotons will stop in the beampipe. If the plasma is contained within the beampipe, the multiple scattering emittance growth of the colliding beams will be difficult to handle. Lastly, if the antiprotons are stopped in a plasma, there must be a means found to remove them from the plasma.

Using a plasma or gas section within the beamline will not serve to cool the beam. The cooling accomplished by coulomb collisions will be more than offset by emittance growth due to multiple scattering. A 10^{18} cm^{-3} plasma corresponds to a pressure of about 30 Torr, leading to a radiation length of 10^4 meters. This radiation length leads to the following expression for multiple scattering emittance growth.

$$\frac{d\epsilon}{dt} = \frac{\pi(1.25 \times 10^5 \text{ m}) (3.0 \times 10^8 \text{ m/s}) \left(\frac{15}{9000}\right)^2}{10^4 \text{ m}} = 1\pi \times 10^4 \text{ m/s} \quad (19)$$

Since the initial antiproton emittance is less than 10^{-3} m-r , the emittance growth due to multiple scattering will occur over of time scale of 10^{-7} seconds.

TOPICS FOR FUTURE CONSIDERATION

Instabilities And Lattice Design

This document has made no mention of the lattice design for the antiproton accumulator ring. A design must be found that has tunes off resonant values, and still incorporates the large beta insertion sections necessary for the electron cooling. In addition, the cooling process will tend to make the antiproton beam shrink in size. This decrease in beam size will cause an increase in the relative space charge contribution to the beam envelope evolution, and will cause a tune shift to occur during the cooling process. This space charge induced tune shift must be small enough so that the antiproton beam does not pass destructive resonances as it cools.

There are many other considerations that need be mentioned. Nothing has been calculated about the various instabilities that may arise, intrabeam scattering and the Z/n instability may be two of the most troubling. The electron cooling force does mitigate against the emittance growth resulting from these factors, but work needs to be done in this area before quantitative statements can be made. Injection and extraction have not been looked at. Electron cooling has never been experimentally tested under these conditions, and there is the

question of whether it can go this high. Plasma instabilities may appear at these densities.

Equilibrium Emittance and Additional Cooling

To do a realistic estimate of the final emittance obtainable in the antiproton accumulator proposed here, studies should be done that include the effect of intrabeam scattering on the final emittance. Also, the beam lattice must be investigated in the presence of space charge effects from the cooling beams, as well as the self space charge. Lastly, more must be known about the electron beam behavior, as it is the angular spread of the electron beam that determines the final angular spread of the antiproton beam. Each of these topics are areas for further research.

When the beam reaches equilibrium in the first antiproton accumulator, it may be sent to additional electron cooling stages. The large decrease in emittance obtained in the first cooler will allow cooling in subsequent stages to proceed with much less stringent requirements on the parameters of the system. As an example, if a 100 fold decrease in emittance is obtained in the first cooler, a second cooler of the same size would only require 1/10 of an ampere to do the cooling in the same amount of time. Since the electron beam current can be reduced, so can the equilibrium emittance obtainable in subsequent stages.

CONCLUSION

Electron cooling of antiprotons may prove to be a possible way to accumulate and cool enough antiprotons to make milligram per year levels. One possible scenario is to use a dedicated cooling ring 50 kilometers in circumference, with electron cooling beams of 100 kiloamp intensities. Even with such intense electron beams advances must be made in target survival and initial production to realize the milligram per year goal. The initial emittance of the antiproton beam assumed here is a factor of ten less than that obtained by simply scaling up the size of the targeted area over what is presently obtainable. Also, the initial mo-

momentum spread of the antiproton beam is a factor of five less than that of existing devices. Since the time required for electron cooling scales as the cube of the velocity of the antiprotons as evaluated in a frame moving with the beam, these improvements are critical to the success of this technique. On the other hand, if further increases in initial antiproton densities are possible, electron cooling will allow for further gains in accumulation.

Many topics need further study. Instabilities may create difficulties. A lattice design for the antiproton ring must be developed including the effects of space charge. The optics of the electron beam systems necessary for the cooling must be developed. A full study of the cooling process should be done that includes intrabeam scattering.

REFERENCES

1. G.I. Budker, The 1966 Proc. Int. Symp. Electron and Positron Storage Rings, Saclay. Atomnaya Energiya 22: 346.
2. L. Spitzer, "Physics of Fully Ionized Gases", (New York: Interscience, 1956) pp. 80-81.
3. G.I. Budker, et al., Particle Accelerators, Vol. 7, 197-211 (1976).
4. M. Bell, et al., Physics Letters, Vol. 87B, No. 3, (1979).
5. T. Ellison, et al., IEEE Trans. Nuc. Sci., Vol. NS-30, No. 4, 2636-2638, (1983).
6. D.L. Friesel et al., IEEE Trans. Nuc. Sci., Vol. NS-32, No. 5, 2421-2423, 1987.
7. D.J. Larson, "Intermediate Energy Electron Cooling for Antiproton Sources", PhD Thesis, 1986.
8. M.L. Sundquist, et al., to be published in AIP conference proceedings of the Washington DC Particle Accelerator Conference, 1987.
9. D.J. Larson, et al., "Intermediate Energy Electron Cooling Applied to the Fermilab Antiproton Source", Low Energy Antimatter, D. Cline, editor, World Scientific, 1986.
10. D.J. Larson, "Design of an Electrostatic Accelerator for use in Intermediate Energy Electron Cooling", submitted to Particle Accelerators, 1987.
11. D.J. Larson, et al., "Toward Multi-GeV electron cooling", AIP Conference Proceedings No. 150, pp. 366-370, 1986.

PRÉCIS OF GROUP II ACTIVITIES

(Note: Group II discussions used as upper bounds for the numbers of antiprotons available the amounts an initial U.S. low energy antiproton facility can deliver - $\sim 10^{14}$ antiprotons per year.

Paper (1) - Nieto and Hughes - discusses the role of quantum theory and special relativity in laying the basis for discovery and understanding of antimatter. Progress is traced up to the CPT theorem, and the role of gravitational interactions is treated. The conceptual position of antimatter in modern understanding of fundamental physics is summarized, after describing how this understanding evolved.

The basic physics case for low energy antiproton research is most compelling. The diversity of the physics involved is very broad, and is summarized in Paper (2) - Bonner and Nieto: Tests of invariance principles; gravity and antiprotons; antiproton annihilation in nuclei; antihydrogen and basic physics tests; formation of cluster ions of antimatter and atomic physics; meson spectroscopy; antimatter storage in normal matter; and tests which invoke higher energies (up to several GeV) for the antiprotons. The comprehensive overview Paper (2) summarizes the arguments for a low energy antiproton facility, and suggests the number of antiprotons desired for 12 basic classes of experiments.

Antiproton annihilation in nuclei: Paper (3) - Smith - produces fundamental insights into production of very high nuclear temperatures; provides information on deep annihilation, strangeness and quark-gluon matter, and production of $\bar{N}NN$ fireballs; and exploits fission as a new tool for studying strangeness of heavy nuclei. For example, antiprotons - nucleus collisions allow exploration of the high temperature region of the nuclear phase diagram. The particle emission from antiproton annihilation: Paper (4) - Smith - is important in determining the fraction of the total annihilation energy release going into heavy

charged particles. This knowledge is critical for use of annihilation energy as a propulsion or compact energy storage source. The paper suggests a greater than previously predicted value for this fraction.

Paper (5) - Sharpe - discusses the phenomenology of exotica and meson spectroscopy in the $\bar{N}N$ channel, and concludes that annihilations can help us understand strongly coupled field theory, that $\bar{P}P$ provides a good general purpose detector, and that $\bar{P}P$ annihilations will provide a very important tool for unravelling of the exotica and insights into whether QCD is the correct strong interaction theory - and, if not, what might lead to a better theory. A variety of experiments has exhibited resonances which do not fit standard patterns. A high luminosity, low energy antiproton source can play a central role in new quantitative tests.

Antiprotons are useful for testing invariance principles (CP, CPT, T) both in their role as antiparticles and as a source of other particles: Paper (6) - Miller. Many types of tests are possible. This paper consolidates prior test results, suggests new tests using antiprotons, and derives estimates for the number of antiprotons which might be needed to get precision tests with good statistics. Up to 10^{12} to $10^{14}/10^{15}$ antiprotons might be desirable, thus emphasizing the high motivation for an intense source in a U.S. initial low energy antiproton facility.

Gravity experiments with antiprotons: Paper (7) - Nieto and Bonner - are motivated in part by apparent non-Newtonian, non-Einsteinian effects suggested by recent experiments, reanalysis, and other work, and in part by quantum gravity, which suggests vector and scalar partners of the graviton - and consequently additive contributions to the Newtonian potential for antimatter, whereas for matter the partners' contributions have opposing signs and hence may nearly cancel. A prediction, based on use of recent mine data, suggests possible magnitudes for the scalar and vector coupling constants and for the force ranges of the additive contributions. The experiment suggested uses as a calibration the hydrogen ion, leading to precision measurements.

The possible storage of antiprotons in relative proximity to normal matter is discussed in Paper (8) - Campbell. While equilibrium storage appears impossible, a variety of schemes for steady-state non-equilibrium storage in a wide spectrum of condensed matter systems cannot now be ruled out. Known limits to stability are discussed, as are down-scaling of macroscopic traps; condensed matter traps; special effects relying on a variety of quantum mechanical mechanisms; and suggested experiments with antiprotons in condensed matter. Muons would likely serve as useful test particles in such fields as developing very small scale traps.

Antihydrogen (\bar{H}) production schemes are reviewed in Paper (9) - Mitchell. Schemes include stimulated radiative recombination, positronium charge exchange, and high density three-body recombination in a trap; with modest technology advances, production rates of $\geq 10^8$ antihydrogen atoms/sec seem attainable. \bar{H} production is of great importance to form a possible basis for very high density storage of antimatter. Basic physics uses of \bar{H} are also exceedingly numerous - e.g., every measurement made with hydrogen would have repetitions with antihydrogen vital to CPT predictions. Normal matter simulations of \bar{H} production can be exploited.

The cluster ion production technique of macroscopic amounts of antimatter is described in Paper (10) - Stwalley. This technique can have very important implications for storing bulk amounts of antimatter. The paper discusses the formation processes, efficiency, etc. first for normal matter and then discusses some complications when antimatter is used. The scheme considers producing \bar{H} , and a catalyst \bar{H}_N^+ ; the individual reaction steps potentially leading to the \bar{H}_N^+ "seed crystal" are reviewed in some detail. Processes leading to bulk amounts of antimatter are then described. Normal matter simulations can be envisaged; normal matter cluster ions are themselves of substantial scientific interest, and of potential importance in producing particle beams for directed energy, fusion, solid state, and other applications.

An extensive Bibliography of Hydrogen Cluster Ions is given in Paper (11) - Stwalley. The over 400 listings discuss formation issues for H_2^+ , H_3^+ , and H_N^+ ($n \geq 4$) in turn; in addition, the H_2^- , H_3^- , and H_N^- species are reviewed (H_2^- is unstable, and probably so is H_3^-). The richness of the experimental and analytical work suggested by this Bibliography will give us a running start on antimatter cluster ion research.

Paper (12) - Forward - discusses experimental work resulting in production of antideuterium, antitritium, antihelium, and prospects for even heavier antinuclei such as antilithium, etc. Results are presented giving production rates of heavy antinuclei, normalized to production rates for antiprotons, as a function of the mass of the antinuclei, and as a function of particle energy. Each added baryon, e.g., appears to lower the production rate by a factor $\sim 10^4$. Production of heavy antinuclei is of very considerable scientific interest and usefulness in itself; in addition; heavy antinuclei might play a role in antimatter cluster ion research.

Paper (13) - Goldman - discusses the physics issues which can be investigated via an Advanced Hadron Facility, and thus comprehensively reviews the primary physics justifications for the facilities described in several papers under Group I activities. Paper (13) considers the fundamental particles and gauge bosons; strong interaction theory; the standard electroweak model; and problems of the standard model, and consequent experimental tests. Precision experimental tests require high intensity, medium energy (~ 30 -75 GeV) accelerator complexes to meet the experimental needs.

Some Major Observations from Group II Activities

- Opportunities are very abundant for explorations with low energy antiprotons.
- New discoveries and exciting results await in tests of invariance principles; antiprotons and gravity; annihilation phenomenology; meson spectroscopy; antihydrogen and basic

physics tests; antimatter cluster ions; antimatter storage in normal matter; production and use of heavy antinuclei.

- We need intense sources of low energy antiprotons to achieve such discovery goals.
- Even for basic science, there are classes of experiments which would exploit the upper portion of the near-term capacities of prospective low energy antiproton sources in the U.S. ($\sim 10^{13}$ to 10^{15} antiprotons/year).
- LEAR has only scratched, and will only scratch, a fraction of the many compelling and attractive low energy antiproton experiments. There is plenty of work for another low energy machine in North America. Such a machine would also be available for international collaborations.
- A low energy antiproton facility, such as the one under consideration in this Workshop, can address very major areas of concern in particle physics today, as emphasized both here and in the prior Fermilab Proceedings (April 1986), in a vital and straightforward way.
- Many of the aims of the program of basic science experimentation discussed by Group II appear generally compatible with, and often expeditable by, use of transportable antiproton storage devices - ion traps (see paper III1) and small rings (see Paper I4).

ANTIMATTER: ITS HISTORY AND ITS PROPERTIES

by

Michael Martin Nieto and Richard J. Hughes

Theoretical Division
Los Alamos National Laboratory
University of California
Los Alamos, New Mexico 87545

ABSTRACT

We review the conceptual developments of quantum theory and special relativity which culminated in the discovery of and understanding of antimatter. In particular, we emphasize how quantum theory and special relativity together imply that antimatter must exist. Our modern understanding of antimatter is summarized in the CPT theorem of relativistic quantum field theory. The implications of this theorem have never been contradicted by any experiment ever done.

I. INTRODUCTION

Given quantum mechanics and special relativity, antimatter's existence is a consequence.¹ However, traces of it can be seen in non-relativistic quantum mechanics and special relativity, independently.

In this survey we begin with a discussion of the discovery of quantum mechanics, and how the interpretation of the wave function was a clue towards the later discovery of antimatter. Schrödinger did not understand his complex wave function. In fact, at first he thought that only the modulus of the wave function was physically significant.

Only later was it realized that the wave function is a complex probability amplitude. This is a key. The probabilistic nature of quantum mechanics only means we have lost classical determinism. But the complex nature of the wave function allows the existence of antimatter. At the time this hint was missed.

Next, after reviewing special relativity and why its strong-reflection (time and space reflection) symmetry does not quite imply antimatter, we discuss the search for a relativistic quantum theory. The Klein-Gordon equation was the first to be discovered, but it failed for the hydrogen-atom spectrum. But later there was triumph with the Dirac equation. This equation has as its basis the desire to take the square-root of the special-relativistic, energy-momentum-mass relation.

The success of the Dirac equation was dramatic. But it had two extra components besides those for the electron. After some confusion over whether these other solutions could represent the proton, it was realized that they had to correspond to a particle of the same mass as the electron but with opposite charge. Imagine the amazement when in

1932 Anderson found this particle in a cloud chamber.

Then began a fascinating period of detective work, as the positive and negative muons, the three pions, and, most significantly to the community, the antiproton were discovered. Finally, in 1957, Lüders² systematized earlier work and published his paper on the CPT theorem. (C=charge conjugation, P=parity, T=time reversal.) This theorem states that for every particle there will be an antiparticle with the same inertial mass, the opposite charge, and the same total decay rate. These properties have been obeyed by every particle ever discovered. This theorem is the foundation of quantum field theory as a description of particle physics up to and including the "standard model" of the strong and electroweak interactions. Even with the discovery of P and CP violation, there is no suggestion of a violation of CPT invariance.

So where does gravity fit in?

Independently of quantum theory, Einstein developed general relativity as a classical (non-quantum) theory. The gravitational field is a tensor field. In its standard, classical form, general relativity does not specifically contain the concept of antimatter. Antimatter is simply another form of energy and has the corresponding weight. Therefore, antimatter must behave in the same way as matter in a classical, general-relativistic, gravitational field.

But even in the era predating modern attempts to unify gravity with the other (quantized) forces of nature, the question was raised of whether antimatter had to have the same weight as matter. In the 1950's there was speculation that antimatter could possibly be repelled by matter, so-called "antigravity".³ Quantum field theory tells us, "No!" However, that was not the end. Modern, quantum field

theories, which attempt to unify all the forces of nature, tell us that the gravitational acceleration of antimatter can be different than that of matter. That fascinating story is the topic of a separate discussion in this Proceedings. You are referred there for the details.⁴

II. The Discovery of Quantum Mechanics.

The great, intuitive breakthrough in atomic physics was Bohr's description of the hydrogen atom in his "old quantum theory," formulated in 1912.⁵ This theory quantized classical orbits. Limited though it was, it correctly predicted the energy levels of hydrogen as

$$E_n = -R/n^2 \quad n = 1, 2, 3 \dots \quad (1)$$

$$R = me^4/(2\hbar^2) \quad (2)$$

In 1926, Schrödinger's wave-mechanics version of quantum theory explained this result from a fundamental viewpoint.⁶ In this new quantum theory, one makes a substitution for the energy, momentum, and position. They become operators in a wave equation:

$$E_{\text{class}} \rightarrow i\hbar(d/dt) , \quad (3)$$

$$p_{\text{class}} \rightarrow -i\hbar \nabla , \quad (4)$$

$$x_{\text{class}} \rightarrow x . \quad (5)$$

The classical energy equation, kinetic energy plus potential energy equals the total energy,

$$E = p^2/(2m) + V(r) \quad (6)$$

is now written in the form

$$E_n \Psi = i\hbar(d/dt)\Psi = [-(\hbar^2/2m)\nabla^2 - V(r)]\Psi \quad (7)$$

The solution to this differential equation yields the same energy levels, E_n , as those obtained by Bohr.

However, one of the aspects of this new theory of operators is that xp is no longer equal to px . In particular,

$$[x, p] = xp - px = i\hbar \quad (8)$$

This equation is the commutator which implies the Heisenberg Uncertainty Relation:

$$(\Delta x)^2(\Delta p)^2 \geq \hbar^2/4 \quad (9)$$

The implication of this relation is that one can never know both the position and the momentum of a particle with infinite precision. This is the place where classical determinism disappears in modern quantum theory.

In the effort to understand this, Schrödinger discovered, what in modern language are called, the coherent states of the harmonic oscillator.^{7,8} These are the wave-function solutions of the quantum

equations of motion. They follow the motion of a classical particle as well as possible. However, wave functions are complex. Schrödinger did not understand what this meant. Below is a reproduction of the translation into English of Schrödinger's remarks.⁸

$$(8) \quad \psi = e^{\pi i \nu_0 t - \frac{A^2}{4} e^{4\pi i \nu_0 t} + 4x e^{2\pi i \nu_0 t} - \frac{x^2}{2}}.$$

Now we take, as is provided for, the real part of the right-hand side and after a short calculation obtain

$$(9) \quad \psi = e^{\frac{A^2}{4} - \frac{1}{2}(x - A \cos 2\pi \nu_0 t)^2} \cos \left[\pi \nu_0 t + (A \sin 2\pi \nu_0 t) \cdot \left(x - \frac{A}{2} \cos 2\pi \nu_0 t \right) \right].$$

The *second* factor in (9) is in general a function whose absolute value is small compared with unity, and which varies very rapidly with x and also t . It ploughs many deep and narrow furrows in the profile of the first factor, and makes a *wave group* out of it, which is represented—schematically only—in Fig. 2.

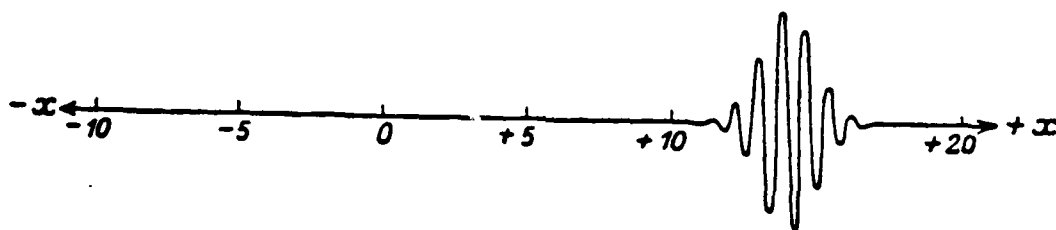


FIG. 2.—Oscillating wave group as the representation of a particle in wave mechanics.

As one can read, Schrödinger originally thought that only the "real part" of the wave function was physically significant. He wanted to ignore the imaginary part, the part which turns out to be critical to the understanding of antimatter. It allows for C conjugation.

It was with the work of Born that the physical significance of the wave function was understood. The wave function is a probability amplitude. It's modulus-squared is the probability density. Since wave functions are only amplitudes, their phases are significant in a relative sense, but not in an absolute sense. This is experimentally seen in quantum interference experiments.

III. Special Relativity.

In 1905 Einstein produced his special theory of relativity.⁹ It describes the kinematics of all of known physics in situations where gravity can be ignored. For a free particle, this theory says that the relationship between mass and (only) kinetic energy is no longer the classical

$$E = (1/2)mv^2 \quad (10)$$

but rather is the new relationship

$$E^2 = (mc^2)^2 + (pc)^2 \quad (11)$$

Special relativity has part of the physics that is needed for antimatter. In particular, there is a symmetry called strong reflection.¹⁰ This involves letting all four coordinates (space and time) be reflected through the origin. The effect of this inversion on the equations of classical electrodynamics is to change the sign of the electric charge. For each solution, then, strong-reflection allows the existence of another. This other solution is similar to what we will call an "antiparticle" solution. However, as we observe below, it is only when quantum theory is introduced that true-antiparticle

solutions appear, that are required.

Now, starting with Bohr's old quantum theory, Sommerfeld had "added" special relativity and had derived the "Sommerfeld formula" for the hydrogen-atom energy levels:¹¹

$$W_{n,\varphi} = mc^2 f(n \equiv \rho + \phi, \phi) , \quad (n, \rho) \leq 0, 1, 2, \dots \quad \phi \leq 1, 2 \dots \quad (12)$$

$$\equiv mc^2 - R [1/n^2 + (\alpha^2/n^4) \{ n/\phi - 3/4 \} \dots] , \quad (13)$$

where

$$f(N, L) = [1 + \alpha^2 / \{ N - L + [L^2 - \alpha^2]^2 \}^{1/2}]^{-1/2} , \quad (14)$$

$$\alpha = e^2 / (\hbar c) . \quad (15)$$

W vs. E denotes that the rest-mass energy has been included in the eigenvalues. ρ and ϕ are radial and angular quantum numbers, of the "quantized orbit" Bohr type. Eq. (13) agreed with the energy levels of the Bohr atom to the level of the principle quantum number, n . The next term, which includes the angular quantum number, ϕ , agreed with the hydrogen atom fine-structure splittings. But from quantum mechanics it was known that the physical interpretation of ρ and ϕ was incorrect, even though phenomenologically they gave the correct energy eigenvalues.

Therefore, an immediate goal in quantum mechanics was to try to add special relativity to Schrödinger's operator ideas. The first attempt was the Klein-Gordon equation,¹² which is the quantum-mechanical form of Eq. (11), with the electromagnetic

potential inserted:

$$[i\hbar(d/dt) - v(r)]^2\Psi = [c^2p^2 + m^2c^4]\Psi \quad (16)$$

The solution for the energy levels is

$$W_{n,\ell} = mc^2 f(n, \ell+1/2) \quad , \quad \ell \leq n+1 \quad (17)$$

$$\equiv mc^2 - R [1/n^2 + (\alpha^2/n^4)\{ n/(\ell+1/2) - 3/4 \} \dots] \quad , \quad (18)$$

ℓ being the angular momentum quantum number.

This result did not agree with the hydrogen atom. We now know that the Klein-Gordon equation describes particles with internal spin-0. Thus, it should be the equation for the pi-mesic atom: a negative pi-meson bound to a nucleus. Ironically, because of technical difficulties, the verification of the spectra of Eq. (18) for the pi-mesic atom did not occur until 1978.¹³ This was long after the situation was understood¹⁴ both theoretically and also from other experiments.

The next step was the equation of Pauli, which incorporated the concept of spin-1/2 electrons. (Spin was the famous discovery of Goudsmit and Uhlenbeck.¹⁵) Pauli gave the Hamiltonian (energy operator) of the hydrogen atom as

$$H = (-\hbar^2/2m)\nabla^2 + V(r) + (2m^2c^2r)^{-1}(dV/dr) \mathbf{L} \cdot \mathbf{S} \quad , \quad (19)$$

where L is the angular momentum operator. S is the spin operator, represented by a (2×2) matrix. Therefore, there are two solutions to the Schrödinger equation, corresponding to spin-up or -down.

The Pauli equation gave agreement with the hydrogen spectra approximation of Eq. (13), with ϕ being replaced by $(j + 1/2)$. " j " is the total angular-momentum quantum number from $J = L + S$. This replacement explained Sommerfeld's semi-ad hoc rule that $\phi \geq 1$. But the Pauli equation obviously was a half-way house to complete understanding. For instance, no one could understand where spin came from. If one took the known "size" of the electron and the value of the angular momentum that the spin value represented, then the edge of the electron would be moving (classically) faster than the speed of light!

IV. The Dirac Equation and Antimatter

The resolution of all this came with the Dirac equation. Note that Eq. (11) can be written as

$$mc^2 = [E^2 - (pc)^2]^{1/2} \quad (20)$$

Dirac wanted to be able to avoid the analogous square root implicit in the Klein-Gordon form of quantum mechanics. Therefore, he searched for some mathematical way in which the quantum operator form of Eq. (20) could be described by

$$mc^2 = [E^2 - p^2c^2]^{1/2} \quad (21)$$

$$= [(E\gamma_0 - \mathbf{p} \cdot \boldsymbol{\gamma}c)^2]^{1/2} \quad (22)$$

so that one could write the equation

$$mc^2\Psi = \{[E - V(r)]\gamma_0 - \mathbf{p}\cdot\boldsymbol{\gamma}c\}\Psi \quad (23)$$

Amazingly, in 1928 Dirac found a solution with the correct mathematical properties. The four γ operators in Eq. (23) were (4 x 4) matrices. Therefore, there were four solutions to the Dirac equation, corresponding to

$$(+E \text{ spin up}, +E \text{ spin down}, -E \text{ spin down}, -E \text{ spin up}). \quad (24)$$

The last two solutions have negative energies. Dirac was so scared of these solutions that when he first attacked the hydrogen atom with his equation he only looked for an approximate solution.¹⁶ It corresponded to the results of Pauli. Later, Darwin and Gordon exactly solved the Dirac equation for the hydrogen atom, and they obtained the correct energy levels as¹⁷

$$W_{n,j} = mc^2 f(n, j+1/2) \quad (25)$$

$$\equiv mc^2 - R [1/n^2 + (\alpha^2/n^4)\{n/(j+1/2) - 3/4\} \dots] \quad (26)$$

As obtained in the Pauli equation, j is the total angular momentum quantum number, corresponding to the operator $\mathbf{J} = \mathbf{L} + \mathbf{S}$.

V. Antimatter, the Negative-Energy States

Now began the fascinating fight to understand the negative-energy solutions of Dirac. For details on what follows, consult the excellent

articles on the history of the Dirac equation and on the early stages of experimental particle physics.¹⁸

A summary can be started with Dirac's above-mentioned fear of the negative-energy solutions. Obviously something was right since the hydrogen atom worked so well. Dirac had to think of some physical explanation of them.

The particles described by the solutions of the Dirac equation were "fermions." Such particles have the property that only one of them at a time can occupy any energy state. In 1930 Dirac¹⁹ proposed that all of the negative energy states are filled with particles, forming what is now known as the "Dirac sea." This state was called the ground state since it had the lowest possible energy. An excitation out of this sea leaves a "hole" in it. It has a positive energy and opposite electric charge to the positive-energy solution. But what were these new particles described by the holes? Dirac suggested that they were protons.

This got Dirac into trouble. Bohr had rejected the physical validity of Dirac's equation.²⁰ Bohr felt Dirac's proposal could not be the ultimate answer since there was no correspondence principle (a well-defined, large-energy, classical limit) for spin, and also because negative energies were "absurd." Later, Oppenheimer pointed out that the holes could not be protons because they had the wrong mass (the hole states had to have the same mass as the positive energy solutions). Also, if they were the protons, they would have decayed.²¹

Faced with these criticisms, Dirac modified his holes to have the same mass as the electrons, and boldly wrote,²² *"A hole, if there were one, would be a new kind of particle, unknown to experimental physics,*

having the same mass and opposite charge to an electron. We may call such a particle an anti-electron. ... Presumably the protons will have their own negative-energy states ... an unoccupied one appearing as an anti-proton."

The stage was set for Carl Anderson,²³ who in 1932 reported the discovery of the anti-electron or positron, as it is now called. He was using a cloud chamber in Millikan's lab. However, this chamber had a piece of lead in it and a magnetic field perpendicular to the vertical. Therefore, high-energy cosmic rays hit the lead, made electron-positron pairs, and the two particles curved in opposite directions in the magnetic field. This showed that the two tracks came from particles with the same momentum but opposite charges. Antimatter had been discovered!

VI. The Understanding of Antimatter

In the following years, we came to understand antimatter.

First, in 1935, Yukawa proposed²⁴ that the strong force must be mediated by a particle of about 100 MeV rest-mass energy because it obviously was short ranged. This meant the potential for the strong force was not of the Newton-Coulomb $1/r$ form, but rather was

$$V(r) = g [e^{-r/\lambda}] / r \quad . \quad (27)$$

In 1937 Anderson and others²⁵ found a particle with a mass of about 200 times that of the electron. But it lived much too long for it to be associated with the strong force. Interestingly, however, it too came in species with both charges.

This part of the story was laid to rest in 1947, when a University of Bristol group found the following processes:²⁶

$$\pi^- \rightarrow \mu^- + \bar{\nu}_\mu \rightarrow e^- + \bar{\nu}_e + \bar{\nu}_\mu + \nu_\mu, \quad (28)$$

$$\pi^+ \rightarrow \mu^+ + \nu_\mu \rightarrow e^+ + \nu_e + \nu_\mu + \bar{\nu}_\mu. \quad (29)$$

The π -mesons were the Yukawa particles that mediate the strong force. The μ particles were the ones found by Anderson and collaborators in 1937. These muons are charged leptons which decay weakly into the electron species of the same charge. Thus, we see that the pions, muons, and electrons come with both particle and antiparticle species. The neutrinos (ν) are the particles (and antiparticles) first postulated by Pauli to conserve energy in the beta-decay of neutrons. Eventually they and their antiparticles were all experimentally shown to exist.

In the 1950's, these and other ideas were systematized in the CPT theorem for quantum field theory.^{2,27} In it, three quantum-mechanical transformations, P, T, and C, are combined. The last of these, C, has as its basis the complex nature of the solutions of quantum mechanics. C changes the "charges" of a particle. In the simplest case this is done by complex-conjugating the wave function and equation. CPT in quantum theory is similar to strong-reflection in classical theory.²⁸ But in quantum theory the complex nature of the fields and equations means that CPT is equivalent to strong-reflection times complex conjugation of the fundamental fields and equations. This new feature, the inherent

complex nature of the system, is what requires the negative-energy solutions, and hence predicts the existence of antimatter.

In a graphic form, the theorem says that if one were to take a motion picture of a physical process, and if one then were to run the film backwards (T), look at it in a mirror and rotate oneself by 180° (P), and change the "charges" or "internal quantum numbers" of the particles, then one would not be able to tell the difference in the laws of physics seen. Put another way, every particle has an antiparticle with

- i) the same (inertial) mass
- ii) the same total lifetime
- iii) the opposite electric charge
- iv) the opposite magnetic moment
- v) the opposite internal quantum numbers.

This theorem has been verified in **every** experiment **ever** done. It is a foundation of modern quantum field theory, and indeed, one does not know how to formulate a mathematically consistent relativistic field theory that does not satisfy this theorem.¹ Even ideas of the separation of matter from antimatter in the early universe are based upon CP violation (and a presumed countermanding T violation), not CPT violation. We have observed and understand the existence of P violation, CP violation, C violation, and we hope to observe T violation.³⁰ But we do not foresee CPT violation, at least in the short term.

VI. The Discovery of the Antiproton

Returning to 1955, the Bevatron was completed at Berkeley with just enough energy (6.2 GeV) to create antiprotons. This was done by

accelerating protons to the maximum energy, colliding them with nuclei, and observing the process

$$p + p \rightarrow 3p + \bar{p} . \quad (30)$$

The actual detection method is described in Ref. 31.

Now, one of us (MMN), being a quantum mechanic and raised after all this was done, always thought, "Why did the discovery of the antiproton earn a Nobel Prize? They should have gotten it if they hadn't found the antiproton!" Then, in preparing this and other discussions related to our antiproton gravity work, we came across and read the 1956 Scientific American article on the discovery of the antiproton.³¹ There it said, *"At this time (1955) several long-standing bets on the existence of the antiproton started to be paid. The largest we know of was for (1955) \$500."*

To us, of our generation, this is simply amazing. We find it absolutely clear that antiparticles exist. We do not see how one can conceive of there not being an antiparticle for every type of particle. It is always difficult to understand the past with one's present viewpoint, and for us this was no exception.

The best recent analogy to this we can think of is that there were those who doubted that the W's and the Z would be discovered at the SPS, the SPS being the accelerator at CERN built to discover them. But that had nothing to do with an antiparticle. That only had to do with there being a correct unification of electromagnetism and the weak interactions. Not finding the W's and Z would be like proton decay not

being seen, which supposedly was the key to unifying the electroweak and the strong interactions³² in the "standard model."^{32,33}

VII. Conclusion

Of course, one must always test for CPT violation. Somewhere it may break down. In fact, there are ideas floating around about how this might happen by a small amount for phenomena on a cosmological scale.³⁴ - (We ourselves have been guilty of such types of speculation.³⁵)

However, except for the case of gravity, CPT is experimentally proven to be correct with precisions ranging up to parts in 10^9 , depending upon the interaction and the phenomenon involved.³⁶ Since the proposed antiproton gravity experiment would be the first involving antimatter, at present we can experimentally say nothing about CPT and gravity. CPT violation would imply a different gravitational interaction than expected. However, as is noted elsewhere in these Proceedings,⁴ that is not necessary. Indeed, new gravitational forces from quantum theory are a more likely possibility to induce unexpected results.

But an important thing to remember is that if any of these speculated violations of CPT turn out to be correct, they would be small, and would have NO effect - period - end of report - NO effect on present-day applied-physics experiments. All such experiments are dealing with the every-day earth. As such they are governed by the electromagnetic interactions which hold both us and also magnets together. Electromagnetism is the interaction for which CPT has been tested to the highest accuracy. Further, quantum electrodynamics is

the quantum theory whose fundamental predictions have been tested to the highest accuracy.³⁷ Finally, recall that it was the fundamental electrically charged particle, the electron, whose antiparticle, the positron, was first discovered and comprehended.

We understand antimatter just as well as we understand matter. Our only problem is that we don't know how to handle antimatter in a matter world. The opposite would be the case for antipeople in an antimatter world, if there are any.

That brings up a final point. Who decides what is matter and what is antimatter? Is it all relative, as our simplist view of the equations of physics might indicate? Or, is nature really telling us something by our not seeing any evidence of antimatter galaxies in the universe? There are some ideas that this "baryon asymmetry" (we do not see antimatter galaxies) is not just a local fluctuation. These ideas hold that baryon asymmetry is a real effect due to CP or CPT violation being much more significant in the early universe.³⁸ If this is correct, then antimatter is not a relative concept. Dirac would have been proven correct.

REFERENCES

1. R. P. Feynman, in Elementary Particles and the Laws of Physics. The 1986 Dirac Memorial Lectures (Cambridge Univ. Press, Cambridge, 1987).
2. G. Lüders, Ann. Phys. (NY) 2, 1 (1957).
3. P. Morrison, Am J. Phys. 26, 358 (1958).

4. M. M. Nieto and B. E. Bonner, in these Proceedings, on looking for new gravitational forces using antiprotons.
5. N. Bohr, Phil. Mag. 26, 1, 476, 857 (1913).
6. E. Schrödinger, Ann. Phys. 79, 361 (1926).
7. E. Schrödinger, Naturwiss. 14, 664 (1926).
8. Translation of Ref. 7 above, in Collected Papers on Wave Mechanics (Blackie & Son, London, 1928), p.41.
9. A. Einstein, Ann. Phys. 17, 891, 905, (1905); 18, 639 (1905).
10. E. C. G. Stüeckelberg, Helv. Phys. Acta 14, 322, 588 (1941); R. P. Feynman, Phys. Rev. 74, 939 (1948).
11. A. Sommerfeld, Atomic Structure and Spectral Lines (Methuen, London, 1934), Chap. V, p. 251. This translation of the 5th German edition gives a physical feeling for the old quantum theory.
12. H. Kragh, Am. J. Phys. 52, 1024 (1984), discusses the 1926 "equation with many fathers."
13. K.-C. Wang, F. Boehm, et al, Phys. Lett. B 79, 170 (1978); L. Delker, et al., Phys. Rev. Lett. 42, 89 (1979).
14. M. M. Nieto, Am. J. Phys. 47, 1067 (1979).
15. S. A. Goudsmit, Phys. Today 29, No. 6, 40 (1976); G. E. Uhlenbeck, ibid. p. 43. Published on the 50th anniversary of the discovery of spin.
16. P. A. M. Dirac, Proc. Roy. Soc. 117, 610 (1928).
17. C. G. Darwin, Proc. Roy. Soc. 118, 654 (1928); W. Gordon, Zeit. Phys. 48, 11 (1928).
18. D. F. Moyer, Am. J. Phys. 49, 944, 1055, 1120 (1981) is a three article series on the discovery of the Dirac electron. Also see, H.

- Kragh, Arch. Hist. Exp. Sci 24, 31 (1981). L. M. Brown and L. Hoddeson, Phys. Today 35, No. 4, 36 (1982), discuss the early history of elementary particle physics.
19. P. A. M. Dirac, Proc. Roy. Soc. A 126, 260 (1930).
 20. See. p. 1056 of the second article in Ref. 18.
 21. J. R. Oppenheimer, Phys. Rev. 35, 562 (1930).
 22. P. A. M. Dirac, April 1931 letter to Van Fleck, quoted in p. 1060 of the second article in Ref. 18.
 23. C. D. Anderson, Science 76, 238 (1932).
 24. H. Yukawa, Proc. Phys.-Math. Soc. Jpn. 17, 48 (1935).
 25. S. H. Neddermeyer and C. D. Anderson, Phys. Rev. 51, 884 (1937); J. C. Street and E. C. Stevenson, Phys. Rev. 51, 1005 (1937); Y. Nishina, M. Takeuchi, and T. Ichimiya, Phys. Rev. 52, 1198 (1937).
 26. C. M. G. Lattes, et al., Nature 159, 694 (1947).
 27. R. F. Streater and A. S. Wightman, PCT. Spin & Statistics, and All That (W. A. Benjamin, New York, 1964), and references therein.
 28. J. S. Bell, Proc. Roy. Soc. A 231, 479 (1955); W. Pauli, in Niels Bohr and the Development of Physics, edited by W. Pauli (Pergamon, New York, 1955), p. 30.
 29. J. J. Sakurai, Invariance Principles and Elementary Particles (Princeton Univ. Press, Princeton, N.J., 1964), Chap. 6, p. 136.
 30. J. Miller, in these Proceedings, on tests of CP violation (and fundamental symmetry experiments) at LEAR.
 31. E. Segrè and C. E. Wiegand, Sci. Am. 194, No. 6, 37 (1956).
 32. S. Weinberg, Dædalus, Proc. Am. Acad. Arts Sci. 106, No. 4, 17 (1977); S. Weinberg, in Ref. 1.

33. T. Goldman, in these Proceedings, on the "standard model."
34. J. F. Donoghue, B. R. Holstein, and R. W. Robinett, *Gen. Rel. and Grav.* 17, 207 (1985).
35. T. Goldman and M. M. Nieto, in Physics with Antiprotons at LEAR in the ACOL Era, edited by U. Gastaldi, R. Klapisch, J. M. Richard, and J. Tran Thanh Van (éditions Frontières, Paris, 1985), p. 639.
36. Particle Data Group, "Review of Particle Properties," *Phys. Lett. B* 170, 1 (1986). See. p. 66, on tests of conservation laws.
37. S. S. Schweber, *Rev. Mod. Phys.* 58, 449 (1986).
38. A. G. Cohen and D. B. Kaplan, Harvard University preprint HUTP-87/A061.

Basic Physics Program For A Low Energy Antiproton Source In North America*

B. E. Bonner

Rice University

Houston, Texas 77251-1892

and

Michael Martin Nieto

Theoretical Division, Los Alamos National Laboratory

University of California

Los Alamos, New Mexico 87545

ABSTRACT

We summarize much of the important science that could be learned at a North American low energy antiproton source. It is striking that there is such a diverse and multidisciplinary program that would be amenable to exploration. Spanning the range from high energy particle physics to nuclear physics, atomic physics, and condensed matter physics, the program promises to offer many new insights into these disparate branches of science. It is abundantly clear that the scientific case for rapidly proceeding towards such a capability in North America is both alluring and strong.

CONTENTS

I. Introduction and Overview.....	2.
II. Tests of Invariance Principles: CP, CPT, and T.....	5.
III. Gravity and \bar{p} 's: $g(\bar{p})/g(H^+)$	8.
IV. Antiproton Annihilation in Nuclei.....	12.
V. Antihydrogen and Basic Physics Tests.....	14.
VI. Meson Spectroscopy.....	19.
VII. Antimatter Storage in Normal Matter.....	22.
VIII. Higher Energy \bar{p} 's.....	27.
IX. Summary and Conclusions.....	30.
X. References.....	33.

*Paper presented at the Second Review and Planning Workshop on Antiproton Science and Technology, October 6-9, 1987, The RAND Corporation, Santa Monica, California.

I. INTRODUCTION AND OVERVIEW

During the past few years there have been numerous workshops and conferences devoted to the science under discussion here. In particular one should mention the series of LEAR workshops^{1,2} the Madison workshop³ on the Design of a Low Energy Antimatter Facility, and the Fermilab workshop⁴ on AntiMatter Physics at Low Energy (AMPLE). In the present article, we extract what appears to be the most compelling of the wide variety of physics that would become accessible, and attempt to give sufficient details to allow one to judge the basic physics case for such a machine.

The guidelines issued for the present workshop indicated a somewhat arbitrary 200 MeV maximum energy for the machine under discussion. The limitations thus imposed on the diversity of physics by such a ceiling, while certainly considerable, will be seen to be far from devastating. Missing from the agenda of such a machine would be the very interesting higher energy topics such as the $\Delta S=1$ CP violation experiment⁵, $\bar{p}p \rightarrow \bar{\Lambda}\Lambda$; the new measurements that could be done in charmonium spectroscopy⁶; and the puzzle⁷ of the enormous deviation from QCD predictions of the ratios for the branching fractions of the J/ψ and the ψ' to exclusive final states. We include a brief discussion of the first and last of these in Section VIII under the "Higher energy \bar{p} 's" heading.

As emphasized by Bob Jaffe⁶ in the Fermilab Proceedings, there are two broad areas of concern in particle physics today. These can be described as the "Origins of the Standard Model" and the "Dynamics of

Confinement in QCD". It is remarkable that a low energy antiproton facility such as the one under consideration here can address both these questions in a vital and straightforward manner.

While it is true that the standard model has enjoyed considerable success, it is less frequently mentioned, but no less true, that there are many parameters and phenomena that are arbitrary and not understood. Examples are i) the sources of weak symmetry breakdown, ii) the origin of CP violation, iii) the origin of quark and lepton masses and angles, and iv) even why $SU(3) \times SU(2) \times U(1)$ should be the fundamental gauge groups chosen by nature. In fact, the absence of proton decay at the 10^{32} year lifetime has cast serious doubt on this simplest version of the standard model. A low energy antiproton machine will contribute to our understanding in this area most directly through precision tests of various invariance principles such as CP, CPT, and T. Therefore, this topic forms one of the cornerstones of the basic physics program for the facility.

The theory of Quantum Chromodynamics has also had its many successes. However, after more than a decade, many fundamental questions are still unanswered. The nature and origin of confinement is still mysterious; the fact that the rich spectrum of particles can be reproduced by naive bag models is astonishing. The absence (so far) of definitive evidence for states⁸ of gluons ($\equiv G$) and/or gluons and quarks may turn out to be fundamental; and yet the large number of particles that have been reported which do not fit into the accepted scheme portends excitement ahead. In the field of meson spectroscopy, a low energy antiproton machine can be used to provide high statistics measurements

of exclusive final states resulting from $\bar{p}p$ and $\bar{p}n$ annihilations, to enable definitive determinations of possible new states.

The various processes which occur when antiprotons annihilate in nuclei offer a rich milieu for uncovering unanticipated phenomena. There have been many speculations and even some calculations⁹ concerning the energy densities to be expected when \bar{p} 's are absorbed in nuclei. Using a reasonable model for the hadronization process, Gibbs and Strottman find that energy densities in the very interesting range of 2 GeV/fm³ for periods of about 2 fm/c should be attainable. Under such conditions we would expect to observe the change of state of nuclear matter to that which is often referred to as "quark-gluon plasma".

A fundamental experiment¹⁰ that has yet to be done is the measurement of the gravitational force on antimatter - the determination of $g(\bar{p})$. Modern theories of gravity predict that the acceleration of protons and antiprotons in the earth's gravitational field will be different¹¹. The difference arises in quantum theories of gravity which have massive partners of the tensor graviton as carriers of the force of gravity. Note especially that this prediction remains regardless of the results from the raft of current experiments searching for anomalous gravitational attraction between matter and matter. A program of experiments with antiprotons to determine the strengths and ranges of these additional components to the gravitational force will be an important activity at a low energy \bar{p} facility.

A variety of precision tests of CPT could be done given a source of antihydrogen atoms. One can envision a measurement of the Lamb shift in

\bar{H}^0 for instance. In addition, precision measurements of the gravitational properties of antimatter may well become feasible if sources of \bar{H}^0 were to become available. Conti and Rich¹² have given estimates of what is achievable using reasonable extensions of presently existing positron sources.

In the remainder of this paper, we summarize the present status of these and some other topics as they relate to low energy antiprotons. In Section IX, we provide a table of characteristics of some of the most interesting of the experiments discussed here; the number of antiprotons required to perform these experiments is also included there.

II. TESTS OF INVARIANCE PRINCIPLES: CP, CPT, AND T

The role of precision tests of invariance principles in uncovering new and unexpected aspects of physical laws as manifest in the different fundamental interactions has a long and fruitful history. Violations of discrete symmetries often herald either a new interaction or subtle modifications to that which has been presumed known. It is fitting that enormous experimental effort continues to be devoted to the search for, and ever more precise measurement of the invariance of the interactions to different combinations of the operations of Charge Conjugation ($C \equiv$ interchange of particle \leftrightarrow antiparticle), Parity Inversion ($P \equiv r \rightarrow -r$) and Time Reversal ($T \equiv t \rightarrow -t$). Modern quantum field theories make the assumption that all physical laws are invariant under the combined operations of CPT. The discovery of CP violation in the neutral kaon

system some 23 years ago has been remarkable because of its uniqueness - it has not been observed in any other system (see also Section VIII A). The combination of CPT invariance and CP violation implies T violation; it has yet to be experimentally verified. As usual, low energy antiprotons offer an important tool for the study of CPT, CP, and T invariance.

The elegant and precise demonstration of CPT invariance in the lepton sector has been accomplished by Dehmelt¹³ and colleagues over the past quarter of a century. They have shown the equality of the inertial masses and the magnetic moments for electrons and positrons isolated in Penning traps. This tests the invariance of the electromagnetic interaction under the CPT operation. The technique will be applied to the proton - antiproton inertial mass determination¹⁴ in a LEAR experiment, PS196. The aim is to test the equality of the masses at a level of 10^{-9} , a great improvement over the current precision of 10^{-4} in the hadron sector. This will provide a test of the strong interaction under CPT. If one could compare the gyromagnetic moments of the proton and antiproton, this would test CPT in both the electromagnetic and strong interactions since the anomalous moments have a complicated source. Other tests of CPT in the electromagnetic interaction come with the study of antihydrogen, discussed in Section V.

In the classic experiments studying CP violation, one examines the 2π and 3π decay modes of the neutral kaon systems, K_L and K_S . The fact that these are mixtures of the K^0 and \bar{K}^0 leads to interference patterns from which one can extract the CP violation parameters: ϵ , ϵ' , η_{00} , and η_{+-} .

It has been emphasized by many authors^{6,15,16} that $\bar{p}p$ annihilation offers the possibility of producing tagged K^0 and \bar{K}^0 initial states. The study of the evolution of these pure states would allow a measurement of the CP parameters in an experiment having very different sources of systematic errors from the usual K_L - K_S experiments. LEAR experiment PS195 has as its goal the study of the 2π and 3π decays of the neutral kaons (CP) as well as testing the equality of the following reaction rates^{17,18,19} (a direct test of T-invariance):

$$\bar{p}p \rightarrow K^- \pi^+ K^0, \quad K^0 \rightarrow \bar{K}^0 \rightarrow \pi^+ e^- \bar{\nu}_e$$

$$\bar{p}p \rightarrow K^+ \pi^- \bar{K}^0, \quad \bar{K}^0 \rightarrow K^0 \rightarrow \pi^- e^+ \nu_e$$

Anticipated precision for the experiment is comparable to or slightly better than the current value for $|\epsilon'/\epsilon|$, and the first time observation of T violation. A more definitive experiment will require a greater number of antiprotons than can be obtained at LEAR.

We emphasize that the study of CP violation in K meson systems has recently assumed added importance. Just a few months ago, the UA1 group at CERN unexpectedly observed large mixing in the $B^0_S \bar{B}^0_S$ system.²⁰ This may mean that there is now a new system in which one can study CP violation, although at a cost that would be astronomical compared to the machine under consideration at this workshop. Indeed, the CP violation in the $B^0_S \bar{B}^0_S$ system should be related to that of the K^0 system. It is, therefore, essential to obtain as accurate and complete a parametrization of the K^0 system as possible, as a tool for trying to

obtain a fundamental understanding of CP violation (its origin rather than the phenomenological Kobayashi - Maskawa parametrization we have now).

Another experiment that was discussed by J. Miller at this workshop is the interference pattern in the 2π decay of the K_L - K_S system as a new and independent means of observing CP violation. Tagged neutral kaons produced by another order of magnitude increase in the number of antiprotons presently available would be essential for the success of such an experiment.

We observe that the equality of the lifetimes of the neutron and the antineutron is a test of CPT in the weak interaction. One should consider whether such an experiment would be useful at a low-energy \bar{p} source.

III. GRAVITY AND \bar{p} 's: $g(\bar{p})/g(H^+)$

Our standard ideas of gravity are really an interesting mixture of classical and quantum physics. The weak equivalence principle tells us that the inertial mass is equal to the gravitational mass:

$$m_I = m_G .$$

The inertial mass is a kinematic quantity; it is the one which enters in Newton's law of force:

$$F = m_I a .$$

On the other hand, the gravitational mass is the gravitational analog of a charge in electromagnetism. It is the quantity which enters in Newton's law of gravitation,

$$F = - G m_G m'_G / r^2 .$$

The principle of the invariance of the laws of physics under the combined operations of CPT tells us that the inertial mass of a particle is equal to the inertial mass of the antiparticle:

$$m_I = \bar{m}_I .$$

From this and Eq. (1) one might make the assumption that

$$m_G = m_I = \bar{m}_I = \bar{m}_G .$$

This would be unwarranted, however, because of the aforementioned observation that m_G is the equivalent of a charge. The fact that the **gravitational** mass of a particle and its antiparticle are not equal does **not** violate CPT. The principle of CPT dictates that an antiapple falls toward an antiearth in the same manner in which an apple falls toward the earth. It is silent concerning the trajectory of an antiapple (read antiproton) toward the earth. Arguments along this line led to an approved experiment¹⁰ (LEAR PS200) to make this fundamental measurement.

In fact, modern attempts to unify gravity with other forces of nature lead to the generic conclusion¹¹ that the gravitational acceleration of the antiproton will not be equal to that of the proton, at some level. At present, these theories are hoped to be renormalizable or finite; they do violate the weak equivalence principle and predict effects that are non-Newtonian. One can mention several of the physical motivations: supersymmetry, dimensional reduction, string theory. The literature concerning this subject is now outrageously large, and growing exponentially.

The fact that none of these theories has yet been proven to be mathematically consistent deters no one. Additionally, the apparent lack of any hope to confront these theories with experiment, such as verifying a particle spectrum, leads to a healthy skepticism concerning their connection with the perceived reality. But they are tantalizing; indeed, they may be giving a hint into what the true physics might be. It is likely that the experiment concerning the gravitational acceleration of an antiproton in the earth's field may bear on this subject.

These modern theories of gravity have many common features. They have spin = 1 and = 0 partners of the graviton, which may couple in a generation-independent way to fermions, and in addition have finite ranges. What phenomenological effects are implied by these new particles? By considering a linearized theory and ignoring relativistic effects, we obtain the following form for a gravitational potential:

$$V(r) = [-Gm_1m_2/r] [1 \pm ae^{-r/v} + be^{-r/s}].$$

(See reference 11 for the complete treatment including the other effects.) The first term, the normal tensor gravity term, is followed by two new, non-Newtonian terms. The vector term has a \pm associated with it, a relative coupling constant, a , and a range, v . The scalar term has a relative coupling constant b and range s . (The ranges are the inverse masses of the graviphoton and graviscalar in appropriate units.)

The minus sign in front of the vector term would correspond to matter repelling matter. This is mathematically the same as the vector photon of electromagnetism: like charges repel. On the other hand, opposite charges (antimatter and matter), attract. The plus sign describes this situation.

One naively expects a and b to be of gravitational strength. (In principle, there could be many components; we parametrize all these as being summed up to be a and b .) Thus, if a and b are of equal magnitude, then for matter-matter interactions the vector and scalar terms would almost cancel. One might observe an effect only in very precise matter - matter experiments. However, for antimatter - matter interactions, the sign in front of the vector term is opposite, and the vector and scalar terms add together. The antimatter - matter interaction displays a new first order effect; in addition, the matter - matter interaction gains a new, second order effect.

The size of the effect depends upon the value of the parameters mentioned above. If these new effects are on the Planck scale, 10^{-33} cm, then they can be considered to be unobservable. If, however, they are on the 200 meter scale, which the "fifth force" advocates would like, then although the effect would be present, it would be undetectable in the approved antiproton experiment. However, if it's on a longer scale, then indeed an effect will be measured..

What size of effect could one have? Stacey, Tuck, and Moore²¹ have done an analysis of the Australian mine data, using both the new vector and a scalar term. They find $(a - b) \approx 0.01$, and allowed ranges up to ≈ 450 km. This result has been put into the PREM model of the earth and integrated to see what effect would be anticipated for the antiproton gravity experiment.¹⁰ The calculated results on the variation of g , as a function of the (set to be equal) ranges, show surprisingly large effects for ranges greater than several kilometers. In particular, for ranges of 40

km, one calculates a 1% effect in the antiproton experiment, which should be measureable. At 450 km one would have a 14% effect, definitely measureable. This is for $a=b=1$; the effect scales with the value of $a(=b)$.

If you add to this the analysis of rapidly-rotating pulsars, which allows values of (a,b) up to $O(100)$, then the expected difference in g for the antiproton could be

$$\Delta g/g = 0.14 \cdot a \cdot v / 450 \text{ km.}$$

The details of the experiment are given elsewhere.¹⁰ Simply stated, antiprotons from LEAR will be decelerated in several stages by the use of degrading foils and Penning traps, eventually cooling them down to approximately 10 K. They will then be tossed up a superconducting drift tube; the cutoff in the arrival time spectrum will provide a measurement of g . More accurately, the comparison between antiprotons and H^- will allow this to be extracted.

Of course, the ultimate gravitational experiment concerning antimatter would be done with neutral antihydrogen. The advent of laser storage and velocity selection techniques for single atoms and magnetic trap devices may eventually open up the possibility for such an experiment.

IV. ANTIPROTON ANNIHILATION IN NUCLEI.

Under what conditions might we expect to form a "quark-gluon plasma" (QGP)? For a start, we believe that a state of quarks and gluons exists inside a nucleon. Given a nucleon radius of 0.8 fm, the matter density, ρ ,

is about 0.5 GeV/fm^3 . For a radius of 0.6 fm , $\rho \approx 1 \text{ GeV/fm}^3$. It seems reasonable to expect that if we can arrange to obtain a density of 1 to 2 GeV/fm^3 over a nuclear volume, we just might observe a change of phase to the long heralded QGP. This region represents an increase in mass density to $\rho/\rho_0 = 6$ times normal nuclear matter density at normal nuclear temperature, or equivalently a temperature of 180 to 200 MeV at normal density. Heavy ion collisions probe the high density-low temperature region whereas energetic \bar{p} - Nucleus collisions may well provide a means to explore the "low" density-high temperature region of the nuclear matter phase diagram.

Qualitative arguments about what incident \bar{p} momentum would maximize the temperature inside the nucleus proceed along the following lines: slow \bar{p} 's annihilate on the surface because of the very large total cross section; the energy quickly escapes the nucleus. At higher \bar{p} energies the annihilation takes place about a fermi inside the nucleus. The annihilation pions, numbering about ten, move mostly forward in the lab frame, and have a high probability of depositing their energy in a small part of the nuclear volume through collisions with several (≈ 5) of the constituent nucleons.

Motivated by such qualitative considerations, Gibbs and Strottman⁹ performed calculations using the Intranuclear Cascade (INC) formalism. Their results show that for 6 and 8 GeV/c antiprotons absorbed on an $A=100$ nucleus, the temperature attains the 180 MeV value where a phase transition is predicted. They also calculate the total amount of energy that is actually absorbed in the nucleus. For 8 GeV/c \bar{p} 's, 6 GeV gets

absorbed. Thus the process is very efficient for putting the energy where it is desired - in the nucleus. The calculated nuclear densities that are attained during the excursion into the high temperature domain are modest: $\rho/\rho_0 = 1.4$ to 1.8 . It is this result that leads to the conclusion that energetic \bar{p} absorption on nuclei provides an alternate route towards a quark-gluon plasma. It complements the more widely discussed relativistic heavy ion collision technique since it utilizes high T - low ρ , instead of the converse.

For a long time the role of strangeness production as a key signature of QGP formation has been emphasized. Close examination of data from a bygone era has led Rafelski²² to conclude that high nuclear temperatures (>100 MeV) have been observed in at least three experiments:

- 1) $\bar{p} d \rightarrow (\text{p}_{\text{spectator}}) K \bar{K} \pi$'s at $1 - 3$ GeV/c,
- 2) $\bar{p} {}^{238}\text{U} \rightarrow \text{neutron}$ with the \bar{p} absorbed at rest, and
- 3) $\bar{p} {}^{181}\text{Ta} \rightarrow \Lambda, K_S$ at 4 GeV/c.

These are discussed in some detail in the article by G. A. Smith in the present proceedings. The conclusion can only be that the opportunities for new discoveries here are excellent.

V. ANTIHYDROGEN AND BASIC PHYSICS TESTS.

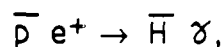
The formation and control of antihydrogen would represent both a technological triumph and a golden opportunity. Methods of obtaining this exotic atom have been studied by several groups.^{12,23,24,25} Once such an

atom is obtained, it will be a veritable CPT laboratory for making fundamental physics tests of quantum electrodynamics. Finally, this would set the stage for the even more demanding project of storing possibly macroscopic quantities of antihydrogen in the form of cluster ions. We examine in more detail these three separate stages of scientific development which would become accessible to study at a North American antiproton source.

A. ANTIHYDROGEN FORMATION

Antihydrogen is composed of the antiparticles of the constituents of hydrogen, viz. an antiproton orbited by a positron. Since both these particles have separately been captured and controlled at low energies in ion traps, it is apparent that the next step is the formation, then control of antihydrogen from these entities.

The first effort in this direction is the proposal²⁷ to merge beams of positrons and antiprotons at LEAR, and observe the following reaction:

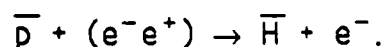


that is, the radiative formation of antihydrogen. To boost the rate of formation of the atom, the CERN group considered using a pulsed dye laser to stimulate capture of positrons to the $n = 2$ Bohr orbit. They calculate that they could produce an antihydrogen atom every few seconds using this technique.

An experiment using normal matter is planned at the University of Western Ontario.²⁵ Using the existing apparatus of the Merged Electron

Ion Beam Experiment, protons and electrons will undergo stimulated radiative recombination to yield experimental results which bear directly on the CERN experiment. As a further step, Rich, et al.²⁷ have proposed using a storage ring to contain the positrons, which should enhance the rate considerably.

Another approach circumvents the necessity of having the relative velocity of the antiproton and positron being so precisely matched. Antiprotons collide with positronium and form antihydrogen in the following reaction:



In the Aarhus collaboration,²³ the idea is to have a beam of antiprotons going through a hollow cylinder of aluminum. A separate beam of positrons enters through a hole in the cylinder, strikes the inside wall, and forms positronium. The first experiment would expect on the order of one antihydrogen atom per second, with dramatic increases foreseen after more work.

The above techniques would produce relatively fast antihydrogen. Colder antihydrogen would come from creation in traps. One should be able to store 10^{10} charged particles per cm^3 in traps at 10 K. This led to the suggestion²⁸ of a pair of nested ion traps, each containing such numbers of positrons and antiprotons. Scenarios were envisioned wherein these particles could be induced to combine in very short times. A complete discussion of these ideas is contained in the article by Mitchell in these Proceedings.

B. BASIC PHYSICS TESTS

After successfully creating antihydrogen, the problem of containment and control becomes imperative, since it is neutral. A natural choice is a magnetic trap.²⁹ Single atoms might be so contained given an appropriate laser to control their velocity. In fact, this may well be the most precise method that one could devise for measuring the gravitational attraction of antimatter to the earth.

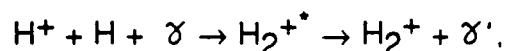
Experiments that would become immediately possible would concentrate on study of the antihydrogen atoms before their ultimate fate of annihilation. Poth³⁰ has emphasized the opportunities offered in atomic and strong interaction physics by studies of antiprotonic and hyperonic atoms. The most obvious fundamental measurements that would be made with antihydrogen, however, would be the tests of CPT for Quantum Electrodynamics.

As discussed in detail in the article by Nieto in these Proceedings, the CPT theorem states that for a given interaction, any measurement made with hydrogen - magnetic moment, transition amplitudes, decay rates, energy levels, energy shifts - would have the analogous quantity in antihydrogen exactly predicted by CPT. The antihydrogen atom would thus allow tests of CPT to be made for the entire set of measurements which form the basis of QED, as we know it, for the hydrogen atom.

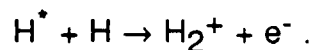
C. CLUSTER IONS

The final topic in this section concerns the formation of cluster ions of antimatter. As Stwalley discusses in these Proceedings, the concept is daunting, but challenging. A cluster ion, denoted by H_N^+ , is an ion composed of N hydrogen atoms with one electron removed, leaving it with a single positive charge. In this case it reduces simply to N protons and (N-1) electrons.

Ultimately what would be desired is to form a very large "seed crystal" consisting of N antihydrogens. This could conceivably then be augmented, a single atom of antihydrogen at a time. Obviously, one can examine the feasibility of this scheme by using ordinary hydrogen. One possible path is to first form H_2^+ by indirect radiative association:



or associative ionization:



Laser-assisted association could be used to make H_3^+ from H_2^+ and H. In principle, one could continue this process to high N, but this involves a complicated knowledge of the spectroscopy for each species. A series of three body interactions may be preferable at this stage.

It is a fortunate circumstance that all these complicated, unknown aspects of cluster ions can be studied with normal matter first. The transition to antimatter will require that the techniques evolved for matter ensure that in the antimatter case, no antimatter comes in contact

with matter, because of the added complication of annihilation. Stwalley covers this aspect of the problem in some detail.

VI. MESON SPECTROSCOPY.

Meson spectroscopy has reached an exciting stage. A variety of experiments find evidence for resonances which do not fit into the standard pattern of $\bar{q}q$ meson nonets. A current table of exotic results which updates Ref. 8 has been prepared by Sharpe and is given here as Table I. Eleven "confirmed oddities" are listed. Good reasons are given in the paper by Sharpe in these Proceedings as to just why none of them fit neatly into our current framework of $\bar{q}q$ nonets. These states could well represent the opening up of a threshold of exotic meson resonances - those which contain constituent gluons.

Such exotic mesons have long been expected in the spectrum of QCD. This follows from an extrapolation of models which can account for the standard pattern of meson nonets, e. g. the MIT bag model or the flux tube model. These models suggest that in addition to q and \bar{q} constituents, there should be independent excitations of gluons - constituent gluons (g). If so, there will be new resonances: glueballs ($G \equiv gg$) and meiktons or hybrids ($\bar{q}qg$). Some of these states have exotic quantum numbers which are not available to $\bar{q}q$ states, e. g. $J^{PC} = 1^{-+}$. We shall refer to all such states as exotic mesons.

It has not yet been proved theoretically, however, that such exotics exist in the spectrum of QCD. Eventually, numerical lattice calculations

TABLE I. Exotic Results in Meson Spectroscopy*

$J^{PC}=0^{+-}, 1^{++}, 1^{+-} \bar{q}q$ nonets filled.
Confirmed oddities are listed here.

<u>Conjectured Structure</u>	<u>Particle Name</u>	J^{PC} —	Isospin —	<u>Mode of Study with \bar{p} source</u>
$G, \bar{q}q$	η or $\tau(1460)$	0^{-+}	0	$\bar{p}p$ at rest
$\bar{q}qg$	f_1 or $E(1420)$	$1^{++} (1^{-+})$	0	"
$G, \bar{q}q$	f_0 or $G(1590)$	0^{++}	0	"
$\bar{q}qg$	ρ' or $C(1400)$	1^{--}	1	"
\bar{q}^2q^2	$X(1480)$	0^{++} or $2^{++}?$		"
G	f_2' or $\theta(1720)$	2^{++}	0	$\bar{p}p$ in flight
$\bar{q}qg, \bar{q}q$	$\xi(2200)$	2^{++} or 4^{++}	0	"
G	$\phi\phi$ (3 states ≈ 2200)	2^{++}	0	"
$\bar{q}q$	$\phi\phi$ (2200)	0^{-+}	0	"

*Table prepared by S. Sharpe, see his article in these Proceedings.

Data from LASS (Kp), MKIII, TPC/MKII, Lepton-F, BNL, MPS, ...

G=gluons.

In no case is interpretation unambiguous.

Need more decay channels--Need more data.

may be able to answer this question from first principles, and provide predictions for the masses of the lightest exotics. Until then, progress can only come from experiments searching for exotic states, measuring their properties, and comparing the experimental results with model predictions. One can then decide between phenomenological models, which in turn will provide better theoretical input to experiment. The goal is eventually to tie both the model and the data it reproduces to the calculations based on first principles. In this way we achieve a quantitative test of QCD, while at the same time obtaining useful phenomenological models for the spectrum of field theories. These can in turn be applied to future theories of matter at shorter distances.

A high luminosity, low energy \bar{p} source can play a central role in such a program. Annihilations at rest enable a detailed study of exotic mesons with masses up to ≈ 1.7 GeV, while annihilations in flight can extend this range up to and beyond the ψ . Present models all suggest that the threshold for exotic mesons lies below 1.7 GeV, and that the number of states increases rapidly with energy. Decay widths increase with increasing mass, so the spectrum can probably only be unravelled for about 1 GeV above threshold. Thus a low energy \bar{p} source will provide a window through which one hopes to view this exotic landscape.

It should be emphasized that a successful search for such states will, of necessity, utilize every known experimental trick one can muster. A good example is quantum number restriction of final states, which helps to reduce the inevitable backgrounds from conventional mesons. When antiprotons annihilate at rest in liquid hydrogen, Stark mixing causes

practically every annihilation to proceed from an initial $L=0$ state. For particular final states, e. g. $\eta\pi^0\pi^0$, $\eta\eta\pi^0$, $\phi\pi^0\pi^0$, this can be especially powerful. Because the branching ratios for such channels are expected to be small, probably in the range 10^{-4} to 10^{-5} , high luminosity will be essential for these measurements.

Another potent experimental strategy is to use the fact that a \bar{p} machine of several GeV/c represents a real ψ factory. It has long been recognized that the most promising way to find unambiguous evidence for glueballs is in the radiative ψ decays: $\psi \rightarrow \gamma X$. In this case X can be a digluon in a color singlet. By using realistic \bar{p} machine parameters of: a) momentum resolution of a few times 10^{-5} (e^- cooling, gas jet target), and b) luminosity of $10^{31} \text{ cm}^{-2} \cdot \text{sec}^{-1}$ (current technology), then one obtains³¹ the astonishing estimate of 10^9 ψ 's produced per year! This is hundreds of times as many ψ 's as have been produced so far in all the e^+e^- collider experiments to date. The two big advantages offered by a \bar{p} machine are as follows: a) luminosity - 10^{31} cf. 10^{29} for e^+e^- machines, and b) very small momentum spread - $\Delta\sqrt{s}/\Gamma_\psi$ is less than one for $\bar{p}p$, cf. ≈ 100 for e^+e^- machines. The fact that much hadronic background accompanies the desired process in the \bar{p} case is an inconvenience that can be managed by modern fast triggering techniques.

VII. ANTIMATTER STORAGE IN NORMAL MATTER

The ability to store antimatter in matter will probably be required if

we are to realize the dream of using antimatter in large-scale practical applications. On the way towards that goal lies an array of solid state physics studies of much interest. Assuming, for example, that a source of antiprotons exists with the appropriate deceleration facilities to make them available at low energies, the question that is addressed by L. Campbell in these Proceedings is as follows: just how many of these antiprotons can be stored by which techniques.¹

The "standard" ways of storing antimatter are in electromagnetic bottles, such as Penning traps. In the section on antihydrogen, we mentioned the possibility of storing an antihydrogen atom in a magnetic bottle; while very interesting for many experimental purposes, it is of limited utility for dense antimatter storage. (The possibility of electromagnetic levitation of solids is skipped here.) In order to store significant amounts of antimatter, new technologies will have to be invented.

One technology could involve direct storage of antiprotons in condensed matter because the electromagnetic force, which prevails there in astonishing complexity, has a much longer range than the strong force which is responsible for the ultimate fate of annihilation of the antiproton. However, an equally important feature of stable condensed matter, Fermi statistics, discourages hope for equilibrium trapping of antiprotons. Nevertheless, the combination of effects like dynamic stabilization and special environments such as the surface of superfluid ^4He may lead to environments that locally trap antiprotons. Even small-scale surface storage would be quite valuable as a nucleation site

for antihydrogen cluster ion formation by providing a mechanism for efficiently conducting the condensation energy to normal matter.

An even longer term version of this question applies to the possibility of neutralizing antiprotons with positrons to produce antihydrogen. Then one would want to know how to store this even more interesting yet difficult to handle species. The interesting chemistry and physics problems associated with this are discussed by Stwalley in these Proceedings.

The basic problem in storage can be understood in the context of Lieb's theorems³² on the absolute stability of matter. Lieb has shown that the stability of large-scale matter is due ultimately to the Pauli exclusion principle. However, there is no Pauli exclusion principle operating between matter and antimatter, so there is nothing *a priori* to prevent their coming together, and hence annihilating. Thus, one is forced to try to avoid the implications of Lieb's theorems.

For charged particles, containment by some configuration of static electric fields is forbidden by Earnshaw's theorem. There are, however, promising avenues to explore in steady-state, nonequilibrium systems (such as storage rings) or those systems in which the decay constant of the instability is long (as in some traps utilizing combinations of electric and magnetic fields). As an obvious first step, one might consider the miniaturization of electromagnetic traps. As Campbell discusses in these Proceedings, existing traps can, in principle, be scaled down in size to the order of 10^{-4} cm, with the consequent maximum densities of order $10^{13}/\text{cm}^3$. Thus, Campbell can "envisage" a cubic meter of these small

traps containing, in principle, up to 10^{18} antiprotons.

However, these would still not be atomic - scale traps. Such a trap has been conceived of by Clark, *et al.*³³ They point out that one could use the "Stark saddle", or force - free location of a particle in an applied external field plus a local ion field. Since this is a saddle, applying a perpendicular magnetic field will only produce metastability, as compared to the stability of a Penning trap. The numbers imply that this concept may be of use in gaseous phase.

There also may be an atomic analog to the storage ring which would make use of the phenomenon of channeling of charged particles in a crystal: the channel ring. This is even more speculative, since it is not known how to fabricate a closed-path channel in a crystal. It is even more difficult to imagine how to arrange a reflection at each end of a straight path. However, one might derive encouragement from the recent, unexpected observation³⁴ of π^- channeling in a helical pattern around lines of atoms in a crystal.

Campbell has estimated the atomic scale trapping parameters which would prevent a stored antiproton from either annihilating directly or being first captured in an atomic orbit and then annihilating. He finds that such a trap could contain an antiproton for a year if the antiproton is kept a few Ångströms away from ordinary matter. Muons have similar trapping characteristics in this respect, and so would serve as good test particles in developing such small scale traps. (It is also mentioned that polaron and exciton states centered about antiprotons in solids provide a rich field of study for theorists interested in antiprotons in solids.)

The problem of storage in solids can be approached from an alternative viewpoint: that of understanding the quantum mechanical properties of particles in potential wells. Just how does a particle tunnel and/or decay from a metastable state to a lower state: that is, to annihilation. Various studies have found that:

- i) By slightly changing the shape of a potential, one can inhibit tunneling unless there is either coupling to other modes or dissipation in the system.
- ii) The exponential decay rate can be modified significantly if the product of the decay itself is unstable.
- iii) In certain coupling situations, muons and protons inside solids can change from a diffusive condition to a trapped condition.
- iv) A charged particle in a lattice can be localized under the action of a time-dependent electric field.
- v) The conditions for localization and/or tunneling in two-level systems have been studied in detail.

Note that the above separate topics and their conclusions are in principle (and sometimes explicitly) related to each other.

All the above ideas suggest that we must rely on experiments to tell us which, if any, of them will yield practical large-scale storage devices. We also note that none of these experiments are presently being done. Although some of the suggestions are admittedly in the "let's see what happens category," this is often the way new phenomena are discovered in

the complicated condensed matter world. It is instructive to mention the example of high temperature superconductors in this connection.

A first, particular suggestion is to see if channeling occurs, and how it occurs, with antiprotons. Equally interesting is what antiprotons will do in superfluid ^4He . Some have suggested that "bubbles" or self-contained cavities might occur, as is the case with electrons³⁵ and positronium.³⁶ Further, there is the possibility that with an applied electric field one can make electron-antiproton states at the surface which do not penetrate the surface (because of the electrons) and thus have a long antiproton annihilation rate.

Three environments where one does not expect long scale trapping to occur are in degenerate liquid ^3He , superconductors, and semiconductors. However, these are all such interesting and exotic substances, that it is worth performing experiments with antiprotons just as a diagnostic tool, let alone for the possible unforeseen surprises that might occur.

VIII. HIGHER ENERGY \bar{p} 's

A. CP VIOLATION IN $\bar{D}D \rightarrow \bar{\Lambda}\Lambda$

It was 23 years ago that CP violation was discovered in the decay of the neutral kaon system ($K^0 \leftrightarrow \bar{K}^0$). In the interim, this puzzling phenomenon has not been observed in any other system than the one in which it was originally discovered. The Standard Model has problems accomodating the magnitude of the violation; myriad extensions to the

standard model have been proposed:

- 1) the Kobayashi Maskawa Model wherein the violation occurs in the coupling of the gauge bosons to the quarks but is generated by the Higgs sector,
- 2) the Weinberg Higgs Model where the violation is found in the Higgs potential and is manifest in the coupling of the Higgs to the quarks,
- 3) the Superweak Model, where again the violation comes from Higgs, but in this model CP violation would be restricted only to the kaon system, and
- 4) the Left - Right Models in which the violation arises from both the effects in 1) and 2).

Whether both $\Delta S=2$ (as in K^0, \bar{K}^0) and $\Delta S=1$ (as in $\bar{p}p \rightarrow \bar{\Lambda}\Lambda$) exhibit CP violation would appear to be an experimental question. The various models of CP violation differ in their predictions⁵ of the magnitude of $\Delta S=1$ $\bar{p}p \rightarrow \bar{\Lambda}\Lambda$ CP violation. They all agree, however, that it is sufficiently small as to make the measurement extremely hard.

The experimental quantities which are expected to be related to the CP violating phases and thus demonstrate CP violation if found to be non-zero are:

$$\Delta = (\Gamma - \bar{\Gamma}) / (\Gamma + \bar{\Gamma})$$

$$C = (\alpha + \bar{\alpha}) / (\alpha - \bar{\alpha})$$

$$B = (\beta + \bar{\beta}) / (\beta - \bar{\beta}).$$

Thus Δ measures the difference in the partial decay width for the $\bar{\Lambda}$ and

the Λ ; C and B reveal differences in the decay parameters, which characterize the angular distribution of the decay products of the hyperon and antihyperon. By using the known $\Delta I = 1/2$ rule and final state π -N interaction, Donoghue⁵ estimates that the magnitudes of the three quantities are related as follows: $B \approx 10 \cdot C \approx 100 \cdot \Delta$. He also finds that the Kobayashi Maskawa Model predicts about $2 \cdot 10^{-5}$ for the value of C, while the Weinberg Higgs Model yields 10^{-4} .

Although a recent LEAR experiment³⁷ with only 4,000 events found that $C = -0.07 \pm 0.09$, consistent with zero, it is obvious that an improvement in precision by a factor of one to ten thousand is not a trivial matter. One will need to measure accurately the symmetric decays $\Lambda \rightarrow p\pi^-$ and $\bar{\Lambda} \rightarrow \bar{p}\pi^+$; between 10^8 and 10^9 events in this channel must be collected and analyzed in order to achieve the required level of precision. The number of antiprotons required is very large, on the order of 10^{14} to 10^{15} .

B. EXCLUSIVE CHARMONIUM DECAYS

As a representative example of the broad class of experiments that study exclusive final states in $\bar{p}p$ annihilation, we mention one of the rare "crisply defined experimental puzzles" in high energy physics which would, incidentally be amenable to study with a high luminosity \bar{p} source. The evidence for this puzzle has been accumulating for many years; Brodsky, Lepage and Tuan⁷ reminded us of its significance in a recent paper.

The decay of the ψ and the ψ' into exclusive final states of hadrons is expected to proceed via three gluons or, occasionally, via a single direct photon. The probability for the decay is proportional to the square of the wave function of the $c\bar{c}$ pair at the origin: $|\psi(0)|^2$. Thus one would expect that the ratio of the branching fractions for ψ' and ψ to hadrons to be the same as for leptons, namely:

$$\begin{aligned} Q_h &\equiv B(\psi' \rightarrow \text{hadrons}) / B(\psi \rightarrow \text{hadrons}) \\ &= B(\psi' \rightarrow e^+e^-) / B(\psi \rightarrow e^+e^-) \\ &= 0.135 \pm 0.023 \end{aligned}$$

For a host of final states such as $\bar{p}p\pi^0$, $2\pi^+2\pi^-\pi^0$, $\pi^+\pi^-\omega$, and $3\pi^+3\pi^-\pi^0$, this expectation has been fulfilled. For the $\rho\pi$ and $K^*\bar{K}$ final states, this is not so:

$$\begin{aligned} Q_{\rho\pi} &< 0.0063 \\ Q_{K^*\bar{K}} &< 0.0027. \end{aligned}$$

These are upper limits only; thus the ratios are at least a factor of 20 and 50 times smaller than expected. An appealing proposed explanation is that a reasonably narrow intermediate state of gluonium exists close to the ψ mass which then couples to hadrons. In essence this makes the denominator of Q_h larger than expected from QCD arguments alone.

Here is an outstanding example of an experiment that is very difficult without a \bar{p} source (see section VI concerning the efficiency of production of ψ 's), but would be relatively straightforward with a machine that would take \bar{p} 's up to 7 GeV/c.

IX. SUMMARY AND CONCLUSIONS

The range of physics topics that has been touched on in the present article is indeed vast. The participants in the Basic Physics Program section of the workshop summarized the experimental requirements for most of the topics that were discussed there. Table II gives the results of these requirements. The degree of difficulty, as defined in the footnote to the table, is indicated for a range of experiments; also given is the number of antiprotons that would be required to perform the experiments. As can be seen there, the range covers the map - from just a few antiprotons to more than 10^{14} . As a reference point, we note that LEAR has provided fewer than 10^{13} \bar{p} 's in any year of operation³⁸ up to the present time. We also mention that the CP violation experiment (PS195) has been approved for a total of 10^{13} \bar{p} 's, but obviously could use at least another order of magnitude in order to do a good measurement of $|\epsilon'/\epsilon|$.

There was much discussion at the workshop about the feasibility of portable sources of \bar{p} 's - a sort of filling station approach. We indicate in the last column of Table II whether the experiment is considered suitable for a portable source.

We have summarized the physics case for proceeding with a Low Energy Antiproton Source in North America. In the opinion of the attendees at the workshop, this case is most alluring, having great potential for new and unexpected discoveries. The time is right for a push for a speedy construction of such a facility.

TABLE II. Characteristics of Low Energy \bar{p} Experiments

<u>Experiment</u>	<u>Difficulty</u> *	<u>No. \bar{p}'s req'd</u>	<u>Portable?</u>
1. $\bar{p}p \rightarrow \bar{\Lambda}\Lambda$, CP violation	Great	$>10^{14}$	No
2. K^0, \bar{K}^0 , CP, & T violation	High	$>10^{14}$	No
3. Inertial $M=\bar{M}$? CPT test	Low	Few	Yes
4. \bar{H}^0 spectra, Lamb, Ry? CPT	High	10^{12}	Yes
5. Gravity: $g(\bar{p})=g(p)$?	High	10^{10}	Yes
6. Hadron Spectroscopy, exotica?	High	10^{12}	No
<hr/>			
7. \bar{p} - A : Quark-Gluon Plasma	Low	10^{14}	No
8. \bar{p} - A : Strange Fireballs, etc.	Low	10^{14}	No
<hr/>			
9. Cold \bar{H} , \bar{H}_2 , \bar{H}^- ... prod ⁿ & manip ⁿ	High	few to $10^{\geq 12}$	Yes
10. Cold e^+ plasma + \bar{p} 's	High	few	Yes
11. Matter/AntiM Collision Dynamics	Low	$>10^6$	Yes
12. Condensed Matter Studies:			
a. \bar{p} atoms	Low	10^6	Yes
b. \bar{p} channeling	Low	10^6	No?
c. \bar{p} 's in dynamic traps	Great	10^6	Yes

*Definition of the different degrees of difficulty:

Great = Don't Know How

High = We Know, But It's Hard

Low = State of the Art.

X. REFERENCES

1. Proceedings of a Workshop on Physics at LEAR with Low-Energy Cooled Antiprotons (May, 1982, Erice), ed. U. Gastaldi and R. Klapisch, (Plenum, New York, 1984).
2. Proceedings of a Workshop on Physics with Antiprotons at LEAR in the ACOL Era (January, 1985, Tignes), ed. U. Gastaldi, R. Klapisch, J. M. Richard, and J. Tran Thanh Van, (Editions Frontieres, Gif sur Yvette, 1985).
3. Proceedings of the Workshop on the Design of a Low Energy Antimatter Facility (October, 1985, Madison), ed D. Cline, (World Scientific, 1987)
4. Proceedings of the First Workshop on Antimatter Physics at Low Energy (April, 1986, Fermilab), ed. B. E. Bonner and L. S. Pinsky, (FNAL Report, 1986).
5. J. F. Donoghue, p. 241 of Ref. 4; J. F. Donoghue, B. R. Holstein, and G. Valencia, Phys. Letts. B 178 (1986) 319.
6. R. L. Jaffe, p. 1 of Ref. 4; M. G. Olsson, p. 119 of Ref 4.
7. S. J. Brodsky, G. P. Lepage, and S. F. Tuan, Phys. Rev. Letts. 59 (1987) 621.
8. S. R. Sharpe, p. 165 of Ref 4, and the present Proceedings.
9. W. R. Gibbs, p. 355 of Ref 4; D. Strottman and W. R. Gibbs, Phys. Letts. B 149 (1984) 288.
10. PS200 at LEAR, "A Measurement of the Gravitational Acceleration of the Antiproton".
11. T. Goldman and M. M. Nieto, Phys. Letts. B 112 (1982) 437; T. Goldman, R. J. Hughes, and M. M. Nieto, Phys. Letts. B 171 (1986) 217; also Phys. Rev. D 36 (1987) 1254.
12. R. S. Conti and A. Rich, p. 97 of Ref.3.
13. P. B. Schwinberg, R. S. Van Dyck, Jr., and H. G. Dehmelt, Bull. Am. Phys. Soc. 24 (1979) 1203; Phys. Rev. Letts. 47 (1981) 1679.
14. CERN LEAR Experiment PS196, FNAL, Mainz, and U. Washington.
15. L. Wolfenstein, p. 227 of Ref 4.
16. R. K. Adair, p. 453 of Ref 2.
17. P. K. Kabir, Phys. Rev. D 2 (1970) 540.
18. N. W. Tanner, p. 483 of Ref. 2.
19. CERN LEAR Experiment PS195; also see the writeup by J. Miller in

the present Proceedings for an excellent, detailed discussion of the physics of this experiment.

20. CERN Courier, p. 17, Oct. 1986.
21. F. D. Stacey, G. J. Tuck, and G. I. Moore, Phys. Rev. D 36, (1987); F. D. Stacey, et al., Rev. Mod. Phys. 59 (1987) 157.
22. J. Rafelski, p. 507 in Ref. 1.
23. B. I. Deutch, et al, Phys. Scr. T. (to be published); see also p. 371 of Ref. 4.
24. H. Poth, p. 325 in Ref. 4.
25. J. B. A. Mitchell, in the present Proceedings.
26. G. Gabrielse, et al., Phys. Rev. Lett. 27 (1986) 2504.
27. A. Rich, et al., in Proc. of the NATO Advanced Research Workshop on Atomic Physics with Positrons (in press).
28. C. F. Driscoll, p. 184 in Ref. 3.
29. D. J. Wineland and W. M. Itano, Physics Today 40 (No. 6), (1987) 34.
30. H. Poth, Proc. of the Conference on the Intersections Between Particle and Nuclear Physics, AIP Conf. Proc. #150, e. D. F. Geesaman (AIP, NY 1986) p. 325.
31. M. S. Chanowitz, p. 393 of Ref. 4.
32. E. H. Lieb, Rev. Mod. Phys. 48 (1976) 553.
33. C. W. Clark, E. Korevaar, and M. G. Littman, Phys. Rev. Lett. 54, 320 (1985).
34. T. H. Braid, et al., Phys. Rev. B 19, 130 (1987).
35. C. G. Kuper, Phys. Rev. 122, 1007 (1961).
36. R. A. Ferrell, Phys. Rev. 108, 167 (1957).
37. LEAR PS185, P. D. Barnes, et al., submitted to Phys. Lett. B; CERN preprint CERN-EP/87-153, 26 August 1987.
38. P. Lefevre, D. Mohl, and D. J. Simon, p. 69 in Ref. 4.

Antiproton Annihilation in Nuclei

Gerald A. Smith*
Laboratory for Elementary Particle Science
Department of Physics
The Pennsylvania State University
University Park, PA 16802 USA

1. Introduction

In this talk I will attempt to develop several ideas which could motivate a long term program of research on annihilation of antiprotons in nuclei at a low energy antiproton facility. To a large extent these ideas, both theoretical and experimental, have evolved as a result of the LEAR program, which has been active at CERN since 1984. Limits of time and space require that I restrict my discussion to a few select topics, which are:

- A. High Nuclear Temperatures by Antimatter-Matter Annihilation;
- B. Deep Annihilation, Strangeness and Quark-Gluon Matter;
- C. $\bar{N}NN$ Fireballs; and
- D. Fission: A New Tool for Studying Strangeness in Heavy Nuclei

I am indebted to the organizers and contributors of the recent IV LEAR Workshop, held at Villars-sur-Ollon, Switzerland on 6-13 September 1987, which I attended and from which I have drawn valuable information for this paper.

2. High Nuclear Temperatures by Antimatter-Matter Annihilation

Strottman and Gibbs [1] have calculated within the framework of the relativistic hydrodynamic and intranuclear cascade models the evolution of nuclear temperature with time after the annihilation of an antiproton or antideuteron on a heavy nucleus. Their results are shown in Fig. 1. Both models provide evidence for extremely high temperatures (> 180 MeV) lasting for several fm/c for incident antiproton momenta above $\sim 6-8$ GeV/c. Nuclear densities peak around 1.4-1.8 times normal nuclear densities in these calculations. At these momenta the antiproton is capable of penetrating the nucleus about one fermi before annihilating, resulting in an efficient deposition of energy.

It is claimed [1] that QCD lattice calculations predict a phase transition from ordinary hadronic matter to a quark-gluon plasma at high temperature (~ 180 MeV) and relatively low nuclear density. Therefore, the situation described by Strottman and

Gibbs looks promising. The immediate question is "What is the signature for the phase transition?" We will speculate on the answer to this question in the next section. In closing this section we note that other authors [2] are somewhat less optimistic on the likelihood of creating the conditions for a phase transition in antiproton-nucleus collisions.

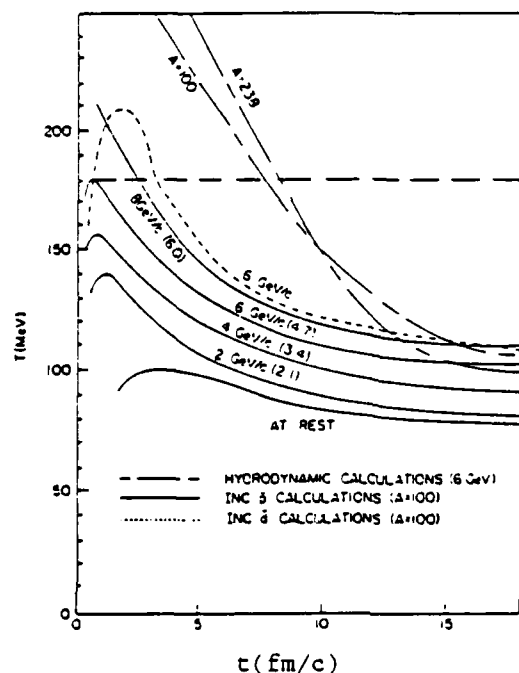


Fig. 1 - Comparison of the temperature obtained as a function of time for the two models considered. The "at rest" absorption occurs on the surface and the annihilation for the other cases takes place on the beam axis just inside the nuclear surface (0.7 fm for the hydrodynamic calculation and 1 fm for the INC). The numbers in parentheses give the actual energy deposited in the nucleus in GeV. The momentum quoted for the \bar{d} is per antinucleon.

3. Deep Annihilation, Strangeness and Quark-Gluon Matter

In his review talk at Villars [3] Jan Rafelski emphasized the importance of searching for unusual conditions in nuclear matter which may confirm the predictions described in the previous section. He also reemphasized his own work on the possibility of forming quark-gluon blobs in a nucleus of mass A [4]. Inside this low density blob of baryon number $b=A-1$, temperatures of the order of about 160 MeV may prevail. Therefore, particles from the disintegration of the blob should show a momentum distribution with a characteristic temperature of ~ 160 MeV, and there

should be an enhanced production of strangeness by at least a factor of five over normal events.

Are there any hints from existing experiments of strange blobs? Rafelski points to three examples, the first of which is shown in Fig. 2 [5]. Here we see plotted the spectator proton momentum distributions for antiproton annihilation on a deuteron in the 1-3 GeV/c momentum range leading to two strange kaons plus several pions. One sees a strong enhancement at proton momenta > 0.3 GeV/c with a temperature $T \approx 160$ MeV. Apparently the strangeness "trigger" is associated with hot protons. Interestingly, such high temperatures are not as prominent when the strangeness "trigger" is eliminated [6].

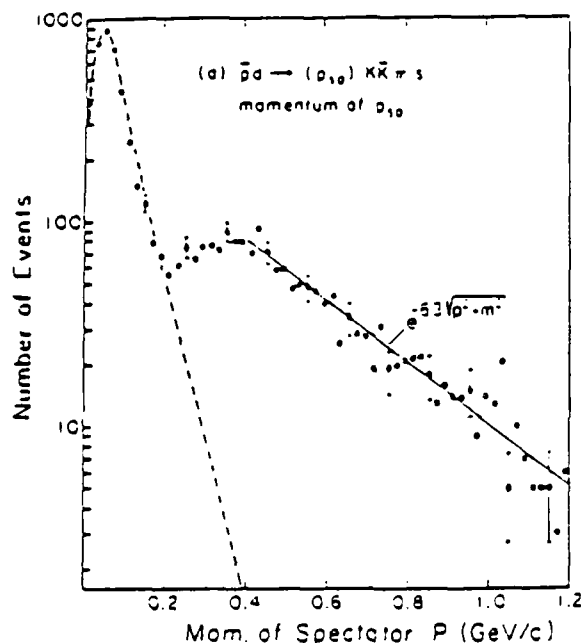


Fig. 2 - Proton spectrum from \bar{p} -d annihilation; $K\bar{K}$ trigger. Dashed line - deuteron-wavefunction. Full line - eyeball fit, $T=160$ MeV.

A second example cited by Rafelski are the recent data from LEAR experiment PS183 on neutron emission from antiproton annihilation at rest in U^{238} , which were presented at Villars [7] and this conference [8]. The neutron momentum spectrum (Fig. 3) shows a high momentum tail with a characteristic temperature of 104 ± 14 MeV and multiplicity of 3.22 ± 0.14 neutrons per annihilation. This temperature, although not as large as the 160 MeV value expected for a quark-gluon blob, is nonetheless larger ($\times 1.5$) than previously measured values for protons in U^{238} [9] and Bi^{209} [10], both at 180 MeV antiproton incident energy. It is important to note that these proton temperatures were obtained from fits to data above ~ 300 MeV/c [9] and ~ 500 MeV/c [10], whereas the neutron temperature was derived from a fit to the full momentum spectrum, including all INC processes (fission,

evaporation and direct scattering terms). It should be especially interesting to see how hot neutrons appear with a strangeness trigger.

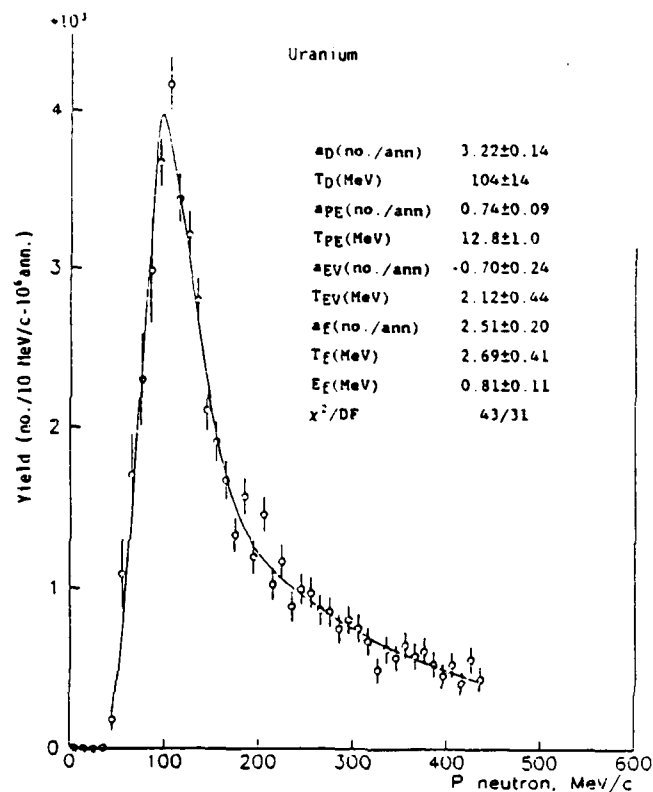


Fig. 3 - PS183(LEAR): Neutron momentum spectrum from uranium with an inclusive trigger and background subtracted.

Finally, Rafelski emphasizes the data on strange particle production (Λ, K_S^0) from 4 GeV/c antiprotons interacting on Ta¹⁸¹ [11], the results from which are seen in Fig. 4. The K_S^0 data peak symmetrically around a rapidity of $y \sim 0.6$ (y is defined as $1/2 \ln[(E+p_L)/(E-p_L)]$, where E and p_L are the total energy and net longitudinal momentum of the particle in the laboratory system). A Lorentz boost to the C.M. translates the K_S^0 data to a symmetric distribution peaked at $y^* = 0$, provided one is in the \bar{p} -3N CM frame (the C.M. moves with a velocity $\beta=0.54$). The Λ^0 data exhibit a peak at $y \sim 0.25$ in the laboratory, with an asymmetric tail on the high rapidity side. A Lorentz boost of these data positions the peak at $y^* = 0$, provided one is in the \bar{p} -13N CM system ($\beta=0.24$). The kinetic energy distributions exhibit temperatures of 135 MeV (K_S^0) and 97 MeV (Λ^0), which in themselves are too low to be evidence for quark-gluon blobs. Nonetheless, the evidence of formation of hot "fireballs" with b as large as 12 is present.

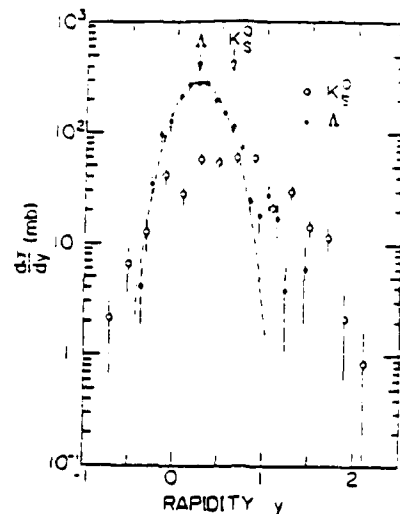


Fig. 4 - Rapidity spectra of K_S^0 and Λ . The dashed curve shows a symmetric curve for the Λ distribution. The centers of the distributions of K_S^0 and Λ are indicated by arrows.

We summarize this section by noting that several experiments have observed hot baryons ($T \geq 100$ MeV) under a variety of conditions emitted from nuclei in association with strangeness. Therefore, a comprehensive experimental program of antiproton annihilation in heavy nuclei with an emphasis on strangeness production appears quite promising and capable of observing the quark-gluon plasma if it exists. A new low energy antiproton facility should allow beams to be accelerated up to several GeV of energy for this purpose.

4. NNN Fireballs

The previous sections have discussed phenomena which may be capable of attaining very high temperatures and triggering a phase transition in nuclear matter. This is very exciting, and should be pursued vigorously, both theoretically and experimentally. But, what do we learn about nuclear matter from such experiments in the unfortunate situation that no phase transition occurs?

Annihilation of antiprotons in nuclei is a complicated process which I believe the previous discussion amply demonstrates. The fireball concept is indeed intriguing, but are there any systems where we have theoretical predictions of rates, etc. and in which we can test the model rigorously? For this purpose, our attention has been drawn to the NNN (b=1) fireball model first discussed by Kahana [12] and developed by Cugnon and Vandermeulen [13]. Their predictions are illustrated in Table 1. In summary, 11.5% of b=1 events involve strangeness, compared to a few % in

$\bar{N}N$ annihilation. Of the 11.5%, 8.8% are hyperon events, which are not produced at all in NN annihilation at low energies. This enhancement in strange particle production would be signaled by, for example, an increase of the K^+/π ratio from $\sim 3\%$ (NN) to $\sim 15\%$ ($\bar{N}NN$). An independent prediction of enhanced strange particle production has also been made recently by Derreth *et al* [14] in a similar model.

Table 1: Predicted branching ratios for $\bar{N}NN$ annihilation ($\sqrt{s} = 3M_N$).

Channel type	Percentage	($\bar{N}\pi$)
$N\pi$'s	88.5	4.73
$N\pi$	5.2×10^{-2}	1.0
$NKK\pi$'s	2.7	1.16
$\Lambda K\pi$'s	2.9	2.51
$\Sigma K\pi$'s	5.5	2.32
$\Xi K\pi$'s	0.4	0.39
all	100	4.42

The simplest nucleus in which to search for $\bar{N}NN$ effects is the deuteron. Surprisingly, only one experiment has published \bar{p} data at low energies which bear on this problem. Based on 6 events, Bizzarri *et al* [15] reported a branching ratio for the $b=1$ reaction $\bar{p}d \rightarrow \pi^-p$ of $(9 \pm 4) \times 10^{-6}$. The theoretical prediction is $\sim 3 \times 10^{-4}$ [13], which suggests perhaps at most a 3% $b=1$ interaction rate. Bizzarri *et al* also reported a rate for $\Lambda^0(\Sigma^0) K^+\pi^-$'s of 3.6×10^{-3} , compared to a theoretical prediction of $\sim 4.7 \times 10^{-2}$ [13], suggesting a 7% $b=1$ rate.

In LEAR experiment PS183 we have attempted to identify the onset of strangeness excess as a function of atomic mass number A , as well as specific examples of $b=1$ reactions. The detector [16] utilized thin (~ 2 mm) C^{12} and U^{238} targets as well as the standard LH_2/D_2 target. Charged particles were momentum analyzed in the spectrometer and their masses measured by time-of-flight, as illustrated in Fig. 5. A clean separation among π , K , p , and d is seen.

(a) Inclusive K^+ Production

We first turn to kaon production as a possible signature of new physics in $\bar{p}A$ annihilation. In Fig. 6 we show K^+ and π^- spectra from hydrogen, deuterium, carbon and uranium targets. The integrated K^+/π^- ratios above 500 MeV/c are 2.3%, 2.8%, 3.0% and 3.0% respectively. A similar trend (2.2%, 3.0%, 3.2% and 3.3%) is seen for K^-/π^- data (not shown). We conclude that the K/π ratio grows $\sim 50\%$ from $A=1$ to $A=238$.

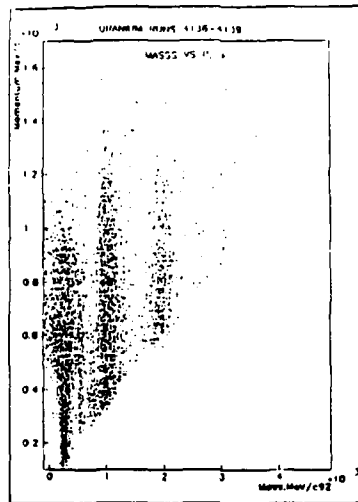


Fig. 5 - PS183(LEAR): Momentum versus mass for particles identified by TOF ($B = 3.5$ kG).

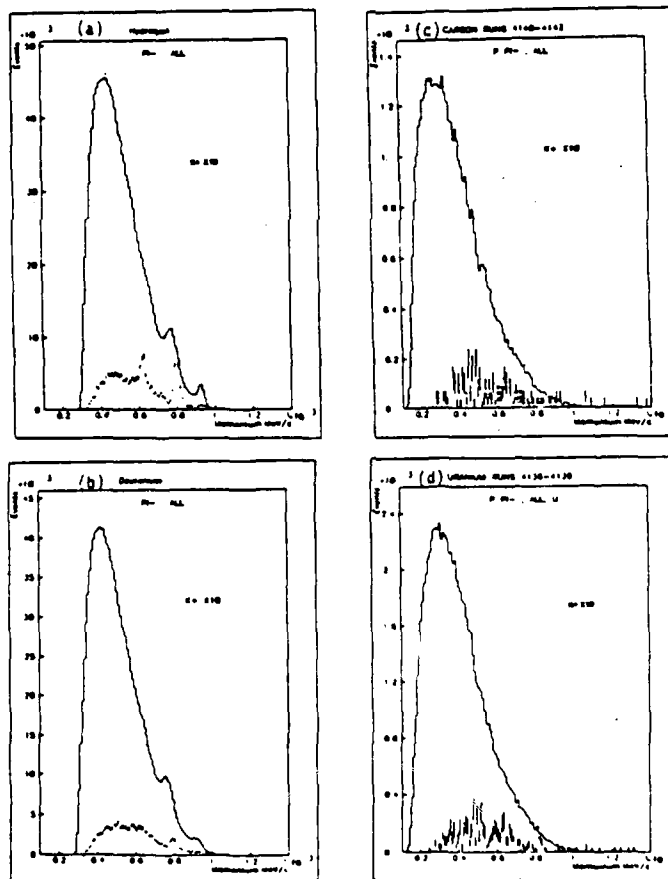


Fig. 6 - PS183(LEAR): K^+/π^- spectra for (a) hydrogen (b) deuterium (c) carbon and (d) uranium.

(b) $\bar{p}d \rightarrow \pi^- p$ ($b=1$)

In Fig. 7 we show plots of momentum versus angle between the particle detected in the magnet and a second away-side particle for charge two events. Very clear clusters of events ($\sim 40 \pi^-$, $\sim 40 p$) are seen at 1250 MeV/c and 180° , exactly where events from $\bar{p}d \rightarrow \pi^- p$ at rest are expected. These ~ 80 events give a branching ratio of $(28 \pm 3) \times 10^{-6}$ per annihilation, which is a factor of three larger than the value quoted by Bizzarri *et al* [15]. This suggests a $b=1$ rate of slightly over 10%.

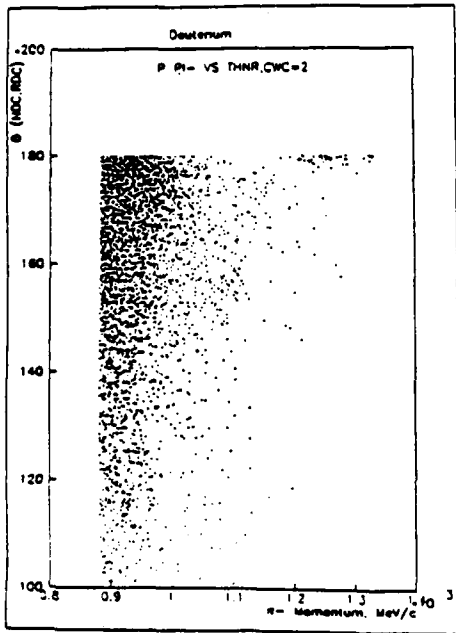


Fig. 7(a) - PS183(LEAR): Pi minus momentum versus the angle between the pi minus and an away-side particle (unidentified) for charge two events.

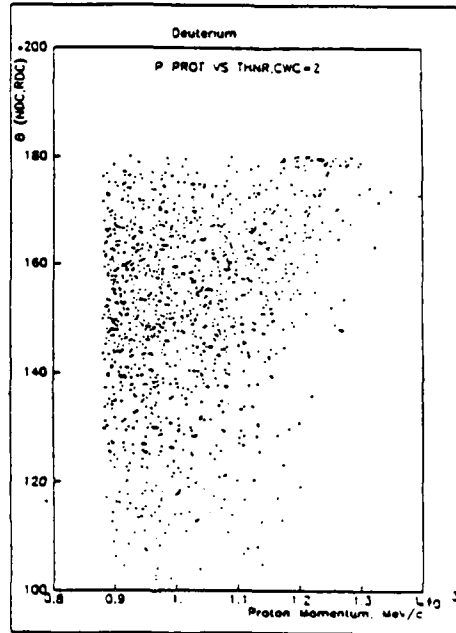


Fig. 7(b) - PS183(LEAR): Proton momentum versus the angle between the proton and an away-side particle (unidentified) for charge two events.

(c) $\bar{p}d \rightarrow \Sigma^- K^+$ ($b=1$)

We have carried out a search for this reaction in charge two events, as it would provide further evidence for the $b=1$ interaction. Experimentally, this is more difficult than reaction (b), as the colinearity of such events is destroyed by the Σ^- decay and the expected location of the K^+ line (1089 MeV/c) is much closer to background from $\bar{N}N$ ($b=0$) $\rightarrow K^+ K^-$ events. At the moment we have no signal, corresponding to a 90% confidence level upper limit of $\sim 8 \times 10^{-6}$ per annihilation, which is slightly larger than the value predicted by theory [13].

In summary, the $\bar{N}NN$ $b=1$ effect has been confirmed in deuterium. The strangeness yield increases with A as expected. The rate for the reaction $\bar{p}d \rightarrow \pi^+p$ suggests a $b=1$ interaction rate of slightly in excess of 10%. In closing, we note that the $b=1$ problem is currently alive with theoretical activity, including in addition to the previously mentioned work that of refs. [17-21].

5. Fission: A New Tool for Studying Strangeness in Heavy Nuclei

At the Villars meeting Sergei Polikanov reviewed hypernuclear physics [22]. The following remarks parallel those of Polikanov, with some effort to distill out highlights.

It is known that the annihilation of antiprotons in complex nuclei yields an enhanced production of Λ^0 hyperons. For example, the inclusive Λ^0 cross section in the experiment of ref. [11] is 193 ± 12 mb, or 2.4 times larger than the inclusive K_S^0 cross section. This suggests that hypernuclear states (Λ^0 hyperons bound in a nucleus) could be produced by stopping antiprotons in nuclear targets. This has been demonstrated successfully by the PS177 group at LEAR [23] utilizing a delay fission technique which will be discussed later. Their results on the lifetimes of states in Bi^{209} and U^{238} are shown in Fig. 8. As one can see, they agree within errors with measurements on nuclei of $A \leq 12$. The very large value for 1 GeV electrons on Bi^{209} [24] will be discussed later.

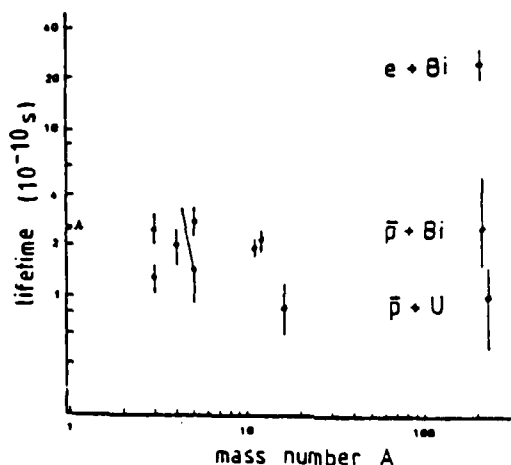


Fig. 8 - PS177(LEAR): Lifetimes of hypernuclei as a function of hypernucleus mass A .

In the case of the lightest hypernuclei, the quasifree mesonic decay $\Lambda \rightarrow N + \pi$ dominates, and the Pauli exclusion principle plays an important role in the decay rate due to the limited energy available to the nucleon. For heavy nuclei the weak

Further to this point, Bychkov [25] has argued that the potential well for heavy hypernuclei may have a minimum at the surface of the nucleus. This leads to a prediction for lifetimes of heavy hypernuclei to be larger for surface states than volume states, since the nuclear density is lower on the surface. Polikanov speculates that the large lifetime for electro-excitation of the hypernuclear state in Bi^{209} [24] may be due to such an effect.

Delayed fission

Prompt fission

Detectors { Identification TOF, dE/dx
Localization x, y

$x = f(v, \tau)$

Amplification:

$$\frac{1}{x} = \frac{R-r}{r} = 270$$

Upstream Downstream

288

We expect this technique to lead to more precise values of heavy Λ° hypernuclear lifetimes in the future. The detector is compact, precise and benefits from the intense, small emittance antiproton beams available at LEAR. This work in time could lead to a better understanding of surface and volume binding in heavy nuclei and the interaction between the Λ° and the nucleon. For example, this interaction may be explained by the overlap of two bags of quarks. Perhaps the most important application of the technique could be a search for the much sought-after doubly strange $H \rightarrow \Lambda^\circ \Lambda^\circ$ dibaryon particle. This particle, which is expected to be relatively stable, could be bound in heavy nuclei, the decay of which would be signaled by a coincidence with fission fragments and two K^+ mesons. A program of introducing K^+ detectors into the PS177 apparatus is presently underway at LEAR [26].

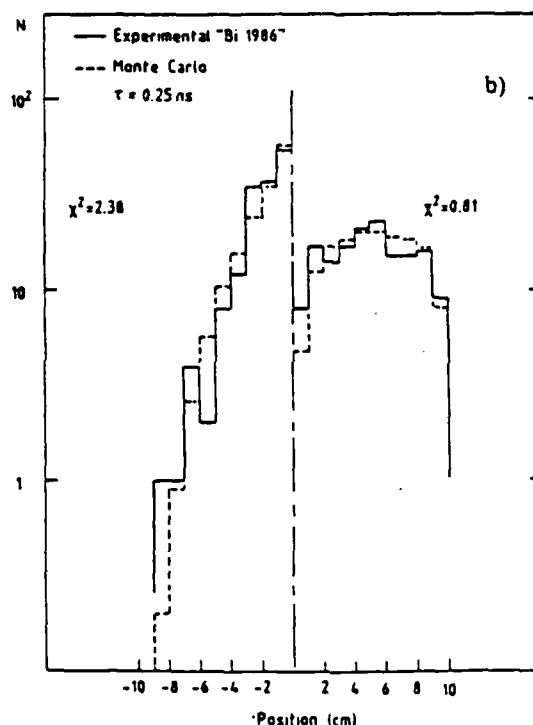


Fig. 10 - PS177(LEAR): Measured and calculated distributions of the positions of delayed-fission fragments from Bi^{209} along the beam direction.

6. Conclusions

Opportunities abound for exploring the nucleus with probes of low energy antiprotons. In our opinion the LEAR program to date has only scratched the surface of new physics that can be revealed by annihilating antiprotons in nuclear matter. Especially

important are conditions of high temperature and the quark-gluon plasma, collective \bar{N} -multinucleon fireballs, and relatively stable states which induce fission in heavy nuclei. A key indicator of these effects is strangeness. As these effects are expected to be very rare, intense, pure, low emittance beams of antiprotons are required. Such beams could be provided by a new low energy antiproton facility.

References and Footnotes

- * Work supported in part by U.S. Air Force grant AFOSR-87-0246.
- [1] D. Ströttman and W.R. Gibbs, Phys. Lett. 149B, 288 (1984).
 - [2] P.L. McGaughey et al, Phys. Lett. 166B, 264 (1986).
 - [3] J. Rafelski, "Deep Annihilation," to appear in the proceedings of the IV LEAR Workshop, Villars-sur-Ollon, Switzerland, 6-13 September 1987.
 - [4] J. Rafelski, Physics at LEAR with Low-Energy Cooled Antiprotons, ed. U. Gastaldi and R. Klapisch, Plenum Press, New York, 1984, p. 507.
 - [5] B.Y. Oh et al, Nucl. Phys. B51, 57 (1973).
 - [6] P.S. Eastman et al, Nucl. Phys. B51, 73 (1973).
 - [7] G. Büche et al, "Search for Unusual Behavior in Neutral and Charged Particle Emission from Antiproton-Nucleus Annihilation at Rest," to appear in the proceedings of the IV LEAR Workshop, Villars-sur-Ollon, Switzerland, 6-13 September 1987.
 - [8] G.A. Smith, "Particle Emission from Antiproton Annihilation at Rest in Uranium," these proceedings.
 - [9] P.L. McGaughey et al, Phys. Rev. Lett. 56, 2156 (1986).
 - [10] D. Garreta et al, "PS184: A Study of \bar{p} -Nucleus Interaction with a High-Resolution Magnetic Spectrometer," Proc. 7th European Symposium on Antiproton Interactions, Durham, U.K., 9-13 July 1984.
 - [11] K. Miyano et al, Phys. Rev. Lett. 53, 1725 (1984).
 - [12] S. Kahana, Physics at LEAR with Low-Energy Cooled Antiprotons, ed. U. Gastaldi and R. Klapisch, Plenum Press, New York, 1984, p. 485.
 - [13] J. Cugnon and J. Vandermeulen, Phys. Lett. 146B, 16 (1984) and LEAR Workshop, Tignes, 1985, p. 559.
 - [14] C. Derreth et al, Phys. Rev. C31, 1360 (1985).
 - [15] R. Bizzarri et al, Lett. Nuovo Cimento, Vol. II, N. 9, 431 (1969).
 - [16] A. Angelopoulos et al, Phys. Lett. 159B, 210 (1985); Phys. Lett. 178B, 441 (1986).
 - [17] L.A. Kondratyuk and M.G. Sapozhnikov, abstract submitted to the IV LEAR Workshop, Villars-sur-Ollon, Switzerland, 6-13 September 1987.
 - [18] S. Nozawa et al, abstract submitted to the XI International Conference on Particles and Nuclei, Kyoto, Japan, 20-24 April 1987.

- [19] S. Nozawa et al, abstract submitted to the IV LEAR Workshop, Villars-sur-Ollon, Switzerland, 6-13 September 1987.
- [20] E. Hernandez and E. Oset, abstract submitted to the IV LEAR Workshop, Villars-sur-Ollon, Switzerland, 6-13 September 1987.
- [21] S. Phatak and N. Sarma, Phys. Rev. C36, 864 (1987).
- [22] S. Polikanov, "Hypernuclei from Antiproton Annihilation in Nuclei," to appear in the proceedings of the IV LEAR Workshop, Villars-sur-Ollon, Switzerland, 6-13 September 1987.
- [23] J.P. Bocquet et al, Phys. Lett. 182B, 146 (1986); Phys. Lett. 192B, 312 (1987).
- [24] V.I. Noga et al, Sov. J. Nucl. Phys. 43, 856 (1986).
- [25] A.S. Bychkov, Sov. J. Nucl. Phys. 40, 259 (1984).
- [26] Amsterdam-Darmstadt-Grenoble-Orsay-Penn State-Saclay-Uppsala-Warsaw-Collaboration (PS177).

Particle Emission from Antiproton Annihilation
at Rest in Uranium

Gerald A. Smith*

Laboratory for Elementary Particle Science
Department of Physics
The Pennsylvania State University
University Park, PA 16802 USA1. INTRODUCTION

The results presented in this paper are the first realization of an experimental program initiated by this author and carried out with the help of many others [1] at the Low Energy Antiproton Ring (LEAR) at CERN. The primary question which we wish to address in this paper is "When an antiproton annihilates at rest in a nucleus, what fraction of the total energy released goes into the kinetic energy of heavy charged particles?" Since such particles readily yield their energy in the form of heat through ionizing collisions with matter, they represent an efficient source of energy for spacecraft propulsion. For a more thorough exposition of this problem, the reader is referred to the report of D.L. Morgan, Jr. [2], which initially inspired this author's interest in this problem.

One of the several objectives of LEAR experiment PS183 is to measure the energy spectrum of neutrons emitted from antiproton annihilation at rest in U^{238} . In this paper we present the first measurement of neutrons down to ~ 1 MeV kinetic energy. Such data are capable of providing information on the probability of fission in the nucleus, and the energy carried by charged fission fragments. Using the intranuclear cascade (INC) model [3-6] as a guide, they can also provide us with an estimate of the energy imparted to protons. Combined with recent results from another LEAR experiment on light nuclei emission, these data indicate that the energy carried by heavy charged particles is larger than previously predicted [2].

2. THE PS183 DETECTOR

The detector (Fig. 1) has been described in detail elsewhere [7]. In 1986 additional neutron counters (N1-4) were installed, and thin (~ 2 mm) targets of carbon and uranium were prepared to replace the liquid hydrogen/deuterium target. Event readout was triggered by charged particles in the spectrometer, whose masses were measured by time-of-flight (Fig. 2). Approximately 35% of the beam stopped in each of the targets.

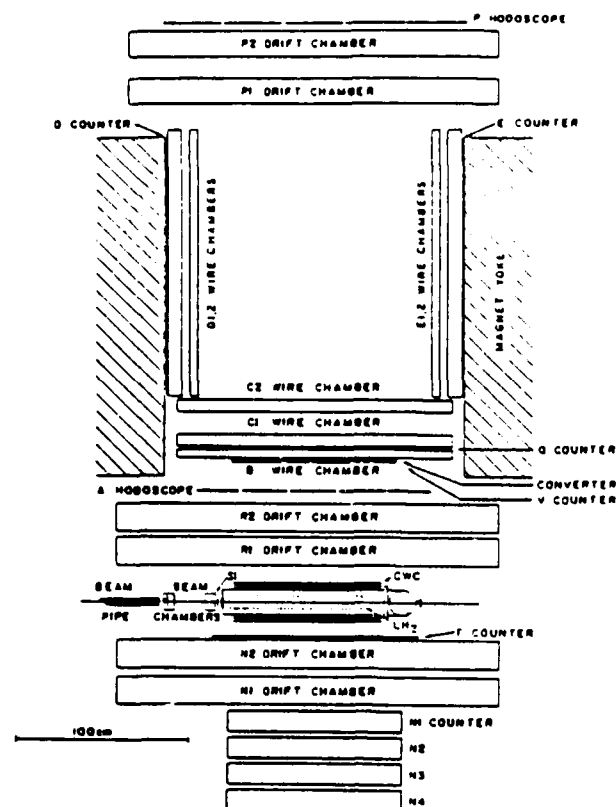


Fig. 1 - The PS183 detector at LEAR.

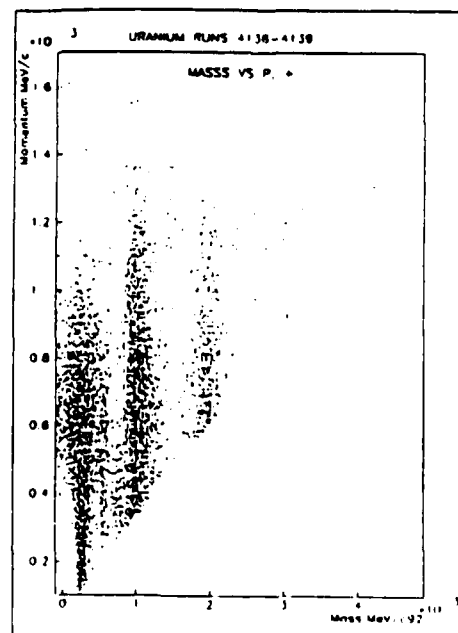


Fig. 2 - Momentum versus mass as determined by time-of-flight for uranium. Clear bands of pions, kaons, protons and deuterons are seen.

3. METHOD OF OBTAINING NEUTRON SPECTRA

Neutron spectra were measured with three NE110 plastic counters, each 100 cm long x 20 cm high x 10 cm deep, placed 79, 93, 107 and 121 cm respectively from the target. Each counter was read out with two RCA 5-inch Quantacon photomultiplier tubes. Neutrons were required to fire at least one counter after a delay of 1.5 ns or more relative to a beam pulse. Gamma-rays were identified by a prompt signal (< 1.5 ns) in a single counter. The individual TOF spectra for carbon and uranium are shown in Fig. 3. Prompt gamma-ray peaks are seen, followed by a broader distribution of neutrons.

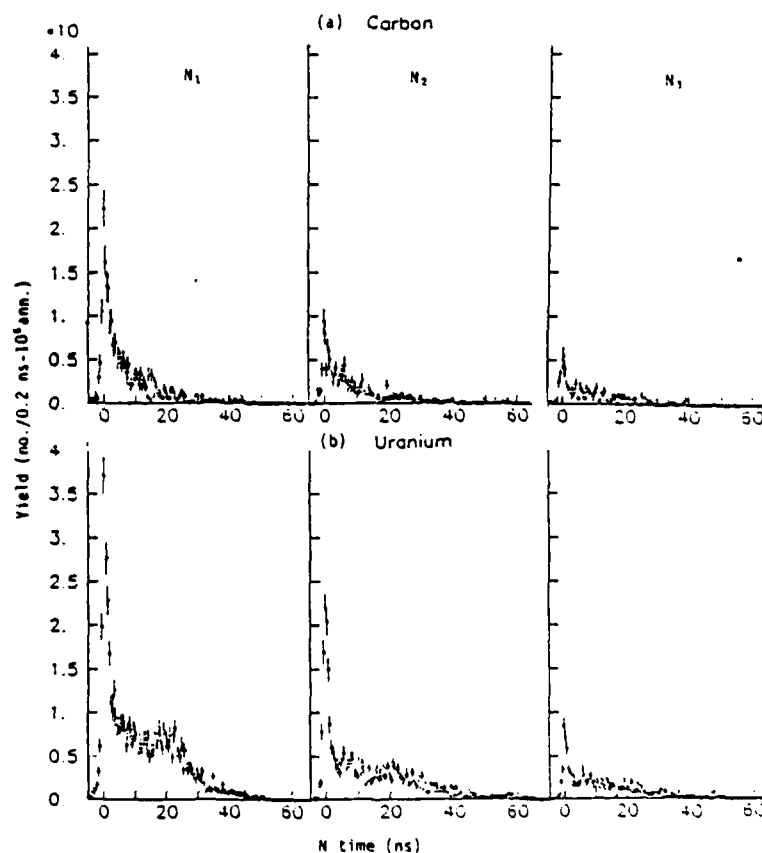


Fig. 3 - TOF spectra taken with an inclusive trigger for (a) carbon and (b) uranium

Hydrogen data served as a calibration of background neutrons due to secondary interactions of particles. We find the neutron momentum spectrum for deuterium, from which the hydrogen spectrum has been subtracted, to be in good agreement, both in shape and magnitude, with a published neutron spectrum [8]. Furthermore, the yield of neutrons (0.41 ± 0.08) agrees with the expectation of the naive spectator model (~ 0.5).

4. NEUTRON SPECTRA FROM URANIUM

We have fit the spectra with a three component Maxwell-Boltzmann (MB) function. For uranium, we have added a fourth term for fission [9]. The components are designated as (1) direct - D (2) pre-equilibrium - PE (3) evaporation - EV and (4) fission - f. The function is

$$Y(E) = \sum_{i=1}^3 a_i E^{\alpha_i} e^{-E/T_i} + a_f \operatorname{sh} \left\{ \frac{2\sqrt{E_f E}}{T_f} \right\} e^{-E/T_f}, \quad (1)$$

where a_i , a_f are intensities, α_i define densities of states (0, 1/2, 1/2 respectively), T_i , T_f are temperatures, and E_f is the mean fission fragment energy per nucleon. The results of the fits for uranium are shown in Fig. 4.

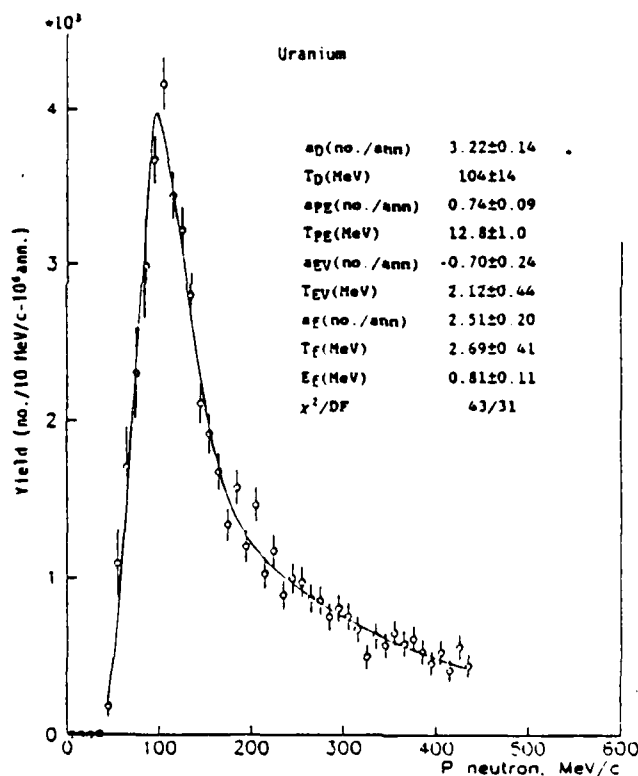


Fig. 4 - Neutron momentum spectrum from uranium with an inclusive trigger and background removed. The inset gives the parameters of the best fit.

5. DISCUSSION OF FISSION RESULTS

Our fission yield (2.51 ± 0.20) and temperature (2.69 ± 0.41 MeV) are somewhat different than those of a stopped negative pion experiment [10] (5.0 ± 1.7 , 1.1 ± 0.1 MeV), although yields differ by less than two standard deviations. We also note that our fission

yields are larger for proton (2.69 ± 0.31) than pion triggers (1.66 ± 0.16 for π^+ , 2.46 ± 0.20 for π^-). These differences may be the result of trigger conditions. By momentum conservation, the trigger pion produces a "jet" of pions in the direction of the neutron counters. One would expect the fission fragments to recoil 90° to this direction. Since fission neutrons are emitted preferentially along the fission fragment direction [9], one would further expect a depletion of fission neutrons at the position of the neutron counters. Such an effect would not be as significant with the proton trigger, as the momentum conservation direction will not be as well defined.

The number of fission neutrons and E_f for the proton trigger (2.69 ± 0.31 , 0.71 ± 0.09 MeV) are consistent with values [9] for fission induced by low energy neutrons [~ 2.4 , ~ 0.5 MeV]. Our fission temperatures [~ 2.7 MeV] are somewhat larger than values measured with low energy neutrons (~ 1.3 - 1.8 MeV), but are consistent with the trend observed with increasing neutron energy [9]. We therefore conclude that our results are consistent with 100% probability for fission. Previous stopped antiproton experiments [11,12] in uranium have reported evidence for fission. However, to the best of our knowledge, this is the first reported measurement of yields of prompt fission neutrons from antiproton annihilation at rest.

6. ENERGY OF HEAVY CHARGED PARTICLES

We now discuss the distribution of energy realized in an antiproton annihilation at rest in U^{238} . The results are given in Table 1. We have used currently available information on fission [9,12], recent data on light nuclear fragments from LEAR [12], charged pion multiplicity data from PS183, and our neutron data (to predict proton multiplicities and energies with the help of the INC model) to complete the table. We note that the total energy (2031 ± 83 MeV) is in agreement with overall mass and energy conservation to within ~ 12 MeV, well within the quoted error.

The most striking feature of Table 1 is the 481 ± 31 MeV of kinetic energy carried by heavy charged particles (fission fragments, protons and light nuclei). This is substantially larger than the prediction of Morgan [2] of 365 ± 30 MeV.

7. GAMMA-RAY ENERGY

We believe it would be quite straightforward to totally contain energy from electromagnetic showers from nuclear γ 's and $\pi^+ \rightarrow 2\gamma$ decays in the same device used to range heavy charged particles. This would result in an additional 402 ± 25 MeV of energy (prompt gamma-rays, plus one-third of the pion energy of Table 1), for a total of 883 ± 39 MeV.

Table 1.

Distribution of Energy from Antiproton Annihilation on U^{238}

<u>Particle</u>	<u>No. Nucleons</u>	<u>Energy (MeV)</u>	<u>Comments</u>
1. <u>Fission fragments</u> (symmetric binary fission with A=110 for each fragment [12])	220	175	Ref. [9], [12]
2. <u>Prompt Gamma-Rays</u> from fission fragments	0	8	Ref. [9]
3. <u>Neutrons</u>	6.47		This expt.
a) Fission*	(2.51)	10 \pm 2	
b) Pre-equilibrium*	(0.74)	14 \pm 2	
c) Direct**	(3.22)	135 \pm 48 359 \pm 48	
4. <u>Protons</u>	2.49		
a) Fission			
b) Pre-equilibrium (neutron value scaled by Z/N)	(0.47)	9 \pm 1	This expt., Ref. [3-6]
c) Direct (neutron value scaled by Z/N)	(2.02)	211 \pm 30 220 \pm 30	This expt., Ref. [3-6]
5. <u>Light Nuclei</u> (d, t, He ³ , He ⁴) 2 deuterons @37 \pm 4 MeV** + 1 alpha @12 \pm 2 MeV**	8.04	86 \pm 8	Ref. [12]
6. <u>Pions</u>	0		
a) K.E.		700 \pm 54	This expt. +
b) Mass		483 \pm 28 1183 \pm 60	This expt. +
Totals	237	2031 \pm 83	

* Ave. energy = $3/2T$. See Eq. (1)** Ave. energy = T . See Eq. (1)+ The ave. charged pion multiplicity is measured to be 2.5 ± 0.2 in this experiment. This is corrected to 3.5 ± 0.2 for all pions. The ave. pion energy (mass) is assumed to be 200 ± 10 (138) MeV [2].**8. CONCLUSIONS**

The first major results from LEAR experiment PS183 lead us to the following conclusions: (1) fission neutrons have been observed from U^{238} , consistent with fission occurring in 100% of antiproton annihilations; (2) neutron data from PS183, combined with recent data from another LEAR experiment on light nuclear fragments, allow us to predict the total energy released to heavy charged particles. This energy is 481 ± 31 MeV, which is 32% larger than predicted earlier; and (3) gamma-ray energy should be

readily converted to heat in the same device used to contain heavy charged particles, leading to a total of 883 ± 39 MeV, or 43% of the total energy available. Further containment of neutron and charged pion kinetic energy and mass (less neutrino-energy) could result in as much as 1858 ± 80 MeV, or 91% of the total energy available.

9. REFERENCES AND FOOTNOTES

* Work supported in part by the U.S. Air Force and the U.S. National Science Foundation.

- [1] Athens-Irvine-Karlsruhe-New Mexico-Penn State Collaboration, LEAR Experiment PS183.
- [2] D.L. Morgan, Jr. "Annihilation of Antiprotons in Heavy Nuclei," AFRPL TR-86-011, April 1986.
- [3] M.R. Clover *et al*, Phys. Rev. C26, 2138 (1982).
- [4] A.S. Iljinov *et al*, Nucl. Phys. A382, 378 (1982).
- [5] M. Cahay *et al*, Nucl. Phys. A393, 237 (1983).
- [6] J. Cugnon and J. Vandermeulen, Nucl. Phys. A445, 717 (1985).
- [7] A. Angelopoulos *et al*, Phys. Lett. 159B, 210 (1985); Phys. Lett. 178B, 441 (1986).
- [8] C. Amsler *et al*, Phys. Rev. Lett. 44, 853 (1980).
- [9] Nuclear Reactions in Heavy Elements, V.M. Gorbachev *et al*, Pergamon Press, 1986.
- [10] H.P. Isaak *et al*, Nucl. Phys. A392, (1983) and references cited therein.
- [11] J.P. Bocquet *et al*, abstract submitted to the IV LEAR Workshop, Villars-sur-Ollon, Switzerland, 6-13 Sept. 1987.
- [12] H. Daniel *et al*, abstracts submitted to the XI International Conference on Particles and Nuclei, Kyoto, Japan, 20-24 April 1987, and the IV LEAR Workshop, Villars-sur-Ollon, Switzerland, 6-13 Sept. 1987; see also T. von Egidy, Nature 328, 773 (1987).

USING $\bar{p}p$ ANNIHILATION TO FIND EXOTIC MESONS*

STEPHEN R. SHARPE

*Stanford Linear Accelerator Center
Stanford University, Stanford, California, 94305*

ABSTRACT

Present data suggests that a number of mesons have been found which cannot be accommodated in standard $\bar{q}q$ multiplets. Theory suggests that such exotic mesons should exist in the spectrum of Quantum Chromodynamics, but provides little guide to their properties. It is argued that a high luminosity, low energy $\bar{p}p$ machine would be a powerful tool with which to search for such exotics.

* Work supported by the Department of Energy, contract DE-AC03-76SF00515.

1. INTRODUCTION

Meson spectroscopy is now at an exciting stage. Results which have accumulated over the last few years have shown that there are very likely a number of "exotic" meson states. I am here using "exotic" to refer to those states that do not fit, in any obvious way, into standard $\bar{q}q$ multiplets. I am not ruling out that some of these states might be squeezed into such multiplets, but I would be very surprised if all can be so accommodated.

The data which suggest these new states come from high statistics studies in hadron collisions and J/ψ decays. However, while the tip of the exotic iceberg has been exposed, it is still surrounded by an impenetrable fog of theoretical uncertainty. Exotic mesons are indeed expected in the spectrum of Quantum Chromodynamics (QCD) – glueballs, meiktons (a.k.a. hybrids, hermaphrodites), $\bar{q}^2 q^2$ states – but so far there are no reliable theoretical predictions of their masses and properties. There is some rough theoretical guidance as to what quantum numbers to expect, and for the ordering of the different multiplets, but little else. Thus it is hard to try to fit the candidates into a scheme that has to be made up as one goes along.

What this situation demands is further guidance from experiment. This it has been receiving in good measure, but more is needed. And here low energy \bar{p} -s can be of great help. Annihilation at rest provides a clear window on exotic states with masses up to ~ 1.7 GeV. Specific spin-parities can be selected by combining the constraints on the quantum numbers of initial and final states. The initial state quantum numbers are constrained because the annihilation occurs in certain atomic $\bar{p}p$ states. The final state quantum numbers can be restricted by looking at simple final states such as $\eta\eta\pi^0$. All the interesting channels can be looked at in this way. Annihilation in flight allows higher mass states to be studied. If a very low spread in the beam energy can be achieved, then a scan for states will be very interesting. Provided the luminosity is high enough, and the detectors can measure photons with good resolution, and have good K/π separation, a low

energy $\bar{p}p$ machine will be an excellent laboratory for exotic mesons.

The remainder of this talk expands upon these claims. I first summarize the theoretical status. Then I enlarge upon why the present experimental situation is so interesting and intriguing. I comment upon some of the possible ideas for interpreting the data. Thirdly, I run through some case studies of final states that I think are particularly interesting for the search for exotics at a $\bar{p}p$ machine. I close with some conclusions.

I have benefitted greatly from the extant reviews of this subject^[1]. I have tried to make this paper self contained, but of necessity details have been omitted, and can be found in these reviews, along with additional references.

2. THEORY

QCD is the only candidate for a theory of the strong interactions. Its stature is based upon a few, somewhat indirect, quantitative tests^[2], and upon a large body of semi-quantitative evidence. A clear example of the latter is the appearance of quark and gluon jets at high energy colliders. Nevertheless, there are no tests which come close to those we have for QED. We cannot, to date, predict the spectrum of the theory from first principles. We cannot even prove that quarks are confined.

Our ignorance about QCD is almost exclusively in the low momentum, long distance regime of particle masses, form factors, reaction cross sections, etc.. Of course, we do know something about this region, based on the $SU(3)$ flavor symmetry, and upon the associated chiral symmetry. We understand why particles come in multiplets, and why the pions and kaons are light, and how the latter couple. What we do not understand is why the spectrum of states, and to some extent their decays, can be explained by relatively simple quark models^[3]. This is worth stressing: though most of the existing mesons and baryons fit well into a scheme in which constituent quarks and anti-quarks interact by a confining potential, we cannot show from first principles why this should be so. In particular,

the constituent quarks of these models are much heavier - ~ 300 MeV - than the bare current quark masses which we put into the QCD Lagrangian. Constituent quarks must be thought of as blobs of glue and $\bar{q}q$ pairs surrounding the bare quark.

Given the success of the quark model many people have speculated that there should be particles in the spectrum other than normal mesons ($\bar{q}q$) and baryons (qqq). If there are constituent quarks, why not constituent gluons, and the glueballs composed of such constituents. There are two levels of objection to this extrapolation. The deepest objection is that gluons have already been accounted for in turning bare quarks into blobs: glueballs are not different from $\bar{q}q$ states. I think this is wrong for two reasons. First, one can make operators out of glue alone with quantum numbers not allowed for $\bar{q}q$ states - spin-parity exotics such as 0^{--} . However, these operators could simply couple to the continuum, rather than create resonances, so this is only suggestive. The second reason is that there are two limits of QCD in which glueballs are certainly distinct from $\bar{q}q$ states: the number of colors $\rightarrow \infty$, and the quark masses $\rightarrow \infty$. The limit of infinite quark masses is pure gauge theory - glue alone - and lattice simulations of this theory have shown fairly conclusively the existence of a spectrum of glueballs of non-zero mass. As one goes from these limiting cases back to QCD, the $\bar{q}q$ states can mix with these glueballs, but both should be present in the spectrum. The weaker objection allows the existence of glueballs, but not of the notion of constituent gluons. Neither of the limits just discussed tells us about the structure of glueballs. They may be hideously complicated entities, requiring numerical simulations to predict their properties. This seems quite possible to me, and though in the following I will often use the language of constituent gluons, this caveat should be borne in mind.

A different path to exotica is to add together more $\bar{q}q$ pairs. The simplest examples are \bar{q}^2q^2 states^[4]. The question of whether such states exist gets to the core of the problem with constituent quarks. For if \bar{q}^2q^2 states do exist, then there should also be \bar{q}^3q^3 states, etc.. A neat answer was provided by

Jaffe^[4] who found in the bag model that nearly all such states would be able to decay classically into two $\bar{q}q$ mesons. Only a few exceptions, most notably the $a_0(980)$ and $f_0(975)$, would be stable. A similar conclusion has been reached within the quark model by Isgur and collaborators^[5], who think of such states as molecules of mesons. Most of these molecules are not bound, the exception being the $\bar{K}K$ system, giving rise to the a_0 and f_0 just below the $\bar{K}K$ threshold. I will discuss this interpretation in the next section. The point I want to make here is that two quite different approaches agree that $\bar{q}^2 q^2$ resonances will not be abundant in the spectrum.

The same need not be true of $\bar{q}qg$ states, i.e. meiktons^[6]. These take the notion of constituent gluons to its logical conclusion: if they exist they can combine with a color octet $\bar{q}q$ pair. There are no fall apart decays, and thus the possibility of a rich spectrum. Indeed, some of the meiktons have spin-parities not available to $\bar{q}q$ mesons. There is another way of thinking about meiktons, which does not depend upon the notion of constituent gluons, and so strengthens the case for the existence of meiktons. To the extent that mesons can be thought of as $\bar{q}q$ pairs bound by a string of color electric flux, one can imagine exciting the string. This gives rise to a meikton, with the string excitation energy playing the role of the constituent gluon mass. Such a picture makes sense in the limit of heavy quarks, and it is possible to do lattice calculations of the excitation energy. The best numbers so far are 1.3 GeV for b quarks and 0.9 GeV for c quarks^[7]. An unfortunate corollary of this result, not directly relevant here but worthy of mention, is that $\bar{b}bg$ and $\bar{c}cg$ states will be above their respective open flavor thresholds.

In summary, I would say that it is almost certain that there is a rich spectrum of exotic states out there waiting to be found. The questions are: Where are they? What do they look like? and How are we to find them? The most important issue is their mass, and this depends on the mass of the constituent gluon. Here, it seems to me, we must depend upon numerical calculations as our major guide. The bag model^[8], the flux tube model^[9], and the QCD sum

rules^[10], all purport to answer this question, but they do not agree. This is perhaps not surprising, since all these methods are being extended beyond the limits within which they are known to work. Lattice QCD allows a calculation from first principles, limited only by computer resources. In the pure gluon theory, methods have matured enough to give a prediction for the 0^{++} and 2^{++} glueball masses^[11]. The 0^{++} is the lightest state, with mass about 1400 MeV, the 2^{++} being about 1.6 times heavier. Addition of dynamical quarks, a next generation calculation, may change these values somewhat, and will allow the states to mix and decay. So these numbers are only rough guides, but it looks to me like a constituent gluon mass of 800 MeV is reasonable. Here I have allowed spin splittings to lower the mass of the scalar glueball from twice the constituent gluon mass. This number is consistent with the extrapolation to light quarks of the string excitation energy discussed above. It should be compared to the 300 MeV constituent mass of light quarks.

Given the constituent gluon mass one can attempt to predict the spectrum of exotic mesons. I shall follow Jaffe *et al.*^[12], who extract some general features common to all models, but be a little bolder (foolhardy?) and give some masses. All numbers are to be taken as uncertain by at least a few hundred MeV.

In addition to the glueballs mentioned above, glueballs with quantum numbers 0^{-+} and 2^{-+} should be among the lightest, with masses higher than their positive parity counterparts. This brings us to about 2 GeV, beyond which there may lie many states, including the exotic spin-parities 1^{-+} and 0^{--} .

The lightest meiktons should appear around 1300 MeV. This is the sum of the constituent masses, less a bit for hyperfine splitting. The quantum numbers of the lightest meiktons are less clear, but among the lightest should be those with $J^{PC} = 0^{-+}, 1^{-+}, 1^{--}, 2^{-+}$. In the bag model, the mass increases along this list, reaching close to 2 GeV at the end. All models find excited states coming in at around this mass, with more and more states appearing as the mass increases further. Each of these J^{PC} s is a nonet of states.

It seems to me, then, that there may be a window of opportunity in the mass range $\sim 1300 - \sim 2000$ MeV. Above this range, there will be a growing number of exotics, as well as of $\bar{q}q$ mesons. Most will be broad and so states will be hard to identify and to disentangle. Within the window, on the other hand, there are a manageable number of states, both exotic and ordinary. Having fewer states in each channel also makes it more likely that some of the exotics will not be significantly mixed with ordinary mesons. It is in this region that a $\bar{p}p$ machine is particularly powerful, and it is here too that a growing number of experimental candidates for exotics have been collecting. To these I now turn.

3. THE PRESENT EXPERIMENTAL STATUS

Exotics must stand out against a background of filled $\bar{q}q$ nonets. Below 1 GeV there are the ground state 0^{-+} and 1^{--} nonets, both of which are filled and well understood. Above 1 GeV, there are the radially excited pseudoscalars and vectors, neither of which are filled, and the orbitally excited nonets with spin-parities $(0, 1, 2)^{++}$ and 1^{+-} . The 2^{++} has long been filled, and, thanks to the efforts of the last 18 months or so, both spin 1 nonets are complete too. Quite a number of higher spin states – higher orbital excitations – are also known, particularly the strange states. But the lightest exotics probably have low spin, and so I shall concentrate on $\bar{q}q$ states of low spin.

Now I come to my list of candidate exotics. This list is not meant to be complete, but rather to indicate that there are a growing number of well documented, though poorly understood, exotics. I use the new notation for particles throughout. First on my list is the $\eta(1460)$ (was iota). This isoscalar, pseudoscalar is very prominent in radiative J/ψ decays, decaying into $\bar{K}K\pi$ with a width $\Gamma \sim 100$ MeV. It appears not to decay into $\eta\pi\pi$ and $\rho\gamma$ ^[13]. It has not been seen in the hadronic decays of the J/ψ , in $\gamma\gamma$ production, or in high energy πp , $\bar{p}p$, or Kp production. It may have been discovered in 1966 in $\bar{p}p$ annihilation at rest^[14]. Thus it appears to be a quarkless state – a prime glueball candidate.

Close by, there is growing evidence for an additional pseudoscalar - the $\eta(1400)$ (known to some as $\eta(1420)$). It is produced in πp scattering, decaying into $\bar{K}K\pi$ and $\eta\pi\pi$ ^[15]. Its status in Kp scattering is less clear. LASS sees no signal^[16], while Lepton-F finds evidence for a state at around 1400 MeV^[17]. They interpret this a 1^{++} state, but Caldwell^[18] suggests that it may be the $\eta(1400)$. It is not seen in two photon production, but may explain part of the $\eta\pi\pi$ signal in radiative J/ψ decay.

All this is rather puzzling. The radially excited pseudoscalar nonet is expected in this mass region, and indeed there is the isovector $\pi(1300)$, and the isoscalar $\eta(1275)$. The $\bar{s}s$ isoscalar is thus expected at ~ 1550 MeV^[3]. There are two possibilities that I can see. (1) Lepton-F is seeing the $\eta(1400)$, which is the required $\bar{s}s$ state, explaining its weak production in two photon and radiative J/ψ decay. (2) LASS is right, and we have another exotic on our hands, leaving no candidate for an $\bar{s}s$ state. In either case, the $\eta(1460)$ remains a prime glueball candidate.

Actually, even the $\eta(1275)$ and $\pi(1300)$ are not completely understood. Crystal ball has looked for both in $\gamma\gamma$ production, the former in $\eta\pi\pi$, the latter in $\pi\pi\pi$. They see no sign of either, and quote the limit^[19]

$$\Gamma(\gamma\gamma \rightarrow \eta(1390)) \times B(\eta(1390) \rightarrow \eta\pi\pi) < 0.27 \text{ KeV}.$$

In fact they see nothing in $\eta\pi\pi$ above the η' . The 2 photon widths of radially excited $\bar{q}q$ states are expected to be of $O(\text{KeV})$, so these limits are beginning to be worrisome for the entire nonet.

I should also mention that in some quark models the second radial excitation of the η also lies in this mass region. Lipkin has pointed out that the mixing of this state with the $\bar{s}s$ radial excitation could be large and obscure flavor tagging arguments^[20]. Nevertheless, I find it hard to see how the present data, and in particular the very large production of the $\eta(1460)$ in radiative J/ψ production, can be explained solely with $\bar{q}q$ states. In any case, $\bar{p}p$ experiments can play a

crucial role in resolving this confusion. Annihilation at rest should be a source of both $\bar{q}q$ and glue-rich states, and so may be a way of producing both $\eta(1460)$ and $\eta(1400)$ at once.

The second exotic is the $1^{++} f_1(1420)$, a.k.a. the E. This has been centrally produced in $\bar{p}p$ and πp ^[21], though not seen in forward production. More recently, a spin 1 state has been seen in $\gamma\gamma^*$ collisions, where the $*$ means off-shell^[22]. Although the exotic negative parity is not ruled out in $\gamma\gamma^*$, positive parity is preferred, and the most economical explanation is that the new state is the 1^{++} state seen earlier.

This assignment leads to a very puzzling problem. The orbitally excited 1^{++} nonet appears now to be filled with the $a_1(1270)$ (was A_1), $K_1(1280/1400)$, $f_1(1285)$ (was D), and the newly added $f'_1(1530)$. This latter state has been seen in Kp production by LASS decaying into $K^*\bar{K}$. It is thus a strong candidate for the $\bar{3}s$ member of the nonet, though its mass is somewhat high. If it does complete the nonet, then the $f_1(1420)$ is an odd-meson-out sitting right in the middle of the nonet.

However, the experimental situation is by no means clear. In some ways the $f_1(1420)$ looks like a light quark state: it is produced in hadronic decays of the J/ψ in association with an ω but not a ϕ ^[23]; the rate of $\gamma^*\gamma$ production suggests considerable light quark content^[22]; and LASS does not see it in Kp production^[16]. However, Lepton-F does see structure in Kp production at the right mass^[17]. This could be 0^{-+} and/or $1^{+\pm}$, as discussed above. So the flavor content of the $f_1(1420)$ is unclear. Furthermore, there is evidence that the $f_1(1285)$ has $\bar{3}s$ content: the decay $J/\psi \rightarrow \phi f_1(1285)$ has been seen^[23], and $f_1(1285) \rightarrow \phi\gamma$ has been measured^[24].

The bottom line here is that there appears to be an extra state, and that no such state is expected in the quark model. It is also hard to think of an explanation for this state even as an exotic - \bar{q}^2q^2 has been suggested^[18], but the mass seems somewhat low. If it were a 1^{-+} state, on the other hand, then it

would fit nicely into the exotic spin-parity meikton nonet^[25]. Or there may be both positive and negative parity states, which would be even more interesting. Clearly, something is going on, but clarification is essential.

Next I turn to the only isovector on my list, the $\rho(1490)$ (was C). This has been seen by the Lepton-F collaboration in πp scattering, decaying into $\phi\pi^0$ in a p-wave. Such a decay should set alarms ringing, since it has long been argued that \bar{q}^2q^2 states with hidden strangeness should decay in this way. Similarly, $\bar{q}qg$ states may decay significantly into this final state. The $\rho(1490)$ sits close to the mass expected of the radially excited vector states. The Particle Data Tables show a $\rho(1600)$, and there may be a $\phi(1680)$. LASS has confirmed the $K_1^*(1790)$ ^[16] which also fits into this nonet. So an second isovector, particularly with such a strange decay (recall that the $\rho(1600)$ decays into 4π and $\pi\pi$ with a large width of $\Gamma \sim 250$ MeV), is probably an exotic.

LASS has also turned up another vector exotic – the $K_1^*(1410)$ ^[16]. This seems too light to be part of the radially excited vector nonet. If the $\rho(1490)$ contains an $\bar{s}s$ pair, then the $K_1^*(1410)$ could be related to it by changing an s quark to a d quark. This is possible in either \bar{q}^2q^2 or $\bar{q}qg$ interpretations. Both would also predict other states nearby: the rest of a nonet if the $\rho(1490)$ is $\bar{q}qg$; the rest of two decuplets of opposite G-parity if it is \bar{q}^2q^2 ^[26]. The $\bar{q}qg$ option seems more plausible to me, since a vector \bar{q}^2q^2 state is orbitally excited and would be expected to be heavier. In either case, it is clearly essential to confirm these new states and study their properties, and a $\bar{p}p$ machine can do this for the $\rho(1490)$.

Another possible exotic is the scalar $f_0(1590)$ (was G). In fact, I do not have very strong reasons to single out this state, as the scalar spectrum is very confused. The quark model predicts an $L=1$ $\bar{q}q$ nonet somewhat above 1 GeV. In addition, \bar{q}^2q^2 states are expected close to the $\bar{K}K$ threshold. Finally, there should be the elusive scalar glueball. The isoscalars, including the glueball, should be broad, given the enormous phase space for $\pi\pi$ decay. This is a theoretical

recipe for a mess, and a mess we indeed have.

The only established isovector is the $a_0(980)$ (was δ), but this is right at the $\bar{K}K$ threshold, which makes it difficult to establish its parameters. Most likely it is a $\bar{K}K$ molecule, or \bar{q}^2q^2 state, but more study is needed. As for the strange states, there is the $K_0^*(1350)$. The \bar{q}^2q^2 hypothesis does not expect stable states above 1 GeV – there should be broad regions of attraction in $K\pi$ and $\pi\pi$ scattering below 1 GeV – so the $K_0^*(1350)$ is most likely a $\bar{q}q$ state. But now to the isoscalars. Two detailed K-matrix analyses have been done, one published^[27], and one preliminary^[28]. Both use essentially all available data pertaining to the scalar isoscalar channel. They agree on $f_0(988)$ (was S^*), and on $f_0(1300)$ (was ϵ). This $f_0(988)$ fits well with the \bar{q}^2q^2 hypothesis, and is the partner of the $a_0(980)$, since both contain a hidden $\bar{s}s$ pair. The $f_0(1300)$ is the broad $\pi\pi$ resonance that has been with us for a long time, and which could be the light quark isoscalar of a $\bar{q}q$ nonet. Ref. 27 find another narrow state close to the $\bar{K}K$ threshold: the $f_0(991)$, decaying into $\bar{K}K$ and $\pi\pi$, which they claim is a candidate for a glueball. On the other hand Ref. 28 find a broad state at around 900 MeV, the ancient ϵ resonance. This might be the remnant of a light quark \bar{q}^2q^2 state, a very broad scalar glueball, or be part of a much distorted $\bar{q}q$ nonet.

Extending their analysis higher up in mass Ref. 28 come to the $f_0(1590)$ (was G). This is a much cleaner state, seen in πp production decaying into $\eta\eta$, $\eta\eta'$ and $4\pi^0$ ^[24]. It is definitely not seen in radiative or hadronic J/ψ decays, which suggests that it is not a glueball. Since it decays predominantly to the η and η' , it might be an $\bar{s}s$ state, but then why does it not decay into $\bar{K}K$? Maybe it is an excited meikton, for which decays to s quarks may dominate, or a \bar{q}^2q^2 state with hidden strangeness, but then why does it not fall apart?

At even higher mass Ref. 28 find a possible $f_0(1650)$ and $f_0(1750)$, and they mention that their final fit may need an additional $f_0(1240)$. Altogether, a lot of isoscalars, but no coherent pattern into which to fit them. Any possible

clarification would be very helpful.

Another possible scalar or tensor exotic is the $X(1480)$,^[29] seen in $\bar{p}p$ and $\bar{p}n$ annihilations, and decaying mainly into $\rho\rho$.

This completes the list of states that can be seen in $\bar{p}p$ annihilation at rest. There are more oddities at higher mass which would be accessible from annihilation in flight. The first is the $f'_2(1720)$ (was θ), which remains a prime candidate for a glueball. It has not been seen so far in hadronic production. It is quite broad, and to search for it the large $\eta\eta$ mode would probably be most effective.

Higher in mass, there are the three tensor states seen in $\pi p \rightarrow \phi\phi n$ ^[30]. These are at masses 2.01, 2.30 and 2.34 GeV, and are all broad. One might expect radially excited $L=1$ tensors at this mass, but not three, and not with this decay. The OZI forbidden nature of the process suggests glueballs, but three states so close in mass seems hard to accomodate in any theoretical scheme. To search for these states in low energy $\bar{p}p$ annihilation will be tricky, since they are so broad, but it is very important to have confirmation of them. They are not seen in J/ψ decays, which goes against the glueball hypothesis.

Conversely, the $\xi(2200)$ is seen in radiative J/ψ decay, possibly in πp production, possibly in Kp production, but not so far in $\bar{p}p$ at LEAR or BNL^[15-31]. It maybe either a 2^{++} or 4^{++} state, which allows me to use its colloquial name. It is very narrow, and thus well suited to a $\bar{p}p$ scan, as long as the momentum spread is small enough. This state may well be a orbitally excited $\bar{q}q$ state^[32], though the meikton hypothesis, and even the Higgs hypothesis, are still possibilities.

4. CASE STUDIES IN $\bar{p}p$ ANNIHILATION AT REST

The particular strengths of $\bar{p}p$ annihilations are two. For annihilation at rest, one can select the spin-parity of particular final states by using information about the initial atomic state. This reduces backgrounds, but will require searching in channels with small branching ratios. The second advantage is that annihilation in flight can scan in mass with very high precision, and thus search for narrow states such as the $\xi(2220)$. Of course, at higher masses one can study the charmonium states, and in particular some states not previously reached^[33]. Such scans are straightforward in principle, however, so I focus my attention on the annihilation at rest. This is also where I have argued that there is the best possibility for unravelling the exotic spectrum of QCD.

Let me begin with some general comments about final states. There seems to be a growing experimental trend to find new states in channels involving mesons containing s quarks: η -s, η' -s, and ϕ -s. This is also where one would expect theoretically that the signal to background for exotics would be best. The signal may be enhanced because most exotic states contain gluons, which may have at least equal coupling to u , d and s quarks. In contrast, $\bar{q}q$ states have to either overcome the OZI rule, if they are made of light quarks, or the difficulty of popping an $\bar{s}s$ pair out of the vacuum, if they are $\bar{s}s$ states, in order to reach final states containing these particles. I am not suggesting that other channels should not be looked in, but I think these channels should be concentrated on when planning detector capabilities.

The beauty of annihilations from rest is that they occur from atomic states with definite J^{PC} . In a liquid target, where there is substantial Stark mixing, nearly all annihilations are from the s-wave, with $J^{PC} = 0^{-+}, 1^{--}$. In a gas target, roughly half of the annihilations come from p-wave states, with $J^{PC} = (0, 1, 2)^{++}, 1^{+-}$. It may be practical to tag the p-wave annihilations by their associated X-rays, and thus separate them from s-wave decays on an event by event basis, with some loss of efficiency. Even if this is not possible, a comparison

of gas and liquid target data should allow a partial extraction of the p-wave component.

Kinematics restricts the search for exotics to the reactions (1) $\bar{p}p \rightarrow \pi X$ and (2) $\bar{p}p \rightarrow \pi\pi X$. In reaction (1) the allowed quantum numbers of X are $0^{++}, 1^{+-}$ from the s-wave atomic states, and $(0, 1, 2)^{-+}, 1^{--}$ from the p-wave states. I am assuming here that lack of phase space restricts the decay to zero orbital angular momentum. Masses for X of up to 1700 MeV can be studied. Reaction (2) yields quantum numbers for X that are the same as those of the initial $\bar{p}p$ state, assuming that the $\pi\pi$ pair in the final state is in a relative s-wave. Here, only masses up to 1550 MeV can be probed. In all cases, the isospin of the initial $\bar{p}p$ can be either 0 or 1, and so the same is true of X .

These considerations mean that decays from atomic s-wave states can search for exotic scalars, pseudoscalars and vectors. Addition of decays from p-wave atomic states allows study of the $J^{PC} = 1^{-+}, 1^{++}$ and 2^{++} , as well as pushing up the mass available in the pseudoscalar and vector channels. The $\bar{q}q$ exotic 1^{-+} is particularly interesting. Thus annihilation from rest allows study of all the spin-parities in which the lightest exotics are expected. For the rest of this section I discuss some final states that seem particularly promising.

$X \rightarrow \bar{K}K\pi$ This decay is allowed for $J^{PC}_X = 0^{-+}, 1^{+\pm}$, and includes the two body decays $\bar{K}K^*$ and $a_0\pi$. One can use it to search for exotic pseudoscalars and axial vectors. If one produces X in association with $\pi\pi$ from an initial s-wave, reaction (2S), then X must be a pseudoscalar, as pointed out by Chanowitz^[34]. Indeed this is the classic channel in which the old E was found. It would be very nice to have more data in this channel, to see if both the $\eta(1400)$ and $\eta(1460)$ are present.

Utilizing initial p-wave states, and reaction (1), one can extend the mass available. One can also, using reaction (2), study 1^{++} states. If the tagging of initial p-wave states is possible, one then has a very nice method of switching between 0^{-+} and 1^{++} . It is harder to make a 1^{-+} , for this requires two units of

orbital angular momentum.

$X \rightarrow \eta\pi\pi$ This is very similar to the previous decay. Since there is uncertainty in the present data on the branching ratios into $\bar{K}K\pi$ and $\eta\pi\pi$, it is very important to do an analysis of both final states.

$X \rightarrow \eta\eta, \eta\eta'$ These final states can only come from scalars or tensors, or from 1^{-+} states for $\eta\eta'$. Unfortunately, the latter channel, which is a good one for meiktons, is very close to the kinematic limit. We can select only the scalars by considering reaction (1S), which is here $\bar{p}p \rightarrow \pi^0\eta\eta'$. This is a particularly nice final state because all the conceivable backgrounds are of interest. These are $a_0\eta$, which allows one to study the a_0 , and $f_2\pi^0$, which is interesting to confirm the $f_2 \rightarrow \eta\eta$ decay. It should be possible to separate f_0 states from f_2 states from the Dalitz plot of the final state.

$X \rightarrow \eta\pi^0$ These decays select appear for isovector particles, with quantum numbers $0^{++}, 1^{-+}, \dots$. By choosing reaction (1S) we again pick out the scalar. This allows one to study the a_0 . To select the exotic quantum numbers one must use reaction (1P). The final state is $\eta\pi^0\pi^0$, which again has few backgrounds. The choice of neutral pions removes any ρ contamination. This leaves the only background as ηf_0 . This may be quite large, but is of interest in its own right as a complementary view of the scalar channel as compared to the $\eta\eta$ decay discussed above.

$X \rightarrow \phi\pi^0$ This is the channel in which the $\rho(1490)$ has been seen. It allows the quantum numbers $1^{+-}, (0, 1, 2)^{--}$. Reaction (1S) selects from these the 1^{+-} , which is of interest because the $h_1(1400)$ may decay to $\phi\pi$. Reactions (2S) and (1P), on the other hand, select out the vector channel. The final state is $\phi\pi^0\pi^0$ for the latter, and in this case the only background is from low mass $\pi\pi$ structure. This is a particularly clean channel. It would also be interesting to replace the ϕ by an ω , though this will be a harder channel to study.

All of these channels will have small branching ratios, perhaps in the range $10^{-4} - 10^{-5}$. Thus high statistics will be essential. It is worth remembering that both the DM2 and Mark III groups have studied over 5 million J/ψ decays, 10% of which are in the intensively studied radiative decay mode. This has allowed these groups to discover a lot of new physics, but is not enough for detailed analysis of all interesting channels. So at least this number of $\bar{p}p$ annihilations will be needed to extract comparable physics.

5. CONCLUSIONS

I hope I have made the case for detailed further study of this exciting mass region. It seems to me reasonable that such study would yield a handful of glueballs and maybe a few partial nonets of meiktons. This study should be carried on with as many different production mechanisms as possible. $\bar{p}p$ annihilations at low energy or at rest can play a central role in these studies.

Acknowledgements: I thank Billy Bonner for inviting me to this workshop, and the other participants for interesting discussions. I thank Marek Karliner and Walter Toki for reading the manuscript.

REFERENCES

1. R. L. Jaffe, Fermilab Antimatter 1986: 1
 S. R. Sharpe *ibid.* 165; H. Lipkin *ibid.* 293; N. Isgur *ibid.* 347
 M. S. Chanowitz, Tsukuba Conf. Hadron 1987:269
 W. Toki *ibid.* 252
 S. U. Chung, preprint BNL-40139 (6/87)
 T. Barnes, preprint UTPT-87-20 (9/87)
2. See, for example, C. Quigg, *Gauge Theories of the Strong, Weak and Electromagnetic Interactions*, Benjamin/Cummings, 1983
3. S. Godfrey and N. Isgur, *Phys. Rev. D* **32** (1985) 189
4. R. L. Jaffe, *Phys. Rev. D* **15** (1977) 267,281
5. J. Weinstein and N. Isgur, *Phys. Rev. D* **15** (1983) 588
 See also Barnes in Ref. 1
6. M. S. Chanowitz and S. R. Sharpe, *Nucl. Phys. B* **222** (1983) 211
 T. Barnes, F. E. Close and F. de Viron, *Nucl. Phys. B* **224** (1983) 241
7. N. A. Campbell, A. Huntley and C. Michael, preprint LTH-178 (6/1987)
8. R. L. Jaffe and K. Johnson, *Phys. Lett.* **60B** (1976) 201
9. N. Isgur and J. Paton, *Phys. Rev. D* **31** (1985) 2910
10. M. A. Shifman, *Zeit. Phys. C* **9** (1981) 347
 C. A. Dominguez and N. Paver, *Zeit. Phys. C* **31** (1986) 591; **32** (1986) 391
 S. Narison, Berkeley High Energy Phys. 1986:709
11. C. Michael and M. Teper, preprint OXFORD-TP-72/87 (10/87)
12. R. L. Jaffe, K. Johnson and Z. Ryzak, *Ann. Phys.* **168** (1986) 344
13. W. Toki in Ref. 1
14. P. Baillon *et al.* , *Nuovo Cimento A* **50** (1967) 393

15. The experimental status has recently been reviewed in T. Tsuru, Tsukuba Conf. Hadron 1987: 233
16. S. Suzuki, Tsukuba Conf. Hadron 1987: 64
17. S. I. Bityukov *et al.* , *Sov. J. Nucl. Phys.* **39** (1984) 735
18. D. O. Caldwell, *Mod. Phys. Lett. A2* (1987) 771
19. S. Cooper, Tsukuba Conf. Hadron 1987: 98
20. H. Lipkin, Fermilab AntiMatter 1986: 293; and references therein
21. T. Armstrong *et al.* , *Phys. Lett.* **146B** (1984) 273
22. For a review see W. Toki in Ref. 1
23. L. Kopke, Berkeley High Energy Phys. 1986:692
24. Yu. Prokoshkin, Tsukuba Conf. Hadron 1987: 28
25. M. S. Chanowitz, *Phys. Lett.* **187B** (1987) 409
26. H. Lipkin, Tsukuba Conf. Hadron 1987: 363
27. K. L. Au, D. Morgan and M. R. Pennington, *Phys. Rev.* **D35** (1987) 1633
28. R. Longacre *et al.* , Tsukuba Conf. Hadron 1987: 50
29. D. Bridges *et al.* , *Phys. Rev. Lett.* **56** (1986) 215
30. R. Longacre *et al.* , Tsukuba Conf. Hadron 1987: 46
31. J. Sculli *et al.* , *Phys. Rev. Lett.* **58** (1987) 1715
32. S. Godfrey, R. Kokoski and N. Isgur, *Phys. Lett.* **141B** (1984) 439
33. M. G. Olsson, Fermilab Antimatter 1986: 119
34. M. Chanowitz, *Phys. Rev. Lett.* **46** (1981) 981

Tests of CP Violation at LEAR

James Miller

Department of Physics

Boston University

Our group at Boston University has joined a collaboration which plans to measure CP violation parameters in the neutral kaon system using the Low Energy Antiproton Ring (LEAR) at CERN, Geneva, beginning in 1988 (experiment # PS195). The plan is to use stopped \bar{p} 's in hydrogen at LEAR to produce K^0 's and \bar{K}^0 's. We will then measure the interference effects in the decay amplitudes to improve current values or in some cases measure for the first time several parameters describing CP violations in the neutral kaon system.

A description of this experiment is appropriate at this conference since a very large number of stopped antiprotons will be required. I will discuss those measurements which can be made at LEAR, and I will also suggest the need for more antiprotons than are currently available in order to extend our knowledge of CP violation.

It is useful for the following discussion to mention the qualitative features of the symmetry operators C, P, and T.

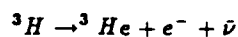
C refers to the operation of charge conjugation, which changes a particle into its antiparticle. For example, a reaction is invariant under charge conjugation if the rate of a reaction and the corresponding reaction with every particle replaced by its antiparticle is the same.

P is the parity operator, in which the direction of each of the three coordinate axes is reversed. The parity operator reverses the direction of vectors like \mathbf{r} and \mathbf{p} , but not pseudovectors like orbital angular momentum or spin. Parity invariance implies, for example, that the rate for a reaction is the same as for the parity-reversed reaction.

T is the time reversal operator, which essentially reverses the direction of a reaction. A reaction is invariant under T if the reverse of the reaction, apart from phase space factors, has the same rate.

The combined symmetry CPT is known experimentally to hold to a high degree. It predicts for example that the magnitude of the masses, charges, magnetic moments, and lifetimes are the same for particles and antiparticles. All existing field theories require this symmetry, since any field theory which satisfies Lorentz invariance, hermiticity, local commutativity, and spin statistics must be CPT invariant. These assumptions are so basic to our understanding of physics that an observation of CPT violation would be earth-shaking indeed. It is not yet clear whether string theories require CPT invariance.

Before the mid-1950's, C, P, and T were thought to be separately conserved in every reaction. It is the usual approach to assume as many symmetries as possible in order to simplify the theories of an interaction, unless experiment shows these symmetries to be incorrect. Parity invariance seemed like a reasonable symmetry, since no one had observed it being violated prior to 1956 (although too much credence had been given to parity invariance and therefore physicists didn't look very hard to check it) and there was no reason to expect that a reaction which could occur in a right handed coordinate system couldn't also occur in a left handed coordinate system. On the other hand, the need for parity invariance was never as compelling as the need for CPT invariance from a theoretical point of view. It was then discovered experimentally that there was a very large (maximal) parity violation in weak interactions (Ambler and Wu). An example is in the beta-decay of tritium



In this type of reaction, it is found that the probability for the electron to be emitted along the direction of the ${}^3\text{H}$ spin is different from the probability to be emitted opposite the spin direction. Applying the parity operator, the directions of the momenta are reversed but

the spin is not. In the parity-reversed reaction we expect the probabilities of production along and opposite the spin direction to be reversed, which is of course not observed, therefore parity is violated. The theories of weak interactions had to be completely reformulated. It is safe to say that since parity violation was discovered, the symmetries which underly theories of reactions have been under much closer scrutiny.

Since CPT is believed to be a good quantum number, and in the 1950's T was known within experimental errors to be invariant to a fairly high accuracy (certainly much better than P), one concluded that C was violated at the same level as P, so that CP, like T, was invariant within experimental errors.

Then, in 1964, an experiment¹ studying the decays of neutral kaons showed that the combined symmetry CP was slightly violated, slightly in the sense that the violation is very small compared to P violation, and in the sense that it is so small that it is hard to measure. In fact, to this day, CP violation has only been detected in the neutral kaon system.

The current understanding of the symmetries is as follows:

CPT is invariant.

For weak interactions:

C and P are maximally violated, and CP has a small measured violation, observed only in K^0 , \bar{K}^0 decays. T must be violated at the same level as CP if one assumes CPT, but this has never been directly measured.

The decay pattern of the neutral kaons is unusual. Decays via the strong interaction are not possible since there are no lighter strangeness = ± 1 particles. Consequently, they decay weakly by the following modes (ignoring for the moment the rarer decay modes which are discussed later): About half the time, they decay into 2 pions

$$K^0 \text{ or } \bar{K}^0 \rightarrow \pi^+ \pi^- \text{ (69\%)} \text{ or } \pi^0 \pi^0 \text{ (31\%)}$$

with a lifetime $\tau_s = .9 \times 10^{-10}s$. This is the K-short (K_S) component. The rest of the time, they can decay into three pions or semileptonically with the much longer decay time $5 \times 10^{-8}s$

$$K^0 \text{ or } \bar{K}^0 \rightarrow \pi^+ \pi^- \pi^0 \text{ (12\%)} \text{ or } 3\pi^0 \text{ (21\%)}$$

$$K^0 \text{ or } \bar{K}^0 \rightarrow \pi^\pm \mu^\mp \nu \text{ (27\%)} \text{ or } \pi^\pm e^\mp \nu \text{ (39\%)}$$

This is the K-long (K_L) component.

This decay scheme is actually *required* by CP invariance, and it was the observed small deviations from this scheme, namely two pion decays at very late times, which first indicated CP violation.

The explanation for this decay scheme is now a familiar one. The most common way to produce neutral kaons is in a reaction involving a strong interaction, which produces states of definite strangeness K^0 or \bar{K}^0 . The kaon has spin 0. The final state consisting of two pions with $J=0$ must be an eigenstate of $CP=+1$. Therefore, if we see a K^0 decay into two pions, and if CP is invariant, then only that portion of the K^0 which has $CP=+1$ can decay into two pions.

Given the property of CP acting on neutral kaon states, $\bar{K}^0 = (CP)K^0$, we can form CP eigenstates:

$$K_1 = \frac{1}{\sqrt{2}}(K^0 + \bar{K}^0), \quad K_1 = +(CP)K_1$$

$$K_2 = \frac{1}{\sqrt{2}}(K^0 - \bar{K}^0), \quad K_2 = -(CP)K_1$$

$$K^0 = \frac{1}{\sqrt{2}}(K_1 + K_2)$$

$$\bar{K}^0 = \frac{1}{\sqrt{2}}(K_1 - K_2)$$

Assuming CP is invariant, $K_S = K_1$ is the mass eigenstate with a short lifetime decaying to two pions, while $K_L = K_2$ is the mass eigenstate with a long lifetime and cannot decay to two pions. In the pioneering experiment of Christiansen, Cronin, Fitch, and Turlay¹, they allowed the K_S component of a neutral kaon beam to decay almost completely. They then detected a small probability of two pion decays from the remaining K_L , a clear indication of CP violation. It has since been established that most of the CP-violation in the 2π decays is due to the CP-impurity of the mass states themselves. Let this be represented by the small number ϵ :

$$K_S = K_1 + \epsilon K_2$$

$$K_L = K_2 + \epsilon K_1$$

It is interesting to see the time progression of, for example, the K^0 (in the approximation $\epsilon \ll 1$):

$$\Psi(t) = \frac{1}{\sqrt{2}}(K_S e^{-M_S t} + K_L e^{-M_L t})$$

$$\Psi(t) = \frac{1}{\sqrt{2}}((K_1 + \epsilon K_2)e^{-M_S t} + (K_2 + \epsilon K_1)e^{-M_L t})$$

$$\Psi(t) = \frac{1}{2}((K^0 + (1 - 2\epsilon)\bar{K}^0)e^{-M_S t} + (K^0 - (1 - 2\epsilon)\bar{K}^0)e^{-M_L t})$$

where $M = im + \frac{\gamma}{2}$, m =rest mass, γ =width.

Then, a typical observable is the rate R for $K^0 \rightarrow 2\pi$ as a function of time:

$$\begin{aligned} R(t) = \text{constant} \times \{ & (1 \mp 2\text{Re}\epsilon)e^{-\gamma_S t} \\ & \pm 2(1 \mp 2\text{Re}\epsilon)\text{Re}\eta_{\pi\pi}e^{-.5(\gamma_S + \gamma_L)t}\cos(\Delta m t) \\ & \pm 2(1 \mp 2\text{Re}\epsilon)\text{Im}\eta_{\pi\pi}e^{-.5(\gamma_S + \gamma_L)t}\sin(\Delta m t) \\ & + (1 \mp 2\text{Re}\epsilon)|\eta_{\pi\pi}|^2 e^{-\gamma_L t} \} \end{aligned}$$

where the upper (lower) signs refer to $\psi(t)$ ($\bar{\psi}(t)$),

$$\eta_{\pi\pi} = \frac{\langle \pi\pi | T | K_L \rangle}{\langle \pi\pi | T | K_S \rangle}$$

$$\Delta m = m_L - m_S = .5 \times 10^{10} s^{-1}$$

$$\frac{1}{\gamma_S} = .9 \times 10^{-10} s, \quad \frac{\gamma_S}{\gamma_L} = 581$$

Because γ_S and Δm have comparable amplitudes, it is possible to observe interference in the decay rate $R(t)$ due to CP violation, in the range $0 \rightarrow 20\tau_S$. It is the several unique aspects of the neutral kaon system which allow CP violation to be seen in their decays and, to this point, in no other system.

The η 's are the ratios of the CP-forbidden $K_L \rightarrow 2\pi$ amplitudes to the CP allowed $K_S \rightarrow 2\pi$, which is just ϵ . To allow for the possibility that there is a CP violation in the decay matrix, the parameter ϵ' is introduced,

$$\epsilon' = \frac{1}{\sqrt{2}} \frac{\langle \pi\pi, I=2 | T | K_2 \rangle}{\langle \pi\pi, I=0 | T | K_1 \rangle}$$

where I refers to the isospin state of the 2π 's and we have

$$\eta_{\pm} = \frac{\langle \pi^+ \pi^- | T | K_L \rangle}{\langle \pi^+ \pi^- | T | K_S \rangle} = \epsilon + \epsilon' = (2.275 \pm 0.021) \times 10^{-3} e^{i(44.6 \pm 1.2^\circ)}$$

$$\eta_{00} = \frac{\langle \pi^0 \pi^0 | T | K_L \rangle}{\langle \pi^0 \pi^0 | T | K_S \rangle} = \epsilon - 2\epsilon' = (2.299 \pm 0.036) \times 10^{-3} e^{i(54 \pm 5^\circ)}$$

In the superweak hypothesis (Wolfenstein)², $\epsilon' = 0$, while milliweak theories predict a range of values. The standard model predicts a non-zero ϵ' of a few $\times 10^{-3}$ via the so-called penguin diagrams. From a theoretical standpoint, it is of paramount importance to establish whether ϵ' is non-zero in order to understand its source and the mechanism responsible for CP violation. Early experiments measured $\epsilon' = 0$ within rather large errors, until a recently announced measurement from CERN, experiment NA31, using $K_L - K_S$ beams,

$$|\frac{\epsilon'}{\epsilon}| = (3.5 \pm .7 \pm .4 \pm 1.2) \times 10^{-3}.$$

This is consistent with predictions based on the standard model. This measurement needs to be confirmed since it is only 2 standard deviations from 0, preferably by another technique. Our CERN experiment (discussed below) will perform the measurement with comparable accuracy by a completely different technique with different sources of systematic errors.

Given the known small value of ϵ' , the difference in phases between η_{+-} and η_{00} should be nearly 0 if CPT is invariant, but the measured value of the difference is $8 \pm 5^\circ$. This is almost two standard deviations from 0, which is uncomfortably large if one is to continue to believe in CPT invariance (see the review by Barmin, et al). Remember the above measured value for ϵ' is only a little more statistically different from 0! The CERN NA31 experiment expects to measure this difference to better than 1° in 1988, and our LEAR experiment will produce a measurement with similar precision.

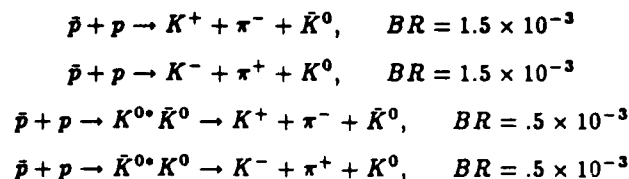
In order to draw a distinction between the proposed LEAR measurement and other measurements of CP violation, I will discuss briefly the two general experimental approaches. Most experiments to date have involved $K_S - K_L$ beams. To get ϵ' from $K_S - K_L$ beams, one measures a ratio of ratios:

$$R = \frac{|\eta_{\pm}|^2}{|\eta_{00}|^2} = 1 + 6 \operatorname{Re}(\frac{\epsilon'}{\epsilon})$$

$$= \frac{(\frac{N_{\pm}^{\pm}}{N_{\pm}^{00}})}{(\frac{N_{\pm}^{\pm}}{N_S^{00}})} = \frac{a}{b} \quad \text{or} \quad = \frac{(\frac{N_{\pm}^{\pm}}{N_S^{\pm}})}{(\frac{N_{\pm}^{00}}{N_S^{00}})} = \frac{c}{d}$$

Here, N is the number of decays per unit time. In a given experiment, one measures separately a and b, or c and d. There have been a number of types of measurements which were cleverly designed to circumvent the systematic problems that are encountered, such as uncertainties in the regeneration amplitude for K_S , or the difficulties of knowing the acceptance of a detector over the extended region where particle decays are being observed, or the difficulty of normalizing the acceptance for neutral decay channels to the charged decay channels.

The approach at LEAR is quite different. Neutral kaons are produced by stopping antiprotons on hydrogen in the following reactions:



The neutral kaons are produced in a well defined state at a well defined time and point in space, and K^0 's and \bar{K}^0 are produced in exactly equal numbers. The systematic advantages are obvious, since all decays can be observed simultaneously by the same detector in the same region of space, there are no uncertainties introduced by K_S regeneration, and the K_0

or \bar{K}^0 are tagged. This experimental approach has not been pursued in the past due to the low branching ratios which make large numbers of antiprotons mandatory. PS195 depends heavily on the LEAR upgraded flux of $2 \times 10^6 \bar{p}/s$.

We can for example minimize the uncertainty in normalization between the $2\pi^0$ decay measurements and the charged 2π decay measurements by determining the η 's from the time-dependent asymmetries:

$$A_{\pi\pi} = \frac{R[\bar{K}^0 \rightarrow \pi\pi] - R[K^0 \rightarrow \pi\pi]}{R[\bar{K}^0 \rightarrow \pi\pi] + R[K^0 \rightarrow \pi\pi]}$$

$$= \frac{2|\eta_{\pi\pi}|e^{\frac{\gamma}{2}t} \cos(\Delta m t - \Theta_{\pi\pi})}{1 + |\eta_{\pi\pi}|^2 e^{\gamma t}} - 2Re\epsilon$$

We can see, from a couple of examples, how the systematic problems from background are minimized by this experimental approach. In the production channel, the main background comes from the numerous

$$\bar{p} + p \rightarrow \pi^+ \pi^+ \pi^- \pi^-.$$

This background has the same effect on both the K^0 and \bar{K}^0 channels. In the 2π decay channel, a major background arises from the semi-leptonic neutral kaon decays. Again, however, the effect is the same for both K^0 and \bar{K}^0 decays.

The apparatus for the proposed LEAR experiment consists of a 2m diameter \times 3m long solenoidal magnet with a field of 0.5 T. At the center is a liquid or compressed gas hydrogen target, where \bar{p} 's can be stopped in a very small volume due to the small momentum spread in the LEAR antiproton beam. The target is surrounded by cylindrical proportional and drift chambers to provide momentum analysis for charged particles. These in turn are surrounded by streamer tubes to provide position information along the axis of the solenoid, then time-of-flight counters and cerenkov counters to identify charged kaons, pions, and electrons, then finally an electron-photon shower sampling calorimeter.

The LEAR experiment is approved for a total of 10^{13} stopped antiprotons, which can be obtained in a couple of months running time if the upgrade at LEAR provides the anticipated increase in flux. In addition to providing competitive measurements of ϵ' and $(\phi_{00} - \phi_{\pm})$, we will also measure a number of other parameters, as shown in the table.

Expected Precision, $10^{13} \bar{p}$

Parameter	Present Precision	Precision, CP-LEAR
$\frac{\epsilon'}{\epsilon}$	$\sim 1.4 \times 10^{-3}$	1.5×10^{-3}
$\phi_{+-} - \phi_{00}$	5°	1°
$ \eta_{+-0} $	$< 1.2 \times 10^{-1}$	$< 6 \times 10^{-4}$
$ \eta_{000} $	$< 10^{-1}$	$< 8 \times 10^{-4}$
Re x	$< 2 \times 10^{-3}$	$< 6 \times 10^{-4}$
Im x	$< 2.6 \times 10^{-3}$	$< 7 \times 10^{-4}$
A_T		$6.4 \times 10^{-2*}$
Δm	4×10^{-3}	$1.2 \times 10^{-3*}$

* indicates relative error

Here,

$$\eta_{\pi\pi\pi} = \frac{\langle \pi\pi\pi | T | K_S \rangle}{\langle \pi\pi\pi | T | K_L \rangle}$$

$$z = \frac{a(\Delta S = -\Delta Q)}{a(\Delta S = \Delta Q)}$$

$$\Delta S = -\Delta Q: \quad K^0 \rightarrow \pi^+ l^- \nu, \quad \bar{K}^0 \rightarrow \pi^- l^+ \bar{\nu}$$

$$\Delta S = \Delta Q: \quad K^0 \rightarrow \pi^- l^+ \bar{\nu}, \quad \bar{K}^0 \rightarrow \pi^+ l^- \nu$$

CP violation has been observed only in the 2π and semi-leptonic decay modes. We expect to observe it in a new decay channel, the 3π decay modes, with an error several standard deviations smaller than the expected level of CP violation.

$\Delta S = -\Delta Q$ is forbidden via weak interactions in the standard model. Currently, the experimental upper limit is only a few percent. The LEAR experiment will produce a much improved upper limit.

T violation has never been directly observed. The LEAR experiment plans to measure T violation directly for the first time. Although observation of the T violation does not require the $\Delta S = \Delta Q$ rule, it is easiest to understand the argument if we assume it to hold exactly. Then, if we observe the decay products $\pi^+ e^- \nu$, a \bar{K}^0 has decayed, while if we observe $\pi^- e^+ \bar{\nu}$, a K^0 has decayed. Then, if we tag the production of a K^0 and measure the decay products $\pi^+ e^- \nu$, then this is equivalent to measuring the rate $K^0 \rightarrow \bar{K}^0$. Similarly, if we tag the production of a \bar{K}^0 and measure the decay products $\pi^- e^+ \bar{\nu}$, then this is equivalent to measuring the rate $\bar{K}^0 \rightarrow K^0$. Therefore, it becomes possible to compare the rates for the time reversed reactions $\bar{K}^0 \rightarrow K^0$ and $K^0 \rightarrow \bar{K}^0$. With the known level of CP violation and assuming CPT invariance, T is not conserved, and these rates must differ by a few tenths of a percent. We expect to measure this T violation quite precisely, through the asymmetry

$$A_T = \frac{P_{\bar{K} \rightarrow K} - P_{K \rightarrow \bar{K}}}{P_{\bar{K} \rightarrow K} + P_{K \rightarrow \bar{K}}}$$

The errors in several of these parameters, for example ϵ' , are dominated by statistical errors, and would benefit from a more powerful antiproton source.

Also of interest are the two photon decays of the neutral kaons,

$$K_S \rightarrow \gamma + \gamma, \quad B.R. = (6.05 \pm .04 \pm .08) \times 10^{-4}$$

$$K_L \rightarrow \gamma + \gamma, \quad B.R. = (2.4 \pm 1.2) \times 10^{-6}$$

(these are new CERN-NA31 measurements). In the helicity basis, the photon states are

$$|++\rangle, |--\rangle, |+-\rangle, |-+\rangle$$

The latter two helicity states are forbidden in the kaon decays by angular momentum conservation.

In order to form eigenstates of CP, we write eigenstates of definite parity:

$$|1\rangle = \frac{1}{\sqrt{2}}(|++\rangle + |--\rangle) \quad (CP)|1\rangle = +|1\rangle$$

$$|2\rangle = \frac{1}{\sqrt{2}}(|++\rangle - |--\rangle) \quad (CP)|2\rangle = -|2\rangle$$

One can define a set of parameters analogous to the 2π decays:

$$\epsilon_1 = \frac{A_L(1)}{A_S(1)}, \quad \epsilon_2 = \frac{A_S(2)}{A_L(2)}, \quad \lambda = \frac{A_L(2)}{A_S(1)}$$

If there is CP violation in the mass matrix only, then

$$\epsilon_1 = \epsilon_2 = \epsilon$$

This decay channel is particularly interesting because it involves CP violation in a new decay matrix. The CP violation in the decay matrix is potentially larger than for the 2π decay modes where there is a large suppression due to the $\Delta I = \frac{1}{2}$ rule; some theories predict that it may be as large as $.1\epsilon$.

Both the K_S and K_L can decay into two photons without violating CP. Therefore, it is very difficult to see the interference effects between K_S and K_L two photon decays in regenerated beams. The ideal approach would be to use tagged K^0 's and \bar{K}^0 's from stopped antiprotons.

Since the 2 photon decay branching ratios are several orders of magnitude smaller than the for 2π decay modes it is clear that many stopped antiprotons are required. To see CP violation in the mass matrix, 10^{13} and 10^{14} stopped p 's are required for 1σ and 3σ measurements, respectively, using decays in the time range $0 \rightarrow 20\tau_S$. 1σ accuracy in the measurement of CP violation in the decay amplitude will require $10^{15} - 10^{16}$ antiprotons using decays in the time range $0 \rightarrow 20\tau_S$. The practical limit with the upgrade is about 10^{13} stopped antiprotons at LEAR.

If the expected systematic advantages of using antiprotons to produce tagged neutral kaons are borne out in the LEAR experiment, then many of our measurements will be limited by the statistics afforded by 10^{13} stopped antiprotons. Given the theoretical importance of understanding CP violation in detail and the fact that the neutral kaon system, after 25 years, is still the richest source of information on CP violation, there will then be a compelling case for building a more powerful stopped antiproton source.

References

1. Christenson, J.H., Cronin, J.W., Fitch, V.L., Turlay, R., Phys. Rev. Lett. **13**, 138(1964).
2. Wolfenstein, L., Phys. Rev. Lett. **13**, 562(1964). Also, see Reviews:
Kleinknecht, K., Ann. Rev. Nucl. Sci. **26**, 1(1976).
Barmin, V.V, et al., Nucl. Phys. **B247**, 293(1984).

LOOKING FOR NEW GRAVITATIONAL FORCES WITH ANTIPROTONS

by

Michael Martin Nieto

Theoretical Division, Los Alamos National Laboratory
University of California
Los Alamos, New Mexico 87545

and

B. E. Bonner

Rice University
Houston, Texas 77251-1892

ABSTRACT

Quite general arguments based on the principle of equivalence and modern field theory show that it is possible for the gravitational acceleration of antimatter to be different than that for matter. Further, there is no experimental evidence to rule out the possibility. In fact, some evidence indicates there may be unexpected effects. Thus, the planned experiment to measure the gravitational acceleration of antiprotons is of fundamental importance.

Perhaps the main thrust of elementary particle physics is the effort to unify, in a quantum field theory, what we call the four forces of nature: the strong nuclear, the electromagnetic, the weak nuclear, and the gravitational forces. Of course this type of effort is not new.

In the last century the experimental work of Faraday and Ørsted laid the foundation for the theoretical work of Maxwell, showing that electricity and magnetism are not two separate forces, but just different aspects of the same force. Also, the last part of Einstein's career was devoted to unsuccessfully trying to unify classical electromagnetism with classical gravity. From our viewpoint, he was doomed to failure because there were other forces that needed to be taken account of, the strong and weak forces.

The 1970's saw the next stage in this drama. Weinberg, Glashow, and Salam devised the electroweak theory, which unifies electromagnetism and the weak interactions. This theory was vindicated in the discovery of the W and Z particles at CERN.

Simultaneously, a model of the strong force, "quantum chromodynamics" or QCD, was developed. Therefore, the next logical step was to try to unify QCD with the electroweak theory. This led to the¹ "standard model" and its simplest unification. One of the main predictions is that the proton is unstable with a lifetime of order 10^{30} years. This long lifetime is because the "X" particle, the particle which typifies the unification mass scale, is so large (10^{15} GeV). Therefore, a process which would occur in the 100's of MeV region (proton decay), would be probing physics at the 10^{15} GeV scale. Unfortunately, proton decay has not been seen at the 10^{32} year lifetime level, so this idea

remains unverified.

However, theoretical physicists have remained undaunted, and are trying to unify gravity with the other three forces, even though the other three have yet to be completely unified among themselves. Such theories are in a class called theories of "quantum gravity".²

As we come to in more detail below, these quantum gravity theories may show macroscopic effects at the 10^{-12} eV level due to a Planck mass (10^{19} GeV) unification scale. This is the same type of effect as was hoped for with proton decay: that it would be mediated at the X-mass unification scale. The difference is that here the energy scale stretches over an even larger regime. In fact, it approaches the 50 orders of magnitudes of energy which defines the field of elementary particle physics. (See Fig. 1.)

In quantum theory one has to look for a new type of gravity because standard Einsteinian gravity (general relativity) cannot be quantized. The divergences obtained in trying to make Einstein's classical theory into a quantum theory are simply too severe. It is to be hoped that any new theory will be renormalizable, or perhaps even finite.

Further, one knows as a matter of principle that metric gravity must be incompatible with quantum mechanics at some level.³ General relativity is a world-line (metric) theory whereas quantum mechanics is a many-path point of view.

The above all emphasizes, as we pointed out in the introduction article to this section,⁴ that our ideas on gravity are really an interesting mixture of classical and quantum physics. The weak equivalence principle states that the inertial mass is equal to the gravitational mass:

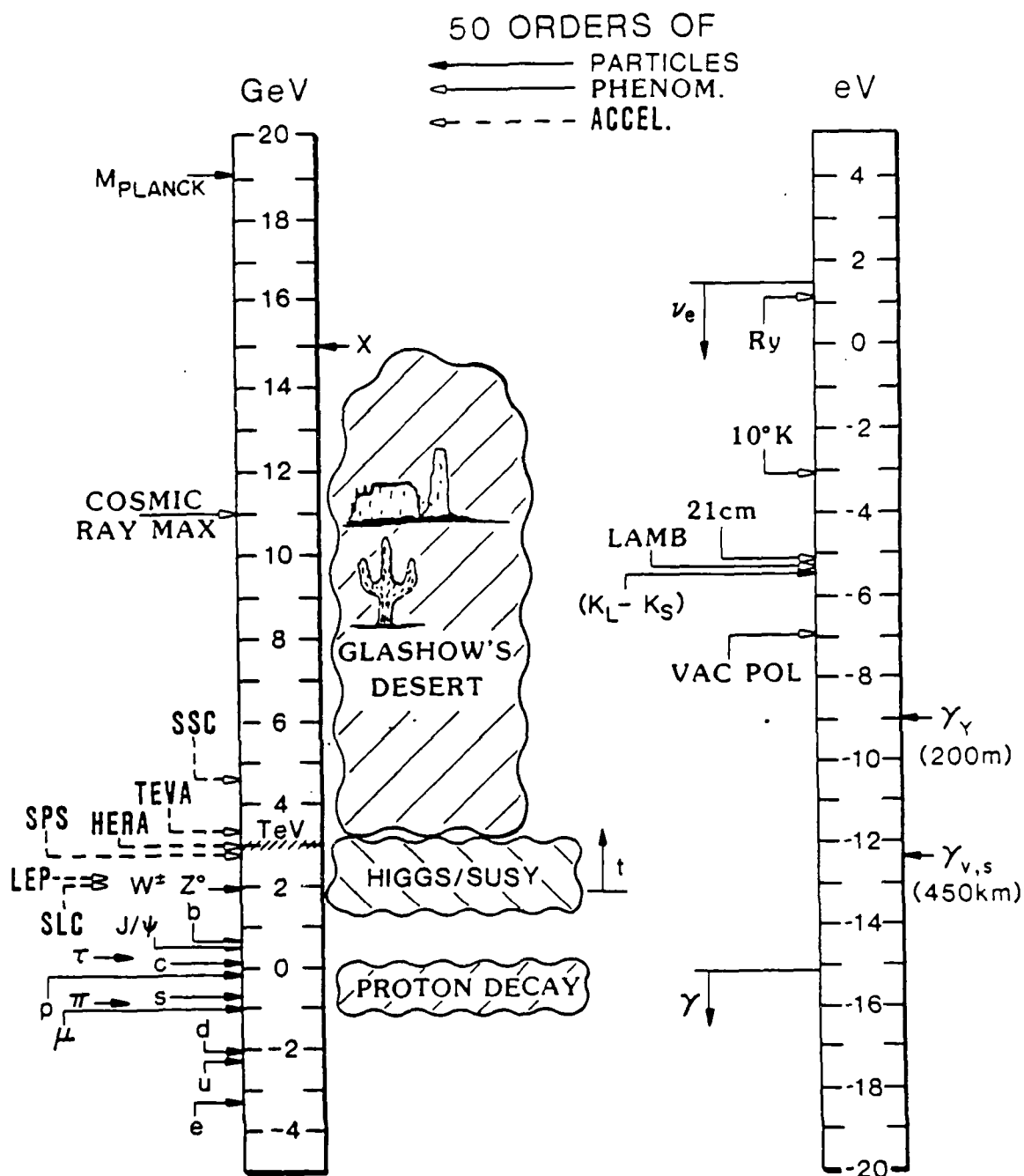


Figure 1. Physics over 50 orders of magnitude in energy. Particle masses are indicated by thick lines, accelerator energies by thin lines, and phenomena by dashed lines. The left-hand sides show established objects and concepts, whereas the right-hand sides show speculated objects and concepts.

$$m_I = m_G . \quad (1)$$

The inertial mass is the kinematic object in Newton's law of force

$$F = m_I a . \quad (2)$$

Contrariwise, the gravitational mass is the charge in Newton's law of gravitation

$$F = -G m_G m_G' / r^2 . \quad (3)$$

Now even though CPT tells us that the inertial mass of a particle is equal to the inertial mass of the antiparticle,

$$m_I = \bar{m}_I \quad (4)$$

this does not imply that

$$m_G = m_I = \bar{m}_I = \bar{m}_G . \quad (5)$$

That is, $m_G \neq \bar{m}_G$ does not necessarily mean that CPT is broken.

If an apple falls to the earth in a certain way CPT only implies that an antiapple falls to an antiearth in the same way. CPT says nothing about how an antiapple (that is to say an antiproton or a positron) falls to an earth. Thus we see that there is nothing wrong, as a matter of quantum principle, for these new theories of quantum gravity to exhibit a violation of the principle of equivalence.

Theories of quantum gravity start from a number of different motivations, such as dimensional reduction, supersymmetry, or string theory. They remain incomplete mathematically and physically. But they do have a common, generic, new prediction:^{2,5} the usual spin-2

graviton now has spin-1 (graviphoton) and spin-0 (graviscalar) partners. These partners are expected to have finite ranges and to couple with approximately gravitational strength to some conserved quantity, such as a fundamental Fermion number. For the static case, this means one would expect a phenomenological gravitational potential to be of the form:⁵

$$V = - Gm_1 m_2 [1 \mp ae^{-r/v} + be^{-r/s}] / r \quad (6)$$

In Eq. (6), a and v (b and s) are the coupling strength normalized to ordinary gravity and the range of the graviphoton (graviscalar). Now tensor and scalar forces are always attractive. However, spin-1 vector forces are attractive between opposite charges and repulsive between like charges. (This is familiar from electromagnetism.) Here the charges are matter and antimatter. Therefore, the $(-)$ sign in front of the vector term of Eq. (6) represents the repulsion of matter to matter and the $(+)$ sign represents the attraction of antimatter to matter.

These theories are saying that there are new vector and scalar gravitational forces which could be macroscopic in their effects. They could approximately cancel in the ordinary world (matter-matter interactions),⁶ and so not have been noticed because there they produce very small second-order effects. However, if one were to measure the gravitational acceleration of antimatter, then the new terms would both add to the normal attraction, and thus could produce a very large first-order effect.⁷

Whether or not a large effect would ensue depends, of course, on the magnitudes of the two ranges v and s and also on the sizes of the coupling constants a and b . As to the coupling constants, they would be

expected to be of order unity since they are normalized to normal gravity. A symmetry breaking could well make them slightly different.

As to the ranges, there are as yet no firm predictions. However, qualitative statements can be made. For very small ranges, of order of the Planck length (10^{-33} cm), although new effects would be produced as a matter of principle, they would not produce effects which could be measured. If the ranges were on the order of 200 m, as advocates of a new "fifth-force" scenario would have,⁸ then there still would be nothing to be seen in the current antiproton gravity experiment. However, in this case there might be measureable effects in precise matter-matter experiments, if the coupling constants a and b and/or the ranges v and s were different.

Finally, ranges on the order of many 10s to 100s of km could yield positive, unexpected results in the antiproton gravity experiment. The question is, "Are such ranges allowed by the data?" The answer, perhaps surprisingly, is, "Yes."

Many people are familiar with the work of Stacey, Tuck, and coworkers analyzing gravity down mine shafts in Australia. Beginning in 1978 and culminating in their recent RMP paper,⁹ they reported an anomalous repulsion which, if analyzed in terms of a single new Yukawa potential, yielded a new term with relative coupling constant of order 0.01 and a range of order 100-1000 m.

They emphasized that their data was not precise enough to restrict the fit to a particular functional form. So, for our program, we requested that they do an analysis in terms of the two new forces predicted by quantum gravity. Stacey, Tuck, and Moore¹⁰ did this. They found that a good fit was allowed as long as $(a-b) \approx 0.01$. Given this,

ranges up to ~450 km were allowed. This result was put into the PREM model of the earth and integrated out to see what the effect would be on the antiproton.⁷ The predictions, with $a=b=1$, are shown in Fig. 2.

The idealized uniform sphere earth is off by a factor of 2, essentially because of the difference in density near the surface of the earth. The real earth's curve is wavy, the waviness corresponds to the fact that you're seeing the different shells become significant. Note that at a 40 km length scale one would obtain a 1% effect in the antiproton experiment, which should be measureable. At 450 km one would have a 14% effect, which definitely would be measureable. This is with $a=b=1$, and the effect scales with $a=b$.

If you add to this the analysis of rapidly-rotating pulsars, which allows values of (a,b) up to $O(100)$ then one can say the expected difference in g for the antiproton could be

$$\Delta g/g \approx a (0.14) (v/450 \text{ km}) . \quad (7)$$

But that is not all the evidence. A number of other experiments have been reported, some finding anomalous results. The most illustrative, for our purposes, are the seemingly contradictory Eötvös experiments by Thieberger¹¹ and by Adelberger's group.¹² Thieberger found that on top of the New Jersey Palisades, a copper sphere neutrally buoyant in water is repelled outward normal to the cliff. Adelberger's group looked for gravitational effects of a small hill on the University of Washington campus. They suspended two pairs of cylinders from a torsion fiber, each pair being of distinct material. Rotating the suspension, they tried to measure a differential torque, caused by one material being closer or farther from the hill. They found

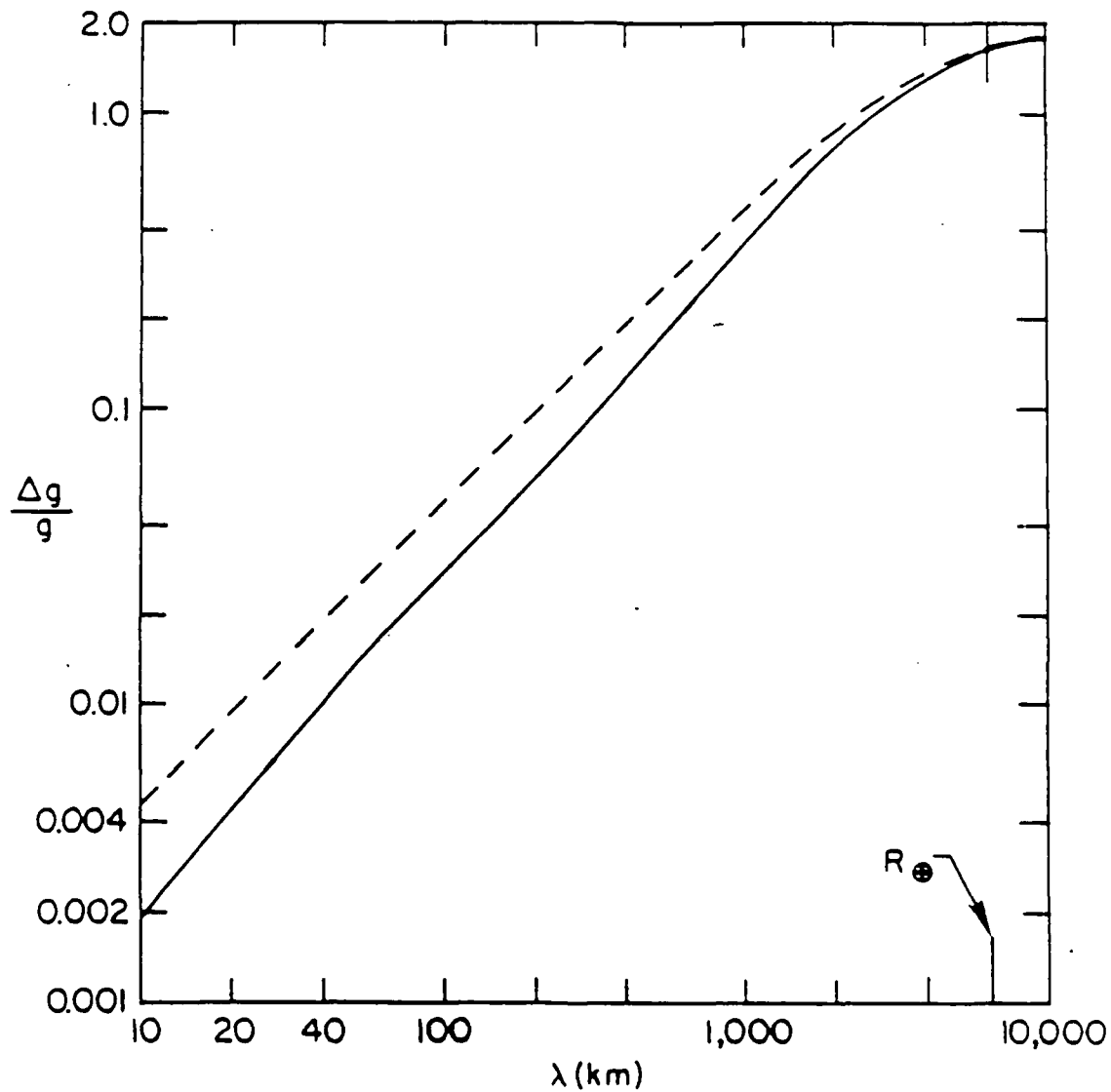


Figure 2. The size of the new effect due to the graviphoton and graviscalar interactions for antimatter as a function of the length scale $v=s=\lambda$. This result is for new coupling constants $a=b=1$, and scales with their values. The lower, solid line is for the earth's real mass distribution, whereas the dashed line is for a uniform mass distribution of the same total mass.

no effect.

If one thinks in terms of a single short-ranged new Yukawa force, as in the fifth force point of view, then these two results appear contradictory. However, if one thinks in terms of two long-ranged forces which approximately cancel, then by geologic accident, the two results are consistent. As observed by Ander, *et al.*,¹³ the Palisades cliff is the edge of a diabase sill which extends all the way into Pennsylvania. This sill has a density of 2.9 g cm^{-3} , which gives a contrast of $+0.2 \text{ g cm}^{-3}$ with the other rock in the region. Taking $(a-b)=0.01$, this sill could account for the effect of Thieberger for a range $r = 200 \text{ km}$.

We mention that another University of Washington group¹⁴ has suspended a ring made of two materials from a torsion fiber. They looked for differential oscillations caused by a mountain near Index, Washington. They found a small, anomalous effect. Even so, this experiment is not inconsistent with the long-range scenario. The geology is not known well enough deep under the Index site to rule out this possibility.

Also, a group from the National Bureau of Standards has performed a modern day Galileo experiment by letting two different materials undergo free fall in a special, evacuated apparatus.¹⁵ They found no effect, but their results are consistent with the positive effect found by the Australians.⁹

From a preliminary version of the ideas expressed above it was proposed¹⁶ that an experiment be done to measure the gravitational acceleration of antiprotons at LEAR (the Low Energy Antiproton Ring) at CERN. Since then a collaboration has been formed to do the

experiment,^{17,18} and the experiment has been approved (PS 200).

Figure 3 is a schematic diagram of the experiment. The output of LEAR (antiprotons of approximate energy 2 MeV) will be decelerated either with an RFQ or by passing through a foil. Then the antiprotons will be captured, cooled, and transferred through a series of electromagnetic traps. Finally, the antiprotons, at approximately 10 °K, will be launched up a superconducting shielded drift tube, guided in the axial direction by a magnetic field.

The actual measurement is a time of flight measurement. For a given length of drift L , the arrival time of the last antiproton which has enough energy to go up a drift tube of length L is given by

$$t = (2L/g)^{1/2}. \quad (8)$$

This value of "g" for the antiproton will be compared to that of the negative hydrogen ion, a particle with the same charge and almost the same mass as the antiproton.

The drift tube used in the antiproton experiment will be an updated version of the tube used by Witteborn and Fairbank to measure the gravitational acceleration of electrons.¹⁹ In this context, we point out that Fairbank is considering doing a modern gravity experiment using positrons.²⁰ Because such an experiment would test for anomalous gravitational coupling to lepton number instead of to baryon number (quark number), it would be complementary to the antiproton experiment. It is to be encouraged.²¹

Ultimately, one would hope someday to be able to do a gravity experiment using neutral antimatter; more specifically, antihydrogen. With electric forces neutralized, such a gravity experiment could be orders of magnitude more precise. The problem, of course, is how to

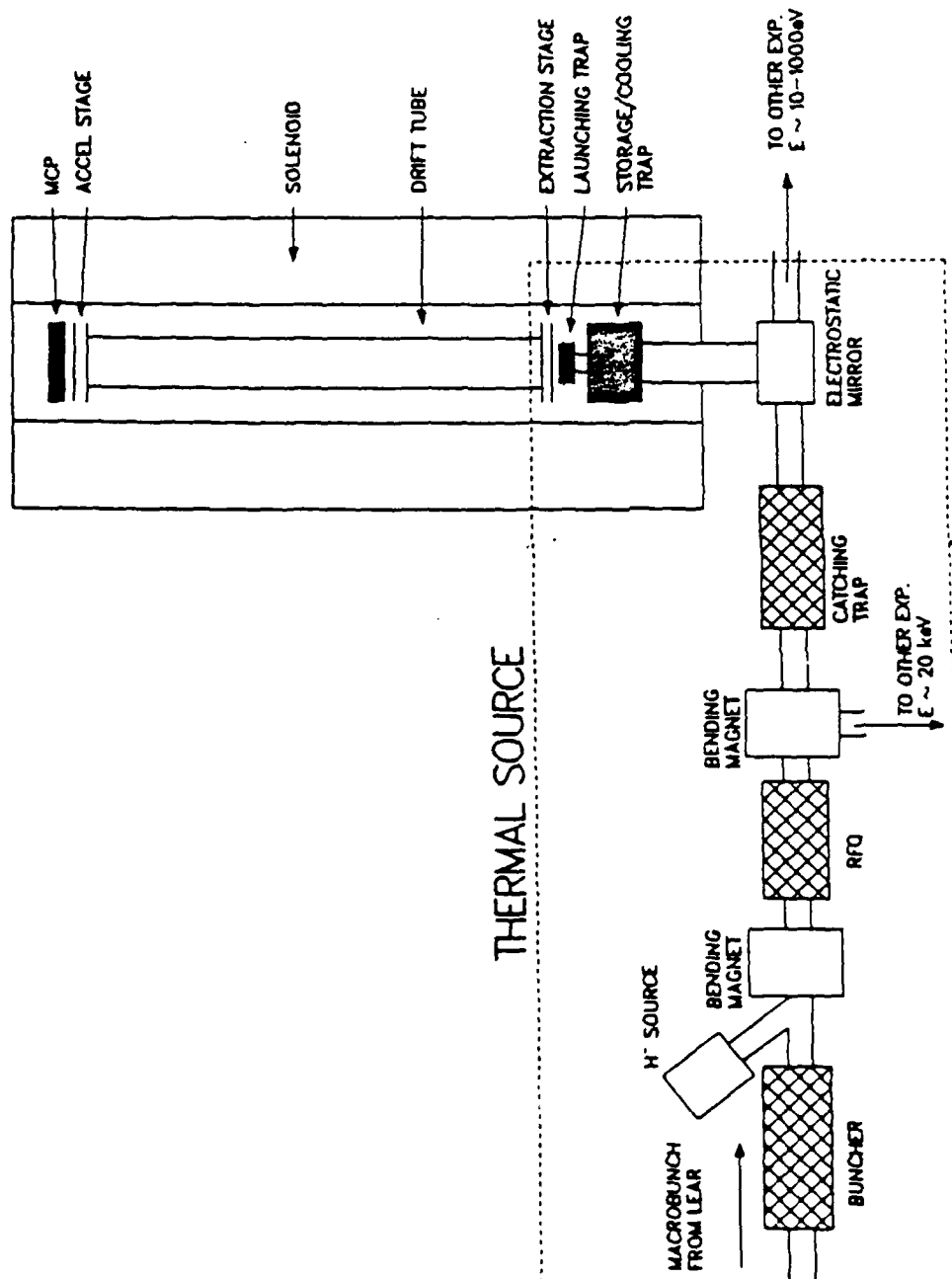


Figure 3. A possible schematic diagram¹⁸ for the antiproton gravity experiment. The diagram is not to scale. The region inside the dotted lines represents a "thermal source" of low to very-low energy antiprotons that would be available for a variety of experiments.

make, let alone contain, antihydrogen. We refer you to the article in these Proceedings by Mitchell.²² He discusses programs aimed at producing antihydrogen. Once antihydrogen is made, the advent of laser storage and velocity selection techniques for single atoms and magnetic trap devices open up the possibility for doing a gravity experiment.

REFERENCES

1. T. Goldman, article in this Proceedings on the "Standard Model".
2. There are many people who deserve credit for the fundamental ideas in this field. A few whom we mention are Fayet, Fujii, Zachos, and especially Joel Scherk. Ref. 5 below contains a detailed bibliography.
3. E. P. Wigner, Rev. Mod. Phys. 29, 255 (1957); Bull Am. Phys. Soc. 24, 633 (1979); H. Salkecker and E. P. Wigner, Phys. Rev. 109, 571 (1958).
4. B. E. Bonner and M. M. Nieto, "Basic Physics Program for a Low Energy Antiproton Source in North America," introductory article to this section of the Proceedings.
5. T. Goldman, R. J. Hughes, and M. M. Nieto, Phys. Lett. B 171, 217 (1986).
6. M. M. Nieto, T. Goldman, and R. J. Hughes, Phys. Rev. D 36, first three articles of a series, Dec. 15 (1987).
7. M. M. Nieto, T. Goldman, and R. J. Hughes, Los Alamos preprint LA-UR-87-3838, submitted to Phys. Rev. D. This is the fourth paper of the series of Ref. 4.
8. E. Fischbach, et al, Phys. Rev. Lett. 56, 3 (1986).
9. F. D. Stacey, G. J. Tuck, G. I. Moore, S. C. Holding, B. D. Goodwin, and

- R. Zhou, Rev. Mod. Phys. 59, 157 (1987).
10. F. D. Stacey, G. J. Tuck, and G. I. Moore, Phys. Rev. D 36, 2374 (1987).
 11. P. Thieberger, Phys. Rev. Lett. 58, 1066 (1987).
 12. C. W. Stubbs, E. Adelberger, et al., Phys. Rev. Lett. 58, 1070 (1987); E. Adelberger, et al., Phys. Rev. Lett. 59, 849 (1987).
 13. M. E. Ander, T. Goldman, R. J. Hughes, and M. M. Nieto, Los Alamos preprint LA-UR-87-2103.
 14. P. E. Boynton, et al., Phys. Rev. Lett. 59, 1385 (1987).
 15. T. M. Niebauer, M. P. McHugh, and J. E. Faller, Phys. Rev. Lett. 59, 609 (1987).
 16. T. Goldman and M. M. Nieto, Phys. Lett. B 112, 437 (1982).
 17. Articles by M. H. Holzschneider and by R. E. Brown, in: Low Energy Antimatter, ed. by D. B. Cline (World Scientific, Singapore, 1986), p. 105 and 120.
 18. N. Jarmie, Nucl. Instrum. Meth. Phys. Res. B24/25, 437 (1987).
 19. F. C. Witteborn and W. M. Fairbank, Phys. Rev. Lett. 19, 1049 (1967).
 20. W. M. Fairbank, in Proceedings of the XXIInd Rencontres de Moriond., edited by J. Tran Thanh Van (Editions Frontieres, Paris, 1987).
 21. T. Goldman, R. J. Hughes, and M. M. Nieto, Phys. Rev. D 36, 1254 (1987).
 22. J. B. A. Mitchell, in these Proceedings.

NORMAL MATTER STORAGE OF ANTIPROTONS

Laurence J. Campbell
Theoretical Division, MS B262
Los Alamos National Laboratory
Los Alamos, NM 87545

ABSTRACT

Various simple issues connected with the possible storage of \bar{p} in relative proximity to normal matter are discussed. Although equilibrium storage looks to be impossible, condensed matter systems are sufficiently rich and controllable that nonequilibrium storage is well worth pursuing. Experiments to elucidate the \bar{p} interactions with normal matter are suggested.

INTRODUCTION

Although it is technically possible, the confinement of \bar{p} as a unneutralized plasma in electromagnetic traps makes no sense for energy storage because the energy density of the required magnetic field is equal to or greater than the rest mass energy density of the confined \bar{p} . This is called the Brillouin limit.¹ (Of course, such storage of \bar{p} for other purposes, as discussed elsewhere in this workshop, makes a great deal of sense.) Therefore, energy storage must be achieved by neutralizing the \bar{p} charge, either directly with e^+ (antihydrogen formation) or indirectly in condensed matter. Both methods confront challenging scientific questions of intrinsic interest. (See the papers by J. B. A. Mitchell and W. C. Stwalley for antihydrogen formation.)

BENEFITS

A. Space charge screening (dense storage)

The density of unneutralized \bar{p} that can be stored in macroscopic electromagnetic traps is ultimately limited by space charge, which must be confined by a magnetic field. A \bar{p} density of only $2.5 \times 10^{13} \text{ cm}^{-3}$ will create a pressure of 100 atmospheres at the surface of a spherical volume 1 cm in radius. Of course, adding positrons to create charge neutrality would be a solution, but, in principle, a deficit of electrons in condensed matter would achieve the same thing, so long as the integrity of the normal matter structure was not affected. Removing only one electron per 100 atoms would be enough to neutralize a \bar{p} storage density of about 10^{22} cm^{-3} in normal matter.

B. Low energy

Although any efficient \bar{p} production process now imagined produces the product at very high kinetic energies, this is an impractical state for storing $10^{22} \bar{p}$ at any density, and especially so at high density. Even at the modest energy of 10 keV the kinetic energy of $10^{22} \bar{p}$ is equivalent to a gram of matter moving at a velocity of 178 km/sec, about 16 times the escape velocity from earth. Should the end use of the \bar{p} require kinetic energies higher than thermal it is a relatively simple matter to accelerate them compared to deaccelerating them, for which a well-defined beam requires the controlled compression of phase space. Condensed matter storage of \bar{p} would be intrinsically low energy storage as would be condensed anti-hydrogen, an attractive alternative.

C. Robustness (vacuum requirements)

Without a specific mechanism in mind it is impossible to predict how robust condensed matter storage would be with all the attendant equipment. However, experience has shown that the condensed matter version of devices, from VLSI chips

to IR detectors, exhibit high reliability. Paradoxically, condensed matter storage would eliminate the requirement for ultra high vacuum since the migration of impurities through a solid is easier to control than their migration through empty space. This is particularly important for low-energy \bar{p} storage for which the vacuum requirements become severe because of the increased cross section for annihilation.

KNOWN LIMITS TO STABILITY

A. Lieb's theorems

Are there any fundamental reasons why no possible combination of matter and antimatter can be stable, i.e., stable intrinsically and in equilibrium? The answer, unfortunately, is yes, and is provided by Elliott Lieb's theorems on the stability of normal matter.² Lieb proves that atoms are stable because of the uncertainty principle, that bulk matter is stable because of the Pauli principle for fermions (which leads to a stronger uncertainty principle), and that thermodynamics is possible because of screening (which permits charge neutrality in bulk matter). These theorems apply with equal force, of course, to antimatter, so that is stable, too. However, combinations of matter and antimatter necessarily involve an interface where there is no Pauli principle between the electrons and positrons and, hence, no stability.

There are two ways around Lieb's theorems. One way is to note that the role of the Pauli principle was crucial only for the leptonic component of matter, not the hadronic. (Solids containing only nuclei having integral spin (bosons) are quite stable.) The fact that protons and neutrons are fermions may be relevant to the stability of neutron stars, but not to ordinary matter. Therefore, the theorems do not strictly address the problem of \bar{p} stability in normal matter. The other escape is to accept the impossibility of equilibrium stability but work for either nonequilibrium

stability in steady state (the basis of \bar{p} storage rings) or a long decay time (the basis of some electromagnetic traps).

B. Intrinsic attraction through induced polarization

If \bar{p} without e^+ avoid Lieb's objections, what is the problem? The problem is not only that Earnshaw's theorem³ prohibits trapping in a static electric field but that a \bar{p} induces attractive electric dipole forces in all neutral, equilibrium matter. Therefore, a thermalized \bar{p} will be attracted to the nearest positive ion in a solid, or to a neutral atomic site, where it will become captured in an atomic orbit and then cascade down the atomic energy levels until annihilation occurs with the nucleus.

C. The question of feasibility

In view of these daunting obstacles what hope can there be for \bar{p} storage in condensed matter? Without its technological importance, shared with \bar{H} condensation, as the ultimate means for energy storage, the problem would be dismissed as too difficult. However, until it can be proven impossible, with the rigor of Lieb's theorems or the second law of thermodynamics, it must be assumed possible because of the astonishing variety of complex and subtle effects that condensed matter continues to reveal. Once a \bar{p} reaches thermal energies its behavior can be dominated by these electromagnetic effects as long as it remains outside the vicinity of nuclei. From another viewpoint, every mole of condensed matter contains 10^{24} force-free positions for \bar{p} -- unstable, though, in one or more directions. To dynamically stabilize a small fraction of these is "all" that is needed.

DOWN-SCALING MACROSCOPIC TRAPS

A. Penning traps to microfabrication to Stark saddles

Can proven macroscopic traps be scaled down to microscopic size? The reduction in size may be carried quite far, although true atomic analogs are not yet known.

Consider a standard Penning trap with electrodes along equipotential lines of the electric potential⁴

$$\phi = A(x^2 + y^2 - 2z^2)$$

in an uniform magnetic field H the z direction. If z_0 and $x^2 + y^2 = r_0^2$ are the locations of the electrodes then A is related to the applied voltage V by

$$A = \frac{V}{2z_0^2 + r_0^2}$$

The three characteristic frequencies are

$$\omega_m = 2cA/H, \text{ magnetron } (c = \text{velocity of light})$$

$$\omega_z = 2 \frac{eA}{m}, \text{ harmonic}$$

$$\omega_c = \frac{eH}{mc}, \text{ cyclotron}$$

There will be a maximum number of charges the trap can hold. For simplicity, take this number N to be that which would cancel a fixed fraction f of the applied field at z_0 when all charges are at the center of the trap,

$$\frac{Ne}{z_0^2} = f4Az_0$$

The effective charge density ρ is then

$$\rho = \frac{N}{2\pi z_0 r_0^2} = \frac{f2z_0^2 V}{\pi e r_0^2 (2z_0^2 + r_0^2)}$$

Consider how this density scales with size. The voltage V must not produce an electric field strength above the value for dielectric or vacuum breakdown, so the scaling of V will be taken as

$$V = E_0 z_0$$

where E_0 is a (safe) constant. Taking the ratio z_0/r_0 to be constant it is seen that ρ scales as $1/z_0$, which implies smaller is better. Assuming constant H , the frequencies

scale as

$$\omega_m \propto 1/z_0$$

$$\omega_z \propto 1/\sqrt{z_0}$$

$$\omega_c = \text{const.}$$

One limit to smaller traps is the lower critical field for stability,

$$H_c = c \frac{2mV}{ez_0^2}$$

This is equivalent to requiring $\omega_m \leq \omega_z/\sqrt{8}$ if $r_0 = \sqrt{2} z_0$. Clearly, H_c scales as $1/\sqrt{z_0}$, so the maximum attainable magnetic field will set a lower limit on the trap size, and an upper limit on the density. If $E_0 = 10^4$ volts/cm and $H_c = 10^6$ gauss (thanks to the new superconductors), then

$$(z_0)_{\min} = 2 \cdot 10^{-4} \text{ cm}$$

and

$$(\rho)_{\max} = 7.26 \cdot 10^{13} \text{ cm}^{-3}$$

This is in the realm of microfabrication, but not quite quantum mechanics. Note that the space charge in each small trap can be neutralized, so there is no build-up of charge as the number of traps is increased. If the total volume of a small trap is five times its storage volume and $f = 0.2$, then a cubic meter of these would contain $10^{18}p$. (The Brillouin limit corresponds to $f = 1$.) The required voltage would be a very modest 2v.

Although miniaturized, these traps are still classical and therefore require a high vacuum and a high, externally imposed magnetic field whose energy density is comparable to the rest energy of the trapped p .

Quantum mechanics does enter for further miniturization, where an atomic analog to the Penning trap exists, as pointed out by Charles Clark, et al.⁵ The so-called Stark saddle is the force-free location of a charge subject to both an external

electric field and the electric field of an ion. This position is unstable only in the direction toward (or away) from ion. Applying a magnetic field perpendicular to the unstable direction leads to closed, classical orbits for the charge's motion around the saddle point. Unlike the Penning trap, in which a magnetic field H perpendicular to a plane with E field instability results in stability, the Stark saddle trap has H perpendicular to a plane with an E field saddle, and the result is metastability. That is, the classical orbits are unstable to small perturbations and correspond to resonances rather than true bound states. For an external field of 5 kV/cm the Stark saddle lies over 600 Å from the ion, so this a phenomenon for gases, not solids.

B. Storage ring to channel ring

The other common macroscopic storage medium for \bar{p} is the storage ring. In principle, it, too, can be down-sized, and this important subject is covered by D. Cline.⁶ Going to even smaller scales, is there an atomic analog? An obvious one would be channeling in a crystal, which would demand some unusual fabrication to make a closed path. It is also possible to imagine (but undoubtedly more difficult to realize) channeling in a straight path with perfect reflection at each end. If lossless channeling occurs for only certain ranges of \bar{p} energy the reflection region would have to be tailored with a varying impedance to minimize turning-point losses. Although no \bar{p} channeling experiments have been done, π^- channeling has been observed in the curious configuration of a helical spiral around lines of atoms.⁷

CONDENSED MATTER TRAPS

A. Generic leakage

Whatever the mechanism for achieving \bar{p} traps there will be a relationship between the size and depth of the trap and the leakage rate to neighboring nuclei where annihilation will occur. This relationship is illustrated here with a simple model.

Let the trap be an equivalent three-dimensional square well of depth $-V_0$ and radius r_0 . Bound states of energy $-\epsilon V_0$ will exist if

$$g = r_0 \sqrt{2mV_0}/\hbar > \pi/2$$

where m is the \bar{p} mass. The wavefunction of the lowest bound state (s wave) will extend outside the well leading to a probability density

$$|\psi(r)|^2 = \frac{A^2}{r_0^3} \left(\frac{r_0}{r}\right)^2 \sin^2 \theta e^{-2\sqrt{1-\epsilon}g(r/r_0-1)}$$

for $r \geq r_0$, where A is a normalization constant and $\theta = \sqrt{1-\epsilon}g$.

This probability density will extend to the nearest nucleus and give an annihilation decay rate. To estimate the distance r_d at which the decay rate is 1 per year assume for simplicity that the proton at r does not change $|\psi|^2$, i.e., the Born approximation, and compare the density $|\psi|^2$ with the 1s state density at the origin of protonium $|\Psi_{10}(0)|^2$, which has a decay rate⁸ of $5 \cdot 10^{18} \text{ s}^{-1}$. That is, solve the following equation for r_d :

$$|\psi(r_d)|^2/|\Psi_{10}(0)|^2 \cdot 5 \cdot 10^{18} = 10^{-8}$$

The results for r_d corresponding to various well strengths are shown in the table below where a trap of radius $r_0 = 10^{-8} \text{ cm}$ is assumed

g	$V_0(\text{ev})$	ϵ_{\min}	$r_d \cdot 10^{-8} \text{ cm}$	$r_d \cdot 10^{-8} \text{ cm}$
π	.81	0.458	8.9	9.5
$3/2\pi$	1.82	0.704	5.3	5.6
3π	7.3	0.909	2.9	3.0
10π	80.8	0.991	1.5	1.6

The table shows that a physically reasonable trap could hold \bar{p} for a year within a few Ångstroms of normal matter, although there is the obvious trade-off between shallow traps (easier to achieve) and larger spacings (harder to achieve).

Actual annihilations will most likely proceed through the capture of a \bar{p} in an atomic state rather than by direct annihilation. To estimate the critical radius r_a for an atomic capture of 1 per year, set the particle flux leaving the well equal to $|\psi(r)|^2$ times $\hbar k/m$, where k is the wavenumber of the \bar{p} in the atomic potential, $k = \sqrt{2m\Delta E}/\hbar$, $\Delta E = me^4/4\hbar^2$ (energy of lowest $\bar{p}p$ state). This flux multiplied by the protonium area $2\pi a_0^2 = 2\pi(2\hbar^2/me^2)^2$ gives the approximate rate of capture (a quantum mechanical engineering estimate!). That is, solve the following equation for r_a ,

$$|\psi(r_a)|^2 \hbar k/m 2\pi a_0^2 = 10^{-8},$$

which has the same form as the previous equation used to find the critical radius r_d for direct $\bar{p}p$ annihilation. Numerically, atomic capture is 10 times more likely, which results in slightly larger r_a as shown in the previous table.

Electrons will not be trapped in these wells unless $\sqrt{m_e/m_p} g > \pi/2$, i.e., $g > 21.4\pi$, much larger than considered above. Even then the traps could not be "poisoned" by electron filling because the heavier particle always wins the competition for the same trap, otherwise the stability of \bar{p} in normal matter would be easier to achieve. Likewise, muons can not be trapped until $g > 1.5\pi$ which is reasonably close to optimum trap depths for \bar{p} . Therefore, μ^- would be a relatively cheap substitute for \bar{p} when testing trap concepts.

3. Polarons

A polaron is a charged particle in a crystal with the accompanying lattice distortions it induces.⁹ In the extensive literature on polarons the particle is usually an electron, but, in principle, it could be an interstitial proton or \bar{p} . The heavier the particle the more dense the phonon cloud around it, and it is known that protons can even be trapped. By itself, the observed phenomenon of proton trapping does not prove that \bar{p} trapping will likewise occur, but it is a promising entrée for theorists into the behavior of \bar{p} in alkali halide crystals. The polaron phenomenon is

responsible for the effective attraction between electrons that leads to superconductivity, which demonstrates its capability for non-trivial effects.

C. Excitons

Excitons are electron-like bound states⁹ and are of interest to the \bar{p} system because they are the quantum unit of the polarization field, and it is precisely on questions of induced polarization that the \bar{p} storage problem hangs. If excitons were large objects spread over many lattice spacings their relevance would be minimal, but, in fact, they may occur localized on one atom. Again, as with polarons, the exciton is a concept with a rich literature of special relevance to theoretical studies of \bar{p} trapping concerned with nonlinear polarization or screening of the \bar{p} charge by holes.

SPECIAL EFFECTS

The following mechanisms are examples of new discoveries and ideas that could lead to a breakthrough in the \bar{p} storage problem.

A. Suppressed barrier penetration

In a study of quantum mechanical tunneling Michael Nieto, et al.,¹⁰ have found that a wave function in a higher-energy well will not necessarily tunnel to a lower-energy well, even in an arbitrarily long time, if there is not dissipation or coupling to other modes. The probability of quantum tunneling is a critical function of the shape of the barrier potential, not just its average height. Temporal modulation of the barrier would seem to be another promising means to control tunneling rates.

B. Quenched decay

E. J. Robinson¹¹ has shown that the well-known exponential decay rate of unstable states can be changed substantially, and even approach zero, if the product of the decay belongs to a continuum that is itself unstable.

C. Self-trapping

Using a model relevant to the quantum diffusion of muons and protons inside metals and at surfaces, F. Guinea, et al.,¹² discovered a transition from diffusive dynamics to a self-trapped state at a critical value of coupling to the environment. This trapping is not related to the self-trapping of polarons mentioned above.

D. Dynamic localization

D. Dunlap, et al.,¹³ calculated the quantum mechanical motion of a charged particle in a lattice under the action of time-dependent electric fields and found a new phenomenon whereby the moving particle became localized within one lattice spacing. Since this localization occurs exactly at a lattice site, it is not directly applicable to \bar{p} , which need to avoid lattice sites. Nevertheless, the concept of dynamic localization, or creating effective traps by parametric modulation, seems a promising mechanism to apply to energy saddle points of \bar{p} in normal matter.

E. Two-level systems

The properties of the two-level quantum system have been recently studied by many people (see the review by A. J. Leggett, et al.¹⁴) and many exact results are known about the tunneling of a particle between two wells in a dissipative environment. The conditions for the particle being localized in one well, decaying, or oscillating between the wells have been delineated in detail.

EXPERIMENTS WITH \bar{p} IN CONDENSED MATTER

The easy availability of low-energy \bar{p} will be a strong impetus to perform experiments in condensed matter. Although most of these will not be intended to test proposed storage mechanisms, the experience gained will build, nevertheless, an invaluable technical base for the critical evaluation of storage feasibility. Predictions of the benefits of condensed matter experiments have consistently missed the most wonderful discoveries, a recent example being the high temperature

superconductors, so the best strategy is to encourage experimentation. The role for theory should be to suggest and interpret, not to proscribe.

A. Atomic decay and strong interactions

The x-rays emitted as a \bar{p} cascades down the atomic states when it is captured by a nucleus are recognized as a powerful diagnostic for studying the $\bar{p}p$ and $\bar{p}N$ interactions at low energies.¹⁵ The effect of the strong interaction shows up as a reduction in the intensity of the last observable transition and as a shift (of order 1. keV) in the low lying atomic states.¹⁶⁻¹⁹ There is also a hyperfine splitting between singlet and triplet s-states (of order 1/4 keV) due to the spin-dependent $\bar{p}N$ interaction.^{20,21} X-rays from $np \rightarrow 1s$ and $nd \rightarrow 2p$ transitions of protonium have been seen¹⁶ and they confirm predictions of strong interaction effects. Other groups have seen strong interaction effects in $\bar{p}N$.^{18,19} Also, the preferential capture and different atomic cascades of the various negative particles, π^- , K^- , Σ^- , and \bar{p} reveal much about low energy cross sections and metastable states.^{22,23} If the atomic deexcitation energy is resonant with an appropriate nuclear E2 excitation it is also possible for radiationless transitions to occur (the atom deexcites by exciting the nucleus).^{24,25} This can provide otherwise inaccessible information about the nuclear potential.

B. Channeling

Unlike the case with μ^+ there is little known about μ^- channeling,^{26,27} which would give useful information about the prospects with \bar{p} . The reason for this is the lack of a μ^- beam or a μ^- source within the solid. The obvious source, a π^- , is captured by a nucleus (as a \bar{p} would be, normally). However, channeling of π^- themselves has been observed and the paths appear to be helical spirals, as mentioned above.⁷ The fact that π^- can channel is most interesting because it is doing so in a lattice of absorbers rather than repellers, and therefore falls outside the usual analysis of channeling.²⁸

C. Potpourri

Because condensed matter is so complicated, many of the scientific breakthroughs arise from unexpected experimental results rather than theoretical discoveries. Therefore, as low-temperature \bar{p} became cheaper they undoubtedly will be inserted in various materials if only "to see what happens." Some of the materials that have been suggested are discussed below.

1. Superfluid ^4He

Superfluid ^4He is one of the most studied and best understood of condensed matter systems. The atoms are the most quiescent of all, with about 10% of them being in a Bose condensate having strictly zero momentum. The atoms also have the highest ionization potential, 24.6 eV, and are correlated into a macroscopic quantum state from the size of the container to an interatomic spacing.

What would \bar{p} do in such an exotic material? It has been suggested they might form "bubbles" or self-containing cavities in the liquid, as other impurities do, such as electrons²⁹ and even positronium.³⁰ Bubble formation, however, does not seem likely because (1) there is no help from the Pauli principle (as with electrons) in pushing away the electron densities of nearby helium atoms and (2) the larger \bar{p} mass reduces the \bar{p} localization energy (zero-point motion) to a scale comparable with the interatomic spacing. Perhaps there will be a barrier to \bar{p} atomic capture because the intermediate state involves a free electron which must form a bubble, which costs 1.3 eV? Alas, there seems no reason to exclude He^- as an intermediate state, for which there is no significant barrier. Impurities are also attracted to the cores of quantized vortex lines, but there is no obvious advantage for \bar{p} stability at such a location. Nevertheless, it will be interesting to see what does happen to \bar{p} in superfluid ^4He .

Another interesting facet of ^4He behavior is its surface, which is microscopically smooth, adjoins a vacuum of arbitrary "hardness" at sufficiently low

temperature, and can support sheets of surface charge on either side.^{31,32} In particular, electrons on the vapor side can be held against the helium surface by applying an electric field; they do not penetrate the surface because of the relatively high energy required to make the bubble state mentioned earlier. Because this electronic surface charge density can be substantial and can be excited in various plasma modes, the possibility exists of finding electron- \bar{p} states that are bound to the surface but have negligible \bar{p} density at the surface. In effect, the \bar{p} would be trapped between the external electric field and the electronic surface charge, which in turn is repelled from the surface by the Pauli principle. One could also introduce other charged species of heavier mass, such as H^- or D^- . As mentioned in the general remarks above, such trapping would have to occur in an excited state.

Even quite small or dilute trapped surface states would be interesting as possible nucleation sites for cluster ion formation, for which the problem is to find a coupling (to normal matter) that can carry away the condensation energy. (See the paper in these proceedings by W. C. Stwalley.)

2. Degenerate liquid ^3He

This is mentioned more to illustrate a general approach to trapping -- prohibit the formation of intermediate states necessary for decay -- than to suggest it will work in this specific instance. At low temperature, the ^3He atoms are in the ground state of a Fermi liquid, which means that all momentum states less than the Fermi momentum, $k_F \approx 0.3 \text{ \AA}^{-1}$ are filled. To the extent that intermediate states of the \bar{p} decay process require the scattering of ^3He atoms into states with $k < k_F$, the decay will be suppressed. The problem is that \bar{p} is a localized perturbation, and it would seem to have no difficulty in confining its interactions to wavelengths $\lambda < 2\pi/k_F$.

3. Superconductors

Many of the features of quantum coherence apply to both superconductors and superfluids, i.e., a superconductor is a charged superfluid in solid, neutralizing

background. Electric and magnetic fields are shielded quite effectively in superconductors over distances comparable to the penetration depth, a length scale present only in charged superfluids and typically having a magnitude of many lattice spacings. Thus, one cannot expect known superconductors to shield and stabilize a \bar{p} in any obvious way on an atomic scale, but what will happen is not clear either since the origin of the effective electron attraction, which gives rise to superconductivity, is a subtle and delicate interplay of electronic and lattice properties, both of which are disturbed by a \bar{p} . A best guess now is that the influence of a \bar{p} impurity will be too local to probe superconductivity, although it could give information on other electronic structure.

4. Semiconductors

A \bar{p} is attracted to positive charge. If there were an effective source of positive charge, other than protons, one could expect \bar{p} trapping. In many respects, especially involving dynamics and transport, the absence of electrons is equivalent to positive charge. This "positive" charge can be either delocalized as holes in a conduction band or localized at ionic lattice vacancies and certain crystal imperfections. Of course, such pseudo positive charge cannot violate the laws of electrostatics, and the earlier remarks on the absence of ground state stability still hold. Nevertheless, the existence of localized exciton states of the \bar{p} -hole system seem possible, in principle, and the model could serve as a fruitful paradigm.

REFERENCES

1. C. F. Driscoll, in Low Energy Antimatter, edited by D. B. Cline (World Scientific, Singapore, 1986), p. 184.
2. E. H. Lieb, Rev. Mod. Phys. 48, 553 (1976).
3. S. Earnshaw, Trans. Cambridge Philos. Soc. 7, 97 (1842).
4. H. G. Dehmelt, Adv. At. Mol. Phys. 3, 536 (1967).

5. C. W. Clark, E. Korevaar, and M. G. Littman, Phys. Rev. Lett. 54, 320 (1985).
6. D. Cline, these Proceedings.
7. T. H. Braid, D. S. Gemmell, et al., Phys. Rev. B19, 130 (1979).
8. B. R. Desai, Phys. Rev. 119, 1385 (1960). This early prediction agrees closely with the recent measurement of the width of the 1s level of protonium: C. A. Baker et al. in Physics with Antiprotons at LEAR in the ACOLE Era, edited by U. Gastaldi et al. (Frontières, Gif-sur-Yvette, France, 1985), p. 219.
9. C. Kittel, Quantum Theory of Solids Wiley, NY, 1966).
10. M. M. Nieto, et al., Phys. Lett. 163B, 336 (1985).
11. E. J. Robinson, Phys. Rev. Lett. 57, 1281 (1986).
12. F. Guinea, V. Hakim, and A. Muramatsu, Phys. Rev. Lett. 54, 263 (1985).
13. D. H. Dunlap and V. M. Kenkre, Phys. Rev. B 34, 3625 (1986).
14. A. J. Leggett, et al., Rev. Mod. Phys. 59, 1 (1987).
15. T. von Egidy, Nature 328, 773 (1987).
16. S. Ahmad, et al., Phys. Lett. 157B, 333 (1985).
17. V. S. Popov, A. E. Kudryavtsev, and V. D. Mur, Sov. Phys. JETP 50, 865 (1979), [Zh. Eksp. Teor. Fiz. 77, 1727 (1979)].
18. G. Backenstoss, et al., Phys. Rev. Lett. 41B, 552 (1972).
19. P. D. Barnes, et al., Phys. Rev. Lett. 29, 1132 (1972).
20. J. M. Richard and M. E. Sainio, Phys. Lett. 110B, 349 (1982).
21. A. M. Green and S. Wycech, Nucl. Phys. A377, 441 (1982).
22. J. G. Fetkavich, et al., Phys. Lett 35B 178 (1971).
23. G. A. Baker, Phys. Rev. 117, 1130 (1960).
24. M. Leon, et al., Nucl. Phys. A322, 397 (1979).
25. C. J. Batty, Nature 322, 487 (1986).
26. D. S. Gemmell, Rev. Mod. Phys. 46, 129 (1974).

27. D. V. Morgan, editor, Channeling: Theory, Observations and Applications (Wiley, NY, 1973).
28. A. W. Sáenz, J. Math. Phys. 26, 1925 (1985).
29. C. G. Kuper, Phys. Rev. 122, 1007 (1961).
30. R. A. Ferrell, Phys. Rev. 108, 167 (1957).
31. C. C. Grimes, Surf. Sci. 73, 379 (1978).
32. G. A. Williams and J. Theobald, Phys. Lett. A77, 255 (1980).

ANTIHYDROGEN PRODUCTION SCHEMES

J.B.A. Mitchell
Department of Physics
The University of Western Ontario
London, Ontario, Canada. N6A 3K7

ABSTRACT

A number of suggested techniques for antihydrogen production are reviewed. These include stimulated radiative recombination, positronium charge exchange and high density recombination in a trap. With moderate technical advances a production rate of 10^8 H per second seems attainable. A normal matter simulation experiment is discussed.

REPORT

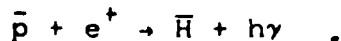
The production of neutral antihydrogen has been recognized as a goal of importance in such diverse areas as Quantum Electrodynamics, Gravitation and rocket propulsion. Nuclei of antimatter can be produced in high energy collisions at a number of accelerators throughout the world. In order to form atoms of antimatter however it is necessary for these nuclei to capture positrons. With normal matter electron capture is easily achieved through charge transfer collisions between the nuclei and a gaseous or solid target, e.g.



For non-resonant charge transfer, the cross section¹ for this process peaks at a few tens of keV falling off at higher energies as $(1/E) \log E$. This means that the cross section is very small at MeV energies and the probability of subsequent reionization in a thick target is high. By reducing the beam energy to low keV energies however it is possible to achieve about 90% neutralization. With antinuclei the situation is very different since one does not have a convenient antimatter target from which to capture positrons. A number of schemes for neutralizing antinuclei are currently proposed employing either the radiative recombination of antinuclei and free positrons or charge exchange between antinuclei and positronium 'atoms'. The purpose of this paper is to analyze the feasibility of these schemes with particular emphasis being given to the former process. A recent review of antihydrogen production techniques has also been given by Rich et al¹.

RADIATIVE RECOMBINATION

An experiment is under consideration at the LEAR facility at CERN² to use merged beams of positrons and antiprotons to generate antihydrogen atoms via the radiative recombination process: -



2.

A detailed description of the theoretical analysis of this experiment has been given by Neumann et al³. The intensities of available antiproton and positron beams are low and are likely to remain so for the foreseeable future so it is imperative that the rate at which positrons and antiprotons recombine be optimized.

When an atom is ionized it must absorb energy in order to eject an electron. The recombination of an ion and an electron therefore involves the removal of some of this energy by some means. For molecular ions, energy can be efficiently removed by conversion of potential energy into kinetic energy. This is achieved through the dissociation of the neutral molecule formed in the recombination, i.e.



and the process is known as dissociative recombination. At thermal energies the time for interaction between an ion and electron in collision is of the order of 10^{-15} seconds. Once formed however the excited intermediate complex AB^{**} has a lifetime against autoionization of $\sim 10^{-13}$ secs. Since this is of the same order as the vibrational period, AB^{**} it can dissociate within this time period thus stabilizing the neutralization process very efficiently. The dissociative recombination processes therefore generally exhibit very large cross sections ($10^{-13} - 10^{-16} \text{ cm}^2$) at thermal energies.

Dissociative stabilization of course is not an available option for a bare nucleus and so the only way in which excess energy can be removed is via the emission of a photon, i.e.



where n is the principal quantum number of the level into which the electron is captured. The problem here is that photon emission is typically a slow process with a characteristic time of $\sim 10^{-9}$ seconds. It is therefore very unlikely to happen during the short electron-ion collisions time and so radiative recombination exhibits a small cross section at thermal energies.

The cross section for radiative recombination of protons into a given level n of H can be calculated using Menzel's expression⁴: -

$$\sigma = A \frac{\nu_0}{\nu} \frac{h\nu_0}{\frac{1}{2}mv_e^2} \cdot \frac{g}{n^3} \quad - - 1$$

where $A = 2.11 \times 10^{-22} \text{ cm}^2$, $g \approx 1$, $h\nu_0 = 13.6 \text{ eV}$. ν is the frequency of the emitted photon and

$$h\nu = \frac{1}{2}mv_e^2 + h\nu_0/n^2 \quad - - 2$$

It can be seen that σ is inversely proportional to $\frac{1}{2}mv_e^2$, the kinetic energy of the electrons and so it is imperative that low interaction energies be achieved in order to have a respectable recombination rate.

MERGED BEAM KINEMATICS

In a merging beam configuration the collision energy in the center of mass frame is given by: -

$$E_{cm} = \frac{1}{2} \mu v_r^2 \quad - - 3$$

$$E_{cm} = \frac{1}{2} \mu (v_i^2 + v_e^2 - 2 v_i v_e \cos \theta) \quad - - 4$$

where v_i and v_e and v_r are the ion, electron and relative velocities respectively, and μ is the reduced mass of the collision system, given by:

$$\mu = m_i m_e / (m_i + m_e) \approx m_e. \quad - - 5$$

In terms of beam energies E_i and E_e this can be written as: -

$$E_{cm} = \mu [E_i/m_i + E_e/m_e - 2(E_i E_e / m_i m_e)^{1/2} \cos \theta] \quad - - 6$$

If we define the reduced ion energy E_+ thus: -

$$E_+ = (m_e/m_i) E_i \quad - - 7$$

then

$$E_{cm} = E_+ + E_e - 2(E_+ E_e)^{1/2} \cos \theta \quad - - 8$$

In merged beam experiments $\theta \approx 0$ and so equation (6) can be written: -

$$E_{cm} = (E_+^{1/2} - E_e^{1/2})^2 \quad - - 9$$

Thus when $E_+ = E_e$, $E_{cm} = 0$.

In practice θ can not be made exactly zero due to beam spreading and this limits the lowest achievable collision energy.

By taking partial derivatives of equation (8) with respect to E_e , E_+ and θ and assuming a gaussian distribution for the uncertainties ΔE_e , ΔE_+ and $\Delta \theta$ in these quantities, an expression for the energy resolution in a merged beam experiment can be shown to be: -

$$\Delta E_{cm} = \left[\left[\left[1 - \left(E_+ / E_e \right)^{1/2} \right] \Delta E_e \right]^2 + \left[\left[1 - \left(E_e / E_+ \right)^{1/2} \right] \Delta E_+ \right]^2 + \left[2 \left(E_e E_+ \right)^{1/2} \theta \Delta \theta \right]^2 \right]^{1/2} \quad - - 10$$

When $E_+ \approx E_e$, the spread in the centre of mass energy is governed primarily by θ and $\Delta \theta$.

An unpublished analysis of merged beam kinematics performed at U. W. O. based upon studies by Taylor et al⁵ at JILA has shown that the most serious limitation to the achievable energy resolution arises from the method of formation of the electron beam. In our experiments at U. W. O. the electrons are produced

4.
from an indirectly heated barium oxide coated cathode which operates at a temperature of $\sim 1000\text{K}$. This means that the electrons are formed with an initial energy spread of about 0.1 eV . In the longitudinal direction this contribution is not a problem as it can be shown using equation (10) that this is significantly deamplified in the center of mass when $E_e \approx E_c$ and can be essentially neglected. The problem arises however due to transverse velocities of the electrons due to their thermal spread. This gives rise to a non zero value of $\Delta\theta$ thus limiting the energy spread given by equation (10).

It is however possible to eliminate electrons with large transverse velocity components and so reduce ΔE_{cm} . The collimation must be carefully designed so if the electron beam is magnetically confined spiralling electrons can manage to pass through small, thin apertures unhindered. This can be prevented by using thick apertures.

Recent results for $e - \text{H}_2^+$ dissociative recombination⁶ taken using the merged beam facility at U.W.O. are shown in Fig. 1.

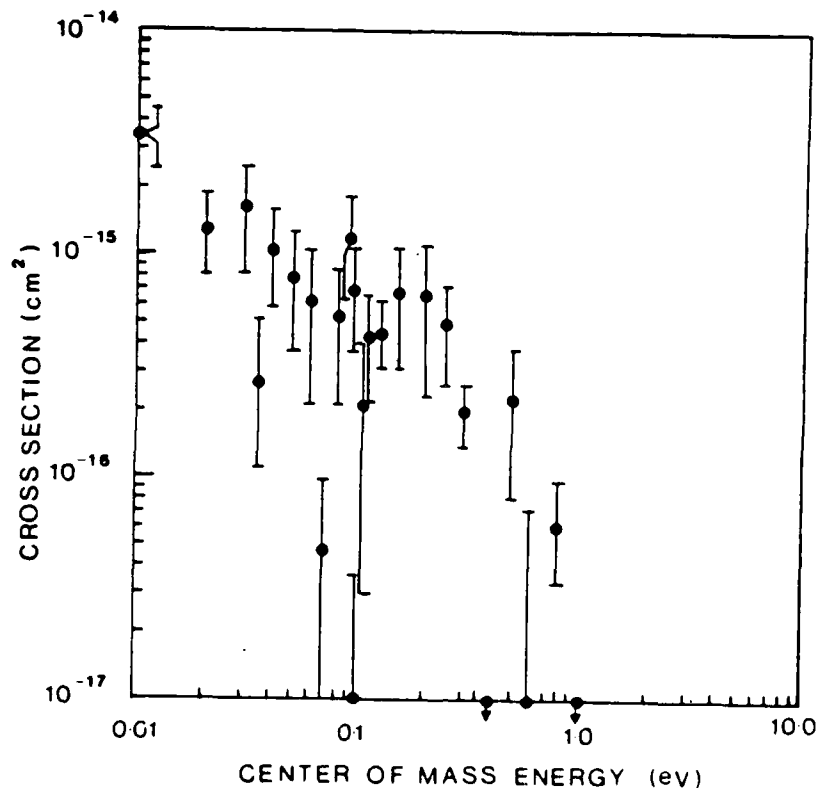


Figure 1: Measured cross sections for $e\text{-H}_2^+$ recombination⁶ showing narrow resonant structures which can be resolved using the merged beam technique. The energy resolution is better than 20 meV .

5.

This process exhibits narrow resonances due to capture into autoionizing, vibrationally excited Rydberg states of H_2 and these have been seen in our experiment. The results shown are very preliminary and much more extensive studies are planned. By examining the resonance at 0.1 eV however it can be seen that the energy resolution achieved in the apparatus is better than 20 meV. This is the first time that the predicted high resolution capability of a merged beam experiment has been demonstrated experimentally.

Other electron-ion merged beam experiments have been performed at Oak Ridge National Lab⁷, CERN⁸ and Novosibirsk⁹, the latter two being electron cooling experiments. In these cases however high current electron beams (0.1 - 1A) are used and the resulting space charge depression limits the lowest achievable interaction energy and the energy spread. The apparatus at U.W.O. employs low current beams, ($E_e \sim 20 \mu A$, $I_i \sim 1 nA$) and space charge effects are not important.

Antihydrogen experiments will inevitably employ low current beams so again the performance should be considerably better than experienced in electron cooling experiments.

The rate of product formation in a binary collision between reagents A and B is given by: -

$$\frac{dN_0}{dt} = \alpha N_A N_B \quad - - 11$$

where N_A , N_B and N_0 are the densities of A, B and the product respectively and α is the rate coefficient which is related to the collision cross section via the relationship.

$$\alpha = \int \sigma v f(v) dv \quad - - 12$$

where v is the relative velocity of A and B and $f(v)$ is the velocity distribution function.

Since in a merged beam experiment the velocity distribution is quite narrow it is acceptable for the purposes of estimating the signal to approximate this expression by: -

$$\alpha \approx \sigma \bar{v} \quad - - 13$$

where \bar{v} is the average collision velocity.

If we consider the situation of N_p antiprotons circulating in a storage ring and interacting with a beam of positrons with a particle density n_e^+ / cm^3 in a merging configuration then using equation (11), the rate of formation of antiprotons is given by:

$$N_{\bar{H}} = \eta N_{\bar{p}} \eta_e^+ \alpha \approx \eta N_{\bar{p}} \eta_e^+ \sigma \bar{v} \quad - - 14$$

where η is the fraction of the storage ring circumference over which the positrons and antiprotons interact.

For relativistic beams this is amended to: -

$$N_{\bar{H}} = \frac{\eta}{\gamma^2} N_{\bar{p}} \eta_e^+ \alpha \quad - - 15$$

where $\gamma^2 = 1/(1-\beta^2)$ and $\beta = v/c$, where $v = v_e = v_i$ is the velocity of the beams in the laboratory frame.

STIMULATED RECOMBINATION

Neumann et al (3) have discussed the possibility of enhancing the electron proton recombination by stimulating the photon emission using a laser beam with the appropriate wavelength.

One can define a gain factor g as the ratio of the stimulated α^{STIM} to spontaneous α^{SPON} recombination coefficient.

$$g = \frac{\alpha^{STIM}}{\alpha^{SPON}} = u(\nu) \frac{B}{A} \quad - - 16$$

where

$$u(\nu) = P/(cF\Delta\nu) \quad - - 17$$

is the spectral energy density of the radiation field of power P and photon beam cross sectional area F . A and B are the Einstein coefficients for spontaneous and stimulated emission which are related by: -

$$A = \frac{8\pi h \nu^3}{c^3} B \quad - - 18$$

ν , the frequency of both the emitted photon and the stimulating photon is related to the velocity of the electrons by: -

$$\frac{mv_0^2}{2} + \frac{E_0}{n^2} = h\nu \quad - - 19$$

and

$$\Delta\nu = \frac{h}{mv_0} \Delta\nu \quad - - 20$$

where $\Delta\nu$ is the spread in the electron velocity. n is the principal quantum number into which the electron is captured and E_0 is the ionization potential of the proton from the $n = 1$ level.

By combining 16, 17, 18 and 20, one gets

$$g = \frac{Pc^2}{F\Delta\nu 8\pi h \nu^3} \quad - - 21$$

In table I the first twelve energy levels for atomic hydrogen are given together with the energy of the photons required to stimulate the recombination of zero energy electrons.

T A B L E I

Energy levels for atomic hydrogen

<u>n</u>	<u>E(ev)</u>	<u>Wavelength (A)</u>
1	-13.6	919.1
2	- 3.4	3676.5
3	- 1.5	8333.0
4	- 0.85	14706.0
5	- 0.54	23148.0
6	- 0.37	33088.0
7	- 0.28	45036.0
8	- 0.21	58824.0
9	- 0.168	74448.0
10	- 0.136	91911.0
11	- 0.11	111213.0
12	- 0.09	132352.0

PROPOSED CERN EXPERIMENT

The CERN^{2,3} group has considered the use of a pulsed dye laser to stimulate capture down to the $n = 2$ state of atomic hydrogen.

Using equation 1 the cross section for spontaneous radiative capture in $n = 2$ at an interaction energy of 0.01 eV is calculated to be:

$$\sigma = 1.4 \times 10^{-19} \text{ cm}^2$$

corresponding to a rate coefficient of

$$\alpha = 8.3 \times 10^{-13}$$

Assuming the electrons to have an energy spread of 0.01 eV and the interaction volume to be cylindrical with a diameter of 1mm then: -

$$P = 3.14 \times 10^{-6} \text{ m}^2$$

$$\Delta\nu = 5 \times 10^{12} \text{ Hz from equation 20}$$

$$\nu(n=2) = 8.18 \times 10^{14} \text{ Hz from equation 19}$$

and equation 21 yields a gain of: -

$$g = 6 \times 10^{-4} P$$

- - 22

where P is the laser power in watts.

Neumann et al have pointed out that although high powered pulsed dye lasers are available, the possibility of reionization of the neutralized atom by a subsequent photon limits the maximum useful power.

8.

If σ_n^h is the photoionization cross section from a given n level of atomic hydrogen then the photoionization rate for one hydrogen atom is

$$Z = \phi \sigma_n^h \quad - - 23$$

where $\phi = P/Ph\nu$ is the photon flux.

If the atom is irradiated for a time τ then

$$Z\tau = \phi \sigma_n^h < 1 \quad - - 24$$

$$\text{hence } \phi \leq \frac{1}{\tau \sigma_n^h}$$

in order that the atom is not reionized. τ is either the lifetime or the laser pulse length, whichever is shorter.

Photoionization cross sections for given n states of atomic hydrogen or hydrogenic ions can be calculated exactly and can be expressed in the form¹⁰ -

$$\sigma = 7.91 \times 10^{-18} \frac{n}{Z_c^2} \left(\frac{\epsilon_n}{\epsilon} \right)^3 \text{ cm}^2$$

where $\epsilon_n = Z_c^2/n^2$; ϵ is the photon energy in rydbergs, Z_c is the atomic number. At threshold, the photoionization cross section for the $n = 2$ level is $1.58 \times 10^{-17} \text{ cm}^2$. The lifetime¹¹ of the $n = 2$ level against spontaneous decay is $2 \times 10^{-9} \text{ s}$ and so substituting into equation 24 yields a maximum usable photon flux of

$$\phi \leq 3 \times 10^{25} \text{ photons cm}^{-2} \text{ sec}^{-1}.$$

This corresponds to a maximum usable power density of 16 MW cm^{-2} . For the 1mm diameter cylindrical interaction region already considered this corresponds to a 0.5 MW power laser pulse.

Using equation 22 and a 1mm diameter interaction region, the maximum gain is 30 yielding a stimulated recombination rate coefficient of:

$$\alpha = 2.5 \times 10^{-11} \text{ cm}^3 \text{ s}^{-1}.$$

Typical experimental parameters³ are

$$\eta N_p = 10^{10}$$

$$\eta_{e+} = 1 \text{ cm}^{-3}$$

and so this would give an antihydrogen production rate of: -

$$N_H = 0.25 \text{ s}^{-1}.$$

The cross sections for radiative recombination to and photo-ionization from the $n = 10$ level are: -

$$\sigma_{\text{RAD}} = 2.86 \times 10^{-20} \text{ cm}^2$$

$$\sigma_{\text{PH}} = 8 \times 10^{-17} \text{ cm}^2$$

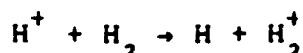
The lifetime of the $n = 10$ level¹¹ is: -

$$\tau = 2 \mu\text{s}$$

and using this value in equation (24) yields a photon flux of 6×10^{21} photons $\text{cm}^{-2}\text{s}^{-1}$. This corresponds to a power density of 135 Watts cm^{-2} or for the 1mm diameter interaction region, to a maximum usable power of 4.2 Watts. This would result in a gain of 42 leading to a stimulated recombination coefficient of: -

$$\alpha_{\text{STIM}} = g\sigma_{\text{RAD}} \bar{v} = 7 \times 10^{-12} \text{ cm}^3 \text{ s}^{-1}$$

The experimental parameters for the MEIBE experiment are listed in Table II and with these it is estimated that the count rate of neutral H atoms will be $\sim 0.25 \text{ s}^{-1}$. The primary background comes from neutralization of the proton beam through charge exchange. At 400 KeV the cross section¹³ for



is $\sim 4 \times 10^{-20} \text{ cm}^2$ and at an operating pressure of 10^{-11} torr a count rate of ~ 0.3 background counts/second is expected. Thus the signal to background ratio will be approximately unity.

For the case of antihydrogen formation in a storage ring the situation is much better as pulsed beams can be used. The lifetime of the level in equation 24 can then be replaced with the pulse length which can be very short ($\sim 1 \text{ ns}$). Thus the maximum usable power density will increase to 2.7×10^5 Watts cm^{-2} or a power of 8.1 KW for a 1 mm diameter interaction region. Given the parameters used earlier this would give an enhanced cross section of $2.3 \times 10^{-15} \text{ cm}^2$ corresponding to a recombination rate coefficient of $\alpha = 1.38 \times 10^{-8} \text{ cm}^3 \text{ s}^{-1}$ at a mean energy of 0.01 eV.

If we consider a 100 KeV, 1mm diameter positron beam with $10^8 \text{ e}^+ / 1 \text{ ns}$ bunch, and a repetition rate of 10 Hz then the mean positron density will be $\sim 2 \text{ s}^{-1}$. With $\eta N_p 10^{10}$ this would give an antihydrogen production rate of

$$N_{\bar{\text{H}}} = 276 \text{ s}^{-1}$$

T A B L E I I

The neutral count rate is given by: -

$$C_n = \sigma \cdot \frac{I_e I_i}{e^2} \left| \frac{v_e - v_i}{v_e v_i} \right| \frac{1}{F} \cdot \frac{1}{\Omega}$$

$$E_i = 400 \text{ KeV} \qquad v_i = 8.785 \times 10^8 \text{ cm s}^{-1}$$

$$E_e = 214.92 \text{ eV} \qquad v_e = 8.725 \times 10^8 \text{ cm s}^{-1}$$

$$E_{cm} = 0.01 \qquad v_{cm} = 5.95 \times 10^6 \text{ cm s}^{-1}$$

$$I_e = 2 \times 10^{-5} \text{ A} \qquad F = 0.03 \text{ cm}^2$$

$$I_i = 1 \times 10^{-7} \text{ A} \qquad e = 1.602 \times 10^{-9} \text{ C}$$

$$L = 10 \text{ cms} \qquad \Omega = 1$$

L is the length of the interaction region. Ω is the detection efficiency for neutrals.

The background count rate is given by

$$I_B = \frac{I_i}{e} \cdot n l \sigma_{10}$$

$$n = 3.2 \times 10^6 \text{ P cm}^{-3}$$

$$l = 30 \text{ cms.}$$

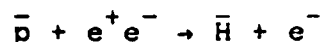
$$\sigma_{10} = 4 \times 10^{-20} \text{ cm}^2 \text{ for } 400 \text{ KeV H}^+ \text{ in H}_2.$$

l is the length of region through which the ion beam moves that can be seen by the neutral detector.

Rich et al¹ have proposed the use of a storage ring to produce a recirculating positron beam. This would allow the mean positron density to be increased by about a factor of 10^6 and so an antihydrogen production rate of $\sim 10^8 \text{ s}^{-1}$ could be achieved.

POSITRONIUM CHARGE EXCHANGE

The positron group at University College, London, England has performed theoretical calculations^{1,4} for the charge exchange process: -



and have designed an experiment to demonstrate this experimentally in conjunction with the atomic physics group at Aarhus in Denmark¹⁵. Initially the experiment will be performed using protons although ultimately the intention is to perform the experiment at LEAR with antiprotons.

The experiment involves inserting a hollow cylinder of aluminum axially into the proton or antiproton beam path. A beam of positrons enters the cylinder through a hole in the side and when it strikes the inside wall positronium 'atoms' are formed with energies ranging from a few meV to 2.6 eV. Para positronium rapidly decays ($\tau = 0.125$ ns) but ortho positronium ($\tau = 142$ ns) is longer lived and so can diffuse through the cylinder. About 75% of the positronium created is in the ortho form.

For a 1 cm diameter cylinder and a positron beam with intensity 10^9 s^{-1} then the average density of positronium atoms is $\sim 100/l \text{ cm}^{-2}$ where $l \sim 1$ cm, is the average axial drift distance over which the positronium atom travels during its lifetime.

Humberston et al have calculated that at 100 KeV (the projected operating energy of LEAR) the cross section for $\bar{p} - p$ charge exchange into the ground state of H is $\sim 10^{-18} \text{ cm}^2$. If we assume that $\sim 10^{10}$ antiprotons can be stored in the ring then

$$R_{\bar{H}} = \eta N_{\bar{p}} n_e^+ \sigma v \sim 0.44$$

where η , the ratio of the interaction region to the ring circumference is $\sim 10^{-4}$ in this experiment.

Recent calculations by Darewych¹⁶ which include capture into excited states of H yield a cross section 2-3 times that quoted above thus raising the formation rate to $\sim 1 \text{ s}^{-1}$.

Other ways to raise the antihydrogen formation rate would be: -

- (a) Lower the collision energy.

A decrease in the antiproton beam energy to ~ 20 KeV would increase the capture cross section by two orders of magnitude.

- (b) Decrease the collision cross sectional area.

The antiproton beam at LEAR is of the order of 1 mm diameter so in principle an increase in positronium density would result from decreasing the diameter of the aluminium containment cylinder. It is not clear however if this would be successful in practice as the positronium could be quenched upon contact with the vessel walls. Investigation of this effect should be one of the goals of the Aarhus experiment.

- (c) Increasing the positron and antiproton beam intensities.

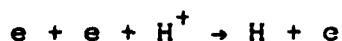
This of course is common to all methods of antihydrogen production. The primary disadvantage however is that there is no possibility for increasing the target density using recirculating techniques.

TRAP FORMATION OF ANTIHYDROGEN

Gabrielse et al¹⁷ have experimentally demonstrated the capture and confinement of antiprotons produced at LEAR, in an electromagnetic trap. Studies of positron, electron and ion trapping have been carried out at a number of centres and the technology is fairly well established.

It would appear to be possible within the confines of today's technology to store electrons (positrons) and protons (anti-protons) in traps with a density of $\sim 10^{10}$ particles cm^{-3} at a temperature of about 10^4K . One can envisage a nested trap which can store positrons and antiprotons simultaneously.

Bates, Kingston and McWhirter¹⁹ have investigated the competition between recombination and collisional ionization in cool hydrogenic plasmas and have deduced rate coefficients for the net "collisional-radiative recombination" of the plasma. At low densities radiative recombination dominates the plasma neutralization. At high densities three body recombination, i.e.



becomes more important.

More recent theoretical treatments of this process have been given by Johnson and Hinnov²⁰, Mansbach and Keck²¹ and Stevefelt et al²².

The latter have expressed the rate coefficient in the form

$$\alpha = \left\{ 1.55 \times 10^{-10} T^{-0.63} + 6.0 \times 10^{-9} T^{-2.18} n(e)^{0.37} \right. \\ \left. + 3.8 \times 10^{-9} T^{-4.5} n(e) \right\} \text{cm}^3 \text{s}^{-1}$$

for $250 \leq T \leq 4000 \text{ K}$ and $10^9 \leq n_e \leq 10^{13} \text{ cm}^{-3}$. It can be seen from this expression that at low temperatures and moderate densities the rate coefficient exhibits at $T^{-4.5}$ temperature dependance and so becomes very large at low temperatures. If extrapolation beyond the limits quoted here is valid then at 10K the recombination rate would be $\sim 1 \times 10^{-3} \text{ cm}^3 \text{ s}^{-1}$. For a trap therefore containing $N_p \approx N_e^+ = 10^{10} \text{ cm}^{-3}$ at 10K the rate of formation of H would be $\sim 10^{17} \text{ s}^{-1}$. What this means of course is that 10^{10} antihydrogen atoms would be produced very rapidly. The ultimate rate of antihydrogen production would therefore be limited by the trap loading time.

ACKNOWLEDGEMENTS

I should like to acknowledge the helpful discussions with Drs. A. Rich, D. Gidley, W. Stwalley, J.W. Humberston, J.W. Darewych and J. Rafelski which contributed much to this paper.

REFERENCES

1. Rich, A., R. Conti, W. Frieze, D.W. Gidley, M. Skalsey, T. Steiger, J. Van House, H. Griffin, W. Zheng and P.W. Zitzewitz, To be published in Proc. NATO Adv. Research Workshop, "Atomic Physics with Positrons", University College, London. 1987.
2. Wolf, A., H. Haseroth, C.E. Hill, J.L. Vallet, C. Habfast, H. Poth, B. Seligmann, P. Blatt, R. Neumann, A. Winnacker and G. zu Putlitz, in "Low Energy Antimatter", ed. B.D. Cline, World Scientific, Singapore 1986, p. 78.
3. Neumann, R., H. Poth, A. Winnacker and A. Wolf, Z. Phys. A., 313, 253, 1983.
4. Menzel, D.H., Ap. J. 85, 330, 1937.
5. Taylor, P.O., K.T. Dolder, W.E. Kauppila and G.H. Dunn, RSI 45, 538, 1974.
6. Hus, H., F. Yousif, C. Noren, A. Sen and J.B.A. Mitchell, Submitted to Phys. Rev. Lett. 1987.
7. Dittner, P.F., S. Datz, P.D. Miller, C.D. Moak, P.H. Stetson, C. Bottcher, W.B. Dress, G.D. Alton and N. Neskovic, Phys. Rev. Lett. 51, 31, 1983.
8. Bell, M., J. Chaney, H. Herr, F. Krienen, P. Moller-Petersen and G. Petrucci, Nucl-Inst. Meth. 190, 237, 1981.
9. Budker, G.I. and A.N. Skrinskii, Sov. Phys. Usp. 21, 277, 1978.
10. Cowan, R.D., "The theory of Atomic Structure and Spectra", Univ. of California Press, Berkeley, 1981.
11. Wiese, W.L., M.W. Smith and B.M. Glennon, Atomic Transition Probabilities, NSRDS-NBS4, Vol. I., U.S. Dept. of Commerce 1966.
12. Auerbach, D., R. Cacak, R. Caudano, T.D. Gaily, C.J. Keyser, J.Wm. McGowan, J.B.A. Mitchell and S.F.J. Wilk, J. Phys. B 10, 3797, 1977.
13. Allison, S.K. and M. Garcia-Munoz, in Atomic & Molecular Processes, eds. Dr. Bates and A. Dalgarno, Academic Press, N.Y. 1962, p. 722.
14. Humberston, J.W. (Personal communication, 1987).
15. Humberston, J.W., M. Charlton, F.M. Jacobsen and B.I. Deutch, J. Phys. B. 20, L25, 1987.
16. Darewych, J.W., J. Phys. B. In Press, 1987.
17. Gabrielse, G. et al, Phys. Rev. Lett. 27, 2504, 1986.
18. Driscoll, C.F. in "Low Energy Antimatter", ed. D.B. Cline, World Scientific, Singapore 1986.
19. Bates, D.R., A.E. Kingston and R.W.P. McWhirter, Proc. Roy. Soc. A267, 297, 1962 and A279, 155, 1962.
20. Mansback, P. and Keck, J., Phys. Rev. 181, 275, 1969.
21. Johnson, L.C. and E. Hinnov, JQSRT 13, 333, 1973.
22. Stevefelt, J., J. Boulmer and J.F. Delpech, Phys. Rev. 12, 1248, 1975.

"The Synthesis of Large Cluster Ions from Elementary
Constituents: A Possible Route to Bulk Antimatter"

W. C. Stwalley

Center for Laser Science and Engineering and
Departments of Chemistry and of Physics and Astronomy
University of Iowa, Iowa City, Iowa 52242-1294

I. Overview	1
II. Introduction	3
III. The Cluster Ion Synthesis Process	4
IV. Individual Reaction Steps	8
A. Formation of H	9
B. Formation of H ⁻	9
C. Formation of H ₂ ⁺	11
D. Formation of H ₂	12
E. Formation of H ₃ ⁺	13
F. Formation of H _N ⁺ ("seed crystal")	13
V. Modifications for Antimatter	14
VI. Temporal Feasibility	14
VII. Financial Feasibility	16
VIII. Summary of Major Issues	16
IX. Acknowledgments	17
X. References	18

I. Overview

The past century has seen the emergence of a fascinating variety of technological developments. Initially, in developments such as the airplane and telephone, the commercial sector played the primary role in these developments. More recently, however, major governments have had the enormous resources required for such major developments and thus have taken the primary role in activities such as fission and fusion weapons, fission and fusion power, rocket development and space exploration, etc. These national priorities have recognized the multifaceted and critical significance of high density energy storage, in particular, with multi-order-of-magnitude improvements in each evolutionary step from chemical energy storage densities to fission to

fusion. There is to the best of my knowledge only one conceivable further multi-order-of-magnitude improvement step possible: antimatter.

Accompanying each of these evolutionary steps, there has been an increase in the magnitude of the scientific and engineering research and development needed to bring the concept to (or closer to) practical reality. In each case, a multidisciplinary approach was essential, combining diverse areas, principally high energy physics (clearly "high" gets higher with time); physics at all lower energies, including nuclear, plasma, atomic, molecular and optical, and solid state; chemistry; electrical and optical engineering; and materials science and engineering. Many feel strongly that it is now appropriate to initiate a similar basic research effort in the area of antimatter. Already, with modest resources at best, antiprotons have been cooled to thermal energies and trapped in an ion trap. This workshop and many other workshops in the past few years (see [FOR 87]) have clearly brought antimatter from the realm of science fiction (à la "Star Trek") to a scientifically credible area in which specific near term goals can be pursued. This article attempts to examine one specific sub-area of antimatter research, namely, the possible production of bulk antimatter by the "cluster ion" approach [BAH 87].

It is important to realize that "antimatter science" very much needs a specific "home" in the federal bureaucracy, such as a program in the Department of Energy. Already, it is clear that the foremost antiproton source in the world (LEAR at CERN near Geneva) is being used primarily to advance the goals of elementary particle physics, which overlap only slightly with the goals of "antimatter science". Likewise, antimatter studies are considered peripheral at best by most atomic and molecular physicists. To obtain acceptable progress in such an evolving field which "falls in the cracks", a specific sponsor is urgently needed.

It is also important to realize that antimatter studies are of

considerable fundamental significance as well as simply a source of high energy density, as documented in these proceedings.

II. Introduction

The goal we have before us is an unprecedented one: to "synthesize" from atomic ("nanoscopic" as opposed to microscopic) constituents bulk macroscopic substances. Moreover, we are to do this for low density antimatter (\bar{p} and e^+) in the absence of contact with ordinary matter, whether in the form of walls, background gas or even radioactive decay fragments. And moreover, we are to do this at technically challenging low temperatures and at unprecedentedly low pressures (not only under static conditions, but also as valves are opened, lasers sent through windows, etc.). Moreover, it is not sufficient merely that each step in the synthesis be scientifically feasible; we must begin to examine questions of rate (throughput) and efficiency (and losses) related to temporal feasibility and financial feasibility as well.

We adopt a single major strategy in addressing the problem of synthesis of bulk quantities of antimatter, the antimatter cluster ion concepts of Bahns, myself and coworkers [BAH 87]. Other strategies include such concepts as storing antimatter in ordinary matter (explored by Larry Campbell in these proceedings); mass production of ultralight ion traps ($m_{\text{trap}} \ll 10^9 N m_{\bar{p}}$), each of which contains a small number N of antiprotons; trapping of antihydrogen atomic gas using lasers and/or magnetic fields [FOR 85]; and magnetic levitation of an antihydrogen molecular solid [FOR 85].

Below we first give an overview of normal matter ion synthesis (Section III) and then discuss the various synthetic steps (Section IV). We then examine complications when antimatter is used (Section V). Finally we discuss rate and throughput issues (Section VI) and efficiency and loss issues (Section VII), and summarize the primary issues which should be studied initially (Section VIII). Note that normal matter ions are of considerable interest.

not only scientifically, but also in connection with ionized or neutral beams for directed energy, fusion, solid state, medical and other applications.

III. The Cluster Ion Synthesis Process

Before examining individual steps in the cluster ion synthesis process [STW 87], it is worth giving a brief overview of the steps involved. Our initial assumptions are as follows:

1. A source of perhaps 10^7 \bar{p} /s is available at energies <1 eV.
2. A source of perhaps 10^7 e^+ /s is available at energies <1 eV.
3. Intense sources of photons (microwave through vacuum ultraviolet) are available.
4. Intense sources of e^- of <1 eV energy are available.
5. Normal matter can be used to fully simulate antimatter in advance of antimatter experiments.
6. High densities of \bar{p} and e^+ (say $\geq 10^{12}/\text{cm}^2$) are unavailable, so most steps must be second order or less in these antimatter constituents. If high density \bar{H} can be achieved, third order processes become possible.

It should also be noted that existence of the proper formation steps for the various intermediate products is insufficient; one must also be able to trap and rapidly cool the intermediate product in the absence of collisions and also rapidly transfer the intermediate product to the next reaction chamber. While these latter steps are not too difficult for charged particles, they are quite difficult for neutral species (H and especially H_2). An overview of important reactions, and trapping, cooling and transfer techniques is given in Table I. Note the convention that the bar over an ion implies a change of all particles to antiparticles; thus \bar{H}^+ is positively charged while \bar{H}_2^- is negatively charged. Most of these processes have been examined in one or more papers in the Proceedings of the Cooling, Condensation and Storage

Table I. Overview of Particle (and Antiparticle) Properties and Characteristics.

particle	e^-	$H^+(\equiv P)$	H	H^-	H_2^+	H_2	H_3^+	H_3	H_4^+	H_4	... H_N^+	H_N
antiparticle	e^+	$\overline{H^+(\equiv P)}$	\overline{H}	$\overline{H^-}$	$\overline{H_2^+}$	$\overline{H_2}$	$\overline{H_3^+}$	$\overline{H_3}$	$\overline{H_4^+}$	$\overline{H_4}$... $\overline{H_N^+}$	$\overline{H_N}$
binding energy in eV	-	-	13.6	0.75	2.6	4.5	4.1	0	0.1	<0.01	... 0.008	0.008
products			H^+, e^-	H, e^-	H^+, H	H, H	H^+, H_2	H, H_2	H, H_3^+	H_2, H_2	H_{N-2}^+, H_2	H_{N-2}, H_2
sensitivities [†] :												
$\lambda < 0.2 \mu$ VUV	-	-	x	x	x	x	x	x	x	x	x	x
$0.2-0.4 \mu$ UV-VIS	-	-	-	x	x	-	(x)	-	(x)	-	x	x
$0.7-100 \mu$ IR	-	-	-	x	-	-	(x)	-	(x)	-	x	x
$\lambda > 100 \mu$ microwave	-	-	-	-	-	-	-	-	-	-	x	x
radiative recomb. (e^-)	*	x	x	-	(x)	-	(x)	-	(x)	-	(x)	-
disso. recomb. (e^-)	*	-	-	-	x	-	x	-	x	-	x	-
assoc. detach. (H^-)	-	-	x	*	-	-	-	x	-	-	-	-
rxn. (H)	-	-	*	-	x	-	x	(x)	x	-	-	-
rxn. (H_2)	-	-	-	-	x	*	-	-	x	-	-	-
neutralization (H^-)	-	x	-	*	x	-	x	-	x	-	x	-
radiative assoc. (H, H_2)	-	-	-	-	-	-	-	-	-	-	x	x
trapping:												
Penning/Paul	x	x	-	x	x	-	x	-	x	-	x	-
laser	-	-	x	(x?)	x?	x?	-	-	-	-	-	-
inhomogeneous magnet	-	-	x	-	-	-	-	-	-	-	x	x
cooling:												
radiative	-	-	-	-	-	-	x	-	x	-	x	x
laser	-	-	x	-	x?	x?	?	-	?	-	-	-
e^-	x	x	-	x	-	-	-	-	-	-	-	-
transfer:												
electrostatic	x	x	-	x	x	-	x	-	x	-	x	-
magnetic	-	-	x	-	-	-	-	-	-	-	-	x
laser	-	-	x	-	(x?)	(x?)	-	-	-	-	-	-

[†] N assumed large ($> 10^3$).[†] All collision partners assumed to be cold.

* Reactant.

of Hydrogen Cluster Ions Workshop, J. T. Bahns, Editor [BAH 87], and extensive references are given there. In addition, a bibliography of several hundred manuscripts (published since 1966) dealing with the positive and negative hydrogen cluster ions is available from the author [STW 87A] and was available at the October 1987 Rand Workshop.

Finally, before enumerating the synthetic steps, we note the catalyst ("seed crystal") strategy in our synthesis [STW 87]. Initially we must synthesize a single cold ($T \leq 1$ K) large cluster ion H_N^+ such that radiative stabilization via photon (γ) emission



is highly efficient compared to loss processes such as



We then grow the ion at a rapid rate to H_{-2N}^+ . The H_{-2N}^+ ion is then fragmented e.g. using

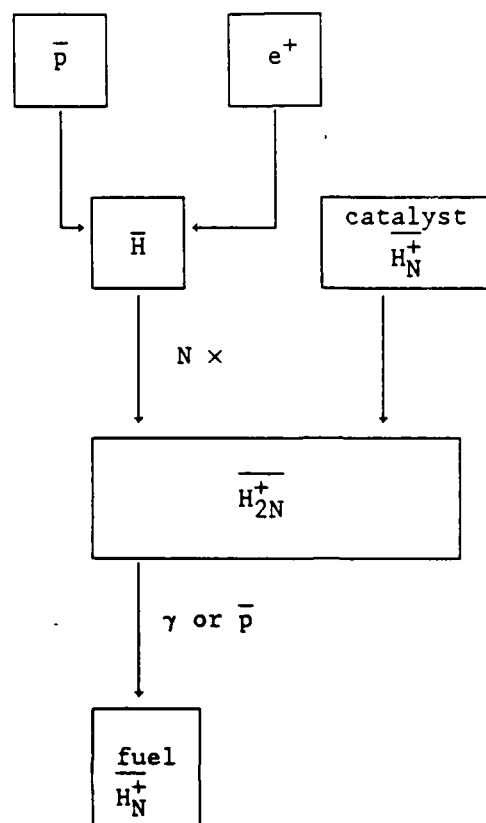


Thus our H_N^+ "seed crystal" has served as a catalyst and rapidly converted N H atoms and 1 H^+ into a H_{N+1}^+ ion.

If good methods for synthesizing and manipulating H_2 can be found, equations analogous to (1)-(4), but with H_2 in place of H , could be used even for very small N ($N = 27$ was estimated in [BAH 86]; recent measurements [KIR 87] suggest a smaller $N \sim 19$). [This is because only -0.008 eV in binding energy must be dissipated when H_2 is added to H_N^+ , versus -4.5 eV when H is added to H_N^+ with N even. (Figure 1b)]

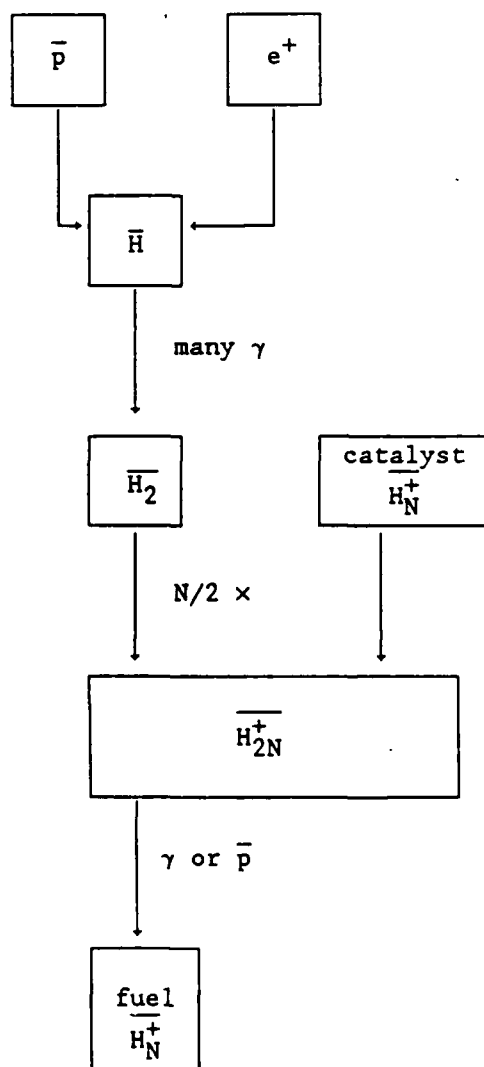
It is essential to stress the importance of this initial chunk of anti-matter (like the caveman's "first flame", the alchemist's "philosopher's stone" or ice-IX in Cat's Cradle). Assuming equations (1)-(4) are correct, once that chunk has been produced (and backups produced and stored), the

Figure 1a. Flow chart for bulk antimatter fuel production using \bar{H} directly.



temporal and financial feasibility questions are reduced greatly (Figure 1). One is then only concerned with \bar{p} , e^+ , H and the "seed crystal" (and possibly H_2 (figure 1b)). This is not true of other storage concepts (see Section II) except the magnetic levitation of antihydrogen "ice" (molecular solid). For this reason, the single most important issue in bulk storage via ions is to establish that equations (1) and (3) (or (4)) do in fact occur rapidly and efficiently for a reasonable N (10^3 - 10^6 ?), with no significant side reactions (such as H_2 boil off) (or $N \sim 19$ if \bar{H}_2 is used). Of course, some other catalyst might be used if one can be found: some extraordinary form of ordinary matter such as H^- -coated liquid helium; or "pseudowalls" of photons, positrons or other particles which do not rapidly destroy the cluster.

Figure 1b. Flow chart for bulk antimatter fuel production using H to make \bar{H}_2 and \bar{H}_2 for cluster growth.



IV. Individual Reaction Steps

How then will we produce this first "seed crystal"? As discussed in [BAH 86], there are a number of conceivable options involving cluster ions: addition of H to positive ions (A^+), addition of H_2 to positive ions (M^+) and analogous processes for negative ions (A^- and M^- respectively). However,

although H^- is stable, H_2^- is not (yielding $H_2 + e^-$ spontaneously) and H_3^- is now thought to be unstable on both experimental [BAE 84] and theoretical [MIC 87] grounds. Although for some larger N , H_N^- must be stable (as $N \rightarrow \infty$, the processes $H_N^- \rightarrow H_N + e^-$ and $H_N \rightarrow H_N^+ + e^-$ require the same positive energy), the value of that N is not established. Thus only the positive ion processes will be considered here.

In what follows, we first list (Table II) the possible options for production and storage of five potentially useful simple reagents: H , H^- , H_2^+ , H_2 and H_3^+ . We then list synthetic sequences involving H^+ , e^- , photons and these reagents which lead potentially to the production of H_N^+ . It should be noted that there is a wide variety of possibilities, so we shall emphasize the simplest (e.g. Figure 2, involving H); determination of the optimal process deserves considerable further study.

A. Formation of H

Formation of H is relatively straightforward by means of spontaneous or stimulated photorecombination; charge transfer from positronium to a proton; or three-body recombination of H^+ with a high e^- density. Brian Mitchell in these proceedings reviews the photorecombination and positronium charge transfer options in detail. He finds the stimulated photorecombination to be superior, and finds recombination to high n states possibly superior to the recombination to the $2p$ state. However, there is one important other option. This three-body recombination option was recently examined by Kells [KEL 87]. Based on the low temperature high e^- density device at La Jolla ($n_{e^-} \approx 10^{10}/\text{cm}^3$, $T \approx 10^{-3}$ eV) described e.g. in [DRI 86], he finds a production rate of $\geq 10^8$ \bar{H}/s possible using a LINAC source with e^+ accretion in a nested Penning trap.

B. Formation of H^-

Two-body recombination of an e^- with H to form H^- plus emission of a

Table II. Overview of possible steps in the "seed crystal" cluster ion synthesis process (* on numbers indicate a currently favored process). For simplicity, substeps are given only in part A.

A. Formation of H

1.* Stimulated Recombination

- a. Cooling of H^+
- b. Cooling of e^-
- c. Stimulated recombination to H (2p or higher state)
- d. Radiative Decay of H (2p or higher state)
- e. Cooling of H
- f. Trapping of H
- g. Transfer of H

2. Positronium Charge Transfer

- a. Cooling of e^+
- b. Formation of positronium (e^+e^-)
- c. Charge Transfer of H^+ with (e^+e^-)
- d. Cooling of H
- e. Removal of e^+

3.* High Density e^- Recombination

- a. Formation of high density low temperature e^-
- b. Injection of H^+ into nested trap with e^-
- c. Formation of H^* (possibly H^- also)
- d. Decay of H^*

4. Spontaneous Recombination (analogous to but also inferior to A. 1.)

B. Formation of H^-

- 1. High e^- Density Recombination (see A. 3. above)
- 2. Photodissociation of H_2 to $H^+ + H^-$
- 3. Spontaneous Recombination of $H + e^-$ (unlikely)

Table II (continued).

C. Formation of H_2^+

- 1.* Associative Ionization
2. Indirect Radiative Association

D. Formation of H_2

- 1.* Reaction of $H_2^+ + H$
- 2.* Indirect Radiative Association
3. Associative Detachment ($H^- + H \rightarrow H_2 + e^-$)
4. Direct Radiative Association (unlikely)

E. Formation of H_3^+

- 1.* Reaction of H_2^+ with H_2
- 2.* Laser-Assisted Association of $H_2^+ +$
3. Laser-Assisted Association of $H^+ + H_2$
- 4.* Three-Body Recombination ($H_2^+ + H + H \rightarrow H_3^+ + H$)

F. Formation of H_N^+

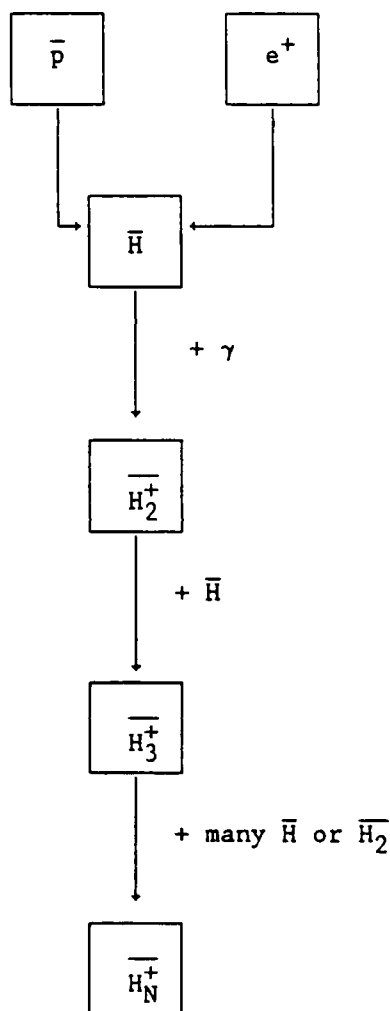
- 1.* Laser-Assisted Association of H_{N-1}^+ and H
 - 2.* Laser-Assisted Association of H_{N-2}^+ and H_2
 - 3.* Sequential Three-Body Recombination
-

photon is presumably a very slow and unlikely process. However, three-body recombination ($2 e^- + H \rightarrow H^- + e^-$) should occur fairly rapidly at high e^- density (although not so rapidly as ($2 e^- + H^+ \rightarrow H + e^-$)). An alternate scheme is the known ion-pair photodissociation process for H_2 ($H_2 + \gamma \rightarrow H^+ + H^-$) [see e.g. CHU 75]. If H^- is an unwanted by-product to H formation by three-body recombination, it can be readily destroyed by photodetachment.

G. Formation of H_2^+

The two leading processes for H_2^+ formation are indirect radiative

Figure 2. Possible flow chart for antimatter catalyst ("seed crystal") production.



association (e.g. $H^+ + H + \gamma \rightarrow (H_2^+)^* \rightarrow H_2^+ + \gamma'$, where $*$ indicates an electronically excited state [BAH 86]) and associative ionization (e.g. $H(3p) + H \rightarrow H_2^+ + e^-$ [WEI 87]). In both cases, H_2^+ cooling will be needed.

D. Formation of H_2

H_2 is the most difficult of the simple species to form and especially to manipulate (trap, cool, transfer). Magnetic traps are difficult (only very

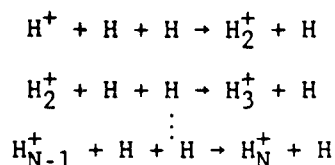
small nuclear and rotational magnetic moments) and there are many vibrational-rotational levels, so laser schemes are inherently complex. Radiative association [WEI 87] is possible, especially through an excited electronic state (e.g. $2H + \gamma \rightarrow H_2^*$ (e.g. $B^1\Sigma_u^+$) $\rightarrow H_2 + \gamma'$), if cold, high density H is available. Alternatives include the well known processes $H_2^+ + H \rightarrow H_2 + H^+$ (reaction/charge transfer) and $H^- + H \rightarrow H_2 + e^-$ (associative detachment).

E. Formation of H_3^+

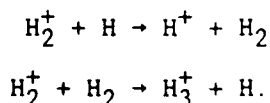
The common way in which H_3^+ forms is via the reaction $H_2^+ + H_2 \rightarrow H_3^+ + H$, but this assumes the availability of H_2 . Alternatively, the laser-assisted association reaction [BAH 86, SAX 87] $H_2^+ + H + \gamma \rightarrow (H_3^+)^* \rightarrow H_3^+ + \gamma'$ or three-body recombination in high density H ($H_2^+ + H + H \rightarrow H_3^+ + H$) might be used.

F. Formation of H_N^+ ("Seed Crystal")

The same laser-assisted processes proposed for H_3^+ should work for H_N^+ , but knowing the spectroscopy in detail for each N is a major undertaking. Conceptually simpler is an additional possibility which arises for the case of a high H density, namely sequential three-body recombination



for which there are many competing and complicating reactions such as



However, a net growth in ion size is expected regardless and collisional relaxation of vibrational energy can be significant. A particularly promising trapping technique for high H density (spin-polarized) is an inhomogeneous magnetic field [PRI 83, HES 86]; this was experimentally realized for Na in [MIG 85]. Alternatives include laser traps [CHU 86] and hybrid laser-magnet traps [STW 84], but for H they require a high power Lyman alpha source [McI

87] and include a "recoil heating" mechanism for which cooling provisions must be made. The recently proposed microwave cooling technique [SIL 87] complements well known laser techniques (since the short wavelength laser radiation required can potentially destroy the molecular ions being produced).

Alternatively, if high density H_2 can be used, H_2 addition in growing the H_N^+ cluster will provide a much smaller thermal load than H addition.

V. Modifications for Antimatter

The discussion in Sections III and IV was primarily for ordinary matter. However, the energetics, spectroscopy, dynamics, etc. for antiparticles and particles of ordinary matter should be virtually identical. The only exception is that the mass of the antiproton may be slightly different from the mass of the proton (currently they agree to 1 part in 10^4). If this is true, there will be scalable differences such as molecular vibration and rotation frequencies, velocities for a given collision energy, small Born-Oppenheimer corrections to potential energy curves and surfaces, changes in zero point energies, etc.

The other difference is that now some matter-antimatter collisions and annihilations can potentially take place. Forward has made a preliminary examination of the topic [FOR 85] and finds that "since the annihilation gamma rays and pions have such great penetrating power, failure of the antihydrogen trap will probably result in a "meltdown" of the antihydrogen container and shielding rather than a violent explosion. A trap failure would be extremely serious, however, and further studies need to be done on antimatter trap failure modes". Experimental studies of cold \bar{p} , \bar{H} , \bar{H}_2 , etc. annihilations are clearly called for.

VI. Temporal Feasibility

The emphasis in this section is on examination of the potential rate of

converting \bar{p} into bulk antimatter (H_N^+) assuming a "seed crystal" is available. The time (and effort) to synthesize the "seed crystal" itself is impossible to predict at this time since there are many possible routes and almost no information about rates except for the smallest clusters.

Referring to Figure 1 and the assumptions at the beginning of Section III, the questions are whether (a) we can produce $10^7 \bar{H}/s$ from $10^7 \bar{p}/s$ and $10^7 e^+/s$ and (b) we can add $10^7 \bar{H}/s$ to our "seed crystal". Based on Kells' analysis [KEL 87], a cold (4.2 K) high density ($10^{10}/cm^3$) e^+ plasma can probably produce the $10^7 \bar{H}/s$ via three-body recombination if the plasma can be achieved (the corresponding e^- plasma has been [DRI 86]). Clearly an experimental program is needed to conclusively answer this question, but it does look promising.

The addition of \bar{H} atoms to a "seed crystal" is limited by the rate of energy removal. In particular as $N \rightarrow \infty$, \bar{H}_N^+ should be very similar to solid molecular hydrogen with a very low temperature (≤ 2 K) being necessary to prevent significant vaporization of \bar{H}_2 molecules. At those temperatures, H_2 (solid) has an extremely low heat capacity and radiates minute amounts of blackbody radiation [FOR 85]. Thus special cooling techniques must be developed to remove heat (-4.5 eV/2 \bar{H} atoms added). If only blackbody radiation provides cooling, then $N \geq 10^9$ is needed before 1 \bar{H}/s can be added (this number N is $\sim 10^6$ if \bar{H}_2 is added instead of \bar{H}). Clearly cooling techniques for \bar{H}_N^+ ions should be studied (e.g. the ion and laser cooling techniques in [WIN 84], [FOR 85], [BRO 86], [JAV 86] and [WIN 87A]). "Sympathetic" cooling [LAR 86, WIN 87] with e^+ is probably ruled out by dissociative recombination, but might work using \bar{p} ions. As noted above, the addition of \bar{H}_2 rather than \bar{H} greatly simplifies the energy removal problem; the temporal feasibility then shifts to a question of the production rate of \bar{H}_2 , but an analysis of the alternatives in Table II.D. has not yet been carried out.

VII. Financial Feasibility

The catalytic or "seed crystal" approach assumes an initial substantial investment in a "seed crystal". The magnitude of that investment is highly uncertain, as in Section VI. However, the operating costs of the "fuel factory" in Figure 1 do not appear to be prohibitive and will probably be significantly less than the accelerator costs. However, the low temperatures and ultralow pressures will not be inexpensive and may generate serious costs. In addition, the safety/failure issues could generate limiting costs.

VIII. Summary of Major Issues

The most important issues in the cluster ion approach from my perspective are summarized in Table III. The appropriate response in terms of research effort is then estimated in Table IV. I have not included critical "engineering" issues such as how to maintain low temperature and ultralow pressure while carrying out a variety of manipulations (trapping, cooling, transferring, diagnosing, etc.) and how to provide for safety and obtain minimal failure rates.

Table III. Summary of Major Issues

1. Given a recyclable "seed crystal", how can bulk antimatter best (throughput, efficiency) be grown from added \bar{H} (or \bar{H}_2)? (i.e. do equations (1)-(4) hold? for what N? what is the best (fastest) cooling method for \bar{H}_N^+ ?)
 2. How can a "seed crystal" best be grown? (i.e. can \bar{H} be stored at high density (10^{18} H/cm³ have been stored at low temperature), e.g. in a magnetic trap? are there important advantages to using \bar{H}_2 or \bar{H}^+ , and, if so, how best are these species produced and manipulated?)
 3. How best can \bar{H} be produced from \bar{p} and e^+ ? (i.e. is the Kells' approach [KEL 87] with 10^{10} e⁺/cm³ at 4.2 K feasible?)
-

Table IV. Recommended Initial Research Efforts Corresponding to the Major Issues in Table III.

	normal matter	antimatter
1. "Seed Crystal" Process (Figure 1)	a. H_N^+ growth demonstrations [equations 1, 2] with H, H_2 b. H_N^+ fragmentation demonstrations [equations 3, 4] with H^+ , γ c. H_N^+ radiative/nonradiative cooling rates determination	-
2. "Seed Crystal" Growth (e.g. Figure 2)	a. H_N^+ stepwise growth (for small N) optimization using H only and using both H_2 and H b. H^+ injection into cold high density H c. H_2 indirect radiative association	d. cold high density \bar{H} production e. cold \bar{H}_2 production
3. \bar{H} formation	a. H^+ injection into cold high density e^- b. $H^+ + e^- + \gamma$ stimulated recombination experiment	c. cold high density e^+ production d. \bar{p} injection into cold high density e^+

IX. Acknowledgments

Discussions at the workshop and in advance with with D. C. Tardy, K. M. Sando, B. Mitchell, W. Kells, B. Augenstein, and especially J. T. Bahns are gratefully acknowledged, as is support from the Rand Corporation.

X. References

- BAE 84 Y. K. Bae, M. J. Coggiola, and J. R. Peterson, "Search for H_2^- , H_3^- , and other Metastable Negative Ions", Phys. Rev. A 29, 2888 (1984).
- BAH 86 J. T. Bahns, K. M. Sando, D. C. Tardy, and W. C. Stwalley, "Proc. of the Hydrogen Cluster Ion Study Group", Proc. Cooling, Condensation, and Storage of Hydrogen Cluster Ions Workshop, 1/8-9/87, A1-64. Edited by J. T. Bahns. University of Dayton Research Institute (1987).
- BAH 87 Proc. Cooling, Condensation, and Storage of Hydrogen Cluster Ions Workshop, 1/8-9/87, Edited by J. T. Bahns. University of Dayton Research Institute (1987).
- BRO 86 L. S. Brown and G. Gabrielse, "Geonium Theory: Physics of an Electron or Ion in a Penning Trap", Rev. Mod. Phys. 58, 233 (1986).
- CHU 75 W. A. Chupka, P. M. Dehmer and W. T. Jivery, "High Resolution Photo-ionization Study of Ion-Pair Formation in H_2 , HD, and D_2 ", J. Chem. Phys., 63, 3929 (1975).
- CHU 86 S. Chu, J. E. Bjorkholm, A. Ashkin and A. Cable, "Experimental Observation of Optically Trapped Atoms", Phys. Rev. Lett. 57, 314 (1986).
- DRI 86 C. F. Driscoll, "Containment of Single-Species Plasmas at Low Energies", in Low Energy Antimatter, D. B. Cline, Editor (World Scientific, Singapore, 1986), p. 184.
- FOR 87 R. L. Forward, "Antimatter Science and Technology Bibliography", unpublished (1987).
- FOR 85 R. L. Forward, "Antiproton Annihilation Propulsion", Air Force Rocket Propulsion Laboratory Report, AFRPL TR-85-034 (1985).
- HES 86 H. F. Hess, "Evaporative Cooling of Magnetically Trapped and Compressed Spin-Polarized Hydrogen", Phys. Rev. B34, 3476 (1986).
- JAV 86 J. Javanainen, "Light-Pressure Cooling of a Crystal", Phys. Rev. A56, 1798 (1986).
- KEL 87 W. P. Kells, " e^+ Accumulation for \bar{H} Production" in Proc. of the Intense Positron Beams Workshop (6/17-19/87), E. H. Ottewitte and W. P. Kells, Editors, in press.
- KIR 87 N. J. Kirchner and M. T. Bowers, "Fragmentation Dynamics of Metastable Hydrogen Ion Clusters H_5^+ , H_7^+ , and H_9^+ : Experiment and Theory", J. Chem. Phys. 91, 2573 (1987).
- LAR 86 D. J. Larson, J. C. Bergquist, J. J. Bollinger, W. M. Itano, and D. J. Wineland, "Sympathetic Cooling of Trapped Ions: A Laser-Cooled Two-Species Nonneutral Ion Plasma", Phys. Rev. Lett. 57, 70 (1986).
- MCI 87 Thomas J. McIlrath, "Long Duration Coherent Lyman-Alpha Sources", Proc. Cooling, Condensation, and Storage of Hydrogen Cluster Ions Workshop, 1/8-9/87, 195. Edited by J. T. Bahns. University of Dayton Research Institute (1987).

- MIC 87 H. H. Michels and J. A. Montgomery, Jr., "The Electronic Structure and Stability of the H_3^- Anion", Chem. Phys. Lett. 139, 535 (1987).
- MIG 85 A. L. Migdall, J. V. Prodan, W. D. Phillips, T. T. Bergeman and H. J. Metcalf, "First Observation of Magnetically Trapped Neutral Atoms", Phys. Rev. Lett. 54, 2596 (1985).
- PRI 83 D. E. Pritchard, "Cooling Neutral Atoms in a Magnetic Trap for Precision Spectroscopy", Phys. Rev. Lett. 51, 1336 (1983).
- SAX 87 R. Saxon, "Overview of Hydrogen Clusters", Proc. Cooling, Condensation, and Storage of Hydrogen Cluster Ions Workshop, 1/8-9/87, 27. Edited by J. T. Bahns. University of Dayton Research Institute (1987).
- SIL 87 I. F. Silvera, "Microwave Cooling of a Gas of Atoms: Spin-Polarized Hydrogen", (preprint) (1987).
- STW 84 W. C. Stwalley, "A Hybrid Laser-Magnet Trap for Spin-Polarized Atoms", Prog. Quant. Electr. 8, 203 (1984).
- STW 87 W. C. Stwalley, "Large Hydrogen Cluster Ions", Proc. of the Workshop on Cooling, Condensation and Storage of Hydrogen Cluster Ions Workshop, 1/8-9/87, 39. Edited by J. T. Bahns. University of Dayton Research Institute (1987).
- STW 87A W. C. Stwalley, "Bibliography of Hydrogen Cluster Ions", unpublished (1987).
- WEI 87 J. Weiner, "Associative Two-Body Condensation in Laser-Cooled Sodium and Hydrogen", Proc. Cooling, Condensation, and Storage of Hydrogen Cluster Ions Workshop, 1/8-9/87, 47-59. Edited by J. T. Bahns. University of Dayton Research Institute (1987).
- WIN 84 D. J. Wineland and W. M. Itano, "High-Resolution Spectroscopy of Stored Ions", Advan. At. Mol. Phys. 19, 135 (1984).
- WIN 87 D. Wineland, "Ion Traps for Large Storage Capacity", Proc. Cooling, Condensation, and Storage of Hydrogen Cluster Ions Workshop, 1/8-9/87, 179. Edited by J. T. Bahns. University of Dayton Research Institute (1987).
- WIN 87A D. J. Wineland and W. M. Itano, "Laser Cooling", Physics Today 34, June (1987).

Bibliography of Hydrogen Cluster Ions

William C. Stwalley

Center for Laser Science and Engineering and
Departments of Chemistry and of Physics and Astronomy,
University of Iowa, Iowa City, Iowa 52242-1294

Introduction

The enclosed bibliography includes the edited results of September 1987 Chemical Abstracts On-Line Searches, plus selected additional references, for the period 1966-1987 for the species H_2^+ (and H_2^-), H_3^+ (and H_3^-), and H_N^+ (and H_N^- , $N \geq 4$), in Sections I, II, and III, respectively. References are roughly in reverse chronological order. Note that H_2^- is not a stable species and the evidence suggests H_3^- is also unstable. All references have been copied or requested through interlibrary loan; thus copies of difficult to obtain articles are available at \$.10/page plus a \$10 service charge from the author. The assistance of Todd Colin and Tom Yang in these searches and partial support from the Rand Corporation are gratefully acknowledged.

Section I: H_2^+ (and H_2^-)

1987

1. Sen, Amarjit; McGowan, J. W.; Mitchell, J. B. A., "Production of Low-Vibrational-State Hydrogen Ions (H_2^+) for Collision Studies", J. Phys. B: At. Mol. Phys. 20(7), 1509-15 (1987).
2. Stine, J. R.; Muckerman, J. T., "Critical Evaluation of Classical Trajectory Surface-Hopping Methods as Applied to the Hydrogen Molecular Ion (H_2^+) + Hydrogen Molecule (H_2) System", J. Phys. Chem. 91(2), 459-66 (1987).
3. Helm, H.; Cosby, P. C.; "Photodissociation Measurement of Rovibrational Energies and Populations of Molecules in Fast Beams", J. Chem. Phys. 86(12), 6813-22 (1987).
4. Xu, E. Y.; Helm, H.; Kachru, R., "Field Ionization of High-Lying States of H_2^+ ", Phys. Rev. Lett. 59(10), 1096-9 (1987).
5. Niedner, G.; Noll, M.; Toennies, J. P.; Schlier, Ch., "Observation of Vibrationally Resolved Charge Transfer in $H^+ + H_2$ at $E_{CM} = 20$ eV", J. Chem. Phys. 87(5), 2685-94 (1987).
6. Schlier, Christoph G.; Vix, Ulrike, "Complex Formation in Proton-Hydrogen Collisions. II. Isotope Effects", Chem. Phys. 113, 211-21 (1987).
7. Weiner, J., "Associative Two-Body Condensation in Laser-Cooled Sodium and Hydrogen", Proc. Cooling, Condensation, and Storage of Hydrogen Cluster Ions Workshop, 1/8-9/87, 47-59. Edited by John T. Bahns. University of Dayton Research Institute (1987).
8. Helm, H., "Photon-Assisted Formation and Cooling of Molecular Hydrogen", Proc. Cooling, Condensation, and Storage of Hydrogen Cluster Ions Workshop, 1/8-9/87, 95-108. Edited by John T. Bahns. University of Dayton Research Institute (1987).
9. Mitchell, J. B. A., "The Role of Electron-Ion Recombination in Bulk Antimatter Production", Proc. Cooling, Condensation, and Storage of Hydrogen Cluster Ions Workshop, 1/8-9/87, 143-56. Edited by John T. Bahns. University of Dayton Research Institute (1987).
10. Bahns, J. T., "Key Problems and Hydrogen Atom Formation", Proc. Cooling, Condensation, and Storage of Hydrogen Cluster Ions Workshop, 1/8-9/87, 219-30. Edited by John T. Bahns. University of Dayton Research Institute (1987).
11. Bahns, J. T.; Sando, K. M.; Tardy, D. C.; Stwalley, W. C., "Proceedings

of the Hydrogen Cluster Ion Study Group", Proc. Cooling, Condensation, and Storage of Hydrogen Cluster Ions Workshop, 1/8-9/87, A1-64. Edited by John T. Bahns. University of Dayton Research Institute (1987).

1986

12. Foster, S. C.; McKellar, A. R. W.; Watson, J. K. G., "Observation and Analysis of the v_2 and v_3 Fundamental Bands of the D_2H^+ Ion", J. Chem. Phys. 85(2), 664-70 (1986).
13. Jensen, Per; Spirko, V.; Bunker, P. R., "A New Morse-Oscillator Based Hamiltonian for H_3^+ : Extension to H_2D^+ and D_2H^+ ", J. Mol. Spectrosc. 115, 269-93 (1986).
14. Wolniewicz, L.; Poll, J. D., "On the Higher Vibration-Rotational Levels of Hydrogen Deuteride Ion (HD^+) and Hydrogen Molecular Ion (H_2^+)", Mol. Phys. 59(5), 953-64 (1986).
15. De Bruijn, D. P.; Neuteboom, J.; Govers, T. R.; Los, J., "Dissociative Decay of $N = 3$ Levels in H_3 . I. Populated in Charge Exchange of Hydrogen Ion (H_2^+) with Cesium", Phys. Rev. A: Gen. Phys. 34(5), 3847-54 (1986).
16. Richards, J. A.; Larkins, F. P., "Photoionization Cross Section Calculations of Molecular Hydrogen and Hydrogen Ion (H_2^+) Using Numerical Continuum Wavefunctions", J. Phys. B: At. Mol. Phys. 19(13), 1945-57 (1986).
17. Chandra, N., "Ab Initio Multichannel Photoionization of Molecular Hydrogen: Photoelectron Angular Distribution for Rotationally Resolved States of Hydrogen Ion (H_2^+)", J. Phys. B: At. Mol. Phys. 19(13), 1959-88 (1986).
18. Blaise, Paul; Henri-Rousseau, Olivier, "On the Quantum Correlation Between the Kinetic and Potential Energies in the Hydrogen Molecular Ion (H_2^+)", C. R. Acad. Sci. Ser. 2, 302(6), 297-302 (1986).
19. Stehle, C.; Feautrier, N., "Absorption or Emission During a Collision: A Test Case Hydrogen Molecular Ion (H_2^+)", J. Phys. (Les Ulis, Fr.), 47(6), 1015-20 (1986).
20. Miao, Jingwei; Yang Beifang; Hao, Shizuho; Jiang, Zengxue; Shi, Miagong; Cue, N., "Internuclear Separations From Foil Breakup of Fast H_2^+ , H_3^+ , D_2^+ and D_3^+ Molecules", Nucl. Instrum. Methods Phys. Res. Sect. B, B13(1-3), 181-3 (1986).
21. Cizek, Jiri; Damburg, R.; Graffi, Sandro; Grecchi, Vincenzo; Harrell, Evans M., II; Harris, Jonathan G.; Nakai, Sachiko; Paldus, Josef; Propin, R.; Silverstone, Harris J., "1/R Expansion for Molecular Hydrogen Ion (H_2^+): Calculation of Exponentially Small Terms and Asymptotics", Phys.

Rev. A: Gen. Phys. 33(1), 12-54 (1986).

22. Liao, C. L.; Ng, C. Y., "Vibrational State Distributions of H_2^+ (v) Resulting From the Hydrogen Ion-Molecule Electron Transfer Reactions $H_2^+ (v'_0 = 0, 1) + H_2(v''_0 = 0) \rightarrow H_2(v') + H_2^+ (v)$ in the Collisional Energy Range of 2-16 eV", J. Chem. Phys. 84(1), 197-200 (1986).
23. Sen, A.; Mitchell, J. B. A., "Production of Vibrationally Cold Ions Using a Radio-Frequency Storage Ion", Rev. Sci. Instrum. 57(5), 754-6 (1986).
24. Bonnie, J. H. M.; Eenshyistra, P. J.; Los, J.; Hopman, H. J., "Influence of the Vibrational Quantum Number of the Resonant State in Resonant Multiphoton Ionization/Dissociation of Hydrogen Molecules", Chem. Phys. Lett. 125(1), 27-32 (1986).

1985

25. Blaise, Paul; Henri-Rousseau, Olivier, "Accuracy of Approximate Wave Functions for the Molecular Hydrogen Ion (H_2^+): Calculation of Standard Deviations for the Hamiltonian in the $2\Sigma_g^+$ State", C. R. Acad. Sci. Ser. 2, 301(13), 907-10 (1985).
26. Tokoro, N.; Oda, N., "Energy and Angular Distributions of Ejected Electrons for Hydrogen-Cluster-Ion (H_n^+ , D_n^+ , $n=1-3$) Impacts on Helium in the Intermediate Energy Region", J. Phys. B: At. Mol. Phys. 18, 1771-80 (1985).
27. Graffi, S.; Grecchi, V.; Harrell, E. M., II; Silverstone, H. J., "The 1/R Expansion for H_2^+ : Analyticity, Summability, and Asymptotics", Ann. Phys. (N. Y.), 165(2), 441-83 (1985).
28. Eaker, Charles W.; Muzyka, Jennifer L., "A Quasiclassical Trajectory Study of the Hydrogen-Deuterium ($(H_2 + D_2)^+$) System", Chem. Phys. Lett. 119(2-3), 169-72 (1985).
29. Primorac, M.; Kovacevic, K., "An Application to Molecular Hydrogen Ion (H_2^+) of Laplace Type Integral Transform and Its Inverse", Z. Naturforsch. A: Phys. Phys. Chem., Kosmophys. 40A(3), 246-50 (1985).
30. Mohlmann, G. R., "Stimulated Raman Scattering from H_2^+ Ions", Chem. Phys. Lett. 115(2), 226-9 (1985).

1984

31. Jungen, Ch., "Unified Treatment of Dissociation and Ionization Processes in Molecular Hydrogen", Phys. Rev. Lett. 53(25), 2394-7 (1984).
32. Brenton, A. G.; Fournier, P. G.; Govers, B. L.; Richard, E. G.; Beynon,

J. H., "The Vibrational Population Distribution of H_2^+ Formed From a Series of Different Precursor Molecules", Proc. R. Soc. London, A, 395(1808), 111-25 (1984).

33. Nicolaides, C. A.; Petsalakis, I. D.; Theodorakopoulos, G., "Theory of Chemical Reactions of Vibronically Excited Molecular Hydrogen ($B^1\Sigma_u^+$). III. Formation of Bound Excited States of the Hydrogen (H_2)₂, (H_2)₃, and (H_2)₅ Clusters", J. Chem. Phys. 81(2), 748-53 (1984).
34. Bae, Y. K.; Coggiola, M. J.; Peterson, J. R., "Search for H_2^- , H_3^- , and Other Metastable Negative Ions", Phys. Rev. A, 29(5), 2888-90 (1984).
35. Damburg, R.; Propin, R. Kh.; Graffi, Sandro; Grecchi, Vincenzo; Harrell, Evans M., II; Cizek, Jiri; Paldus, Josef; Silverstone, Harris J., "1/R Expansion for Hydrogen Molecular Ion (H_2^+): Analyticity, Summability, Asymptotics, and Calculation of Exponentially Small Terms", Phys. Rev. Lett. 52(13), 1112-5 (1984).
36. Lee, Chyuan Yih; DePristo, Andrew E., "Semiclassical Investigation of Vibrational State and Molecular Orientation Effects in Electron Transfer Reactions for the Hydrogen (H_2^+/H_2) Collision", J. Chem. Phys. 80(3), 1116-26 (1984).
37. Kutina, R. E.; Edwards, A. K.; Pandolf, R. S.; Berkowitz, J., "UV Laser Photodissociation of Molecular Ions", J. Chem. Phys. 80(9), 4112-9 (1984).

1983

38. Lee, Chyuan Yih; DePristo, Andrew E., "A Simple Model for the Interaction Potentials in Electron-Transfer Reactions: Application to the Molecular Hydrogen Ion/Molecular Molecular (H_2^+/H_2) System", J. Am. Chem. Soc. 105(23), 6775-81 (1983).
39. Semenova, N. V., "Quasiclassical Calculation of Low-Lying Terms of Hydrogen (H_2^+) Ion", Vestn. Leningr. Univ., Fiz., Khim. 3, 72-6 (1983).
40. Samsonov, B. F., "Calculation of Diatomic Molecules by the MO LCAO Method. Excited States of Hydrogen Ion (H_2^+)", Izv. Vyssh. Uchebn. Zaved., Fiz. 26(8), 115-7 (1983).
41. Chu, Shih I; Laughlin, Cecil; Datta, Krishna K., "Two-Photon Dissociation of Vibrationally Excited Molecular Hydrogen Ion (H_2^+). Complex Quasi-Vibrational Energy and Inhomogeneous Differential Equation Approaches", Chem. Phys. Lett. 98(5), 476-81 (1983).
42. Brenton, A. G.; Beynon, J. H.; Richard, E. G.; Fournier, P. G., "Rotational Predissociation of H_2^+ Ions of Different Precursor Origins", J. Chem. Phys. 79(4), 1834-45 (1983).

43. Ozaki, Jiro; Tomishima, Yasuo, "Monte Carlo Solutions of Schroedinger's Equation for Molecular Hydrogen (H_2^+) Ion in Strong Magnetic Fields. II", J. Phys. Soc. Jpn. 52(4), 1142-7 (1983).
44. Khersonskii, V. K., "Frequencies and Probabilities of the Vibrational Transitions of Molecular Hydrogen Ion (H_2^+) in the Magnetic Field of a Neutron Star", Astron. Zh. 60(1), 105-9 (1983).

1982

45. Samsonov, B. F., "Calculation of Diatomic Molecules by the MO LCAO Method. $1s\sigma_g$ and $2p\sigma_u$ States of H_2^+ and $1s\sigma$ State of HeH_2^+ ", Izv. Vyssh. Uchebn. Zaved., Fiz. 25(10), 117-9 (1982).

1981

46. Sataka, Masao; Shirai, Toshizo; Kikuchi, Akira; Nakai, Yohta, "Ionization Cross Sections for Ion-Atom and Ion-Molecule Collisions. I. Ionization Cross Sections for Hydrogen and Helium Ions H^+ , H_2^+ , H_3^+ , He^+ and He^{++} Incident on H, H_2 , and He", Nippon Genshiryoku Kenkyusho, [Rep.] JAERI-M, JAERI-M-9310, 65 Pp. (1981).
47. Cue, N.; Edwards, A. K.; Gemmell, D. S.; Kanter, E. P.; Kutina, R., "UV-Laser Photofragmentation of a 2-MeV Molecular Hydrogen Ion (H_2^+) Beam", Ann. Isr. Phys. Soc., 4 (Mol. Ions, Mol. Struct. Interact. Matter), 194-7 (1981).
48. Sonnleitner, Stephanie A.; Beckel, Charles L.; Colucci, Anthony J.; Scaggs, E. Rodney, "Rational Fraction Representation of Diatomic Vibrational Potentials. V. The $3d\sigma_g$ State of H_2^+ ", J. Chem. Phys. 75(4), 2018-20 (1981).

1980

49. Anderson, S. L.; Hirooka, T.; Tiedemann, P. W.; Mahan, B. H.; Lee, Y. T., "Photoionization of Hydrogen [$(H_2)_2$] and Clusters of Oxygen Molecules", J. Chem. Phys. 73(10), 4779-83 (1980).
50. Huber, B. A.; Schulz, U.; Wiesemann, K., "Cross Sections for Slow Ion Production and Charge Transfer in $H_3^+(D_3^+)-H_2(D_2)$ Collisions", Phys. Lett. A, 79A(1), 58-60 (1980).
51. Kaschiev, M. S.; Vinitskii, S. I.; Vukajlovic, F. R., "Hydrogen Atom H and Hydrogen (H_2^+) Molecule in Strong Magnetic Fields", Phys. Rev. A, 22(2), 557-9 (1980).
52. Nir, D.; Navon, E.; Mann, A.; Rosner, B., "Relations Between the Dissoci-

ation Cross Section of H_2^+ Ions and the Charge Exchange Cross Sections of Their Fragments", Phys. Lett. A, 77A(2-3), 150-2 (1980).

53. Koyano, Inosuke; Tanaka, Kenichiro, "State-Selected Ion-Molecule Reactions by a Threshold Electron-Secondary Ion Coincidence (TESICO) Technique. I. Apparatus and the Reaction $H_2^+ + H_2 \rightarrow H_3^+ + H$ ", J. Chem. Phys. 72(9), 4858-68 (1980).
54. Semenov, V. E., "Calculation of the Cross Section for Photoionization of a Molecular Hydrogen Ion H_2^+ Based on Gaussian Functions", Opt. Spektrosk. 48(4), 723-7 (1980).
55. Oda, Nobuo; Urakawa, Junji; Tokoro, Nobuhiro; Nojiri, Hiroshi, "Ionizing Collisions of Hydrogen Cluster Ions (H^+ , H_2^+ , H_3^+) of Intermediate Energies with Gases", Iongen to Sono Oyo, Shinpojumu, 4th, 205-8. Ion Kogaku Kondankai: Kyoto, Japan. (1980).

1979

56. Hirooka, Tomohiko; Anderson, Scott L.; Tiedemann, Peter W.; Mahan, Bruce H.; Lee, Yuan T., "Photoionization of Molecular Hydrogen Dimer $(H_2)_2^+$ ", Koen Yoshishu - Bunshi Kozo Sogo Toronkai, 64-5. Chem. Soc. Japan: Tokyo, Japan. (1979).
57. Dastidar, K. Rai; Bose, M.; Dastidar, T. K. Rai, "Electron Cooling Through Resonant Collisions with Hydrogen (H_2^+) Molecular Ion", J. Phys. Soc. Jpn. 47(6), 1955-8 (1979).
58. Boikova, R. F., "Ion-Ion Recombination of Molecular Hydrogen Ion (H_2^+) and Hydrogen Ion (H^+)", Vestn. Leningr. Univ., Fiz., Khim. 2, 103-5 (1979).
59. Moiseyev, Nimrod; Corcoran, Chris, "Autoionizing States of Diatomic Hydrogen and Hydrogen Ion (H_2^+) Using The Complex-Scaling Method", Phys. Rev. A, 20(3), 814-7 (1979).
60. Propin, R. Kh., "Exponentially Small Part of the Molecular Hydrogen (H_2^+) Ion Wave Function", Latv. PSR Zinat. Akad. Vestis, Fiz. Teh. Zinat. Ser. 3, 7-12 (1979).
61. Hashemi-Attar, Ali-Reza; Beckel, Charles L.; Keepin, William N.; Sonnelitner, Stephanie A., "A New Functional Form for Representing Vibrational Eigenenergies of Diatomic Molecules. Application to Hydrogen Molecular Ion (H_2^+) Ground State", J. Chem. Phys. 70(8), 3881-3 (1979).
62. Strand, Michael P.; Reinhardt, William P., "Semiclassical Quantization of the Low-Lying Electronic States of Hydrogen Molecular Ion (H_2^+)", J. Chem. Phys. 70(8), 3812-27 (1979).
63. Bishop, David M.; Cheung, Lap M., "Natural Orbital Analysis of Nonadia-

batic H_2^+ Wave Functions", Int. J. Quantum Chem. 15(5), 517-32 (1979).

64. Dastidar, K. Rai; Dastidar, T. K. Rai, "Dissociative Recombination of H_2^+ , HD^+ , and D_2^+ Molecular Ions", J. Phys. Soc. Jpn. 46(4), 1288-94 (1979).
65. Van der Hart, Johanna A.; Mulder, J. J. C., "Ab Initio CI LCAO Calculations of the Lowest Core-Excited Σ Resonant States of H_2^+ ", Chem. Phys. Lett. 61(1), 111-4 (1979).

1978

66. Beck, D. R.; Nicolaides, C. A., "How Many Bound States do Hydrides H^- and H_2^- Have?", Chem. Phys. Lett. 59(3), 525-8 (1978).
67. Teloy, E., "Proton-Hydrogen (H_2 , D_2) Differential Inelastic and Reactive Scattering At Low Energies", Electron. At. Collisions, Proc. Int. Conf., 10th, Meeting Date 1977, 591-603. Edited by: Watel, Guy. North-Holland: Amsterdam, Neth. (1978).
68. Veselov, M. G.; Rekasheva, T. N., "Extension of the LCAO Method [Hydrogen (H_2^+) Ion Calculation]", Vestn. Leningr. Univ., Fiz., Khim. (2), 14-6 (1978).
69. Tame, B. R.; Ritchie, Burke, "Continuum States for Hydrogen Molecule: A Study of Convergence in $e^-H_2^+$ Scattering Equations", J. Chem. Phys. 68(8), 3595-9 (1978).
70. Stine, J. R.; Muckerman, J. T., "Charge Exchange and Chemical Reaction in the $H_2^+ + H_2$ System. I. Characterization of the Potential Energy Surfaces and Nonadiabatic Regions", J. Chem. Phys. 68(1), 185-94 (1978).

1977

71. Gentry, W. Ronald; Ringer, Geoffrey, "On the Possibility That Electronically Excited Products May Be Formed in the Reaction $H_2^+ + H_2 \rightarrow H_3^+ + H$ ", J. Chem. Phys. 67(11), 5398-9 (1977).
72. Douglass, Charles H.; McClure, Donald J.; Gentry, W. Ronald, "The Dynamics of the Reaction $H_2^+ + H_2 \rightarrow H_3^+ + H$, with Isotopic Variations", J. Chem. Phys. 67(11), 4931-40 (1977).
73. Malkhasyan, R. T.; Zhurkin, E. S.; Tunitskii, N. N., "Excitation of Hydrogen Ions (H_3^+) and Dependence of the Cross Section of the Secondary Ionic-Molecular Reaction $H_3^+ + Ar \rightarrow ArH^+ + H_2$ on Excitation Energy of the H_3^+ Ion", Khim. Vys. Energ. 11(6), 400-2 (1977).
74. Top, Zvi H.; Baer, Michael, "Incorporation of Electronically Nonadiabatic Effects Into Bimolecular Reactive Systems. II. The Collinear ($H_2 + H^+$,

$H_2^+ + H$ System", Chem. Phys. 25(1), 1-18 (1977).

75. Steinborn, E. Otto; Weniger, E. J., "Advantages of Reduced Bessel Functions as Atomic Orbitals. An Application to the Hydrogen Ion (H_2^+)", Int. J. Quantum Chem., Symp., 11 (Proc. Int. Symp. At., Mol., Solid-State Theory, Collision Phenom., Comput. Methods), 509-16 (1977).
76. Hyatt, D.; Careless, P. N.; Stanton, L., "A Simple Ab-initio Potential Surface for the Reaction $H_3^+(H_2, H_2)H_3^+$ in C_{2v} Symmetry", Int. J. Mass Spectrom. Ion Phys. 23(1), 45-50 (1977).
77. Auerbach, D.; Cacak, R.; Caudano, R.; Gaily, T. D.; Deyser, C. J.; McGowan, J. Wm.; Mitchell, J. B. A.; Wilk, S. F. J., "Merged Electron-Ion Beam Experiments I. Method and Measurements of ($e-H_2^+$) and ($e-H_3^+$) Dissociative-Recombination Cross Sections", J. Phys. B: Atom. and Molec. Phys. 10(18), 3797-820 (1977).

1976

78. Alvarez, Ignacio; Cisneros, Carmen; Barnett, C. F.; Ray, J. A., "Negative-Ion Formation From Dissociative Collisions of H_2^+ , H_3^+ , and HD_2^+ in Molecular Hydrogen, Helium, and Xenon", Phys. Rev. A, 14(2), 602-7 (1976).
79. Adamov, M. N.; Ivanov, A. I., "Calculation of Electric Field Gradient in Hydrogen Ion (H_2^+) on a Four-Center Base From Slater Type Functions", Vestn. Leningr. Univ. Fiz., Khim. (1), 28-31 (1976).
80. Vestal, M. L.; Blakley, C. R.; Ryan, P. W.; Futrell, J. H., "Crossed-Beam Study of the Reaction $H_3^+(D_2, H_2)D_2H^+$ ", J. Chem. Phys. 64(5), 2094-111 (1976).
81. Ozenne, J.-B.; Durup, J.; Odom, R. W.; Pernot, C.; Tabché-Fouhaillé, A.; Tadjeddine, M., "Laser Photodissociation of the Isotopic Hydrogen Molecular Ions. Comparison Between Experimental and Ab Initio Computed Fragment Kinetic Energy Spectra", Chem. Phys. 16, 75-80 (1976).

1975

82. Rekasheva, T. N., "Calculation of the Hydrogen (H_2^+) Molecular Ion", Tr. Leningr. Korablestroit. Inst. 97, 60-1 (1975).
83. Barsuk, A. A.; Zenchenko, V. P.; Rusanov, M. M., "Hydrogen Molecular Ion H_2^+ in a Magnetic Field", Tezisy Dokl. Soobshch.-Konf. Molodykh Uch. Mold., 9th, Meeting Date 1974, 50. Edited by: Lazarev, A. M. "Shtiintsa": Kishinev, USSR. (1975).
84. Lees, A. B.; Rol, P. K., "Merging Beams Study of the $D^+(H_2, H)HD^+$ and

$H_2^+(D,H)HD^+$ Reaction Mechanisms", J. Chem. Phys. 63(6), 2461-5 (1975).

85. Bishop, David M.; Shih, Shing-Kuo; Beckel, Charles L.; Wu, Fun-Min; Peek, James M., "Theoretical Study of H_2^+ Spectroscopic Properties. IV. Adiabatic Effects for the $2p\pi_u$ and $3d\sigma_g$ Electronic States", J. Chem. Phys. 63(11), 4836-41 (1975).
86. Hiraoka, K.; Kebarle, P., "Temperature Dependence of Third Order Ion Molecule Reactions. Reaction $H_3^+ + 2H_2 = H_5^+ + H_2$ ", J. Chem. Phys. 63(2), 746-9 (1975).
87. Hiraoka, K.; Kebarle, P., "Determination of the Stabilities of H_5^+ , H_7^+ , H_9^+ , and H_{11}^+ From Measurement of the Gas Phase Ion Equilibria $H_n^+ + H_2 = H_{n+2}^+$ ($n = 3, 5, 7, 9$)", J. Chem. Phys. 62(6), 2267-70 (1975).
88. Robiette, Alan G., "Variation Theorem Applied to Hydrogen Ion (H_2^+). Simple Quantum Chemistry Computer Project", J. Chem. Educ. 52(2), 95-6 (1975).

1974

89. Elford, M. T.; Milloy, H. B., "Mobility of H_3^+ and H_5^+ Ions in Hydrogen and the Equilibrium Constant for the Reaction $H_3^+ + 2H_2 = H_5^+ + H_2$ at Gas Temperatures of 195, 273, and 293 K", Aust. J. Phys. 27(6), 795-811 (1974).
90. Lees, A. B.; Rol, P. K., "Merging Beams Study of the $H_2^+(H_2,H)H_3^+$, $H_2^+(D_2,H)HD_2^+$, and $D_2^+(H_2,H)HD_2^+$ Reaction Mechanisms", J. Chem. Phys. 61(11), 4444-9 (1974).
91. Wendell, K. L.; Rol, P. K., "Merging Beams Study of the Reaction $H_2^+(D,H)HD^+$ ", J. Chem. Phys. 61(5), 2059-61 (1974).
92. Malkhasyan, R. T.; Zhurkin, E. S.; Tikhomirov, M. V.; Tunitskii, N. N., "Charge Exchange of Argon($1+$) and Hydrogen(H_2^+) Ions with Deuterium Molecules in Reactive Collisions At Up to 100 eV, and Formation of Deuterium (D_3^+) Ions in Ion-Molecule Reactive Collisions Involving the Charge-Exchanged Deuterium (D_2^+) System", Khim. Vys. Energ. 8(2), 189-91 (1974).
93. Van Asselt, N. P. F. B.; Maas, J. G.; Los, J., "Laser Induced Photodissociation of H_2^+ and D_2^+ Ions", Chem. Phys. 5, 429-38 (1974).
94. Peart, B; Dolder, K. T., "Collisions Between Electrons and H_2^+ Ions. V. Measurements of Cross Sections for Dissociative Recombination", J. Phys. B: Atom. Molec. Phys. 7(2), 236-43 (1974).
95. Davydkin, V. A.; Rapoport, L. P., "Two-Photon Ionization of Molecular Hydrogen Ion (H_2^+)", Opt. Spektrosk. 36(2), 244-9 (1974).

1973

96. Bunker, P. R., "Nonadiabatic Effects on the Vibrational Intervals of Hydrogen Molecular Ion [H_2^+]", J. Mol. Spectrosc. 46(3), 504-5 (1973).
97. Zhurkin, E. S.; Kaminskii, V. A.; Tikhomirov, M. V.; Tunitskii, N. N., "Cross Sections of Hydrogen (H_2^+) and Deuterium (D_2^+) Ion Dissociation in the 0.1-2 KeV Range", Zh. Tekh. Fiz. 43(2), 405-9 (1973).
98. Beckel, C.; Shapi, M.; Peek, J. M., "Theoretical Study of H_2^+ Spectroscopic Properties. II. The $2p\pi_u$ Electronic State", J. Chem. Phys. 59(10), 5288-93 (1973).

1972

99. Stewart, Ronald F., "Finite-Difference Solution of the United Atom, One-Center Expansion for H_2^+ ", Mol. Phys. 24(4), 879-83 (1972).
100. Bochvar, D. A.; Tutkevich, A. V., "Chemical Bonding and Entropy of Electron Density Distribution in Molecules. II. Characteristics of Electron Density Distribution in the H_2^+ Molecular Ion", Zh. Strukt. Khim. 13(4), 678-81 (1972).
101. Herrero, F. A.; Doering, J. P., "Superelastic Collisions of Vibrationally Excited H_2^+ with Atoms and Molecules", Phys. Rev. Lett. 29(10), 609-11 (1972).
102. Sauers, I.; Fitzwilson, R. L.; Ford, J. C.; Thomas, E. W., "Angular Distribution of Metastable Hydrogen Formed by Dissociation of H_2^+ ", Phys. Rev. A, 6(4), 1418-24 (1972).
103. Ali, M. K.; Meath, W. J., "A Floating One-Center Perturbation Treatment for H_2^+ -Like Molecules", Int. J. Quantum Chem. 6(5), 949-66 (1972).
104. Peart, B.; Dolder, K. T., "Collisions Between Electrons and H_2^+ Ions. III. Measurements of Proton Production Cross Sections at Low Energies", J. Phys. B, 5(8), 1554-8 (1972).
105. Tung, Eleanor W.; Sanders, William A., "Simple Perturbation and Perturbation-Variation Treatments of the $1s\sigma_g$ and $2p\sigma_u$ States of H_2^+ ", Int. J. Quantum Chem. 6(4), 717-23 (1972).
106. Dolder, K.; Peart, B., "Proton Production by Collisions Between Electrons and H_2^+ . Comments", J. Phys. B, 5(6), L129-L131 (1972).
107. Taylor, Howard S.; Thomas, Lowell D., "Short-Lived Resonant State of H_2^+ ", Phys. Rev. Lett. 28(17), 1091-2 (1972).
108. Rundel, R. D., "Proton Production in Collisions Between Electrons and H_2^+

Ions", J. Phys. B, 5(4), L76-8 (1972).

109. Weinhold, Frank; Chinen, Allan B., "Variational Wave Functions for H_2^+ ", J. Chem. Phys. 56(8), 3798-801 (1972).
110. Von Busch, Friedrich; Dunn, Gordon H., "Photodissociation of H_2^+ and D_2^+ : Experiment", Phys. Rev. A 5(4), 1726-43 (1972).
111. Ozenne, J.-B.; Pham, D.; Durup, J., "Photodissociation of H_2^+ by Monochromatic Light with Energy Analysis of the Ejected H^+ Ions", Chem. Phys. Lett. 17(3), 422-4 (1972).

1971

112. Kelkar, V. K.; Bhalla, K. C.; Khubchandani, P. G., "Study of the Hydrogen Molecule Using H_2^+ Molecular Orbital", Mol. Phys. 22(6), 1141-3 (1971).
113. Peart, B.; Dolder, K. T., "Collisions Between Electrons and H_2^+ Ions. I. Measurements of Cross Sections for Proton Production", J. Phys. B, 4(11), 1496-505 (1971).
114. Laurenzi, Bernard J., "Green's Function for the Hydrogen Molecular Ion H_2^+ ", J. Chem. Phys. 55(6), 2681-4 (1971).
115. Jackson, M.; McEachran, R. P.; Cohen, M., "James Wave Function for the Ground State of H_2^+ ", Chem. Phys. Lett. 10(2), 143-5 (1971).
116. Borkman, R. F., "Electric Quadrupole Moments for H_2^+ , H_2 , and H_3^+ from a Point-Charge Model", Chem. Phys. Lett. 9(6), 624-6 (1971).
117. Borisov, M. S.; Vetchinkin, S. I., "Threshold Photoionization of the H_2^+ Molecular Ion in the United Atom Model", Opt. Spektrosk. 30(3), 409-12 (1971).
118. Kawaoka, Kenji; Borkman, Raymond F., "Single-Center Calculations on the Electronically Excited States of Equilateral H_3^+ Ion", J. Chem. Phys. 54(10), 4234-8 (1971).
119. Trivedi, P. C., "Wave Functions for H_2^+ ", J. Phys. B, 4(4), 420-3 (1971).
120. Bishop, David M., "Cubic and Quartic Force Constants for H_2^+ ", J. Chem. Phys. 54(6), 2761-2 (1971).
121. Katriel, J.; Adam, Gabriel, "Exact Analytic Evaluation of the H_2^+ Force Constant", Chem. Phys. Lett. 8(2), 191-4 (1971).

1970

122. Borkowski, Jozef, "Calculations of the Photoionization Cross Section of H_2^+ from $1\sigma_g$ State by Using Some Approximate Wave Functions", Bull. Soc. Sci. Lett. Lodz, 24(3), 4 Pp. (1970).
123. Mueller, Hans, "Theoretical Study of Hydrogen Polymers. I. Calculation of the Proton Affinities of H , H_2 , and H_3^+ ", Z. Chem. 10(12), 478-9 (1970).
124. Silters, E.; Ustinov, N. N.; Yurkevich, V. E.; Bolotin, A. B., "Calculation of the Energy Spectrum and Wave Functions of the H_2^+ Ion Electron", Str. Mol. Kvantovaya Khim., 138-42. Edited by: Brodskii, A. I. "Naukova Dumka": Kiev, USSR. (1970).
125. Jasperse, J. R., "Method for One Particle Bound to Two Identical Fixed Centers: Application to H_2^+ ", Phys. Rev. A, [3]2(6), 2232-44 (1970).
126. Tunitskii, N. N.; Zhurkin, E. S.; Tikhomirov, M. V., "Effect of the Excitation of H_2^+ and D_2^+ Ions on the Cross Section of Their Dissociation During a Collision with Atoms and Molecules At 0.1-2 keV", Pis'ma Zh. Eksp. Teor. Fiz. 12(6), 312-4 (1970).
127. Weingartshofer, A.; Ehrhardt, Helmut; Hermann, V.; Linder, F., "Measurements of Absolute Cross Sections for (e, H_2) Collision Processes. Formation and Decay of H_2^- Resonances", Phys. Rev. A, [3] 2(2), 294-304 (1970).
128. Schaad, Lawrence J.; Hicks, W. V., "Equilibrium Bond Length in H_2^+ ", J. Chem. Phys. 53(2), 851-2 (1970).
129. Chang, Edward S.; Temkin, Aaron, "Rotational Excitation of Diatomic Molecular Systems. II. H_2^+ ", J. Phys. Soc. Jap. 29(1), 172-9 (1970).
130. Csizmadia, Imre G.; Kari, R. E.; Polanyi, John C.; Roach, A. C.; Robb, M. A., "Ab-initio SCF-MO-CI Calculations for H^+ , H_2 , and H_3^+ Using Gaussian Basis Sets", J. Chem. Phys. 52(12), 6205-11 (1970).
131. Burt, J. A.; Dunn, Jerry L.; McEwan, M. J.; Sutton, M. M.; Roche, A. E.; Schiff, Harold I., "Ion-Molecule Reactions of H_3^+ and the Proton Affinity of H_2 ", J. Chem. Phys. 52(12), 6062-75 (1970).
132. Beckel, Charles L.; Hansen, Bertle D. III, "Theoretical Study of H_2^+ Ground Electronic State Spectroscopic Properties", J. Chem. Phys. 53(9), 3681-90 (1970).
133. Jackson, Malcolm; McEachran, Robert P.; Cohen, Maurice, "Second-Order Perturbation Treatment of the Ground State of H_2^+ ", J. Chem. Phys. 52(1), 102-6 (1970).

1969

134. Jefferts, Keith B., "Hyperfine Structure in the Molecular Ion H_2^+ ", Phys. Rev. Lett. 23(26), 1476-7 (1969).
135. Calvert, J. McI.; Davison, William Donald, "Numerical Single-Center Calculation of the Polarizabilities of H_2^+ ", Chem. Phys. Lett. 4(6), 327-30 (1969).
136. Bishop, David M.; Macias, A., "Ab Initio Calculation of Harmonic Force Constants. II. Application to Gaussian Wavefunctions for H_2^+ ", J. Chem. Phys. 51(11), 4997-5001 (1969).
137. Temkin, Aaron; Vasavada, K. V.; Chang, Edward S.; Silver, A., "Scattering of Electrons From H_2^+ . II", Phys. Rev. 186(1), 57-66 (1969).
138. Stecher, Theodore P.; Williams, David A., "Interstellar H_2^+ Molecule", Astrophys. Lett. 4(3), 99-101 (1969).
139. Lyon, William D.; Matcha, Robert L.; Sanders, William A.; Meath, William J.; Hirschfelder, Joseph O., "Erratum: Perturbation Treatment of the Ground State of H_2^+ ", J. Chem. Phys. 51(7), 3151-2 (1969).
140. Latimer, C. J.; Browning, R.; Gilbody, H. B., "Dissociation and Charge Transfer in 1.4-46 keV $H_2^+-H_2$ Collisions", Proc. Phys. Soc., London (At. Mol. Phys.), [2]2(10), 1055-9 (1969).
141. Bochvar, D. A.; Borodzich, R. M.; Tutkevich, A. V., "Chemical Bonding and Entropy of Electron Density Distribution in Molecules. I. H_2^+ and H_2 ", Zh. Strukt. Khim. 10(3), 530-2 (1969).
142. Brandas, Erkki; Goscinski, O., "Symmetry-Adapted Second-Order Energy. Some Comments and Results for H_2^+ ", J. Chem. Phys. 51(3), 975-83 (1969).
143. Meierjohann, B.; Seibt, W., "Collision-Induced Dissociation of H_2^+ Ions Energy and Angular Dependence", Z. Phys. 225(1), 9-25 (1969).
144. Luke, S. K., "Radiofrequency Spectrum of H_2^+ ", Astrophys. J. 156(2)(Pt. 1), 761-9 (1969).
145. Radel, Stanley R.; Gorman, Ronnie; Cutler, Carol; Kahn, Luis, "Geometric-Mean Variation Function for the Hydrogen Molecular Ion H_2^+ ", J. Chem. Phys. 50(8), 3642-4 (1969).
146. Leventhal, Jacob J.; Friedman, Lewis, "Energy Transfer in the De-Excitation of H_3^+ by H_2 ", J. Chem. Phys. 50(7), 2928-31 (1969).
147. Conroy, Harold, "Molecular Schrödinger Equation. X. Potential Surfaces for Ground and Excited States of Isosceles H_3^{++} and H_3^+ ", J. Chem. Phys. 51(9), 3979-93 (1969).

148. Luke, S. K.; Hunter, G.; McEachran, Robert P.; Cohen, Maurice, "Relativistic Theory of H_2^+ ", J. Chem. Phys. 50(4), 1644-50 (1969).
149. Peek, James M., "Discrete Vibrational States Due Only to Long-Range Forces: $^2\Sigma_u^+$ ($2p\sigma_u$) State of H_2^+ ", J. Chem. Phys. 50(10), 4595-96 (1969).
150. Gersten, Joel I., "Evaluation of the Lamb Shift for the Hydrogen Molecule-Ion", J. Chem. Phys. 51(8), 3181-5 (1969).

1968

151. Dunn, Gordon H., "Photodissociation of H_2^+ and D_2^+ : Theory and Tables", Joint Inst. Lab. Astrophys., Rep. No. 92, 55 Pp. (1968).
152. Tunitskii, N. N., "Effect of the Excitation of H_2^+ And D_2^+ Ions in the Reaction in Which They Take Part", Teor. Eksp. Khim. 4(5), 695-8 (1968).
153. Winter, Nicholas Wilhelm; McKoy, Vincent, "Numerical One-Center Calculation of the ns-(σ) Rydberg Series of H_2^+ ", J. Chem. Phys. 49(10), 4728-30 (1968).
154. Bishop, David M., "Calculation of the Electric Field Gradient at the Nucleus in H_2^+ ", J. Chem. Phys. 49(8), 3718-22 (1968).
155. Burke, P. G., "Potential Energy Curves of H_2^- ", Proc. Phys. Soc., London, At. Mol. Phys. [2]1(4), 586-8 (1968).
156. Main, I. G.; Durell, J. L.; Sareen, R. A., "Search for the Formation of H_2^- Ions From 40-keV H_2^+ Ions in Hydrogen", Proc. Phys. Soc., London, At. Mol. Phys. [2] 1(4), 755-7 (1968).
157. Hayden, Howard C.; Amme, Robert C., "Vibrational Excitation Effects on Charge-Transfer Processes Involving H_2^+ and D_2^+ Between 70 and 1000 eV", Phys. Rev. 172(1), 104-9 (1968).
158. Damburgs, R.; Propin, R. Kh., "Asymptotic Expansion of the Electronic Terms of the Hydrogen Molecular Ion H_2^+ ", Latv. PSR Zinat. Akad. Vestis, Fiz. Teh. Zinat. Ser. (1), 50-9 (1968).
159. Jefferts, Keith B., "Rotational Hyperfine Structure Spectra of Hydrogen Molecular Ions", Phys. Rev. Lett. 20(2), 39-41 (1968).
160. Blicharski, Jerzy S., "Radio-Frequency Transitions and Nuclear and Electron Polarization for Hydrogen Molecular Ions H_2^+ ", Can. J. Phys. 46(7), 823-9 (1968).
161. Hughes, Raymond Hargett; Kay, David B.; Stigers, C. A.; Stokes, E. D., "Production of Hydrogen Atoms in the 3s State by the Dissociation of Fast H_2^+ and H_3^+ Projectiles on Impact with Hydrogen, Helium, Argon, and

Neon", Phys. Rev. 167(1), 26-9 (1968).

162. Neynaber, Roy H.; Trujillo, S. M., "Study of $H_2^+ + H_2 \rightarrow H_3^+ + H$ Using Merging Beams", Phys. Rev. 167(1), 63-6 (1968).
163. Richardson, C. B.; Jefferts, K. B.; Dehmelt, H. G., "Alignment of the H_2^+ Molecular Ion by Selective Photodissociation. II. Experiments on the Radio-Frequency Spectrum", Phys. Rev. 165(1), 80-7 (1968).

1967

164. Solov'ev, E. S.; Il'in, R. N.; Oparin, V. A.; Fedorenko, N. V., "Production of Highly Excited Hydrogen Molecules and Atoms by Fast H_2^+ and H_3^+ Ions Passing Through Hydrogen, Neon, and Magnesium and Sodium Vapor", Zh. Eksp. Teor. Fiz. 53(6), 1933-41 (1967).
165. Oksyuk, Yu. D., "Effect of Vibrational Excitation on the Dissociation of the Molecular Hydrogen Ion Under Electron and Proton Bombardment", Opt. Spektrosk. 23(3), 366-73 (1967).
166. Bhalla, K. C.; Khubchandani, P. G., "A Variational Function for the Ground State of H_2^+ ", Proc. Phys. Soc., London, 92(3), 529-30 (1967).
167. Dance, D. F.; Harrison, M. F. A.; Rundel, Robert D.; Smith, A. C. H., "A Measurement of the Cross Section for Proton Production in Collisions Between Electrons and H_2^+ Ions", Proc. Phys. Soc., London, 92(3), 577-8 (1967).
168. Eliezer, Isaac; Taylor, Howard S.; Williams, James Kendree, Jr., "Resonant States of H_2^+ ", J. Chem. Phys. 47(6), 2165-77 (1967).
169. McQuarrie, Donald A.; Hirschfelder, Joseph O., "Intermediate-Range Intermolecular Forces in H_2^+ ", J. Chem. Phys. 47(5), 1775-80 (1967).
170. Cohen, Maurice; McEachran, Robert P.; McPhee, Sheila D., "Approximate Molecular Orbitals. IV. The $3d_g$ and $4f_u$ States of H_2^+ ", Can. J. Phys. 45(8), 2533-42 (1967).
171. Carlson, Charles M., "Use of Linear Nonsymmetric Eigenvalue Equations for a Sum-Over-Points Approach: Application to H_2^+ ", J. Chem. Phys. 47(2), 862-3 (1967).
172. Silbey, Robert, "Perturbation of Calculation of the Energy of the First Excited State ($2p\sigma$) of H_2^+ ", J. Chem. Phys. 46(10), 4026-8 (1967).
173. Komarov, I. V.; Slavyanov, S. Yu., "Wavefunctions and Electron Terms of the H_2^+ Molecular Ion for Large Internuclear Distances", Zh. Eksp. Teor. Fiz. 52(5), 1368-77 (1967).

174. Patel, Jashbhai C., "Accurate Wavefunction of H_2^+ ", J. Chem. Phys. 47(2), 770-4 (1967).
175. Peek, James M.; Green, Thomas Allen; Weihofen, W. H., "Theory of High-Energy Inelastic Collisions Between Molecular Systems. Dissociation of H_2^+ with H_2 ", Phys. Rev. 160(1), 117-24 (1967).
176. Zare, Richard N., "Dissociation of H_2^+ by Electron Impact: Calculated Angular Distribution", J. Chem. Phys. 47(1), 204-15 (1967).
177. Henderson, Richard C.; Ebbing, Darrell D., "Calculations of Electric Field Gradients in H_2^+ and H_2 Using Single-Center Wavefunctions", J. Chem. Phys. 47(1), 69-72 (1967).
178. Adamov, M. N.; Rebane, T. K.; Evarestov, R. A., "Polarizability of the H_2^+ Ion", Opt. Spektrosk. 22(5), 709-13 (1967).
179. Doverspike, L. D.; Champion, Roy L., "Ion-Molecule Reactions of D_2^+ with D_2 and H_2 ", J. Chem. Phys. 46(12), 4718-25 (1967).
180. Leventhal, Jacob J.; Moran, Thomas F.; Friedman, Lewis, "Molecular Resonant Charge-Transfer Processes; $H_2^+-H_2$ and $N_2^+-N_2$ ", J. Chem. Phys. 46(12), 4666-72 (1967).
181. Pavlik, Philip I.; Blinder, Seymour M., "Relativistic Effects in Chemical Bonding: The H_2^+ Molecule", J. Chem. Phys. 46(7), 2749-51 (1967).
182. Peek, James M., "Theory of Dissociation of H_2^+ by Fast Electrons", Phys. Rev. 154(1), 52-6 (1967).
183. Dunn, Gordon H.; Van Zyl, Bert, "Electron Impact Dissociation of H_2^+ ", Phys. Rev. 154(1), 40-51 (1967).
184. McClure, Gordon W., "Dissociation of H_2^+ Ions in Collision with Hydrogen Atoms: 3 to 115 keV", Phys. Rev. 153(1), 182-3 (1967).
185. Lefaivre, Jean, "Energy of H_2^+ Ions by the L.C.A.O. Method", Can. J. Phys. 45(1), 228-30 (1967).
186. Hunter, G.; Pritchard, H. O., "Born-Oppenheimer Separation for Three-Particle Systems. III. Applications", J. Chem. Phys. 46(6), 2153-8 (1967).
187. Buchheit, K.; Henkes, W., "Untersuchung der Massenverteilung von Wasserstoff-Agglomerat-Ionen in Einem Massenspektrometer mit Energiezerlegung", Z Angew. Phys. 24(4), 191-6 (1967).

1966

188. Williams, James Francis; Dunbar, D. N. F., "Charge Exchange and Dissociation Cross Sections for H_1^+ , H_2^+ , and H_3^+ Ions of 2- to 50-keV Energy Incident Upon Hydrogen and the Inert Gases", Phys. Rev. 149(1), 62-9 (1966).
189. Dei-Cas, Renato; Fumelli, Michele; Girard, Jean Pierre; Prevot, Francois; Valckx, Franciscus P. G., "Dissociation of Hydrogen Molecular Ions by the Lorentz Force", Nucl. Fusion, 6(3), 212-4 (1966).
190. Dunken, Helga H.; Gottschlich, Klaus, "Relation Between Axial Electron Density and Bond Energy for Various Approximation Functions in H_2^+ ", Z. Phys. Chem. (Leipzig), 233(3-4), 231-6 (1966).
191. Bottiglioni, Franco; Coutant, Jacques; Gadda, Erio, "Dissociation of H_2^+ and H_3^+ in a Lithium Plasma", J. Phys. (Orsay, Fr.), 27(9-10), 599-604 (1966).
192. Dutton, J.; Llewellyn-Jones, Frank; Rees, Walter D.; Williams, Edward Malcolm, "Motion of Slow Positive Ions in Gases. IV. Drift and Diffusion of Ions in Hydrogen", Philos. Trans. R. Soc. London, Ser. A, 259(1100), 339-54 (1966).
193. Valckx, Franciscus P. G.; Verveer, Philippe, "Vibrational Dissociation and Cascade Dissociation of H_2^+ Ions by Collisions with Gas Molecules", J. Phys. (Orsay, Fr.), 27(7-8), 480-4 (1966).
194. Cohen, Maurice; Dorrell, Brenda H.; McEachran, Robert P., "Approximate Molecular Orbitals. II. The $2p\pi_u$ and $3d\pi_g$ States of H_2^+ ", Can. J. Phys. 44(11), 2827-38 (1966).
195. Cohen, Maurice; McEachran, Robert P., "Approximate Molecular Orbitals. I. The $1s\sigma_g$ and, $2p\sigma_u$ States of H_2^+ ", Can. J. Phys. 44(11), 2809-25 (1966).
196. Nielsen, Svend E.; Dahler, John S., "Theory of the Dissociative Recombination and Associative Ionization of Hydrogen", J. Chem. Phys. 45(11), 4060-79 (1966).

Section II: H_3^+ (and H_3^-)

1987

1. Okumura, M; Yeh, L. I.; Lee, Y. T., "Infrared Spectroscopy of the Cluster Ions $H_3^+ \cdot (H_2)_n$ ", preprint, submitted to Journal of Chemical Physics.
2. Berblinger, Michael; Schlier, Christoph, "Classical Radiation Spectra of Long-Lived H_3^+ Complexes, preprint.
3. Le Coz, Georges; Tuffin, Firmin, "A Study of a Collision Process Creating Molecular Ions of Hydrogen (H_3^+) and Deuterium (D_3^+)", C. R. Acad. Sci. Ser. 2, 304(8), 295-300 (1987).
4. Schlier, Christoph G.; Vix, Ulrike, "Complex Formation in Proton-Hydrogen Collisions. II. Isotope Effects", Chem. Phys. 113, 211-21 (1987).
5. Mitchell, J. B. A., "The Role of Electron-Ion Recombination in Bulk Antimatter Production", Proc. Cooling, Condensation, and Storage of Hydrogen Cluster Ions Workshop, 1/8-9/87, 143-56. Edited by John T. Bahns. University of Dayton Research Institute (1987).
6. Bahns, J. T., "Key Problems and Hydrogen Atom Formation", Proc. Cooling, Condensation, and Storage of Hydrogen Cluster Ions Workshop, 1/8-9/87, 219-30. Edited by John T. Bahns. University of Dayton Research Institute (1987).
7. Bahns, J. T.; Sando, K. M.; Tardy, D. C.; Stwalley, W. C., "Proceedings of the Hydrogen Cluster Ion Study Group", Proc. Cooling, Condensation, and Storage of Hydrogen Cluster Ions Workshop, 1/8-9/87, A1-64. Edited by John T. Bahns. University of Dayton Research Institute (1987).
8. Niedner, G.; Noll, M.; Toennies, J. P.; Schlier, Ch., "Observation of Vibrationally Resolved Charge Transfer in $H^+ + H_2$ at $E_{CM} = 20$ eV", J. Chem. Phys. 87(5), 2685-94 (1987).
9. Crofton, M., "Infrared Spectroscopy of H_3^+ ", Proc. Cooling, Condensation, and Storage of Hydrogen Cluster Ions Workshop, 1/8-9/87, 119-24. Edited by John T. Bahns. University of Dayton Research Institute (1987).
10. Bowers, M. T., "Formation and Reactivity of Small Hydrogen Cluster Ions", Proc. Cooling, Condensation, and Storage of Hydrogen Cluster Ions Workshop, 1/8-9/87, 61-72. Edited by John T. Bahns. University of Dayton Research Institute (1987).
11. Saxon, R., "Overview of Hydrogen Clusters", Proc. Cooling, Condensation, and Storage of Hydrogen Cluster Ions Workshop, 1/8-9/87, 27-37. Edited by John T. Bahns. University of Dayton Research Institute (1987).

12. Johnson, B. R., "Semiclassical Vibrational Eigenvalues of H_3^+ , D_3^+ , and T_3^+ by the Adiabatic Switching Method", J. Chem. Phys. 86(3), 1445-50 (1987).
13. Michels, H. H.; Montgomery, J. A. Jr., "The Electronic Structure and Stability of the H_3^- Anion", Chem. Phys. Lett. 139(6), 535-9 (1987).
14. Hamilton, I., "Vibrational Spacings for H_3^+ ", J. Chem. Phys. 87(1), 774-6 (1987).

1986

15. Vojtik, Jan; Spirko, Vladimir; Jensen, Per, "Vibrational Energies of H_3^+ and Li_3^+ Based on Diatomics-in-Molecules Potentials", Collect. Czech. Chem. Commun. 51(10), 2057-62 (1986).
16. Tennyson, Jonathan; Sutcliffe, Brian T., "The Infrared Spectrum of H_3^+ and Its Isotopomers. A Challenge to Theory and Experiment", J. Chem. Soc., Faraday Trans. 2, 82(8), 1151-62 (1986).
17. Child, M. S., "Semiclassical Method for the Determination of Narrow Multichannel Resonances: Application to Hydrogen Molecular Ion (H_3^+)", J. Phys. Chem. 90(16), 3595-9 (1986).
18. Pan, Fu Shih; Oka, Takeshi, "Calculated Forbidden Rotational Spectra of the Hydrogen Ion (H_3^+)", Astrophys. J. 305(1, Pt. 1), 518-25 (1986).
19. Miao, Jingwei; Yang Beifang; Hao, Shizuho; Jiang, Zengxue; Shi, Miangong; Cue, N., "Internuclear Separations From Foil Breakup of Fast H_2^+ , H_3^+ , D_2^+ and D_3^+ Molecules", Nucl. Instrum. Methods Phys. Res. Sect. B, B13(1-3), 181-3 (1986).
20. Sen, A.; Mitchell, J. B. A., "Production of Vibrationally Cold Ions Using a Radio-Frequency Storage Ion", Rev. Sci. Instrum. 57(5), 754-6 (1986).
21. Helm, Hanspeter, "Observation of High-n Rydberg Series ($7 < n < 49$) of the H_3 Molecule", Phys. Rev. Lett. 56(1), 42-5 (1986).
22. Foster, S. C.; McKellar, A. R. W.; Peterkin, I. R.; Watson, J. K. G.; Pan, F. S.; Crofton, M. W.; Altman, R. S.; Oka, T., "Observation and Analysis of the ν_2 and ν_3 Fundamental Bands of the H_2D^+ Ion", J. Chem. Phys. 84(1), 91-9 (1986).
23. J. B. A. Mitchell, "Dissociative Recombination of Molecular Ions", 185-222, Atomic Processes in Electron-Ion and Ion-Ion Collisions, Edited by F. Brouillard, Plenum Publishing Corp. (1986).
24. Sen, Amarjit; Mitchell, J. B. A., "Production of H_3^+ Ions with Low Internal Energy for Studies of Dissociative Recombination", J. Phys. B: At. Mol. Phys. 19, L545-9 (1986).

1985

25. Tokoro, N.; Oda, N., "Energy and Angular Distributions of Ejected Electrons for Hydrogen-Cluster-Ion (H_n^+ , D_n^+ , $n=1-3$) Impacts on Helium in the Intermediate Energy Region", J. Phys. B: At. Mol. Phys. 18, 1771-80 (1985).
26. Spirko, V.; Jensen, Per; Bunker, P. R.; Cejchan, A., "The Development of a New Morse-Oscillator Based Rotation-Vibration Hamiltonian for H_3^+ ", J. Mol. Spectrosc. 112, 183-202 (1985).
27. Shpirko, V., "Vibration-Rotation Hamiltonian of X_3 Type Molecules in Internal Coordinates. Vibrational Spectrum of Hydrogen (H_3^+) Molecule", Aktual. Probl. Spektroskopii. Materialy Simp. Uchenykh Sots. Stran po Nov. Probl. Spektroskopii, Moskva, 18-22 Uyunya, 1984, M. 26-9 From: Ref. Zh., Fiz. (A-Zh.) 1985, Abstr. No. 8D65 (1985).
28. Adams, N. G.; Smith, D., "Dissociative Recombination of Triatomic Hydrogen Cation (H_3^+), Oxomethylum, Nitrogen Hydride (N_2H^+) and Monoprotonated Methane (CH_5^+)", NATO ASI Ser., Ser. C, 157(Mol. Astrophys.), 657-9 (1985).
29. Tennyson, Jonathan; Sutcliffe, Brian T., "A Calculation of the Rovibrational Spectra of the H_3^+ , H_2D^+ and D_2H^+ Molecules", Mol. Phys. 56(5), 1175-83 (1985).
30. Levin, F. S.; Shertzer, J., "Channel-Coupling Array Analysis of Electron Correlation in Hydrogen Molecular Ion (H_3^+)", Phys. Rev. A: Gen. Phys. 32(4), 2062-7 (1985).
31. Phillips, T. G.; Blake, Geoffrey A.; Keene, Jocelyn; Woods, R. Claude; Churchwell, E., "Interstellar Hydrogen Ion (H_3^+): Possible Detection of the $1_{10} \rightarrow 1_{11}$ Transition of H_2D^+ ", Astrophys. J. 294(1, Pt. 2), L45-8 (1985).
32. Amano, T., "Difference-Frequency Laser Spectroscopy of Molecular Ions with a Hollow-Cathode Cell: Extended Analysis of the ν_1 Band of H_2D^+ ", J. Opt. Soc. Am. B 2(5), 790-3 (1985).
33. Saito, Shuji; Kawaguchi, Kentarou; Hirota, Eizi, "The Microwave Spectrum of the H_2D^+ Ion; The $2_{20} \leftarrow 2_{21}$ Transition", J. Chem. Phys. 82(1), 45-7 (1985).
34. Okumura, M; Yeh, L. I.; Lee, Y. T., "The Vibrational Predissociation Spectroscopy of Hydrogen Cluster Ions", J. Chem. Phys., 83(7), 3705-6 (1985).

35. Amano, T.; Watson, J. K. G.; "Observation of the ν_1 Fundamental Band of H_2D^+ ", J. Chem. Phys. 81(7), 2869-71 (1984).
36. Watson, J. K. G.; Foster, S. C.; McKellar, A. R. W.; Bernath, P.; Amano, T.; Pan, F. S.; Crofton, M. W.; Altman, R. S.; Oka, T., "The Infrared Spectrum of the ν_2 Fundamental Band of the Hydrogen (H_3^+) Molecular Ion", Can. J. Phys. 62(12), 1875-85 (1984).
37. Mitchell, J. B. A.; Ng, C. T.; Forand, L.; Janssen, R.; McGowan, J. William, "Total Cross Sections for the Dissociative Recombination of Hydrogen (H_3^+), Hydrogen-Deuterium (HD_2^+) and Deuterium (D_3^+)", J. Phys. B, 17(24), L909-13 (1984).
38. Preiskorn, Aleksandra; Woznicki, Wieslaw, "Variational Calculations for the Ground State of Triatomic Hydrogen Ion (H_3^+)", Mol. Phys. 52(6), 1291-301 (1984).
39. Adams, Nigel G.; Smith, David; Alge, Erich, "Measurements of Dissociative Recombination Coefficients of H_3^+ , HCO^+ , N_2H^+ , and CH_5^+ at 95 and 300 K Using the FALP Apparatus", J. Chem. Phys. 81(4), 1778-84 (1984).
40. Eaker, Charles W.; Schatz, George C., "Semiclassical Vibrational Eigenvalues of Triatomic Molecules: Application of the FFT Method to Sulfur Dioxide, Water, Hydrogen Ion (H_3^+) and Carbon Dioxide", J. Chem. Phys. 81(5), 2394-9 (1984).
41. Carrington, Alan; Kennedy, Richard A., "Infrared Photodissociation Spectrum of the Hydrogen (H_3^+) Ion", J. Chem. Phys. 81(1), 91-112 (1984).
42. MacDonald, Jeffrey A.; Biondi, Manfred A.; Johnsen, Rainer, "Recombination of Electrons with Hydrogen (H_3^+ and H_5^+) Ions", Planet. Space Sci. 32(5), 651-4 (1984).
43. Burton, P. G.; Von Nagy-Felsobuki, E.; Doherty, G.; Hamilton, M., "Vibration Spectrum of Triatomic Hydrogen Ion (H_3^+): A Model Hamiltonian", Chem. Phys. 83(1-2), 83-8 (1984).
44. Bae, Y. K.; Coggiola, M. J.; Peterson, J. R., "Search for H_2^- , H_3^- , and Other Metastable Negative Ions", Phys. Rev. A, 29(5), 2888-90 (1984).
45. Warner, H. E.; Conner, W. T.; Petrnmichl, R. H.; Lemoine, B., "Laboratory Detection of the $1_{10} \rightarrow 1_{11}$ Submillimeter Wave Transition of the H_2D^+ Ion", J. Chem. Phys. 81(5), 2514 (1984).
46. Bogey, M.; Demuynck, C.; Denis, M.; Destombes, J. L.; Lemoine, B., "Laboratory Measurement of the $1_{10} - 1_{11}$ Submillimeter Line of H_2D^+ ", Astron. Astrophys. 137(2), L15-6 (1984).

47. Lubic, Karen G.; Amano, T., "Observation of the ν_1 Fundamental Band of D_2H^+ ", Can. J. Phys. 62(12), 1886-8 (1984).
48. Kutina, R. E.; Edwards, A. K.; Pandolf, R. S.; Berkowitz, J., "UV Laser Photodissociation of Molecular Ions", J. Chem. Phys. 80(9), 4112-9 (1984).

1983

49. Gellene, Gregory I.; Porter, Richard F., "Experimental Observations of Excited Dissociative and Metastable States of Triatomic Hydrogen Radical (H_3) in Neutralized Ion Beams", J. Chem. Phys. 79(12), 5975-81 (1983).
50. Oka, Takeshi, "The Hydrogen (H_3^+) Ion", Mol. Ions: Spectrosc., Struct. Chem., 73-90. Edited by: Miller, Terry Alan; Bondybey, Vladimir E. North-Holland: Amsterdam, Neth. (1983).
51. Mitchell, J. B. A.; Forand, J. L.; Ng, C. T.; Levac, D. P.; Mitchell, R. E.; Mul, P. M.; Claeys, W.; Sen, A.; McGowan, J. William, "Measurement of the Branching Ratio for the Dissociative Recombination of Triatomic Hydrogen (H_3^+) + Electron", Phys. Rev. Lett. 51(10), 885-8 (1983).
52. Gaillard, M. J.; De Pinho, A. G.; Poizat, J. C.; Remillieux, J.; Saoudi, R., "Experimental Study of the Triatomic Hydrogen Molecule Through the Collisional Sequence $H_3^+ \rightarrow H_3 \rightarrow H_3^+$ Undergone by Fast Beams in Argon", Phys. Rev. A, 28(3), 1267-75 (1983).
53. Yamaguchi, Yukio; Gaw, Jeffrey F.; Schaefer, Henry F., III, "Molecular Clustering about a Positive Ion. Structures, Energetics, and Vibrational Frequencies of the Protonated Hydrogen Clusters H_3^+ , H_5^+ , H_7^+ , and H_9^+ ", J. Chem. Phys. 78(6, Pt. 2), 4074-85 (1983).
54. Montgomery, D. L.; Jaecks, D. H., "Three-Body Dissociation of H_3^+ ", Phys. Rev. Lett. 51(20), 1862-4 (1983).
55. Elford, M. T., "The Heat of Dissociation of H_5^+ Derived from Measurements of Ion Mobilities", J. Chem. Phys. 79(12) 5951-9 (1983).
56. Hirao, K; Yamabe, S., "Theoretical Study on the Structure and Stability of Hydrogen Ion Clusters H_n^+ and H_n^- ($n = 3, 5, 7, 9, 11, 13$)", Chem. Phys. 80, 237-43 (1983).

1982

57. Poluyanov, L. V., "One Model of High Single-Electron Excitations in the Hydrogen Ion (H_3^+)", Zh. Strukt. Khim. 23(1), 16-21 (1982).

1981

58. Rayez, J. C.; Rayez-Meaume, M. T.; Massa, L. J., "Theoretical Study of the Hydride (H_3^-) Cluster", J. Chem. Phys. 75(11), 5393-7 (1981).
59. Adams, N. G.; Smith, D., "A Laboratory Study of the Reaction $H_3^+ + HD = H_2D^+ + H_2$: The Electron Densities and the Temperatures in Interstellar Clouds", Astrophys. J. 248(1, Pt. 1), 373-9 (1981).
60. Goh, S. C.; Swan, J. B., "Collisional Dissociation and the Binding Energy of Hydrogen Molecular Ion (H_3^+)", Phys. Rev. A, 24(3), 1624-5 (1981).
61. Sataka, Masao; Shirai, Toshizo; Kikuchi, Akira; Nakai, Yohta, "Ionization Cross Sections for Ion-Atom and Ion-Molecule Collisions. I. Ionization Cross Sections for Hydrogen and Helium Ions H^+ , H_2^+ , H_3^+ , He^+ and He^{++} Incident on H, H_2 , and He", Nippon Genshiryoku Kenkyusho, [Rep.] JAERI-M, JAERI-M-9310, 65 Pp. (1981).
62. Shy, J.-T.; Farley, John W.; Wing, William H., "Observation of the Infrared Spectrum of the Triatomic Molecular Ion H_2D^+ ", Phys. Rev. A (24(2), 1146-9 (1981).

1980

63. Carney, Grady D., "Rotation Energies for Deuterated Hydrogen (H_3^+) Oscillators in Zero-Point States of Vibration", Chem. Phys. 54(1), 103-7 (1980).
64. Oka, Takeshi, "Observation of the Infrared Spectrum of H_3^+ ", Phys. Rev. Lett. 45(7), 531-4 (1980).
65. Carney, G. D.; Porter, R. N., "Ab Initio Prediction of the Rotation-Vibration Spectrum of H_3^+ and D_3^+ ", Phys. Rev. Lett. 45(7), 537-41 (1980).
66. Kyrala, George A.; Tolliver, David E.; Wing, William H., "Production of H_3^+ , HeH^+ and He_2^+ Ion Beams Using a Coaxial Electron-Impact Ion Source", Int. J. Mass Spectrom. Ion Phys. 33(4), 367-82 (1980).
67. Anderson, S. L.; Hirooka, T.; Tiedemann, P. W.; Mahan, B. H.; Lee, Y. T., "Photoionization of Hydrogen [$(H_2)_2$] and Clusters of Oxygen Molecules", J. Chem. Phys. 73(10), 4779-83 (1980).
68. Huber, B. A.; Schulz, U.; Wiesemann, K., "Cross Sections for Slow Ion Production and Charge Transfer in $H_3^+(D_3^+)-H_2(D_2)$ Collisions", Phys. Lett. A, 79A(1), 58-60 (1980).
69. Oda, Nobuo; Urakawa, Junji; Tokoro, Nobuhiro; Nojiri, Hiroshi, "Ionizing Collisions of Hydrogen Cluster Ions (H^+ , H_2^+ , H_3^+) of Intermediate Energies with Gases", Iongen to Sono Oyo, Shinpojumu, 4th, 205-8. Ion Kogaku Kon-

dankai: Kyoto, Japan. (1980).

70. Koyano, Inosuke; Tanaka, Kenichiro, "State-Selected Ion-Molecule Reactions by a Threshold Electron-Secondary Ion Coincidence (TESICO) Technique. I. Apparatus and the Reaction $H_2^+ + H_2 \rightarrow H_3^+ + H$ ", J. Chem. Phys. 72(9), 4858-68 (1980).
71. Shy, J.-T.; Farley, J. W.; Lamb, Willis E. Jr.; Wing, William H., "Observation of the Infrared Spectrum of the Triatomic Deuterium Molecular Ion D_3^+ ", Phys. Rev. Lett. 45(7), 535-7 (1980).
72. Carney, G. D., "Refinements in the Vibrations Frequencies of H_3^+ and D_3^+ ", Mol. Phys. 39(4) 923-33 (1980).

1979

73. Dyachenko, G. G.; Nemukhin, A. V.; Stepanov, N. F., "Approximation of Potential Surfaces and Solution of a Vibration Problem for the Molecular Hydrogen Ion (H_3^+)", Vestn. Mosk. Univ., Ser. 2: Khim. 20(5), 416-22 (1979).
74. Hirao, Kimihiko; Yamabe, Shinichi, "Structure and Stability of Cluster Ions H_n^+ ($n=3,5,7,9,11$)", Koen Yoshishu - Bunshi Kozo Sogo Toronkai, Siga Med. Coll., Ohtsu, Japan, Chem. Soc. Japan, 260-1 (1979).
75. Dykstra, Clifford E.; Swope, William C., "The Hydrogen Ion (H_3^+) Potential Surface", J. Chem. Phys. 70(1), 1-3 (1979).
76. Hirooka, Tomohiko; Anderson, Scott L.; Tiedemann, Peter W.; Mahan, Bruce H.; Lee, Yuan T., "Photoionization of Molecular Hydrogen Dimer (H_2)₂", Koen Yoshishu - Bunshi Kozo Sogo Toronkai, 64-5. Chem. Soc. Japan: Tokyo, Japan. (1979).
77. Garcia, R.; Rossi, A.; Russek, A., "Dissociating States of the H_3^- System", J. Chem. Phys. 70(12), 5463-7 (1979).
78. Bader, Richard F. W.; Nguyen-Dang, T. Tung; Tal, Yoram, "Quantum Topology of Molecular Charge Distributions. II. Molecular Structure and its Change", J. Chem. Phys. 70(9) 4316-29 (1979).

1978

79. Saute, Marcel; Laforgue, Alexandre, "Correlation, Ionization, and Attachment Operators Studied as an Example of Triatomic Hydrogen and H_3^+ Complexes in a Diagrammatic Method Extended to Open Shell Systems", J. Chim. Phys. Phys.-Chim. Biol. 75(7-8), 679-88 (1978).
80. Gaillard, M. J.; Gemmell, D. S.; Goldring, G.; Levine, I.; Pietsch, W.

J.; Poizat, J. C.; Ratkowski, A. J.; Remillieux, J.; Vager, Z.; Zabransky, B. J., "Experimental Determination of the Structure of Hydrogen Ion (H_3^+)", Phys. Rev. A, 17(6), 1797-803 (1978).

81. Siegbahn, P.; Liu, B., "An Accurate Three-Dimensional Potential Energy Surface for H_3 ", J. Chem. Phys. 68(5), 2457-65 (1978).
82. Dykstra, Clifford E.; Gaylord, Arthur S.; Gwinn, William D.; Swope, William C.; Schaefer, Henry F. III, "The Uncoupled Symmetric Stretching Frequency of H_3^+ ", J. Chem. Phys. 68(8), 3951-2 (1978).
83. Yamabe, S.; Mirao, K.; Kitaura, K., "Theoretical Study on the Stability and the Structure of H_n^+ ($n = 3, 5, 7, 9, 11$)", Chem. Phys. Lett. 56(3), 546-8 (1978).
84. Bardo, Richard D.; Wolfsberg, Max, "The Adiabatic Correction for Nonlinear Triatomic Molecules: Techniques and Calculations", J. Chem. Phys. 68(6) 2686-95 (1978).
85. Stine, J. R.; Muckerman, J. T., "Charge Exchange and Chemical Reaction in the $H_2^+ + H_2$ System. I. Characterization of the Potential Energy Surfaces and Nonadiabatic Regions", J. Chem. Phys. 68(1), 185-94 (1978).

1977

86. Lupu, D.; Bucur, R. V., "Properties Suggesting H_3^+ -Type Clusters in Some Metallic Hydrides", J. Phys. Chem. Solids, 38(4), 387-91 (1977).
87. Gentry, W. Ronald; Ringer, Geoffrey, "On the Possibility That Electronically Excited Products May Be Formed in the Reaction $H_2^+ + H_2 \rightarrow H_3^+ + H$ ", J. Chem. Phys. 67(11), 5398-9 (1977).
88. Douglass, Charles H.; McClure, Donald J.; Gentry, W. Ronald, "The Dynamics of the Reaction $H_2^+ + H_2 \rightarrow H_3^+ + H$, with Isotopic Variations", J. Chem. Phys. 67(11), 4931-40 (1977).
89. Malkhasyan, R. T.; Zhurkin, E. S.; Tunitskii, N. N., "Excitation of Hydrogen Ions (H_3^+) and Dependence of the Cross Section of the Secondary Ionic-Molecular Reaction $H_3^+ + Ar \rightarrow ArH^+ + H_2$ on Excitation Energy of the H_3^+ Ion", Khim. Vys. Energ. 11(6), 400-2 (1977).
90. Hyatt, D.; Careless, P. N.; Stanton, L., "A Simple Ab-initio Potential Surface for the Reaction $H_3^+(H_2, H_2)H_3^+$ in C_{2v} Symmetry", Int. J. Mass Spectrom. Ion Phys. 23(1), 45-50 (1977).
91. Ahlrichs, Reinhart; Votava, Christian; Zirz, Constantin, "Comment: The Bound $^3\Sigma_u^+$ Excited Level of H_3^+ ", J. Chem. Phys. 66(6), 2771-2 (1977).
92. Auerbach, D.; Cacak, R.; Caudano, R.; Gaily, T. D.; Deyser, C. J.; Mc-

Gowan, J. Wm.; Mitchell, J. B. A.; Wilk, S. F. J., "Merged Electron-Ion Beam Experiments I. Method and Measurements of $(e-H_2^+)$ and $(e-H_3^+)$ Dissociative-Recombination Cross Sections", J. Phys. B: Atom. and Molec. Phys. 10(18), 3797-820 (1977).

1976

93. Orient, O. J., "Study of Plasma-Produced Hydrogen (H_3^+) Ions During the Decay Period in Helium-Hydrogen Mixtures", J. Phys. B, 9(15), 2731-6 (1976).
94. Alvarez, Ignacio; Cisneros, Carmen; Barnett, C. F.; Ray, J. A., "Negative-Ion Formation From Dissociative Collisions of H_2^+ , H_3^+ , and HD_2^+ in Molecular Hydrogen, Helium, and Xenon", Phys. Rev. A, 14(2), 602-7 (1976).
95. Vestal, M. L.; Blakley, C. R.; Ryan, P. W.; Futrell, J. H., "Crossed-Beam Study of the Reaction $H_3^+(D_2, H_2)D_2H^+$ ", J. Chem. Phys. 64(5), 2094-111 (1976).
96. Carney, G. D.; Porter, R. N., " H_3^+ : Ab Initio Calculation of the Vibration Spectrum", J. Chem. Phys. 65(9), 3547-65 (1976).
97. Johnsen, Rainer; Huang, Chou-Mou; Biondi, Manfred A., "Three-Body Association Reactions of H^+ and H_3^+ Ions in Hydrogen from 135 to 300 K", J. Chem. Phys. 65(4), 1539-41 (1976).

1975

98. Lees, A. B.; Rol, P. K., "Merging Beams Study of the H_3^+ System", C. R. - Symp. Int. Jets Mol. 5th, Paper No. D₃, 8 Pp.. Com. Int. Jets Mol., C/o Dr. F. Marcel Devienne: Peymeinade, Fr. (1975).
99. Anderson, James B., "Random-Walk Simulation of the Schroedinger Equation. Hydrogen Ion (H_3^+)", J. Chem. Phys. 63(4), 1499-503 (1975).
100. Hiraoka, K.; Kebarle, P., "Temperature Dependence of Third Order Ion Molecule Reactions. Reaction $H_3^+ + 2H_2 = H_5^+ + H_2$ ", J. Chem. Phys. 63(2), 746-9 (1975).
101. Hiraoka, K.; Kebarle, P., "Determination of the Stabilities of H_5^+ , H_7^+ , H_9^+ , and H_{11}^+ From Measurement of the Gas Phase Ion Equilibria $H_n^+ + H_2 = H_{n+2}^+$ ($n = 3, 5, 7, 9$)", J. Chem. Phys. 62(6), 2267-70 (1975).
102. Aberth, W.; Schnitzer, R.; Anbar, M., "Observations of the Diatomic and Triatomic Hydrogen Negative Ions", Phys. Rev. Lett. 34(26), 1600-3 (1975).

1974

103. Elford, M. T.; Milloy, H. B., "Mobility of H_3^+ and H_5^+ Ions in Hydrogen and the Equilibrium Constant for the Reaction $H_3^+ + 2H_2 = H_5^+ + H_2$ at Gas Temperatures of 195, 273, and 293 K", Aust. J. Phys. 27(6), 795-811 (1974).
104. Peart, B.; Dolder, K. T., "Measurements of the Dissociative Recombination of Hydrogen (H_3^+) Ions", J. Phys. B, 7(14), 1948-52 (1974).
105. Lees, A. B.; Rol, P. K., "Merging Beams Study of the $H_2^+(H_2, H)H_3^+$, $H_2^+(D_2, H)HD_2^+$, and $D_2^+(H_2, H)HD_2^+$ Reaction Mechanisms", J. Chem. Phys. 61(11), 4444-9 (1974).
106. Schaad, L. J.; Hicks, W. V., "Gaussian Basis Configuration Interaction Calculations on Twenty Electronic States of H_3^+ . A Bound $^3\Sigma_u^+$ Excited Level", J. Chem. Phys. 61(5), 1934-42 (1974).

1973

107. Bauschlicher, Charles W. Jr.; O'Neil, Stephen V.; Preston, Richard K.; Schaefer, Henry F. III, "Avoided Intersection of Potential Energy Surfaces: The ($H^+ + H_2$, $H + H_2^+$) System", J. Chem. Phys., 59(3), 1286-92 (1973).

1972

108. Leu, Ming-Taun, "Recombination of Electrons with Positive Ions of the Type H_3^+ , H_5^+ , $H_3O^+ \cdot (H_2O)_n$, and HCO^+ at Thermal Energies", 79 Pp. Avail. Univ. Microfilms, Ann Arbor, Mich., Order No. 73-13,190 From: Diss. Abstr. Int. B 1973, 33(12)(Pt. 1), 5998 (1972).
109. Patch, R. W., "Observability of the H_3^+ Fundamental Spectrum", J. Chem. Phys. 57(6), 2594-5 (1972).
110. Huang, Jan-Tsyu J., "Analytical Self-Consistent-Field Energy Expression for Ground-State H_3^+ Ion", J. Chem. Phys. 56(6), 3176-7 (1972).

1971

111. Huang, Jan-Tsyu J., "Simple Diatomics-in-Molecules Energy Expression for M_3^+ and Its Application to H_3^+ ", J. Chem. Phys. 55(10), 5136-7 (1971).
112. Kawaoka, Kenji; Borkman, Raymond F., "Electric, Magnetic, and Spectral Properties of H_3^+ Ground State Calculated From Single-Center Wave Functions", J. Chem. Phys. 55(9), 4637-41 (1971).

113. Middleton, C. R.; Payne, M. F.; Riviere, A. C., "Dissociation of H_3^+ Ions at 410, 510, and 550 keV in Molecular Hydrogen Gas", J. Phys. B, 4(10), L88-L91 (1971).
114. Duben, Anthony J.; Lowe, John P., "Correlation Studies on H_3^+ . II. Electron Densities and Expectation Values", J. Chem. Phys. 55(9), 4276-82 (1971).
115. Duben, Anthony J.; Lowe, John P., "Correlation Studies on H_3^+ . I. Wave Functions", J. Chem. Phys. 55(9), 4270-5 (1971).
116. Huntress, W. T., Jr., "Ion Cyclotron Resonance Power Absorption. Collision Frequencies for CO_2^+ , N_2^+ , and H_3^+ Ions in Their Parent Gases", J. Chem. Phys. 55(5), 2146-55 (1971).
117. Preston, Richard K.; Tully, John C., "Effects of Surface Crossing in Chemical Reactions: The H_3^+ System", J. Chem. Phys. 54(10), 4297-304 (1971).
118. Borkman, R. F., "Electric Quadrupole Moments for H_2^+ , H_2 , and H_3^+ from a Point-Charge Model", Chem. Phys. Lett. 9(6), 624-6 (1971).
119. Kawaoka, Kenji; Borkman, Raymond F., "Single-Center Calculations on the Electronically Excited States of Equilateral H_3^+ Ion", J. Chem. Phys. 54(10), 4234-8 (1971).

1970

120. Duben, Anthony J., "First Order Density Matrices From Configuration Interaction Wavefunctions for H_3^+ ", 138 Pp. Avail. Univ. Microfilms, Ann Arbor, Mich., Order No. 71-16,594 From: Diss. Abstr. Int. B 1971, 32(1), 152 (1970).
121. Stecher, Theodore P.; Williams, David Arnold, "Interstellar H_3^+ ", Astrophys. Lett. 70(1), 59-60 (1970).
122. Sumin, L. V.; Gur'ev, M. V., "Mechanism of Ion-Molecular Reactions of the Formation of H_3^+ in Hydrogen and CD_5^+ in Deuteriomethane", Dokl. Akad. Nauk SSSR, 193(4), 858-61 [Phys Chem] (1970).
123. Borkman, Raymond F., "Single-Center Configuration-Interaction Calculations on the Ground State of H_3^+ ", J. Chem. Phys. 53(8), 3153-60 (1970).
124. Somorjai, R. L.; Yue, C. P., "Integral Transform Gaussian Wave Functions for H_3^{2+} and H_3^+ ", J. Chem. Phys. 53(5), 1657-61 (1970).
125. Mueller, Hans, "Theoretical Study of Hydrogen Polymers. I. Calculation of the Proton Affinities of H, H_2 , and H_3^+ ", Z. Chem. 10(12), 478-9 (1970).

126. Csizmadia, Imre G.; Kari, R. E.; Polanyi, John C.; Roach, A. C.; Robb, M. A., "Ab-initio SCF-MO-CI Calculations for H^- , H_2 , and H_3^+ Using Gaussian Basis Sets", J. Chem. Phys. 52(12), 6205-11 (1970).

127. Burt, J. A.; Dunn, Jerry L.; McEwan, M. J.; Sutton, M. M.; Roche, A. E.; Schiff, Harold I., "Ion-Molecule Reactions of H_3^+ and the Proton Affinity of H_2 ", J. Chem. Phys. 52(12), 6062-75 (1970).

1969

128. Leventhal, Jacob J.; Friedman, Lewis, "Energy Transfer in the De-Excitation of H_3^+ by H_2 ", J. Chem. Phys. 50(7), 2928-31 (1969).

129. Preuss, H.; Janoschek, R., "Wave-Mechanical Calculations on Molecules Taking all Electrons into Account", J. Mol. Structure 3, 423-8 (1969).

130. Conroy, Harold, "Molecular Schrödinger Equation. X. Potential Surfaces for Ground and Excited States of Isosceles H_3^{++} and H_3^+ ", J. Chem. Phys. 51(9), 3979-93 (1969).

131. Poshusta, R. D.; Haugen, J. A., "Ab Initio Predictions for Very Small Ions", J. Chem. Phys. 51(8), 3343-51 (1969).

1968

132. Joshi, Bhairav D.; Anand, S. C., "Overlap Matrix Elements and Related Integrals Involving R_{12}^k -Type Correlation Function for H_3^+ in One-Center Expansion Approximation", Indian J. Pure Appl. Phys. 6(12), 656-64 (1968).

133. Macias, A., "Configuration-Interaction Study of the H_3 -System. II. Expanded Basis", J. Chem. Phys. 49(5), 2198-209 (1968).

134. Albritton, D. L.; Miller, T. M.; Martin, D. W.; McDaniel, E. W., "Mobilities of Mass-Identified H_3^+ and H^+ Ions in Hydrogen", Phys. Rev. 171(1), 94-102 (1968).

135. Macias, A., "Configuration-interaction Study of the H_3 System. I. 1s Orbitals", J. Chem. Phys. 48(8), 3464-8 (1968).

136. Wu, Ay-Ju A.; Ellison, Frank O., "Method of Diatomics-in-Molecules. VII. Excited Singlet States of H_3^+ ", J. Chem. Phys. 48(4), 1491-6 (1968).

137. Christoffersen, Ralph E.; Shull, Harrison, "Nature of the Two-Electron Chemical Bond. VII. Multicenter Bonds and H_3^+ ", J. Chem. Phys. 48(4), 1790-7 (1968).

138. Hughes, Raymond Hargett; Kay, David B.; Stigers, C. A.; Stokes, E. D., "Production of Hydrogen Atoms in the 3s State by the Dissociation of Fast H_2^+ and H_3^+ Projectiles on Impact with Hydrogen, Helium, Argon, and Neon", Phys. Rev. 167(1), 26-9 (1968).
139. Neynaber, Roy H.; Trujillo, S. M., "Study of $H_2^+ + H_2 \rightarrow H_3^+ + H$ Using Merging Beams", Phys. Rev. 167(1), 63-6 (1968).
140. Hopkinson, A. C.; Holbrook, N. K.; Yates, K.; Csizmadia, I. G., "Theoretical Study on the Proton Affinity of Small Molecules Using Gaussian Basis Sets in the LCAO-MO-SCF Framework", J. Chem. Phys. 49(8), 3596-601 (1968).
141. Wu, Ay-Ju; Ellison, Frank O., "Method of Diatomics-in-Molecules. VIII. Excited Triplet States of H_3^+ ", J. Chem. Phys. 48(11), 5032-7 (1968).
142. Ritchie, Calvin D.; King, Harry Frederick, "Theoretical Studies of Proton-Transfer Reactions. I. Reactions of Hydride Ion with Hydrogen Fluoride and Hydrogen Molecules", J. Am. Chem. Soc., 90(4), 825-33 (1968).

1967

143. Albritton, D. L.; Miller, T. M.; Moseley, J. T.; Martin, D. W.; McDaniel, E. W., "Mobilities of Mass-Identified H_1^+ and H_3^+ Ions in Hydrogen", Phenomena Ioniz. Gases, Int. Conf., Contrib. Pap., 8th, Vienna, 12. Springer-Verlag: Vienna, Austria. (1967).
144. Kutzelnigg, Werner; Ahlrichs, Reinhart; Labib-Iskander, I.; Bingel, Werner A., "Hartree-Fock and the Correlation Energies of the H_3^+ Ion and Their Dependence on the Nuclear Configuration", Chem. Phys. Lett. 1(10), 447-50 (1967).
145. Schwartz, Maurice Edward; Schaad, Lawrence J., "Ab Initio Studies of Small Molecules Using 1s Gaussian Basis Functions. II. H_3^+ ", J. Chem. Phys. 47(12), 5325-34 (1967).
146. Conroy, Harold; Bruner, Buddy L., "Molecular Schroedinger Equation. VI. Results for H_3 and Other Simple Systems", J. Chem. Phys. 47(3), 921-9 (1967).
147. Solov'ev, E. S.; Il'in, R. N.; Oparin, V. A.; Fedorenko, N. V., "Production of Highly Excited Hydrogen Molecules and Atoms by Fast H_2^+ and H_3^+ Ions Passing Through Hydrogen, Neon, and Magnesium and Sodium Vapor", Zh. Eksp. Teor. Fiz. 53(6), 1933-41 (1967).
148. Pfeiffer, Gary V.; Huff, Norman T.; Greenawalt, E. M.; Ellison, Frank O., "Method of Diatomics in Molecules. IV. Ground and Excited States of H_3^+ , H_4^+ , H_5^+ and H_6^+ ", J. Chem. Phys. 46(2), 821-2 (1967).

149. Considine, James P.; Hayes, Edward F., "Single-Center Wave Functions for H_3^+ and H_3 ", J. Chem. Phys. 46(3), 1119-24 (1967).
150. Buchheit, K.; Henkes, W., "Untersuchung der Massenverteilung von Wasserstoff-Agglomerat-Ionen in Einem Massenspektrometer mit Energiezerlegung", Z. Angew. Phys. 24(4), 191-6 (1967).

1966

151. Schwartz, Maurice Edward, "Hellmann-Feynman Theorem and the Correlation Energy of H_3^+ ", J. Chem. Phys. 45(12), 4754-5 (1966).
152. Williams, James Francis; Dunbar, D. N. F., "Charge Exchange and Dissociation Cross Sections for H_1^+ , H_2^+ , and H_3^+ Ions of 2- to 50-keV Energy Incident Upon Hydrogen and the Inert Gases", Phys. Rev. 149(1), 62-9 (1966).
153. Joshi, Bhairav D., "Study of the H_3^+ Molecule Using Self-Consistent-Field One-Center Expansion Approximation", J. Chem. Phys. 44(9), 3627-31 (1966).
154. Pearson, A. G.; Poshusta, R. D.; Browne, J. C., "Some Potential-Energy Surfaces on H_3^+ Computed with Generalized Gaussian Orbitals", J. Chem. Phys. 44(5), 1815-8 (1966).
155. Lester, William A. Jr.; Krauss, Morris, "Some Aspects of the Coulomb Hole of the Ground State of H_3^+ ", J. Chem. Phys., 44(1), 207-12 (1966).
156. Devienne, F. Marcel; Roustan, Jean C., "Existence and Some Properties of Triatomic Molecular Jets of Hydrogen", C. R. Acad. Sci., Ser. A B (See CHASAP and CHDBAN), 263B(25), 1389-92 (1966).

Section III: H_N^+ (and H_N^- , $N \geq 4$)

1987

1. Okumura, M.; Yeh, L. I.; Lee, Y. T., "Infrared Spectroscopy of the Cluster Ions $H_3^+ \cdot (H_2)_n$ ", preprint, submitted to Journal of Chemical Physics.
2. Mongtomery, J. A. Jr.; Michels, H. H., "On the Structure of the Ground State of H_6^+ ", J. Chem. Phys. 87(1), 771-3 (1987).
3. Hobza, P.; Schneider, B.; Sauer, J.; Carsky, F.; Zahradnik, R., "MP4 Interaction Energies and Basis Set Superposition Errors for the Molecular Hydrogen ($(H_2)_2$) Dimer", Chem. Phys. Lett. 134(5), 418-22 (1987).
4. Metropoulos, A.; Nicolaides, C. A., "Towards Understanding the Stability of the H_4^+ (C_{3v}) Cluster", Z. Phys. D: At., Mol. Clusters, 5(2), 175-80 (1987).
5. Theodorakopoulos, G.; Petsalakis, I. D.; Nicolaides, C. A., "Potential Energy Hypersurfaces of the Hydrogen Tetraatomic Molecule in the Ground and the First Two Singlet Excited Electronic States", THEOCHEM, 34(1-2), 23-31 (1987).
6. Yamaguchi, Yukio; Gaw, Jeffrey F.; Remington, Richard B.; Schaefer, Henry F. III; "The H_5^+ Potential Energy Hypersurface: Characterization of Ten Distinct Energetically Low-Lying Stationary Points", J. Chem. Phys. 86(9), 5072-81 (1987).
7. Hiraoka, Kenzo, "A Determination of the Stabilities of $H_3^+(H_2)_n$ with $n = 1-9$ from Measurements of the Gas-Phase Ion Equilibria $H_3^+(H_2)_{n-1} + H_2 = H_3^+(H_2)_n$ ", J. Chem. Phys. 87(7), 4048-55 (1987).
8. Kirchner, N. J.; Bowers, M. T., "An Experimental Study of the Formation and Reactivity of Ionic Hydrogen Clusters: The First Observation and Characterization of the Even Clusters H_4^+ , H_6^+ , H_8^+ , and H_{10}^+ ", J. Chem. Phys. 86(3), 1301-10 (1987).
9. Kirchner, N. J.; Bowers, M. T., "Fragmentation Dynamics of Metastable Hydrogen Ion Clusters H_5^+ , H_7^+ and H_9^+ : Experiment and Theory", J. Phys. Chem. 91, 2573-82 (1987).
10. Forward, R., "Prospects for Antiproton Production and Propulsion", Proc. Cooling, Condensation, and Storage of Hydrogen Cluster Ions Workshop, 1/8-9/87, 9-26. Edited by John T. Bahns. University of Dayton Research Institute (1987).
11. Saxon, R., "Overview of Hydrogen Clusters", Proc. Cooling, Condensation, and Storage of Hydrogen Cluster Ions Workshop, 1/8-9/87, 27-37. Edited by John T. Bahns. University of Dayton Research Institute (1987).

12. Stwalley, W. C., "Large Hydrogen Cluster Ions", Proc. Cooling, Condensation, and Storage of Hydrogen Cluster Ions Workshop, 1/8-9/87, 39-45. Edited by John T. Bahns. University of Dayton Research Institute (1987).
13. Bahns, J. T., "Introduction to the Workshop on Cooling, Condensation and Storage of Hydrogen Cluster Ions", Proc. Cooling, Condensation, and Storage of Hydrogen Cluster Ions Workshop, 1/8-9/87, 1-7. Edited by John T. Bahns. University of Dayton Research Institute (1987).
14. Bowers, M. T., "Formation and Reactivity of Small Hydrogen Cluster Ions", Proc. Cooling, Condensation, and Storage of Hydrogen Cluster Ions Workshop, 1/8-9/87, 61-72. Edited by John T. Bahns. University of Dayton Research Institute (1987).
15. Yamaguchi, Yukio; Gaw, Jeffrey F.; Remington, Richard B.; Schaefer, Henry F. III, "The H_5^+ Potential Energy Hypersurface. Characterization of Ten Distinct Energetically Low-Lying Stationary Points", Proc. Cooling, Condensation, and Storage of Hydrogen Cluster Ions Workshop, 1/8-9/87, 73-9. Edited by John T. Bahns. University of Dayton Research Institute (1987).
16. Montgomery, J. A. Jr.; Michels, H. H., "Electronic Structure and Stability of Small Cation and Anion Hydrogen Clusters", Proc. Cooling, Condensation, and Storage of Hydrogen Cluster Ions Workshop, 1/8-9/87, 81-94. Edited by John T. Bahns. University of Dayton Research Institute (1987).
17. Crofton, M., "Infrared Spectroscopy of H_3^+ ", Proc. Cooling, Condensation, and Storage of Hydrogen Cluster Ions Workshop, 1/8-9/87, 119-24. Edited by John T. Bahns. University of Dayton Research Institute (1987).
18. Yeh, L. I.; Okumura, M.; Myers, J. D.; Lee, Y. T., "Vibrational Spectroscopy of the Hydrogen and Hydrated Hydronium Cluster Ions", Proc. Cooling, Condensation, and Storage of Hydrogen Cluster Ions Workshop, 1/8-9/87, 125-41. Edited by John T. Bahns. University of Dayton Research Institute (1987).
19. Mitchell, J. B. A., "The Role of Electron-Ion Recombination in Bulk Antimatter Production", Proc. Cooling, Condensation, and Storage of Hydrogen Cluster Ions Workshop, 1/8-9/87, 143-56. Edited by John T. Bahns. University of Dayton Research Institute (1987).
20. Bahns, J. T., "Key Problems and Hydrogen Atom Formation", Proc. Cooling, Condensation, and Storage of Hydrogen Cluster Ions Workshop, 1/8-9/87, 219-30. Edited by John T. Bahns. University of Dayton Research Institute (1987).
21. Bahns, J. T.; Sando, K. M.; Tardy, D. C.; Stwalley, W. C., "Proceedings of the Hydrogen Cluster Ion Study Group", Proc. Cooling, Condensation, and Storage of Hydrogen Cluster Ions Workshop, 1/8-9/87, A1-64. Edited by John T. Bahns. University of Dayton Research Institute (1987).

1986

22. Cardelino, B. H.; Eberhardt, W. H.; Borkman, R. F., "Ab Initio SCF Calculation on Lithium-Hydrogen (Li_nH_m) Molecules and Cations with Four or Less Atoms", J. Chem. Phys. 84(6), 3230-42 (1986).
23. Roszak, S.; Sokalski, W. A.; Hariharan, P. C.; Kaufman, Joyce J., "Procedure Supplementing SCF Interaction Energies by Dispersion Term Evaluated in Dimer Basis Set within Variation-Perturbation Approach", Theor. Chim. Acta, 70(2), 81-8 (1986).
24. Yeh, L. I.; Okumura, M.; Lee, Y. T., "The Vibrational Predissociation Spectroscopy of Hydrogen Cluster Ions", 813-8 in "Electronic and Atomic Collisions", Edited by D. C. Lorents, W. E. Meyerhof, J. R. Peterson, Elsevier Science Publishers B. V., NY (1986).

1985

25. Okumura, M.; Yeh, L. I.; Lee, Y. T., "The Vibrational Predissociation Spectroscopy of Hydrogen Cluster Ions", J. Chem. Phys., 83(7), 3705-6 (1985).

1984

26. Nicolaides, C. A.; Theodorakopoulos, G.; Petsalakis, I. D., "Theory of Chemical Reactions of Vibronically Excited Diatomic Hydrogen ($\text{B}^1\Sigma_u^+$). I. Prediction of a Strongly Bound Excited State of Tetraatomic Hydrogen", J. Chem. Phys. 80(4), 1705-6 (1984).
27. Kirchner, Nicholas J.; Gilbert, James R.; Bowers, Michael T., "The First Experimental Observation of Stable Hydrogen (H_4^+) Ions", Chem. Phys. Lett. 106(1-2), 7-12 (1984).
28. MacDonald, Jeffrey A.; Biondi, Manfred A.; Johnsen, Rainer, "Recombination of Electrons with Hydrogen (H_3^+ and H_5^+) Ions", Planet. Space Sci. 32(5), 651-4 (1984).
29. Beuhler, R. J.; Friedman, L., "Cluster Ion Formation in Free Jet Expansion Process at Low Temperatures", Ber. Bunsenges. Phys. Chem. 88, 265 (1984).
30. Moser, H. O., "Time of Flight Spectroscopy of Sub-meV Cluster Ions in the Mass Range $1\text{-}10^6$ Atoms per Charge", Rev. Sci. Instrum. 55(12), 1914-23 (1984).
31. Kutina, R. E.; Edwards, A. K.; Pandolf, R. S.; Berkowitz, J., "UV Laser Photodissociation of Molecular Ions", J. Chem. Phys. 80(9), 4112-9 (1984).

1983

32. Jungen, Martin; Staemmler, Volker, "Rydberg States of the Hydrogen Tetramer (H_4)", Chem. Phys. Lett. 103(3), 191-5 (1983).
33. Pulay, Peter, "Variational Formulation and Gradient Evaluation for Coupled Electron Pair Approximations: A Model Study", Int. J. Quantum Chem., Quantum Chem. Symp. 17, 257-63 (1983).
34. Takahashi, Mitsuo; Fukutome, Hideo, "Projected BCS Tamm-Dancoff Method for Molecular Electronic Structures", Int. J. Quantum Chem. 24(6), 603-21 (1983).
35. Brown, Richard E.; Colpa, Johannes Pieter, "SCF and CI Studies of Hund's Rules for the Effects of Electronic Correlation and Delocalization. I", Int. J. Quantum Chem. 24(6), 593-602 (1983).
36. Wilson, S.; Jankowski, K.; Paldus, J., "Applicability of Nondegenerate Many-Body Perturbation Theory to Quasi-Degenerate Electronic States: A Model Study", Int. J. Quantum Chem. 23(5), 1781-802 (1983).
37. Yamaguchi, Yukio; Gaw, Jeffrey F.; Schaefer, Henry F., III, "Molecular Clustering about a Positive Ion. Structures, Energetics, and Vibrational Frequencies of the Protonated Hydrogen Clusters H_3^+ , H_5^+ , H_7^+ , and H_9^+ ", J. Chem. Phys. 78(6, Pt. 2), 4074-85 (1983).
38. Beuhler, R. J.; Ehenson, S.; Friedman, L., "Hydrogen Cluster Ion Equilibria", J. Chem. Phys. 79(12), 5982-90 (1983).
39. Elford, M. T., "The Heat of Dissociation of H_5^+ Derived from Measurements of Ion Mobilities", J. Chem. Phys. 79(12) 5951-9 (1983).
40. Hirao, K.; Yamabe, S., "Theoretical Study on the Structure and Stability of Hydrogen Ion Clusters H_n^+ and H_n^- ($n = 3, 5, 7, 9, 11, 13$)", Chem. Phys. 80, 237-43 (1983).
41. Huber, H.; Szekeley, D., "Near-Hartree-Fock Energies and Geometries of the Hydrogen Clusters H_n^+ (n (odd) ≤ 13) Obtained with Floating Basis Sets", Theor. Chim. Acta 62, 499-506 (1983).
42. Raynor, S.; Herschbach, D. R., "Electronic Structure of H_n^+ and HeH_n^+ Clusters", J. Phys. Chem. 87, 289-93 (1983).

1982

43. Wright, L. R.; Borkman, R. F., "Ab Initio Studies on the Stabilities of Even- and Odd-Membered Hydrogen (H_n^+) Clusters", J. Chem. Phys. 77(4), 1938-41 (1982).

44. Borisov, Yu. A., "The Functional of the Electron Density for Atoms and Molecules", Chem. Phys. Lett. 93(2), 197-200 (1982).

45. Beuhler, R. J.; Friedman, L., "Hydrogen Cluster Ions", Phys. Rev. Lett. 48(16), 1097-9 (1982).

1981

46. Chanut, Y.; Martin, J.; Salin, R.; Moser, H.O., "Production and Beam Analysis of Energetic Small Hydrogen Cluster Ions for Study of Their Interactions with Targets and Their Structure", Surface Science 106(1-3), 563-8 (1981).

47. Moser, H. O.; Falter, H. D.; Hagena, O. F.; Henkes, P. R. W.; Klingelhöfer, "Cluster Ion Acceleration as a Means of Producing Multiampere Particle Beams in the Energy Range of 1 eV to 1 keV/Atom", Surface Science 106, 569-75 (1981).

1980

48. Yano, K.; Bee, S. H., "Mass Analyses of Cluster Ion Beams by Wein Filter", Jap. J. of Appl. Phys. 19(6), 1019-25 (1980).

49. Huber, H., "Geometry Optimization in Ab Initio SCF Calculations. The Hydrogen Clusters H_n^+ ($n = 7, 9, 11, 13$)", Chem. Phys. Lett. 70(2), 353-7 (1980).

50. Anderson, S. L.; Hirooka, T.; Tiedelmann, P. W.; Mahan, B. H.; Lee, Y. T., "Photoionization of $(H_2)_2$ and Clusters of O_2 Molecules", J. Chem. Phys. 73(10), 4779-83 (1980).

1979

51. Hirao, Kimihiko; Yamabe, Shinichi, "Structure and Stability of Cluster Ions H_n^+ ($n=3,5,7,9,11$)", Koen Yoshishu - Bunshi Kozo Sogo Toronkai, Siga Med. Coll., Ohtsu, Japan, Chem. Soc. Japan, 260-1 (1979).

52. Bunker, P. R., "Symmetry in Molecular Hydrogen Dimer $((H_2)_2)$, Molecular Deuterium Dimer $((D_2)_2)$, Hydrogen Deuteride Dimer $((HD)_2)$, and H_2 - D_2 Van der Waals Complexes", Can. J. Phys. 57(12), 2099-105 (1979).

53. Vojtik, J.; Polak, R., "On the Multidimensional "Avoided Surface Crossing" Problem", Chem. Phys. 42(1-2), 177-82 (1979).

54. Van Lumig, A.; Reuss, J.; Ding, A.; Weise, J.; Rindtisch, A., "Double Differential Fragmentation Cross Section Measurements of H_{2n+1}^+ Ions, $n \leq 7$ ", Mol. Phys. 38(2), 337-51 (1979).

55. Huber, H., "Geometry Optimization in Ab Initio SCF Calculations. Floating Orbital Geometry Optimization Applying the Hellmann-Feynman Force", Chem. Phys. Lett. 62(1), 95-9 (1979).

56. Sapse, A. M.; Rayez-Meaume, M. T.; Rayez, J. C.; Massa, L. J., "Ion-Induced Dipole H_n^+ Clusters", Nature 278, 332-3 (1979).

1978

57. Van Lumig, A.; Reuss, J., "Collisions of Hydrogen Cluster Ions with a Gas Target, at 200-850 eV Energy", Int. J. Mass Spectrom. Ion Phys. 27(2), 197-208 (1978).

58. Polak, R.; Vojtik, J.; Schneider, F., "Analysis of DIM Energy Hypersurfaces for Some Hydrogenic and Lithium Clusters", Chem. Phys. Lett. 53(1), 117-20 (1978).

59. Stine, J. R.; Muckerman, J. T., "Charge Exchange and Chemical Reaction in the $H_2^+ + H_2$ System. I. Characterization of the Potential Energy Surfaces and Nonadiabatic Regions", J. Chem. Phys. 68(1), 185-94 (1978).

60. Cobb, M.; Moran, T. F.; Borkman, R. F.; Childs, R., "Ab Initio Potential Energy Curves for $H_2-H_2^+$ Interactions", Chem. Phys. Lett. 57(3), 326-30 (1978).

61. Yamabe, S.; Hirao, K.; Kitaura, K., "Theoretical Study on the Stability and the Structure of H_n^+ ($n = 3, 5, 7, 9, 11$)", Chem. Phys. Lett. 56(3), 546-8 (1978).

1976

62. Polak, R., "Diatomics-in-Molecules Study on the Stability of the H_4^+ Ion", Chem. Phys. 16(3), 353-9 (1976).

63. Krenos, J. R.; Lehmann, K. K.; Tully, J. C.; Hierl, P. M.; Smith, G. P., "Crossed-Beam Study of the Reactions of Molecular Hydrogen(+) with Molecular Deuterium and Molecular Deuterium(+) with Molecular Hydrogen", Chem. Phys. 16(1), 109-16 (1976).

64. Arifov, U. A.; Lugovskoi, V. B.; Makarenko, V. A., "Emission of Negative Ions During Irradiation of Metals by Microsecond Pulses of Ruby Laser Radiation", Izv. Akad. Nauk SSSR, Ser. Fiz. 40(8), 1702-6 (1976).

65. Johnsen, Rainer; Huang, Chou-Mou; Biondi, Manfred A., "Three-Body Association Reactions of H^+ and H_3^+ Ions in Hydrogen from 135 to 300 K", J. Chem. Phys. 65(4), 1539-41 (1976).

1975

66. Carsky, Petr; Zahradnik, Rudolf; Hobza, Pavel, "Semiempirical Estimates of the Correlation Energy in Small Clusters of Hydrogen Atoms", *Theor. Chim. Acta*, 40(4), 287-95 (1975).
67. Hiraoka, K.; Kebarle, P., "Temperature Dependence of Third Order Ion Molecule Reactions. Reaction $H_3^+ + 2H_2 = H_5^+ + H_2$ ", *J. Chem. Phys.* 63(2), 746-9 (1975).
68. Hiraoka, K.; Kebarle, P., "Determination of the Stabilities of H_5^+ , H_7^+ , H_9^+ , and H_{11}^+ From Measurement of the Gas Phase Ion Equilibria $H_n^+ + H_2 = H_{n+2}^+$ ($n = 3, 5, 7, 9$)", *J. Chem. Phys.* 62(6), 2267-70 (1975).
69. Aberth, W.; Schnitzer, R.; Anbar, M., "Observations of the Diatomic and Triatomic Hydrogen Negative Ions", *Phys. Rev. Lett.* 34(26), 1600-3 (1975).
70. Ahlrichs, R., "Theoretical Study of the H_5^+ System", *Theoret. Chim. Acta* 39, 149-60 (1975).

1974

71. Elford, M. T.; Milloy, H. B., "Mobility of H_3^+ and H_5^+ Ions in Hydrogen and the Equilibrium Constant for the Reaction $H_3^+ + 2H_2 = H_5^+ + H_2$ at Gas Temperatures of 195, 273, and 293 K", *Aust. J. Phys.* 27(6), 795-811 (1974).

1973

72. Harrison, S. W.; Massa, L. J.; Solomon, P., "Binding Energy and Geometry of the Hydrogen Clusters H_n^+ ", *Nature* 245(141), 31-2 (1973).
73. Salmon, W. I.; Poshusta, R. D., "Polarized-Orbital Valence-Bond Calculations on the Ground State Properties of H_5^+ ", *J. Chem. Phys.* 59(9), 4867-70 (1973).
74. Van Deursen, A.; Reuss, J., "Measurements of Intensity and Velocity Distribution of Clusters from a H_2 Supersonic Nozzle Beam", *Int. J. of Mass Spectrom. and Ion Phys.* 11, 483-9 (1973).

1972

75. Leu, Ming-Taun, "Recombination of Electrons with Positive Ions of the Type H_3^+ , H_5^+ , $H_3O^+ \cdot (H_2O)_n$, and HCO^+ at Thermal Energies", 79 Pp. Avail. Univ. Microfilms, Ann Arbor, Mich., Order No. 73-13,190 From: Diss. Abstr. Int. B 1973, 33(12)(Pt. 1), 5998 (1972).

76. Bennett, S. L.; Field, F. H.; "Reversible Reactions of Gaseous Ions. VII. The Hydrogen System", J. Am. Chem. Soc. 94(25), 8669-72 (1972).

1971

77. Arifov, U. A.; Pozharov, S. L.; Chernov, I. G.; Mukhamediev, Z. A., "Ionic-Molecular Reactions in Hydrogen at High Pressures", High Energy Chemistry 5, 69 (1971).

1969

78. Clampitt, R.; Gowland, L., "Clustering of Cold Hydrogen Gas on Protons", Nature 223, 815-6 (1969).

1968

79. Schwartz, M. E.; Schaad, L. J., "Ab Initio Studies of Small Molecules Using 1s Gaussian Basis Functions. III. LCGTO SCF MO Wavefunctions of the Three- and Four-Electron Systems He_2^+ , He_2 , and Linear H_3 , H_4^+ , H_4 ", J. Chem. Phys. 48(10), 4709-15 (1968).

1967

80. Pfeiffer, Gary V.; Huff, Norman T.; Greenawalt, E. M.; Ellison, Frank O., "Method of Diatomics in Molecules. IV. Ground and Excited States of H_3^+ , H_4^+ , H_5^+ and H_6^+ ", J. Chem. Phys. 46(2), 821-2 (1967).
81. Buchheit, K.; Henkes, W., "Untersuchung der Massenverteilung von Wasserstoff-Agglomerat-Ionen in Einem Massenspektrometer mit Energiezerlegung", Z Angew. Phys. 24(4), 191-6 (1967).

PRODUCTION OF HEAVY ANTINUCLEI: REVIEW OF EXPERIMENTAL RESULTS

Dr. Robert L. Forward
Senior Scientist
Hughes Research Laboratories
3011 Malibu Canyon Road
Malibu, California 90265 USA

23 April 1987

PRODUCTION OF HEAVY ANTINUCLEI: SUMMARY OF EXPERIMENTAL RESULTS

Dr. Robert L. Forward
Hughes Research Laboratories
Malibu, California 90265 USA

ABSTRACT

Antinuclei heavier than antiprotons, such as antideuterons, antitritons, antihelium-3, and larger antinuclei, might be useful in the initial phases of the nucleation and growth of antihydrogen cluster ions from antiprotons and antielectrons (positrons). The heavier antinuclei could possibly be used as seed catalysts to initiate the growth of a cluster ion, or to broaden or increase the number of infrared emission lines for radiation cooling purposes, or to break the symmetry of the smaller cluster ions, thus changing the large difference in binding energy between clusters with even versus odd numbers of atoms. There also may be other uses for heavy antinuclei, antiatoms and excited antiatom species that will be discovered once it is realized that small quantities can be obtained using variations on present antiproton production, capture, and trapping techniques. This paper summarizes the experimental work to date on the production of antideuterium, antitritium, and antihelium nuclei, and the prospects for production of heavier antinuclei such as antilithium. The general experimental trend is that the ratio of production of antideuterons to antiprotons is 10^{-4} , antitritium and antihelium-3 to antiprotons is 10^{-8} , and each added baryon lowers the production rate by another factor of 10^{-4} . A typical facility using high energy protons striking metal targets can produce about 10^{15} antiprotons per day (about a nanogram), of which only 0.1% or 10^{12} (about a picogram) is captured. Thus, if special collection apparatus were used to separate out these heavier antiparticles and the collection efficiency was the same as that for antiprotons (0.1%), then along with the 10^{12} antiprotons being captured there would be 10^8 antideuterons, 10^4 antitritons and antihelium-3 nuclei, and 1 antihelium-4 nuclei. In addition, there are alternative proposals for producing antideuterium through colliding beams of antiprotons that may ultimately prove to be more effective in producing significant quantities of captured antideuterons. Extension of these techniques to colliding beams of heavy antinuclei may even allow fabrication of small amounts of very heavy antinuclei that are not feasible using the straight proton-target production approach.

INTRODUCTION

The availability of small numbers of heavy antinuclei may be useful in certain scientific and technological areas. Some examples would be the use of antideuterium and antitritium in the initial phases of antihydrogen cluster ion nucleation and growth, or the use of antihelium or antilithium with their multiple ionization states as a catalyst for antihydrogen cluster ion or antihydrogen ice crystal growth. Muon catalyzed fusion of antideuterium and antitritium to produce antihelium and an antineutron could also be attempted to search for any anomalous results from the use of antiparticles.

This paper is a brief review of the experimental results reported in the literature on the relative formation rates of heavy antinuclei. Most of this work was done in the 1970s, soon after the particle accelerator energies were sufficient to produce heavier antiparticles than antiprotons. After a brief flurry of papers, interest in production of heavy antinuclei dropped off and later papers only mention the production of heavy antinuclei in passing with the major emphasis being on searches for more exotic particles with approximately the same masses.

The threshold for production of antiprotons in pp collisions is 5.6 GeV, for antideuterons it is 15 GeV, for antitritium and antihelium-3 it is 28 GeV, for antihelium-4 it is 45 GeV, etc. For the efficient production of antinuclei it is necessary that the incident proton energy be considerably greater than these threshold values. For example, as the incident particle energy is increased from 30 to 70 GeV, the yield of antideuterons increases by more than an order of magnitude.

The production rate of heavy nuclei varies with a large number of parameters, the incident particle type and energy, the target type, and the output heavy antinuclei type, energy (momentum), and production angle. The variations with incident particle type, target nuclei type, and production angle turn out to be small (<50%). Even e^+e^- beam collisions give almost the same rates as proton-target interactions at the same center of mass energy. The major variation in production rate is the variation with output antiparticle type, with the antiproton production rate being a few percent of the pion production rate, the antideuteron production rate being 10^{-4} of the antiproton production rate, and succeeding antinuclei being down another factor of 10^{-4} for each additional antibaryon.

The simple model¹ that seems to fit the data is that it is necessary that several antinucleon-nucleon pairs be produced simultaneously, and that the antinucleons travel off in nearly the same direction at the same speed so they are close enough to "stick" together to form an antinucleus.

Most of the experimental measurements surveyed are reported as a ratio of the production of the heavy antinuclei at a given

momentum and production angle compared to the number of negative pions with the same momentum and production angle, because this is an easy measurement to make. Sometimes this ratio is (or can be) converted to the number of heavy antinuclei at a given momentum and production angle compared to the number of antiprotons at the same momentum and production angle. Less seldom the absolute production rate of pions is also determined (or estimated) and an absolute production cross section for the heavy nuclei from the given target nucleus is given. There are small but significant differences in production rates from different target materials.

HEAVY ANTINUCLEI EXPERIMENTAL RESULTS

The first report of the production of antideuterons seems to have been in 1965 at the Alternating Gradient Synchrotron (AGS) at Brookhaven National Laboratory by a team from Columbia University¹. They used the 30 GeV (BeV in 1960s notation) proton beam from the AGS on a beryllium target. About 200 heavy antinuclei events were reported and the ratio of antideuterons to negative pions at this low energy was only 5.5×10^{-8} . No firm evidence was found for antitritium. This team barely beat out another group in Europe² who also observed antideuterons using the 19.2 GeV/c proton beam from the CERN Proton Synchrotron. Their antideuteron to negative pion production ratio was 8×10^{-9} . In 1969 an IHEP-CERN Collaboration³ made measurements at incident proton energies of 43, 52, and 70 GeV, and a number of antideuteron energies and production angles. This was followed in 1971 by further measurements at low antideuteron momenta by an IHEP team⁴, again using 70 GeV protons on aluminum targets. The results of all the IHEP experimental measurements at 70 GeV is shown in Figure 1. At the peaks of the 70 GeV production curves, which occurred around 13 GeV/c secondary particle momentum, the ratio of antiprotons to pions was about 3×10^{-2} , and the ratio of antideuterons to pions was about 3×10^{-6} , giving a ratio of antideuterons to antiprotons of about 10^{-4} .

The same IHEP team^{5,6} also reported in 1971 the first observation of antihelium-3 from 70 GeV protons on aluminum. A total of five antihelium-3 particles were observed out of 2.4×10^{11} particles (mostly negative pions) passing through the apparatus. The ratio of the differential cross section for the production of doubly ionized antihelium-3 nuclei at a momentum of 20 GeV/c compared to the negative pion at a momentum of 10 GeV/c was measured as 2×10^{-11} . In 1974, essentially the same group⁷ reported the production of four antitritium nuclei with 70 GeV protons on aluminum. The production ratio of antitritons to negative pions was about 10^{-11} . Although the statistics of the heavier nuclei are bad, it is possible to draw a trend curve of the relative production ratio. The (sparse) data for 70 GeV proton on aluminum production ratios of antideuterons, antitritons, and antihelium-3 nuclei with respect to antiprotons (instead of negative pions) is shown in Figure 2.

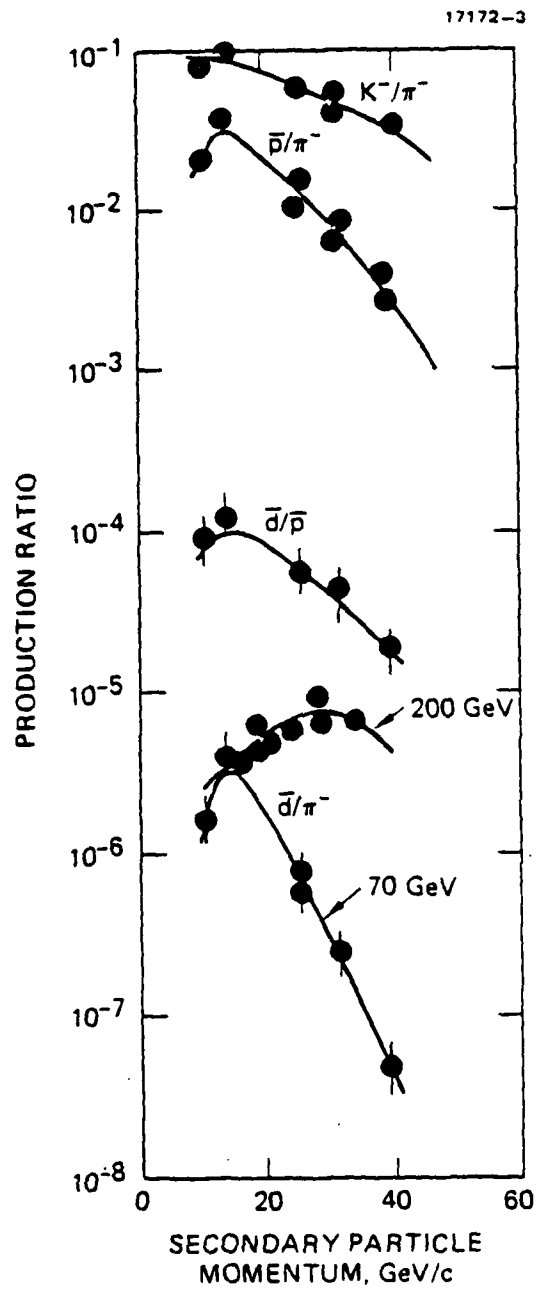


Figure 1 - Secondary particle production ratios as a function of secondary particle momentum for 70 GeV protons^{3,4} and 200 GeV protons⁸ on aluminum targets.

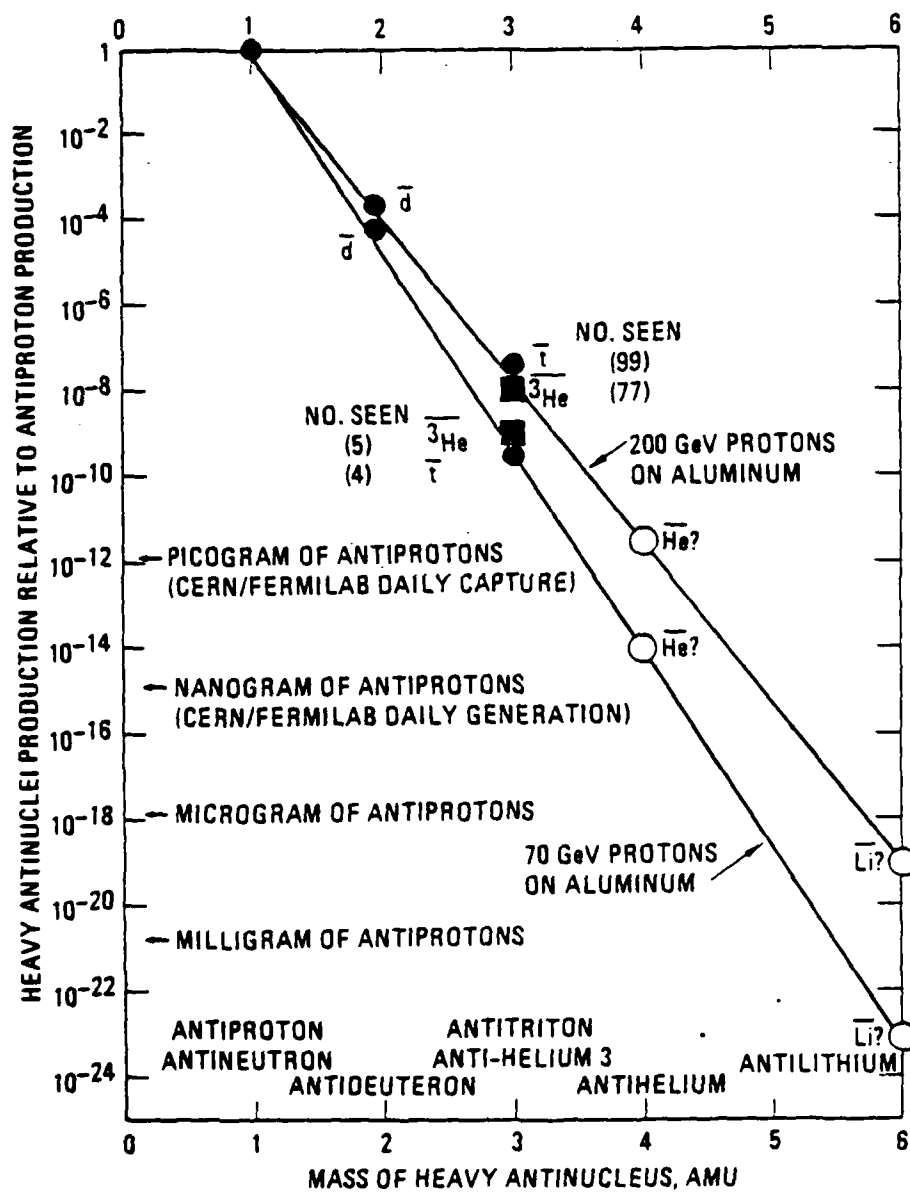


Figure 2 - Heavy antinuclei production ratio compared to the antiproton production ratio as a function of secondary antinucleus baryon number.

With the advent of the 200 GeV SPS machine at CERN, experiments were initiated in 1978 that produced copious quantities of antideuterons, ten antihelium-3 nuclei, and three antitritium nuclei⁸. The production ratio of antideuterons to negative pions was measured as a function of the secondary particle momentum and as shown in Figure 1, a broad peak was found at 30 GeV/c compared to the 13 GeV/c for antideuterons produced by 70 GeV protons. Later experiments⁹ in 1979 increased the number of heavier antinuclei to 99 antitritons and 94 antihelium-3 nuclei. From this data the relative production ratio compared to negative pions is 3×10^{-2} for antiprotons, 4.6×10^{-6} for antideuterons, 1.3×10^{-9} for antitritium, and 3×10^{-10} for antihelium-3. This is also plotted in Figure 2 with the heavier antinuclei production ratios given as the production rate with respect to antiprotons rather than negative pions. At that time all the available data¹⁻¹² on the production of antideuterons at low transverse momentum seemed to show a smooth trend as shown by the open data points in Figure 3 taken from Bozzoli, et al.⁸ There was an increase in antideuteron production rate with increasing incident proton energy, leveling off at about 5×10^{-6} antideuterons per negative pion above 200 GeV. The solid line drawn through the data points is the square of the production ratio for antiprotons to negative pions at half the antideuteron momentum, as a simple model for the antideuteron production ratio.

Measurements in 1978 of the ratio of production of deuterons to antideuterons in proton-proton beam collisions at the CERN ISR Collider¹² at a center-of-mass energy of 53 GeV (1400 GeV equivalent p->N energy) gave a value of 3.8 deuterons to antideuterons, which is close to the square of the ratio of protons to antiprotons. This gives credence to the simple model¹ that if (anti)deuterons are produced as the result of the overlap of two produced (anti)nucleons, then the deuteron to antideuteron ratio should equal approximately the square of the ratio of protons to antiprotons at the same transverse momentum per (anti)nucleon.

Later experiments in 1985 that included correction factors for relative absorption of negative pions and antideuterons gave a value of 5.8×10^{-6} antideuterons per negative pion¹³. Then more data points were generated by other experiments with the highest energies being reached by experiments that involved protons colliding with protons. The data for the antideuteron to negative pion production ratio as a function of the equivalent incident beam momentum in many different experiments with different targets and different secondary momentum is shown as the filled spots in Figure 3 taken from Thron, et al.¹³ The smooth trend with a leveling off above 200 GeV is now not so clear, and there could be a possibility that the production ratio of antideuterons (and presumably the heavier antinuclei) is increasing with increasing production energy above 200 GeV.

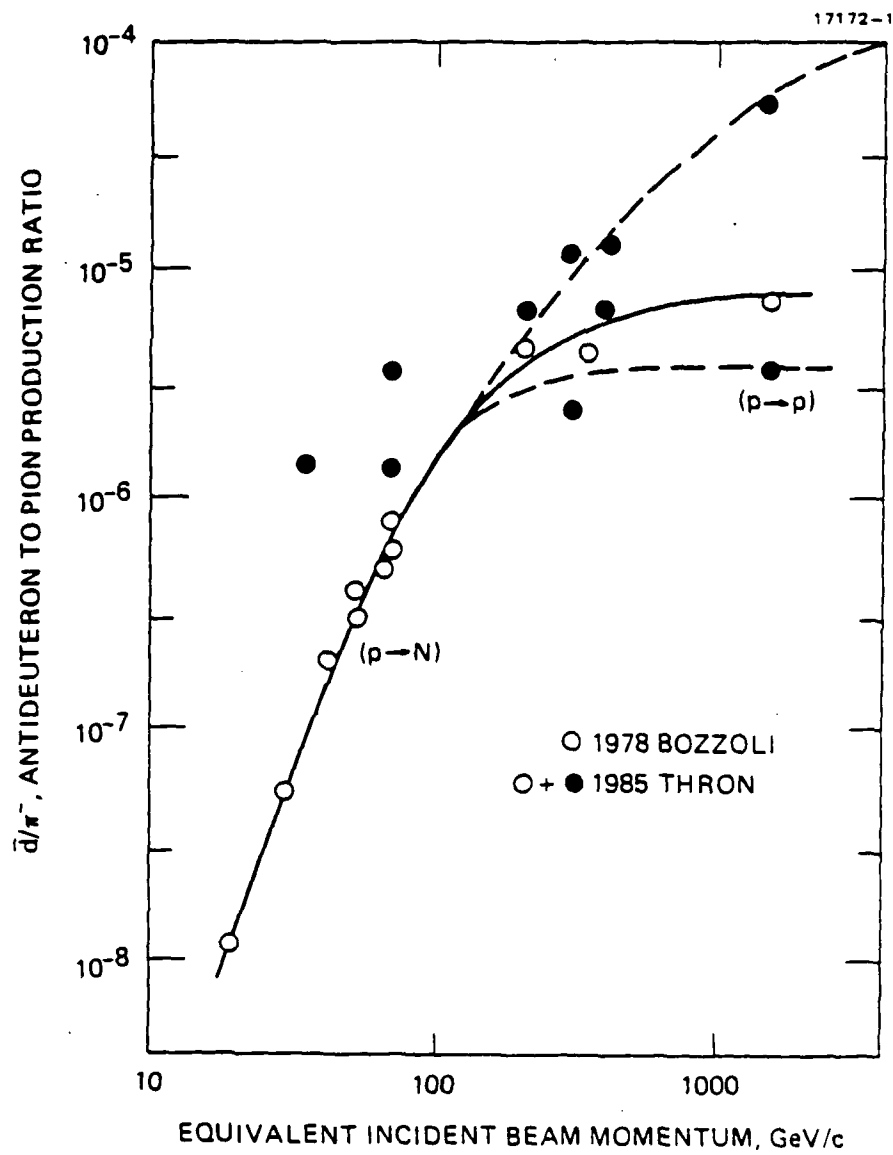


Figure 3 - Antideuteron to negative pion production ratio as a function of effective incident proton beam momentum.

Antideuterons have also been observed in electron-positron annihilation collisions at 10 GeV center-of-mass energy in the ARGUS detector at the DORIS II storage ring at DESY in Hamburg, Germany¹⁴. A total of six candidates passed the selection criteria for antideuterons. The production rate for antideuterons was about 2×10^{-5} per hadronic event compared to a production rate for antiprotons of 2×10^{-1} per hadronic event, or a ratio of antiprotons to antideuterons of 10^{-4} , similar to that observed in proton-proton or proton-target interactions.

PRODUCTION CROSS SECTIONS

A few production cross sections have been given in some of the papers. To convert production cross sections per target nucleus (usually ^{27}Al or ^9Be) to production cross sections per nucleon, the accepted procedure is to divide by $A^{2/3}$, which is 9 for Al and 4.33 for Be.

For 30 GeV/c protons on Be: ¹	
antideuterons at 5 GeV/c	$7 \times 10^{-33} \text{ cm}^2/\text{sr} \cdot (\text{GeV}/c) \cdot \text{Be}$
For 70 GeV/c protons on Al: ⁴	
antideuterons at 13 GeV/c	$3 \times 10^{-30} \text{ cm}^2/\text{sr} \cdot (\text{GeV}/c) \cdot \text{Al}$
antitritons at 25 GeV/c	$1.0 \pm 0.6 \times 10^{-35} \text{ cm}^2/\text{sr} \cdot (\text{GeV}/c) \cdot \text{Al}$
antihelium-3 at 20 GeV/c	$2.0 \times 10^{-35} \text{ cm}^2/\text{sr} \cdot (\text{GeV}/c) \cdot \text{Al}$
For 200 GeV/c protons on Be: ⁹	
antihelium-3 at 21 GeV/c	$1.3 \pm 0.3 \times 10^{-34} \text{ cm}^2/\text{sr} \cdot (\text{GeV}/c) \cdot \text{Be}$
antihelium-3 at 47.4 GeV/c	$1.9 \pm 0.3 \times 10^{-34} \text{ cm}^2/\text{sr} \cdot (\text{GeV}/c) \cdot \text{Be}$
antitritons at 23.7 GeV/c	$7.6 \pm 0.9 \times 10^{-34} \text{ cm}^2/\text{sr} \cdot (\text{GeV}/c) \cdot \text{Be}$

SUMMARY OF EXPERIMENTAL RESULTS

If we extrapolate the data to date on the production of heavy antinuclei as shown in Figure 2, we can predict that at machine energies above 200 GeV, that for 10^{12} antiprotons captured (roughly one day's production at CERN or Fermilab) we could expect to capture 10^8 antideuterons, 10^5 antitritons, 10^4 antihelium-3 nuclei, and 1 antihelium-4 nuclei. Antilithium will have to wait for higher machine energies, greater beam currents, and especially better collection efficiencies.

Since machines exist that make large numbers of antiprotons using proton-target interactions, it is relatively simple to consider the installation of a diverter and a collection ring after the target and focusing lens to capture other particles than antiprotons. It might even be possible to make such an installation without significantly affecting the collection of antiprotons. It was estimated¹⁵ in 1982 that the Antiproton Accumulator could store 2 antideuterons per production pulse at 3.5 GeV/c. At 7 GeV/c this number would be increased by a factor of 40. Another factor of 80 could be gained in the production rate if antideuteron beams of 30 GeV/c were produced from 200 GeV

primary protons. Thus, for planning purposes, it is probably best to assume that if antideuterons or heavier antinuclei are urgently needed for some critical scientific experiments or to overcome some bottleneck in the development of antimatter technology, that they can be obtained using the same machines that are presently producing antiprotons. There are alternate methods for producing heavy antinuclei, however, and they may have some advantages.

ALTERNATE HEAVY ANTINUCLEI PRODUCTION CONCEPTS

Since cooled antiproton beams are now available at low energy at CERN and high energy at Fermilab, it is possible to consider using these beams for the production of antideuterons through the reaction $\bar{p} + \bar{p} \rightarrow d + \pi^-$. The process occurs in 8% of all $\bar{p}\bar{p}$ reactions. The details of arranging the reactions and capturing the resulting deuterons are discussed in two papers^{15,16}. In principle the reaction could be iterated to produce antihelium ions and perhaps heavier antinuclei, although there have been no publications discussing this concept in any detail.

It is also well known that negative muons can be used as a catalyst to initiate fusion of a DT molecule to produce He^4 and an energetic fusion neutron. Once we have copious amounts of trapped neutral antihydrogen molecules with a large component of antitritium and antideuterium nuclei, we could attempt the formation of antihelium-4 by subjecting the trap to a positive muon beam.

ACKNOWLEDGMENTS

This research was supported by the Air Force Rocket Propulsion Laboratory through Contract F04611-86-C-0039.

REFERENCES

- ¹D.E. Dorfman, J. Eades, L.M. Lederman, W. Lee, and C.C. Ting, "Observation of Antideuterons", Physical Review Letters 14, 1003-1006 (14 June 1965).
- ²T. Massam, Th. Muller, B. Righini, M. Schneegans, and A. Zichichi, "Experimental Observation of Antideuteron Production", Il Nuovo Cimento 39, 6574-6578 (1 September 1965).
- ³F. Binon, P. Duteil, V.A. Kachanov, V.P. Khromov, V.M. Kutyin, V.G. Lapshin, J.P. Peigneux, Yu.D. Prokoshkin, E.A. Razuvaev, V.I. Rykalin, R.S. Shuvalov, V.I. Solianik, M. Spighel, J.P. Stroot, and N.K. Vishnevsky, "Production of Antideuterons by 43 GeV, 52 GeV, and 70 GeV Protons", Physics Letters 30B, 510-513 (24 November 1969).

⁴Yu.M. Antipov, N.K. Vishnevskii, Yu.P. Gorin, S.P. Denisov, S.V. Donskov, F.A. Ech, A.M. Zaitsev, V.A. Kachanov, V.M. Kut'in, L.G. Landsberg, V.G. Lapshin, A.A. Lebedev, A.G. Morozov, A.I. Petrukhin, Yu.D. Prokoshkin, E.A. Razuvaev, V.I. Rykalin, V.I. Solyanik, D.A. Stoyanova, V.P. Khromov, and R.S. Shuvalov, "Production of Negative Particles with Low Momenta by 70-BeV Protons", *Yad. Fiz.* 13, 135-138 (January 1971) [English translation: *Soviet Journal of Nuclear Physics* 13, 78-79 (July 1971)]; essentially the same data and graphs also appeared in: Yu.M. Antipov, S.P. Denisov, S.V. Donskov, Yu.P. Gorin, V.A. Kachanov, V.P. Khromov, V.M. Kut'in, L.G. Landsberg, V.G. Lapshin, A.A. Lebedev, A.G. Morozov, A.I. Petrukhin, Yu.D. Prokoshkin, E.A. Razuvaev, V.I. Rykalin, V.I. Solyanik, D.A. Stoyanova, R.S. Shuvalov, N.K. Vishnevskii, F.A. Yetch, and A.M. Zaytzev, "Production of Low Momentum Negative Particles by 70-GeV Protons", *Physics Letters* 34B, 164-166 (1 February 1971).

⁵Yu.M. Antipov, N.K. Vishnevskii, Yu.P. Gorin, S.P. Denisov, S.V. Donskov, F.A. Ech, G.D. Zhilchenkova, A.M. Zaitsev, V.A. Kachanov, V.M. Kut'in, L.G. Landsberg, V.G. Lapshin, A.A. Lebedev, A.G. Morozov, A.I. Petrukhin, Yu.D. Prokoshkin, E.A. Razuvaev, V.I. Rykalin, V.I. Solyanik, D.A. Stoyanova, V.P. Khromov, and R.S. Shuvalov, "Observation of Antihelium 3", *Yad. Fiz.* 12, 311-322 (August 1970) [English translation: *Soviet Journal of Nuclear Physics* 12, 171-172 (February 1971)].

⁶Yu.D. Prokoshkin, "Particles of Antimatter", *Die Naturwissenschaften* 59, 281-284 (1972).

⁷N.K. Vishnevskii, M.I. Grachev, B.I. Rykalin, V.G. Lapshin, V.I. Solyanik, Yu.S. Khodyrev, V.P. Khromov, B.Yu. Baldin, L.S. Vertogradov, Ya.V. Grishkevich, Z.V. Krumshstein, R. Leiste, Yu.P. Merekov, V.I. Petrukhin, D. Pose, A.I. Ronzhin, I.F. Samenkova, V.M. Suvorov, G. Chemnitz, N.N. Khovanskii, B.A. Khomenko, M. Szawlowski, G.A. Shelkov, and J. Schuler, "Observation of antitritium nuclei", *Yad. Fiz.* 20, 694-708 (October 1974) [English translation: *Soviet Journal of Nuclear Physics* 20, 371-378 (April 1975)].

⁸W. Bozzoli, A. Bussiere, G. Giacomelli, E. Lesquoy, R. Meunier, L. Moscoso, A. Muller, R. Rimondi, and S. Zylberajch, "Production of d, t, ³He, anti-d, anti-t, and anti-³He by 200 GeV Protons", *Nuclear Physics* B144, 317-328 (1978).

⁹W. Bozzoli, A. Bussiere, G. Giacomelli, E. Lesquoy, R. Meunier, L. Moscoso, A. Muller, D.E. Plane, R. Rimondi, and S. Zylberajch, "Search for Long-Lived Particles in 200 GeV/c Proton-Nucleon Collisions", *Nuclear Physics* B159, 363-382 (1979).

¹⁰J.A. Appel, M.H. Bourquin, I. Gaines, L.M. Lederman, H.P. Parr, J.-P. Repellin, D.H. Saxon, J.K. Yoh, B.C. Brown, and J.-M. Gaillard, "Heavy Particle Production in 300 GeV/c Proton-Tungsten Collisions", *Physical Review Letters* 32, 428-432 (25 February 1974).

¹¹M.G. Albrow, D.P. Barber, P. Benz, B. Bosnjakovic, J.R. Brooks, C.Y. Chang, A.B. Clegg, F.C. Ernè, P. Kooijman, F.K. Loebinger, N.A. McCubbin, P.G. Murphy, A. Rudge, J.C. Sens, A.L. Sessions, J. Singh, and J. Timmer, "Search for Stable Particles of Charge >1 and Mass $>$ Deuteron Mass", Nuclear Physics B97, 189-200 (1975).

¹²W.M. Gibson, A. Duane, H. Newman, H. Ogren, S. Henning, G. Jarlskog, R. Little, T. Sanford, S.L. Wu, H. Bøggild, B.G. Duff, K. Guettler, M.N. Prentice, and S.H. Sharrock, "Production of Deuterons and Antideuterons in Proton-Proton Collisions at the CERN ISR", Lettere Al Nuovo Cimento 21, 189-194 (11 February 1978).

¹³J.L. Thron, T.R. Cardello, P.S. Cooper, L.J. Teig, Y.W. Wah, C. Ankenbrandt, J.P. Berge, A.E. Brenner, J. Butler, K. Doroba, J.E. Elias, J. Lach, P. Laurikainen, J. MacLachlan, J.P. Marriner, E.W. Anderson, A. Breakstone, and E. McCliment, "Search for Heavy Charged Particles and Light Nuclei and Antinuclei Produced by 400-GeV Protons", Physical Review D31, 451-463 (1 February 1985).

¹⁴ARGUS Collaboration, "Observation of Antideuteron Production in Electron-Positron Annihilation at 10 GeV Center of Mass Energy", Physics Lett. 157B, 326-332 (18 July 1985).

¹⁵D. Möhl, K. Kilian, H. Pilkuhn, and H. Poth, "Production of Antideuterons in Antiproton Rings", Nuclear Instruments and Methods 202, 427-430 (1982).

¹⁶H. Koch, K. Kilian, D. Möhl, H. Pilkuhn, and H. Poth, "Antideuterons at LEAR", pp. 877-880, Proceedings Workshop on Physics at LEAR with Low-Energy Cooled Antiprotons, Erice, Italy (9-16 May 1982).

THE STANDARD MODEL AND ITS PROBLEMS:

The Physics Background For an Advanced Hadron Facility

T. Goldman

Theoretical Division, Los Alamos National Laboratory
Los Alamos, New Mexico 87545

ABSTRACT

The particles and the interaction structures of the standard model of the strong and electroweak interactions are introduced. This systematization of all known particle physics phenomena raises new questions regarding repetitions of the particle types and regarding their masses. These questions are discussed and some of the experiments which seek to illuminate them, and to provide precision tests of the standard model, are described.

TABLE OF CONTENTS

1. Introduction
2. The Fundamental Particles and Gauge Bosons
3. Strong Interactions
 - 3.1 The QCD Lagrangian
 - 3.2 The QCD Coupling Strength
 - 3.3 Phenomenology from QCD
 - 3.4 Quark Masses in QCD
 - 3.5 Experimental Evidence for QCD
 - 3.6 The Problem with QCD
4. The $SU(2) \times U(1)$ Electroweak Model
 - 4.1 The Electroweak Lagrangian
 - 4.2 The Electroweak Coupling Constants
 - 4.3 Vector Boson Masses
 - 4.4 Weak Interactions of Leptons
 - 4.5 Fermion Masses
 - 4.6 Weak Interactions of Quarks
 - 4.7 Family Repetitions and Quark Masses
 - 4.8 Strong Interaction Corrections to the Electroweak Interactions
5. Problems of the Standard Model and Experimental Tests
 - 5.1 Family Problems and Their Mass Scales
 - 5.2 Family Problems and Fermion Masses
 - 5.3 Precision Tests of the Standard Model
6. Conclusion
7. References

1. INTRODUCTION

Particle physics has advanced tremendously in the past 40 years. The strong and weak forces have been "solved" in a sense similar to the status of quantum electrodynamics in the late 1940's; that is, we have field theories with so much beauty and phenomenological backing that enormous calculational and experimental efforts are now considered warranted to test their detailed predictions.

The "standard model" consists of the $SU(3)_c$ gauge field theory called quantum chromodynamics and the spontaneously broken $SU(2)_W \times U(1)_B$ gauge field theory known as the "electroweak model". These theories define spin 1 (vector) gauge fields which describe the transmission of the strong and weak forces, just as the photon transmits the electromagnetic force. The eight massless "gluons" fill an adjoint representation of the $SU(3)_c$ group, and the three massive intermediate vector bosons of the weak force the W^+ , W^- and Z , fill the adjoint representation of the $SU(2)_W$ group.

In addition to these vector bosons, the standard model includes several fermions, and one scalar field, called Higgs' boson. This last is an as yet unobserved remnant of the spontaneous symmetry breaking which is the technical means used to generate masses for the W and Z bosons. The fermions come in repeating sets, called families (or generations). This repetitiveness forms the basis of the serious and completely unresolved puzzle which is one of the most important problems that an Advanced Hadron Facility can address. In this paper, the standard model will be described, with some reference to the successes, which have led to its broad acceptance. More importantly, the problems with it and the unanswered questions which it raises will also be indicated, especially those which can be addressed by experiments[†] at an Advanced Hadron Facility.

2. THE FUNDAMENTAL PARTICLES AND GAUGE BOSONS

The Standard Model is defined by a product of three symmetry groups: $SU(3)_c \times SU(2)_W \times U(1)_B$. It is a non-Abelian gauge field theory based on these groups. The quantum rules for such theories require that they contain

[†]These are, in general, complementary to experiments at the proposed Superconducting Super Collider, which are primarily directed at questions which have answers lying beyond the standard model.

eight vector bosons (gluons) from the $SU(3)_C$ factor, three from $SU(2)_W$ and one from $U(1)_B$. The completely specify the theory, we must also specify that other representations of particles are present.

All of the fermions of the Standard Model are shown in Table I and their masses are shown in Table II.

TABLE I Fermion Families of the standard model.

$$\begin{pmatrix} u_r, u_b, u_g \\ d_r, d_b, d_g \end{pmatrix}_L \quad \begin{pmatrix} \nu_e \\ e^- \end{pmatrix}_L \quad (d_r, d_b, d_g)_R \quad (u_r, u_b, u_g)_R \quad (e^-)_R$$

u = up quark, d = down quark, e = electron, ν_e = electron-type neutrino

$$\begin{pmatrix} c_r, c_b, c_g \\ s_r, s_b, s_g \end{pmatrix}_L \quad \begin{pmatrix} \nu_\mu \\ \mu^- \end{pmatrix}_L \quad (s_r, s_b, s_g)_R \quad (c_r, c_b, c_g)_R \quad (\mu^-)_R$$

c = charm quark, s = strange quark, μ = muon, ν_μ = muon-type neutrino

$$\begin{pmatrix} t_r, t_b, t_g \\ b_r, b_b, b_g \end{pmatrix}_L \quad \begin{pmatrix} \nu_\tau \\ \tau^- \end{pmatrix}_L \quad (b_r, b_b, b_g)_R \quad (t_r, t_b, t_g)_R \quad (\tau^-)_R$$

t = top quark, b = bottom quark, τ = tau, ν_τ = tau-type neutrino

r = red, b = blue, g = green: the three colors of QCD

u, c, t have electric charge $+ 2/3 e$.

d, s, b have electric charge $- 1/3 e$.

In addition, a weak $(SU(2)_W)$ isodoublet of Higgs scalars is required to describe the symmetry breaking evident in the electroweak $(SU(2)_W \times U(1)_B)$ sector. These Higgs scalars provide the mechanism to generate masses for the fermions and for three of the vector bosons. There is, as yet, no direct experimental evidence for these scalars. There is indirect evidence from the W and Z masses, which suggest that three of the four scalars have been absorbed into these vector bosons.

Except for these scalars, all of the basic interactions of the standard model are produced by the exchange of vector bosons between the fermions. Gluon exchanges bind quarks into hadrons and are ultimately the origin of the strong interactions. Meson exchange pictures of hadron-hadron interactions are higher order effects from this point of view.

TABLE II

Members of the three known quark-lepton families and their masses. Each family contains one particle from each of the four types of fermions: charged leptons with an electric charge of -1 (the electron, the muon, and the tau); neutral leptons (the electron neutrino, the muon neutrino, and the tau neutrino); quarks with a electric charge of $2/3$ (the up, charmed, and top quarks); and quarks with an electric charge of $-1/3$ (the down, strange, and bottom quarks). Each family also contains the antiparticles of its members. Family membership is determined by mass, with the first family containing the least massive example of each type of fermion, the second containing the next most massive, and so on. What, if any, dynamical basis underlies this grouping by mass is not known, nor is it known whether other, heavier families exist.

<u>First Family</u>	<u>Second Family</u>	<u>Third Family</u>
electron, e $0.511 \text{ MeV}/c^2$	muon, μ $105.6 \text{ MeV}/c^2$	tau, τ $1782 \text{ MeV}/c^2$
electron neutrino, ν_e $<0.00002 \text{ MeV}/c^2$	muon neutrino, ν_μ $<0.3 \text{ MeV}/c^2$	tau neutrino, ν_τ $<56 \text{ MeV}/c^2$
up quark, u $\approx 5 \text{ MeV}/c^2$	charmed quark, c $\approx 1500 \text{ MeV}/c^2$	top quark, t $>40,000 \text{ MeV}/c^2(?)$
down quark, d $\approx 10 \text{ MeV}/c^2$	strange quark, s $\approx 170 \text{ MeV}/c^2$	bottom quark, b $\approx 4500 \text{ MeV}/c^2$

The electroweak bosons include the photon, and the recently discovered W^+ , W^- and Z vector bosons (at 81 and 93 GeV/c^2). It is the exchange of these massive bosons which is responsible for all known weak interactions, such as nuclear β -decay and neutrino scattering.

What follows are more detailed, separate descriptions of the strong and electroweak factors of the Standard Model.

3. STRONG INTERACTIONS

Let us first present the physics of the strong interactions. In the minimal standard model, mesons (π, ρ, K, \dots) and baryons ($N, N^*, \Delta, \Lambda, \dots$) are to be completely described in terms of quarks combining to make color-singlet composite states. To satisfy the spin-statistics theorem, each of these quarks must come in three states of an internal symmetry called color. Each set of these three states forms a triplet representation of the $SU(3)_c$ group, as indicated by the r, b, g subscripts in Table I. (This is a different $SU(3)$ from the "Eight-fold Way" based on the u, d, s

quarks.) The gauge theory based on this group is called Quantum Chromodynamics.

3.1 The QCD Lagrangian

The assumption of local symmetry leads to a Lagrangian whose form is highly restricted. Only the quark and gluon fields are necessary to describe the strong interactions, and so the most general Lagrangian is

$$L_{\text{QCD}} = -\frac{1}{4} F_{\mu\nu}^a F_{\mu\nu}^a + i \sum_i \bar{\psi}_i \gamma^\mu D_\mu \psi_i + \sum_{ij} \bar{\psi}_i M_{ij} \psi_j, \quad (3.1)$$

assuming CP invariance, and where

$$F_{\mu\nu}^a = \partial_\mu A_\nu^a - \partial_\nu A_\mu^a + g_s f_{abc} A_\mu^b A_\nu^c. \quad (3.2)$$

The sum on a in the first term is over the eight gluon fields A_μ^a . The second term represents the coupling of each gluon field to an SU(3) current of the quark fields, called a color current. This term is summed over the index i , which labels each quark type and is independent of color. Since each quark field ψ_i is a three-dimensional column vector in color space, the covariant derivative, D_μ , is defined by

$$D_\mu \psi_i = \partial_\mu \psi_i - \frac{1}{2} i g_s A_\mu^a \lambda_a \psi_i, \quad (3.3)$$

where λ is a generalization of the three 2×2 Pauli matrices of SU(2) to the eight 3×3 Gell-Mann matrices of SU(3), and g_s is the QCD coupling. Thus, the color current of each quark has the form $\bar{\psi} \lambda_a \gamma^\mu \psi$. The left-handed quark fields couple to the gluons with exactly the same strength as the right-handed quark fields, hence parity is conserved in the strong interactions.

The gluons are massless because the QCD Lagrangian has no spinless fields and therefore no obvious possibility of spontaneous symmetry breaking. Of course, if motivated for experimental reasons, one could add scalars to the QCD Lagrangian and spontaneously break SU(3) to a smaller group. For the remainder of the discussion, we assume that QCD is not spontaneously broken.

The third term in Eq. 3.1 is a mass term. In contrast to the electroweak theory, this mass term is allowed, even in the absence of spontaneous symmetry breaking, because the left- and right-handed quarks are assigned to the same multiplet of SU(3). The numerical coefficients M_{ij} are the elements of the quark mass matrix; they can connect quarks of equal electric charge. The L_{QCD} of Eq. 3.1 permits us to redefine the QCD quark fields so that $M_{ij} = m_i \delta_{ij}$. The mass matrix is then diagonal and each quark has a definite mass, which is an eigenvalue of the mass matrix. We will re-appraise this situation when we describe the weak currents of the quarks.

3.2 The QCD Coupling Strength

Successfully extracting detailed predictions of the L_{QCD} of Eq. 3.1 is very difficult. Analysis of the electroweak theory is simple because the couplings are always small, regardless of the energy scale at which they are measured, so that a classical analysis is a good first approximation to the theory. The quantum corrections are, for most processes, only a few percent.

In processes that probe the short-distance structure of hadrons, the quarks inside the hadrons interact weakly, and here the classical analysis is again a good first approximation because the coupling, g_s , is small. However, for Yang-Mills theories in general, the renormalization group equations of quantum field theory require that g_s increases as the squared-momentum transfer, q^2 , decreases until the momentum transfer equals the masses of the vector bosons. For large q^2 ,

$$\alpha_s(q^2) = g_s^2/4\pi = \frac{\alpha_s(\mu^2)}{1 + b\alpha_s(\mu^2)\ln(q^2/\mu^2)} \quad (3.4)$$

where μ^2 is some reference scale usually chosen to be greater than 1 GeV², and Eq. 3.4 describes the variation of α_s away from that reference value. (The quantity b is a pure number calculated from one-loop Feynman diagrams.) For $q^2 < \mu^2$, however, the logarithm is negative and $\alpha_s(q^2)$ grows as q^2 decreases. It quickly exceeds the range of validity of the perturbation theory used to derive Eq. 3.4. It is widely speculated that this growth produces the confinement of quarks (and gluons), so that only color neutral hadronic states are observed in nature. This speculation is

now receiving support from lattice QCD calculations. Lacking spontaneous symmetry breaking to give the gluons mass, QCD contains no mechanism to stop the growth of g_s , and the quantum effects become more and more dominant at larger and larger distances (smaller q^2 values). Thus, analysis of the long-distance behavior of QCD, which includes driving the hadron spectrum, requires solving the full quantum theory implied by Eq. 3.1. This analysis is proving to be very difficult.

3.3 Phenomenology from QCD

Even without the solution of L_{QCD} , however, some conclusions can be drawn. The quark fields ψ_i in Eq. 3.1 must be determined by experiment. Phenomenological analyses determine their masses (as they appear in the QCD Lagrangian), which are given in Table II. If these results are substituted into Eq. 3.1, we can derive a beautiful result from the QCD Lagrangian. In the limit that the quark mass differences can be ignored, Eq. 3.1 has a global SU(3) symmetry that is identical to the Eightfold-Way SU(3) symmetry. Moreover, in the limit that the u, d, and s masses can be ignored, the left-handed u, d, and s quarks can be transformed by one SU(3) and the right-handed u, d, and s quarks by an independent SU(3). Then QCD has the "chiral" SU(3)×SU(3) symmetry that is the basis of current algebra. The sums of the corresponding SU(3) generators of chiral SU(3)×SU(3) generate the Eightfold-Way SU(3). Thus, the QCD Lagrangian incorporates in a very simple manner the symmetry results of hadronic physics of the 1960s. The more recently discovered c (charmed), b (bottom), and t (top) quarks are easily added to the QCD Lagrangian. Their masses are so large and so different from one another that the SU(3) and SU(3)×SU(3) symmetries of the Eightfold-Way and current algebra cannot be usefully extended to larger symmetries. (The predictions of, say, SU(4) and chiral SU(4)×SU(4) are not easy to reconcile with experiment.)

3.4 Quark Masses in QCD

It is important to note that the quark masses are undetermined parameters in the QCD Lagrangian and therefore must be derived from some other more complete theory or inserted phenomenologically. These arise from coupling to Higgs scalars in the electroweak Lagrangian (see later), which are also free parameters. Thus, the Standard Model provides no

constraints on quark masses, so they must be obtained from experimental data.

The mass term in the QCD Lagrangian (Eq. 3.1) has led to new insights about the neutron-proton mass difference. The quark content of a neutron is "udd" and that of a proton is "uud." If the u and d quarks had the same mass, then we would expect the proton to be more massive than the neutron because of the electromagnetic energy stored in the "uu" vs. the "dd" system. Since the masses of the u and d quarks are arbitrary in both the QCD and the electroweak Lagrangians, they can be adjusted phenomenologically to account for the fact that the neutron mass is 1.293 MeV/c² greater than the proton mass. This experimental constraint is satisfied if the mass of the d quark is about 3 MeV/c² greater than that of the u quark. In a way, this is unfortunate, because we must conclude that the famous puzzle of the n-p mass difference will not be solved until the Standard Model is extended enough to provide a theory of the quark masses.

3.5 Experimental Evidence for QCD

The long distance behavior of QCD is dominated by the growth of the coupling, g_s . The absence of experimental observations of free quarks and gluons is consistent with the extrapolation of this growth beyond the perturbative regime. Many nonperturbative models have been developed to describe this confinement of the color degrees of freedom: linearly rising potentials, strings, flux tubes, and bags. These all do reasonably well at reproducing the mass splittings of mesons and baryons. Even hadron sizes, however, are much more difficult to calculate. The meson-baryon coupling strength, and the momentum dependence of their vertices, are not reliably obtained. Although direct calculations of the QCD path integral by lattice techniques offer significant promise, they are still in a primitive state.

In view of this, one might well ask what experimental basis exists for accepting QCD. This is actually better founded than the tenuous relation between the putative confinement property of QCD and the absence of observed free quarks, or even the qualitative correspondence with the observed hadron spectrum. There is a very good semi-quantitative agreement between QCD calculations (including an inferred effective potential) and the properties of states composed of heavy quarks and antiquarks, such as

the c and b quarks. This is due to the fact that in these heavy quark-antiquark systems, all of the dynamics occur at short distances, with the separation always being within a few tenths of a fermi (fm).

The best evidence for QCD is found in scattering involving short distance dynamics. This includes the hadron jets predicted and found in e^+e^- annihilation into quarks and antiquarks (which appear experimentally as several hadrons moving in similar directions -- a "jet") and especially the quark, antiquark, gluon three-jet final states. In the latter, the measured angular distributions accurately confirm the predictions of QCD. Jet distributions in high momentum transfer hadron-hadron scattering also support QCD predictions, but are less definitive as quantum loop corrections produce significant, but not precisely calculated, corrections. Finally, the pattern of scaling violations in deep inelastic lepton-hadron scattering is consistent with the predictions of QCD.

3.6 The Problem with QCD

The problem of QCD is that it is not understood beyond the perturbative, short distance regime. It must be extended to longer distance scales. In none of the above, however, has QCD been applied directly to nuclei. Deep inelastic lepton scattering results have suggested that the quark distributions in nuclei are not just the sum of distributions in nucleons. This raises the prospect that QCD can be studied at long ($\gg 1$ fm) distance scales in nuclei, and that there are new effects to be studied.

An Advanced Hadron Facility provides secondary beams of mesons (pions and kaons) and of nucleons and antinucleons at energies appropriate for such studies of QCD at longer ranges. In the nuclear medium, for instance, the changes in the properties of baryon and meson states from their free space characteristics depend on the degree to which quark propagation is enhanced beyond 1 fm. Although first family mesons and baryons will provide a great deal of information (via formation and propagation of deltas and N^* 's), it is already apparent that this will not be sufficient, of itself.

Tremendous advantages in clarity of interpretation and understanding of experiments can be afforded by the "radioactive tracer" of strangeness. Introducing the strange quark (lightest quark of the second family) into the systems under study, especially nuclei via kaon beams, or by associated production using first family beams at higher energies, provides a

distinguishable marker with which to follow energy, momentum, and quantum number flow within the nuclear medium. (Any of the quarks from the second or third families could be used, but the extreme masses of the c , b and t make them much harder to produce in experimentally useful quantities.)

Thus, the propagation of a particular quark may be followed, elucidating the properties of QCD in its most interesting (non-perturbative) regime. This is a problem of great interest within the standard model (as material properties remain of interest within the electrodynamic theory of atoms). For problems that primarily involve new physics beyond the standard model, we must turn to the electroweak interactions.

4. THE $SU(2) \times U(1)$ ELECTROWEAK MODEL

Before the electroweak model was proposed over twenty years ago, the electromagnetic and charge-changing weak interactions were well known. If the weak interactions can change electrons to electron neutrinos, then the group representations must at least include doublets, so that $SU(2)$ is the smallest possible group. Various schemes were tried that did not agree with experiment. The hypothesis of the extra $U(1)$ factor was challenged many times until the discovery of the weak neutral current at CERN in 1972 in a neutrino scattering experiment. That discovery established that the local symmetry of the electroweak theory had to be at least as large as $SU(2) \times U(1)$, despite the theoretical awkwardness of having two factors.

4.1 The Electroweak Lagrangian

The Lagrangian includes many pieces. The kinetic energies of the vector bosons are described by L_{Y-M} . The three weak bosons W^+ , W^- , and Z have masses acquired through spontaneous symmetry breaking, so we need to add a scalar pieces L_{scalar} to the Lagrangian in order to describe the observed symmetry breaking. The fermion kinetic energy L_{fermion} includes the fermion gauge boson interactions, analogous to the electromagnetic interactions. Finally, we add terms that couple the scalars with the fermions in a term L_{Yukawa} . The significance of the Yukawa term is that it provides for a description of the masses of the quarks and charged leptons

Thus, the electroweak Lagrangian has the form

$$L_{\text{electroweak}} = L_{Y-M} + L_{\text{scalar}} + L_{\text{fermion}} + L_{\text{Yukawa}} \quad (4.1)$$

(The reader may find this construction to be *ad hoc* and ugly. However, it is important to remember that, at present, the Standard Model is the pinnacle of success in theoretical physics and describes a broader range of natural phenomena than any theory ever has, which is not to say that it is the end.)

The Yang-Mills piece is completely analogous to that for QCD, with only the structure constants for SU(2) replacing those for SU(3) in Eq. 3.2.

The scalar Lagrangian requires inclusion of a representation of scalar fields, called Higgs' bosons. These develop a nonzero vacuum expectation value to break the symmetry similar to the way a spontaneous magnetization field breaks rotational symmetry in a ferromagnetic system. In the minimal version of the theory, these scalars form a complex doublet with four degrees of freedom. After the spontaneous symmetry breaking, three of the four scalar degrees of freedom are "eaten" by the weak bosons. Thus, just one scalar should be observable as an independent neutral particle, called the Higgs particle. It has not yet been observed experimentally, and is the most important particle in the standard model that does not yet have a direct phenomenological verification. (The minimum number of scalar fields in the standard model are these four. Experimental data could eventually require more.)

4.2 The Electroweak Coupling Constants

SU(2)×U(1) has two factors, and there is an independent coupling constant for each factor. The coupling for the SU(2) factor is called g , and the U(1) coupling is g' . The two couplings can be written in several ways. The U(1) of electrodynamics is a linear combination of the U(1) factor and the third component of the weak isospin. The electromagnetic coupling is, as usual, denoted by e and its value is $\sqrt{4\pi\alpha} \approx 0.3$. The other coupling can then be parameterized by an angle θ_w . The relations among g , g' , e , and θ_w are

$$e = gg' / \sqrt{g^2 + g'^2} \text{ and } \tan \theta_w = g' / g \quad (4.2)$$

In the electroweak theory, both couplings must be evaluated experimentally and cannot be calculated in the standard model. (This is also true for the strong coupling constant.)

4.3 Vector Boson Masses

Under the spontaneous symmetry breakdown, the vacuum expectation value of the scalars produces mass terms for the vector bosons. If we call the vacuum expectation value $v/\sqrt{2}$, then the charged (W^+, W^-) bosons have a mass squared of

$$M_W^2 = g^2 \frac{v^2}{4} \quad (4.3)$$

A combination of the remaining two vector bosons will also have a mass; this is the Z^0 . The Z^0 mass squared is

$$M_Z^2 = (g^2 + g'^2) v^2 / 2, \quad (4.4)$$

and the photon is, of course, massless. The ratio of the squares of the W and Z masses satisfies

$$\frac{M_W^2}{M_Z^2 \cos^2 \theta_w} = 1 \quad (4.5)$$

The ratio is termed ρ and its deviation from 1 is a test of the standard model. Values for M_W and M_Z have recently been measured at the CERN proton-antiproton collider: $M_W = (80.8 \pm 2.7) \text{ GeV}/c^2$ and $M_Z = (92.9 \pm 1.6) \text{ GeV}/c^2$. The ratio M_W/M_Z calculated with these values agrees well with that given by $\cos \theta_w$. (The angle θ_w is usually expressed as $\sin^2 \theta_w$ and is measured in neutrino-scattering experiments to be $\sin^2 \theta_w = 0.224 \pm 0.015$.)

4.4 Weak Interactions of Leptons

The form of L_{fermion} is analogous to that for electrodynamics. There is no mass term. Mass terms violate the $SU(2) \times U(1)$ symmetry. We will see later that the electron mass will reappear as a result of modification of L_{Yukawa} due to spontaneous symmetry breaking, just as the vector boson masses arise from coupling to the Higgs' scalars.

After simplifying some expressions, we find that L_{lepton} for the electron lepton and its neutrino is

$$\begin{aligned}
 L_{\text{lepton}} = & i\bar{e}\gamma^\mu\partial_\mu e + i\bar{\nu}_L\gamma^\mu\partial_\mu\nu_L - e\bar{e}\gamma^\mu e A_\mu \\
 & + \frac{g}{\sqrt{2}}\left[\bar{\nu}_L\gamma^\mu e_L W_\mu^+ + \bar{e}_L\gamma^\mu\nu_L W_\mu^-\right] \\
 & - \frac{g\cos\theta_w}{2}\left[\tan^2\theta_w(2\bar{e}_R\gamma^\mu e_R + \bar{e}_L\gamma^\mu e_L) - \bar{e}_L\gamma^\mu e_L\right]Z_\mu \\
 & - \frac{g}{2\cos\theta_w}\bar{\nu}_L\gamma^\mu\nu_L Z_\mu.
 \end{aligned} \tag{4.6}$$

The first two terms are just the kinetic energies of the electron and the neutrino. (Note that the electron field $e = e_L + e_R$.) The third term is the electromagnetic interaction with electrons of charge $-e$, where e is defined in Eq. 4.2. The coupling of A_μ to the electron current does not distinguish left from right, so electrodynamics does not violate parity. The fourth term is the interaction of the W^\pm bosons with the weak charged current of the neutrinos and electrons. Note that these bosons are blind to right-handed electrons. This is the reason for maximal parity violation in beta decay. The final terms predict how the weak neutral current of the electron and that of the neutrino couple to the neutral weak vector boson Z° .

If the left- and right-handed electron spinors are written out explicitly, with $e_L = (1 - \gamma_5)e/2$, the interaction of the weak neutral current of the electron with the Z° is proportional to $\bar{e}\gamma^\mu[(1 - 4\sin^2\theta_w) - \gamma_5]eZ_\mu$. This prediction provided a crucial test of the standard model. Since $\sin^2\theta_w$ is very nearly $1/4$, the weak neutral current of the electron is very nearly a purely axial current, that is, a current of the form $\bar{e}\gamma^\mu\gamma_5 e$. This crucial prediction was tested in deep inelastic scattering of polarized electrons and in atomic parity-violation experiments. The results of these experiments went a long way toward establishing the standard model. The test also ruled out models quite similar to the standard model. There are many more tests and predictions of the model based on the form of the weak currents, but this would greatly lengthen our

discussion. The electroweak currents of the quarks will be described after fermion masses.

4.5 Fermion Masses

We now discuss the last term in Eq. 4.1, L_{Yukawa} . The interaction between the scalars and spinors has the form:

$$L_{\text{Yukawa}} = G_Y \bar{\Psi} \phi \Psi \\ = G_Y (\bar{\Psi}_L \phi \Psi_R + \bar{\Psi}_R \phi^\dagger \Psi_L) \quad (4.7)$$

where ϕ is the Higgs' doublet. We first discuss the case where Ψ describes the electron and its neutrino. If the neutrino has no right-handed component, then it is massless. If ν_R is included, then the neutrino mass is another free parameter; it is excluded in the minimal model. When the neutral Higgs' boson is replaced by its vacuum expectation value, the Yukawa terms for the electron produce the electron mass term,

$$m_e = G_e v / \sqrt{2} \quad (4.8)$$

so the electron mass is proportional to the vacuum expectation value of the scalar field. The general Yukawa coupling G_Y has been replaced by the particular one for the electron, G_e .

As the G_Y -values are free parameters in the electroweak theory, they must be determined phenomenologically from v and the fermion mass. The value of v can be obtained from the value of g and the W -mass, by using Eq. 4.3. The value of g may be inferred from the electromagnetic coupling and the weak angle θ_w , by using Eq. 4.2. Using $m_e = 0.000511$ GeV, we find $G_e = 2.8 \times 10^{-6}$ for the electron.

There are more than nine Yukawa couplings, including those for the μ and τ leptons and the three quark doublets as well as terms that mix different fermions of the same electric charge. The standard model in no way determines the values of these Yukawa coupling constants. Thus, only extensions of the standard model address the full fermion mass matrix.

The electroweak theory predicts, to very high accuracy, all of the interactions of leptons. For example, aside from electromagnetic phenomena, the electroweak theory predicts the detailed structure of μ and

τ decay, and the neutral and charged current scattering of neutrinos on electrons. These predictions are absolute, given the W and Z masses, and the value of $\sin^2\theta_w$ inferred from them. In fact, accurate predictions require the inclusion of radiative corrections which intrinsically depend on the renormalizability of the theory. There are no observed deviations from these predictions at the present levels of accuracy. Further tests require a knowledge of the electroweak properties of quarks, which we describe next.

4.6 Weak Interactions of Quarks

The weak currents of the quarks are determined in the same way as the weak currents of the leptons. Let us begin with just the u and d quarks. Their electroweak assignments are as follows: the left-handed components u_L and d_L form an $SU(2)$ doublet and the right-handed components u_R and d_R are $SU(2)$ singlets.

The charged currents of quarks are entirely analogous to those of leptons (see section 4.4). The contribution to the Lagrangian due to interaction of the weak neutral current $J_\mu^{(nc)}$ of the u and d quarks with Z^0 is

$$L_{(nc)} = \frac{e}{\sin\theta_w \cos\theta_w} J_\mu^{(nc)} Z_0^\mu, \quad (4.9)$$

where

$$\begin{aligned} J_\mu^{(nc)} = & \left[\frac{1}{2} - \frac{2}{3} \sin^2\theta_w \right] \bar{u}_L \gamma_\mu u_L - \frac{2}{3} \sin^2\theta_w \bar{u}_R \gamma_\mu u_R \\ & + \left[-\frac{1}{2} + \frac{1}{3} \sin^2\theta_w \right] \bar{d}_L \gamma_\mu d_L + \frac{1}{3} \sin^2\theta_w \bar{d}_R \gamma_\mu d_R. \end{aligned} \quad (4.10)$$

This pattern is repeated when we include the other quarks.

4.7 Family Repetitions and Quark Masses

So far we have emphasized the construction of the QCD and electroweak Lagrangians for just one lepton-quark "family" consisting of the electron and its neutrino together with the u and d quarks. Two other lepton-quark families are established experimentally: the muon and its neutrino along with the c and s quarks and the τ lepton and its neutrino along with the t

and b quarks. Just like $(\nu_e)_L$ and e_L , $(\nu_\mu)_L$ and μ_L , and $(\nu_\tau)_L$ and τ_L form weak-SU(2) doublets: e_R , μ_R and τ_R are each SU(2) singlets. Similarly, the weak quantum numbers of c and s and of t and b echo those of u and d: c_L and s_L form a weak-SU(2) doublet as do t_L and b_L . Like u_R and d_R , the right-handed quarks c_R , s_R , t_R , and b_R are all weak-SU(2) singlets.

This triplication of families cannot be explained by the standard model, although it may eventually turn out to be a critical fact in the development of theories which extend the standard model. (The quantum numbers of the quarks and leptons are summarized in Tables I and II.)

All these quark and lepton fields must be included in a Lagrangian that incorporates both the electroweak and QCD Lagrangians. It is quite obvious how to do this: the standard model Lagrangian is simply the sum of the QCD and electroweak Lagrangians, except that the terms occurring in both Lagrangians (the quark kinetic energy terms $i\bar{\psi}_i \gamma^\mu \partial_\mu \psi_i$ and the quark mass terms $\bar{\psi}_i M_{ij} \psi_j$) are included just once. Only the mass term requires comment.

The quark mass terms appear in the electroweak Lagrangian in the form from L_{Yukawa} analogous to Eq. 4.8. In the electroweak theory quarks acquire masses only because SU(2)×U(1) is spontaneously broken. However, when there are three quarks of the same electric charge (such as d, s, and b), the general form of the mass terms is the same as in Eq. 3.1, $\bar{\psi}_i M_{ij} \psi_j$, because there can be Yukawa couplings between d and s, d and b, and s and b. Nevertheless, there is no reason for the fields obtained directly from the electroweak symmetry breaking to be these mass eigenstates, and in fact they are not.

We illustrate this for the case of two families of quarks. Let us denote the quark fields in the weak currents with primes and the mass eigenstates without primes. There is freedom in the Lagrangian to define $u = u'$ and $c = c'$. If we do so, then the most general relationship among d, s, d', and s' is

$$\begin{bmatrix} d' \\ s' \end{bmatrix} = \begin{bmatrix} \cos \theta_c & -\sin \theta_c \\ \sin \theta_c & \cos \theta_c \end{bmatrix} \begin{bmatrix} d \\ s \end{bmatrix} \quad (4.11)$$

The parameter θ_c , the Cabibbo angle, is not determined by the electroweak theory (it is related to ratios of various Yukawa couplings) and is found experimentally to be about 13°.

(When the b and c(=c') quarks are included, the matrix in Eq. 4.11 becomes a 3×3 matrix involving four parameters that are evaluated experimentally. The fourth parameter permits a description of CP violation in the standard model. The standard form of this [Kobayaski-Maskawa (KM)] mixing matrix is:

$$\begin{bmatrix} d' \\ s' \\ b' \end{bmatrix} = \begin{bmatrix} c_1 & s_1 c_3 & s_1 s_3 \\ -s_1 c_2 & c_1 c_2 c_3 - s_2 s_3 e^{i\delta} & c_1 c_2 s_3 + s_2 c_3 e^{i\delta} \\ s_1 s_2 & -c_1 s_2 c_3 - c_2 c_3 e^{i\delta} & -c_1 s_2 s_3 + c_2 c_3 e^{i\delta} \end{bmatrix} \begin{bmatrix} d \\ s \\ b \end{bmatrix}$$

$$c_i = \cos \theta_i \quad s_i = \sin \theta_i \quad i = 1, 2, 3 \quad (4.12)$$

where θ_1 , θ_2 , and θ_3 are three real mixing angles and δ is a CP violating phase parameter.)

The correct weak currents are then given by Eq. 4.10 if all quark families are included and primes are placed on all the quark fields. (See Table I.) The weak currents can be written in terms of the quark mass eigenstates by substituting Eq. 4.11 (or its three-family generalization) into the primed version of Eq. 4.10. The ratio of amplitudes for $s \rightarrow u$ and $d \rightarrow u$ is the $\tan \theta_c$; the small ratio of the strangeness-changing to strangeness-nonchanging charged-current amplitudes is due to the smallness of the Cabibbo angle. It is worth emphasizing again that the standard model alone provides no understanding of the value of this angle.

If the neutrinos have masses, then similar effects to Eq. 4.11 must be discussed in the lepton sector, also. This leads to the phenomena of neutrino oscillations, and neutrino decays.

This discussion of the electroweak properties of quarks has been very brief; they are just like leptons, except for a slightly different weak hypercharge. Yet the whole host of weak nuclear and particle decays is, in principle, now understood. We say, in principle, because QCD can produce significant corrections to the basic interactions.

4.8 Strong Interaction Corrections to the Electroweak Interactions

The charged-current weak interactions described above are purely left-chiral. Figure 1a shows a Feynman graph which produces an innocuous renormalization of these left-chiral fermions (such as u_L and d_L) in the pure electroweak theory. However, for quarks, there are also gluonic

couplings. Figure 1b, called a "penguin" diagram, shows a strong interaction correction to Fig. 1a. The gluon couples another quark to the first one, and detailed calculation shows that, to a good approximation, this produces an effective four-fermion coupling of electroweak strength. However, because the gluon couples equally to left- and right-chiral quarks (the strong interactions conserve parity), the result is an effective parity-violating, left-right current-current interaction. This is different from that found for fermions with no strong interactions (leptons). Thus, nonleptonic decays of hadrons appear to involve a more complicated weak Hamiltonian. Furthermore, the usual large QCD effects at large distances (due to the growth of the coupling constant) make large contributions to these decays and so they are difficult to analyze precisely.

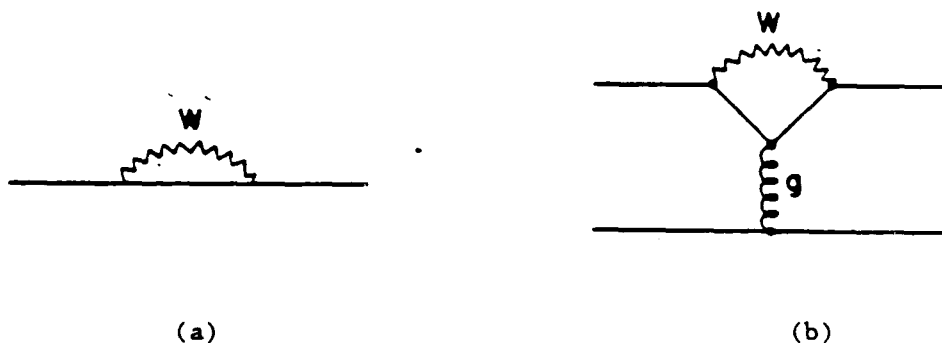


Figure 1. One-loop Feynman diagrams for (a) weak interaction corrections to quark propagation, and (b) combined weak and strong interaction effect in quark-scattering. This latter is called a "penguin" diagram. The straight lines represent quarks, the sawtooth represents a weak interaction vector boson (W, Z, and A), and the curly line represents a gluon.

Other areas where QCD must have significant effects include: the axial vector nucleon coupling ($g_A/g_V = -1.262 \pm 0.005$), which differs from the bare quark value ($g_A/g_V = -1$); and the enhancement of $1/2$ unit isospin changing weak decays over $3/2$ unit ones ($\Delta I = 1/2$ rule).

Thus, it has been nuclear decays, with their effect of quantum number filtering, which have dominantly confirmed the systematics of the electroweak theory. In general, only semileptonic interactions have been useful. One particularly noteworthy case is the parity violating asymmetry in deep inelastic polarized electron-nucleon scattering which confirms the value of $\sin^2\theta_w$.

5. PROBLEMS OF THE STANDARD MODEL AND EXPERIMENTAL TESTS

All of the mesons and baryons and their strong, weak, and electromagnetic interactions, and the nuclei and atoms formed from them, can be described, in principle, by combinations of these fermions and their couplings to the gauge bosons, but many physicists feel that a set of 58 fundamental elements is still too many. There are other problems as well. Why are there three "gauge groups", $SU(3)_C$, $SU(2)_W$, and $U(1)_B$, instead of one? Where does gravity fit in? Are the quarks and leptons really separate, or is there a dynamics that relates them? Do they have a common substructure, that is, are they composite also? Why are there three families, or are there more?

Theories that identify the known dynamical symmetry groups as subgroups of a larger, encompassing group are known as Grand Unified Theories (GUTs). Here both quarks and leptons appear in the same representation of this "unifying" group, and so one predicts dynamical relations between them. The most startling of these predictions is that a proton will decay into leptons and mesons. Major non-accelerator experiments are searching for evidence of proton decay.

Inclusion of gravity is a sort of "super" unification; it requires the introduction of "supersymmetry", a dynamical symmetry between bosons and fermions. Technical problems with this approach (it has too few degrees of freedom) led to serious consideration of composite quarks and leptons where the multiplicity of families reflects the existence of a substructure.

The questions raised here can go well beyond the standard model, but there are still problems closer to home. In Sec. 3.6, the problem of QCD was briefly discussed. There is great hope that this is indeed a problem of understanding a known, correct theory in greater depth. The electroweak problems of family and fermion mass, however, like grand unification, intrinsically take us beyond the standard model. The principle tools for

this effort are searches for decays between families which are not predicted by the standard model, and precision tests of amplitudes, especially for rare processes, which are predicted to occur.

The high fluxes of kaons and other mesons, hyperons and neutrinos provided in the secondary beams of an Advanced Hadron Facility naturally provide great opportunities for precision tests of the standard model and for rare decays searches. In both cases, raw statistical power is improved. But even more so, the quality (brightness and lack of contamination) of these beams, or of even specially built tertiary beams, can be crucial for further advances. In this section, we describe a few of the processes of greatest interest.

5.1 Family Problems and Their Mass Scales

Decays from one family to another, which depend on presumed "family gauge bosons", analogous to those of the standard electroweak model, but inducing transitions between members of different families with the same electric charge, have not been observed. Table III lists a few representative processes that could provide the needed information and the present experimental limits for them.

TABLE III Experimental limits on some family nonconserving processes. The branching ratio is the fraction, of the total number of decays, occurring to a specific final state. [From the Particle Data Group, LBL.]

Process	Branching ratio limit
$\mu^+ \rightarrow e^+ \gamma$	$< 1.7 \times 10^{-10}$
$\mu^+ \rightarrow e^+ \gamma \gamma$	$< 3.8 \times 10^{-10}$
$\mu^+ \rightarrow e^+ e^+ e^-$	$< 2.4 \times 10^{-12}$
$\pi^+ \rightarrow \mu^+ e^-$ or $\mu^- e^+$	$< 7 \times 10^{-8}$
$K^+ \rightarrow \pi^+ \mu^+ e^-$	$< 7 \times 10^{-9}$
$K^+ \rightarrow \pi^+ \mu^+ e^-$	$< 5 \times 10^{-9}$
$K_L \rightarrow \mu^+ e^-$ or $\mu^- e^+$	$< 2 \times 10^{-9}$

The observation of one of the decay modes listed in Table III would constitute direct evidence for a family-nonconserving interaction. It would also provide a measurement of the mass scale associated with family

symmetry breaking. The weak interactions are rare processes with slow rates due to the large (~100 GeV) dynamical scale set by the W and Z boson masses. We can interpret the absence of observed family changing decays as being due to a similar, but larger, dynamical scale associated with the breaking of "family symmetry", that is the mass, M_F , of the "family gauge vector boson" is large. The stringent limit on $K_L \rightarrow \mu e$ shown in Table III allows us to put a lower bound on M_F .

If we assume that the strange and (anti)down quarks in the kaon annihilate to form a virtual massive family boson that emits the final observed muon and electron, the rate (Γ) for this decay process will be given (roughly) by

$$\Gamma \sim \frac{g^4}{M_F^4} M_K^5. \quad (5.1)$$

The fourth power of M_F appears just as M_W and M_Z do in ordinary weak processes (in G_F^2 , the Fermi constant squared). A "grand unification" prejudice appears in the assumption that the "family coupling constant" is similar to that for the weak (g) and electromagnetic interactions.

The branching ratio limit in Table III can be used in Eq. (5.1) to obtain a lower bound on M_F :*

$$M_F \geq 10^5 \text{ GeV}. \quad (5.2)$$

The scale in Eq. 5.2 is not directly accessible by high energy accelerators in the foreseeable future. The Superconducting Super Collider (SSC), which is presently being considered for construction in the next decade, will reach 10^4 GeV and is estimated to cost several billion dollars. We cannot expect to be able to do something yet ten times larger for a long time.

Our experimental knowledge of the scale in Eq. 5.2, however, does not arise from such a brute force approach but rather from a precise measurement at a level of a few parts in 10^9 . Since Γ varies as M_F^{-4} , it is necessary to improve the present branching ratio limit by four orders of

* Certain chirality properties of the family interaction could require that two of the five powers of M_F in Eq. 5.1 be replaced by the muon mass, m_μ . However, after taking a fourth-root to obtain Eq. 5.2, there is little difference.

magnitude to search for a value of M_F in the 10^3 TeV (10^6 GeV) range. This will be quite feasible at an AHF where kaon fluxes on the order of 10^8 /sec will be produced. (Raw fluxes would be larger but some flux will be traded for higher quality beams to reduce backgrounds and minimize systematic errors.) A typical solid angle times efficiency factor for an inflight decay experiment is on the order of 10%. Thus, 10^7 K's per second could be examined for the decay mode of interest. A branching ratio larger than 10^{-12} could be found in one day of running. A full year of beam time would be sensitive down to the 10^{-14} level. Of course, we do not know if a positive signal will be found at even this tiny level. Nonetheless, the need for such an observation to elucidate family dynamics drives us to make the attempt.

We must also investigate the possibility that family symmetry is governed by a massless scalar boson, which has been called the familon. As is generally true for such scalars, the strength of its coupling falls inversely with the mass scale (F) at which the family symmetry is spontaneously broken. Cosmological arguments suggest a lower bound on F very near to its upper bound from laboratory experiments:

$$10^9 \text{ GeV} < F < 10^{12} \text{ GeV} . \quad (5.3)$$

The familon should appear in the two-body decays such as $\mu \rightarrow e + f$ or $s \rightarrow d + f$. The latter appears in $K^+ \rightarrow \mu^+ + f$, where the familon is unseen and the π^+ appears at a momentum of 227 MeV/c. This is a special case of the class of experiments called $K \rightarrow \pi + \text{nothing}$. Improved searches for the familon will require very precise and high resolution measurements of meson-decay spectra.

The neutrino sector offers another arena to search for evidence of nonconservation of family quantum numbers. Neutrino radiative decay has been sought in ν_μ beams with the result of a bound on the lifetime of $\tau_\nu > 10^5 \text{ sec} (m_\nu/\text{MeV})$ for decay into a lighter neutrino plus a photon. If the muon family were not distinct from any other, the naive expectation for τ would be $10^3 \text{ sec} (m_\nu/m_\mu)^5$.

Better evidence may be found in neutrino scattering experiments. The decay of positive muons produces muon-family anti-neutrinos and electron-family neutrinos as long as family quantum numbers are preserved. If these neutrinos are subsequently scattered in nuclear targets, they should

produce only positive muons and electrons, respectively. A LAMPF experiment has confirmed that no negative muons or positrons are produced at a level of about 5%. Since positive pions decay overwhelmingly ($10^4:1$) into positive muons and muon-family neutrinos, subsequent scattering of these neutrinos should produce only negative muons; this, too, has been accurately confirmed.

From the above, it is clear that at present no evidence exists in any (electric charge) neutral process mediated by a Z^0 -like boson for a nonconservation of a family quantum number, i.e., neutral family-changing interactions. Is it possible that these quantum numbers are exactly preserved? Are the family superselection rules as inviolate as those for electric charge and angular momentum? The answer to this is unequivocally NO! We know beyond a shadow of a doubt that family must be a broken symmetry. To see this, one needs only to examine the mass spectrum of the fermions in Table II.

5.2 Family Problems and Fermion Masses

All of the fermion masses violate the electroweak symmetry. However, the pattern of mass splittings within each family and between families all show that family symmetry is also broken. More importantly, because we do not know the mass scale or understand the pattern of the family symmetry breaking, we also cannot determine the mass scale for the electroweak breaking in the fermion sector. If the interactions responsible for family symmetry breaking subtract from the electroweak masses, the scale of the latter could be consistent with the W and Z masses.

Other evidence for family symmetry breaking can be found in weak decays mediated by the charged bosons W^+ and W^- . We know from π and K decays that both the strange quark s and the down quark d decay into the up quark but with significantly different strengths; the down quark has the greater strength. This was discussed in Sec. 4.7 (see Eqs. 4.11-12). This difference between the mass and weak-interaction eigenstates shows that the full Hamiltonian (of the world) cannot be diagonalized in a manner that defines conserved family quantum numbers.

The generalization of this formalism to the three-family case produces an important relation between family nonconservation and CP nonconservation (time reversal noninvariance). [Recall Eq. 4.12.] If family symmetry were exact, the angles in the KM matrix would vanish; then the CP-violating

phase δ would be absorbed in the b-quark field and could not contribute to the observed CP nonconservation. Detailed studies of CP violation in the neutral kaon system are feasible to unprecedented levels at an AHF.

Returning to the discussion of fermion masses, the neutrino masses are especially interesting, as they appear to be very small. The question of neutrino mass is complicated by their lack of electric charge and a peculiarity of the CPT theorem. The latter guarantees the existence of a spin-down (negative helicity) anti-particle state as a partner for every spin-up (positive helicity) particle state but it does not require a spin-down particle state. (We choose the spin quantization axis parallel to the momentum.) When the particles are massless, we can speak of positive and negative helicity or, equivalently, chirality, which just refers to the handedness (as in the right hand rule for the Poynting vector) of the combination of spin rotation and linear momentum. However helicity is not a Lorentz invariant quantity for a massive state, as the particle may be brought to rest and then accelerated in the opposite direction thus changing the sign of its helicity. The chirality, on the other hand, is a Lorentz invariant. Thus, if a particle has mass it requires that either an additional spin down particle state exists (Dirac case) or that particle and antiparticle are indistinguishable (Majorana case).

The latter is impossible when there is a conserved charge, such as electric charge, which distinguishes the particle and antiparticle. Neutrinos, however, carry only weak charge, which is not conserved due to the spontaneous breaking of electroweak symmetry. Indistinguishability of the neutrino and its antineutrino means that lepton number is not conserved; the mass term reflecting this indistinguishability is termed a Majorana mass. Because of the possibility of this Majorana mass in addition to the standard Dirac mass, the neutrino mass matrix is more complicated than that for the other fermions.

Thus the question of neutrino mass is very important and different types of searches are being undertaken. One class of experiment looks for massive neutrinos in decays such as $\pi \rightarrow \mu \nu$ and $K \rightarrow \mu \nu$; the effect appears as a small spike in the lepton energy distribution above the background of multibody decays. Another possibility is to detect a distortion of the π^+ spectrum in $K^+ \rightarrow \pi^+ \nu_i \bar{\nu}_i$ caused by the closing of phase space due to the ν_i mass. This method is sensitive to neutrino masses in the range 50 to 150

MeV/c², independent of the overall rate normalization. These experiments also afford precision tests of predictions of the standard model.

Another consequence of massive neutrinos is the possibility of neutrino oscillations. If the neutrino types have mass and mix in the same general manner as quarks, beams of neutrinos will oscillate from one type into another as one moves away from the neutrino source, just as occurs in the $K^0 - \bar{K}^0$ system. The probability of finding the neutrino state $|b\rangle$ orthogonal to $|a\rangle$ at a distance x is:

$$P_{a \rightarrow b} = \sin^2 (2\theta) \sin^2 \left[\frac{\pi x}{L} \right] \quad (5.4)$$

for relativistic neutrinos with mixing angle θ , where the neutrino oscillation length, L , is given by

$$L = (2.5 \text{ metres}) \left[\frac{E}{\text{MeV}} \right] \left[\frac{\Delta m^2}{\text{eV}^2} \right]^{-1} \quad (5.5)$$

$$\text{and } \Delta m^2 = m_a^2 - m_b^2$$

Although the general case of three neutrino types is more involved, Eqs. (5.4-5) already contain the generally important implications for experiments that attempt to discover neutrino mass effects in this way. From (5.4) it is clear that the largest signal is obtained at $x = L/2$. Even there, the signal is small if θ is small. Thus, experiments require many neutrino scattering events and as small a background as possible for maximum sensitivity to small values of θ . However, the flux of neutrinos always falls off as x increases for any fixed size detector due to the declining solid angle subtended. Thus, for a given Δm^2 , the smallest value of E (and so, L) is desirable. Unfortunately, neutrino cross sections fall rapidly with decreasing energy. For any observation process with an energy threshold, the optimum energy will be not far above that threshold. For example, to detect muon neutrinos, they must have sufficient energy to produce muons. Finally, as for small θ , small Δm^2 reduces the signal strength at any given distance, x . This again puts a premium on maximizing the number of detectable events using the high flux available from an AHF.

5.3 Precision Tests of the Standard Model

The questions about family have been considered in the context of possible extensions to the minimal standard model. However, even if we were completely convinced of the validity of the standard model it would be necessary to subject it to the most detailed test possible. (This is also a classic way to look for new physics.) Three such tests are highlighted here. Perhaps the most outstanding precision test is $\nu_\mu e$ scattering. It would allow a clean, high precision measurement of θ_W , which would test the electroweak theory at the one-loop level of quantum field theory; this is a stringent test, analogous to the Lamb shift or $g-2$ for quantum electrodynamics.

The problem of CP nonconservation is one of the great mysteries of our generation. It has been seen only in the neutral kaon system and the experimental evidence does not dictate a unique theoretical interpretation. One of the strengths of the standard model is a natural parameterization of CP nonconservation. It is very important, therefore, to make measurements with adequate precision to see if this represents the proper explanation.

In principle, CP nonconservation can be studied in other, heavier quark systems, namely $D^0(-c\bar{u}) - \bar{D}^0$, $B^0(-b\bar{d}) - \bar{B}^0$, and $T^0(-t\bar{u}) - \bar{T}^0$, but there are two obstacles to this. One problem is that the CP-nonconserving effects arise only in communicating channels between particle and antiparticle, which are a smaller fraction here of the total decay amplitude than for kaons. The K^0 and \bar{K}^0 both largely decay to two and three pions, so that unitarity promotes $K^0 - \bar{K}^0$ mixing. Such modes are Cabibbo (or KM) suppressed for the heavier mesons, and the dominant channels do not communicate to this order in the weak interaction; e.g., $D^0 - c\bar{u} \rightarrow s\bar{u}$, while $\bar{D}^0 - \bar{c}u \rightarrow \bar{s}u$ and the s and \bar{s} do not mix under the strong interaction. The other problem is a small production rate, $< 10^9/\text{yr}$ vs. the 10^9 K's/sec possible at an AHF. Thus, one must search for a smaller fractional effect in a smaller available data set. Clearly, the strange quark offers the better window on family symmetry and CP nonconservation.

The process $K^+ \rightarrow \pi^+ + \text{"nothing else seen"}$ was introduced as a way to search for the familon. It is also an important test of the standard model via the rate for the allowed mode $K^+ \rightarrow \pi^+ + \nu_1 + \bar{\nu}_1$ for all light neutrino types, i. As for CP violation this process occurs through a one-loop quantum field theoretic correction to the standard electroweak theory. It

is interesting in itself for two reasons: 1) it depends on quark mixing differently from CP nonconservation and so allows independent study of the quark mixing matrix elements; 2) it depends on the number of light neutrino types, N_ν . Because the latter number is expected to be determined in Z^0 decay studies, an uncertainty in the hadronic overlap matrix element can be determined. Present estimates place the branching ratio in the range $N_\nu \times (10^{-9} - 10^{-10})$. If this experiment yielded a discrepancy with the N_ν value determined from Z^0 decay it would be evidence for new physics or that at least one of the neutrinos has a mass greater than about 200 MeV/c².

6. CONCLUSION

The experiments referred to above will require a variety of high quality beams to be available at an AHF just as muon beams at LAMPF have enabled the world-leading searches for family nonconservation in the decays $\mu \rightarrow e\gamma$ and $\mu \rightarrow e\gamma\gamma$. Of particular importance are the high flux and high quality stopping kaon beams for QCD studies and the high flux and well defined multi-GeV kaon beams for electroweak studies. The extra flux at an AHF also provides unique opportunities to obtain desirable experimental conditions for other meson decay studies. For example, a momentum-analyzed K^+ beam could be used to produce, by charge exchange scattering, a narrow momentum bite neutral kaon beam with a flux in the latter comparable to present day unanalyzed beams. Similarly, a narrow-band neutrino beam at an AHF could equal or exceed the flux in present wide-band beams.

For neutrino oscillation experiments, the high flux of neutrinos at modest energies allows maximization of the statistical power of experiments while minimizing backgrounds. An AHF complex can provide high flux, low-energy ν_μ beams with exceptionally little ν_e contamination for experiments searching for $\nu_\mu \rightarrow \nu_e$, clean beams at the intermediate energies optimum for studying ν_μ disappearance, and unparalleled intensities of ν_e and $\bar{\nu}_e$ at energies suitable for studying ν_μ appearance.

In addition to the need to deepen our understanding within the standard model, extensions may be well required. The example that has been concentrated on here is the family symmetry problem, which is as fundamental and important a problem as Grand Unification, and it may well be a completely independent one. The known bound of 100 TeV on the scale of family dynamics is an order of magnitude beyond the direct reach of even

foreseeable accelerators, such as the Superconducting Super Collider. These dynamics, however, may be accessible in studies of rare kaon decays, meson and hyperon decays, neutrino oscillations, and careful studies of CP nonconservation. This high-precision frontier is complementary to the high-energy frontier. To undertake these experiments at the required levels of precision requires intense fluxes of particles from the second or later families. Only particles from the second family can be produced at the required intensities. The high intensity, medium-energy accelerator complex of an AHF is a highly cost-effective means to meet these experimental needs.

7. REFERENCES

On the Standard Model and Unification

P. Langacker, Proceedings of the 1985 International Symposium on Lepton and Photon Interactions at High Energies", Kyoto publication by the Organizing Committee, Yukawa Hall, Kyoto University.

R. C. Slansky, Los Alamos Science, No. 11, Summer/Fall 1984, published by Los Alamos National Laboratory.

T. Goldman, Advances in Nuclear Physics, Vol. 18, in press.

On Experiments at an Advanced Hadron Facility:

Physics and Plan for a 45 GeV Facility, Los Alamos manuscript LA-10720-MS, May 1986.

LAMPF-II Proposal, Los Alamos preprint, LA-UR-84-3982 (Dec. 1984).

Report of the AGS-II Task Force, Brookhaven User Group (Feb. 1984), ed. by G. A. Smith.

Proceedings of the 3rd LAMPF-II Workshop, Los Alamos, LA-9933-C (2 Vols.), July 1983, ed. by J. C. Allred, T. S. Bhatia, Kit Ruminer and Beverly Talley.

Physics with LAMPF-II, Los Alamos proposal, LA-9798-P, June 1983.

Proceedings of the 2nd LAMPF-II Workshop, Los Alamos LA-9572-C (2 Vols.) July 1982, ed. by H. A. Thiessen, T. S. Bhatia, R. D. Carlini and N. Hintz.

Intense Medium Energy Sources of Strangeness, (UC-Santa Cruz, 1983) AIP Conf. Proc. No. 102, Particles and Fields Subseries No. 31 (AIP, N.Y., 1983), ed. by T. Goldman, H. E. Haber and H.F.-W. Sadrozinski.

Proceedings of the Workshop on Nuclear and Particle Physics at Energies Up to 31 GeV: New and Future Aspects, Los Alamos LA-8775-C (Jan. 1981), ed. by J. D. Bowman, L. S. Kisslinger and R. R. Silbar.

PRÉCIS OF GROUP III ACTIVITIES

(Note: Group III discussions generally used as upper bounds for the numbers of antiprotons available the amounts an initial U.S. low energy antiproton source can deliver - 10^{14} antiprotons per year. Exceptions occur in papers 5 and 7.

Paper (1) - Hynes, et al - discusses the principles of a design for a large portable ion trap storing $\sim 10^{13}$ antiprotons at 25-50 KeV. The particles are confined in a cylindrical plasma volume 100 cm. long, 4 cm. in diameter; the vacuum is $< 10^{-12}$ Torr, giving a storage time of ~ 30 to 100 days or better; the magnetic field is 10T. A complete installation, including all support equipment, can easily fit into a large truck. The point design can be scaled to smaller storage levels and storage assemblies.

Paper (2) - Solem - discusses the general theoretical basis for opacity and equation-of-state measurements. The basic question here is whether antiprotons can be used for experiments in extreme states of matter without the current needs for large and expensive centralized facilities available to relatively few researchers. A "table-top" tool using antiprotons from a portable storage device would open up this research area to a much wider audience. The main areas of interest include high temperature, high pressure, high secondary particle (pions, γ s, etc.) flux research, and work such as described in several papers of Group II.

Paper (3) - Morgan - discusses some of the information base necessary if one is to evaluate critically, and perform realistic conceptual and implementation designs for, antimatter propulsion engines (rocket or air-breathing). The promise of using antiprotons in propulsion awaits not only orders-of-magnitude increase in antiproton production, but also a detailed understanding of how antiprotons and their annihilation products interact with matter.

The two main issues for these engines are: 1) getting the antiprotons to annihilate where they are wanted, and 2) getting the annihilation energy deposited where desired. A variety of experiments is described which contribute to full scale engine model design, assess basic feasibility, allow code verification and calibration, and permit design optimization.

Paper (4) - Callas - describes a generic experimental apparatus with which many antiproton engine - related processes could be investigated, using modifications of current high energy particle detector technology. The paper identifies key research issues, and uses the proposed experimental apparatus with quantities of antiprotons consistent with quantities deliverable from assumed low energy antiproton facilities.

Paper (5) - Cassenti - discusses the underlying calculations and the systematic attributes of a specified class of antimatter engines, and establishes the efficiencies attainable with magnetic deflection in a vacuum, effects of propellant density, etc. A parametric study is presented, showing effects of propellant choice, mass ratios, and magnetic fields, over wide ranges.

Paper (6) - Takahashi - describes fundamental aspects of antiproton annihilations interacting in a DT mixture, using the muons produced by decay of the annihilation produced pions and exploiting muon catalyzed fusion in several propulsion schemes. The reaction chains possible here can substantially amplify the basic annihilation energy release. Schemes are also suggested for non-accelerator production of heavy antinuclei, using muons from annihilation produced pions. Heavy antinuclei are of basic physics interest, as well as being potentially useful as condensation sites for antimatter, one of the uses suggested here.

Paper (7) - Takahashi and Powell - speculates on possibilities which might serve to increase significantly antiproton production yields and lower costs for producing these antiprotons. Paper (7) suggests substantial increases in antiproton production when multiple collisions are taken into account, with estimated total yields increasing almost

linearly with incident proton energy above 200 GeV. These estimates depend on a number of simplifying assumptions whose validity and degree of optimism need further suggested testing and analysis. Antiproton production costs are estimated for a range of power costs and accelerator/target costs.

Paper (8) - Kalogeropoulos et al - introduces what may be one of the most compelling near-term and high payoff applied science uses for low energy antiprotons.

Imaging appears to be perhaps the most promising single near-term application for antiprotons. As an example of the potential of antiprotons, 10^7 antiprotons could give the same quality image as a CT scan, with 1/15 the dose and none of the artifacts that can clutter a CT image.

For therapy the doses must be increased one or two orders of magnitude, and at those levels more information is needed about the local energy deposition in biological targets. One potential immediate application for antiprotons in therapy is as a tool for testing, monitoring, simulating, and improving proton and heavy ion therapies.

The third interesting area for medical experimentation with antiprotons, using x-ray emissions or nuclear gammas, is in the general area of "mesic chemistry" or imaging elemental atoms in-vivo or in-vitro.

Preliminary experimental trials of these biomedical applications can be undertaken at BNL (or LEAR).

Paper (9) - Greszczuk - reviews suggested uses of antiprotons for quantitative non-destructive evaluation (NDE) of materials, measuring local densities and density gradients; new material processing techniques; defect healing in materials; identification of material compositions. Comparing use of CT and antiprotons for inspecting a critical component suggests that use of antiprotons might speed up this process by a very large factor.

The contents of paper (10) - Forward - are self-explanatory. The paper reflects an intensive bibliographic search on the 10 major topics identified, brought up to a date of August, 1987. Interested readers and researchers can thus access antimatter information of direct interest.

Some Major Observations from Group III Activities

- The technology is ripe for developing a family of portable ion traps, complementary to use of portable storage rings, storing antiprotons in various amounts up to $\sim 10^{13}$ particles, and allowing transport to and use at laboratories removed from FNAL, BNL.
- A number of potential applied science and applications - related uses for antiprotons employ antiproton amounts deliverable by a first U.S. low energy antiproton source ($\sim 10^{14}$ antiprotons per year) and appear attractive and worthy of further study.
- Basic tools, experimental procedures, instrumentation, etc. for a great deal of applied science research are comparable to those needed for basic science work, so that these two streams of effort should reinforce each other.
- As with the basic science case, the possibility of pursuing near-term, useful applied science research emphasizes the vital needs for a U.S. low energy antiproton source and development of associated enabling tools, such as portable storage devices.
- Joint pursuit of basic and applied science at levels allowed by a first U.S. low energy antiproton source ($\sim 10^{14}$ antiprotons/year) gives prospects for fast progress in assessing feasibility and utility of concepts requiring much larger antiproton amounts.

Portable Pbars, Traps that Travel

S. D. Howe, M. V. Hynes, and A. Picklesimer

Los Alamos National Laboratory
Los Alamos, NM 87545

Abstract

The advent of antiproton research utilizing relatively small scale storage devices for very large numbers of these particles opens the possibility of transporting these devices to a research site removed from the accelerator center that produced the antiprotons. Such a portable source of antiprotons could open many new areas of research and make antiprotons available to a new research community. At present antiprotons are available at energies down to 1 MeV. From a portable source these particles can be made available at energies ranging from several tens of kilovolts down to a few millielectron volts. These low energies are in the domain of interest to the atomic and condensed matter physicist. In addition such a source can be used as an injector for an accelerator which could increase the energy domain even further. Moreover, the availability of such a source at a university will open research with antiprotons to a broader range of students than possible at a centralized research facility. This report focuses on the use of ion traps, in particular cylindrical traps, for the antiproton storage device. These devices store the charged antiprotons in a combination of electric and magnet fields. At high enough density and low enough temperature the charged cloud will be susceptible to plasma instabilities. Present day ion trap work is just starting to explore this domain. Our assessment of feasibility is based on what could be done with present day technology and what future technology could achieve. We conclude our report with a radiation safety study that shows that about 10^{11} antiprotons can be transported safely, however the federal guidelines for this transport must be reviewed in detail. More antiprotons than this will require special transportation arrangements.

1 Introduction

Antiprotons have been available for research in high energy physics since their discovery in 1955 (Ref. [1]). The advent of the new cooling technology at CERN [2] and later at FermiLab [3] has made these particles available at energies down to a few MeV [4] and has opened many new research avenues in nuclear and particle physics. Through a series of additional deceleration stages, the energy of the antiprotons can be lowered to a few tens of kilovolts (or lower). These energies are suitable for storage in ion traps.

Ion traps have been in use in atomic physics for several decades and are commonly very compact structures [5,6]. A number of large ion traps, those capable of storing large numbers of ions have been in use in the United States [7] and in Japan [8]. These structures are still compact when compared with the very large storage rings commonly used in high energy physics. Recently, the possibility of storing very large numbers of antiprotons in ion traps has been discussed [9,10,11]. The fact that these structures will be relatively compact raises the additional possibility of their being portable. Such a portable source of antiprotons could be filled at a production facility and then transported to a remote university or other research laboratory. In addition the antiprotons could be made available at a variety of energies from several tens of kilovolts down to a millivolt. These energies are of interest to the atomic, condensed matter, or chemical physicist. Thus a low energy source of antiprotons could make these particles available to a new research community. Moreover, the fact that the source can be made available at the home institution of the researchers will allow for a wider research community involvement than would be possible at the production facility itself. In addition there will be a broader range of student involvement in this research. If the remote research lab has an accelerator, the portable antiproton source can serve as an injector so that much higher energies can be obtained. These higher energies are those of conventional interest to nuclear physics. However, there is not much known at present about the nucleon-antinucleon interaction. This too would be a new frontier of research.

Two review articles have already very thoroughly discussed the storage of very large numbers of ions in traps [12,13]. In this report we build on the foundation laid by these works and explore specific design considerations for such a portable source. In outlining the design problem there are three main issues:

- How many antiprotons are required for a significant research program?
- How long do the antiprotons have to be stored?
- How safe is the transport and storage of the source?

Evidently these three issues have interlocking answers. Some research in atomic and condensed matter physics requires only a handful of antiprotons, whereas other research in these areas or in nuclear physics requires enormous quantities. Transporting a handful of antiprotons is an almost trivial safety problem whereas a very large number could present a hazard.

In the sections that follow each of these major design issues are discussed and their impact on the design is assessed.

2 How Many

2.1 How Many Do You Want?

Because much of the research that would be done with a portable source is in areas that have not had antiprotons available before, it is difficult to assess how many antiprotons they could need. In a typical experiment at LEAR between 100 — 1000 hours of beam time are allocated depending on the experimental requirements. These experiments are generally in nuclear and particle physics with a few in atomic physics. With the flux at LEAR of 10^9 per hour the total number of antiprotons used ranges from 10^{11} — 10^{12} . Thus to keep even with this current beam availability for experiments total storage capacities in this range are required. Because the portable source technology could become available a few years from now and because much of the research that could be done is not well defined at present, it is probably prudent to plan a system for about an order of magnitude larger than this range. Thus we will consider as the upper limit to the question of "how many do you want", the range 10^{12} — 10^{13} .

Naturally for some research programs several orders of magnitude fewer may be required. Thus we will also consider the impact on the point design of storing fewer particles.

2.2 How Many Can You Get?

The answer to the question of "how many can you get" at present is zero. No accelerator facility in the world today is in the business of filling storage bottles with antiprotons for transport to a remote research site. They are in the business of providing beams of antiprotons for basic research on-site. Moreover, this research is peer reviewed by a program advisory committee which recommends to the director of the facility beam allocations on the basis of scientific merit and technical competence. In addition every facility requires experimenters to design according to a well defined safety code and has standard practice for radiation hazards. Ultimately the liability rests with the facility. It must show a path of diligence directed at avoiding accidents. These issues will be difficult enough to resolve for the case of a facility in the United States providing antiprotons to a remote research site also in the United States. Trying to resolve them in an international arena is probably near impossible. Because there is no facility in the United States that can provide the low energy beam suitable for additional deceleration to ion trap energies, the answer to how many can you get really waits on the building of such a facility and the setting in place of the proper agreements of responsibility, research oversight, etc..

Recently, the building of such a low energy facility at FermiLab has been discussed. Such a facility, given funding, could be operational early in the next decade. The antiproton flux at such a facility could be as high as 10^{10} per hour. To obtain the 10^{12} — 10^{13} antiprotons would still take 100 — 1000 hours of beam. This would represent an enormous impact on the on site research program. It is unlikely that this many antiprotons would be allocated to off-site research. Unless there is a significant increase in the flux at the discussed facility at FermiLab, or yet another facility is built, any off-site research program will have to settle for fewer antiprotons.

Thus to answer the question how many can you get, at least early in the next decade, if the FermiLab facility is built, and if there is no new technical breakthrough at FermiLab, and if no other facility is built, and if the impact on the on-site research program is to be minimized, is probably between 10^{11} — 10^{12} antiprotons. This would take at a flux of 10^{10} per hour between 10 — 100 hours. Normally a facility is in operation about half of the year. This is in part to

reduce operating costs but also to effect repairs on equipment that is down or to make facility modifications. We propose that a viable off-site research program would involve about 10 locations with bottles to fill. If a week at the start and end of the operating schedule were allocated to fill all the bottles, then each facility would have about 10^{11} antiprotons for its research program. This amount of commitment to an off-site program is probably within the capability of such a facility as that discussed at FermiLab without impacting the on-site research in a serious way. Efficient utilization of this schedule requires that the storage time for the particles at the off-site location be about 6 months.

2.3 How Many Can You Store?

Regardless of how many total particles you can get, for portability the design will always be driven towards smaller storage devices. This means ultimately that the density of the antiprotons in the storage device will be as high as possible. There are physical limits, however, to how high a density is possible. There are also considerations based on what has been achieved with current day technology. Thus there are two paths through the question "how many can you store". What can be done in principle and what can be done as a reasonable extension of existing technology. The path through what can be done in principle requires that a research program addressing the technical issues to which we have no answers, be initiated. The path through existing technology is much more reliable for a practical design that we would build tomorrow. Because the actual use of portable traps is a few years away we try to address both paths.

2.3.1 What Can You Store in Principal?

Ion traps use a combination of electric and magnetic fields to achieve confinement. Electric fields are used to achieve axial confinement whereas magnetic fields are used for the radial confinement. In the radial direction a force balance must be achieved between the Lorentz force and the centrifugal force so that the particle orbits can be stable. The details of this radial force balance have been discussed in previous review articles and the reader is referred to them for more information. The exact balance of the radial forces is termed the Brillouin Limit [14]. The Brillouin limit obtains in detail at zero temperature, or at low enough temperatures so that the Debye length is short compared to the dimensions of the charge cloud. Nevertheless, you can not do any better than this limit for the density of the charge cloud. This limit is given by

$$n_0 \leq \frac{B^2}{8\pi mc^2} \quad (1)$$

where n_0 is the ion density, B is the magnitude of the applied magnetic field and, mc^2 is the rest mass energy of the stored particle. To stay below this limit the total energy in the magnetic field must exceed that contained in the rest mass energy of the contained particles. As a design guide and to provide a more visual appreciation of the magnitudes involved we display the Brillouin limit in Fig. 1. In the figure the limiting density in units of AMU/cm^3 is plotted as a function of magnetic field. For systems with densities and field strengths above the contour, the orbits of the stored particles will be unstable. For systems that locate below the contour the orbits will be stable. The plotted points are a selection of reported values of density and field strengths reported in the literature in Refs. [12,15] (by no means a complete survey). These points show that the closest anyone in this limited survey has come to the limit at high field strengths is about within

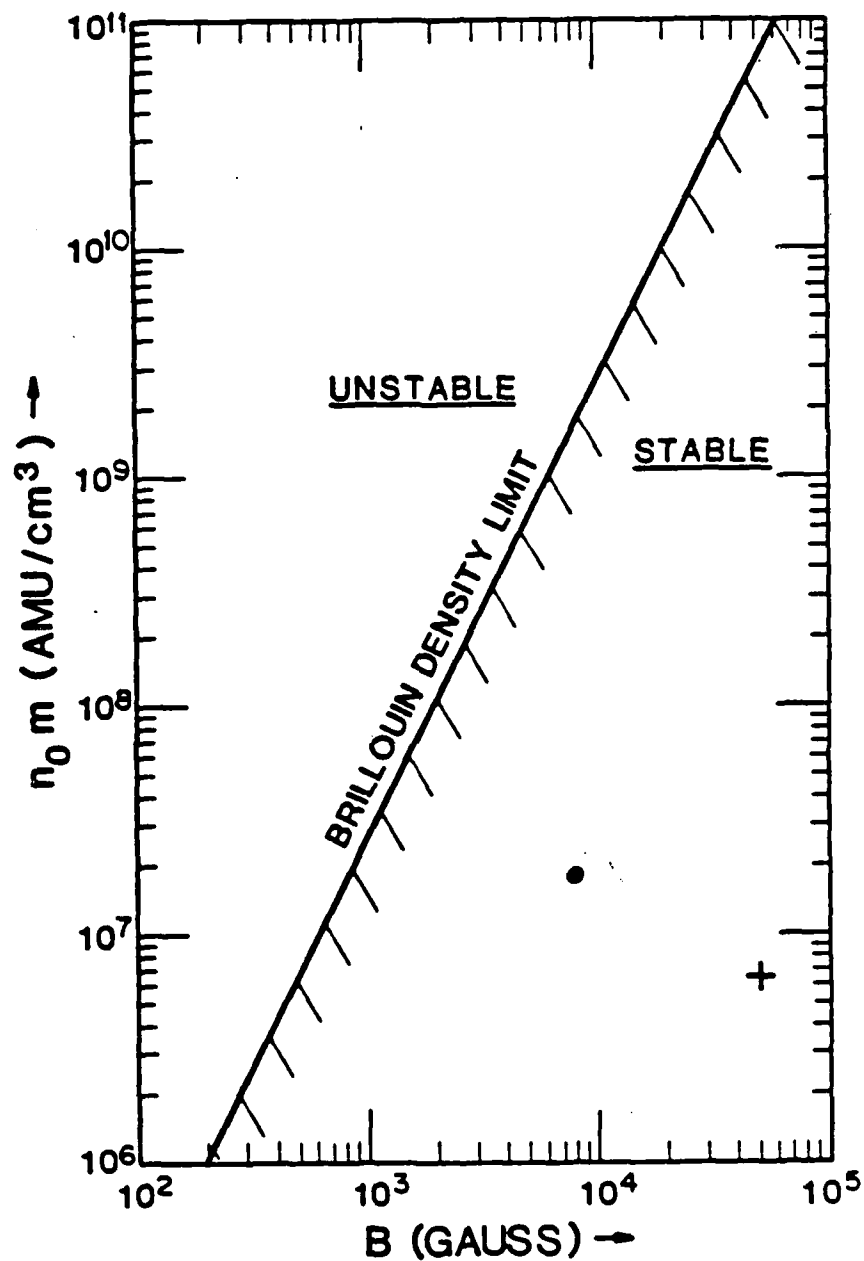


Figure 1: The Brillouin limit on the density in ion traps is shown as a function of magnetic field strength and density. Below the contour shown the particle orbits will be stable, whereas above the contour the orbits will not be. The density is in units of AMU/cm³. The points represent reported values of density and magnetic field strength reported in the literature.

2 orders of magnitude. Thus, for our storage system we must stay well below the limit to achieve stability with a high degree of confidence.

Recently, it has been suggested that ion traps could be used for large scale storage of antiprotons for energy source applications [16]. The Brillouin limit on the storage density in ion traps requires that the energy in the magnetic confining field be greater than or equal to the energy contained in the rest mass of the stored particles. Because the rest mass energy is what can in principle be extracted for these applications, massive storage in ion traps is simply not very attractive: you'll have more energy stored in the form of the magnetic field. For these applications a technology beyond ion traps is required. However, ion traps can provide an intermediate technology that will allow the research in higher density storage concepts to move forward.

The relationship between the rest mass energy and the magnetic field energy at the Brillouin limit suggests a figure-of-merit for storage concepts for energy applications. In ion traps, because of the Brillouin limit, the ratio of the rest mass energy to the magnetic field energy must be less than 1. More advanced storage concepts will have to exceed this value. For realistic energy applications the energy in the fields used to confine the particles or to achieve some sort of dynamic equilibrium must be very small compared to the rest mass energy of the stored particles. The figure-of-merit would thus be much greater than 1.

2.3.2 Plasma Physics Considerations

An important break point in the number density stored in a trap is determined by the onset of collective effects. This onset is characterized by comparing the Debye length with other lengths in the system. If the Debye length is larger than the dimensions of the charge cloud, no collective effects should be present. In fact, by definition, we do not even have a plasma, only a collection of charged particles behaving independently [17]. For Debye lengths less than the dimensions of the charge cloud there will be collective effects. Although the original work by Debye was for the shielding of a charge in an electrolyte (an overall neutral system), the concept of the Debye length for a nonneutral plasma has much utility [18].

The Debye length can be written as

$$\lambda_D = \left[\frac{kT}{4\pi e^2 n_0} \right]^{\frac{1}{2}} \quad (2)$$

where T is the temperature of the particles and n_0 is the number density. To visualize the quantities involved, this expression is plotted in Fig. 2. In this figure are plotted contours of constant Debye length on a grid of number density and plasma temperature. Three values of the Debye length are shown, 0.1, 1.0, and 10.0 cm. For cylindrically shaped charge clouds the dimension of interest will be the radius of the cylinder. This dimension will be smaller than the length of the cylinder (for the cases we envision here) and will provide us with a worst case scenario. Because the cylinders of interest will be between 1 - 10 cm in diameter the onset of collective effects should lie between these two contours shown in Fig. 2.

2.3.3 Electrostatics

A final limitation on the number of particles that can be stored is given by their space charge potential. The geometry of the cylindrical traps considered here is shown in Fig. 3. In the figure three electrodes are shown with the location of the plasma column also indicated. The central

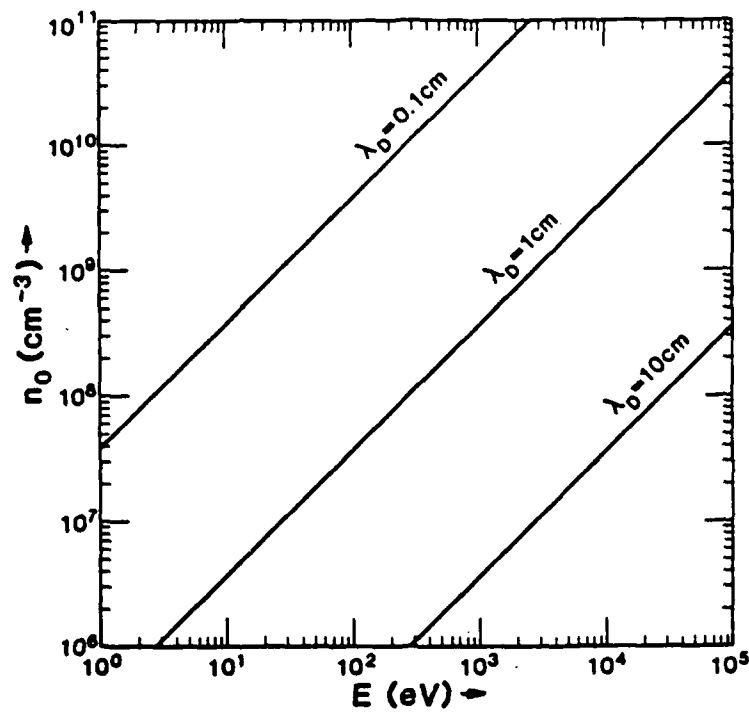


Figure 2: Contours of constant Debye length are plotted on a grid of number density and plasma temperature.

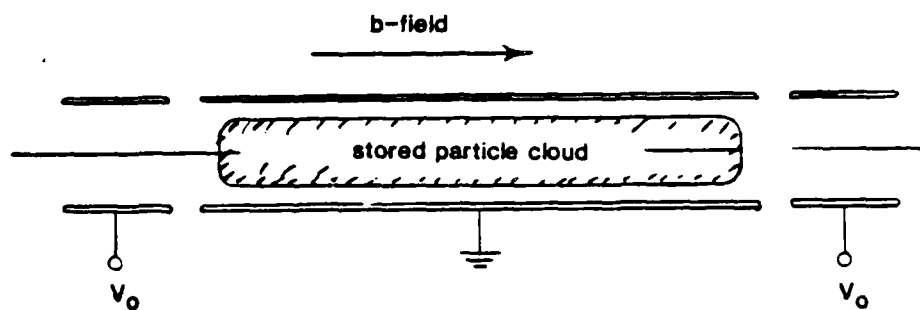


Figure 3: Schematic geometry of cylindrical traps.

electrode is shown grounded whereas the outer two electrodes are at a potential that will confine the particles. For the cylindrical traps considered here the potential at $r=0$ is given by [12]

$$\Phi_0 = -1.4 \times 10^{-7} \frac{N_T}{L} \left(1 + 2 \ln \frac{R_w}{R_p}\right) (\text{Volts}) \quad (3)$$

where N_T is the total number of stored charges in cm^{-3} , L is the length of the cylinder in cm, R_w is the radius of the grounded cylindrical electrode, and R_p is the radius of the plasma. To achieve axial confinement the potential applied to the outer two electrodes shown in Fig. 3 must exceed this potential by several times the kinetic energy of the stored particles. To store 10^{12} antiprotons in a 100 cm long trap with $R_w = 1.5R_p$ would require voltages in excess of 2500 Volts. This seems initially a modest voltage. However, this voltage scales as the number of stored particles. The likelihood of storing as much as a milligram of unneutralized antiprotons ($\sim 6 \times 10^{20}$) seems rather remote.

2.4 Impact on Point Designs

The Brillouin limit gives a relationship between the number density and the applied magnetic field. To achieve high densities in the trap, high magnetic fields will be required. Magnetic fields of up to 10 Tesla can be achieved in solenoids from a number of manufacturers and even higher fields may be possible with a design effort. However, there is a limit to the maximum field given by the strength of materials.

The Debye length gives us a relationship between the transverse size of the charge cloud, the temperature of the stored particles, and the number density. To avoid collective effects which could lead to instabilities for charge clouds between 1 - 10 cm in radius the design is driven to higher temperatures to achieve larger number densities. If we ignore the importance of the Debye length compared to the size of the charge cloud we eventually must do something about the possibility of instabilities in the plasma. The physics of nonneutral plasmas is not very well understood. Only recently with the work of the UCSD [12] and NBS [13] groups has some of the physics started to come to light. The design decision is between keeping the charged cloud single particle in nature which drives us to higher temperatures or to wrestle with the collective effects which are at present not well understood. Ultimately to achieve higher densities the physics of the collective effects will have to be understood. This is a critical issue in the design and will require a research effort to resolve.

The electrostatics of the plasma require modest voltages for storage of $10^{12} - 10^{13}$ particles. However, the actual voltages used must exceed the space charge potential by several times the kinetic energy of the stored particles. Storage of very large quantities of unneutralized antiprotons seems rather remote.

3 How Long?

3.1 Introduction

The storage time for particles in a Penning trap is ultimately limited by the loss rates arising from collisions with residual gas molecules and from collisions among the ions themselves. These loss rates depend on the collision frequency and on the size of the cross sections for these reactions that

lead to particle loss from the trap. However, the frequency of collisions (per ion) with residual gas molecules depends solely on the density of the residual gas, whereas the self-collisions of the ions depend solely on the density of the stored ions. At sufficiently high densities where the Debye length is small compared to the dimensions of the contained plasma, the ion-ion collisions will lead to collective effects and possible plasma instabilities.

The collisions with residual gas is a vacuum issue whereas the collective effects are a plasma physics issue. As stated earlier the physics of the collective effects must be ultimately understood to achieve very high densities in the storage system. In addition there will be instabilities associated with the mechanical alignment of the system with the magnetic field. These fabrication difficulties have been discussed in Ref. [12] where it is suggested that active feedback could be used for defeating this loss process. These loss processes also require a research effort for resolution before an informed design can move forward. Here we focus on the vacuum issue, the design consequences arising from simple collisions with residual gas molecules, and the limitations imposed by the space charge potential.

3.2 Vacuum Requirements

The density of the residual gas can be written using the ideal gas law as

$$\frac{N}{V} = \frac{P}{RT} \quad (4)$$

In this expression the density is proportional directly to the pressure and inversely to the temperature. Thus if the gas temperature is 10 or 100 times less than room temperature, the pressure has to be reduced 10 or 100 times also just to keep a constant density level. Thus it is the ratio of the pressure and temperature that is the important quantity that determines the density and it is the density that is a determining factor for the loss rates. In our calculations we have evaluated the loss rates for room temperature and liquid nitrogen temperature to illustrate the importance of this point.

The density of particles in the ion trap can be evaluated using rather specific assumptions about the trap geometry and potential settings. This is important only for the self-collision loss rates. For residual gas collision losses, only the total number of ions is important. For the antiproton there are no measurements of these cross sections. There are however good calculations from which we can make a worst case estimate. For all these processes hydrogen is the gas that is the subject of the calculation. In the ultra-high vacuum required for long storage times this gas will be the most abundant. However, the cross section for helium and other gases were uniformly lower than for hydrogen when the data was available. Thus the hydrogen cross section is the worst case. For the antiproton the cross section calculation is for atomic hydrogen. However this can be extended to molecular hydrogen due to the similarities in the ionization potential. The details of our calculations for the loss rates for antiprotons are presented in Ref. [19].

3.2.1 The $\bar{p} + H_2$ Cross Section.

Measurements of the total annihilation total cross section in H_2 have been reported down to a lab energy of 2 MeV in the hydrogen bubble chamber work of Ref. [20]. To estimate our vacuum requirements, the cross section for energies below 50 keV is needed. Because of the lack of data, our estimate must be guided by theory. At very low energies the scale for the annihilation cross

section is set by an atomic process in which the antiproton replaces an electron in an atom as it approaches and is thus captured in a bound state. Once in a bound state, the antiproton cascades to an ultimate annihilation at the nucleus. Two calculations are available in the literature for the very low energy antiproton capture cross sections of interest for the storage/cooling trap [21,22]. These calculations are valid for antiproton capture on hydrogen for center-of-mass energies $10^{-5} \text{ eV} \leq E \leq 1 \text{ eV}$. They agree to about a factor of $\sqrt{2}$, the work reported in Ref. [21] being higher. To obtain a worst case estimate, we use this higher cross section which is written as

$$\sigma_A = 3\pi a_0^2 \left(\frac{T_0}{T} \right)^{\frac{1}{2}}, \quad (5)$$

where a_0 is the Bohr radius ($0.519 \times 10^{-8} \text{ cm}$). $T_0 = \alpha m_e c^2$, α is the fine structure constant, and $T = \frac{1}{4} m_p v_{12}^2$ is the total center-of-mass energy in the $p - \bar{p}$ system.

Because of the ultra-high vacuum we expect in the design and the high bake-out temperature ($\sim 400^\circ\text{C}$) that will be used, most of the residual gas will be hydrogen. However, this hydrogen will be in molecular form, i.e., H_2 . Using the above cross section ignores some of the physics involved in the capture by the H_2 molecule. For the purpose of our estimate, however, this approximation is justified based on the similarity of the ionization potential for H (13.6 eV) and H_2 (15.6 eV) [23] which is the principle feature driving the physics of the cross section quoted above. Although the H_2 molecule has twice as many electrons as the H atom, the differing reduced mass compensates. For the storage trap system, the particle energies could be between $1 \leq E \leq 50,000 \text{ eV}$, and the cross section of Eq. 5 is not valid in this energy regime. The work of Ref. [21] gives an approximate cross section for $1 \leq E \leq 13 \text{ eV}$ as

$$\sigma_A = \pi R_0^2 \left(1 - \frac{V(R_0)}{T} \right) \quad (6)$$

where $R_0 = 0.64a_0$ (Ref. [24]), $V(R_0) = -e^2/R_0 + T_0$ and T again is the center-of-mass energy of the collision. However, the cross section for higher energies is still required. At present no estimates exist for this cross section. However, for the purpose of estimating the vacuum requirements for the storage trap, this cross section can be crudely bounded. Near 2 MeV the cross section behaves as

$$\sigma_A = \pi \lambda^2 \quad (7)$$

where $\lambda = h/p$ [20]. This cross section scales as $1/v_{12}^2$, just as in the 1-13 eV cross section scales, but with a different magnitude. Certainly at these low energies the true value of the cross section is bounded from below by $\pi \lambda^2$. To estimate an upper bound, observe that for energies above $\sim 13 \text{ eV}$, there is considerable extra energy available after ionization and the antiproton is so energetic that capture into a bound state becomes very unlikely, even allowing for an additional radiative process [21]. Thus, the cross section is certainly bounded from above by a simple continuation of the $1/v_{12}^2$ slope already established by the behavior in the 1-13 eV regime. The cross sections at issue are plotted in Fig. 4 for the center-of-mass energy range of interest. The curves illustrate the upper and lower bounds under discussion. The atomic cross section of hydrogen, πa_0^2 is plotted as well for reference.

To obtain "worst case" estimates of the vacuum requirements for the storage trap, we parameterized the upper bound as shown in the figure as

$$\sigma_A = \frac{\kappa}{v_{12}^2} \quad (8)$$

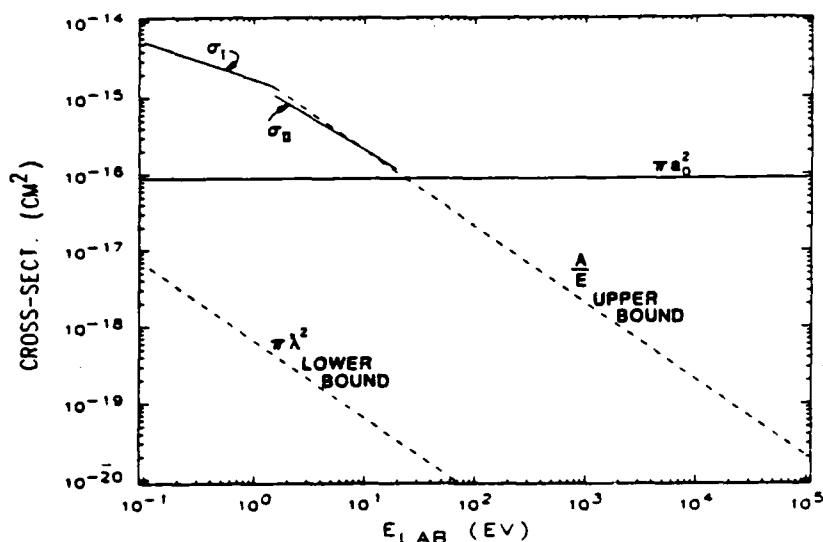


Figure 4: Total annihilation cross sections as a function of center-of-mass energy. Upper and lower bounds are as labeled.

and evaluate the rate integrals [19].

3.2.2 Results

For a binary gas system the loss rate can be expressed as

$$-\frac{dN}{dt} = \frac{N}{t_{1/e}} \quad (9)$$

where $t_{1/e}$ is the time required for the number of particles to fall to $1/e$ of the initial value. We refer to this time as the "time constant" in the plots that follow which display our results using the formalism derived in the first section of this report. In Fig. 5 we show the time constant for the $\bar{p} + H_2$ reaction using the worst case cross section discussed earlier. In the figure we show this time constant plotted versus the laboratory "temperature" of the stored antiprotons over a range of energies appropriate for the storage trap system. Also in the figure we show the time constant for several different vacuum situations (10^{-11} , 10^{-12} , 10^{-13} Torr) and two different values for the background gas temperature (77 K, 300 K).

The overall trend in this figure is for the time constant to decrease with decreasing energy. This simply reflects the trend of the cross section which is to increase with decreasing energy (see Fig. 4). Another overall feature from the plot is that for a fixed pressure, a lower background gas temperature makes for a shorter time constant. Although the lower temperature for the gas does lower the overall energy of the collisions and thus samples a bigger cross section, the dominant effect that leads to lower time constants is the increase in gas density at the lower temperature but fixed pressure (see Eq. 4). The difference between the results for different pressures is also driven by the change in density.

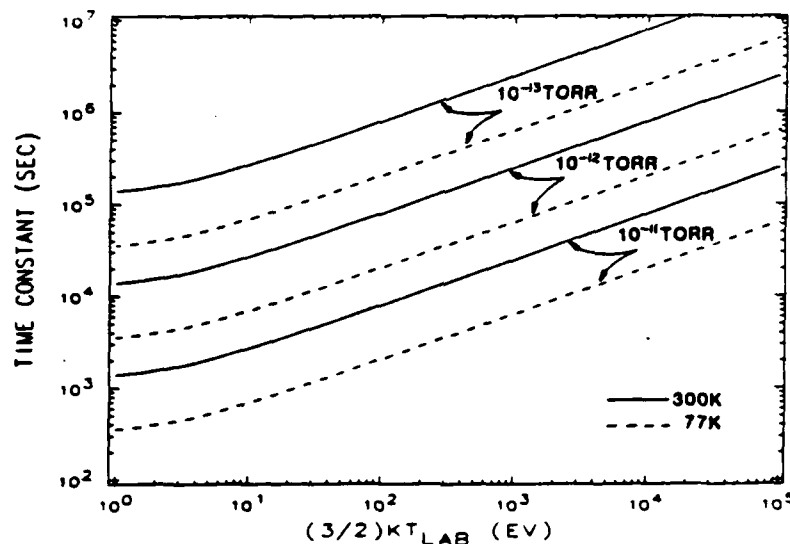


Figure 5: The time constant ($t_{1/e}$) for the reaction $\bar{p} + H_2$ versus the laboratory temperature of the stored antiprotons. The ambient pressures and temperatures of the background H_2 gas are as indicated.

3.3 Electrostatics

Finally we return again to the issue of the electrostatics of the trap and stored particles. In an earlier section we discussed the space charge potential of the charge cloud in the trap and how the potential on the confinement electrodes had to exceed this value by several times the kinetic energy of the stored particles. Because the velocities (we assume) can be described by a Boltzmann distribution, some of the particles will always be in the high velocity tail. We are concerned with these particles escaping over the potential barrier provided by the voltage on the outer electrodes (see Fig. 3) which provides the confinement in the axial direction.

The one dimensional distribution function of interest for the axial velocities can be written as

$$P(v) = N \exp\left(-\frac{mv^2}{2kT}\right) \quad (10)$$

where N is a normalization constant, v is the particle velocity, and T is the temperature. From this distribution we know that the expectation value of the energy in the axial direction is

$$\langle E_z \rangle = \frac{1}{2} kT \quad (11)$$

whereas the expectation value for the total energy in all three directions is given by

$$\langle E_T \rangle = \frac{3}{2} kT \quad (12)$$

By setting the potential at the outer electrodes at some value equal to or greater than the average energy of the stored particles in the z -direction we allow the particles with energies above this value to escape over the potential barrier. Two questions become important: How many particles

are above a given cutoff in energy and how fast does this tail of the distribution get repopulated with particles? How many particles are above a given cutoff is a matter of integrating the above distribution function from the cutoff out to infinity. A summary of results on this question is shown in the following table

Cutoff	Remainder
$2 \times \langle E_z \rangle$	3.17E-1
$4 \times \langle E_z \rangle$	4.55E-2
$6 \times \langle E_z \rangle$	2.70E-3
$8 \times \langle E_z \rangle$	6.25E-5
$10 \times \langle E_z \rangle$	5.88E-7

In this table the cutoff is taken to be a multiple of the energy in the z-direction and the result is shown as the remaining fraction of particles above the cutoff. For example if we take the cutoff to be 4 times the energy in the z-direction then 4.55% of the particles will be lost.

The question of how long it takes for this to happen is an issue of how long it takes for the distribution function to repopulate the tail. This issue was addressed by Spitzer [25] who derived a "self-collision time" for this process as

$$t_c = \frac{11.4 A^{1/2} T^{3/2}}{n_o Z^4 \ln \Lambda} \quad (13)$$

where A is the mass of the ion in AMU, T is the plasma temperature in K, n_o is the particle density in cm^{-3} , Z is the atomic number of the ion, and $\ln \Lambda$ is the natural log of a shielding length ratio that is about 20 for the cases of interest here (see [25] for more details). We can naively take this "self-collision" time to be representative of the time it will take for the distribution to repopulate the tail.

From these two considerations we can derive a loss rate for the particles escaping over the potential barrier at the end of the trap to be

$$-\frac{dN}{dt} = \frac{\kappa N}{t_c} \quad (14)$$

where κ is the fraction of the tail that remains over the potential barrier (see previous table) and t_c is the "self-collision" time derived by Spitzer. We can express the time constant, as before for the vacuum losses, by defining the $t_{1/e}$ time for this process to be

$$t_{1/e} = \frac{t_c}{\kappa} \quad (15)$$

Thus we find that the $t_{1/e}$ time for this loss process is considerably longer than the "self-collision" time because only a fraction of the distribution is being acted upon.

3.4 Impact on Point Design

The "bottom line" from all of these considerations is that for long term storage of antiprotons, high energies are preferred to low energies because the cross section for capture and subsequent annihilation decreases with increasing energy. From the results in Fig. 5 the time constant for

storage at 20 keV in a room temperature system at 10^{-12} Torr is about 10^6 seconds, whereas for storage at 1 eV in the same conditions the time constant is about 1.5×10^4 seconds. This rather dramatic difference in the time constants is simply due to the change in the cross section with energy; cross sections are larger for lower energies.

Let us assume that we store the antiprotons at 20 keV in a room temperature system at 10^{-12} Torr. The time constant of 10^6 seconds corresponds to only 11.5 days. This is far short of the 6 month storage time that we arrived at earlier based on how many antiprotons could be supplied from a production facility for an off-site research program (see Section 2.2). If the storage vacuum system operated between 10^{-14} – 10^{-13} Torr, the storage time would be about 6 months. However, this is an extremely difficult vacuum to achieve in a large system. In small completely sealed systems operating at cryogenic temperatures it has been suggested that extreme vacuums beyond the 10^{-14} range could be possible [26]. Measurements using a residual gas analyzer on such a system confirmed this possibility down to 10^{-14} Torr [27]. Very recently, a vacuum of 10^{-17} Torr has been reported in a liquid helium system [28]. This pressure at liquid helium temperature is roughly equivalent to 10^{-15} Torr at room temperature in terms of the gas density. At Los Alamos we have designed a room temperature system which we calculate will operate in the 10^{-13} Torr range. All these results are tantalizingly close to the operating range we require for long term storage, but have not been engineeringly demonstrated for a large system. Before we get too far a field with designing a vacuum system beyond the edge of present day technology we point out that our estimate of the cross section for capture-annihilation is a "worst case" value. The true value could be as much as 2 orders of magnitude smaller in the energy regime above ~ 100 eV. A two orders of magnitude smaller cross section would bring the required operating range of the system for 6 months storage times to between 10^{-12} – 10^{-11} Torr. This vacuum range is achievable with present day technology for large systems at room temperature with careful design.

There is no doubt that the cross section for capture/annihilation decreases with increasing energy. The crucial design information we require is what is the true value of this cross section. From our "worst case" estimate for the 6 months storage time we require a system that is beyond the demonstrated performance of present day systems. If the cross section is significantly smaller the system can be built without a development program researching new vacuum techniques. Before we can make a serious design decision for the vacuum system we need to know how big these cross sections are. This is a critical measurement that our systems require.

4 How Safe

In the event that the confining electric fields fail in the trap, the antiprotons will annihilate rapidly producing a very short rise-time burst of energetic pions and gamma-rays. The energy spectra of the emitted particles are shown in Fig. 6. The average energies of the pions and gamma-rays are 243 MeV and 196 MeV respectively. The corresponding range of the pions in lead is 100 g cm^{-2} . To stop 90% of the pions with a spectrum as shown in the Figure would require $\sim 1000 \text{ g cm}^{-2}$.

A potential problem exists, however, in the generation of secondary neutrons and gamma-rays from $\pi(X,n)Y$ reactions. Typically, the cross sections for these reactions are hundreds of millibarns. Consequently, significant secondary fluxes can be produced if high Z shield material is used around the annihilation point. Addition of more shielding to stop the secondary particles may raise the shield mass to unacceptable levels. Thus, a low Z material to stop the pions with reduced neutron production may also be incorporated inside of the lead shield to reduce radiation levels.

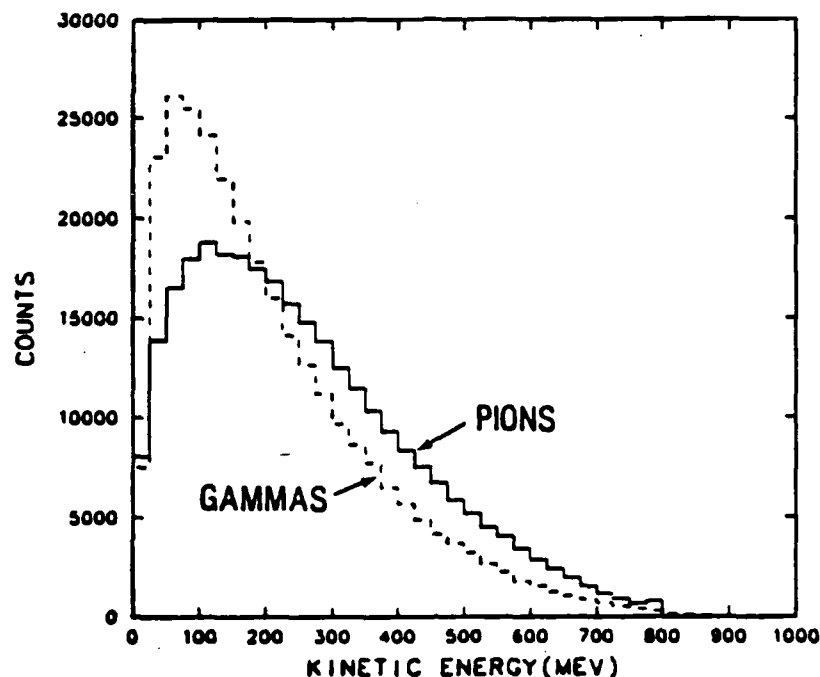


Figure 6: Energy spectra of emitted particles from $p\bar{p}$ annihilation.

Preliminary calculations of the radiation dose as a function of standoff distance is shown in Fig. 7 for different thicknesses of lead. The calculations were made using a modified version of the High Energy Transport Code (HETC) and the Monte Carlo Neutron Photon (MCNP) transport code. The HETC was changed to allow emission of pions and gamma-rays according to the spectra in Fig. 6. The spectra were generated at a point source inside of a simulation of the ion trap components. The results seen in Fig. 7 show that the dose increases with lead thickness up to a point and then decreases as expected. These results indicate that approximately 20-30 cm of lead are needed to shield individuals at a distance of 5 m (approximate distance to the next lane of traffic on a highway) to safe levels for a trap containing 10^{11} particles. Also plotted in the figure is a single calculation for a composite borated/graphite/lead shield. The mass of the composite was about $\sim 60\%$ of the lead required to allow an equivalent dose. These calculations indicate that a shield mass of approximately 10 tons of lead is needed to safely transport the portable source.

5 Point Designs

5.1 Introduction

Finally we are at the point where we can start to investigate specific designs for the storage traps. Because there are several physics and engineering related unknowns in the design choices we have at hand, the designs we generate here must be regarded as rather speculative. Nevertheless, we can make an assessment on the relative difficulty, as far as we can estimate at present, of implementing a given design. The biggest engineering uncertainty is in the attainable vacuum for the storage system. In moderate size systems $10^{-12} - 10^{-13}$ Torr are possible. However, if vacuums of 10^{-16}

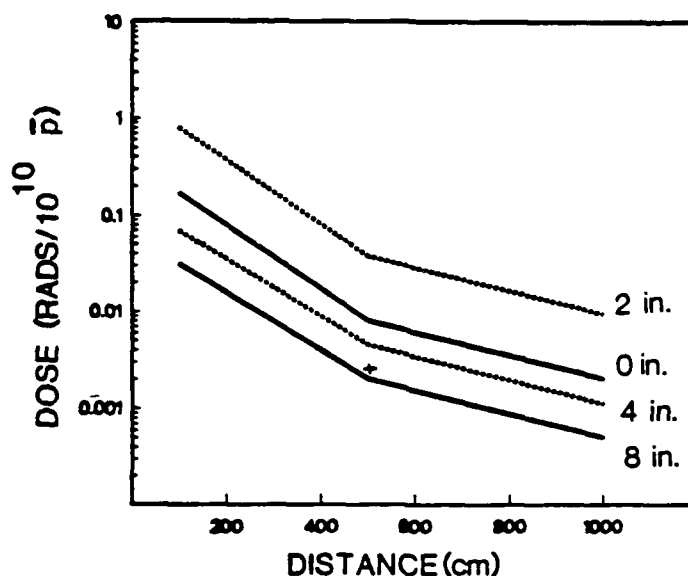


Figure 7: Radiation dose as a function of standoff distance.

can be achieved, much of the design can be simplified; the energy of the stored particles can be lowered which will lower the required voltages on the electrodes and the storage times can be substantially longer than the 6 months we are aiming for. Naturally, there is a trade-off between the number of particles stored, the space charge potential they generate and the required voltages on the electrodes. Thus for very large numbers of particles, the required voltages will still be high, even though the vacuum problem is minimal. The biggest physics issues involved are the value of the annihilation/capture cross section as a function of energy, and our understanding of the plasma physics issues associated with high density storage at low temperature.

Two design paths are presented here; either we can assume that we stay within existing or reasonable extensions of engineering practice for the vacuum system and other components, and we avoid all dealing with the plasma physics uncertainties, or we presume that we can achieve arbitrarily good vacuums and have solved all the plasma physics problems. Naturally the first path will lead to a system that we can more accurately estimate the cost and scale of whereas for the second path the system cost and scale is just an educated guess. For both paths we will assess the storage of 10^{12} and fewer antiprotons.

5.2 The Cautious Design

Here we assume that we can achieve vacuums of 10^{-12} - 10^{-13} Torr and that we operate in a density/temperature regime that will make the properties of the stored cloud single particle in nature (no plasma problems). As mentioned previously we have designed a system at Los Alamos that we estimate can achieve these vacuums. Although this system has not been built we have confidence that about 10^{-13} Torr will be attained. From Fig. 5 we see that a $t_{1/e}$ time of about

115 days is possible with 10^{-13} Torr at a storage temperature of 20 keV. Although this does not meet our design goal of 6 months, it is almost certain that the cross section we have used for the 115 days estimate is much too large. Thus we could achieve the 6 months storage time with reasonable certainty perhaps even with less stringent vacuum requirements. This points again to how important a measurement of these cross sections is to the design. Because we will mount the trap inside the bore of a reasonably sized solenoid, we know that the radius of the charge cloud must be about 1 - 2 cm. Let's select 2 cm and refer to Fig. 2 to determine what density is required to keep the Debye length larger than this value. From the figure, we can estimate that the Debye length for a charge cloud at a temperature of 20 keV at a density of about 10^9 is about 3 cm. With this density and temperature we can assume that the radial plasma effects will be small.

The confining fields for the storage of the particles is the next step. Because we wish to minimize the plasma effects, we select using Fig. 1, a magnetic field that will keep us a factor of 100 away from the Brillouin limit. At a density of 10^9 a 6 Tesla field will provide this factor of safety. The "self-collision" time for a charged cloud with this density and temperature is (see Eq. 13) about 1100 seconds. To keep the loss rate from particles penetrating the potential barrier at the ends of the trap on the same scale as the losses from the vacuum we need to use a voltage that is 53.3 kV larger than the space charge potential. This numerical value is $8 \times \langle E_z \rangle$ (see the preceding Table). Recall that $E_z = \frac{1}{3} E_T$. To calculate the space charge potential we use Eq. 3. First to keep within the density limitations for a cloud at 10^9 density and for storing 10^{12} particles we require a length of about 80 cm. To keep things easy let's just make this length 100 cm. Using Eq. 3 we then calculate that the charge cloud will generate about 2.5 kV of space charge potential. If we simply design the electrostatic system for 60 kV we will easily keep the penetration loss rate to a minimum. Voltages of 60 kV are readily available and are rather typical of the voltages that are used in ion sources. Thus standard design practice for sources can be used.

A schematic view of this design is shown in Fig. 8. In the figure we show the solenoid, major vacuum system components, beam dumps/plugs, and beam extraction section. These components along with support electronics, cryogenic support equipment and liquified gases, and a portable power system make up a portable source. The source and support equipment can fit into the back of a rather standard trailer. The total weight of the source is about 5 tons. The total weight of the shielding is about 10 tons giving a total weight of 15 tons, well within the load capabilities of normal tractors that we envision hauling the source. We estimate very roughly that the cost for equipment only (excluding the tractor trailer) will be about 250 K\$.

If we want to store and transport 10^{11} antiprotons the source just described just get about 1 meter shorter. All of this length is taken up in the solenoid. The remaining support equipment remains basically the same. Thus for 10^{11} particles the source looks basically the same although a bit smaller. The radiation hazard is less and the shielding could be reduced but this is only a small factor in the overall size. For still fewer particles the solenoid will not get smaller, only the density will diminish bringing us further from the plasma instabilities that we have avoided originally. We estimate the cost for this source to be about 150 K\$.

5.3 The "Pie-in-the-Sky" Design

Here is where we throw all caution to the wind and design based on achieving arbitrarily good vacuum and having solved all the problems associated with the plasma physics unknowns. Otherwise we stick to standard good engineering practice for the other components.

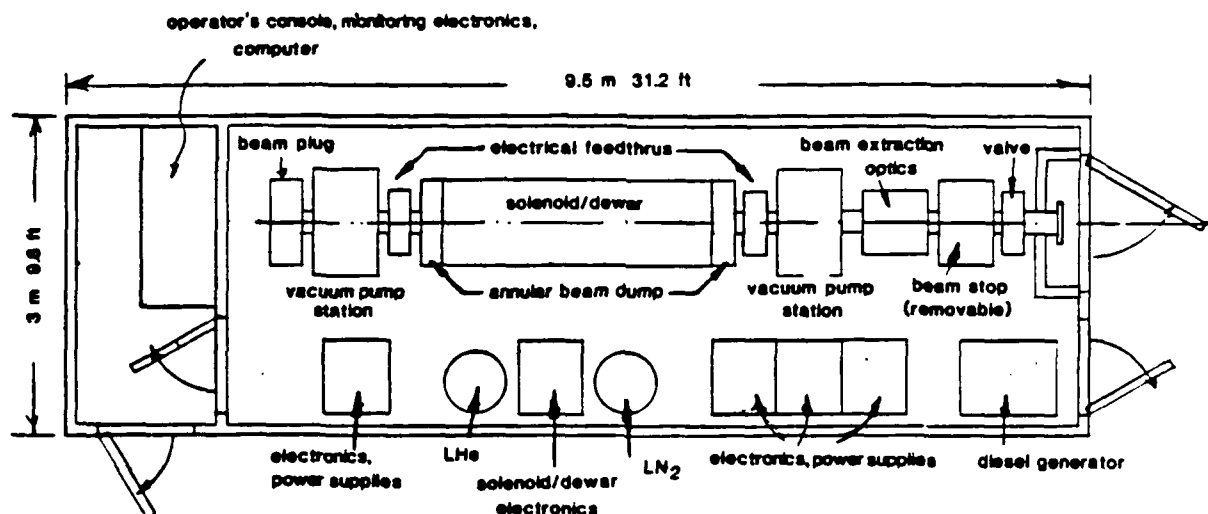


Figure 8: Schematic view of the portable source showing major equipment items.

Let's not fool around and go right for the Brillouin limit at 10 Tesla which gives us a storage density of $2.6 \times 10^{11} \text{ cm}^{-3}$. We don't worry about the Debye length for this plasma because we have solved all those problems in our imaginary senario. To store 10^{12} antiprotons we need a mere 4 cm^3 approximately. If we make the plasma column about 3 cm long, the space charge potential generated by the stored particles is about 47 kV, well within the 50 - 60 kV voltage practice from ion sources. So if we design for 50 kV we should be safe. Remember that because we can achieve arbitrarily good vacuum we have no concern about losses and can store the particles at very low kinetic temperatures.

The only way we can conceive of a vacuum system capable of extreme vacua is through using a totally enclosed cryogenic system. Thus the two vacuum pump stations present in the previous design can be eliminated, although some pumping is required to keep the vacua between the dewar walls at a reasonable level and to provide roughing on the main system. The dewar itself will only be about 0.5 meter long and only 1 feedthru section will be needed. The beam stops and radiation shielding, and beam extraction optics sections remain basically the same. These changes reduce the length of the source itself by about 3 m. Thus the overall length of this imaginary source would be about 6.5m. For fewer numbers of particles the required equipment will largely remain the same. The overall length of the source does not change.

6 Conculsion and Summary

Because of the limitations imposed by the Brillouin limit on the density of charged particles in an ion trap, the use of such traps in energy source applications presently seems very remote. However, the use of ion traps in a broad range of basic research offers many new avenues of investigation. In particular antiprotons can now be made available at energies of interest to the atomic and condensed matter physicist. Because it is in this area that higher density storage may be possible, the development of ion traps is an enabling technology.

Although preliminary prototype traps can and should be designed now, the complete final design of a portable source of antiprotons suitable for basic research at an off-site location is at present not possible. The design process has too many uncertainties associated with our lack of knowledge of the plasma physics issues, of the capture/annihilation cross sections, and the engineering uncertainties associated with designing ultra-high vacuum systems. Nevertheless we have attempted to study some of the problems of the design and have generated a skeleton outline of what such a source could look like. In the process we have identified several critical issues that must be addressed if the fabrication of such a source is to be carried out.

The first critical issue is the the input from the research community of users of such a source on what will constitute a research program at their home institution and how many particles are needed for such a program. We have schematically presented several sources scaled to the particle number and estimated quantities based on availability from such a facility as that discussed at FermiLab. Because of safety requirements in transportation the size of such a source does not continue to get much smaller below about 10^{11} particles. Although the radiation hazard for this many antiprotons or less is very small, the guaranteed safe arrival of the source requires these measures. The size of the sources we have discussed fit into a rather modest size trailer easily hauled by standard tractors.

The next critical issue in the design is how long does the off-site research location need to store the particles. We estimated that about 6 months is reasonable but even this time was uncertain because of the lack of knowledge of the capture/annihilation cross sections and uncertainties associated with plasma instabilities and fabrication and alignment of the system. To address the cross section uncertainties requires an experimental program of measurement. This program must be completed before the final design and fabrication of portable sources for basic research at off-site locations is possible. To address the plasma issues will require another research program in non-neutral plasma physics. We feel that the design of sources can be accomplished to avoid many of the problems of plasma instabilities, however the source we presented as our cautious design is still beyond the existing state of the art. A program directed at studying these issues so that the state-of-the-art can be extended must be carried out.

The final critical issue is associated with the transportation of hazardous material on the Nation's highways. The radiation hazard from 10^{12} antiprotons is acceptable for a radiation worker, however for the average citizen it is over the federal guidelines. The hazard from fewer antiprotons is at the natural background level, however the guidelines, we understand, are for no additional dose for the average citizen, period. All this points toward the requirement of establishing new federal regulations for the transport of the source, at least on the highway. Other means of transport are naturally possible, and should be considered by a working group specifically charged with studying this problem.

The full design of a portable source is possible with an effort in the areas just described. The final ingredient that is required is a production facility in the United States to fill the sources. The facility discussed at FermiLab could meet this requirement. Such a facility would be unique in the world in that it would have both an on-site and off-site research program in antimatter physics. With the support of such a potentially broad and multidisciplinary research community, such a source could be built, given funding, by the early part of the 1990's.

References

- [1] O. Chamberlain, E. Segre, C. Wiegand, and T. Ypsilantis, *Phys. Rev.* 100, 1947 (1955).
- [2] "Design Study $\bar{p}p$ Facility", CERN Report, CERN/PS/AA 78-3.
- [3] C. Hojvat and A. Van Ginneken, *Nucl. Instrum. Meth.* 206, 67 (1983).
- [4] D. Allen, E. Asseo, S. Baird, J. Bengtsson, M. Chanel, J. Chevallier, et al., CERN Report, CERN/PS 87-26 (LEAR), March 1987.
- [5] H. Dehmelt, *Adv. At. Mol. Phys.* 3, 53 (1967).
- [6] D. J. Wineland, W. M. Itano, and R. S. Van Dyck, Jr., *Adv. At. Mol. Phys.* 19, 135 (1983).
- [7] J. H. Malmberg and C. F. Driscoll, *Phys. Rev. Letts.* 44, 654 (1980).
- [8] T. Arikawa, in *Electronic and Atomic Collisions*, J. Eichler, I. V. Hertel, and N. Stolterfoht eds., Elsevier Science Publishers B. V., 1984, p. 239.
- [9] L. J. Campbell, W. R. Gibbs, T. Goldman, D. B. Holtkamp, M. V. Hynes, N. S. P. King, et al., LAUR-84-3572.
- [10] W. Kells, *IEEE Trans. Nucl. Sci.* NS32, 1770 (1985).
- [11] J. H. Billen, R. E. Brown, L. J. Campbell, K. R. Crandall, T. Goldman, D. B. Holtkamp, et al., Los Alamos Report, LAUR-85-3737.
- [12] C. F. Driscoll, in "Low Energy Antimatter", D. B. Cline, ed., World Scientific Press, Singapore 1986, p. 184.
- [13] D. J. Wineland, in *The Proceedings of the Workshop on the Cooling, Condensation, and Storage of Hydrogen Cluster Ions*, SRI International, Menlo Park CA January 8-9 1987.
- [14] L. Brillouin, *Phys. Rev.* 67, 260 (1945).
- [15] J. J. Bollinger and D. J. Wineland, *Phys. Rev. Letts.* 53, 348 (1984).
- [16] R. L. Forward, AFRPL-TR-85-034.
- [17] I. Langmuir, *Phys. Rev.* 33, 954 (1929).
- [18] R. C. Davidson, *Theory of Nonneutral Plasmas*, Benjamin, 1974.
- [19] M. V. Hynes, A. Picklesimer, and W. G. Robertson, LAUR-87-3054.
- [20] D. Cline, J. English, and D. D. Reeder, *Phys. Rev. Lett.* 27, 71 (1971).
- [21] L. Bracci, G. Fiorentini, O. Pitzurra, *Phys. Letts.* 85B, 280 (1979).
- [22] D. L. Morgan and V. W. Hughes, *Phys. Rev.* A7, 1811 (1973).
- [23] H. M. Rosenstock, K. Draxl, B. W. Steiner, and J. T. Herron, *J. Phys. Chem. Ref. Data* 6, 71 (1977).

- [24] A. S. Wightman, Phys. Rev. 77, 521 (1950).
- [25] L. Spitzer, Jr., Physics of Fully Ionized Gases, Interscience Publishers, 1962.
- [26] J. P. Hobson, J. Vac. Sci. Technol. 10, 73 (1973).
- [27] W. Thompson and S. Hanrahan, J. Vac. Sci. Technol. 14, 643 (1977).
- [28] P. A. Ekstrom, University of Washington, private communication, 1987.

EXTREME STATES OF MATTER:
COULD ANTIPROTONS BE USED TO POWER TABLE-TOP
EQUATION OF STATE OR OPACITY EXPERIMENTS?

Johndale C. Solem
Physics Department
University of Illinois at Chicago

Prepared for RAND Workshop, October 6-9, 1987,
on Antiproton Science and Technology

**EXTREME STATES OF MATTER: COULD ANTIPROTONS BE USED TO POWER
TABLE-TOP EQUATION-OF-STATE OR OPACITY EXPERIMENTS?**

ABSTRACT

I discuss the use of antiproton-driven fission to measure high-temperature opacities and to obtain Hugoniot points for high-pressure equations of state (EOS). The best experimental techniques utilize a unique property of antiproton beams: their ability to penetrate matter and deposit their energy at an occluded location. This property combined with the promise of small portable antiproton traps could make antiproton drivers competitive with more mature technologies, some of which require costly centralized facilities not available to most researchers.

I compare techniques for opacity measurement and find that experiments using the heat capacity of the target for energy storage, as opposed to black-body radiation, are most feasible within the scope of foreseeable technology. Measurements in the 100 eV regime require about two orders of magnitude increase in antiproton number and about three orders of magnitude reduction in pulse length* (compared with values suggested by a previous author-see text). Substantial relaxation of these requirements could be achieved with less-than-ideal experiments that necessitate numerical simulation for their interpretation.

I find that EOS experiments are possible today and that two orders of magnitude improvement in both antiproton number and pulse length* could make antiproton drivers competitive with nuclear-explosive drivers for conducting EOS experiments at ultrahigh pressure.

*Note: See the Epilogue to this paper to update the most recent information on these possibilities.

INTRODUCTION

Polikanov¹ has suggested that the high beam quality and high capacity of the LEAR storage ring could be used to produce high-specific-energy-microexplosions. He suggests that the stored antiprotons be dumped in a fissile-isotope target to obtain local amplification of the annihilation energy by fission. The author's estimates suggest that 6×10^{11} antiprotons, whose total annihilation energy is 180J, should deposit about 16J locally by the fission-enhanced process, the rest of the energy being carried away by the pions and subsequent electromagnetic cascade. A $300 \text{ MeV}\cdot\text{c}^{-1}$ beam would stop in $0.2 - 0.5 \text{ mg}$ of uranium, the dump time is $\sim 1\mu\text{s}$, resulting in $\sim 5 \times 10^4 \text{ MW}\cdot\text{gm}^{-1}$. Presently LEAR can store $\sim 10^9$ antiprotons and will be upgraded to 10^{10} , so the estimate of 6×10^{11} is not unreasonable².

It has been suggested that such microexplosions could be used to study extreme states of matter. If antiprotons were available in portable traps or storage rings, perhaps such studies could be carried out in small laboratories. Such "table-top" tools would allow research to be conducted almost anywhere and without the need for large centralized facilities.

The properties most often mentioned in connection with extreme states of matter are opacity and equation-of-state (EOS). This paper addresses the fundamental requirements for opacity and EOS experiments and compares the potential antiproton source with other energy sources. I do not address use of this table-top tool as a source of energetic particles and gammas interacting in interesting ways with external targets. This is an exciting possibility and worthy of further investigation.

OPACITY

The paucity of experimental opacity data at temperatures above an eV reflects the fundamental difficulty of conducting laboratory experiments. It is both expensive and arduous to space-time compress enough energy for good measurements. Fusion lasers had been proposed as laboratory instruments to supply the requisite energy densities, but as

will be shown, the total energy requirements are very costly if not prohibitive.

Rossland Mean Opacities Classical Experiment

The most straightforward method of measuring mean opacities is to fill the center of a spherical cavity with black-body radiation and observe the emergence of a radiation diffusion front. Figure 1 shows how this classical method of opacity measurement could be adapted to an antiproton driver. The fissile target is small compared to the cavity volume and its heat capacity is small compared to the vacuum radiation field at the temperatures of interest. Because of its size, the target can expand a great deal (explode) without disturbing the cavity wall.

The energy of the black-body radiation is

$$E_{bb} = \frac{4\sigma}{c} VT^4. \quad (1)$$

where σ is the Stephan Boltzman constant, V is the cavity volume and T is the temperature inside. Because of the fourth-power dependence, the driving temperature is expected to diminish only slightly as the diffusion front travels through the cavity wall -- it is a very stable power supply. For a good experiment there are several requirements: (1) the wall must be many mean free paths (mfp) thick; (2) the energy in the wall E_w at temperature T must be much less than E_{bb} ; (3) the thickness of the wall Δr must be a small fraction of the cavity radius r in order to avoid significant effects from spherical divergence of the diffusion wave; (4) the port that admits the antiprotons must either close before much radiation energy leaks out or have a small area compared to the whole sphere; and (5) the preheating that occurs in the wall, owing to the pion shower and subsequent electromagnetic cascade that accompanies the annihilation, must be small compared to the energy from the diffusion front.

First we consider the energy requirement. Say we want the wall to be n mfp thick. Then

$$\Delta r = \frac{n}{\kappa \rho}, \quad (2)$$

where κ is opacity and ρ is density. The energy in the wall when the diffusion wave has propagated through is

$$E_w = \frac{4\pi r^2 C_v T}{\kappa} n, \quad (3)$$

where C_v is the wall specific heat. The temperature in the cavity will drop as the wall heats up. If T_i and T_f are the initial and final radiation temperatures in the cavity, then

$$\frac{T_i}{T_f} = \left[\frac{E_{bb} + E_w}{E_{bb}} \right]^{1/4} = [1 + \epsilon]^{1/4}, \quad (4)$$

where $\epsilon = E_w/E_{bb}$. Combining Eq(1) and Eq(3), we find the radius of the cavity

$$r = \frac{3cC_v}{4\sigma\kappa T^3} \frac{n}{\epsilon}. \quad (5)$$

To use a concrete example, let us consider an experiment to measure the opacity of lead. A good measurement would require several mfp, so say $n=10$. Also assume we want no more than a 1% drop in the cavity temperature, which would make $\epsilon \approx 0.04$. The lead opacity is approximately $2 \times 10^5 T^{-1} \text{ cm}^2 \cdot \text{gm}^{-1}$, where T is in eV, and its specific heat is $5 \times 10^{11} \text{ erg} \cdot \text{gm}^{-1} \cdot \text{eV}^{-1}$ and $4\sigma/c = 1.37 \times 10^2 \text{ erg} \cdot \text{cm}^{-3} \cdot \text{eV}^{-4}$. For a temperature of 1 KeV, we find $r = 13.6 \text{ cm}$, an enormously large sphere. Needless to say, the energy required for this ideal experiment is well beyond that which can be supplied by a table-top antiproton source. The requisite energy is large, even if we dramatically reduce our requirements. For example, if we allow the temperature to drop 10% and require only 5 mfp, we obtain $r = 5.2 \text{ mm}$ for $T = 1 \text{ KeV}$, which corresponds to a total deposited energy of $E_{\text{bb}} + E_w = 1.2 \times 10^7 \text{ J}$. Thus it is reasonable to conclude that schemes using energy stored in the vacuum radiation field are not amenable to a table-top power source.

At higher temperatures the approximation of Eq(3) does not hold and the energy requirement can be dominated by the wall. Also, the wall becomes so thick as to violate the spherical divergence requirement.

The pulse of energy from the antiproton reaction must occur on a time-scale that is short compared to the time for sound to traverse the shell. Otherwise the measurement of the diffusion wave will be complicated by hydrodynamic motion. At high temperature, the sound speed in lead is about $6.8 \times 10^4 T \text{ cm} \cdot \text{s}^{-1}$. From Eq(2), the transit time is $6.5 \times 10^{-12} n T \text{ s}$. If $n = 10$ and $T = 1 \text{ KeV}$, the transit time is about 2 ns. This means the antiproton pulse must annihilate in less than a nanosecond.

Non-Classical Opacity Experiment

The classical experiment described above requires too much energy for measurements at low temperature and spherical divergence considerations as well as extreme spatial compression of the antiprotons makes it appear exceedingly difficult at high temperatures. These difficulties derive from the peculiar nature of occluded black-body radiation used for energy storage.

An alternative is to use the specific heat of a material for energy storage. Figure 2 shows an opacity experiment that might be within the reach of near-future technology if the pulse length were short enough. The inner sphere is uranium. The antiproton beam is focused on the inner sphere and its energy distribution is adjusted so the Bragg peak of all the antiprotons is within the inner sphere and it is heated uniformly. Minimal heating will occur in the spherical shell. To heat the 100 μ -radius inner sphere to 100 eV will require about 400 J or about 1.5×10^{13} antiprotons, using Polikanov's estimate for deposited/annihilation energy ratio. The outer shell is ~ 10 mfp thick at 100 eV, which for lead is only 4.4. μ m. The heat capacity of the shell is 12% of the sphere, so the temperature will drop, but not dramatically. The sound transit time of the shell is only 0.6 ns. Hydrodynamic motion may be a problem.

Monochromatic Opacities

In the discussions above we have considered measuring Rossland mean opacity by the rate of radiation diffusion. If the difficulties described above could be overcome, we could also measure monochromatic opacities.

One method of monochromatic opacity measurement is analogous to an astrophysical technique commonly referred to as "limb darkening". This technique has been studied extensively in connection with laser-driven opacity experiments by Hoffman, et al⁴. The underlying theory is that the intensity observed from a radiator is a function of the angle of view, hence the sun appears darker at its limbs because the radiation passes through more of the solar atmosphere⁵. The intensity observed at an angle θ and frequency ν is given by

$$I_v(\cos\theta) = \frac{1}{\cos\theta} L \left[B_v(\tau_v) \right], \quad (6)$$

where L is the Laplace transform of the Planck function B_v which is a function of optical depth τ_v . From $B_v(\tau_v)$ we can determine the temperature $T(\tau_v)$. If we make a careful measurement at many different frequencies, we could calculate $dT/d\tau_v$ at fixed temperature and obtain relative opacities.

$$\frac{\kappa_{v1}}{\kappa_{v2}} = \frac{dT/d\tau_{v1}}{dT/d\tau_{v2}}. \quad (7)$$

This method does not measure absolute opacity, another technique must be employed to provide a benchmark. It is also very susceptible to experimental error because it relies on calculated derivatives. Laser-driven experiments were found difficult to interpret because of roughness on the plasma surface.

Another monochromatic opacity measurement technique has been described by Zel'dovich and Raizer⁶. They suggest observing the brightness temperature T_{br} as a strong shockwave emerges from a material surface. The radiating layer is somewhat behind the vacuum interface but not very deep. It provides a measure of the opacity by the equation

$$\frac{\gamma+1}{2(\gamma-1)} t \int_0^{T_w} \rho \kappa_v(T) \frac{c_s(T)}{T} dT = 1, \quad (8)$$

where γ is the usual ratio of specific heats ($\gamma = C_p/C_v$). The generalization from a polytropic gas EOS to a real EOS will require numerical techniques and fairly good understanding of the EOS in the region of interest. Absolute measurement of T_{br} as a function of t will require very clever instrumentation. But this technique does not require storage of energy. In principle, any emergent shockwave could yield opacity information and could be coupled with the EOS experiments described later in this paper.

By time-resolved spectroscopy of the emergent radiation diffusion wave, it also may be possible to acquire opacity information when the medium is out of local thermodynamic equilibrium (LTE). In fact, such spectroscopy will be required to ensure LTE when we are attempting Rossland mean opacity measurements.

Less-Than-Ideal Opacity Experiments

The experiments described here attempt to minimize competing process in an attempt to produce clean opacity measurements with little additional calculation. If the pulse length and antiproton number are not practically achievable, it is possible to relax the requirements by accepting more complicated, less-than-ideal experiments. The three requirements that could be relaxed to greatest profit are: (1) that spherical divergence be kept to a minimum; (2) that there be little hydrodynamic motion; and (3) that the energy be deposited in a time that is short compared to the time for the diffusion wave to propagate through the wall. The relaxation of any or all of these requirements will make it necessary to use a hydrodynamics and radiation flow computer code for interpretation of the data. But if the experiments are simple enough to execute, a great deal of data may become available for many different materials at many different temperatures, which will constrain the uncertainties introduced by computer code interpretation.

It may also be possible to use less-than-ideal geometries to obtain higher radiation temperatures. If we depart from spherical symmetry, a number of more complicated geometries become available that might achieve higher energy densities. For example, we could use the phased-

conical collapse of a cylindrical shell to obtain a smaller volume of higher temperature radiation. All such mechanisms require larger total energies but can tolerate longer pulses. They convert a lot of low-grade heat into a bit of high-grade heat with concomitant increase in entropy.

Summary

Conversion of annihilation and fission energy into black body radiation would provide the best experimental arrangement for measuring Rossland mean opacities, but the energy requirements are prohibitive. Storing the energy in specific heat may be feasible and could be used for measuring opacities up to $\sim 100\text{eV}$. This technique utilizes a unique property of the antiproton energy source: the ability to penetrate outer layers and deposit energy predominantly inside a target. In addition to measuring Rossland means, monochromatic opacities might be measured by limb-darkening techniques or by observing brightness temperature at shock emergence. Less-than-ideal opacity experiments could extend the measurement ranges or reduce requirements on antiproton number or bunch space-time compression, at the cost of added computational complexity.

EQUATION OF STATE

Understanding EOS is important to solving a multitude of problems in geophysics, astrophysics, the theory of solids, the behavior of high explosives and nuclear explosives, and a wide range of related sciences. Static studies, now with high-precision diamond anvil presses, are limited to less than one Mbar ($1\text{ bar} = 10^6\text{ dyn}\cdot\text{cm}^{-2} \equiv 1\text{ atm}$). For higher pressures, it is necessary to study the shock compression of the materials. High-explosive and chemical-propellant experiments can extend the pressure range up to about 7 Mbar⁷. Two-stage light gas guns can reach as far as 10 Mbar⁸. Techniques using nuclear explosives⁹⁻¹² have further extended the range of dynamic pressures, most recently to over 60 Mbar^{11,12}. But these experiments are expensive and infrequent. In an effort to reduce cost and increase the repetition rate a variety of laboratory - scale shock driving techniques¹³ have been developed,

including rail guns, magnetically accelerated foils, and laser ablation targets. Also, not all interested researchers have access to nuclear explosives.

Theory of Measurement

When a material is shocked, the following conservation laws must be obeyed:

$$\frac{\rho}{\rho_0} = \frac{D}{(D-u)} \quad \text{mass} \quad (9)$$

$$P - P_0 = \rho_0 D u \quad \text{momentum}$$

$$\left[(E - E_0) + \frac{1}{2} u^2 \right] \rho_0 D = P u, \quad \text{energy}$$

where the subscript ₀ refers to the initial (unshocked) state, E is specific internal energy, u is particle velocity, P is pressure, and D is shock velocity. These shock-jump conditions are known as the Rankine-Hugoniot equations, and the locus of all possible states that can be reached from a given initial state is called the Hugoniot. Measurement of any two of the quantities (P, ρ, E, D, u) locates a point on the Hugoniot.

Early nuclear explosive experiments⁹ obtained points on the Hugoniot of molybdenum by measuring D and u. Shock velocity D was obtained by determining the transit time between two points: the luminescence of shock emergence was observed through light pipes at two depths. Particle velocity was obtained by observing Doppler shifts of neutron resonances in a gold foil embedded in the moving molybdenum. This technique produced a well defined Hugoniot for molybdenum, which is now used as a standard.

Once the standard was established, it was only necessary to measure one variable, the shock velocity, to determine Hugoniot points for other materials by a method called impedance matching¹⁰⁻¹². In impedance-matching experiments, the shock passes first through the standard (molybdenum) and then into the test material. The shock velocities in the standard D_s and the test material D_t are measured by transit time. Conservation of momentum and the measured D_s establish straight lines in the P - u plane with slope ρD . The intersection of the line for the standard with the known Hugoniot determined its pressure and particle velocity. At the interface, the shock propagates into the test material and simultaneously generates a backward moving wave in the standard, which can be either a rarefaction or a shock. Particle velocity and pressure are continuous across the interface. A point on the Hugoniot of the test material in the P - u plane is then established by the intersection of the straight line $P = (\rho_0 D)_t u$ either with the reflected shock Hugoniot or the release isentrope of the standard.

Laser Experience

By far the greatest experience with ultrahigh pressure shocks in the laboratory has been gained through the use of high-energy short-pulse lasers developed for the Inertial Confinement Fusion Program. Preliminary experiments¹⁴⁻¹⁷ used ultrafast streak cameras¹⁸ to measure shock velocity by observing the luminescence of emerging shocks on stepped targets 10-50 μm thick (see Figure 3). The laser spot size was adjusted to have a large diameter compared to the target thickness. Pulses from Nd-glass lasers at 1.06 μm were used in all early experiments and pressure as high as 18 Mbar¹⁷, in aluminum were obtained at an intensity of $3 \times 10^{14} \text{W-cm}^{-2}$. This was well within the domain previously accessible only to nuclear explosives.

A series of exploratory impedance-match experiments¹⁹⁻²² followed. Experiments with gold overlays on aluminum²⁰ produced data at 3 Mbar in the aluminum and 6 Mbar in the gold. Similar experiments with copper overlays²² measured shock velocities corresponding to 2-8 Mbar in aluminum and 4-8 Mbar in copper. Error limits on the latter data were

established within 10%²². A problem that was anticipated at an early stage was the possibility of preheating^{21,23} the shocked materials with suprathermal electrons produced in the laser-generated plasma. The problem was mitigated, if not completely eliminated, by inserting a thin layer of high-z material (gold)^{21,22} between the laser plasma end of the target and the shock speed measurement end of the target. This layer would also tend to stabilize the shock as it traversed the shock-speed-measurement region. Later experiments²⁵ showed that higher pressures would be obtained with shorter wavelength (0.35 μ m) laser. This was owing to increased light absorption and reduced preheating from suprathermal electrons.

Antiproton-Driven Experiments

The laser-driven experiments can be used as a paradigm for antiproton-driven experiments. Many of the concepts and problems are similar: (1) both must be executed on a microscopic scale; (2) recording and target fabrication techniques are similar; (3) we must account for suprathermal electron preheat in laser experiments, we must account for energetic meson and electromagnetic cascade preheat in antiproton experiments. One conspicuous difference is the pulse length. Antiprotons are fermions and do not benefit from Bose condensation. Furthermore, antiprotons are charged, making it even more difficult to achieve high densities in the same portion of phase space.

Estimates of Shock Pressures

What kind of shock pressure can we expect? To answer this question, let us look at an idealized experiment emphasizing the unique features of an antiproton source. The most conspicuous feature is the ability to deposit energy predominantly deep within a target, specifically where the residual range¹ is less than 10 mg \cdot cm⁻². In laser driven experiments the shock is generated by blow off from the laser-heated region. This has been analyzed extensively^{28,29} and is not a very efficient way of converting driver energy into shock energy. Using the penetrating feature of an antiproton beam allows us to utilize nearly all the fission energy. Imagine we are trying to generate a

shockwave in uranium by focusing the antiprotons to the center of a sphere. Let us assume that all the fission energy is deposited in an embedded sphere of initial radius R_0 . The sphere will expand during the pulse, but to a good approximation the energy continues to be deposited in the same uranium that was initially enclosed in R_0 . We will call this the "heated sphere". The expanding heated sphere compresses the uranium ahead of it with a shockwave. The mass of the compressed region is

$$M = \frac{4}{3} \pi (R^3 - R_0^3) \rho_0, \quad (10)$$

where R is the shock radius. The equation of motion is

$$\frac{d}{dt}(MU) = 4\pi R^2 P_h, \quad (11)$$

where P_h is the pressure in the heated sphere. The shock is assumed to be strong, so

$$U = \frac{2}{\gamma + 1} \frac{dR}{dt}, \quad (12)$$

and

$$P_s = \frac{2}{\gamma + 1} \rho_0 \left(\frac{dR}{dt} \right)^2, \quad (13)$$

where P_s is the shock pressure. If we can relate the pressures by a constant

$$P_h = \alpha P_s, \quad (14)$$

then substituting Eqs(10) and (12) in the left of Eq(11) and Eqs(13) and (14) into the right, and integrating we obtain

$$\frac{dR}{dt} = a(R^3 - R_o^3)^{\alpha-1}, \quad (15)$$

where a is a constant of integration. We now evaluate, the two constants. The total energy is approximately

$$E = \frac{1}{2} MU^2 + \frac{4}{3} \pi R^3 \frac{P_h}{\gamma-1}, \quad (16)$$

if we take only internal energy in the heated sphere and only kinetic energy in the shocked region. Substituting Eqs(10) and (12) in the kinetic term and Eqs(13) and (14) in the internal term and using Eq(15) for the derivatives, we get

$$E = a^2 \frac{8}{3} \pi \rho_o \frac{(R^3 - R_o^3)^{2\alpha-1}}{(\gamma+1)^2} + \alpha R^3 \frac{(R^3 - R_o^3)^{2\alpha-2}}{\gamma^2 - 1} \quad (17)$$

The constants can now be evaluated at two limits: early time ($R \approx R_0$) and late time ($R \gg R_0$). For each we want the energy to increase linearly with time.

Early Time

Define $x = R - R_0$. Ignoring the kinetic term Eq(17) becomes

$$E = a^2 \frac{8}{3} \pi \rho_0 \alpha R^2 \frac{(3R_0^2 x)^{2\alpha-2}}{\gamma^2 - 1}. \quad (18)$$

Integrating Eq(15), we find the energy is proportional to time if $\alpha = 4/3$, so

$$x = \frac{\sqrt{8a^3}}{9} R_0 t^{3/2}, \quad (19)$$

and Eq(18) becomes

$$E = a^3 \frac{64\pi}{9} \frac{\rho_0 R_0^5}{\gamma - 1} t, \quad (20)$$

and

$$a^3 = \frac{3\dot{E}}{16m} \frac{\gamma-1}{R_0^2}, \quad (21)$$

where m is the mass of the heated sphere. The shock radius is

$$R = R_0 + \left[\frac{\gamma-1}{6} \frac{\dot{E}}{m} \right]^{1/2} t^{3/2}, \quad (22)$$

and the shock pressure is given by Eq(13) as

$$P_s = \frac{3}{4} \left[\frac{\gamma-1}{\gamma+1} \right] \frac{\dot{E}}{m} \rho_0 t. \quad (23)$$

The radius of the sphere is found from Eq(12);

$$R_h = R_0 + \left[\frac{2}{3} \frac{\gamma-1}{(\gamma+1)^2} \frac{\dot{E}}{m} \right]^{1/2} t^{3/2}. \quad (24)$$

Late Time

If we neglect R_0 compared to R , the total energy in Eq(17) increases directly with time when $\alpha = 7/4$. The radius of the shock is found to be

$$R = \left[\frac{25}{4} \frac{(\gamma+1)(\gamma^2-1)}{(8\gamma-1)} \frac{\dot{E}}{m} \right]^{1/5} (R_0 t)^{3/5}, \quad (25)$$

and the shock pressure is

$$P_s = \frac{18}{25} \left[\frac{25}{4} \frac{\gamma-1}{(8\gamma-1)\sqrt{\gamma+1}} \frac{\dot{E}}{m} \right]^{2/5} R_o^{6/5} \rho_o t^{-4/5}. \quad (26)$$

From the density behind the shock $\rho = \rho_o (\gamma+1)/(\gamma-1)$, we find the radius of the heated sphere:

$$R_h = \left[\frac{2}{\gamma+1} \right]^{1/3} \left[\frac{25}{4} \frac{(\gamma+1)(\gamma^2-1)}{(8\gamma-1)} \frac{\dot{E}}{m} \right]^{1/5} (R_o t)^{3/5}, \quad (27)$$

which completes the analysis²⁶.

Example EOS Experiments

We are now in position to look at some concrete examples. Polikanov¹ asserts that LEAR could dump 6×10^{11} antiprotons into a uranium target in 10^{-6} s, and this would deposit 16J resulting in $\sim 5 \times 10^4$ MW-gm⁻¹. This is consistent with a heated-sphere radius $R_o = 0.16$ mm, weighing about 0.3 mg. If we assume $\gamma \approx 1.2$ for uranium at the temperature and pressures we are dealing with, then at the end of the 1 μ s pulse, the heated sphere (Eq.27) reaches a radius $R_h = 0.66$ mm and the shock (Eq.25) reaches a radius $R = 0.68$ mm. The shock pressure (Eq.26) is a feeble $P_s = 2.84 \times 10^{10}$ erg-cm⁻³ = 28 Kbar, easily reached with black powder.

If we make the pulse much shorter, say a factor of 10 so that $t=0.1$ μ s and $\dot{E}/m = 5 \times 10^{18}$ $\text{erg}\cdot\text{gm}^{-1}\cdot\text{s}^{-1}$, we get into the region of the early time solution. For this case, at the end of the pulse, the heated sphere will have expanded (Eq.24) to $R_h = 0.276$ mm and the shock will have expanded (Eq.24) to $R = 0.288$ mm and the shock pressure (Eq.23) will have reached a respectable 650 Kbar. Further decrease in the pulse length will not help. Equation (23) shows that the shock pressure is proportional to E_t , which is the total energy deposited. Thus unless we increase the number of antiprotons, we are stuck with 650 Kbar -- not enough to do anything new.

If we could keep the pulse short enough to stay in the early-time regime, the shock pressure (Eq.23) will be proportional to the number of antiprotons. If we have enough energy to get into the late-time regime, the shock pressure (Eq.26) is proportional to the 0.4 power of the number of antiprotons and the -1.2 power of the pulse length.

Retaining a heated sphere $R_0 = 0.16$ mm, which is primarily determined by specific ionization along the antiproton path, we examine the dependence of the shock pressure on the number of antiprotons and pulse length. If we retain $E t^2 < 5 \times 10^{-3}$ m, we will stay in the regime of early-time solutions, and for fixed pulse length, the shock pressure Eq.(23) will be proportional to the antiproton number. Thus with $\dot{E}/m = 5 \times 10^{20}$ and $t = 1$ ns, we could obtain 6.5 Mbar, which is competitive with early laser-driven experiments^{15,17}. In the near term, shortest pulse at 300 MeV C^{-1} is probably 0.01 μ s and for the intermediate term we may be limited to about 10^{14} antiprotons, which would give a shock pressure of about 55 Mbar, quite competitive with nuclear-explosive-driven experiments. But to achieve this is a formidable technical challenge, perhaps worth the expenditure if antiproton based table-top tools can get into interesting experimental regimes with less investment in facilities and apparatus.

Caveat to Guide or Thinking

Why has the laser-driven EOS work stopped? Changing programmatic needs is one answer. But more importantly the nuclear-explosive work has been so successful¹² in verifying the SESAME EOS library²⁷ that there seems little motivation to continue. Rumor holds that laser-driven EOS work continues in Israel and France, and has reached the 100 Mbar regime. But such work is apparently classified.

Summary

Rather substantial improvements over Polikanov's¹ assumptions for pulse length and total number of antiprotons must be realized for this technology to compete with extant technologies for obtaining ultrahigh pressure EOS data.** The capabilities projected by Polikanov¹ are barely competitive with high-explosive drivers. We must wrestle with the difficult question of whether EOS research with antimatter is sufficiently motivated when it is not now being actively pursued by other means.

Conclusions

Two qualitative features of the projected antiproton energy source make it attractive for microscale opacity and EOS experiments.

- If small portable storage rings or traps with capacities of 10^{14} particles become available, such experiments could be conducted almost anywhere with minimum investment in facilities.
- The unique energy-deposition profile that allows antiprotons to deposit energy deep within a target substantially simplifies both opacity and EOS experiments and enhances their efficiency.

Substantial technical advances are needed to obtain the pulse lengths required by such experiments. But if antiproton sources become

**See the Epilogue for newer information.

readily available and inexpensive, they will undoubtedly be used to study these aspects of the extreme states of matter. In addition, use of such a table-top as a powerful source of particles and radiation for phenomenology studies external to the source merits additional investigation.

EPILOGUE

As a result of the RAND Workshop on Antiproton Science and Technology, some of the conclusions of this paper are slightly modified.

- I. The research³⁰ reported by Professor Smith suggests that the quantity of antiprotons required in each of the examples above may be somewhat less. Energetic light nuclei (d, t, He³, He⁴) and pre-equilibrium protons produced in \bar{p} - U reactions increase estimates of local energy deposition by a factor of 1-1/2 to 2 over the estimates given by Polikanov¹, which included fission fragments only. Thus estimates of the number of antiprotons required for each experiment might be reduced by as much as a factor of two.
- II. With clever storage ring technology² it appears possible to produce pulse lengths of 10 ns and perhaps as short as 1 ns in the near future. The availability of antiproton pulses in this range makes opacity experiments considerably more tractable and within the scope of near term technology.
- III. Preliminary calculations had shown that preheating of the test material, owing to the flux of neutrons, photons, and pions, was not serious enough to worry about. However, Professor Smith reported that about 9 MeV of the energy of each fission is imparted to pre-equilibrium protons³⁰. These protons could deposit a substantial fraction of their energy in the test material. Understanding of the preheat, which in principle could be calculated to a high degree of accuracy, is imperative to the design of each experiment. While it is unlikely to prohibit any of the experiments described above, preheat will add complexity to their interpretation.

More research is certainly in order. Transport calculations will be required to refine estimates of both local deposition and preheat. These should be combined with numerical calculation of the hydrodynamics and radiation flow in each experiment. More accurate estimates of pulse-length limitation would greatly enhance our capability to delineate the parameter space accessible to these experiments.

Figure 1.

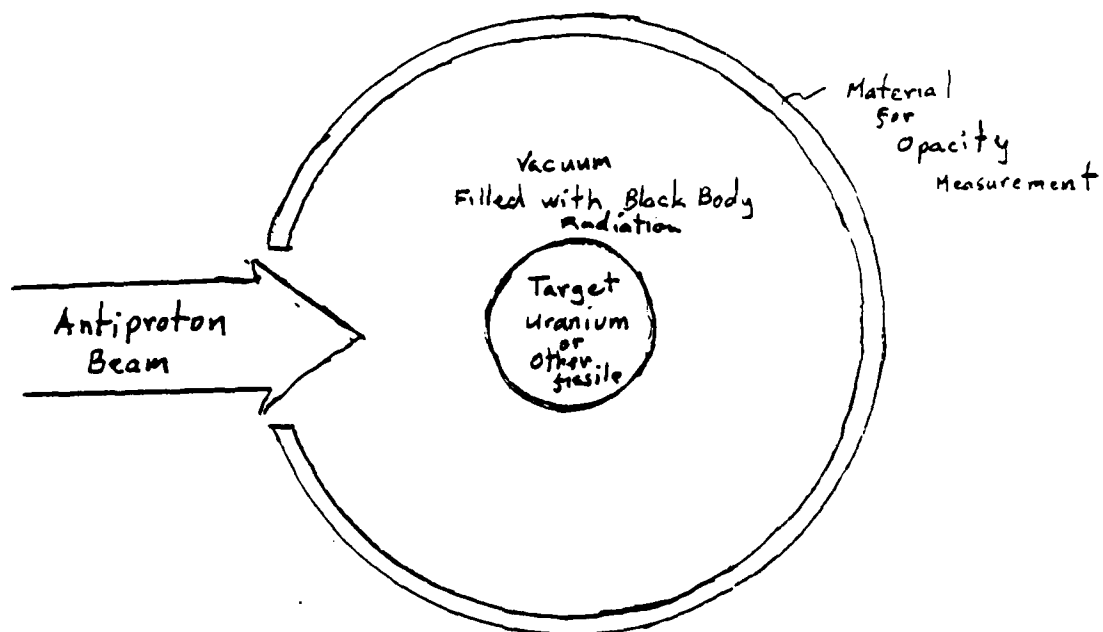


Figure 2.

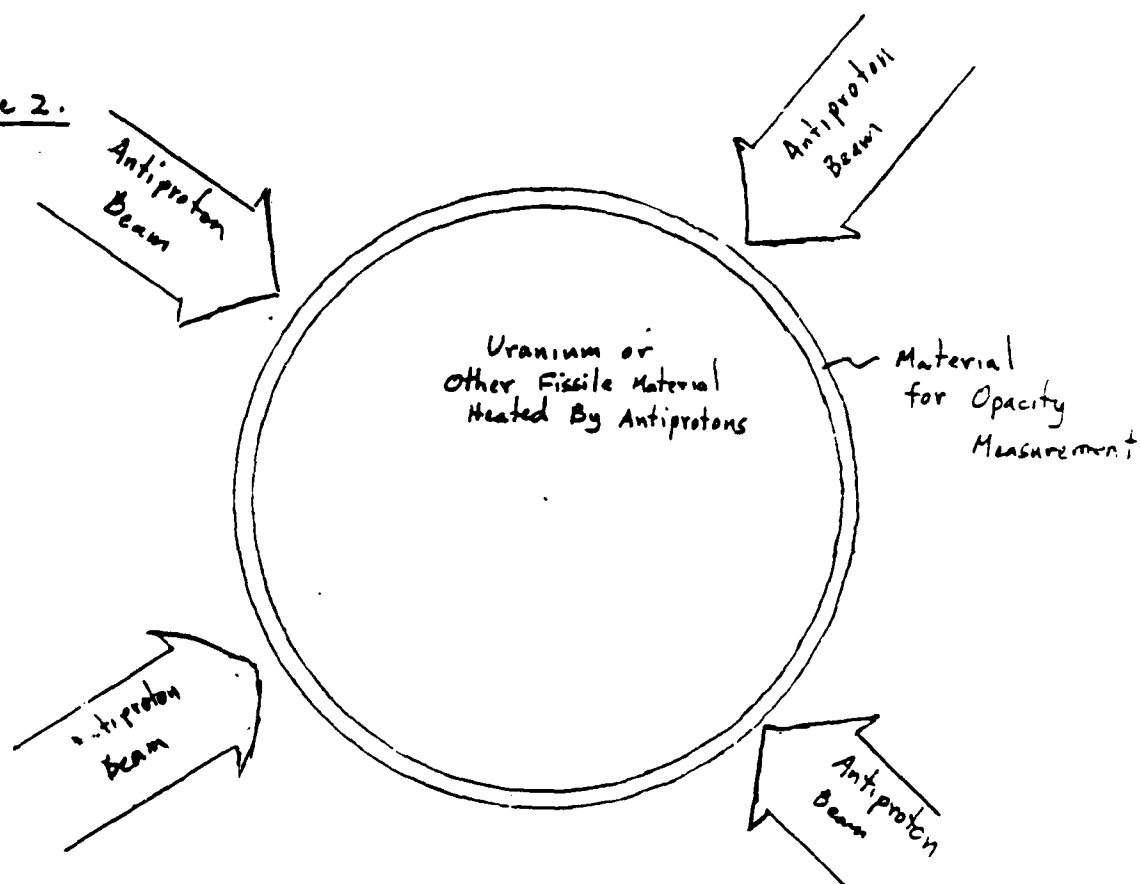


FIGURE CAPTIONS

- Fig. 1. *Classical Opacity Experiment* Single beam of antiprotons is passed through a port in cavity wall and heats fissile target in center. Exploding target fills cavity with black-body radiation. Diffusion wave passes through cavity wall.
- Fig. 2. *Non-Classical Opacity Experiment* Antiproton beams converge on target and deposit energy primarily in central region where Bragg peak and annihilation occur. Energy reservoir is specific heat of fissile material, not radiation. Diffusion wave passes through cavity wall.
- Fig. 3.a. *Typical Experimental Setup for Laser-Driven EOS Measurement* (from Ref. 19) Laser light is focused onto target in vacuum chamber. Rapid heating drives shockwave into foil. Streak camera records luminosity as shock emerges at different steps on back of foil. Time intervals give shock velocities.
- Fig. 3.b. *Typical Streak Camera Trace* Shock emerges at different times giving shock velocity in gold and aluminum. If aluminum EOS is well known, a point on the gold Hugoniot is determined. This same technique can be used to conduct impedance-match experiments in antiproton-driven experiments.

REFERENCES

1. S. Polikanov, *Could Antiproton Be Used to Get a Hot, Dense, Plasma, in Physics at LEAR with Low-Energy Cooled Antiprotons*, Ugo Gastaldi and Robert Klapisch, eds.
2. Private Communication, Gerald A. Smith, Pennsylvania State University.
3. Private Communication, J.F. Barnes, Los Alamos National Laboratory.
4. N.M. Hoffman, L.W. Miller, and J.M. Mack, *The Limb-Darkening Opacity Experiments Using a Laser-Heated Plasma*, Los Alamos Scientific Laboratory report LA-7484-MS (October 1978). Also see L.W. Miller, H.W. Kruse, P.J. Kruse, D.E. Bartram, N.M. Hoffman, and J.M. Mack, *Design and Operation of a Time-Gated Optical System for Measuring the Angular Distribution of Light Emitted from Laser Targets*, SPIE Vol. 190 LASL Optics Conference (1979), pp. 430-437.
5. A.K. Pierce and J.H. Waddell, *Analysis of Limb-Darkening Observation*, R.A.S. Memoirs 68, 89-112 (1961).
6. Ya. B. Zel'dovich and Yu.P. Raizer, *Physics of Shock Waves and High-Temperature Hydrodynamics Phenomena*, Vol. 2, (Academic Press, New York, 1967), pp. 770-777.
7. J.A. Morgan, *High Temperature-High Pressure* 6, 195 (1974). Also see R.G. McQueen, S.P. Marsh, J.W. Taylor, J.N. Fritz, and W.J. Carter, in *High-Velocity Impact Phenomena*, R. Kinslow, ed. (Academic, New York, 1970), p. 293.
8. A.C. Mitchell and W.J. Nellis, *J. Appl. Phys.* 52, 3363 (1981).
9. C.E. Ragan III, M.G. Silbert and B.C. Diven, *Shock Compression of Molybdenum to 2.0 TPa or by means of a Nuclear Explosion*, *J. Appl. Phys.* 48, 2860-2870 (1977).
10. C.E. Ragan III, *Ultrahigh-Pressure Shock-wave Experiments*, *Phys. Rev. A* 21 458-463 (1980).

11. C.E. Ragan III, *Shock Compression Measurements at 1 to 7 TPa*, Phys. Rev. A. 25, 3360-3375 (1982).
12. C.E. Ragan III, *Shock-wave Experiments at Three-fold Compression*, Phys. Rev. A. 29, 1391-1402 (1984).
13. Sec XI, *Dynamic Pressures - Experimental Techniques*, in High Pressure Science and Technology, Vol. 2, B. Vodar and Ph. Marteau, eds. (Pergamon, New York, 1980), pp. 958-1008.
14. J.C. Solem and L.R. Veesser, *Exploratory Laser-Driven Shock Wave Studies*, Los Alamos Scientific Laboratory report LA-6997-MS (November 1977).
15. L.R. Veesser and J.C. Solem, *Studies of Laser-Driven Shock Waves in Aluminum*, Phys. Rev. Lett. 40, 1391-1394 (1978).
16. J.C. Solem and L.R.-Veesser, *Laser-Driven Shock Wave Studies*, in Behavior of Dense Media under High Dynamic Pressure, J. Yuon, ed. (Commissariat a l'Energie Atomique, Paris, pp. 463-476 1978).
17. R.J. Trainor, J.W. Shaner, J.M. Auerbach, N.C. Holmes, *Ultrahigh Pressure Laser-Driven Shock Wave Experiments in Aluminum*, Phys. Rev. Lett. 42, 1154-1157 (1979).
18. L.R. Veesser, A.J. Lieber, and J.C. Solem, *Planar Streak Camera Laser-Driven Shockwave Studies*, in Proceedings of the International Conference on Lasers' 79 (STS Press, McLean, VA, 1980) pp. 45-48.
19. J.C. Solem, L.R. Veesser, and A.J. Lieber, *Impedance-Match Experiments using Laser-Driven Shock Waves* in High Pressure Science and Technology, Vol. 2, B. Vodar and Ph. Martean, eds. (Pergamon, New York, 1979) pp. 971-973.
20. L.R. Veesser, J.C. Solem, and A.J. Lieber, *Impedance Match Experiments using Laser-Driven Shock Waves*, Appl. Phys. Lett. 35, 761-763 (1979).
21. R.J. Trainor, N.C. Holmes, and R.A. Anderson, *Ultrahigh Pressure Laser-Driven Shock Wave Experiments*, in Proceedings of the American Physical Society Topical Conference on Shockwaves in Condensed Matter (APS, New York, 1981).

22. N.C. Holmes, R.J. Trainor, R.A. Anderson, L.R. Veaser, and G.A. Reeves, "Impedance-Match Experiments using High Intensity Lasers (APS, New York, 1982) pp. 160-163.
23. R.J. Trainor, H.C. Graboske, K.S. Long, and J.W. Shaner, *Application of High-Power Lasers to Equation-of-state Research at Ultrahigh Pressures*, Lawrence Livermore Laboratory report UCRL-52562 (1978).
24. R.J. Trainor and Y.T. Lee, *Analytic Models for Design of Laser-Generated Shock-Wave Experiments*, Phys. Fluids 25, 1898-1907 (1982).
25. R.J. Trainor, N.C. Holmes, R.A. Anderson, E.M. Campbell, W.C. Mead, R.J. Olness, R.E. Turner, and F. Ze, *Shock Wave Pressure Enhancement using Short Wavelength Laser Irradiation*, Appl. Phys. Lett. 43, 542-544 (1983).
26. This analysis roughly follows the treatment given by Ya. Zel'dovich and Y. Raizer, *Physics of Shock Waves and high-Temperature Phenomena*, Vol. 1 (Academic, New York, 1966) pp. 93-99. also see G. Chernyi, Dokl. Akad. NaukSSSR 112, 213 (1957).
27. B.T. Bennett, J.D. Johnson, G.I. Kerley, and G.T. Reed, Los Alamos Scientific Laboratory report LA-7130. Also see LASL 79-62 and LALP-83-4. Also see K.S. Long, D. Young, F.H. Ree, in *Shock Waves in Condensed Matter-1981*, API Conf. Proc. No. 78, W.J. Nellis, L. Seaman, and R.A. Graham, eds. (AIP, New York, 1982) pp. 213-217. Also see G.I. Kerley, in *Proceedings of Eighth Symposium on Thermophysical Properties*, Vol. II, J.V. Sengers, ed. (American Society of Mechanical Engineers, New York, 1981), pp. 159-164.
28. C. Fauginon and C. Floux, *Hydrodynamic Behavior of Solid Deuterium under Laser Heating*, Phys. Fluids 13, 386-391 (1970).
29. R.J. Trainor and Y.T. Lee, *Analytic Models for Design of Laser-Generated Shock-Wave Experiments*, Phys. Fluids 25, 1898-1907 (1982).
30. G.A. Smith, *Particle Emission from Antiproton Annihilation at Rest in Uranium*, PSU HEP/87-12.

INITIAL LABORATORY PROPULSION TESTING

David L. Morgan, Jr.

728 Polaris Way, Livermore, CA 94550

(For the Rand Workshop on Antiproton Science and Technology,
Santa Monica, CA, October 6-9, 1987)

ABSTRACT

Investigation of the physics relevant to the design and feasibility of antiproton annihilation propulsion engines reveals a lack of knowledge in some crucial areas. The stopping rate of antiprotons in matter is not known for energies below about 10 KeV (some possible models are presented here). The annihilation rate for antiprotons in some relevant materials has never been measured, and it is not known for antiproton energies below a few tens of MeV in nearly all others. Experiments to obtain this knowledge could probably be carried out with no more than about 10^7 antiprotons.

The amount and distribution of annihilation energy deposited within hypothetical engines is difficult to predict. Experiments requiring roughly 10^7 or 10^8 antiprotons could measure this deposition. Some of these experiments use actual, full scale models of the engines that are capable of simulating engine performance in a number of ways. For roughly 10^8 antiprotons the experiments could provide useful information on engine design, verify modelling codes, and help determine feasibility of the engine concepts.

A. INTRODUCTION

The design of engines and systems to achieve propulsion from the annihilation energy of antiprotons is largely determined by how antiprotons and their annihilation products interact with matter. Investigation of these interactions reveals a number of pertinent physical processes and quantities relevant to engine design that require experimentation for their understanding and determination. The interactions also determine some of the conditions (e.g. antiproton energy) under which experiments pertinent to other parts of the propulsion system should be conducted.

In designing an annihilation engine there are two main issues to consider. First, how does one get the antiprotons to annihilate only where desired (Section C of this report), and second, how does one transfer the energy of the annihilation products to the working medium that provides thrust (Section D). Consideration of these issues reveals a number of pertinent gaps in our knowledge (e.g. stopping and annihilation of antiprotons with energies from about 1 eV to a few KeV), and experiments to fill these gaps are suggested in Section E. That section also contains suggestions for full scale engine simulation experiments. It appears that the suggested experiments can be conducted with numbers of antiprotons that are orders of magnitude within the 10^{14} antiprotons per year that might be produced by a postulated U.S. low energy antiproton production facility. Section B of this report is a brief review of possible engine types and how these engine concepts deal with the two issues.

The production and storage of antiprotons and antihydrogen, which are necessary for annihilation propulsion, are dealt with in other reports of this workshop.

Background information on the use of antiproton annihilation for propulsion may be obtained from the references, including my JBIS article [1] and, in particular, Forward's comprehensive work [2]. Among other articles containing shorter reviews are those by Augenstein [3], Pace [4], and Howe and Hynes [5]. Section B of this report is intended to provide some background information. It may be important to point

out here that particle-antiparticle annihilation provides, according to present-day physics, the greatest conceivable amount of on-board stored energy per unit mass (9×10^{16} Joules/kg) and that use of this "ultimate" form of propulsion may be possible within a few decades.

B. ENGINE TYPES

Proposed annihilation engine types may be categorized according to the physical state of the predominant substance within the engine. Hence the types: solid core, gas core, plasma core, and beam core. The substance may be one or both of annihilation medium and propellant. The distinction, in this manner, of the first three types is principally related to the ease with which the annihilation energy is transferred to the propellant. Thus, it is a density distinction with transferral being "easiest" in the solid core case.

In their overall appearance, annihilation engines resemble rocket engines (or a jet engine in the case of an air-breathing variety of solid-core engine). There is a combustion chamber wherein annihilation and transferral of energy to the propellant occur and an exhaust nozzle. In some cases the combustion chamber and nozzle consist of magnetic fields.

The annihilation products referred to are mainly positive and negative pions and gamma rays (each with a few hundred MeV of kinetic energy) when antiprotons annihilate with the protons of hydrogen. The same products are produced, along with protons and neutrons (with kinetic energies around 100 MeV each) and some light nuclei of lower energy, when antiprotons annihilate in the nucleus of a heavier element. The annihilation energy of an antiproton is 1876.5 MeV, twice its mass energy since it annihilates with a proton of equal mass or with a neutron of nearly equal mass. The annihilation energy goes into both the kinetic energies and mass energies of the annihilation products. When an antiproton annihilates with a proton, the average numbers and kinetic energies of products are: 1.5 positive pions with 235 MeV each, 1.5 negative pions with 235 MeV each, and four gammas with 200 MeV each. The gammas come from the decay, in about 10-16 seconds, of an average of two neutral pions which are initially produced. About 4% of the

annihilation energy goes into the kinetic and mass energy of kaons. Annihilation of an antiproton with a neutron gives about the same result except that the number of negative pions is about one more than the number of positive pions.

1. Solid-Core Engines

For this engine type [3,5,6], a solid that is a heavy element with a very high melting point (e.g. tungsten) is the medium that absorbs the energy of the annihilation products. The antiprotons may annihilate in this solid or in another substance placed within the solid. The propellant is a gas (preferably hydrogen) which absorbs heat while passing through channels in the solid. The total distance intersecting the solid along the path of any particle (or gamma ray) from an annihilation point to the edge of the solid need only be a few to several centimeters for the solid to absorb a high fraction of the annihilation energy [2]. Roughly 75% of the annihilation energy can be converted to exhaust energy.

For suitable antiproton energies, the distance (range) from the point at which the antiproton enters the solid to the point at which it annihilates is much less than the distance that the annihilation products must travel to transfer their energy to the solid (see results of sections C and D). Thus the antiprotons are provided with an open channel into the solid so that they may annihilate near the center rather than near an edge. Solid-core engines as described above are limited in specific impulse to about 1000 s because the temperature of the propellant cannot exceed the melting point of the solid. Nevertheless, this value is about double that of the best chemical engines. Air breathing solid-core engines would be suitable as aircraft engines, and as rocket engines their specific impulse is ideal for many possible missions in the earth-moon environment. The use of such engines in single-stage, earth-to-orbit vehicles has been considered by Froning [7].

2. Gas-Core Engines

In gas-core engines [8] a gas serves as both annihilation medium and propellant. It follows from the stopping power formulae that the distances that must be travelled in a gas by annihilation products to

deposit their energy are considerably greater than any currently reasonable size of a rocket engine, so the engine is placed in a magnetic field of sufficient strength (a few to several tesla, depending on engine size, in a "bottle" configuration) to confine the charged annihilation products within the engine while they deposit their energy. (The antiprotons are injected along the symmetry axis where their direction is parallel to the magnetic field.) Thus, the energy of the annihilation gamma rays (and neutrons, if the gas is not hydrogen) is lost.

Because the walls of the engine can be cooled by propellant flow through them into the engine, the propellant can be heated to a much higher temperature than the highest melting point of solids. Howe and Hynes at Los Alamos National Laboratory have determined that a propellant temperature of 9000 K is possible [9], giving a specific impulse of about 2500 s (the authors of reference 9 use 1500 s, 2500s is the theoretical maximum for 9000 k). In gas-core engines the gas density is about ten to thirty times that at STP. Cassenti [10] has shown that for such densities and no leakage of the charged products through the magnetic field and out of the engine, nearly 47% (the theoretical maximum) of the annihilation energy goes to heat the gas. At lower densities, the time for energy transferral is long enough so that the charged pions decay into muons (and neutrinos) and the muons decay into electrons and positrons (and neutrinos). This leads to the loss of a substantial portion of the energy into neutrinos. At very low density (assuming no leakage) only 9% of the annihilation energy goes into heating (or 18% if the positrons from muon decay manage to transfer all of their kinetic energy to the gas before annihilating with electrons of the gas to form gammas). Gas-core engines are ideal for many high performance missions in the earth-moon environment and for transit to nearby planets. Assuming some of the heating of the gas when passing through the walls is from heat deposited in the wall by annihilation gammas, about fifty percent of the annihilation energy is converted to exhaust energy.

3. Plasma-Core Engines

Plasma-core engines [1] have some similarity to gas-core engines. Here, however, the propellant has a much lower density (on the order of 10^{16} to 10^{17} atoms or ions/cm³) and is heated to temperatures at which it is highly ionized. Annihilation occurs within this plasma, but not necessarily with nuclei of the plasma itself. The annihilation medium may be a beam of neutral atoms or molecules injected from the side. The magnetic field ("bottle" plus connected "nozzle" configuration) serves the additional purpose of confining the plasma and directing the exhaust; the combustion chamber and nozzle do not necessarily have solid walls. Because of the low density, the charged annihilation products have a greater tendency to escape from the field before they have transferred their energy. It may therefore be necessary to pulse the magnetic field. In its "strong" configuration the field confines the products within the combustion chamber until energy transfer is complete. In its "weak" configuration the field strength at one end lessens to allow the plasma to proceed into the magnetic nozzle.

Depending on the specific design, the plasma density may be so low in these engines that the kinetic energy of the pions and their decay muons does not transfer to the plasma before decay of the muons into electrons or before leakage of the pions or muons. Thus much of the annihilation energy that resides in the pions can be lost. The kinetic energy of the charged nuclear fragments that result from antiproton annihilation in a heavy nucleus [11] transfers much more readily to the plasma because the mass of these fragments (mainly protons, with some deuterons, tritons, helions, alphas, etc.) is much greater than the pion and muon masses. Thus, whereas the inert propellant, which constitutes most of the plasma, may be chosen to be hydrogen, it might be advantageous to make the neutral cross beam in which the antiprotons annihilate be a heavy element.

Smith [12] has recently shown that about 15% of the annihilation energy goes into kinetic energy of charged fragments when antiprotons annihilate, at rest, in uranium. This figure is significantly above the previous estimate of 10% [11]. Smith also states that nearly 100% of

the annihilations result in fission of the nucleus, confirming an estimate of Polikanov [13]. When the kinetic energy of the fission fragments is added, the total kinetic energy of charged fragments is about 25% of the annihilation energy.

Plasma core engines appear capable of specific impulses of a few to several thousand seconds and are therefore suitable for high-performance missions within the solar system which are essentially impossible for chemical propulsion. Assuming no leakage of the pions or their decay daughters, but using Cassenti's 9% minimum figure for the pion energy transferred, about twenty five percent or thirty five percent of the annihilation energy is converted to exhaust energy when annihilation is in a heavy element cross beam, with the higher figure applying when a fission element is employed.

4. Beam-Core Engines

In beam-core engines [1] the antiprotons annihilate in a vacuum with a crossing beam of atoms or molecules. Both beams have a density of about 4×10^{12} particles or atoms per cubic centimeter. A magnetic field directs the charged annihilation products forming an exhaust that consists of the products themselves. If the crossing beam is hydrogen, the specific impulse is about 3×10^7 since the exhaust speed of the charged pions produced by annihilation of the antiprotons with the protons of hydrogen is nearly that of light. These engines are suitable for interstellar travel where spacecraft speeds near light speed are desirable. About forty percent of the annihilation energy is converted to exhaust energy.

5. Other Types

Augenstein has mentioned a concept for a liquid core engine [3] which bears some similarity to the solid-core concept. A liquid with a very high boiling point is heated by annihilation while being held in place by centrifugal force in a rotating solid of high melting point. The hydrogen propellant is bubbled from holes in the solid through the liquid, keeping the part of the liquid in contact with the solid cooler than the solid's melting point, but absorbing heat while it passes through and attaining a temperature approaching the boiling point of the liquid. Specific impulses around 2000 s may thus be possible. It is

not clear how the hot hydrogen exhaust avoids all solids, including the engine walls.

Engines with properties between those of a gas-core engine and a plasma-core engine are possible. In fact, a single engine type might be possible that could transform from one to the other through intermediate configurations, just by varying the propellant and antiproton flow rates and the magnetic field strength. The same is true for variation between plasma-core and beam-core engines, but with at least some of the intermediate types having dual exhaust velocities.

A pulsed, solid/plasma-core engine has been alluded to by Augenstein [3] and Vulpetti [14] and discussed by Howe and Hynes [15]. In this concept, a chunk of solid is converted into a plasma by a pulse of antiprotons. The plasma is then directed by a magnetic field to form an exhaust, and the process is repeated with other chunks. To demonstrate that this concept is feasible, it must be shown that an antiproton pulse of sufficient strength to vaporize and ionize the solid can be delivered into the chunk in a time less than the time it takes the plasma to expand to a density that is insufficient to absorb the annihilation energy. If a small crystal or a large cluster of antihydrogen is used in place of the pulse of bare antiprotons, then it must be shown that the annihilation will complete with a similar rapidity.

Vulpetti has proposed a solid/beam-core engine concept that differs from the beam-core engine in two main respects. It is pulsed, and the annihilation occurs in one of a number of sequential solid pellets, each small enough so that nearly all charged annihilation products escape from the solid and form the exhaust. Each pellet is shot crosswise through the engine and is hit at a point where there is a hole into the pellet by a pulse of antiprotons when it reaches the engine's symmetry axis. The pellet is then followed by others as each is captured and recycled (the annihilation energy absorbed is insufficient to melt a pellet). This concept permits annihilation levels of nearly 100% with antiprotons at KeV and MeV energies, while such a level requires antiproton energies of about 1 eV or less in the antiproton-hydrogen crossed beam annihilation of the ordinary beam-core engine. The low

energies, at the high antiproton currents required (several amps), may be difficult to achieve, due to the high charge densities involved. Depending on pulse duration and rate, the charge densities at the high energies might be significantly less.

Nordley has proposed an antimatter - electric power engine [16]. Here annihilation occurs in what has some similarity to a solid-core engine, but the power is used to generate electricity, which is then used to accelerate a propellant by electric propulsion techniques. Although this dual method adds complexity and weight, it offers a wide range of specific impulses that can be between those of the plasma- and beam-core engines, with roughly similar overall efficiencies. The engine thrust is fairly low (as with the beam-core engine), but with the high specific impulses available, it can accomplish deep space missions involving great distances (hundreds or thousands of a.u.'s to light years) in times much less than conventional means.

Billen [17], Takahashi [18], and Rafelski [19] have proposed that muon catalyzed fusion be employed to enhance the energy available in antiproton annihilation. Here one designs what is similar to a gas-core or plasma-core engine, but with deuterium and tritium constituting all or part of the propellant, and with a density and a magnetic field strength (values within the range for the current concepts of those engines would suffice) such that the charged pions decay to muons within the engine. The negative muons then catalyze fusion between deuterium and tritium nuclei (producing a neutron and an alpha particle). If one negative muon can catalyze 150 to 200 fusions (the approximate maximum currently observed) then an additional energy of about 5 GeV per antiproton is produced. Of this, most is in the kinetic energy of the neutron which will escape in ordinary sized systems without transferring much energy. Only about $3/4$ GeV is in the kinetic energy of the alphas, which will be transferred rapidly to the inert propellant. This extra energy is, nevertheless, sufficient to at least double or triple the efficiency of a plasma-core engine. However, it is probable at the temperature of the plasma-core engine and possible at the temperature of a gas-core engine that the number of fusions per muon is considerably less than the maximum currently observed [9]. Another possible problem

is producing and handling the tritium (very radioactive) required, although it may be possible to breed it within the engine.

An annihilation engine operating at a temperature around 10^8 (as with the specific concept for a plasma-core engine in reference 1) could cause fusions in any deuterium and tritium within it without help from muons. Thus one can imagine annihilation engines in which a substantial part of the energy is derived from fusion, or fusion engines in which antiproton annihilation acts as an initial trigger to start fusion and, possibly, help maintain it. Such ideas are mentioned in reference 9. Gsponer and Hurni [20] have conceived a means to obtain fusion energy in a bomb configuration by using antiprotons to initiate a pure fusion reaction.

C. SLOWING AND ANNIHILATION OF ANTIPROTONS

Considering the slowing and annihilation of antiprotons in matter and their relevance to engine design reveals an incomplete knowledge of relevant stopping and annihilation rates. This knowledge gap can be filled in by the experiments suggested in Section E.

The location of a region within a substance where annihilation occurs depends on the rates (per unit distance) at which antiprotons annihilate and at which they slow down in the substance. Both of these quantities depend on the energies of the antiprotons. At very high energies the antiprotons will pass through a given thickness of the substance with very little annihilation. At very low energies they will annihilate at the surface of the material, which reduces energy transferral for all but solid-core engines. It is shown below that for a hydrogen annihilation medium there is a range of antiproton energies between roughly 0.1 eV and 10 MeV that is most suitable for injection of antiprotons into the annihilation medium, with the exact energy depending on engine type and size and on the density and composition of the annihilation medium. For some heavier elements it is shown that this range may not exist; there may be no energy that allows penetration of the antiprotons to the point where annihilation is desired without a substantial portion of the antiprotons being annihilated on the way in.

Figure 1 shows the stopping rate $-dE/d(\rho x)$ for antiprotons in hydrogen as a function of their kinetic energy, E , where ρ is the hydrogen density and x is the position of the antiproton. Integration of $-[dE/d(\rho x)] \cdot 1/\rho$ between energies E_1 and E_2 gives the distance travelled by the antiproton while slowing down from energy E_2 to energy E_1 . To obtain the stopping rate I used the Bethe formula with $I=13.6$ eV for energies above 6.3 KeV where energy loss is predominantly due to ionization of the medium by antiproton-electron collisions. At lower energies I used formulae from models I developed for the processes: elastic collisions of antiprotons with atoms, adiabatic ionization of atoms by antiprotons, and rearrangement annihilation. The models and formulae are given in the appendix. For energies below the peak in the collision-ionization rate at 20 KeV, the rate drops off rapidly and is zero for the energy less than or equal to about 6.2 KeV. For these latter energies the other processes continue to slow the antiprotons. Although rates for these processes are initially much lower, they are working on a proton with much lower energy at this point, so the slowing is very rapid. This latter fact is illustrated in Table 1 where the values of $D(\rho x)$ (change in the value of ρx) traversed as the antiproton energy drops through chosen energy ranges is given. Also shown in the table are actual distances traversed for various densities of hydrogen for the same drops in energy.

Figure 2 shows the antiproton annihilation rate $dP/d(\rho x)$ as a function of E . For energies above 27.2 eV the coulomb-corrected direct annihilation formula of Morgan and Hughes is employed [21]; for energies below 27.2 eV a formula based on their work on antiproton-hydrogen rearrangement annihilation is employed. At low energies the presence of the negatively charged antiproton reduces the effective charge of the proton binding the electron in a hydrogen atom. Thus the atom may adiabatically ionize. Below 27.2 eV the energy of the antiproton in the center of mass system is less than 13.6 eV (the binding energy of the electron) so if the hydrogen atom is adiabatically ionized, the antiproton must become bound to the proton to conserve energy. It then eventually annihilates with the proton. The cross section for this

rearrangement-annihilation process is orders of magnitude greater than the direct annihilation cross section.

The annihilation rate per energy loss is $-dP/dE = (dP/d(\rho x)) / (-dE/d(\rho x))$. The integral of this quantity between E_1 and E_2 (E_2 greater than E_1) gives the value of DP for that energy range, and the probability that an antiproton starting at E_2 has annihilated by the time it reaches E_1 is $1-\exp(-DP)$. Values of DP are also given in Table 1. For determining annihilation probabilities over more than one range, the sum of the DP's is used in place of DP. For large numbers of antiprotons the annihilation probability is equal to the fraction that have annihilated.

Table 1 may be used to determine suitable injection energies for annihilation engines. For instance, the of about 55.4 cm in a hydrogen gas-core engine (with the density 20 times that at STP) before the annihilation rate becomes substantial. The value, 55.4 cm, is the sum of the Dx's in the gas-core column beginning at the range of $10^7 - 10^6$ eV and continuing down until DP becomes substantial, and that value is suitable for an engine of a particular size for which 55.4 cm from the entrance point puts the annihilation region in the center of the combustion chamber. The annihilation history may be read from the DP column. For the first 54.5 cm of the path (i.e. most of it), while the antiproton energy is decreasing from 10 MeV to 1 MeV, about 1.5 percent of the antiprotons annihilate. In the next roughly 0.874 cm, the energy decreases to 27.2 eV, and about 0.5 percent of the remaining antiprotons annihilate. Then in the final 0.03 microns the remaining 96 percent of the antiprotons annihilate as their energy drops below 27.2 eV. This short distance for the final annihilation does not occur in reality because of straggling in the stopping distance, a phenomenon not considered here.

The "plasma..." column in Table 1 gives Dx's for unionized hydrogen atoms at a density of the plasma in a plasma-core engine and is intended as a rough approximation to that case. For the 6300 - 1000 eV energy range the value of Dx is much larger than adjacent values. In this energy range, slowing by collisional ionization has cut off to zero while the energy is still sufficiently high that the slowing due to

adiabatic ionization and elastic collisions is still relatively small. Whereas such a "coasting" effect would not occur in a fully ionized plasma, it would be present to some degree in partially ionized plasmas of hydrogen-medium engines midway between gas core and plasma core. It would also be present, but at a higher energy, in plasma core engines with a heavy element for the medium, where the atoms would not be fully ionized. The proper injection energy can be very sensitive to the degree to which this phenomenon is present. Thus it is important to experimentally determine stopping rates at energies below the collisional-ionization cutoff. My models for the energy loss at such energies are only approximations, and it is not clear that I have included all processes that contribute to energy loss.

The last row of Table 1 shows that an injection energy of 0.1 eV results in about 90 percent of the antiprotons annihilating in a distance of about 12 cm within hydrogen at a density appropriate to a beam-core engine. Since the product of this distance (as the size of an annihilation region) with the density is a minimum value for annihilation engines, the 0.1 eV is approximately a lower limit for the injection energies. Thus, injection energies of about 0.1 eV to 10 MeV are required by annihilation engines, and this represents the antiproton energy range for any experiments that might be conducted on the transport and injection of antiprotons. (Such experiments might involve simulation of antiprotons with negative hydrogen ions, for which production facilities currently exist [22].)

Table 2 gives approximate values of DP , $D(\rho x)$, and Dx for antiprotons in a heavy element such as xenon, tungsten, or uranium. Values of DP are very approximate, being extrapolated from high energy data involving elements of medium atomic weight. That data is summarized in Figure 3 of reference 11. The extrapolation involves the use of the known electron-positron annihilation cross section and the assumption that the cross section is proportional to the area of the nucleus. The values of Dx are for a gas-core engine with the same atomic number density as for the hydrogen gas-core engine of Table 1. [The use of a heavy element in a gas-core engine might result in transferral of more annihilation energy to the propellant as it does in

a plasma-core engine.] It may be seen that there is no injection energy that permits most of the annihilation to occur in a small region. If one aims for a distance to the annihilation region of about 120 cm for instance, DP is about 13., so essentially all of the antiprotons will have annihilated before reaching that point. Thus a substantial fraction of the annihilations will occur near the entrance point, resulting in energy leakage and problems associated with the deposit of large amounts of energy into the nearby portion of the engine wall. This circumstance arises because the direct annihilation rate rises faster with atomic number, for fixed number density of the atoms of the annihilation medium, than does the stopping rate. It is therefore important to experimentally determine the direct annihilation cross section for heavy elements at energies from about 1 to 100 MeV.

D. DEPOSITION OF ANNIHILATION ENERGY

A fundamental, but surmountable, difficulty with the energy transferral is that in any kind of homogeneous medium the range of all or most of the annihilation products (particles) is much greater than the range of antiprotons for all desirable antiproton energies. Thus if an antiproton is injected into a substance, the depth at which it annihilates is much less than the range of the annihilation products in the same substance. Therefore, at least about half of the annihilation energy escapes through the surface through which the antiproton entered.

This difficulty is overcome in the solid-core engine by providing a free pathway into the solid for the antiproton, so that when it annihilates it is nearly surrounded by a sufficient thickness of the solid so that nearly all of the annihilation products deposit their energy in the solid. It is overcome for the charged annihilation products in the gas-core and plasma-core engine types by use of a strong magnetic field that confines these particles within the propellant while they travel long distances in their orbits.

Essentially all of the pion energy will be transferred to the propellant in hydrogen gas-core engines after the pions have passed through about 100 gm/square cm [23]; for a heavy element the corresponding number is about 350 gm/square cm. In most cases the pions

will have decayed to muons before depositing all their energy, but in cases where a significant amount of the pion kinetic energy remains, the muons continue in about the same direction and have about the same stopping properties as pions. The figures correspond to a path length of about 1 kilometer and 40000 kilometers for the gas and plasma-core engines of table 1, where the propellant stopping medium is hydrogen, and about 3.5 kilometers and 140000 kilometers when it is a heavy element. Over the larger of these distances, the muons will decay into electrons and positrons (and neutrinos) before stopping. The electrons and positrons are strongly held by the magnetic field and the electrons rapidly transfer their energy to the propellant, while the energy of the neutrinos and perhaps the positrons (through annihilation with propellant electrons into gamma rays) is lost. Hopefully an appropriate calculation of stopping in a plasma will substantially reduce the distances. As pointed out in Section B3, the protons and other charged nuclear fragments produced when annihilation occurs in a heavy element transfer their energies in much shorter distances.

In any case, a strong magnetic field of a few to several tesla is required to keep the charged annihilation products within the combustion chamber while they circuit thousands of times. During this time the particles will undergo numerous collisions with propellant atoms leading to outward drift across the magnetic field lines. It is possible that avoidance of this drift will require fields that are prohibitively high. It is also possible that plasma instabilities will occur in the plasma-core engine. Investigation of these possibilities requires experiments that will simulate such engines with the numbers of transportable antiprotons that might be available in a few years.

E. PROPOSED EXPERIMENTS

In the following, I make rough estimates of the numbers of antiprotons required for the proposed experiments. I assume that the antiprotons to be used have been stored in a trap and that they can be extracted and accelerated or decelerated (if they come out at higher than the desired energy) to the energies necessary for the experiments (about 100 eV to 100 MeV).

1. Stopping of Antiprotons and Other Charged Particles

The rate $-dE/d(\rho x)$, at which antiprotons lose energy in unionized matter needs to be determined for antiproton energies around and below about 10 KeV where slowing due to collisional ionization (and excitation) of the electrons drops off to zero. Knowledge of the rate is important, for low density neutral or partially ionized stopping media, in choosing an antiproton injection energy that places the annihilation region near the center of the engine. At the same time the energy loss rate has to be determined for antiprotons in a plasma for similar reasons, and the energy loss rates for charged pions and other charged annihilation products in a plasma must be determined to aid in modeling energy transferral. For the stopping of antiprotons and the other charged particles in plasmas, particle energies of a few eV to a few hundred MeV are of interest. Whereas protons could be used to simulate antiproton slowing at high KeV energies and above, they would not suffice for lower energies where the energy loss mechanisms are known to be or are likely to be charge dependent [24].

The experimental apparatus, in idealized form, for such an experiment might consist of a tube containing the stopping material in gaseous form. Antiprotons (or the other charged particles) of known energy and intensity are injected at one end while at the other end is a device that measures the intensity and energy distributions of the emerging particles. Varying the density of the gas in the tube thus allows energy loss (and attenuation, in case absorptive processes, like annihilation, are present) to be determined as a function of ρx . The gas can be ionized to make measurements as a function of ionization level by passing an electric current through the gas or by irradiating it.

For low energy particles, energy and angle straggling will be important and the apparatus may have to consist of a chamber with a number of detectors inside to account for the different paths followed by the different particles.

The effects of straggling are in themselves important to measure, since they affect the minimum volume within which antiproton annihilation can be made to occur. This is also relevant to using antiprotons for EOS experiments. If density is chosen so that the antiprotons come to rest and annihilate within the chamber, then detectors could determine the spatial distribution of annihilation points.

To estimate the number of antiprotons required to determine $dE/d(px)$ for antiproton energies from about 1 eV to 100 MeV, I assume four initial energies of 10^2 , 10^4 , 10^6 , and 10^8 eV. For each of these energies, 10 values of px are employed (giving 40 values of E as a function of px) and for each combination of initial energy and px , an average of 50 angles (i.e., detection at 50 different annular locations perpendicular to the initial direction of the antiproton). Each measurement consists of the detection and energy determination of a single antiproton. If nine out of ten antiprotons are lost prior to detection and the measurements are made for ten combinations of material and ionization level, then 10^7 antiprotons are required.

2. Antiproton Annihilation

The cross section for annihilation of antiprotons at energies in the low MeV range and below is poorly known. Theoretical predictions have not been checked. Knowledge of the cross section is important for knowing the ionization energies that make annihilation occur at the desired location and for knowing whether or not the ionization region can be localized. Measurements of the annihilation cross section could be made simultaneously with the experiment described above by placing an appropriate detector array along the tube to detect annihilation products. The number of annihilations per antiproton, per decrease in antiproton energy by one decade, varies from about 10^{-4} to 1 (Table 1). With an average of 2500 measurements for each px , 10^7 antiprotons should more than adequate.

3. Annihilation Energy Deposition

To gain knowledge for design and feasibility studies of annihilation engines it is important to determine experimentally the distribution of energy deposited in substances by antiproton annihilation for a number of substances of different atomic weight. Such knowledge would also provide verification and calibration for computer codes that calculate the energy distribution.

Callas [25] has described an experiment to determine the spatial and spectral distribution of annihilation energy deposited in an engine-like geometry in a magnetic field. The detection apparatus for this experiment permits each annihilation product to be followed in space after it exits the annihilation and energy transferral regions. Thus, for each value of p_x upon exiting, and for each substance employed, a spatial-energy distribution can be obtained with a sufficient number of measurements. If we assume 100 values of p_x , 10 combinations of annihilation material and energy-transferral material, 10 values for the magnetic field, one hundred measurements each to get the energy distribution, and nine out of ten antiprotons lost, then 10^7 antiprotons are required. It is presumed here that a single antiproton energy is chosen for each combination of materials and p_x such that the antiprotons annihilate within the annihilation region.

4. Solid-Core Engines

A full scale model, capable of variation, of a solid-core engine, or a large portion of it, should be constructed. A design for aircraft propulsion might be appropriate. Injection of relatively small numbers of antiprotons would allow measurement of where annihilation energy is deposited, and this information could be used to form or to calibrate the energy deposit portion of a computer code that simulates the engine. The code could then be used to suggest changes in the model. Other phases of the experimentation would involve heating the engine by means other than annihilation and flowing the inert propellant through it. The end result would be the demonstration that a solid-core engine could be constructed that is capable of producing a given thrust and specific impulse while remaining intact. It is important to demonstrate, in the process, that any radioactivity or radiation could be contained within

the engine or surrounding shields. If each trial with the model required no more than the number of antiprotons as in the above experiment, then about 10^8 would suffice for this experiment.

5. Gas and Plasma-Core Engines

These proposed experiments resemble the "Annihilation Energy Deposition" experiment (no. 3), and in fact some of the information sought here might be determined in that experiment if the medium were a gas or plasma of controllable ionization level placed in a magnetic field. Here, however, the intent is to construct fairly realistic models of gas and plasma-core engines and to measure the annihilation energy deposited with detectors placed within the model. Energy deposition would be measured both as a function of location in the engine and as a function of time after a pulse of antiprotons enters the engine. Other important purposes for this experiment are to measure drift of the charged products and plasma and to determine the presence and nature of any plasma instabilities that might occur.

The models should be constructed with approximately those dimensions (a size of a few meters) that currently exist for such concepts [26], and should employ magnetic fields shaped as in those concepts with strengths that vary from a few tesla up to values that are as close as practical to the thirty tesla maximum appearing in the concepts. Smaller scaled models would require proportionately larger fields so that the radii of the charged particle orbits is the same fraction of engine diameter.

For measuring energy deposition, the gas in the gas-core engine need not be heated but only have densities (variable) appropriate to those of the concept. In the plasma-core simulation, however, it is necessary, in addition to choosing appropriate densities, to heat the medium to form a plasma of controllable ionization level, since the ionization level is likely to influence the energy deposition. Heating could be accomplished by electric discharge or irradiation. Irradiation might be preferable, since it is possible that an electric discharge would cause instabilities that would not otherwise be present. To achieve essentially full ionization in a hydrogen plasma, a temperature much lower than in an actual engine would suffice, but if the heating

were sufficient to raise the temperature to that of a real engine, then plasma drift and instabilities also could be investigated.

Antiprotons are injected in pulses at appropriate energies and in numbers only sufficient to make the measurements. For both engine concepts the experiments will give the fraction of annihilation energy deposited in various media as a function of magnetic field strength and density. For the plasma-core concept, deposition as a function of ionization level is also determined and is additionally determined as a function of time. This piece of information is important for deciding what the pulse rate of the plasma-core engine should be if it must act in a pulsed mode.

The results of the experiments, if sufficiently high magnetic fields can be attained, will allow the determination of engine parameters that maximize the fraction of annihilation energy deposited, and thereby determine what that fraction is. Values of the fraction are important for evaluating the feasibility of these engine concepts.

Since the detectors must be placed within the apparatus, they must occupy a relatively small volume or else their presence would introduce significant perturbations on the results. Hence an overall detection efficiency that might be 10 to 100 times less than for the Callas apparatus. However, since the specificity of the designs being investigated is greater, fewer combinations of annihilation material and energy transferral material need be employed. Also, since statistical accuracy is not as important when working with an actual model, about 10^7 antiprotons would suffice for each level of ionization, so that about 10^8 would probably be required altogether.

CONCLUSIONS

There are a number of issues relevant to the performance and feasibility of the various concepts for rocket engines that provide propulsion from antiproton annihilation. Table 3 lists the issues that have been investigated or discussed in this report along with five of the engine types described in Section B. An entry in the table that connects an issue with an engine type indicates a relatively strong need for information to resolve the issue for the engine type. The experiments suggested in Section E can go a long way toward resolving most of these issues.

Current information on antiproton annihilation and stopping in matter is adequate to show that the annihilation region can be localized in solid-core and beam-core engines and is adequate to give good estimates of the antiproton energies required. It appears that localization in gas-core and plasma-core engines can be accomplished when the stopping medium (propellant) is hydrogen, but more information on the slowing of antiprotons is needed to predict the required injection energies. For unionized hydrogen, energy loss rates of antiprotons are needed for energies in the low keV energy range down to a few eV (models proposed here may not be adequate). For ionized hydrogen the rates are needed for MeV energies down to a few eV. For heavy elements it is possible that the annihilation region cannot be adequately localized in a uniform medium. Information on both energy loss and ionization rates of antiprotons in heavy elements is needed for eV through MeV energies.

The spatial distribution and energy spectrum of annihilation energy deposited in the solid of solid-core engines or in the gas or plasma propellant of gas-core or plasma-core engines is not known adequately to demonstrate the feasibility and/or capability of these engines. Experimental information is needed for the creation and calibration of computer codes that predict the deposition, in particular in the presence of a magnetic field. Energy deposition is of lesser importance

for a beam-core engine, where the charged annihilation products form the exhaust.

The performance, feasibility, and design specifics of a plasma-core engine depend greatly on how strong a magnetic field is needed to confine the plasma and on whether or not any possible plasma instabilities can be avoided. Investigation of these issues probably requires experimentation with a full scale model of the engine which needs only relatively small numbers of antiprotons while simulating some of their effects with external sources of heat.

It is principally the high specific impulses and in part the high thrusts, along with the high exhaust energy per unit mass of propellant, that provide large advantages for annihilation propulsion over other means. To achieve these characteristics requires high rates of energy production and consequently high temperatures and radiation levels. It must be demonstrated that such can be the case without damage to the engine components, and other parts of the vehicle, through the use of cooling, shielding, and obtaining a high temperature difference between the outer and inner portions of the combustion chamber. The experiments with full scale engine models would provide information for the calibration of computer codes that could predict possible damage.

The experiments suggested in Section E can provide much of the information needed to resolve most of the issues. Estimates of the numbers of antiprotons required for each experiment, about 10^8 or less, are orders of magnitude less than the annual production rate of transportable antiprotons that is envisioned for a near-future, low-energy, U.S. antiproton production facility.

ACKNOWLEDGMENTS

I am grateful to the following people in regard to presentations they made at the workshop session on propulsion, suggestions for the work reported here, help in locating relevant reports, and the numerous pieces of pertinent information they provided: John Callas, Brice Cassenti, Robert Forward, David Froning, Bill Halouiakas, Steven Howe, Michael Hynes, Theodore Kalogeropoulos, Gerald Nordley, Scott Pace, Jan Rafelski, Gerald Smith, Hiroshi Takahashi, and Bruno Augenstein.

REFERENCES

1. D.L. Morgan, Jr., Concepts for the design of an antimatter annihilation rocket, J. British Interplanetary Society 35, 405 (1982).
2. R.L. Forward, Antiproton annihilation propulsion, AFRPL TR-85-0334, Air Force Rocket Propulsion Laboratory, Edwards Air Force Base, CA, September, 1985, (p 113-116).
3. B.W. Augenstein, Some examples of propulsion applications using antimatter, July 1985, The Rand Corporation, Santa Monica, CA.
4. S. Pace, Applications of antimatter to space propulsion, Rand Graduate School, 16 March 1987, The Rand Corporation, Santa Monica, CA.
5. S.D. Howe and M.V. Hynes, Antimatter propulsion: status and prospects, Proceedings of the Manned Mars Mission Workshop, Huntsville, Alabama, June 1985.
6. G. Vulpetti and E. Pieragostini, Matter-antimatter annihilation engine design concept for Earth-space missions, IAF-86-178 (pre-print), 37th Congress of the International Astronautical Federation, Innsbruck, Austria, October 4-11, 1986, Pergamon Press, New York, 1986.
7. H.D. Froning, Jr., Investigation of antimatter airbreathing propulsion for single-stage-to-orbit ships, MDC H2618, McDonnell Douglas Astronautics Company, Huntington Beach, CA, July 1987 (presented to 38th Congress of the International Astronautical Federation, Brighton, United Kingdom, October 10-17, 1987).
8. B.N. Cassenti, Radiation shield annalysis for antimatter rockets, AIAA-87-1813, AIAA/SAE/ASME/ASEE 23rd Joint Propulsion Conference, June 29 - July 2, 1987, San Diego, CA; (see also ref. 2).
9. S.D. Howe and J.D. Metzger, Survey of antiproton-based propulsion concepts and potential impact on a manned Mars mission, Preprint LA-UR-87-2191, Los Alamos National Laboratory, 1987 (submitted to J. of Propulsion and Power).
10. B.N. Cassenti, talk at Rand Workshop on Antiproton Science and Technology, Santa Monica, CA, October 6-9, 1987.
11. D.L. Morgan, Jr., annihilation of antiprotons in heavy nuclei, Air Force Rocket Propulsion Laboratory, TR-86-011, December, 1985.

12. G.A. Smith, Particle emission from antiproton annihilation at rest in uranium, PSU HEP/87-12, Rand Workshop on Antiproton Science and Technology, Santa Monica, CA, October 6-9, 1987.
13. S. Polikanov, Letter to author, 28 November 1985.
14. G. Vulpetti, A concept of low-thrust relativistic-jet-speed high efficiency matter-antimatter annihilation propulsion system, IAF-83-397, 34th Congress of the International Astronautical Federation, October 9-15, 1983, Budapest, Hungary.
15. J.L. Callas, private communication, September, 1987.
16. G.D. Nordley, Application of antimatter - electric power to interstellar propulsion, IAA-87-609, 38th Congress of the International Astronautical Federation, Brighton, United Kingdom, October 10-17, 1987.
17. J.H. Billen et al., Los Alamos National Laboratory report LA-UR-85-3737, 1985.
18. H. Takashi, talk at Rand Workshop on Antiproton Science and Technology, Santa Monica, CA, October 6-9, 1987; private communication, April 1987.
19. J. Rafelski, talk at Rand Workshop on Antiproton Science and Technology, Santa Monica, CA, October 6-9, 1987.
20. A. Gsponer and J.P. Hurni, Antimatter Induced Fusion and Thermonuclear Explosions, Atomkernenergie-Kerntechnik 49, 198 (1987).
21. D.L. Morgan, Jr. and V.W. Hughes, Atomic processes involved in matter-antimatter annihilation, Phys. Rev. D 2, 1389 (1970), Atom-antiatom interactions, Phys. Rev. A 7, 1811 (1973); D.L. Morgan, Jr., Antiproton - hydrogen atom annihilation, Air Force Rocket Propulsion Laboratory, TR-86-019, May 1986.
22. V. Haloulakos, talk at Rand Workshop on Antiproton Science and Technology, Santa Monica, CA, October 6-9, 1987.
23. Ref. 2, p 114.
24. M.H. Martir, A.L. Ford, J.F. Reading, and R.L. Becker, Excitation and ionisation in collisions of negatively charged projectiles with atoms, J. Phys. B 15, 1729 (1982); W. Brandt and G. Basbas, Antiparticle excitation of atomic inner shells, Phys. Rev. A 27, 576 (1983).

25. J.L. Callas, Antimatter spacecraft propulsion experiments with current antiproton production rates, Rand Workshop on Antiproton Science and Technology, Santa Monica, CA, October 6-9, 1987.
26. Ref. 2, p 122,124; Ref. 1.

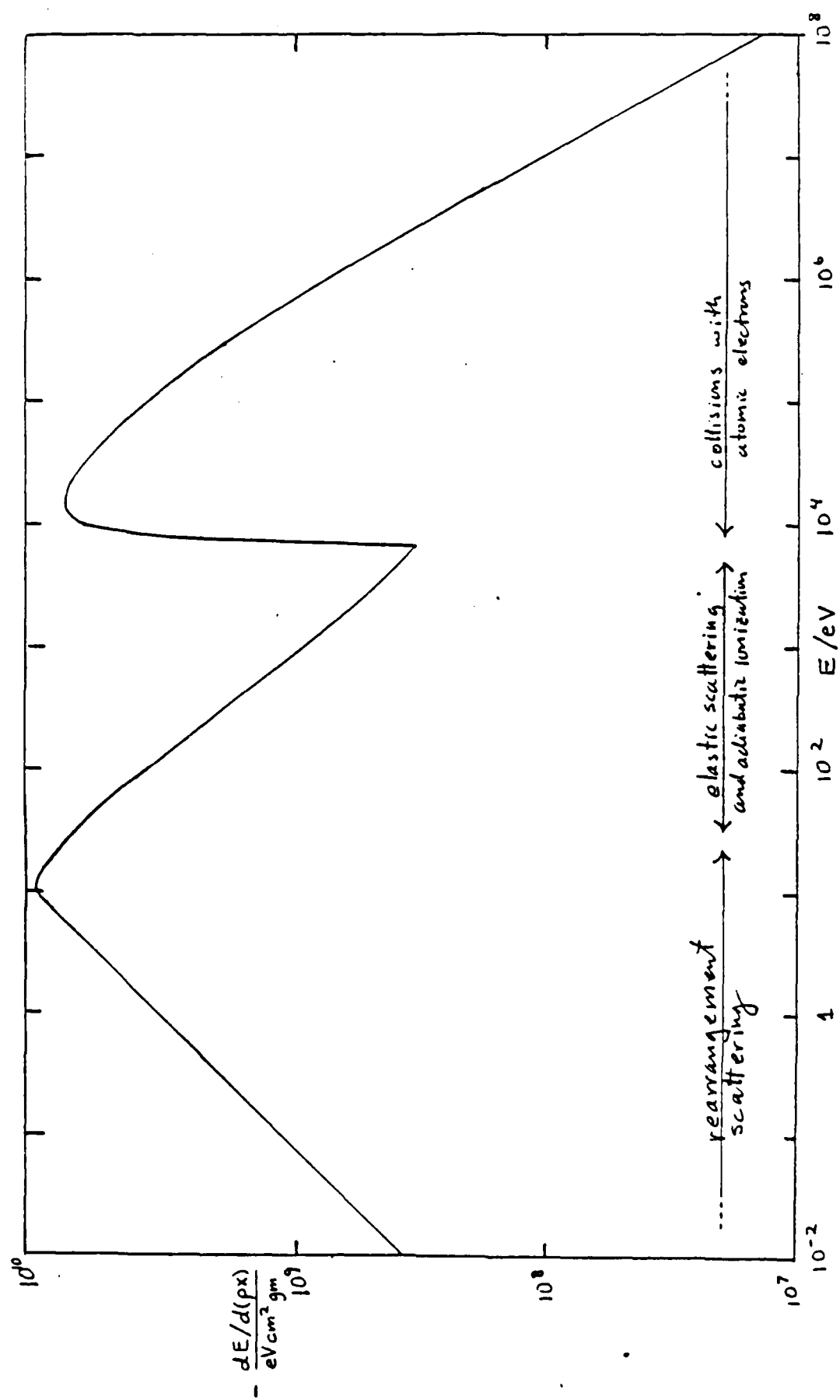


Figure 1. Stopping power for antiprotons of lab energy E in hydrogen.

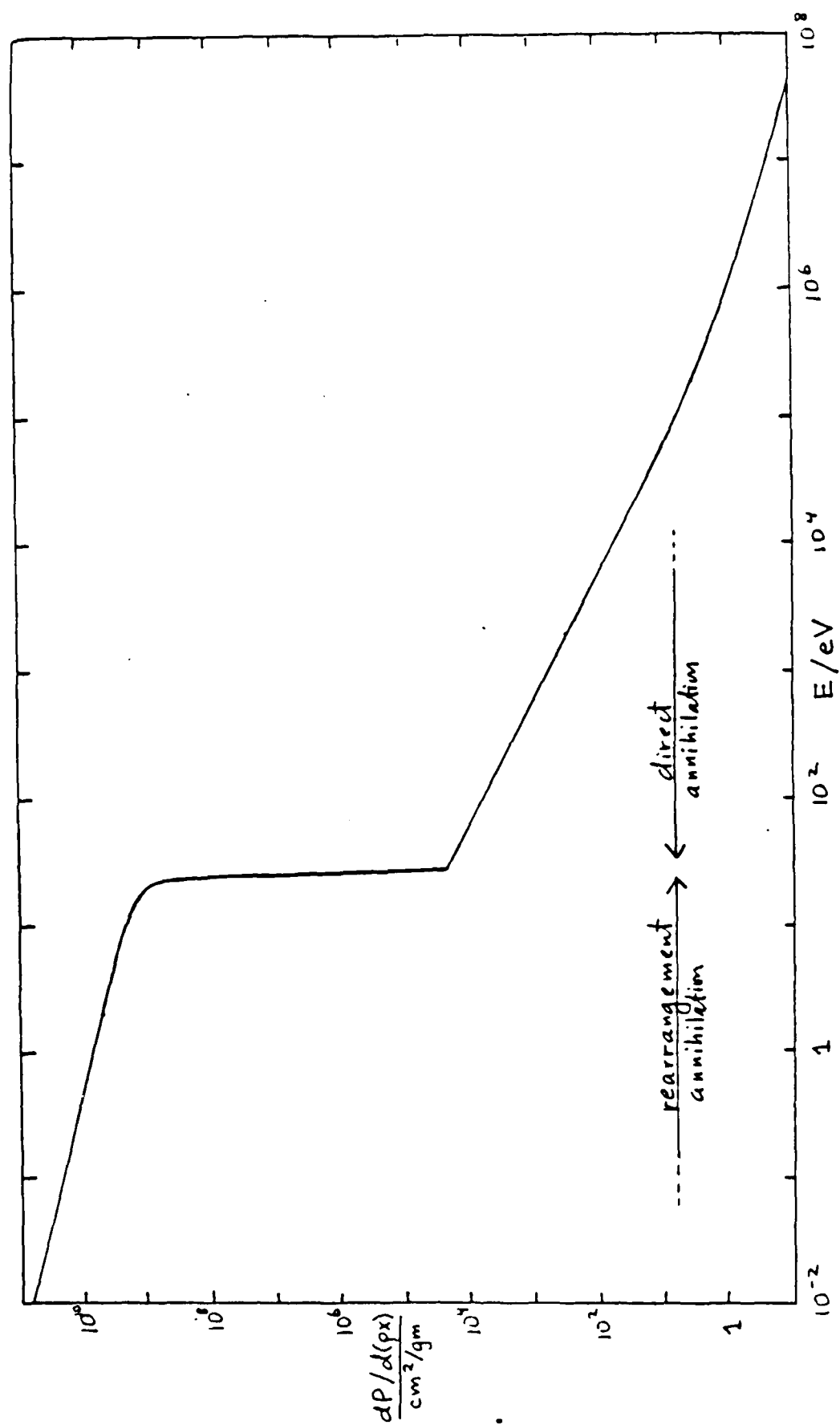


Figure 2. Probability of annihilation per gx for antiprotons in hydrogen.

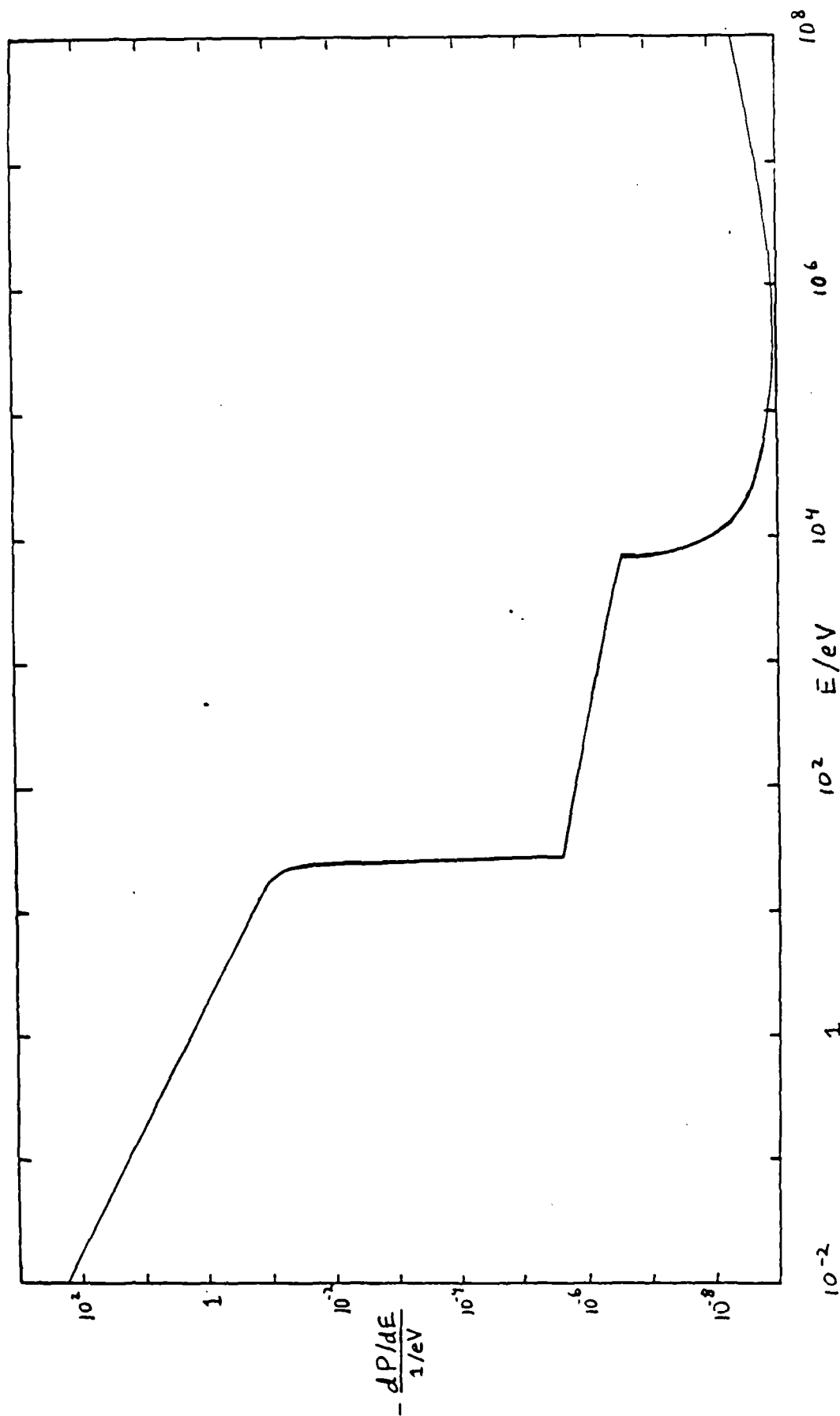


Figure 3. Antiproton annihilation probability in hydrogen per decrease in energy.

Table 1. Antiproton in Hydrogen.

E/eV Range	DP	D(px)/gm/cm ²	Dx/cm		
			gas core $g = 8.9 \times 10^{-4} \frac{gm}{cm^3}$	plasma core $g = 2.5 \times 10^{-8} \frac{gm}{cm^3}$	beam core $g = 6.5 \times 10^{-12} \frac{gm}{cm^3}$
$10^9 - 10^8$	7.20	305.	3.42×10^5	1.22×10^{10}	
$10^8 - 10^7$	0.309	3.68	4.13×10^3	1.47×10^8	
$10^7 - 10^6$	0.0155	0.0486	54.5	1.94×10^6	
$10^6 - 10^5$	1.19×10^{-3}	7.65×10^{-4}	0.858	3.06×10^4	
$10^5 - 10^4$	2.68×10^{-4}	1.43×10^{-5}	0.0160	572.	
$10^4 - 6300$	1.30×10^{-4}	1.36×10^{-6}	1.53×10^{-3}	54.5	
$6300 - 10^3$	2.12×10^{-3}	1.13×10^{-5}	1.26×10^{-2}	451.	
$10^3 - 10^2$	7.89×10^{-4}	6.33×10^{-7}	7.10×10^{-4}	25.3	
$10^2 - 27.2$	1.41×10^{-4}	1.38×10^{-8}	1.55×10^{-5}	0.552	
$27.2 - 10$	2.02	1.16×10^{-9}	1.31×10^{-6}	0.0466	
$10 - 1$	4.61	1.23×10^{-9}	1.38×10^{-6}	0.0491	
$1 - 0.1$	4.61	3.88×10^{-10}	4.35×10^{-7}	0.0155	
$0.1 - 0.0316$	2.30	7.85×10^{-4}	8.80×10^{-8}	0.00314	
$27.2 - 20$	0.637	4.22×10^{-10}			65.2
$20 - 15$	0.575	3.40×10^{-10}			52.6
$15 - 10$	0.811	4.03×10^{-10}			68.1
$10 - 3.16$	2.30	7.85×10^{-10}			121.
$3.16 - 1$	2.30	4.42×10^{-10}			68.3
$1 - 0.316$	2.30	2.48×10^{-10}			38.4
$0.316 - 0.1$	2.30	1.40×10^{-10}			21.6
$0.1 - 0.0316$	2.30	7.85×10^{-11}			11.8

Table 2. Antiproton in Heavy Element

E/eV Range	DP	D(x)/gm/cm ²	DX/cm
			$\rho = 0.164 \text{ gm/cm}^3$
$10^9 - 10^8$	192.	1020.	6200.
$10^8 - 10^7$	13.0	19.4	118.
$10^7 - 10^6$	1.03	0.405	2.47
$10^6 - 10^5$	0.119	9.56×10^{-3}	0.0583
$10^5 - 10^4$	0.0536	3.58×10^{-4}	2.18×10^{-3}
$10^4 - 6300.$	0.0346	4.54×10^{-5}	2.77×10^{-4}

Table 3. Issues of greater importance for five engine concepts. Numbers are subsections of Section E suggesting an experiment that can help resolve the issue. Parentheses indicate experiments providing relevant information. "n.e." means no relevant experiment is suggested.

Issue	Engine Type				
	solid core	solid/ plasma	gas core	plasma core	beam core
Localization of Annihilation, in antiproton energy loss hydrogen and annihilation rates heavy el. →			1,2	1,2	
Annihilation Energy Deposition:					
Location and Spectrum	3,4	3	3,5	3,5	
Effect of Mag. Field (orbital drift)			3,5	3,5	
Desirability of Fission				5	
Plasma Confinement and Stability				5	
High Isp, Thrust w/o damage to:					
Core	4				
Wall			5		
Magnet		(3)	5	5	(3)
Vehicle, Payload, Environment	4	(4)	5	5	(4,5)
Injection of large low energy → no. of antiprotons short pulse →		n.e.			n.e.

APPENDIX

1. Stopping Power Formulae

The nonrelativistic Bethe formula is used, but the log term is integrated over a distribution of ionization potentials rather than putting in shell corrections (it is important to have the formulae valid below the cutoff of the simple Bethe formula). This distribution is such that I , the average ionization potential (adjusted slightly relative to standard definitions to remove the slight effect of the shell corrections on the choice of its value), is the geometric mean of an $IMIN$ and an $IMAX$. $IMAX$ is the ionization potential of the innermost electrons, $IMAX = (N/2)^2 \cdot 24.5$ eV, where N is the atomic number of the stopping material. As with the standard definition, $I \approx N \cdot 13$ eV for most elements, and $IMIN \approx (I/N)^2 / (6.1 \text{ eV})$.

$$\text{For } E \geq c_2 IMAX, \quad \frac{dE/(e^2/a_0)}{dx/a_0} = \frac{-c_1 N}{E} \ln \frac{E}{c_2 I};$$

$$\text{For } c_2 IMIN \leq E \leq c_2 IMAX,$$

$$\frac{dE/(e^2/a_0)}{dx/a_0} = \frac{-c_1 N \left(\ln \frac{E}{c_2 IMIN} \right)^2}{2E \ln(IMAX/IMIN)};$$

$$\text{For } E \leq c_2 IMIN, \quad dE/dx = 0;$$

$$\text{where } c_1 = 2\pi \frac{m}{m_e} (a_0^3 n) \frac{e^2}{a_0}, \quad c_2 = \frac{1}{4} \frac{m}{m_e},$$

where e = the electronic charge

a_0 = the first Bohr radius

m = the antiproton mass

m_e = the electron mass

n = the number of atoms per volume

For hydrogen the above is not employed. In that case I used the ordinary Bethe formula (equivalent to the first equation above for dE/dx) with $I = 13.6$ eV. Some elements for which $I = N \cdot 13$ eV is off by more than 10% are He ($I/N=24.5$ eV), Be ($I/N=16$ eV), N ($I/N=11.3$ eV), and Ca ($I/N=11.3$ eV).

2. Energy Loss by Elastic Collisions with Atoms

Here I model the atom as one where all electrons are in a single hydrogenic orbital with ionization potential energy equal to the above I . The first order perturbation energy between an antiproton and such an atom is then fit with a cut-off coulomb potential energy,

$$V = -\frac{N}{r} + \frac{N}{r_c}, \quad V=0 \text{ for } r > r_c,$$

and then I calculate classical scattering in this potential energy. The result is that

$$\frac{dE/(e^2/a_0)}{dx/a_0} = 6\pi u (a_0^3 n) N \sqrt{I_H/I} f[A]$$

where

$$f[A] = \frac{A}{1-2A} \left(1 - 2 \frac{(1-A)^2}{1-2A} \ln \left| \frac{1}{A} - 1 \right| \right)$$

where

$$A = \frac{(1+u)N}{6} \sqrt{\frac{I}{I_H}} \frac{e^2/a_0}{E}$$

where

$$u = \frac{m}{M}, \quad I_H = e^2/2a_0 \text{ is the ionization energy of hydrogen}$$

and M is the mass of the atom.

3. Adiabatic Ionization

For the energy loss by adiabatic ionization above that which is automatically included in the elastic collision formula (the elastic effects of the adiabatic ionization interaction), I use for antiprotons in hydrogen,

$$\frac{dE}{d(\rho x)} = -2.94 \cdot 10^8 \frac{\text{eV cm}^2}{\text{gm}} \left[1 - \left(1 + \sqrt{\frac{31.73}{E/\text{eV} + 66.51}} \right)^{-3} \right] \left(1 + \frac{66.51 \text{ eV}}{E} \right)$$

The formula is obtained by modelling the wave function of the emitted electron as a time dependent gaussian in a time varying central field. That field, through various approximations and assumptions, represents the effect of the antiproton on the electron.

4. Rearrangement Energy Loss and Annihilation

Here it is assumed that the antiproton-atom potential energy is $-e^2 a / (2r^4)$, where a is the polarizability of the atom and r is the antiproton-atom separation, for r larger than a few Bohr radii and gradually changes to $-N/r$ for small r . Solving the classical orbits and assuming that whenever $r < R_c (=0.63 a_0$ for hydrogen) an electron is emitted and the antiproton is captured, gives the annihilation cross section equal to

$$\sigma_a = \pi \sqrt{\frac{2(1+\mu)e^2 a}{E}}$$

which gives

$$dP/d(\rho x) = 7.05 \cdot 10^9 \frac{\text{cm}^2 (\text{eV})^{1/2}}{\text{gm}} \sqrt{E}$$

for hydrogen where, as usual here, E is the antiproton kinetic energy in the lab frame.

Since these collisions are dominated by an inelastic process and because several angular momentum waves are involved, the elastic scattering cross section is equal to the annihilation cross section. Assuming hard sphere scattering,

$$\frac{dE}{dx} = -n \sigma_a * 2\mu E / (1+\mu)^2$$

I have estimated (last entry of reference 21) that for an antiproton on a hydrogen atom, the annihilation cross section should be multiplied by about 0.80 to account for the possibility of reversal of rearrangement. The corresponding factor for other than hydrogen has not been determined.

5. Direct Annihilation

Theoretical results for the electron-positron annihilation and experimental results for antineutron-proton annihilation [G. Smith, private communication, October 1987] suggest that the antiproton-proton annihilation cross section should have the form

$$\sigma_a = \text{const.} * \frac{c}{v}$$

where c is the speed of light and v is the relative velocity (=velocity in lab frame). Fitting this to data at around 20 Mev and above and adding the coulomb correction gives

$$\sigma_a \approx 0.19 \frac{\gamma}{1-e^{-\gamma}} \frac{c}{v} \pi r_o^2$$

with

$$\gamma = 2\pi\alpha c/v$$

where r_o is the classical electron radius and σ is the fine structure constant. For direct antiproton - hydrogen atom annihilation, the same formula is used since it appears that electron screening does not alter the coulomb correction for any energies of interest.

1 September 1987

ANTIMATTER SPACECRAFT PROPULSION EXPERIMENTS
WITH CURRENT ANTI-PROTON PRODUCTION RATES

John L. Callas

Jet Propulsion Laboratory

ABSTRACT

Facilities for the production of anti-protons at the rate of 10^{12} anti-protons per day could provide an opportunity for valuable experiments in antimatter propulsion research. Of critical importance to the viability of antimatter propulsion is the effective coupling of the antimatter annihilation energy to an expellant fluid to produce directed thrust. In addition, the possibility of induced secondary reactions (e.g., fusion, fission) might enhance energy production for propulsion by orders-of-magnitude, thereby reducing antimatter requirements for flight. This paper identifies the key research issues for antimatter spacecraft propulsion technology and outlines a series of antimatter propulsion experiments for their investigation utilizing current anti-proton production levels.

INTRODUCTION

For effective antimatter spacecraft propulsion (i.e., high thrust, high specific impulse), efficient use must be made of the antimatter annihilation energy. On average, anti-proton annihilations at rest produce three charged and two neutral pions [1]. Each neutral pion subsequently decays into two gamma rays. The average kinetic energies are 243 MeV and 196 MeV for the charged pions and gamma rays respectively [1]. The neutral particles result in a large fraction of the energy, from the matter-antimatter annihilation, to be lost directly without energy deposition to a working fluid/expellant. The remaining fraction of annihilation energy is distributed among energetic charged particles. The fraction of the annihilation energy distributed among charged particles as kinetic energy is estimated at approximately 0.38 [2]. These charged particles, because of their high kinetic energy, have to traverse large quantities of matter before transferring a significant fraction of their energy to the working fluid. Some current high specific impulse (Isp) designs harness only about 8% of the annihilation energy for propulsion [1].

Techniques must be developed to increase the coupling of the annihilation energy to an expellant fluid while maintaining high Isp in order for antimatter propulsion to be effective. These techniques might include the application of strong magnetic fields for charged particle confinement or the use of heavy elements for increased annihilation energy coupling. Heavy elements, such as tungsten or uranium, can be used either as solid core targets which absorb the annihilation energy and heat and expellant fluid or as the target/expellant material itself. In addition, the possibility of inducing secondary reactions (e.g., fusion, fission) to enhance energy production must be investigated.

This paper identifies the key research issues for an antimatter spacecraft propulsion system and describes an apparatus for antimatter propulsion research which makes use of quantities of antimatter consistent with current anti-proton production levels.

Anti-Proton Facilities

The Low-Energy Anti-proton Ring (LEAR) at CERN currently produces 10^{12} anti-protons per day [3]. Individual experiments receive 5×10^6 anti-protons per second with beam momentum continuously scannable from 100 MeV/c to 2 GeV/c and beam lifetime of up to 3 hours [3]. In addition, plans exist for a proposed U.S. low energy anti-proton facility at either Fermilab or Brookhaven National Laboratory (BNL) [4]. This facility is envisioned to produce 10^{14} to 10^{15} anti-protons per year with momenta less than 200 MeV/c. These facilities (either current or planned) could provide antimatter production levels sufficient to address some of the research issues associated with antimatter propulsion technology.

Research Issues

The primary research issue associated with the feasibility of an anti-matter propulsion system is the effective use of the annihilation energy. The physics which determines the effective energy coupling is primarily dependent on the cross sections and their respective branching ratios for annihilation, the spectra of the products from annihilation, and the energy deposition of these products in various materials.

Many experiments at LEAR have made initial determinations of the cross sections and branching ratios for anti-proton annihilation with protons and neutrons at various incident beam energies [5]. However, the cross sections and branching ratios for reactions of interest to propulsion have not been investigated and need to be determined. These reactions include the annihilation at rest of anti-protons with protons and various nuclei which compose the target/expellant.

The coupling of the annihilation energy to the working fluid is directly related to the energy deposition of the annihilation products. Development of effective energy coupling techniques requires the understanding of the energy deposition profiles for each of the annihilation products. The rate of energy deposition in a material of incident particles is proportional to the density of the material. Therefore, the energy deposition can be increased through the use of heavy elements in the working fluid or by increasing the distance spent in the working fluid by magnetic confinement.

Additional energy production might be produced by induced secondary reactions. Some possible concepts for these secondary reactions include fission, thermally induced fusion and muon catalyzed fusion [1]. If heavy elements are used to compose the expellant fluid, induced fission with a net energy release might be realized. In addition, the heavy fission products will couple energy more effectively to bulk of the working fluid [2].

Thermally induced fusion reactions involving D-T fuel require plasma temperatures of 10 KeV. For the small antimatter quantities envisioned for this experiment, it might be possible to observe a limited number of induced fusion reactions in the locality of the annihilation site in the target where temperatures might become sufficient. If fissile material is added to the plasma, a staged reaction of antimatter initiated fission followed by fission initiated fusion might proceed.

Each anti-proton annihilation produces approximately three muons from pion decay. If sufficient containment enables the muons to thermalize in the plasma, it is possible that muon catalyzed fusion might proceed. Current research indicated that this process requires temperatures of less than 1000 K [1]. Therefore, muon-catalyzed fusion could contribute only in low-temperature antimatter thruster applications unless a high temperature resonance is found.

ANTIMATTER PROPULSION EXPERIMENTAL APPARATUS

To understand and eventually influence the coupling of annihilation energy to directed thrust, it is necessary to investigate each of the physical factors involved. An apparatus for this purpose is described below and diagrammed in Figure 1. The apparatus consists of a beam degraded to lower the beam energy, a flexible target system to test various samples, a set of "magnetic confinement" magnets, a mass spectrometer for the identification of reaction fragments and two systems of particle detectors for particle tracking and identification.

Since current facilities (i.e., LEAR) produce anti-proton beams with momentum above 100 MeV/c, it is necessary to decelerate the anti-proton beam down to a momentum of a few keV/c in order to investigate annihilations near rest where propulsion systems will operate. This can be accomplished by the insertion of a beam degrader into the anti-proton beam upstream of the apparatus (as shown in Figure 1). The use of degrader will result in a substantial loss in beam flux. First results by experiments at LEAR indicate that a small fraction (10^{-5}) of the anti-protons survive the degrader with energy less than 3 keV/c [3]. However, this would still provide "cool" anti-proton flux levels sufficient for experimentation. Rates of 50 anti-protons per second can be reasonably expected. Other beam deceleration techniques employing radio-frequency quadrupoles (RFQ) are being developed at both CERN and Los Alamos which would preserve a significantly larger fraction of the incident anti-proton beam [6]. Such techniques might be realized for application to this experiment.

To investigate magnetic confinement techniques, a pair of superconducting solenoid magnets is positioned around the interaction region (target system). This magnet assembly is designed to produce a magnetic field of approximately 20 Teslas. Each magnet is intended to operate separately such that either a divergent magnetic "nozzle" configuration can be produced with one solenoid operating or a magnetic "bottle" configuration can be produced with both solenoids operating (see Figure 2). The magnetic "bottle" is intended to provide confinement of the energetic charged annihilation products (pions) and the expellant plasma until the annihilation products become thermalized (i.e., give up their energy to the plasma). Confinement times will depend on plasma density, magnetic field strength and annihilation product energies. The magnetic "nozzle" configuration will be tested for confinement characteristics which might adequately contain the charged annihilation products and permit their thermalization during the plasma thrust expansion.

A pair of concentric semiconductor vertex detector arrays is positioned within the inner solenoid magnets and encloses the target region. These detectors can monitor individual charged particles which emerge from the interaction region. These devices will provide the first level of tracking and identification of charged annihilation products. In addition, they will assess the effectiveness of the containment procedures by observing exiting charged particles during confinement studies with the inner solenoid magnets.

The next level of particle tracking and identification is a concentric array of particle detectors (with high degrading power) which encloses the target region. This array also includes an external solenoid magnet for particle momentum and charge sign determination. Fine energy resolution and tracking resolution are required for particle identification and trajectory determination. Many configurations on the design and arrangement of such a detector array have already been considered in numerous high energy physics experiments [7]. Experimental design details may be found in Reference 7. An existing configuration could be exploited for this experiment.

Critical to the determination of induced fission or fusion is the identification of heavy nuclei produced by the annihilation reaction or any secondary reactions. A mass spectrometer is configured near the interaction region for this task. This will permit the identification of heavy nuclei from secondary reactions and the extent of their production. In addition, it will identify the fragmentation of target nuclei from the annihilation reaction.

The target system will consist of several interchangeable devices which will permit the study of various target materials. A gas injector system will be used to investigate antimatter annihilations in hydrogen (i.e., with free protons). This injector will produce a proton density within the interaction region sufficient for complete anti-proton annihilation. It will be used primarily for cross section and annihilation spectra determinations. A device for positioning solid cores in the interaction region will be used to investigate solid core thrusters of tungsten and graphite. The size of the interaction region will be able to permit the positioning of solid cores up to 30 cm in diameter and 30 cm in length. Magnetic confinement studies utilizing the inner solenoid magnets will require a pellet/droplet injection system. The system will introduce into the interaction region sufficiently dense targets of hydrogen, deuterium-tritium, or heavy elements to serve as "inertial" targets for the antimatter beam. Precise metering and positioning of the pellets or droplets is critical.

SUMMARY

This antimatter propulsion apparatus represents a possible experimental opportunity which can be performed at existing or planned anti-proton facilities to investigate several critical issues relating to an effective antimatter propulsion system. Because its design and operation is similar to current experiments (e.g., LEAR experiments), existing high-energy particle detectors could be modified to this configuration, thereby reducing costs and short-cutting development and construction time. Antimatter propulsion experiments could conceivably be performed within the next five years.

ACKNOWLEDGMENTS

The author would like to acknowledge the invaluable contributions of Joel C. Sercel of the Jet Propulsion Laboratory, Steven D. Howe of Los Alamos National Laboratory, and David Morgan and Charles Orth of Lawrence Livermore National Laboratory.

REFERENCES

1. Howe, S. D. and Metzger, J. D., "Survey of Antiproton-Based Propulsion Concepts and Potential Impact on a Manned Mars Mission," LA-UR-87-2191.
2. Morgan, D. L., "Annihilations of Antiprotons in Heavy Nuclei," AFRPL TR-86-011.
3. Landau, R., "Future Physics at LEAR," CERN-EP/86-136.
4. Augenstein, B. W., Draft-Issues for October 1987 Rand Workshop, Rand Corp. (June 1987).
5. Kilian, K., Proc. 3rd LEAR Workshop on Physics With Antiprotons at LEAR in the ACOL Era, Tignes, 1985, Eds. Gastaldi, U., Kalpisch, R., Richard, J. M. and Tran Thanh Van, J. (Editions Frontieres, Gif-sur-Yvette, 1985).
6. Boltezar, E. et al., Proc. Linear Accelerator Conference, Santa Fe, 1981, Eds. Jameson, R. A. and Taylor, L. S. (LAMPF, Los Alamos, 1982), p. 302; Biscari, C. and Iazzourene, Proc. 3rd LEAR Workshop, Tignes, 1985, p. 115.
7. Gidal, G., Armstrong, B. and Rittenberg, A., "Major Detectors in Elementary Particle Physics," LBL-91 UC-34D (May 1985).

JPL ANTIMATTER INTERACTION EXPERIMENT

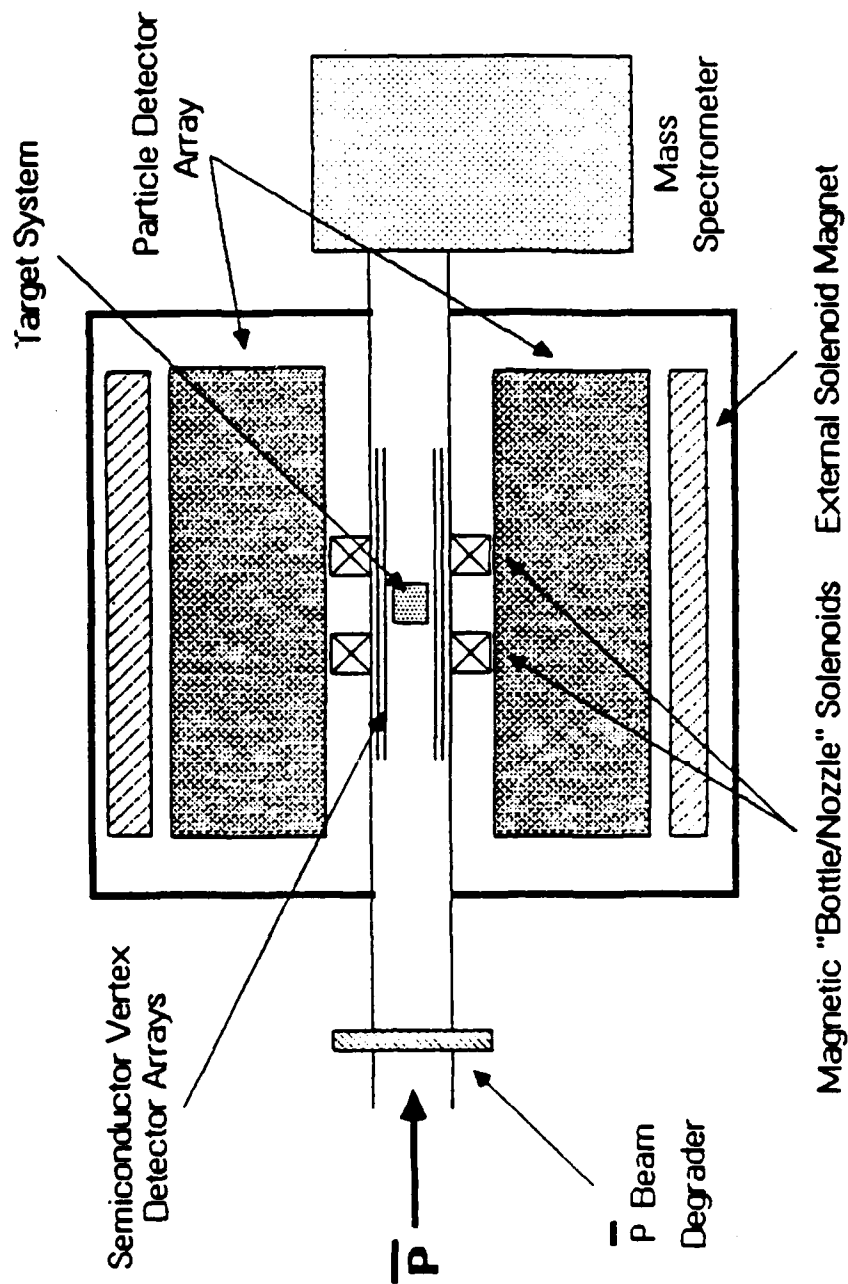


Figure 1

JPL MAGNETIC SOLENOID CONFIGURATIONS

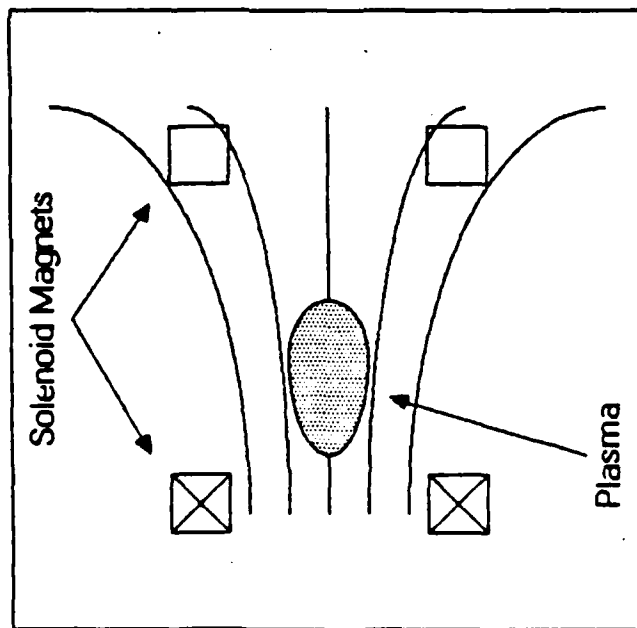
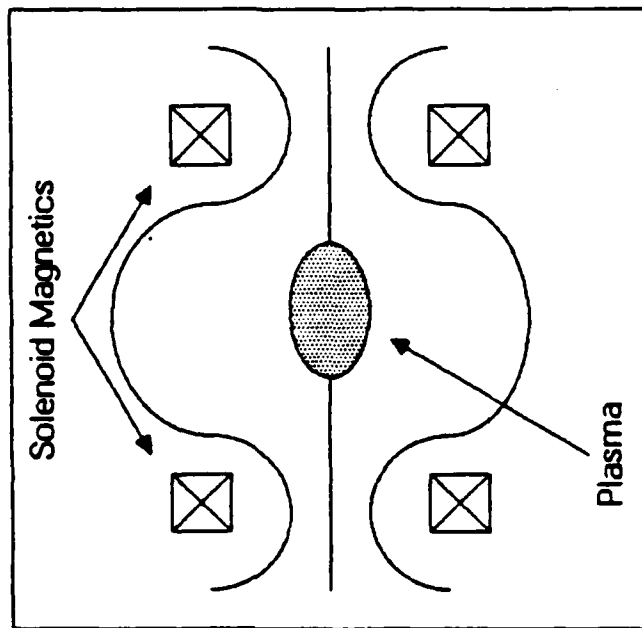


Figure 2

Energy Transfer in Antiproton Annihilation Rockets

B. N. Cassenti
United Technologies Research Center
East Hartford, Connecticut 06108

ABSTRACT

A review of previously published work on energy transfer in antiproton annihilation rockets is presented. The work includes energy spectra for the annihilation products, annihilation energy deposition in propellents, confinement of annihilation products by magnetic fields, efficiency of energy transfer to propellents, and optimization of propulsion systems based on mass annihilation. The calculations indicate that typically about one-third of the annihilation energy can be absorbed by a propellant.

INTRODUCTION

The first investigation of antimatter propulsion systems were carried out by Sanger¹ with an emphasis on the photon rocket. The photons would be created by combining equal numbers of electrons and positrons, but it was difficult to devise methods for directing the resulting gamma rays into a collimated beam. Storing the positrons also presented a difficult problem without a known realistic solution. A JPL report was the first technical investigation on proton-antiproton annihilation. At this time Morgan³ investigated atom-antiatom annihilation for propulsion and suggested further analyses. In Ref. 4, Forward: (1) summarized methods for generating and storing antiprotons, and (2) suggested using the pions resulting from the annihilation directly to provide thrust or using the pions to heat a propellant. Morgan⁵ then discussed systems for storing, extracting, and transporting antimatter and presented details for a specific engine design. In Ref. 6, Cassenti predicted the energy spectra for the products resulting from proton-antiproton annihilations in a vacuum and in liquid hydrogen. Additionally, in Ref. 6 an extension to relativistic speeds of a solution, first developed by Depprey,² was presented for minimizing the amount of

antimatter required. In 1985, Forward,⁷ completed an Air Force study on the feasibility of developing propulsion systems using milligrams of antimatter. In Ref. 8, Cassenti showed it may be possible to reduce the amount of antimatter required for specific missions by up to 35 percent by varying the propellant and antimatter flow rates. Cassenti⁹ also demonstrated that a rocket using a standard DeLaval nozzle could be used if the annihilation products are trapped in a combustion chamber by magnetic fields. In Ref. 10 a comparative cost study of antiproton and chemical propulsion systems showed that antiproton propulsion would always be more effective in missions requiring large changes in speed.

In 1985 Vulpetti¹¹ also presented a summary of all aspects of antiproton propulsion. In 1986, Morgan¹² examined the effect of atomic rearrangement on antiproton-hydrogen annihilation at extremely low energies. Vulpetti¹³⁻¹⁵ has since examined a thermal transfer engine, for missions to the nearer planets. The engine consists of high density, high atomic number cylindrical shells which absorb the energy of the annihilation products and transfer them to a propellant. Howe and Metzger¹⁶ have examined in detail in a NERVA type engine for use in Mars missions. In Ref. 17, there is some discussion that fusion (or fission) systems may be more cost effective than antiproton annihilation even for high speed missions. In Ref. 17 some of the disadvantages for annihilation engines were associated with radiation shielding, but more recent analyses¹⁸ have indicated that the radiation shielding may not be as difficult as first thought. In any case detailed comparisons of fission, fusion, and annihilation engines should be performed and designs developed so that optimum configurations can be developed.

This paper will concentrate on the transfer of the annihilation energy directly to a propellant and will not compare specific engine designs. The work in Refs. 6, 8 and 9 will be summarized in some detail.

Proton-Antiproton Annihilation^{6,9}

The proton-antiproton annihilation reaction⁶ proceeds through several steps. The initial reaction products consist of two or more mesons. Most of these mesons are pions, but some kaons are also produced. The reaction usually proceeds by

$$p + \bar{p} \rightarrow m\pi^0 + n\pi^+ + n\pi^- \quad (1)$$

where m and n are approximately 1.60. The charged pions (π^\pm) are not stable and decay into muons (μ) and neutrinos (ν) or anti-neutrinos ($\bar{\nu}$), while the neutral pions (π^0) decay into gamma rays (γ)

$$\pi^0 \rightarrow \gamma + \gamma \quad (2)$$

$$\pi^+ \rightarrow \mu^+ + \nu_\mu \quad (3)$$

$$\pi^- \rightarrow \mu^- + \bar{\nu}_\mu \quad (4)$$

The muons decay according to

$$\mu^- \rightarrow e^- + \nu_\mu + \bar{\nu}_e \quad (5)$$

$$\mu^+ \rightarrow e^+ + \bar{\nu}_\mu + \nu_e \quad (6)$$

The charged pions, the muons, and the electrons readily interact (e.g., by ionizing atoms) with matter. The neutral pions react only with nuclei. Their extremely short life means that the interaction must occur at the annihilation site. Since neutrinos have a negligible interaction with matter and the gamma rays are too energetic to readily interact with matter their energy is lost. The charged particles can be directed or trapped by magnetic fields. There are two possible methods for extracting thrust from the annihilation. The charged pions, muons, and electrons can be formed into a collimated exhaust or the charged particles can be used to heat propellant. Only the second of these will be considered here.

Annihilation Dynamics⁶

The initial products of the reaction will be mostly neutral and charged pions. The average energy of the pions is about 390 MeV taking 1.6 of each of

the three types of pions per reaction gives a total of 1870 MeV which is the total energy of the initial proton and antiproton. A fair fit to the distribution, See Fig. 1, occurs for

$$\frac{dN}{N_0 dE} = \left(\frac{2}{\bar{E} - E_0} \right) \left[\frac{2(E - E_0)}{\bar{E} - E_0} \right] e^{-\frac{2(E - E_0)}{\bar{E} - E_0}} \quad (7)$$

where N_0 is the total number of pions,

dN is the number of pions between energies E , and $E+dE$,

E_0 is the rest mass of the pion (139.6 MeV), and,

\bar{E} is the average pion energy (390 MeV)

The quantity $E - E_0$ is the kinetic energy.

The neutral pions will decay according to Eq. (2) while the charged pions will decay by Eqs. (3) and (4). Consider the decay of a neutral pion the energy of the resulting gamma rays can be determined from the conservation of momentum (and energy) as

$$E_1 = \frac{1}{2} E_\pi \left[1 + \cos \phi \sqrt{1 - \left(\frac{E_{0\pi}}{E_\pi} \right)^2} \right] \quad (8)$$

$$E_2 = \frac{1}{2} E_\pi \left[1 - \cos \phi \sqrt{1 - \left(\frac{E_{0\pi}}{E_\pi} \right)^2} \right] \quad (9)$$

where E_π is the energy of the neutral pion

$E_{0\pi}$ is the rest mass of the neutral pion (135 MeV),

E_1 and E_2 are the energies of the photons, and,

ϕ is the angle in the center of mass frame of reference between the direction of the pion's motion and the direction of the gamma ray emitted with energy E_1 .

The energy of the pion is random and governed by Eq. (7) and the angle ϕ is taken so that all directions are equally likely. The probability density is then

$$\frac{dN}{N_0 d\phi} = \frac{1}{2} \sin \phi \quad (10)$$

which represents the number of photons with energy E_1 between angle ϕ and $\phi+d\phi$.

The results indicate that the gamma ray energy distribution can be represented using Eq. (7) and an average energy of approximately 200 MeV. Although all directions need not be equally likely for all types of unstable particles, this assumption will be used to simplify all subsequent analyses.

A Monte Carlo simulation using Eqs. (8) through (10) was performed on 1000 neutral pions producing the energy distribution shown in Fig. 2. In a similar manner the energies of the muons and neutrinos resulting from the decay of the charged pions, Eqs. (3) and (4) can be determined from

$$E_\mu = \frac{E_\pi}{2} \left\{ 1 + \left(\frac{E_{0\mu}}{E_{0\pi}} \right)^2 + \left[1 - \left(\frac{E_{0\mu}}{E_{0\pi}} \right)^2 \right] \sqrt{1 - \left(\frac{E_{0\pi}}{E_\pi} \right)^2} \cos \phi \right\} \quad (11)$$

$$E_\nu = \frac{E_\pi}{2} \left[1 - \left(\frac{E_{0\mu}}{E_{0\pi}} \right)^2 \right] \left[1 - \sqrt{1 - \left(\frac{E_{0\pi}}{E_\pi} \right)^2} \cos \phi \right] \quad (12)$$

where E_μ is the energy of the muon,

E_ν is the energy of the neutrino,

$E_{0\mu}$ is the muon rest energy (105.7 MeV), and

$E_{0\pi}$ is the pion rest energy (139.6 MeV).

Figures 3 and 4 present the resulting muon and neutrino energies from the decay of the charged pions. Note that about 22 percent of the energy is lost to neutrinos.

The decay of the muons is considerably more complicated since its dominant decay mode is into three particles from Eqs. (5) and (6). For this case the conservation of momentum (and energy) is not sufficient to determine the energies of the resulting particles. The energies of the electrons, or positrons, can be approximated with a probability density given by⁶

$$\frac{dN}{N_0 dz} = 3z^2 (2-z) \quad (13)$$

where $z = P_e / P_{\max}$ is the normalized electron momentum

P_e is the electron momentum

$P_{\max} = 523.85 \text{ MeV/c}$.

In Eq. (13) all electron emission directions are assumed to be equally likely and the rest mass of the electron has been neglected with respect to the rest mass of the muon. Once the electron's energy, by a Monte Carlo analysis, is found in the coordinate system moving with the muon, the energy can be transformed to the laboratory reference frame. The energy of the two neutrinos emitted is now the difference between the muon and the electron energies. The energy of the electron is given by

$$E_e = \frac{E_\mu}{E_{0\mu}} \left[c P_{\max} z + \sqrt{1 - (E_{0\mu}/E_{0\mu})^2} \sqrt{(c P_{\max} z)^2 - E_{0e}^2} \cos \phi \right] \quad (14)$$

where z is chosen by Eq. (13), and

E_{0e} is the electron rest mass, which can be taken to be zero.

Figures 5 and 6 present the energy distributions for the electrons, or positrons, and for the total of the two neutrinos. The energy appears to be about equally divided between the three particles, with about 70 percent of the energy lost to the neutrinos.

Figures 1 through 6 imply that the efficiency in directing magnetically the annihilation products changes with the products directed. If 100 percent of the charged pions are ejected in a collimated beam the efficiency would be 67 percent. If, instead, 100 percent of the muons are ejected in a collimated beam, but the pions are not, the efficiency would be 52 percent. If only the electrons and positrons are directed the efficiency would be about 18 percent. Some positrons and electrons may be annihilated before they can be directed but nearly all of the positrons can be annihilated by injecting sufficient quantities of slowly moving matter. Then the efficiency would drop to about nine percent.

Instead of combining equal amounts of matter and antimatter, a small mass of antiprotons could be injected into a large mass of liquid hydrogen (LH_2). The resulting charged pions would then collide with the hydrogen atoms and transfer some of their energy to the hydrogen atoms. After the pions decay the muons would do the same and also the electrons or positrons. Figure 7 presents the energy lost per unit distance for pions and muons in LH_2 . The same Monte Carlo simulation, as previously performed, can now be modified to include the energy lost to the liquid hydrogen. The life of the particle can be chosen according to

$$\frac{dN}{N_0 dT} = \frac{1}{\bar{T}} e^{-T/\bar{T}} \quad (15)$$

where dN/N_0 is the fraction of particles decaying between T and $T+dT$

T is the time in the reference frame of the particle, and
 \bar{T} is the average life of the particle.

The energy lost per unit time in the particles reference frame is given by

$$\frac{dE}{dT} = c \sqrt{\left(\frac{E}{E_0}\right)^2 - 1} \frac{dE}{dx} \quad (16)$$

where dE/dx can be taken from Fig. 7.

The results of this simulation are presented in Figs. 8 through 12. Note that over half the pions stop and nearly all the muons should stop before decaying. The efficiency for heating the liquid hydrogen is now about 45 percent but no charged particles are being directed and a more conventional rocket results. If the positrons are not used the efficiency falls to 42 percent. An efficiency of 40 percent implies a specific impulse possibly as high as 2 million seconds.

The analysis can be extended to any density of hydrogen atoms by noting that probability for a collision is proportional to the atomic density and then performing the Monte Carlo simulations at different densities. In Fig. 13 the efficiency for conversion in an infinite combustion chamber can be accurately approximated by

$$\eta_{\infty} = \ln \left[\frac{1.592(n/n_0) + 0.007414}{n/n_0 + 0.006776} \right] \quad (17)$$

as shown in Fig. 13.

These results apply only to a hydrogen propellant; for propellents with heavier nuclei, more neutral pions can be absorbed in the nucleus, producing an increase in efficiency. Assuming that: 1) an infinite atomic weight nucleus would trap all of the neutral pions, 2) the gain in efficiency exponentially approaches the infinite atomic weight nucleus, and 3) annihilations with carbon nuclei are about 7 percent more efficient in producing charged particles can be attributed to the absorption of neutral pions, then the gain g for heavier nuclei is approximately

$$g = 1.5 - 0.5e^{-0.013(\bar{z}-1)} \quad (18)$$

where \bar{z} is the average atomic weight of the propellant per atom.

Liquid Propellant Engine⁹

Several factors must be considered in the design of an engine powered by proton-antiproton annihilation. The most important of these is the confinement of the exhaust products. Confining the annihilation products

(i.e., the charged pions, muons, and electrons) allows them to heat a propellant, such as hydrogen, significantly reducing the amount of antimatter required in a finite combustion chamber. These charged particles can be confined by surrounding the combustion chamber with current-carrying coils. The resulting magnetic field will cause the charged particles to move along a helical path. The particles can be reflected at the ends of the combustion chamber by greatly increasing the magnetic field intensity at the ends.

The analysis in Ref. 9 indicated that for the engine of Fig. 14 and Table 1 the fraction of pions trapped, $f_{T\pi}$ can be approximated by

$$f_{T\pi} = \sqrt{1 - \frac{B_{\min}}{B_{\max}}} - \beta e^{-\beta} \ln \left[\sqrt{\frac{B_{\max}}{B_{\min}}} + \sqrt{\frac{B_{\max}}{B_{\min}} - 1} \right] \quad (19)$$

where

$$\beta = \frac{q_c B_{\min} R_c}{\bar{E} - E_0} \gg 1 \quad (20)$$

where q is the electron charge
 c is speed of light
 R_c is the chamber radius
 \bar{E} is the average pion energy
 E_0 is the pion rest mass energy
 B_{\min} is the central magnetic field, and
 B_{\max} is the end magnetic field.

Assuming that the fractional energy retained is equal to the fraction of particles trapped and assuming that the same fraction of muons and electrons is lost, the efficiency of the magnetic confinement is

$$\eta_m = f_{T\pi}^3 \quad (21)$$

where the cube is present because there are three possible particle losses (pions, muons, and electrons).

The total efficiency η will be taken as the product of the factors in Eqs. (17), (18), and (21), or

$$\eta = \eta_m \eta_{\infty} g \quad (22)$$

The amount of matter to be annihilated, half of which is antimatter, can be calculated from (see Table 1)

$$m_a = \frac{C_p (T_c - T_{inj})}{\eta c^2} m_p \quad (23)$$

where c is the speed of light and η the fraction of the annihilation energy transferred to the propellant. Generally, η will depend on the magnetic field strengths, the chamber density, and the atomic weight of the individual atoms. The quantity η for the baseline mission is about 0.35, from Eq. (22) and Table 1.

The annihilated mass flow rate, from Eq. (24), is given by

$$\dot{m}_a = \frac{C_p (T_c - T_{inj})}{\eta c^2} \dot{m}_p \quad (24)$$

the energy added to the propellant is given by

$$\Delta E = m_a c^2 \quad (25)$$

The standard rocket nozzle equations can be used to determine the engine design parameters. The baseline mission (Fig. 14 and Table 1) is mission from low earth orbit to geostationary orbit and back to low earth orbit. The minimum speed change for such a mission is 5.5 km/s. For a payload of 10 metric tons, and an efficiency η of 0.35, the amount of mass to be annihilated is approximately 8 mg, of which 4 mg is antihydrogen nuclei. The rocket would use a 50 kG field in the central region of the combustion chamber and a 50 kG at the ends. A field of 500 kG is not within current practice. The current necessary to maintain at least a 50 kG intensity is approximately 90 kA for a chamber length of 2 m and 400 turns. If the superconductor Nb_3Sn is used for the 50 kG coil a 50 kA/cm² current density could be supported.¹⁵ Assuming a

specific gravity of 8.5, the coil weight is approximately 3.75 metric tons.¹⁶ Using high-strength aluminum (75 ksi) for the combustion chamber and assuming spherical ends, the combustion chamber mass is approximately 1.7 metric tons. Assuming the nozzle is 0.3 tons the total mass for the coils, nozzle, and combustion chamber is 5.75 tons. Assuming another 2.5 tons for support equipment (refrigeration, pumps, guidance and control systems, aeroassist system, and radiation shielding) leaves at least 1.5 tons for the payload out of the 10 ton final mass.

Parametric Study

Variations in several of the parameters with respect to the baseline design in Fig. 14 and Table 1 were examined to determine the amount of annihilated mass required and the combustion chamber temperatures that would result.

In Figs. 15 and 16, 10 propellents were considered and the results are shown. The amount of annihilated mass increased with molecular weight, approximately doubling at a molecular weight of 40 when compared to hydrogen. However, the combustion temperature increased exponentially with the molecular weight, making hydrogen the most desirable propellant, in spite of the fact that there is only one proton in the nucleus. Note that at the higher temperatures, a significant amount of ionization (and dissociation) may occur, invalidating the perfect gas law used in standard rocket engine analyses.

In Figs. 17 and 18 various mass ratios are presented and show a shallow minimum in the annihilated mass at a mass ratio (initial mass to final mass) of about 5. Note that even a mass ratio of 2 does not double the amount of mass that must be annihilated. On the other hand, at a mass ratio of 2 the combustion chamber temperature is rising rapidly, greatly increasing the technical problems related to cooling and structural reliability.

A significant technical challenge will be associated with the high magnetic field strengths. This may be alleviated with the application of advanced superconductors. Figures 19 and 20 present the annihilated mass

required for variations in the magnetic field configurations. A decrease to a 25 kG central field will double the amount of mass to be annihilated and the amount of annihilated mass at this point is rising steeply with decreasing strengths. The approximations made in developing the fraction of energy retained become inaccurate below a strength of about 50 kG (for a 2 m diameter chamber). From Fig. 20, the end field strength can probably be halved without a significant increase in annihilated mass.

Figures 21 and 22 show that there are no significant changes in the annihilated mass with changes in the chamber pressure and area ratio.

Only the baseline mission 5.5 km/s change in velocity has been considered to this point, but higher velocity missions were also examined and the results are presented for various final velocities (i.e., total velocity change) in Figs. 23 and 24. Note that as in the previous figures only a single parameter, including propellant, is varied from the baseline mission in Table 1. In Fig. 23 there is a significant increase in the annihilated mass at about 400 km/s. This corresponds to the decrease in efficiency at relative atomic hydrogen densities of 10^{-2} in Fig. 13. From Fig. 24 at 400 km/s the hydrogen is beginning to dissociate and therefore the ideal gas laws used in standard rocket analyses are becoming inaccurate.

Annihilated Mass Minimization⁸

From Fig. 17 it can be seen that there is a broad minimum in the amount of mass that needs to be annihilated (with respect to propellant used) to perform a mission. Minimizing the amount of annihilated mass (half of which is antimatter) will alleviate the problems associated with antimatter production and storing. For this purpose consider a combustion chamber which has injected into it matter to be annihilated, m_a , and propellant to be heated, m_p . Exhausted from the rocket will be heated (i.e., ionized) propellant and/or a collimated beam of photons of energy, E_λ . If the propellant is exhausted with a velocity βc relative to the rocket, where c is the speed of light, and if η represents the fraction of the annihilation energy which is used to heat the propellant, then energy balancing gives

$$\dot{m}_p c^2 + \eta \dot{m}_a c^2 = \dot{E}_\lambda + \frac{\dot{m}_p c^2}{\sqrt{1-\beta_e^2}} \quad (25)$$

where

$$(\dot{}) = \frac{d()}{d\tau}, \text{ and}$$

τ is the time in the reference frame of the rocket. The momentum flux out the exhaust is

$$\dot{p} = ma = \frac{\dot{m}_p \beta_e c}{\sqrt{1-\beta_e^2}} + \frac{\dot{E}_\lambda}{c} \quad (26)$$

These equations yield

$$\frac{dm_a}{d\theta} = -\frac{m}{\eta} \left[\frac{\cosh \theta_e - 1}{(1-\zeta)\sinh \theta_e + \zeta(\cosh \theta_e - 1)} \right] = -G_1(\theta_e)m \quad (27)$$

$$\frac{dm}{d\theta} = -\frac{m}{\eta} \left[\frac{\cosh \theta_e - 1 + \eta(1-\zeta)}{(1-\zeta)\sinh \theta_e + \zeta(\cosh \theta_e - 1)} \right] = -G_2(\theta_e)m \quad (28)$$

where $m = m_a + m_p + m_f$ is the current mass of the rocket

$\dot{E}_\lambda = \zeta \eta \dot{m}_a c^2$ defines the parameter ζ

$\beta = \tanh \theta$, $\beta_e = \tanh \theta_e$ are the rocket, and exhaust speeds (relative to the speed of light), and

$a = c\dot{\theta}$ defines the rate of change of the velocity parameter, θ , in terms of the acceleration, a .

$$m_a = 0 \text{ at } \theta = \theta_f \quad (29)$$

$$m = m_f \text{ at } \theta = \theta_f \quad (30)$$

where θ_f is the final value of the velocity parameter.

For constant exhaust velocities, $\beta_e c$, and small final velocities ($\theta_f \ll 1$), the minimum annihilated mass is⁹

$$\frac{m_{ai}}{m_f} = 0.7721 \frac{\beta_f^2}{\eta(1-\zeta)} \quad (31)$$

where $\beta_f = \theta_f$ the mass of propellant required is⁸

$$\frac{m_{pi}}{m_f} = 3.922 \quad \text{or} \quad (32)$$

$$\frac{m_i}{m_f} = 1 + \frac{m_{pi}}{m_f} = 4.922$$

as shown in Fig. 17.

For a variable exhaust velocity (i.e., variable propellant and annihilated mass flow rates) and small final velocities the equations can be solved via the Euler equation to yield⁸

$$\frac{m_{ai}}{m_f} = \frac{\theta_f^2}{2\eta(1-\zeta)} \frac{MR}{MR-1} \quad (33)$$

where

$$MR = \frac{m_i}{m_f} = 1 + \frac{m_{pi}}{m_f}$$

The minimum annihilated mass required is given by an infinite mass ratio or from Eq. (33)

$$\frac{m_{ai}}{m_f} = 0.5 \frac{\beta_f^2}{\eta(1-\zeta)} \quad (34)$$

which is 65 percent of the amount required for constant mass flow rates. The case for relativistic final speeds can be found in Ref. 8.

Conclusion

Recent calculations have shown that it may be possible to devise propulsion systems based on antiproton annihilation that may achieve efficiencies of 35 percent or more.

REFERENCES

1. Sanger, E., Zur Theorie der Photoneraketen, Ingenieur-Archiv V., 21, p. 213 (1963).
2. Papailou, D. D. (ed.), Frontiers in Propulsion Research, JPL Technical Memorandum 33-722 (1975).
3. Morgan, D. L., Investigation of Matter Antimatter Interaction for Possible Propulsion Applications. NASA CR-141356 (1974).
4. Forward, R. L., Antimatter Propulsion. Journal of the British Interplanetary Society, 35, p. 391 (1982).
5. Morgan, D. L., Concepts for the Design of an Antimatter Annihilation Rocket. Journal of the British Interplanetary Society, 35, p. 405 (1982).
6. Cassenti, B. N., Design Considerations for Relativistic Antimatter Rockets. Journal of the British Interplanetary Society, 35, p. 396 (1982).
7. Forward, R. L., Antiproton Annihilation Propulsion. Journal of Propulsion and Power, 1, p. 370 (1985).
8. Cassenti, B. N., Optimization of Relativistic Antimatter Rockets. Journal of the British Interplanetary Society, 37, p. 483 (1984).
9. Cassenti, B. N., Antimatter Propulsion for OTV Applications. Journal of Propulsion and Power, 1, p. 143 (1985).
10. Forward, R. L., B. N. Cassenti, and D. Miller, Cost Comparison of Chemical and Antihydrogen Propulsion Systems for High Delta-V Missions. AIAA 85-1455, AIAA/SAE/ASME/ASEE 21st Joint Propulsion Conference, Monterey, CA, July 8-10, 1985.
11. Vulpetti, G., Antimatter Propulsion for Space Exploration. IAA-85-491, 36th Congress of the International Astronautical Federation, Stockholm, Sweden, October 7-12, 1985.
12. Morgan, D. L., Antiproton-Hydrogen Atom Annihilation. AFRPL TR-86-019, Air Force Rocket Propulsion Laboratory (1986).
13. Vulpetti, G., A Further Analysis About the Liquid-Propellant Thermal Antimatter Engine Design Concept. Acta Astronautica, 15, p. 551 (1987).

14. Vulpetti, G. and E. Pieragostini, Matter-Antimatter Annihilation Engine Design Concept for Earth-Space Missions. IAF-86-178, 37th Congress of the International Astronautical Federation, Innsbruck, Austria, October 4-11, 1986.
15. Vulpetti, G., M. Pecchioli and Rosa Maria, Simultaneous Optimization of Payload Mass and Antimatter Energy for a Fully-Reusable Single-Stage-to-orbit Launch Vehicle. IAF-87-330 presented at the 38th Congress of the International Astronautical Federation, October 10-17, 1987.
16. Howe, S. D. and I. D. Metzger, Survey of Antiproton-Based Propulsion Concepts and Potential Impact on a Manned Mass Mission. LA-UR-87-2191, Los Alamos (1987). Submitted to the Journal of Propulsion and Power.
17. Borowski, S. K., A Comparison of Fusion/Antiproton Propulsion System for Interplanetary Travel. AIAA-87-1814, AIAA/SAE/ASME/ASEE 23rd Joint Propulsion Conference, San Diego, CA, June 29-July 2, 1987.
18. Cassenti, B. N., Radiation Shield Analysis for Antimatter Rockets. AIAA-87-1813, AIAA/SAE/ASME/ASEE 23rd Joint Propulsion Conference, San Diego, CA, June 29-July 2, 1987.

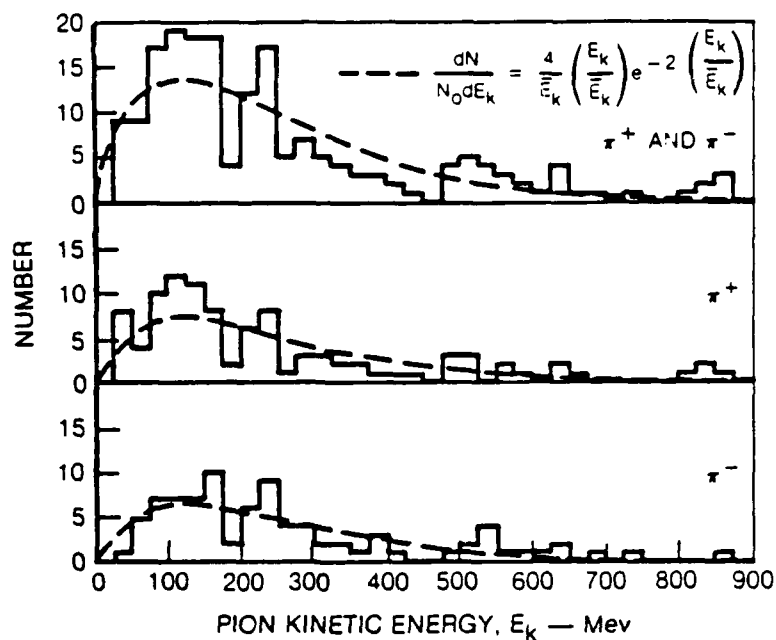


Figure 1 Charged pion energy distribution from low energy proton-antiproton reactions (from Ref. 6)

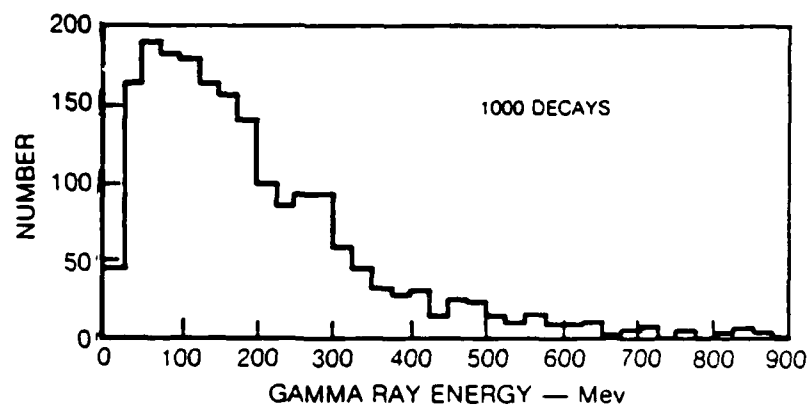


Figure 2 Neutral pion decay gamma ray energy distribution (from Ref. 6)

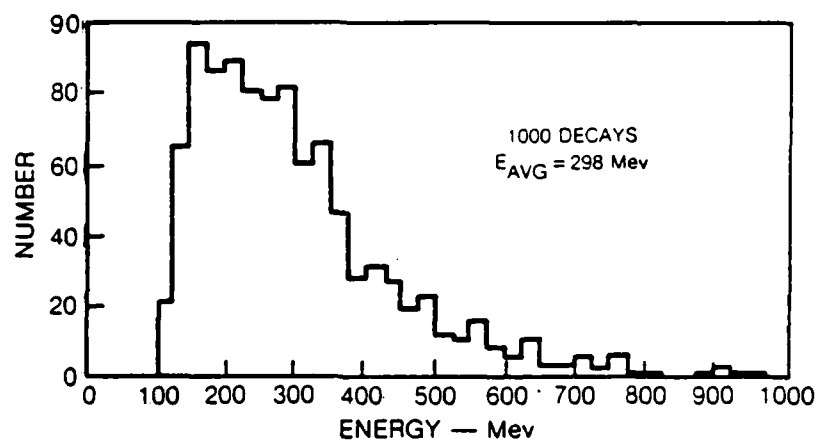


Figure 3 Muon energy distribution in vacuum from pion decay (from Ref. 6)

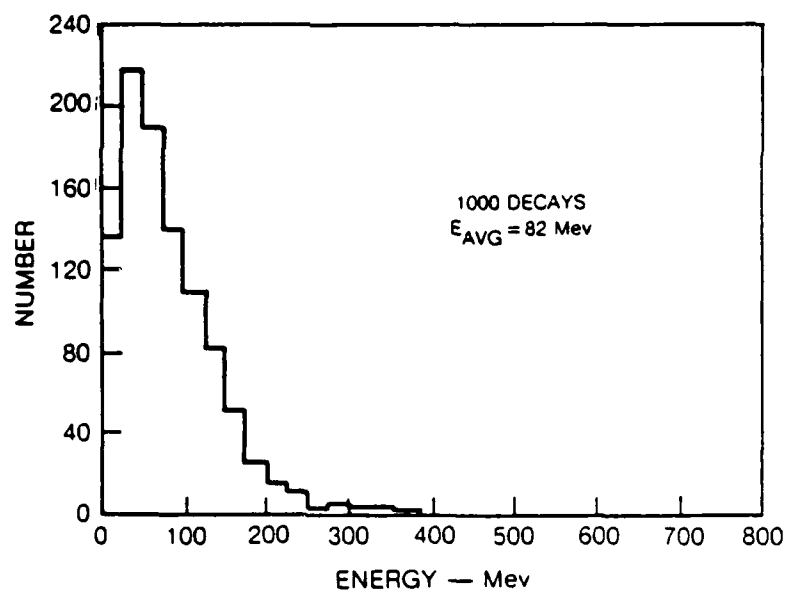


Figure 4 Neutrino energy distribution in vacuum from pion decay (from Ref. 6)

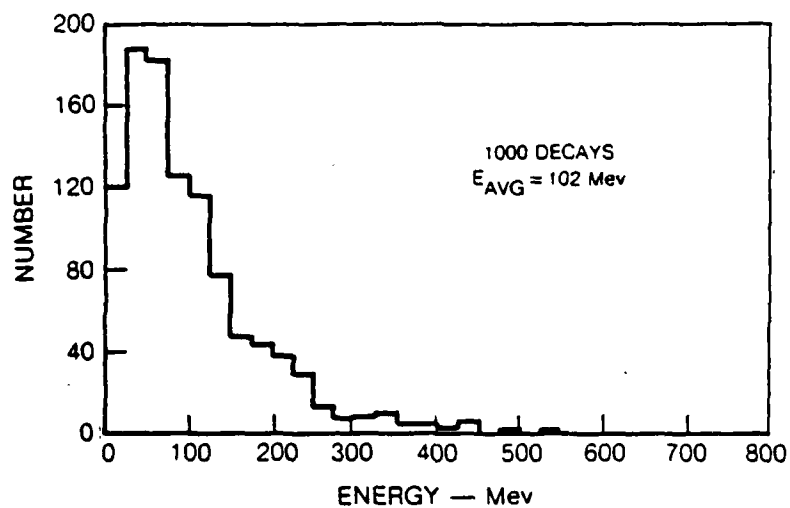


Figure 5 Electron energy distribution in vacuum from muon decay (from Ref. 6)

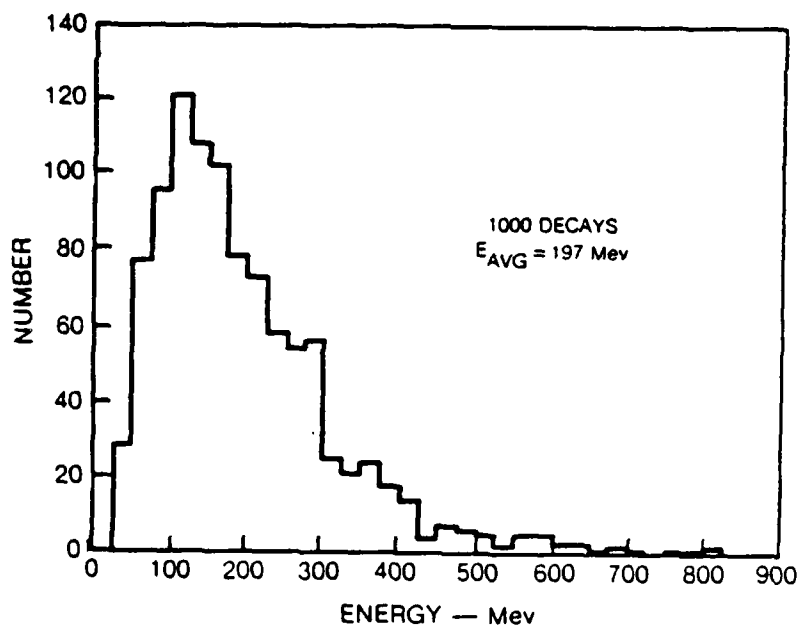


Figure 6 Total neutrino energy distribution in vacuum from muon decay (from Ref. 6)

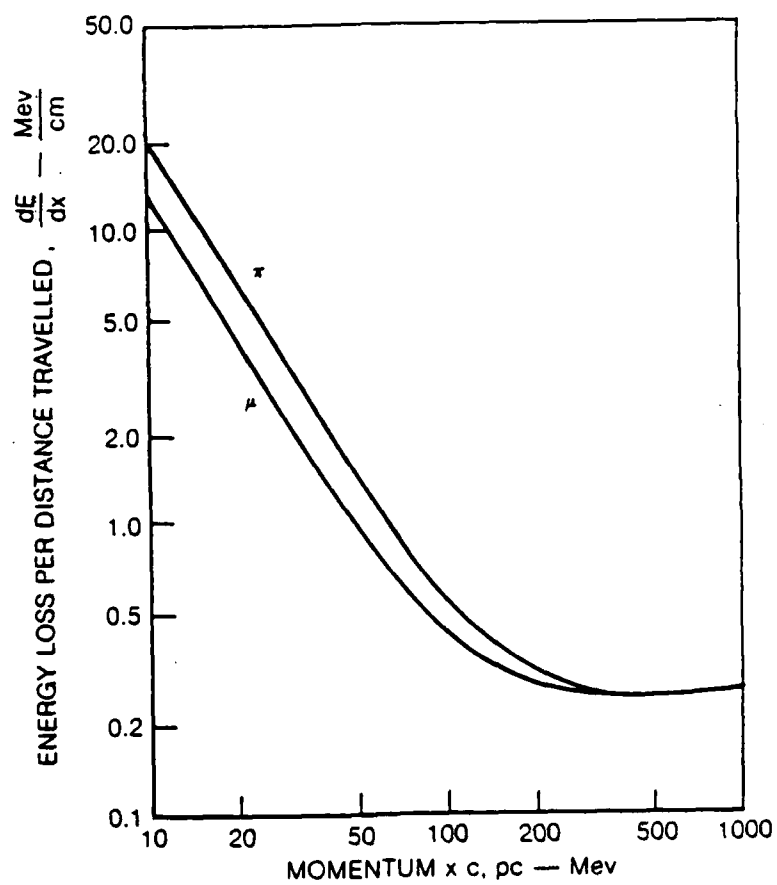


Figure 7 Energy loss in liquid hydrogen (from Ref. 6)

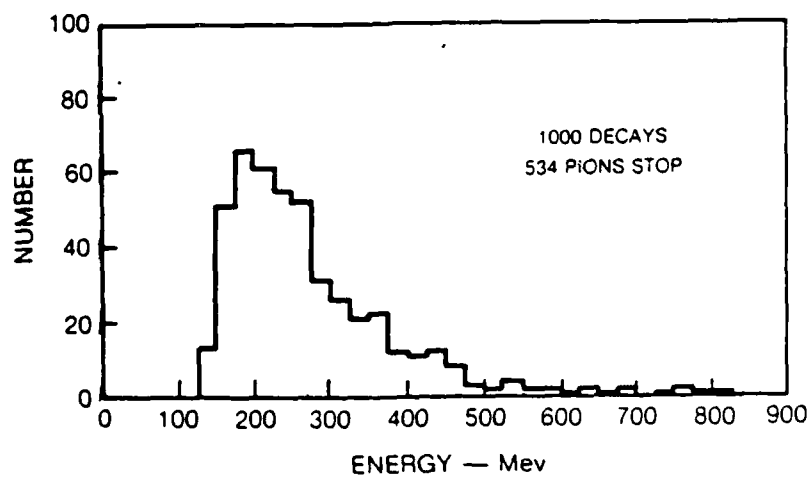


Figure 8 Final energy distribution of moving pions in liquid hydrogen (from Ref. 6)

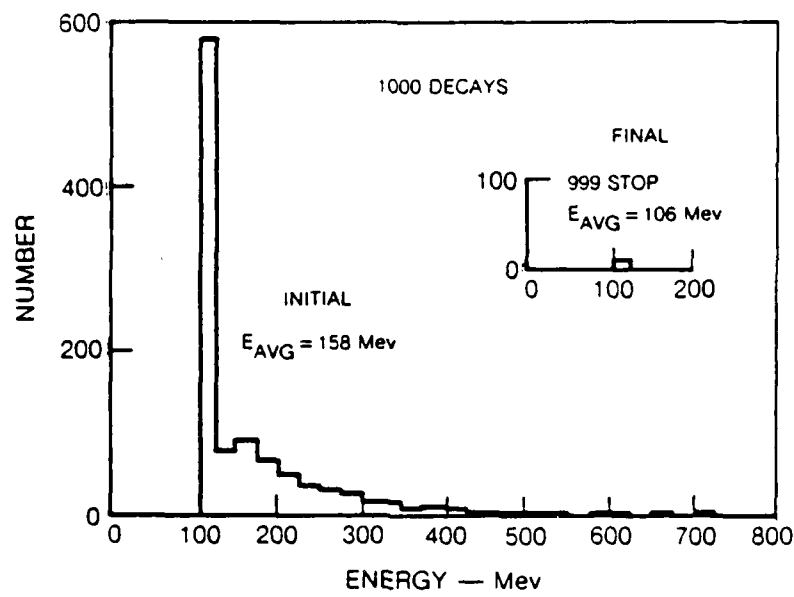


Figure 9 Muon energy distribution in liquid hydrogen from pion decay (from Ref. 6)

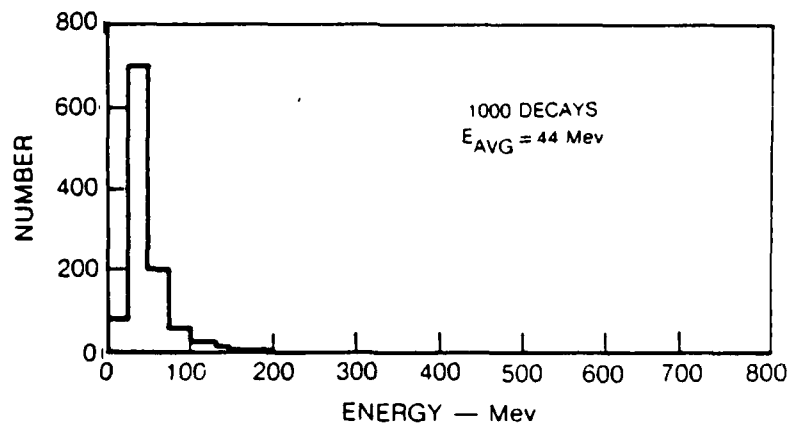


Figure 10 Neutrino energy distribution in liquid hydrogen from pion decay

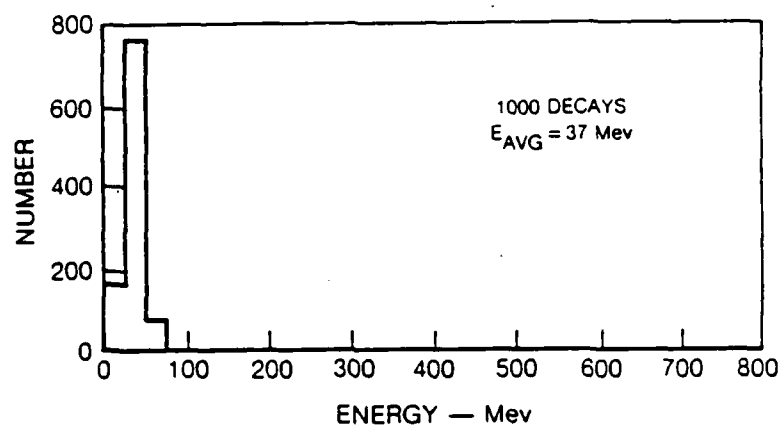


Figure 11 Electron energy distribution in liquid hydrogen from muon decay (from Ref. 6)

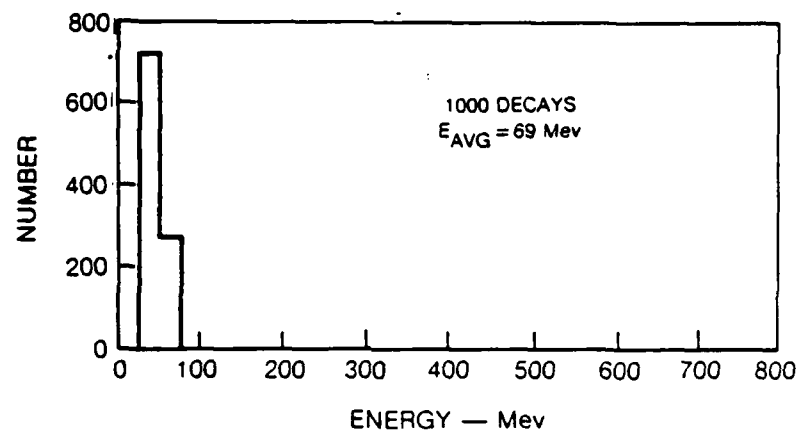


Figure 12 Total neutrino energy distribution in liquid hydrogen from muon decay (from Ref. 6)

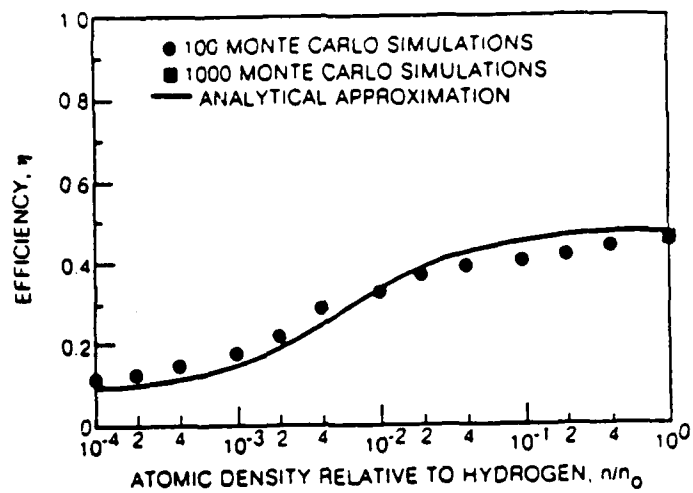


Figure 13 Efficiency for annihilation energy transfer in an infinite combustion chamber (from Ref. 9)

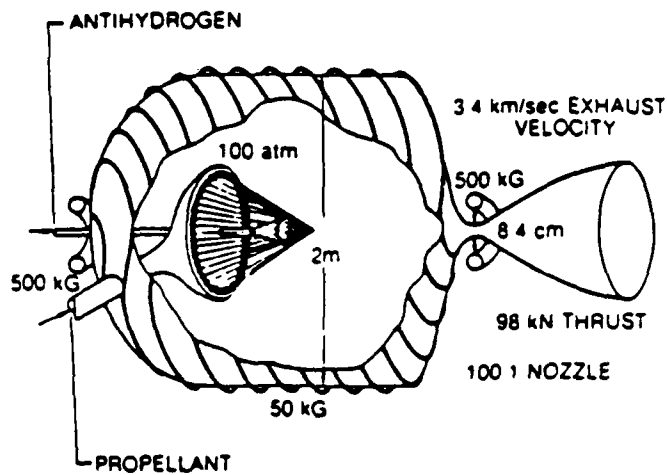


Figure 14 Schematic of OTV antimatter rocket (from Ref. 9)

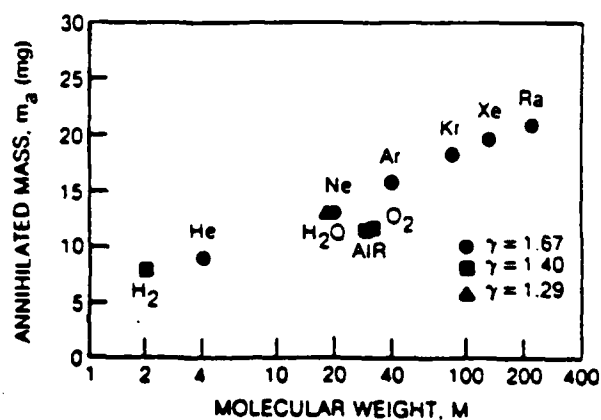


Figure 15 Annihilated mass for various propellents (from Ref. 9)

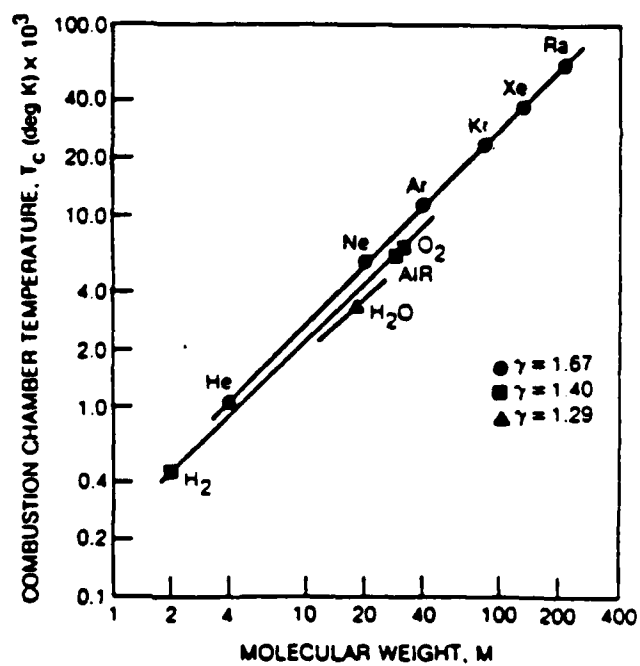


Figure 16 Combustion chamber temperature for various propellents (from Ref. 9)

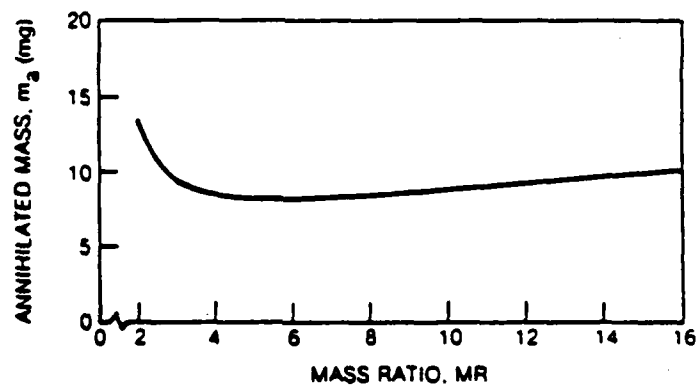


Figure 17 Annihilated mass for various ratios of initial mass to final mass (from Ref. 9)

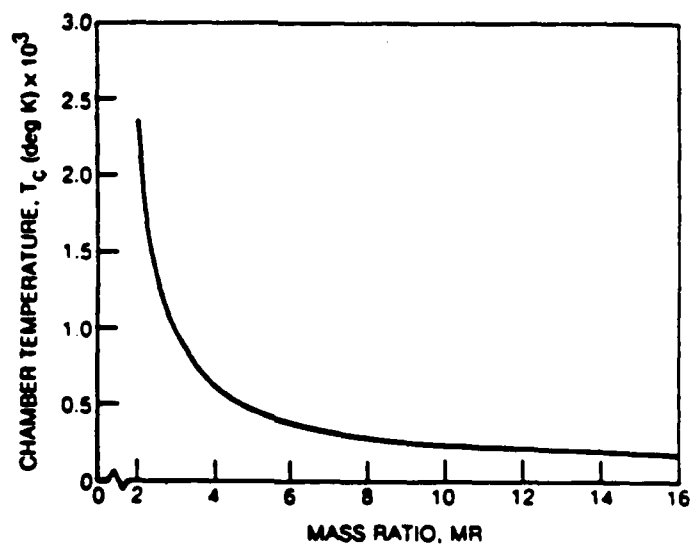


Figure 18 Combustion chamber temperature for various mass ratios (from Ref. 9)

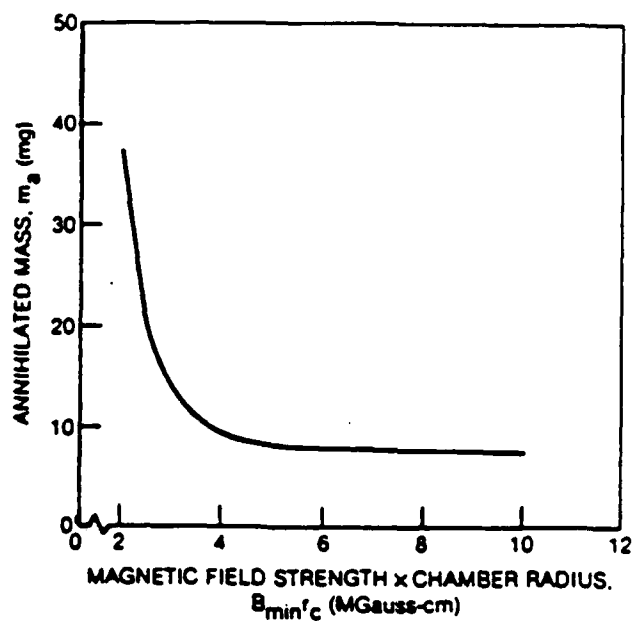


Figure 19 Annihilated mass for various central magnetic field strengths (from Ref. 9)

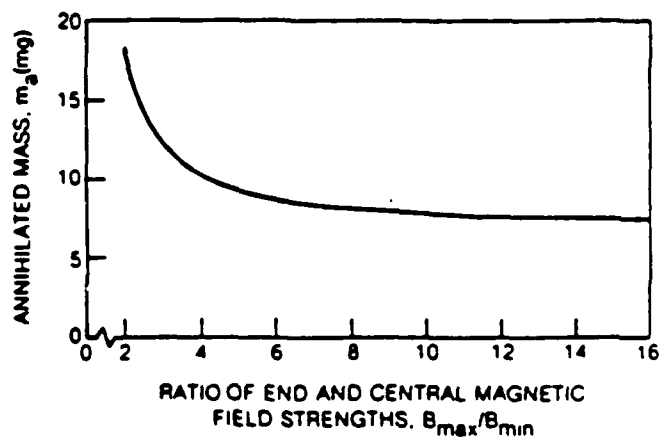


Figure 20 Annihilated mass for various end magnetic field strengths (from Ref. 9)

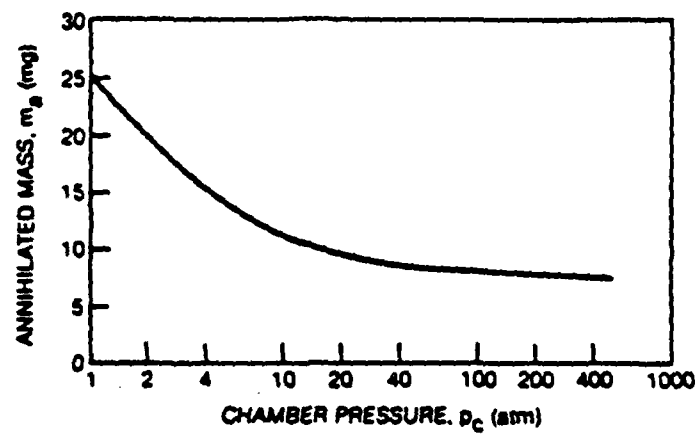


Figure 21 Annihilated mass for various chamber pressures (from Ref. 9)

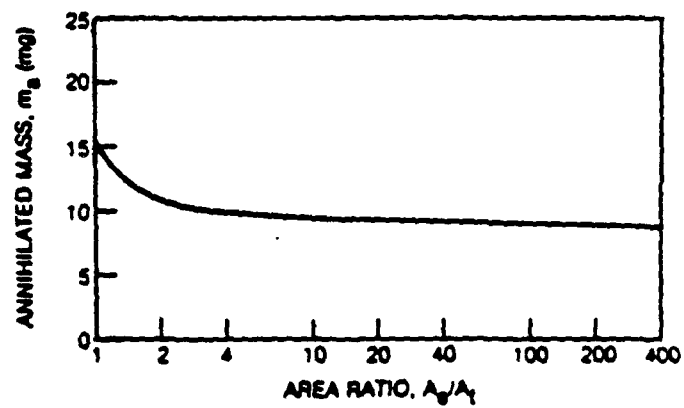


Figure 22 Annihilated mass for various area ratios (from Ref. 9)

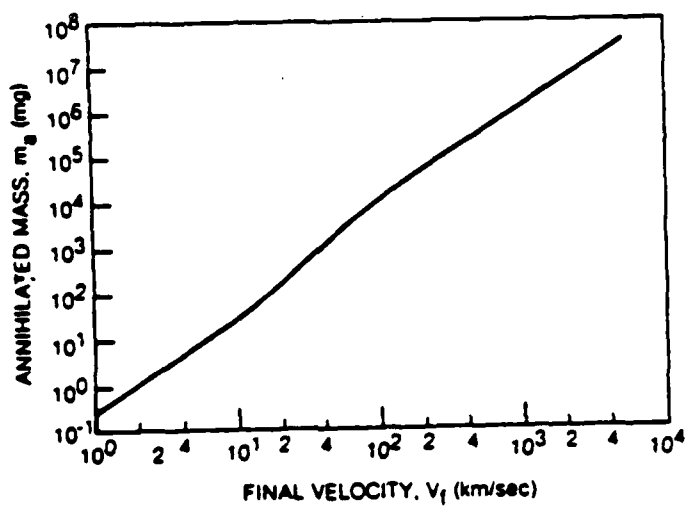


Figure 23 Annihilated mass for various final velocities (from Ref. 9)

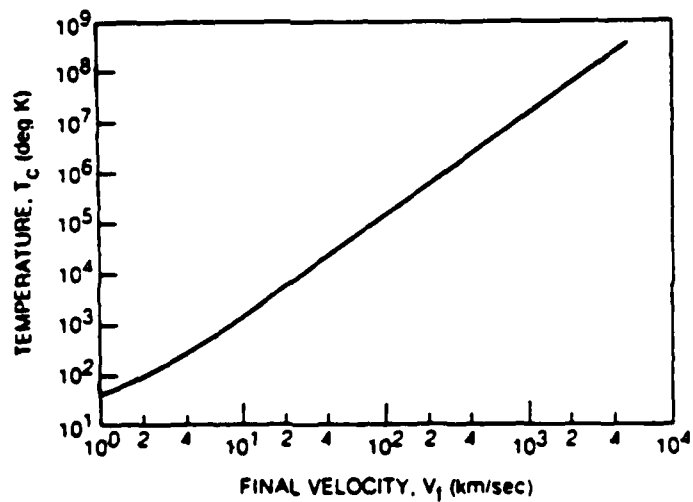


Figure 24 Combustion chamber temperature for various final velocities (from Ref. 9)

SOME THOUGHTS ON THE MUON-CATALYZED FUSION PROCESS FOR ANTIMATTER
PROPULSION AND FOR THE PRODUCTION OF HIGH A MASS NUMBERS ANTINUCLEI

Hiroshi Takahashi
Brookhaven National Laboratory
Upton, New York 11973

Prepared for the Rand Workshop on Antiproton Science and Technology
October 6-9, 1987

ABSTRACT

The muon-catalyzed fusion process has a very valuable role for antiproton science and technology. Several schemes of propulsion energy enhancement of the antiproton-fueled propulsion using the muon-catalyzed fusion are discussed. Production of high A mass antinuclei by the muon-catalyzed fusion using the clustered antihydrogen molecule and quark-gluon plasma formation by annihilation of the produced high A antimatter with regular nuclei are discussed.

INTRODUCTION

The possibility of using a muon-catalyzed fusion for energy production has been resurrected 30 years after the first discovery of muon-catalyzed fusion (1-3). The molecular formation of dtu is via a resonance mechanism, and this rate is faster than the rate which was expected from the early theoretical calculation. After this resonance formation mechanism was discovered (4), experimental observations were carried out. More than 160 fusions per muon have been observed by Jones' group at Los Alamos (5,6) and Breunlich's group at SIN (7). This value of 160 is much higher than the previously theoretically estimated maximum value of 100, and an extensive theoretical calculation is being carried out to explain this high fusion rate. The muon-catalyzed fusion process provides a very valuable approach for antiproton science and technology. In this paper, the use of muon-catalyzed fusion for a spacecraft propulsion energy source and for the production of high A antinuclei will be discussed.

The use of the muon-catalyzed fusion for spacecraft propulsion has been discussed by Subotowich (8). In his scheme, the muon would be produced by decay of mesons created by using a high-energy particle accelerator. The proton accelerator would have to be in the spacecraft, making the payload very high. If the spacecraft uses antiprotons as fuel, pions can be generated from the antiproton annihilation process, eliminating the heavy proton accelerator.

When antiprotons are annihilated in low-energy collisions with protons, pions and Kaons, etc., are produced with high-energy momentum (9). If these charged, high velocity particles interact with a magnetic field in a reactor engine, the short interaction makes the thrust very small. Furthermore, γ -rays produced from short-lived π^0 decay do not interact with the magnetic field, and their energy is lost unless the γ -rays are converted to a charged particle by some nuclear reaction. To get much higher thrust, it has been proposed to annihilate antiprotons with high A nuclei (9,10).

The annihilation of an antiproton with a proton produces π^- mesons. A portion of the π^- mesons collide with nuclei, producing charged particles. The remaining π^- mesons decay into μ^- and ν_μ . If the low-energy μ^- meson

is used for muon-catalyzed fusion of dt, then $160 \times 17.6 \text{ MeV} = 2.8 \text{ GeV}$ energy can be obtained from this process. Of the 17 MeV reaction energy, 14 MeV is carried by a fast neutron. Conversion of this neutron energy to charged particle energy is desirable, and the neutron can be used to generate new tritium by absorption in Li. The dt fusion also produces a 3.4 MeV α particle. We thus get an energy release of $160 \times 3.4 \text{ MeV} = 0.55 \text{ GeV}$ as charged particles, which is substantial. There is the possibility of increasing the number of fusions per muon above 160. However, this requires a high-density dt mixture. When the mixture density is reduced, the reaction rate for a muon-catalyzed fusion cycle becomes small. In particular, the dt₂ molecule formation rate becomes a bottleneck for muon-catalyzed fusion.

A high density mixture is not practical for spacecraft from a technical and economic point of view. The high-density mixture requires a small reaction zone and large inventory cost for tritium. In the following section, approaches for reducing the equivalent mixture density but not reducing the molecular formation rate are discussed.

The production of high A antinuclei is important for antimatter technology: 1) with high A antimatter condensation sites, anti-hydrogen molecules could then be readily generated with no need for wall catalysis, and 2) metallic antimatter such as anti Li (11) could be easily stored in the strong magnetic field created by a superconductor. Muon-catalyzed fusion process is very suitable for producing high A antinuclei, because the process occurs at very low temperatures. This approach is discussed in the following section.

Heterogeneous Mixture (12) (Liquid Droplet, Ice Form)

As discussed above, the number of muon-catalyzed fusions per muon is proportional to the density of the dt mixture. However, when the dt mixture is in the form of liquid droplets or crushed ice, then muon-catalyzed fusions can take place inside a small volume since the mean free path for the various reaction processes is very small, as shown in Table I. Once the muon is stopped in the droplet, it stays until muon-catalyzed fusion occurs. When fusion occurs, the muon gets some energy from this fusion

reaction. If this energy is high, the muon leaves the droplet and travels through droplets, until it is captured by another droplet and catalyzes dt fusion inside. Since this travel time between droplets consumes some of its lifetime, the number density of the droplet can be determined from the study of the energy which the muon gets from dt fusion.

In the case of the power plant (13), this liquid droplet scheme or crushed ice requires refrigeration after going through the turbine and the cost of the refrigeration is quite high and not economical. But in the case of spacecraft propulsion, the heated dt mixture is exhausted from the engine.

Laser Enhancement of dtu Molecular Formation (14)

The most important reaction step for shortening the dtu fusion cycle is dtu molecular formation. As shown in the Table 1, the reaction processes of the capture by deuterons or μ transfer from d to t and ut slowing down, are much faster than the dtu molecular formation process. The formation of dtu molecules is a resonance process, and energy conservation requirements have to be satisfied. For low-density targets, energy conservation is satisfied by exciting from the ground D-D molecular state to the excited $((dtu-d)-2e)$ molecular state, and the reaction rate is determined by this excitation process. For high density targets, energy conservation can be satisfied by giving the excess energy to surrounding molecules (third body). The D_2 molecule participating in dtu molecular formation collides with the surrounding molecule, reducing the required energy of excitation of the $((dtu-d)-2e)$ molecule and increasing the formation rate. In a thin gas target, the probability of collision between D_2 molecules is small, reducing the formation rate. But if we irradiate the dt mixture, with a high intensity laser, energy can be transferred to this third body photons, satisfying energy conservation and increasing dtu molecular formation rate.

Figure 1 shows the effect of the laser enhancement of dtu molecular formation. This analysis indicates that to enhance 100 times faster than the nonlaser irradiating dt, mixture can be done with a laser intensity of $10^{11} \sim 10^{12}$ w/cm² and frequencies of $\nu = 11.4$ and 11.9×10^{13} rad/sec.

Besides using a laser to enhance dtu molecular formation rate, a high-intensity x-ray laser could be used to reactivate muons captured by the alpha products from fusion (12,15). A coherent laser can ionize muons captured in the α -u ground state, even if the laser has lower energy than the ionization energy, by coherent multiphoton excitation. Due to the small muonic Bohr radius, high laser intensity is probably required to ionize the muon.

The cross section of direct multiphoton ionization of muon from the α u ground state is expressed as:

$$\sigma(\omega, \Omega) = \frac{8^2 \pi k^3 C}{\omega_0^2} \sum_{n=1}^{\infty} \frac{J_n^2 (eAk/mc\omega_0)(a/z)^3}{[1 + (a/z)^2 (k - nk_0)^2]} \quad (1)$$

where ω_0 , k_0 are the angular frequencies and wave vectors, a is the muonic Bohr radius, k is the emitting muon wave vector, J_n is the n th order Bessel function, A is the vector potential, and z is the atomic number of the nucleus. In deriving Eq. (1) the laser field is treated as a classical field due to its high coherence. Figure 1 shows the cross section for various vector potential A as functions of the laser frequency.

To derive Eq. (1) it was assumed that there is no excited states between ground state and the continuous state. However, in fact there are many excited states in this interval. By tuning frequency, we can use the resonance process for the ionization. The ionization cross section becomes very high at certain laser frequencies, which reduces substantially the required laser intensity for muons ionization.

Use of the Clustered Hydrogen

When the hydrogen molecule is charged, hydrogen clusters become stable with shallow potential depth. Many configurations of clustered hydrogen exist. Such clusters are very important for creating antihydrogen molecules from antihydrogen atoms by a combination process that does not involve a wall (16). Hydrogen clusters could be suitable for dtu molecule formation. As discussed before, the third body is very important for a fast formation

rate. Hydrogen atoms in the cluster play the role of the third body in the same way as surrounding molecules in a high-density target. This, even without having a high density target, fast formation rate might be achieved. The reaction rate formula used for the hydrogen molecule (17,18,19) can be extended to estimate the rate of the resonance formation of dtu molecules using hydrogen clusters, which are composed with N nuclei, as follows:

$$\lambda = \sigma v N_0 \quad (2)$$

$$v d\sigma = 2\pi h^{-1} |T_{fi}|^2 \delta(E_f - E_i) Y(\epsilon, \epsilon_T) d\epsilon \quad (3)$$

The matrix element of the transition

$$|T_{fi}|^2 = \left| \int \prod_j^{N+1} d\vec{r}_j d\vec{r}_u \bar{\Psi}_f(\vec{r}_u, \vec{r}_1 \dots \vec{r}_{N+1}) H_{int} \bar{\Psi}_i(\vec{r}_u, \vec{r}_1, \dots, \vec{r}_{N+1}) \right|^2 \quad (4)$$

$$H_{int} = \sum_{j=3}^{N+1} \hat{d}_{oj} \frac{\partial U_j(\rho_j)}{\partial \rho_j} \quad (5)$$

$$\vec{\rho}_j = \vec{r}_j - \vec{r}_a$$

where r_a is the center of mass coordinate of dtu($\vec{r}_2, \vec{r}_1, \vec{r}_u$) and $\bar{\Psi}_i(\vec{r}_u, \vec{r}_1 \dots \vec{r}_{N+1}) + \bar{\Psi}_f(\vec{r}_u, \vec{r}_1 \dots \vec{r}_{N+1})$ are respectively the initial wave and final functions.

Shock Wave Application

In order to increase the density of gas target, shock wave could be applied using the dtu fusion process itself, or by some other means like laser irradiation. In the shock wave, the following mass, momentum and energy conservation condition have to be satisfied (20,21).

$$\rho/\rho_0 = D/(D-u)$$

$$P - P_0 = \rho_0 D u \quad (6)$$

$$[(E - E_0) + 1/2 u^2] \rho_0 D = P_u$$

where ρ is density, P is pressure, u is particle velocity, D is shock velocity and E is specific internal energy, and the subscript o refers to the initial unshocked state.

If shock velocity is close to the particle velocity, then the mixture density ρ is substantially increased, and 3rd body collisions enhance the rate of dtu molecule formation. On the other hand, the limiting density ratio across the shock wave is a function of specific heat ratio (γ) as

$$\frac{\rho}{\rho_o} = \frac{\gamma + 1}{\gamma - 1} \quad (7)$$

The limiting density ratio for diatomic gas $\gamma = 7/5$ (assuming that the vibrational modes has not been excited) becomes 6. If on the other hand full vibrational excitation is assumed, then $\gamma = 9/7$ and the density ratio becomes 8. In order to create much high density ratios, many successive shock waves could be applied with good spatial and temporal tailoring of the shock waves, in the same way as inertial confinement fusion.

Another way to increase this limiting ratio is use of the clustered molecule discussed above. This cluster molecule has γ which is close to 1, making the limiting ratio very high. However, applying shock waves to the target increases gas temperature dissociating the clustered hydrogen. Detailed calculations that takes into account the shock wave propagation and the change of state, are required to apply this shock wave method to muon catalyzed fusion.

Focused μ^- Beam and Clustered H_2 Ice or Liquid Droplet

If high intensity μ^- focused beams can be realized, such beams could be focused into the H_2 ice or liquid droplets with dimensions on the order of 1 cm dia. This would then cause a large number of fusions in such droplets. If the temperature of droplet reached $\sim 1000^\circ\text{C}$, the velocities of D_2 and T_2 molecules become 1.9×10^5 cm/sec and 1.56×10^5 cm/sec, respectively. During the muon lifetime of 2.2×10^{-6} sec, these molecules move at most only 0.3 ~ 0.4 cm, which is less than the droplet radius. Since this fusion process does not require high temperature fusion, the high density can be achieved by irradiating muons on the surface of the liquid droplet and ice

similar to the initial fusion concept. It is interesting to calculate the hydrodynamic behavior of this droplet under the pulsed irradiation of muon flux.

Anti-High A Nuclei Production by Muon Catalyzed Fusion

R. Forward (22) suggests using muon-catalyzed fusion to make \bar{d} or \bar{t} nuclei from \bar{P} using the μ^+ which is the anti particle of μ^- . The μ^+ catalyzed fusion appears attractive for making antinuclei. Production of antinuclei by accelerator methods does not appear practical. First, the amount of antiproton produced by using high current high energy accelerator is very small, so that the production of large amount of \bar{H}_2 which could be needed for a large target size, is not practical. Second, antinuclei production using high energy \bar{P} collision will be very inefficient because the cross section of fusion is small. When \bar{P} 's collide with high A antinuclei, rather than two particles fusing together, the ejection of antiparticles, such as antineutrons, from the high A antinuclei becomes predominant.

Another alternative is a high temperature fusion plasma. This has severe problems of confining high energy antiparticles without collision with a surrounding wall or boundary layer. In contrast the process of producing high A antinuclei production by μ^+ has much less severe problems. Muon catalyzed fusion can take place in a low temperature environment. Reaction rate can be enhanced by using the clustered antihydrogen, laser enhancement, and liquid droplet techniques discussed above. However, in fusion processes which produce antineutrons, such as $(\bar{d}t\mu^+)$ fusion, escape of the antineutrons and subsequent reactions become a problem for high rates of antinuclei production, and we should seek to suppress these fusion reactions in mass production.

The benefit of high A antiatoms such as \bar{Li} (11), is due to the fact that this metallic material can be stored in a magnetic field "bottle" created by superconductors. To make high \bar{Z} antiparticles, many μ^+ should be attached to the high \bar{Z} antinuclei for neutralization. Thus a focusing technique for μ^+ beams will be required.

To get higher A antinuclei than $\overline{\text{Fe}}$ (anti-iron) nuclei, which is the most stable, binding of nuclei by using many μ^+ is necessary. The reaction for producing higher A antinuclei than $\overline{\text{Fe}}$ from lower A antinuclei is endothermic and requires the kinetic energy between two antinuclei. The kinetic energy can be gained by binding with μ^+ mesons. The spatial dimension of the muonic molecule is 207 times small than the electronic molecule, and the momentum 207 times higher, the high kinetic energy between the two bound nuclei may satisfy the endothermic energy requirement.

Another way of making high A antinuclei is to use antineutrons produced from fusion reactions, but the intensity of antineutron must be so small, that the large yield cannot be expected. If we can make very high A antinuclei such as $\overline{\text{U}}^{238}$, they would be a useful tool for producing a quark-gluon plasma, which is presently planned to create from realistic heavy ion collisions. To efficiently annihilate these two nuclei and produce a quark-gluon plasma, some acceleration of the heavy nuclei might be required, but it would be very low in energy compared to the relativistic heavy ion collision process.

We have discussed here the production of high A antinuclei using μ^+ and antiparticles. But the feasibility of these experiments can be tested using μ^- mesons and the ordinary nuclei, and we should carry out such tests.

CONCLUSION

A main objective of antimatter research is the potential use of antimatter for spacecraft propulsion. By using muons from the antiproton annihilation process to produce muon catalyzed fusion, propulsion energy can be increased. Several schemes, such as heterogenous mixture, crushed ice form, and clustered ion form mixture, appear to allow efficient use of muons even in a low density mixture.

High intensity laser irradiation at the proper frequency can enhance the muon molecular formation rate, and also strip muons that are stuck to the fusion product alphas. Application of shock waves in a propulsion reactor chamber potentially could increase reaction rate.

Another application of the muon catalyzed fusion process is the production of high A and Z antinuclei. These nuclei cannot be effectively produced by thermonuclear reactions because of the high temperature environment and low density mixture. Muon catalyzed fusion using positive muons appears desirable for producing such antinuclei under the conditions of a small quantity of the antinuclei material and a nonviolent environment. Because of the low density and low temperature conditions possible with this process, control of antimatter is much easier than with a production process based on thermonuclear reactions.

With a high intensity muon beam, creation of the high A and Z nuclei can be carried out in a similar fashion to dt μ fusion. The annihilation of high A, Z antinuclei with ordinary nuclei, using the moderate energy accelerator should create a quark-gluon plasma without requiring relativistic heavy ion-heavy ion collisions.

Muon catalyzed fusion process thus appears to be an important tool for expanding antimatter science and technology. Some of the necessary techniques can be developed through experiments using μ^- mesons and conventional nuclei; it is of worth to pursue this scientific and technical field.

ACKNOWLEDGMENT

The author would like to express his thanks to Dr. Augenstein and Dr. R. Forward for introducing him to this exciting scientific field. Research carried out under the auspices of the U. S. Air Force, Rocket Propulsion Laboratory.

REFERENCE

1. L.W. Alvarez, H. Brander, and F.S. Crawford, et al. Phys. Rev. 105 (1957) 1127.
2. Ya B. Zeldovich and S.S. Gerstein. Usp. Fiz. Nauk 71 (1960) 581 (Sov. Phys. Yshekhi) 3 (1961) 593.
3. S.S. Gerstein and L.I. Ponomarev in "Muon Physics," vol. III, ed. V. Hughes and C. S. Wu (Atomic Press, New York 1975).
4. E.A. Vesman, Zh. Eksp. Theoz. Fiz. Pisma 5 (1967) 113 (English Translation. Sov. Phys. JETP Letter. 5 (1967) 91).
5. S.E. Jones et al. Phys. Rev. Lett. 51 (1983) 1757. Phys. Rev. Letter 56 (1986) 588.
6. A. J. Caffrey et al. Muon catalyzed fusion 1 (1987) 53-66.
7. W.H. Breunlich et al. Muon catalyzed fusion 1 (1987) 67-88.
8. M. Subotowich. Journal of British Interplanetary Society 39 (1986) 312.
9. D. Morgan. This proceeding.
10. G. Smith. This proceeding.
11. J. C. Solem. Private communication.
12. H. Takahashi. Muon catalyzed fusion 1 (1987) 375.
13. Yu V. Petrov. Nature 285 (1980) 466; Muon catalyzed fusion 1 (1987) 351.
14. H. Takahashi. Proc. of UCF-87, Leningrad Nuclear Physics Institute, May 25-31.
15. H. Takahashi and A. Moats. Atomkernenergie - Kerntechnik 43 (1983) 188.
16. W.C. Strwalley. This proceeding.
17. S.I. Vinitzky, L.I. Ponomarev, I.V. Puzynin et al., Zh. Eksp. Theor. Fiz 74 849 (1978) [Sov. Phys. JETP 47 444 (1978)].
18. L.I. Menshikov. Yad. Fiz. 42 (1985) 1184 (Sov. J. Nucl. Phys. 42 750 (1985)).
19. M. Leon. Phys. Rev. Lett. 52, 605 (1984).
20. Ya.B. Zeldovich and Yu.P. Raizer Physics of Shock Waves and High Temp.
21. J.C. Solem. This proceeding.
22. R. Forward. Private communication, 1986.

FIGURE LEGENDS

Fig. 1. (dtu) molecular formation rate as function of laser intensity.

Fig. 2. Ionization cross section due to coherent X-ray. E_x : X-ray energy; E_0 : ionization energy; A : vector potential in units of volt.

Table 1

The mean free paths of du and tu (with room temperature kinetic energy)
in the liquid hydrogen density d - t mixture

Process	λ mean free path (in units of cm)
$(du)_{1S} + t + (tu) + d$	5×10^{-4}
$du + D_2 \rightarrow [(ddu)d_2e]_v$	7.1×10^{-1}
$tu + D_2 \rightarrow [(dtu)d_2e]_v$	1.4×10^{-4}
$tu + DT \rightarrow [(dtu)t_2e]_v$	
$tu + T_2 \rightarrow [(t + u)t_2e]_v$	4.2×10^{-1}

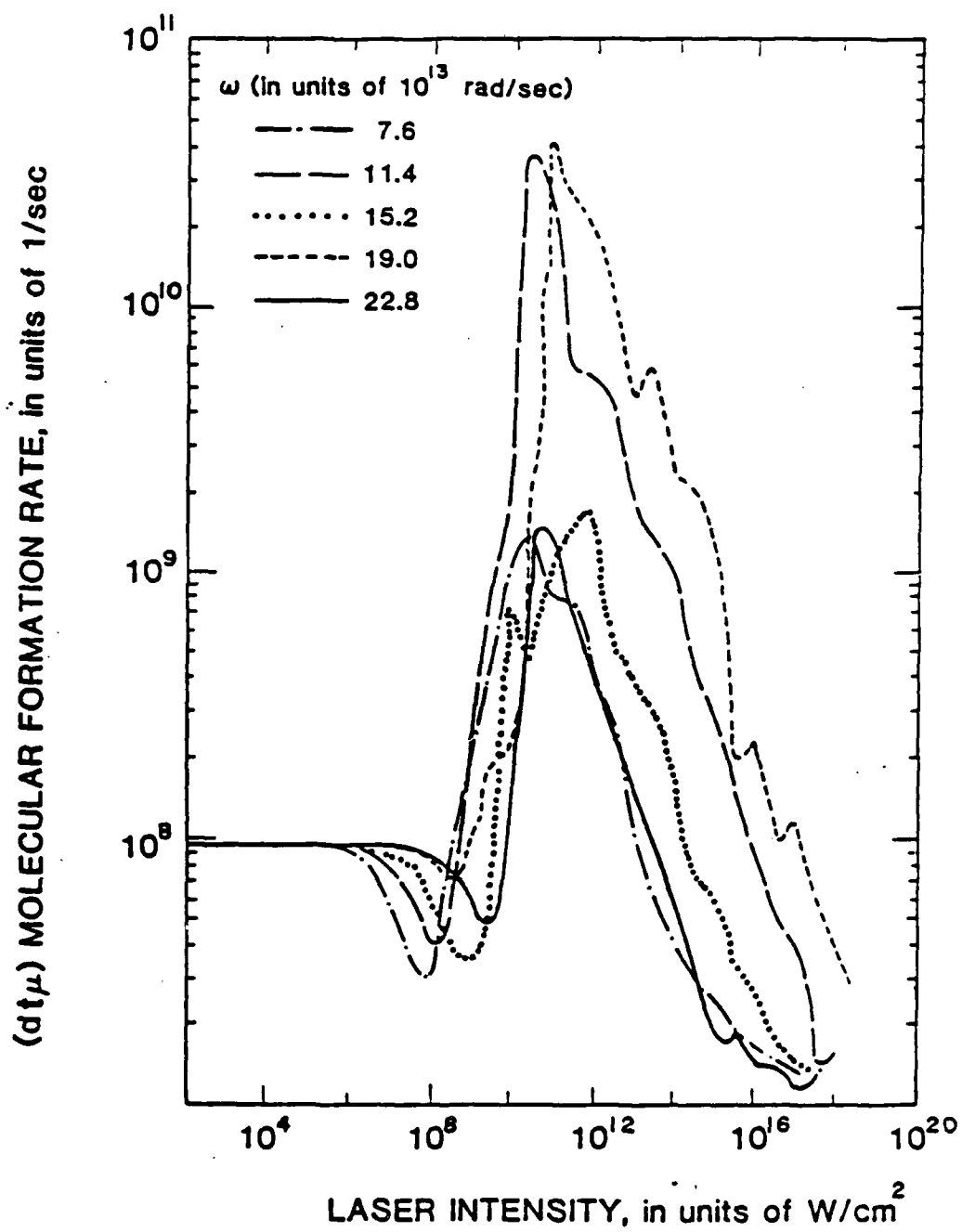


FIGURE 1

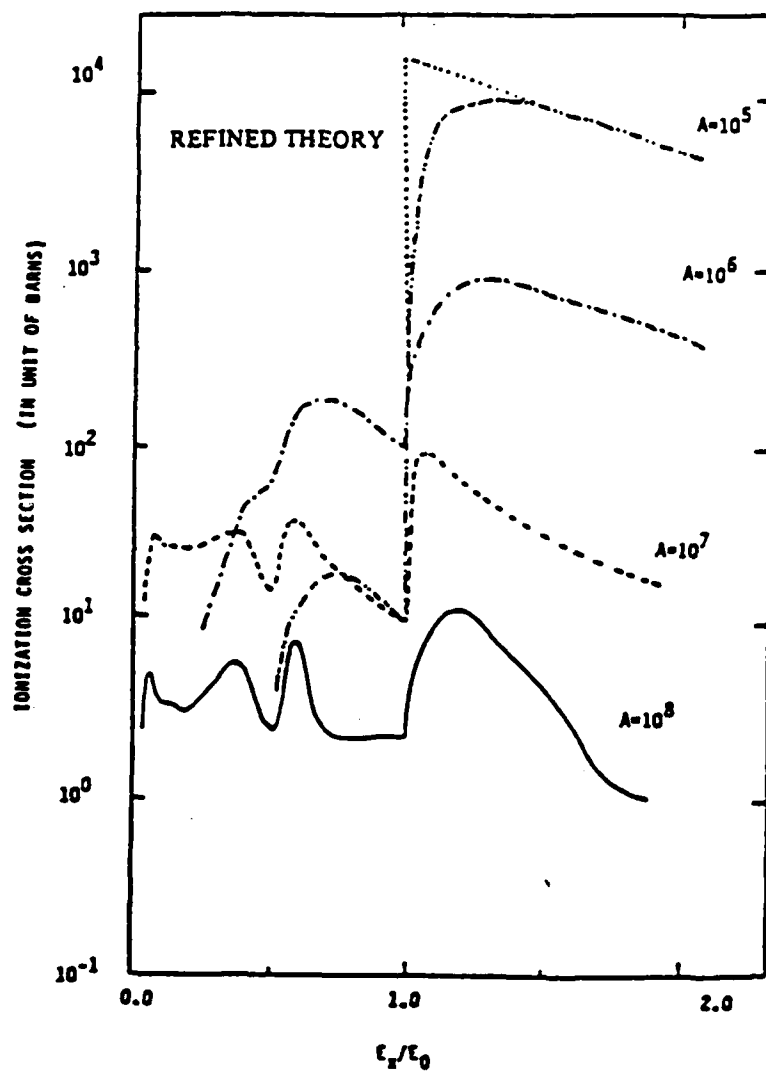


FIGURE 2

Multiple Collision Effects on the Antiproton

Production by High Energy Proton

(100 GeV - 1000 GeV)

Hiroshi Takahashi

James Powell

Brookhaven National Laboratory

Upton, New York 11973

Prepared for Rand Workshop, Oct. 6-9, 1987 on Antiproton Science and Technology.

ABSTRACT

Antiproton production rates which take into account multiple collision are calculated using a simple model. Methods to reduce capture of the produced antiprotons by the target are discussed, including geometry of target and the use of a high intensity laser. Antiproton production increases substantially above 150 GeV proton incident energy. The yield increases almost linearly with incident energy, alleviating space charge problems in the high current accelerator that produces large amounts of antiprotons.

INTRODUCTION

The production of antiprotons which have been used for high energy physics and low energy antiproton annihilation studies has generally been carried out with a thin target of heavy metal. The thin target is used because it allows present collecting devices to capture only a small momentum bite of antiprotons, which are produced with wide momentum spread (1-6). In order to increase capture of antiprotons, lithium lens and horn type devices have been studied (1,2).

To produce and to collect the large amount of antiproton needed for performing antigravity experiments (7) or for spacecraft propulsion (8,9,10), several schemes for collecting antiprotons with large angular and momentum spread have been proposed. One such approach is a large solenoidal coil with high magnetic field (11). If antiprotons with large angular and momentum spread can be collected by these devices, then a thick target instead of a thin target can be used. In thick targets, secondary particles created by proton-nucleus collisions, such as pions or leading protons, can produce additional antiprotons in successive collisions.

In this paper, antiproton production due to multiple collisions is studied. The study indicates: (1) that above 150 GeV incident proton energy, substantial numbers of antiprotons are produced by successive collisions, and (2) antiproton yield increases almost linearly with incident proton energy.

Cross Sections for antiproton, π^\pm meson and leading proton production.

In high energy P-P collisions, the sum of elastic and diffractive cross sections is about 20% of the total cross section. Protons which have been elastically or diffractively scattered have nearly as much energy as the incident proton. Such protons can produce antiprotons in successive collisions with the target. Protons produced as leading protons also have significant energy and can produce antiprotons in successive collisions.

The cross section of $P(P,P)P$ is shown in Figure 1a as a function of $X = P_1/P_{1\max}$ (12). The longitudinal momentum spectrum for leading protons calculated from the cross section in the laboratory system is shown in Figure 2. As shown in the figure, the leading proton has a large longitudinal momentum.

The longitudinal momentum spectra of mesons produced from P-P collision (cross section of $P(P,\pi)X$) as a function of X is shown in Figure 1b and in the laboratory coordinate system in Figure 3. The mesons produced at X close to 1 are very small momentum. Antiproton production cross sections from the P-P and π^\pm -P collisions calculated from the Hojvat and Van-Ginnken's (1) empirical formula are shown in Figure 4. In the energy region less than 150 GeV incident particle energy, π^\pm mesons have larger antiproton production cross section than protons (see also ref. 13). This large antiproton production cross section of the pions contribute substantially to antiproton production. Roughly 1/3 of antiproton production is contributed each from proton, π^+ and π^- particles.

Antiproton yield by multiple collisions.

Using these cross sections discussed in the previous section and assuming that no contribution from processes of $\pi^\pm(P,P)\pi^\pm$, and no capture of the produced antiproton in the collision with the nuclei, the yield of the antiproton from primarily, secondary, etc. collisions are calculated. Figure 5 shows the antiproton yield as function of incident proton energy.

The antiproton yield from multiple collisions becomes substantial above 150 GeV incident proton energy. At 200 GeV incident energy, antiproton yield due to secondary collisions is comparable to that from primary collisions. At 700 GeV incident energy, production from secondary collisions is about twice that from primary collisions.

For thin targets, where antiproton production is mostly due to primary collisions, antiproton yield above 150 GeV incident proton energy increases slowly. Yield is not proportional to incident energy and the most effective incident proton energy for antiproton production is a broad band around 200 GeV.

Total antiproton production due to multiple collisions is almost proportional to incident proton energy above 150 GeV. The energy cost for antiproton production does not change above this energy. Thus from the energy economy point of view, increasing incident proton energy does not benefit energy cost. However, when large amounts of antiproton are required, such as

for spacecraft propulsion, increasing incident proton energy reduces the beam current needed for a desired antiproton production rate. Reducing beam current alleviates problems associated with space charge in the high current accelerated beam.

Taking into account antiproton production from elastically and diffractively scattered protons and leading mesons in (π ,P) collisions (which are neglected in this calculation), the yield of the antiproton becomes little higher than the value calculated here. However, the assumption that the produced antiprotons are not captured by target nuclei overestimates antiproton yield. The fraction of the produced antiprotons that are captured by target nuclei depends strongly on target geometry and incident beam profile. This issue is addressed in the section on targetry.

So far we have considered antiproton production in P-P collisions. It is expected that higher yields can be obtained from proton-high A nucleus collisions. The mechanism for antiproton production is taken as follows. When a quark in one nucleon collides with a quark in the other nucleon, a color string is stretched between these two quarks. Pions, baryons and antibaryons are then produced from the hadronization of the stretched string. The quark that collides with the other quark, which is called a wounded quark, does not collide with other quarks before leaving the nucleus. In the case of proton-proton collisions the usually only one quark-quark collision occurs and the probability of making second quark-quark collisions occur is very small. In the case of proton collisions with high A nuclei, the probability of second and third quark-quark collisions is high. Since the proton has two up quarks and one down quark, the number of stretched strings in a proton-high A nucleus collision is limited to 3.

In these calculations, pion and leading proton production in collision between a proton and a high A nucleus collision are calculated with the nucleus factor for antiproton production used by Hojvat and Van-Ginneken (1). Since the mechanism of leading proton production is different from antiproton production, this assumption overestimates antiproton yield in a multiple collision process. The calculated yield for a proton collision with a tungsten nucleus is shown in Figure 6. The antiproton yield for proton-tungsten

collisions is approximately a factor of three greater than for proton-proton collisions. The author was informed (2) that the empirical formula for anti-proton production in proton-high A nuclei collisions overestimates the cross section at low $X = P_{\parallel}/P_{\parallel \text{ max}}$, compared to the experiment. As shown in the Figure 4, antiproton production for meson-proton collision is larger than for proton-proton collisions below 200 GeV. This is interpreted as follows. Pions are composed of a quark and antiquark. To produce antiprotons which are composed of two anti-up quarks and one anti-down quark, the quark of the pion is replaced by one antidiquark. In the proton-proton collision, however, three antiquarks must be created from the quark sea surrounding the colliding proton. Pion based production is thus energetically more favorable than the proton based production at low incident energies.

If pion could be accelerated in a short distance (because of its short rest frame lifetime of 2.6×10^{-8} sec) by laser acceleration, pions might be useful particles for producing antiprotons. In the multiple collision process, the favorable nature of pions for producing antiprotons is used effectively.

Targetry

We assumed in this calculation that the produced antiprotons are not captured by the target. The validity of this assumption depends on target geometry and beam profile. Evaluation of the absorption effect should be carried out using more detailed Monte Carlo calculations for various target geometries and beam profiles. One way to reduce absorption is to use a fine line solid target (i.e., small diameter) or a fine heavy metal jet target similar to that proposed for laser accelerators by Palmer (14,15). As shown in Figures 2,3, and 7 the longitudinal momentum of the produced antiproton is very small compared to the that of the leading proton and produced pions. The transverse momenta of these particles is on the order of 0.6 GeV/c. Produced antiprotons thus have more sideward emission than the leading proton and produced pions. Thus when high energy protons are injected into a slender long line target or liquid jet, the leading protons and the produced pions tend to stay inside the target and contribute to antiproton production by second and third multiple collisions. The produced antipions escape from the target and their capture by target nuclei is reduced.

By running a large electric current through a metallic target in the opposite sense to that of a lithium lens system (which focuses antiprotons), the produced antiprotons will be defocused and kicked away from the target (without much disturbance of the leading protons and pions), further reducing antiproton capture.

In addition, the proton distribution in the beam can be more intense in the periphery ("hollow beam"), allowing antiprotons produced near the target surface to easily escape. Another possibility for reducing antiproton capture, controlling, and slowing down antiprotons is a high intensity laser. Acceleration of charged particle using high intensity lasers has been proposed. Instead of using microwaves with a large cavity structure, laser irradiation of a suitably shaped micro structure can create strong electric fields which accelerate charged particles. Present technology can make micro structures of materials such as Si using lasers or electron beams, which would correspond to an electric field accelerating electrons on the order of 1 GV/m. To create an electric field of 1 GV/cm, a laser intensity of 2.7×10^{15} W/cm² is required. This is calculated from

$$I = \frac{C}{4\pi} \left(\frac{e}{2a_0^2} \right)^2 = 1.8 \times 10^{16} \text{ W/cm}^2 \quad (1)$$

where a_0 is the Bohr radius and the electric field of

$$E = \left(\frac{e}{2a_0^2} \right) = 2.57 \times 10^9 \text{ volt/cm} \quad (2)$$

The laser intensity of 2.7×10^{15} W/cm² can be created using present technology.

For antiproton production, the high intensity laser would irradiate the micro structured surface of the target at the same time as the proton injection. The resultant antiprotons emitted transversely from the target surface would then be controlled by the electric field created by the laser irradiation. Surface structure design and laser intensity depend on the control

scheme for the antiprotons and the injected proton profile. It appears worthwhile to further pursue the concept of using a laser to control produced antiprotons and mesons.

The increased yield of antiprotons achievable with a multiple collision target greatly reduces cost of the product. Table 1 illustrates the cost potential using such targets for a range of power costs and accelerator/target costs.

Table 1
Production Cost/Rate for Anti-Protons Using Multiple Collision Targets

Basis: 1mA beam current (Avg) @ 1000 GeV (1000 MW)
50% efficient beam (electric to beam)
0.35 Tev beam energy per anti-proton produced
15% fixed charges per year
80% duty factor
100% collection of anti-protons

Accelerator/Target Capital Cost	Anti-proton Cost (Million \$/mg) Power Cost	
	2¢/KWH	10¢/KWH
1 \$/watt	0.6	2.2
10 \$/watt	2.4	4.4

Production Rate = 700 mg/year (80% duty factor)

Anti-matter cost ranges from a low of 0.6 Million \$/milligram to a high of 4.4 M\$/mg, depending on input costs. Even the highest cost is probably acceptable.

Power costs range from 2¢/KWH to 10¢/KWH, depending on location (e.g., low cost hydro versus a fossil or nuclear plant). Previous cost estimates for the accelerator/target components of an accelerator-breeder system indicate approximately 1.5 \$/watt; the range of 1 to 10 \$/watt should cover the cost for an anti-proton system.

Most of the accelerator cost will be for rf power which can be estimated reasonably accurately. The actual target cost is more uncertain but it should be relatively low. The target probably will be a single fine jet of liquid lead. In practice, a number of separate targets will probably be required with beam splitting or switching to limit average current to the target. No single target would be able to handle 1000 megawatts of beam deposition.

The cost of the anti-proton collection and cooling system will probably decimate the target cost, and is difficult to estimate. However, the \$1 to \$10/watt range should provide sufficient margin for this component.

Total production rate from such a facility is 700 milligrams/year, which would provide for a large spacecraft propulsion effort. The facility power input requirement of 2000 megawatts is well within current U.S. capability.

CONCLUSION

This study shows that multiple collisions substantially increase anti-proton production of 150 GeV and above incident proton energies. At 200 GeV, total production is approximately twice that of a single collision; above 200 GeV, yield increases almost linearly with incident proton energy. In order to make large amounts of antiproton, we can then increase incident proton energy instead of increasing beam current which creates a space charge problem in the beam. (This is not effective for thin targets, since yield is nonlinear with energy.) In the case of multiple collisions, capture of the produced anti-protons by the target is a potential problem. Capture of antiprotons can be avoided by using slender long targets or laser irradiation on a microstructured target surface. Evaluation of these approaches should be detailed Monte Carlo calculation, carried out by an investigation of how to collect anti-protons produced with large phase space.

In this paper, antiproton production from tungsten targets was calculated using a simple factor to describe the effect of target mass number on the antiproton production. This appears to overestimate both the leading proton production in the high energy range and antiproton production. This shortcoming should be corrected using models based on quark cascade theory.

In the case of a target with high A nuclei, many neutrons and anti-neutrons will be created along with the antiprotons. These are neglected in this calculation. Antiproton production through high energy neutron and anti-neutron reactions should also be taken into account, along with antideuteron, antitritium and strange particle production.

ACKNOWLEDGMENT

This research was carried out under the auspices of the U.S. Air Force Rocket Propulsion Laboratory. The authors would like to express their thanks to Profs. D. Cline and F. Mills for their valuable discussions.

REFERENCES

1. C. Hojvat and A. VanGinneken, "Calculation of Antiproton Yields for the Fermi Antiproton Source," Nuclear Instrumentation and Methods, 206 (1983) 67-83.
2. F.E. Mills, "Scaleup of Antiproton Production Facilities to 1 mg/yr," Fermi National Accelerator Lab. Sept. 30 (1987).
3. D. Cline, "The Development of Bright Antiproton Sources and High Energy Density Targetting," Proc. 11th Int. Conf. High Energy Accelerator, Geneva (1980).
4. T. Goldman, "Large Hadron Facility Adaptation," this proceeding.
5. E. Blackmore, "TRIUMF KAON Factory," this proceeding.
6. D. Lowenstein and Y. Lee, This proceeding
7. B.E. Bonner and M.M. Nieto, "Basic Physics Program for A. Low Energy Antiproton Facility," this proceeding.
8. D.L. Morgan, "Concepts for the Design of an Antimatter Annihilation Rocket," Journal of the British Interplanetary Society, 35 (1982).
9. R.L. Forward, "Antiproton Annihilation Propulsion," AFRPL TR-85-034, Air Force Rocket Propulsion Laboratory. Edwards Air Force Base, CA, Sept. (1985).
10. B.W. Augenstein, "Concepts, Problems, and Opportunities for use in Annihilation Energy," An annotated Briefing on Near-Term RDT&E. To Assess Feasibility, RAND Note N-2302-AF/AC, Rand Corp., Santa Monica, CA 90406.
11. D. Cline, This proceeding
12. V.V. Anisovich, M.N. Kobrinsky, J. Nyiri, and Yu. M. Shabelski, "Quark Model and High Energy Collision," World Scientific, Singapore (1985).
13. B.N. Cassenti, this proceeding.
14. R.B. Palmer, "A Laser-Driven Grating Linac," Particle Accelerators, 11 (1980), 81-90.
15. R.B. Palmer, N. Baggett, J. Claus, R. Fernow, et al., "Laser Plasma Linac," Proc. on Int. Conf. on Lasers 1984, San Francisco, CA. Nov. 26-30, 1984 (BNL-35737).

FIGURES

- 1a. The longitudinal center of mass momentum distribution of leading proton produced by the proton-proton collision, as function of Feynman $X = P_1/P_{1\max}$.
- 1b. The longitudinal center of mass momentum distribution of π^+ meson produced by the proton-proton collision as function of Feynman $X = P_1/P_{1\max}$.
2. The longitudinal laboratory momentum spectra of leading proton produced by the proton-proton collision.
3. The longitudinal laboratory momentum spectra of the π^+ mesons produced by the proton-proton collision.
4. The antiproton production rates in the proton-proton, and π^+ mesons proton collision as functions of the incident proton and π^+ meson energy.
5. The antiproton production rates in the multiple proton-proton collisions as the function of the proton energy initial incident.
6. The antiproton production rates in the multiple proton-tungsten collision as the function of the initial proton incident energy.
7. The laboratory system antiproton spectra produced by proton-proton and π^+ meson proton collisions.

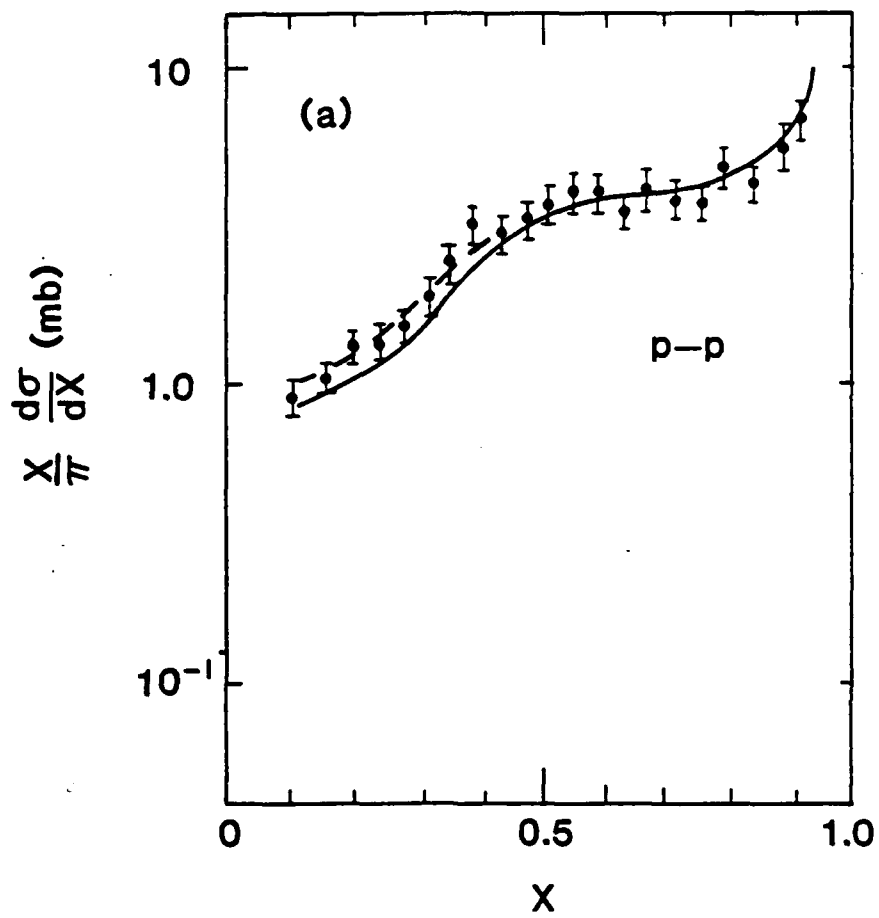


FIGURE 1a

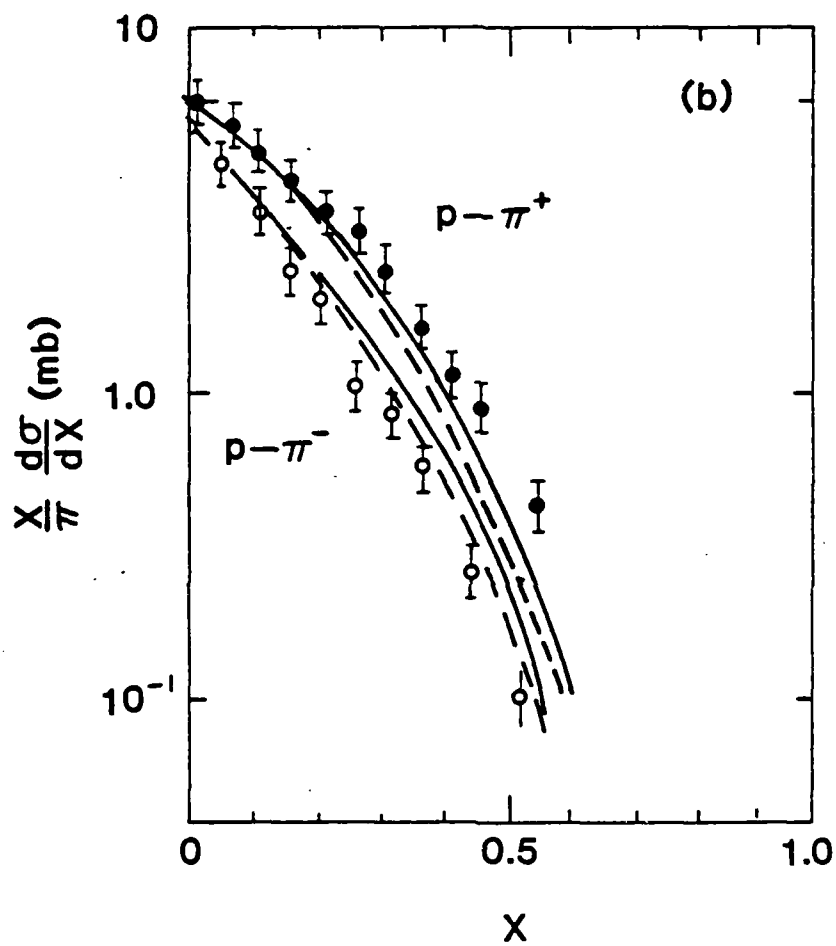


FIGURE 1b

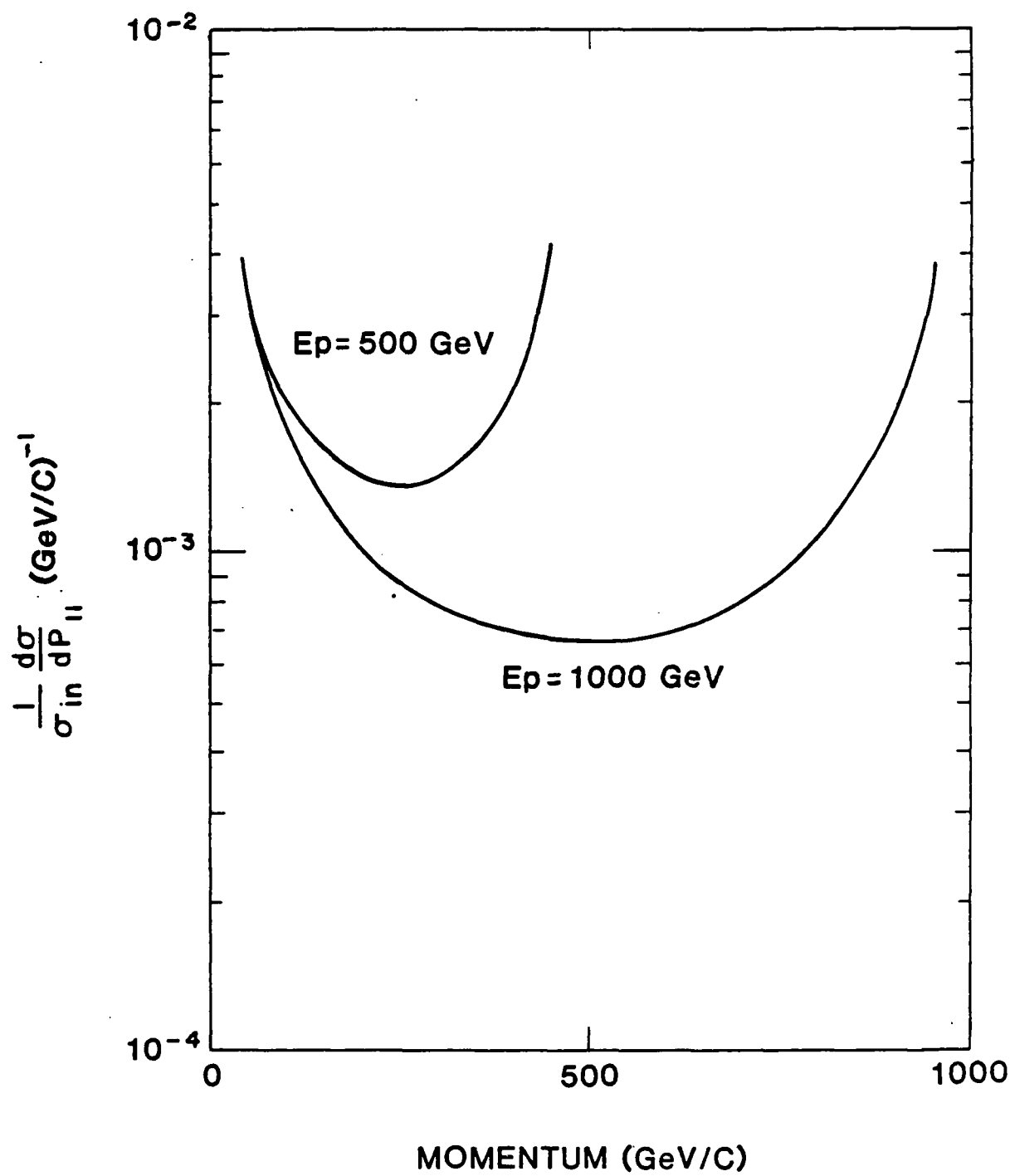


FIGURE 2

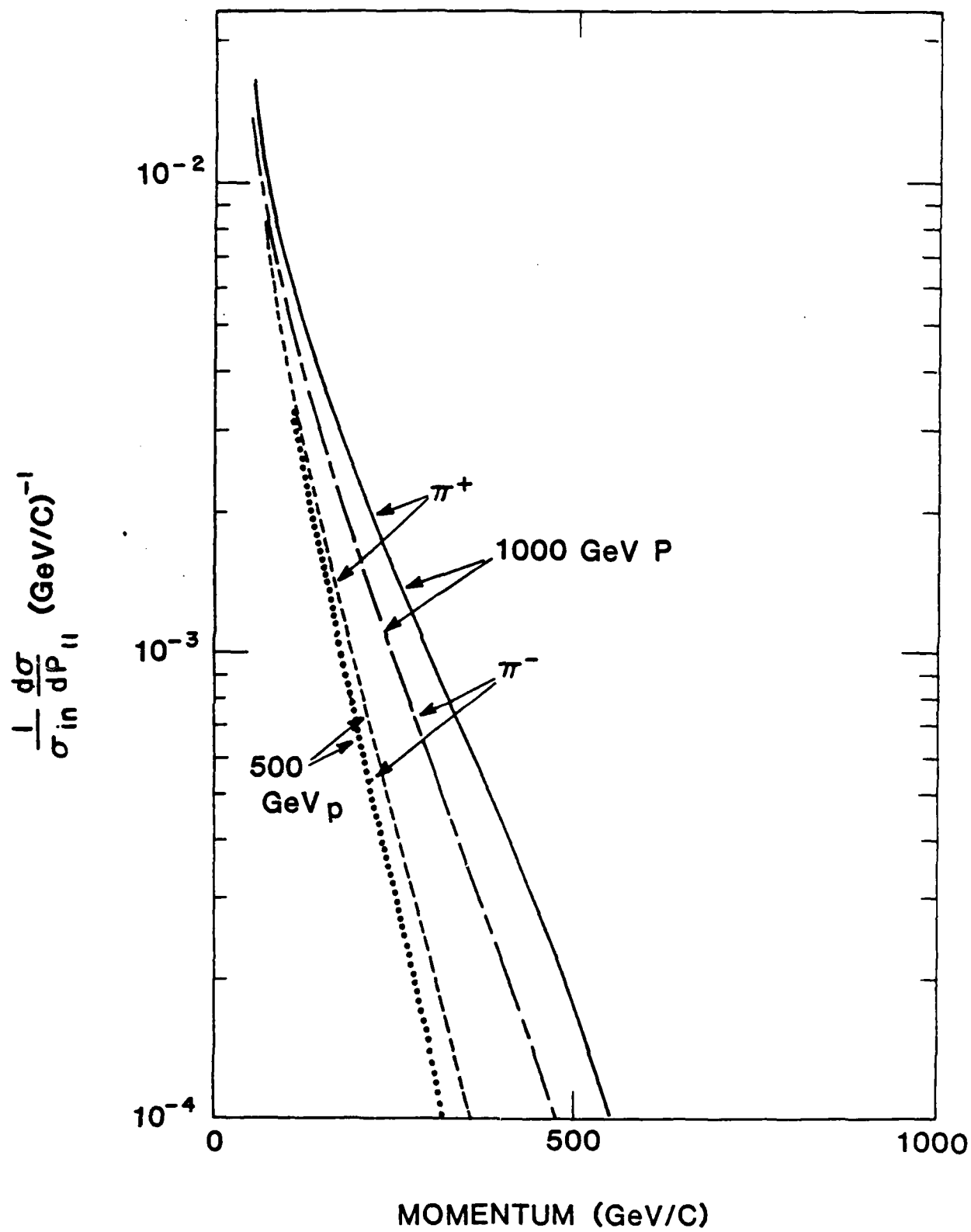


FIGURE 3

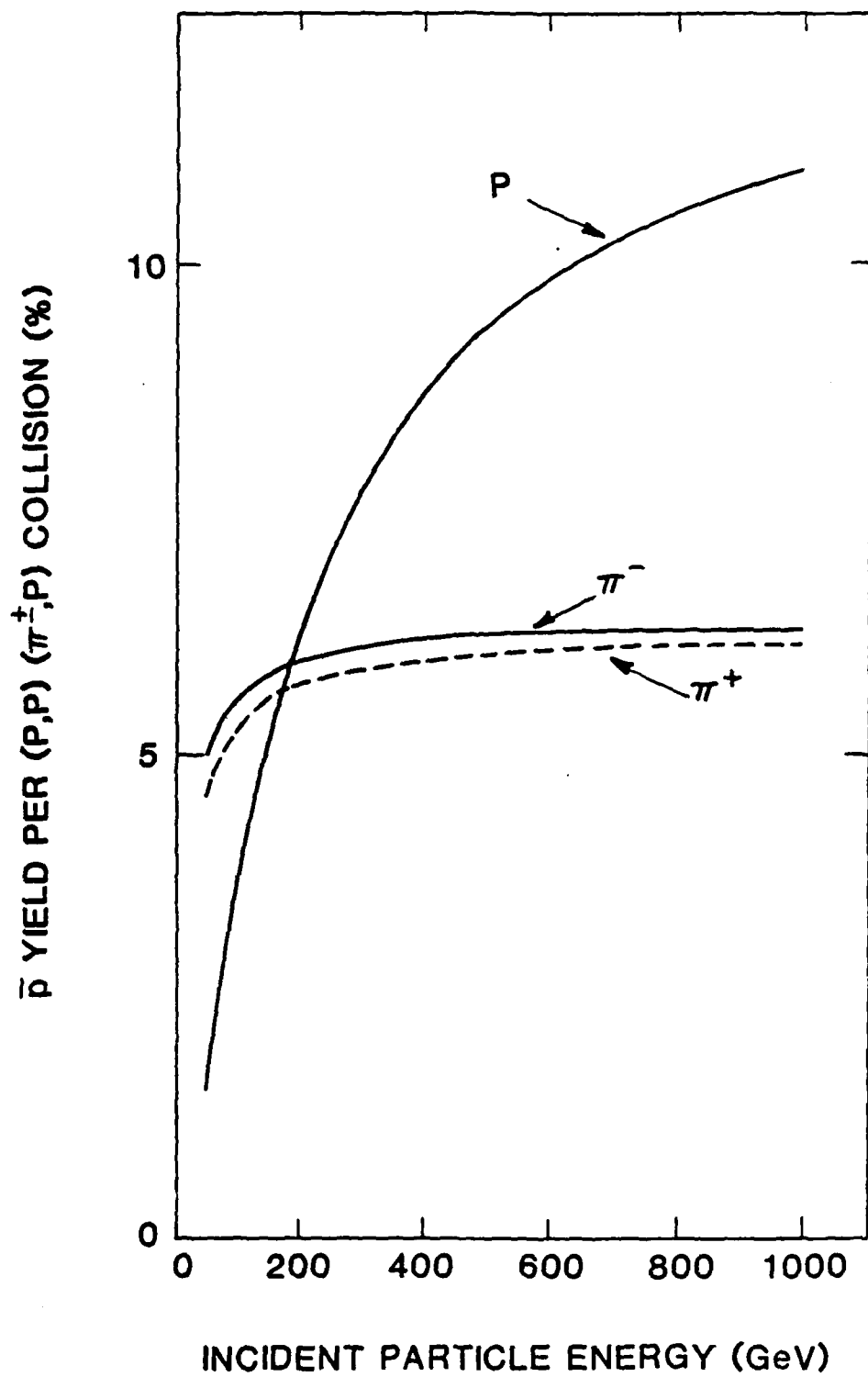


FIGURE 4

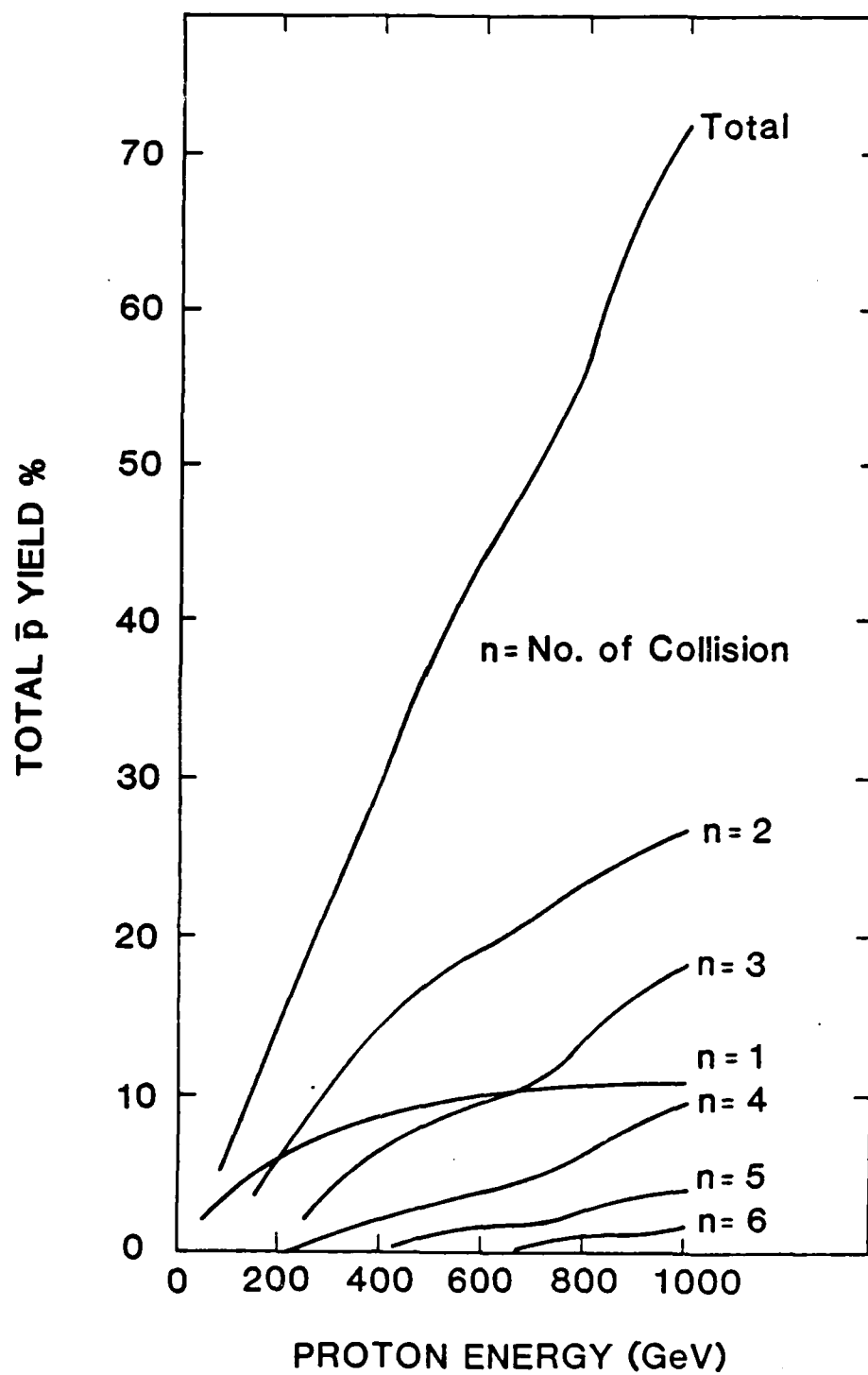


FIGURE 5

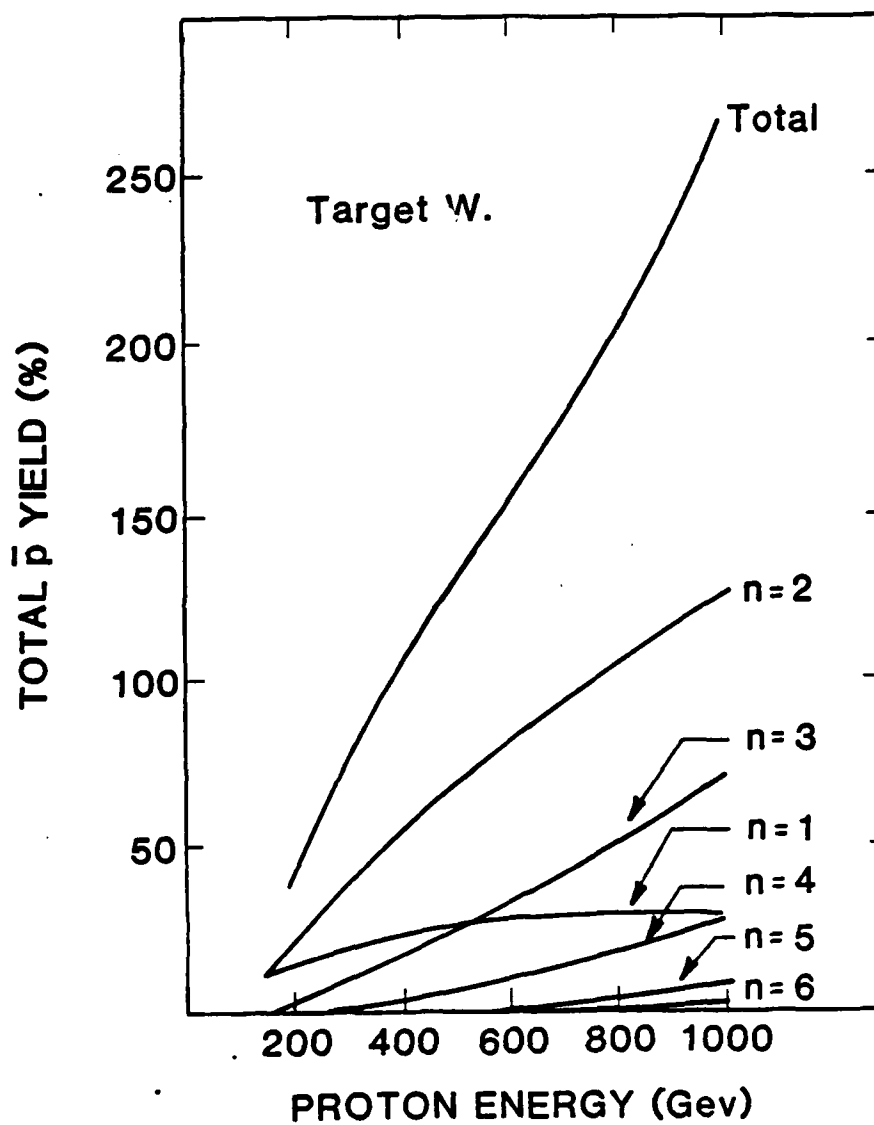


FIGURE 6

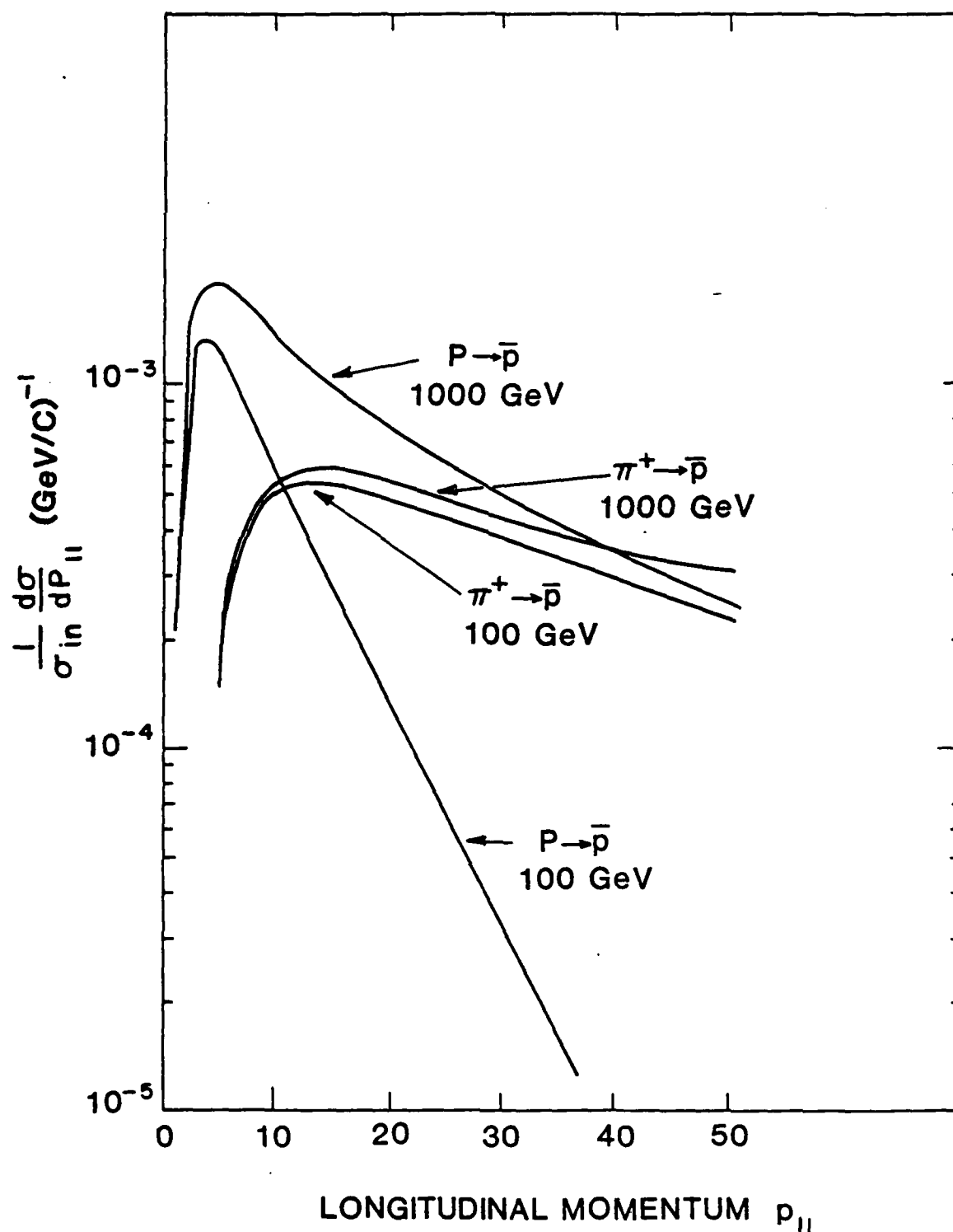


FIGURE 7

BIOMEDICAL POTENTIAL OF ANTIPROTONS

T. Kalogeropoulos⁵, J. Archambeau³, D. Bassano⁶, G. Bennett¹, B. Gottchalk²,
L. Gray⁵, A. Koehler², R. Muratore⁵, and M. Urie⁴

¹*Brookhaven National Laboratory, Upton, NY 11979*

²*Harvard Cyclotron, Harvard University, Cambridge, MA 02138*

³*Loma Linda Medical Center, Loma Linda, CA 92354*

⁴*Massachusetts General Hospital, Boston, MA 02114*

⁵*Department of Physics, Syracuse University, Syracuse, NY 13244*

⁶*Department of Radiology, SUNY Health Science Center, Syracuse, NY 13210*

Abstract

Antiprotons are presently produced in sufficient quantities at accelerator centers and efforts are under way to store and transport them to users anywhere. These developments make timely a closer look at their potential outside particle physics. This paper explores their potential to biomedical research and applications. The relevant interactions of low energy antiprotons, such as stopping power, annihilations and antiprotonic atoms, are reviewed. Imaging of the electronic density and elemental composition are discussed and compared with present techniques. The advantage of antiprotons over other charged particles for tumor treatment and as simulators for precise radiation delivery are discussed. These considerations show that the antiproton is of high promise to biomedical research and the practice of medicine. Finally, an exploratory experimental program is proposed which can be carried out in an existing beam at the Brookhaven AGS or at the CERN LEAR facility.

I. INTRODUCTION

Applications to medicine have been found for all stable particles known to physicists, such as protons, heavy ions, photons, phonons, electrons and positrons. The notable exception is the antiproton (\bar{p}) in spite of the fact that physicists have been using it since its discovery about thirty years ago.¹ It is the objective of this paper to familiarize everybody with the antiproton and direct attention to its biomedical potential. This includes treatment, imaging and chemical analysis.

The antiproton, like the proton and other charged particles, exhibits a Bragg peak; the maximum dose is delivered near the maximum depth of penetration of the beam, sparing distal normal tissue. The resulting physical dose distribution is more nearly ideal for antiprotons than for other particles, and the presence of emissions with high Linear Energy Transfer (LET) provides an enhanced biological effect.

The small and well-defined interaction region characteristic of the \bar{p} is uniquely determined by the incident beam energy and the composition and density of the medium traversed. In addition, each antiproton interaction produces a number of charged and neutral particles with sufficient energy to exit the body. Imaging the interaction region is improved by the charged particles since their trajectory is readily measured. Finally, the chemical composition and even molecular structure at depth appear to be assayable because of their effects on the antiproton interaction process. All of these features suggest the potential for unique diagnostic applications, and for precise control of therapeutic applications.

The antiproton is the "anti" of the proton in the same way as the positron is the "anti" of the electron. (It is amusing to contemplate the consequences if the positron had been named antielectron. Imagine the psychology involved in giving someone an antielectron source or injecting antielectrons into someone's body). Besides its unfortunate name the fact that it is created and generally disappears shortly afterwards makes the antiproton "exotic". In this context, the antiprotons are not at all different than photons (light, x-rays,

γ -rays, etc.) or phonons (sound). Antiprotons, photons, and phonons are "man-made" at an instant in matter and "disappear" by interacting with matter. Their differences are in the energies involved. The energy involved in creating an antiproton is about a hundred thousand times larger than in creating an x-ray photon. The difference in energy scale and the negative charge of the antiproton are at the root of the problems and opportunities.

The high energy of protons required for antiproton production is indeed a real obstacle to antimatter applications in general and biomedical in particular. In order that these applications become routine, antiprotons need to be available at the hospital site. Thanks to their charge and stability in vacuum the antiprotons can be stored in magnetic rings or traps ("bottles"), and this is done today at CERN and Fermilab. Missing, however, are transportable bottles of antiprotons which can be taken anywhere. In this workshop, proposals^{2,3} are being presented for developing such transportable antiproton sources. Because there are no fundamental problems in the development of such bottles, it is only a question of time and effort before they become available. We guess that such bottles after their development will cost about half a million dollars and last indefinitely.

Important considerations in antimatter applications are the cost and the quantity of bottled antiprotons. With present technology a dedicated factory of antimatter can transfer antiprotons to the bottles at about a few \$ per 10^9 antiprotons⁴ and the efficiency of antiproton technology has been steadily improving over the years (Fig.1). At present the best facility in the world for antiprotons with energy appropriate to biomedical applications is at CERN where they are stored in the Low-Energy-Antiproton-Ring (LEAR) and are used in particle physics research at the rate of 10^6 \bar{p} /sec. A similar facility can be built at Fermilab or Brookhaven at a cost⁵ of about 20 M\$. In view of these developments, it is time to seriously explore the biomedical potential of antiprotons.

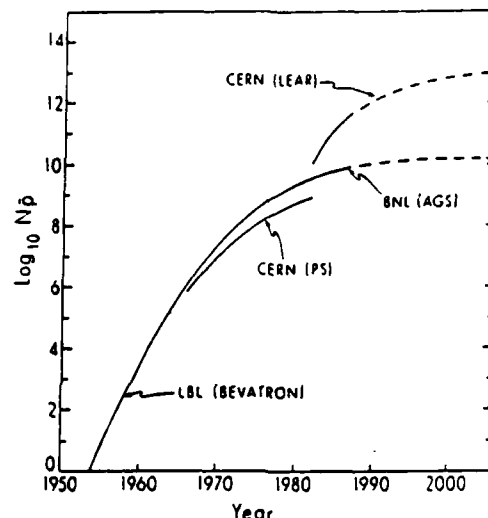


Fig. 1. Evolution of the typical number of stopping antiprotons used per experiment.

We hope to make apparent the uniqueness and versatility of antiprotons in this paper and we will propose an exploratory and development program. Antiproton beams can be directed to any part of the body and stopped with a precision of about 1 mm depending on the depth. The stopping point of every antiproton can easily be measured with an accuracy of 1 mm by extrapolation of the trajectories of annihilation products. Upon coming to rest the antiprotons are caught by the nuclei and form antiprotonic ("exotic") atoms. The capture rate is sensitive to the concentration of the nuclei and the local chemistry. Exotic atoms emit characteristic penetrating x-rays which can be used to measure the local elemental composition and chemical environment. Signatures for all nuclei are available. When finally the antiprotons annihilate in a nucleus, about 1/20 of the rest energy is transferred to the medium within a few mm of the annihilation vertex via nuclear fragments; antiprotons are thus ideal for radiation therapy.

Section II discusses interactions of antiprotons and in Section III the $\bar{p}N$ annihilation properties and their application to imaging (ASTER). In Section IV antiproton energy deposition and comparisons to other particles are presented. In Section V antiprotonic atoms are discussed. Section VI discusses elemental imaging. Section VII outlines a research program and in Section VIII the summary and conclusions are presented.

II. ANTIPROTONS IN MATTER

We briefly discuss here the main features of antiproton interactions with matter relevant to biomedical applications. Fig.2 summarizes the average features of an antiproton entering matter. The initial kinetic energy (E) of the antiproton is transferred along its path to the electrons of the medium until all of its kinetic energy has been dissipated and the antiproton comes to "rest". The mechanism of this energy transfer is independent of the sign of the charge⁶. Protons or antiprotons with the same initial energies come to rest at the same depth.

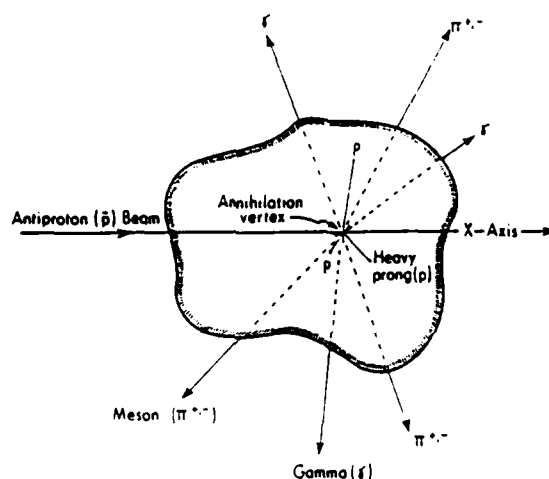


Fig. 2. An "average" annihilation event (star) produced by stopping antiprotons in matter. The indicated gammas are only those from π^0 decays. In addition, one expects nuclear gammas from the excitation of the nucleus and x-rays from the deexcitation of antiprotonic atoms.

The antiproton, in contrast to the proton which becomes hydrogen upon coming to rest, is captured by a nucleus and forms an excited *antiprotonic atom*. It cascades towards the ground state by emission of *penetrating characteristic x-rays* which are the *fingerprints* of the nucleus. Finally, it is captured from some atomic level by the nucleus and *annihilates* with either a proton or a neutron. The available energy of annihilation is equal to ~ 1880 MeV, twice the antiproton rest mass (mc^2) energy. This energy is transferred to about five pions on the average and in $\sim 5\%$ of the annihilations a kaon pair is emitted as well. About a third of the energy goes to neutral pions (π^0). Each π^0 decays within a few

microns from the annihilation point into two energetic gammas (γ). About 10% to 20% of the annihilation energy is transferred to the nucleus via pion interactions. This energy goes mainly into protons (*heavy fragments*) and neutrons and a small fraction is expected to go into gammas characteristic of the nucleus (*nuclear γ -rays*).

A small fraction of the antiprotons will not come to rest, but instead interact with a nucleus *in-flight* and either annihilate or scatter. The fraction of the in-flight interactions depends primarily on the incident antiproton energy. The features of the in-flight annihilations are similar to those at rest, except that x-rays are absent, and a larger fraction of the annihilation energy goes into nuclear excitation.

A. The Slowdown Process

The theory of the energy loss of charge particles moving in matter is well developed. In a chemical compound or mixture the stopping power (dE/dx), in MeV/cm, is given to within a few percent⁷ by

$$-\frac{1}{\rho} \frac{dE}{dx} = \frac{0.30708}{\beta^2} \cdot \sum \frac{Z_i \cdot C_i}{A_i} \{f(\beta) - \ln I_i\} \quad (1)$$

where ρ is the density (g/cm³) of the medium, β is the velocity (v/c) of the moving particle, $f(\beta) = \ln(2mc^2\beta^2/(1-\beta^2)) - \beta^2$, m is the mass of the electron (0.51 MeV/c²), and Z_i , A_i , C_i , I_i (MeV) are atomic number, weight, concentration, and excitation potential of the i^{th} element, respectively.

1. Bragg Peak

Because of the $1/\beta^2$ dependence, which is proportional to $1/E$ for $\beta \ll 1$, the stopping power dE/dx increases rapidly towards the end point. For heavy particles such as protons and antiprotons this energy loss is characterized by the sharp *Bragg peak*. The sharpness of the peak is shown in Fig.3 for a proton in water. This feature is exploited in proton and heavy ion radiation therapy.⁸

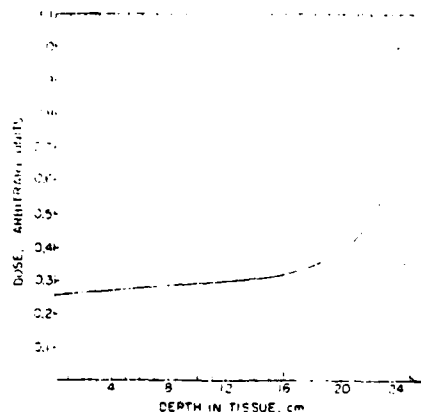


Fig. 3. The Bragg peak of protons in water.

2. Stopping Range

Integration of (1), until the kinetic energy is dissipated, yields the depth (*range*) in the medium at which the particle comes to rest. The dependence of the stopping range (\bar{R}) in water as a function of the incident antiproton kinetic energy is shown in Fig.4. Any part of the human body can be reached with antiprotons with energy of 200 to 250 MeV (equivalent to 25 to 37 cm of water).

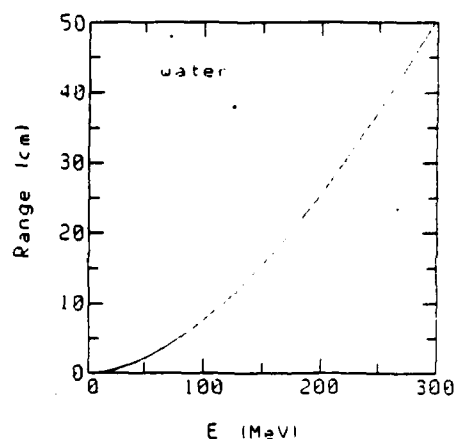


Fig. 4. The stopping range of antiprotons in water as a function of incident kinetic energy.

The stopping power given by (1) represents *average* energy loss. The stopping range differs from particle to particle due to the statistical nature of the energy transfer to the medium and this is called *straggling*. The distribution of the stopping points around the mean is almost a Gaussian with a standard deviation (σ_s) given by⁹

$$\sigma_s = \bar{R} \cdot \sqrt{(200m_e/m)} \cdot f(E/mc^2) \quad (2a)$$

where m is the mass of the particle (antiproton) and $f \approx 3\%$ to 4% in the region of interest. Thus, for antiprotons of interest

$$\sigma_s = 1.1 \times 10^{-2} \times \bar{R} \quad (2b)$$

and at $\bar{R} = 25$ cm, $\sigma_s = 3$ mm. Fig.5 shows the computer simulated distribution of antiprotons with an average range of 10 cm in water. The entering beam is monochromatic and the Gaussian around the stopping point is a result of straggling.

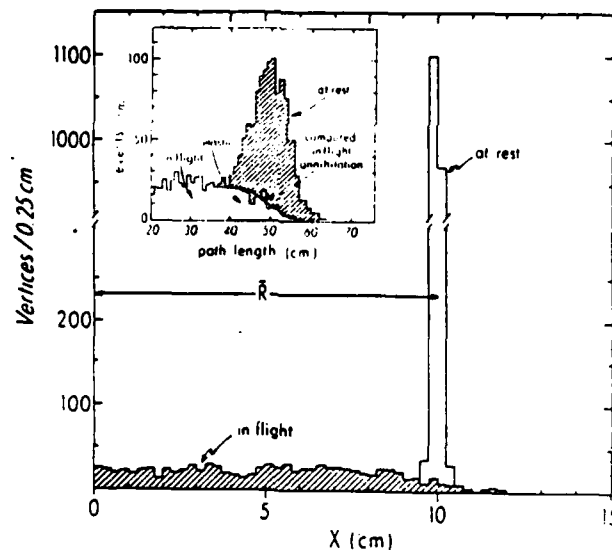


Fig. 5. Computer simulation of annihilation vertices along the beam in water. The broadening of the stopping peak is indicated by considering a monochromatic beam of antiprotons in water. The width is due to straggling. Insert shows distribution of vertices in liquid hydrogen (density = 0.076 g/cm^3) produced in a beam with a $\delta p/p \approx \pm 3\%$ from Ref. 12.

3. Lateral Dispersion

A pencil beam after traversing a medium will be laterally spread about the beam axis as a result of Coulomb scattering. Of interest here is the distribution of the stopping points

to a plane normal to the beam and at \bar{R} . The rms of the distribution of the projected stopping points projected to an axis normal to the beam has been calculated following Fowler and Perkins ¹⁰. The following dependence on range has been obtained:

$$\sigma_{\perp}(\text{mm}) = 0.264R^{0.963} \quad (3)$$

where R is the mean range in water in cm. Thus, a pencil beam of antiprotons of 200 MeV stops at 25 cm and its lateral spread projected to an axis normal to the beam is 5.9 mm while the longitudinal spread (straggling) is 3 mm.

These Coulomb effects have to be considered carefully in any application. They are strongly dependent on the mass of the particle and the medium. Fig. 6 shows the trajectory of an antiproton and a K^+ (half the antiproton mass) near their stopping points in emulsion which has a density of 3.5 larger than water. Even near their stopping point where scattering is maximum the antiprotons travel almost on a straight line.



Fig. 6. Stopping antiprotons in emulsion from Ref. 26. Note the difference in scattering between the antiproton and the K^+ (track 1).

B. In-Flight Interactions

Antiprotons travelling in a medium may encounter a nucleus and undergo annihilation

or interaction. The total antiproton cross-section¹¹ in mb is parametrized as follows in terms of the atomic weight (A) and antiproton momentum (p) in GeV/c:

$$\sigma_A^T = 600 \times (1 + 0.17/p) \times (A/12)^{2/3} \quad (4a)$$

About 62% of the interacting in-flight antiprotons annihilate and 38% scatter. In hydrogen the cross-section¹² is given by

$$\sigma_H^T = 66 + 52/p. \quad (4b)$$

Fig.7 shows the fraction of the stopping antiprotons as a function of stopping range in water. Thus the majority of the antiprotons which enter the human body come to rest. The distribution of the in-flight annihilations along the beam is shown in Fig.5. The in-flight annihilations can be discriminated easily from those at rest due to the narrow width of the at rest annihilations. Moreover, after collisions which result from elastic or inelastic (other than annihilation) nuclear interactions, the annihilation point is not along the beam and can thus be easily discriminated. Most of the biomedical applications depend on the information provided by stopping antiprotons. The in-flight interactions contribute to the "background" events but they can be discriminated on an event by event basis.

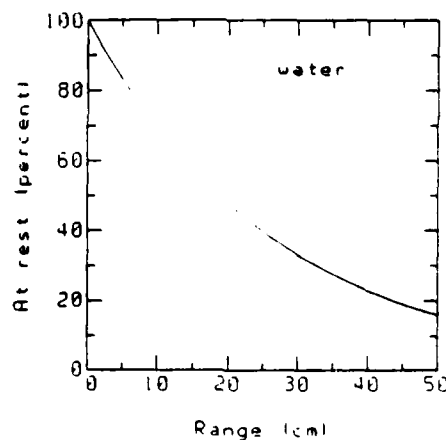


Fig. 7. Fraction of the antiproton annihilations at rest (without prior scattering) as a function of stopping range in water.

III. ANNIHILATION PRODUCTS

A. Charged Pions

Examples of antiproton annihilations stopping in a bubble chamber within a magnetic field are shown in Fig. 8. The bubble density along the path of the particles is proportional to dE/dx , which in turn is proportional to $1/\beta^2$. The antiprotons, as they come to rest ($\beta \rightarrow 0$) form dense tracks, while the annihilation products, (π^\pm) are moving faster ($\beta \approx 1$), and their bubble density is minimum. Measurement of the curvature of the pion tracks provide their spectra which are shown in Fig.9. For our purposes, these spectra¹³ are described well by

$$N_\pi(p) \propto p^2 \cdot \exp(-p/124) \quad (5)$$

where p is in MeV/c. The average kinetic energy is about 200 MeV and is sufficient for the pions to escape the body without stopping (Fig. 10a) or interacting (Fig.10b). Thus, with a cylindrical detector¹⁴ surrounding the body, such as that shown in Fig.11, the pion directions can be measured and the annihilation point determined by the intersection of the antiproton and the charged pion trajectories. This feature is *unique* to antiparticles and in contrast, protons, alphas, etc. do not provide *external* signatures of the stopping point. This feature in combination with other properties is central to most envisioned biomedical applications.

The reconstruction of the stopping point depends upon the detection of at least one charged pion which exits the target without nuclear scattering. Because the charged pion multiplicity¹² is three (see insert in Fig.9), and because pions penetrate water readily, high vertex reconstruction efficiency can be achieved.

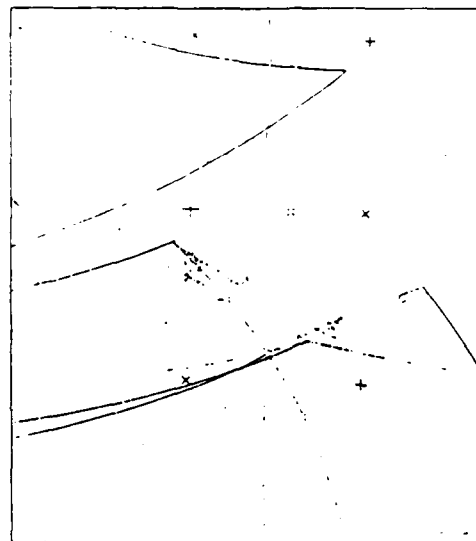


Fig. 8. Examples of annihilations photographed in a deuterium bubble chamber. (Spacing between fiducial marks is 10 cm.) Four antiprotons enter from the left and are heavily ionizing because of their low velocity. The light tracks emanating from the vertices are the charged pions and the heavy positive track from the annihilation on the top is a "heavy prong" which in this case is a proton.

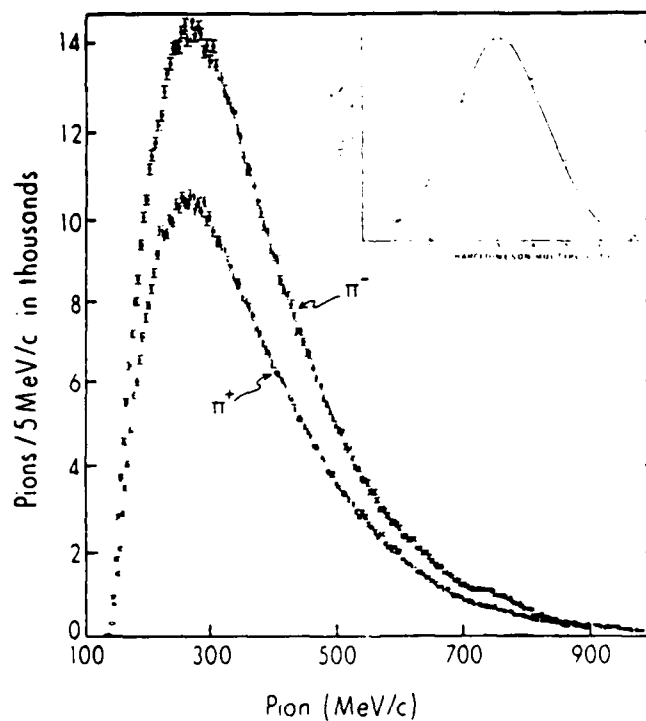


Fig. 9. The charged π^+ , π^- spectra from stopping antiproton annihilations in deuterium from Ref. 13. The threshold of the spectrum is due to the spectrometer acceptance. Insert shows the charged pion multiplicity from Ref. 12.

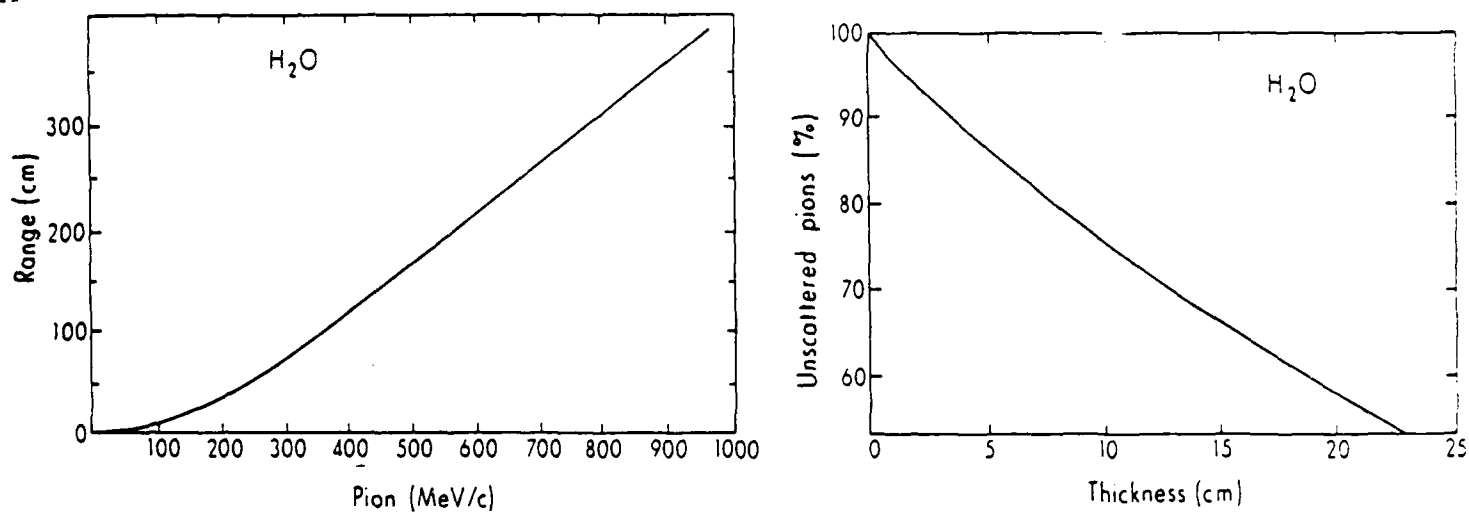


Fig. 10. (a) Charged pion range in water as a function of incident momentum. (b) Unscattered pions going through water as a function of target thickness..

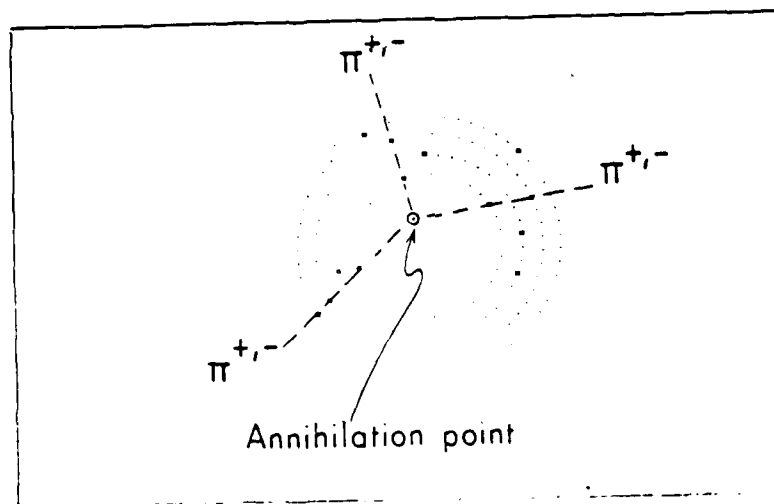


Fig. 11. An example of an annihilation on a neutron producing three charged pions and seen by a four-layer cylindrical drift chamber. Dots are locations of sense wires and those with crosses are those with signals from an AGS experiment (Ref. 14). This chamber provides the information which determines the directions of the charged particles in three dimensions. The diameter of the inner cylinder is about 40 cm.

B. Neutral Pions

About 1/3 of the annihilation energy goes into 1.5 neutral pions¹⁵ (π^0) on the average. Each π^0 decays within microns of the annihilation point into two γ -rays. The γ -ray multiplicity is therefore three per annihilation on the average. The spectrum¹⁶ of these gammas is shown in Fig.12 and fits well to the function

$$N_\gamma(E) \propto E \cdot \exp(-E/104) \quad (6)$$

where E is the γ -energy in MeV.

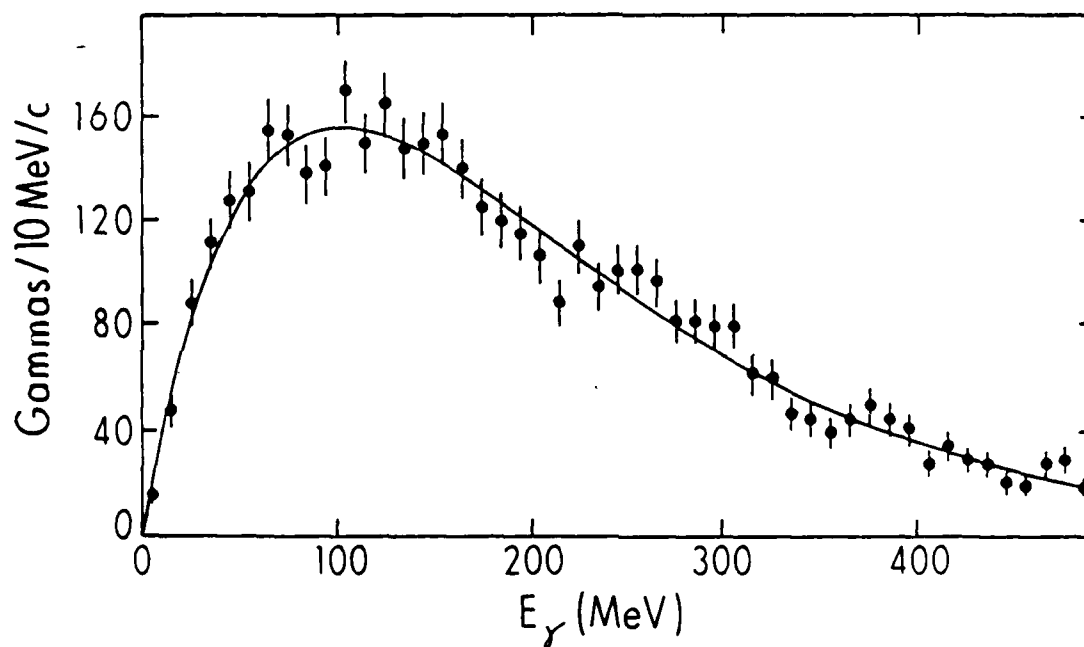


Fig. 12. The γ -ray spectrum of $\pi^0 \rightarrow 2\gamma$ decays from stopping antiprotons in deuterium from Ref. 16. The curve is a fit with the function $E \cdot \exp(-E/T)$ where $T = 104$ MeV.

These energetic gammas can provide another way of determining the coordinates of the annihilation point. In principle, they can determine the vertex more accurately than the charged pions which undergo Coulomb scattering, but measurement errors are typically smaller with charged particles than with γ -rays. Fig.13 shows a photograph of a $\bar{p}p$ annihilation into $3\pi^0$ ($\rightarrow 6\gamma$). The γ -rays were detected by a 72 steel layer spark chamber¹⁷ which surrounds the annihilation point. Extrapolation of the lines drawn thru the γ showers intersects the vertex.

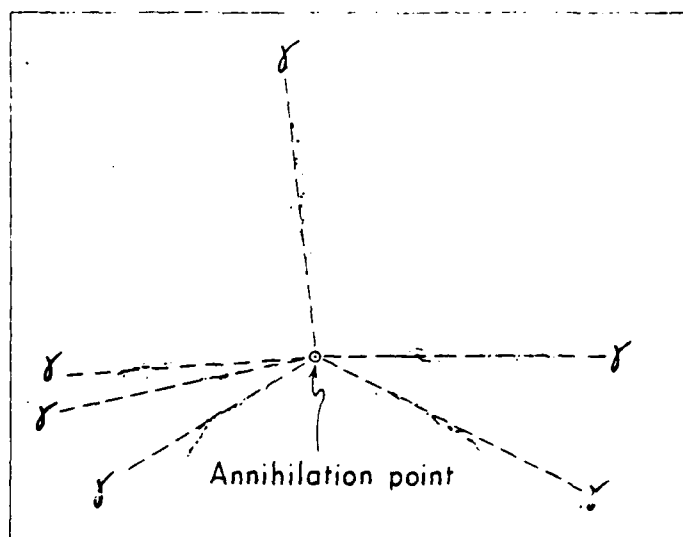


Fig. 13. An antiproton-proton annihilation into $3\pi^0 \rightarrow 6\gamma$ seen by a 4π spark chamber from an AGS experiment (Ref. 17). The eye-drawn lines through the showers extrapolate to the annihilation vertex.

C. Imaging the Electron Density

1. Antiprotonic Stereography

Gray and Kalogeropoulos proposed¹⁸ to use the dependence of the stopping range of antiprotons on incident energy and produce 3-dimensional images. This technique is in principle different than other imaging techniques, such as CT's with x-rays¹⁹ or charged particles²⁰, where one measures integrals of absorption or energy loss along the beam. These transmission techniques require irradiation of a plane from many directions and a mathematical inversion (the Radon transformation or equivalent) before the "density" over the plane is inferred. These transmission techniques can create artifacts²¹.

ASTER (Antiprotonic Stereography) measures dE/dx directly at any point in the target which, via eqn.1, is well defined in terms of the concentration of constituents. Briefly, the method consists of measuring along the beam

$$\Delta E / \Delta \bar{R} \equiv (E_1 - E_2) / (\bar{R}_1 - \bar{R}_2). \quad (7)$$

which is proportional to the average density of electrons between points 1 and 2. Such measurements over the volume of interest are used for imaging. The points 1 and 2 can

be as close as one wishes as long as one measures \bar{R}_1 and \bar{R}_2 with sufficient accuracy. Moreover, the accuracy of $\Delta E/\Delta \bar{R}$ depends upon the ratio $\sigma_{\bar{R}}/\Delta \bar{R}$ if the error of ΔE is negligible. Thus both the resolution ($\Delta \bar{R}$) along the beam and contrast (rms standard deviation of $\Delta E/\Delta \bar{R}$) depend upon $\sigma_{\bar{R}}$. The rms standard deviation of the range, $\sigma_{\bar{R}}$, is given by

$$\sigma_{\bar{R}} = \sigma_v / \sqrt{N_{\bar{p}}} \quad (8)$$

where σ_v is the reconstructed vertex error per antiproton and $N_{\bar{p}}$ is the number of antiprotons used in the measurement of \bar{R} . Thus resolution and contrast along the beam axis are not in principle limited. The resolution transverse to the beam is approximately equal to σ_v .

Fig.14a summarizes the various uncertainties which contribute to σ_v in water.¹⁸ It shows the dependence on beam energy spread (σ_E), straggling of the antiproton (σ_s), and Coulomb scattering of the charged pions going through 10 cm of water and extrapolated to the vertex (σ_m). The error of the pion Coulomb scattering dominates for thick (> 10 cm) targets. However, if one could construct a γ -ray detector of high (< 10 mradians) directional accuracy then the σ_m contribution to σ_v would become negligible in comparison to the antiproton straggling. We have simulated antiproton annihilations at the center of a spherical water phantom. The charged pions going through the phantom provide, by extrapolation, the vertex. The contribution of each pion has been weighted according to its momentum (energetic pions have less Coulomb scattering) and an angular geometrical factor. Assuming that measuring errors are negligible the vertex reconstruction rms error shown in Fig. 14b has been obtained. The dependence of σ_v on the radius is:

$$\sigma_v(mm) = 5.1 \times 10^{-2} \times R^{3/2} \quad (9)$$

where R is in cm. This yields e.g., 1.6 mm at $R = 10$ cm. In summary, a σ_v of 1 mm or less can be achieved. Fig.15 shows an example²² of an ASTER computer simulation of a planar phantom 1 mm thick. The important features of ASTER are:

- ♠ Three dimensional imaging can be done as fast as the electronics determining the vertex allows. (There are no mechanical movements!).
- ♠ (As in photography, where the field of view is adjustable) the volume to be imaged is adjustable. Thus, one may image only the region(s) of interest.
- ♠ Furthermore, ASTER measures dE/dx directly, just as photography measures light intensity. In short, ASTER is three dimensional volume "photography".
- ♠ There are no fundamental limitations in resolution along the beam or in $\Delta E/\Delta \bar{R}$ accuracy which is essential for contrast of different densities. The limitations come from the number of antiprotons used. Transverse to the beam, the resolution is perhaps limited by σ_{\perp} (eqn.3) or at best by vertex reconstruction accuracy.

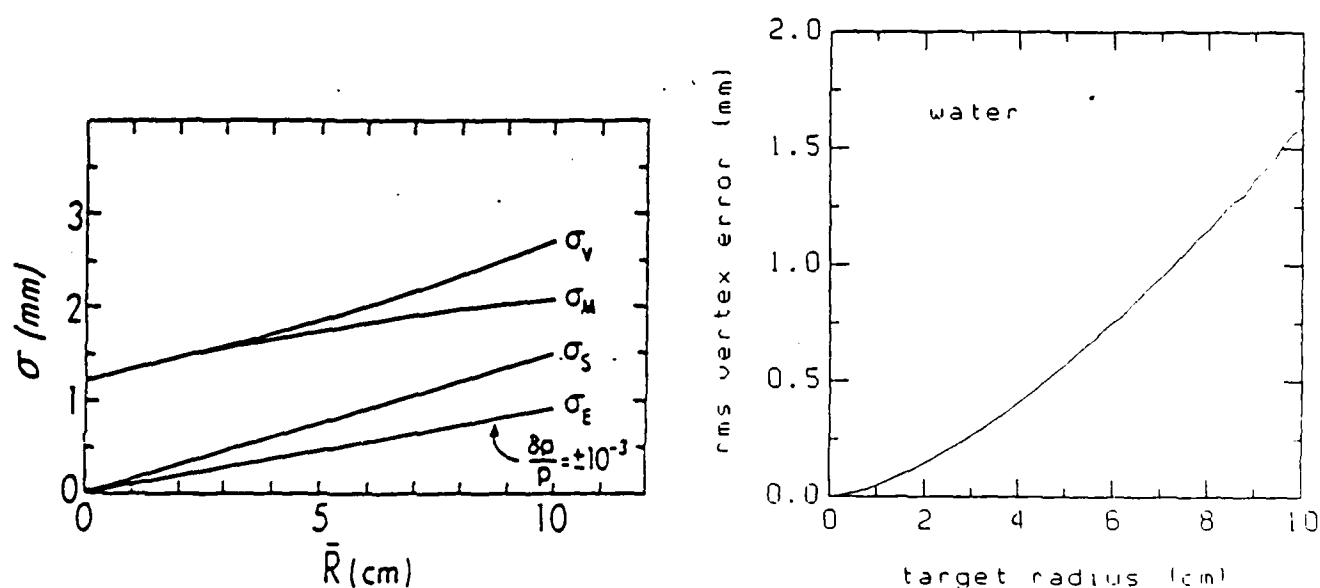


Fig. 14. Vertex position errors along the beam. (a) σ_E is rms standard deviation in stopping position due to the incoming beam momentum spread of 10^{-3} . σ_s is the rms error of the stopping point due to antiproton straggling. σ_m is the rms error from the extrapolation of charged pion tracks which is a combination of measuring (1 mm) and Coulomb scattering in 10 cm of water. The overall vertex error is $\sigma_v = (\sigma_E^2 + \sigma_s^2 + \sigma_m^2)^{1/2}$. (b) Ultimate vertex reconstruction error based on charged pions at the center of a spherical water target as a function of the radius.

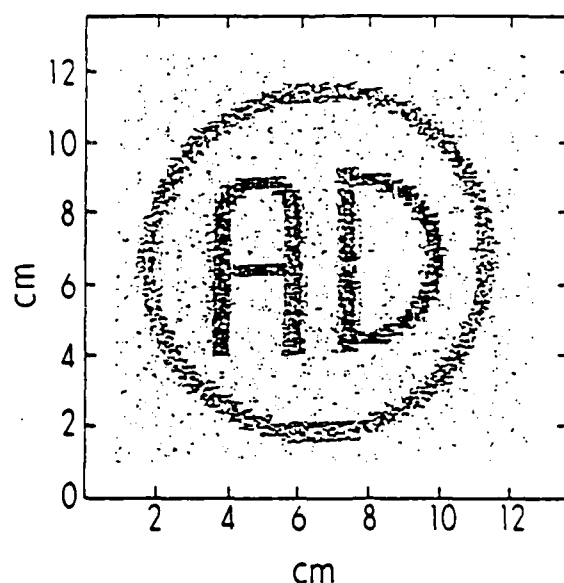


Fig. 15. Computer simulated ASTER of a phantom imbedded in water. The number of dots is proportional to the measured density minus the water density. The thickness of the target is 1 mm and the scanning has been made on a $1 \times 1 \text{ mm}^2$ grid.

It was estimated²³ that about 10^9 antiprotons are needed to image a volume of 1500 cm^3 (e.g., a human head) with 1% rms $\Delta E/\Delta \bar{R}$ point measurements over a grid of $2 \times 2 \times 2 \text{ mm}^3$ and σ_v given by Fig.14. This number can be reduced substantially by better vertex determination, larger grid size, or larger $\Delta E/\Delta \bar{R}$ errors. For example, if one improves σ_v by a factor of two then the number of antiprotons decreases by a factor of four; or if the grid size increases to $3 \times 3 \times 3 \text{ mm}^3$ then $N_{\bar{p}}$ decreases (see eqn. 10) by a factor of $1.5 \times 1.5 \times 1.5^2 = 11$; or if the $\Delta E/\Delta \bar{R}$ error increases by a factor of two, then $N_{\bar{p}}$ decreases by a factor of four. If the head was imaged with a 3-dimensional grid of 3 mm with point $\Delta E/\Delta \bar{R}$ errors of 2% and a detection system minimizing the vertex error then 10^7 antiprotons would be needed which are equivalent to a head dose of $\sim 10 \text{ mrad}$ s.

2. X - Ray CT Versus ASTER

An x-ray CT scan measures x-ray absorption which is proportional to the density of electrons. ASTER also measures a similar quantity. (By contrast NMR measures hydrogen density). Therefore both ASTER and x-ray CT imaging measure, to first order, the electronic density. In a CT scan one measures the electronic density $\rho(x,y)$ of a planar

section (tomos) of thickness, Δz , where the z axis is normal to the plane. Thus, the density $\rho(x,y)$ of the section is projected onto the xy plane with pixel size $\Delta x \cdot \Delta y$. Scans with $\Delta z = 1\text{cm}$, $\Delta x = \Delta y = 1\text{ mm}$ and $\delta\rho/\rho \approx 0.5\%$ (equivalent to 2 rads) are routinely made in hospitals.

Consider the corresponding ASTER imaging where the antiprotons are brought normal to the plane. It can be easily shown using eqn.13 of Ref.18 that

$$N_{\bar{p}}^{\text{rest}} = 2 \cdot (A/\Delta x \Delta y) \cdot (\sigma_v/\Delta z)^2 / (\delta\rho/\rho)^2 \quad (10)$$

where A is the area of the slice and $N_{\bar{p}}^{\text{rest}}$ is the number of antiprotons annihilating at rest or about 80% of the entering. Using the same parameters as above ($\Delta x = \Delta y = 1\text{ mm}$, $\Delta z = 1\text{ cm}$, $\delta\rho/\rho = 0.5\%$), $A = 10 \times 10\text{ cm}^2$ and $\sigma_v = 1\text{ mm}$, a total of 10^7 antiprotons are needed. (Their present cost is a few cents!). This number can in principle be decreased by about two orders of magnitude if the vertex is reconstructed using $\pi^0 \rightarrow \gamma$ -rays.

The dose of radiation is

$$\text{Dose (rads)} = \frac{10^{-7}}{6} \times \frac{N_{\bar{p}} \cdot E_{\bar{p}}}{A \cdot \Delta z} \quad (11)$$

where $E_{\bar{p}}$ is the average deposited energy per antiproton to the imaged volume. We estimate on the basis of Ref.23 that $E_{\bar{p}}$ is about 90 MeV with contributions from the slowing down of the antiproton (45 MeV), charged pions (8 MeV), neutrons (3 MeV), γ -rays (1 MeV) and charged nuclear fragments (30 MeV). Thus the radiation dose from imaging the slice is about 150 mrad, a factor of 13 smaller than the CT imaging of identical quality. At 2 rads ASTER can produce pictures with 0.5 mm pixel size, slice thickness 5 mm, and $\delta\rho/\rho = 0.5\%$.

If radiation dose is not a problem, ASTER can yield pictures of any desired quality down to three dimensional pixel size of about 0.5 mm depending on depth while CT is already operating near its practical limits. Moreover, ASTER can image any part of the section, has no deconvolution artifacts, can be done in much less than 1 sec, employs a simpler detector which does not require calibrations.

3. Antiprotonic CT

The antiprotons can be used like protons for charged particle tomography²⁰. The advantage of charged particle tomography over x-ray tomography is lower dose and smaller slice thickness (~ 1 mm). The advantage of antiprotons over protons is the simplicity of the apparatus. For example, the energy of the exiting antiproton can be deduced easily by measuring for example its stopping point in water.

4. Stopping Power In Biological Media

ASTER images dE/dx and therefore the contrast of organs and abnormalities depends on the accuracy of dE/dx measurements and differences in dE/dx among adjacent organs. Koehler and Johnson²⁴ have made in vivo measurements of dE/dx (relative linear stopping power) which are reproduced in Fig. 16. The dE/dx varies from about a half (gray/white matter) percent to three percent among various soft and non-fatty tissues. These measurements imply that ASTER with point measurement errors of about a half percent is expected to produce good quality diagnostic images. If one uses a 3-D pixel size of 2 mm, abnormalities with volumes of $(0.2 \text{ cm})^3 \approx .008 \text{ cm}^3$ can be detectable which are almost a factor of 100 smaller than with CT scans.

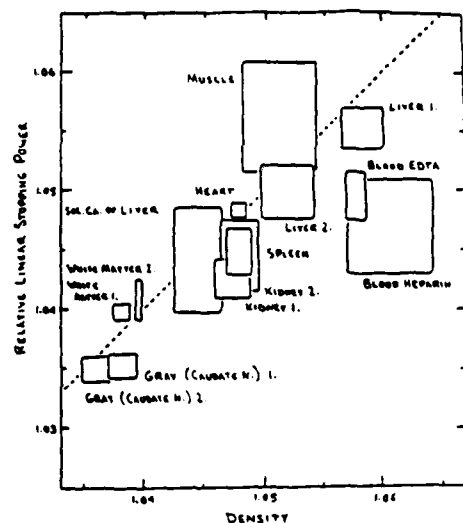


Fig. 16. Results of stopping power and density measurements on non-fatty tissues. For each tissue the range of measured values obtained is indicated by the dimensions of the rectangle. The dotted line represents a one-to-one correspondence between linear stopping power and density.

5. Micro - ASTER

It is of practical importance to raise the question of whether imaging at the micron level is possible with ASTER. To be more specific we looked at whether we can do the same quality CT imaging as was done recently at the Brookhaven light source²⁵. The imaged samples of $(500 \mu\text{m})^3$ were made with pixel size of $2.8 \mu\text{m}$ and accuracy of 2%. Because of the small mass of the target the vertex can be measured with an rms error of less than $10 \mu\text{m}$ (see eqn. 9). Using eqn. 10 we deduce that the same quality pictures can be made by using two antiprotons per pixel or a total of about $10^5 \bar{p}$. This micron imaging may find special applications in biomedical science as well, because of speed and the information being directly computerized.

IV. ENERGY PROFILES AND THERAPY

A. Nuclear Fragments

Study of annihilations in emulsion²⁶ have shown that $393 \pm 36 \text{ MeV}$ are transferred to the nucleus per annihilation. This goes mainly into protons and neutrons. Recent work at LEAR shows that a great wealth of information is provided by the capture of antiprotons in nuclei²⁷.

1. Heavy Prongs

The charged nuclear fragments, mainly protons, are called "heavy prongs" because of their high ionizing power (LET) which is due to their low energy. Their spectra and multiplicity in emulsion nuclei²⁶ are shown in Fig.17. On the average 144 MeV per annihilation are given off to the three heavy prongs. A proton with an average energy of 43 MeV travels about 1.5 cm in water but because many of them peak at energies below 43 MeV (Fig.17c), they stop closer to the vertex on the average.

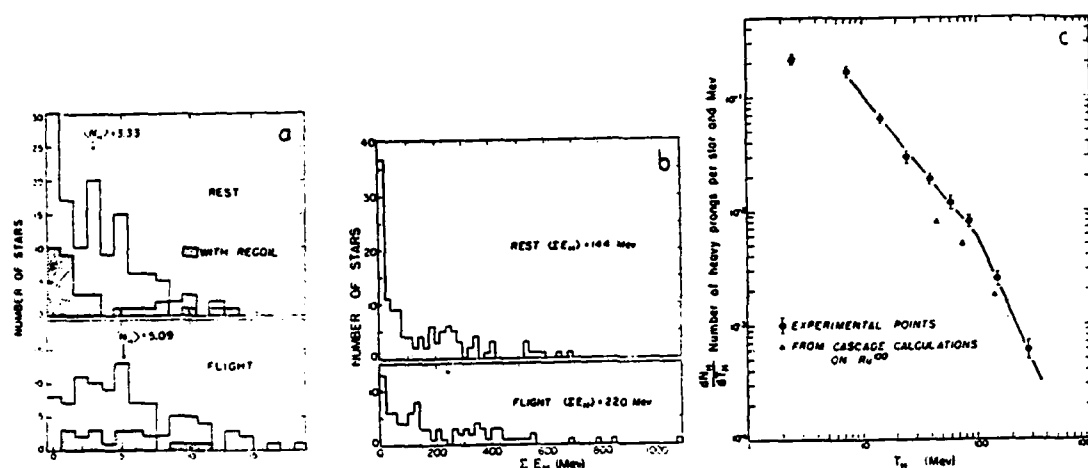
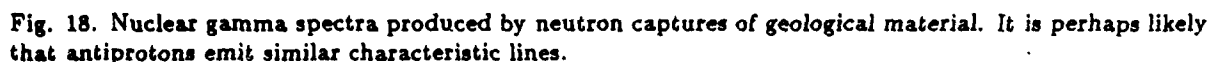


Fig. 17. Heavy prongs released by the excitation of emulsion nuclei by at rest and in flight annihilations. (a) number of events versus heavy prong multiplicity. (b) number of events versus total energy released into heavy prongs assumed to be protons. (c) spectrum of heavy prongs assumed to be protons.

2. Neutral Fragments and Nuclear γ - Rays

The energy going into neutrals is a factor of 1.7 larger than that going into the heavy prongs. Nuclear cascade calculations²⁸ show that most of this energy goes into neutrons. Most of these neutrons escape from the body.

A small fraction of the neutral energy must be going into nuclear γ -rays with typical energies of a few MeV. Nothing is known experimentally about them at present but it is reasonable to assume that they will be similar perhaps to those observed (Fig.18) in neutron captures²⁹. These γ -rays are expected to exhibit peaks in their energy spectrum which are characteristic of nuclear transitions.



Gray and Kalogeropoulos considered antiprotons for radiation therapy²³. They simulated the energy profiles of the energy deposited by the charged particles, namely, the antiprotons, charged pions, and heavy prongs. Fig.19a shows the energy projected along the beam for four incident beam energies stopping at various depths in water. The sharp peak in the stopping region is the result of the antiproton Bragg peak further enhanced by nuclear fragments. These nuclear fragments, being high in dE/dx (LET), have a high Relative Biological Effect (RBE), an effect which has to be accounted for in calculating the dose equivalent from the absorbed dose calculated above. The peak decreases with depth because of antiproton losses due to the in-flight interactions.

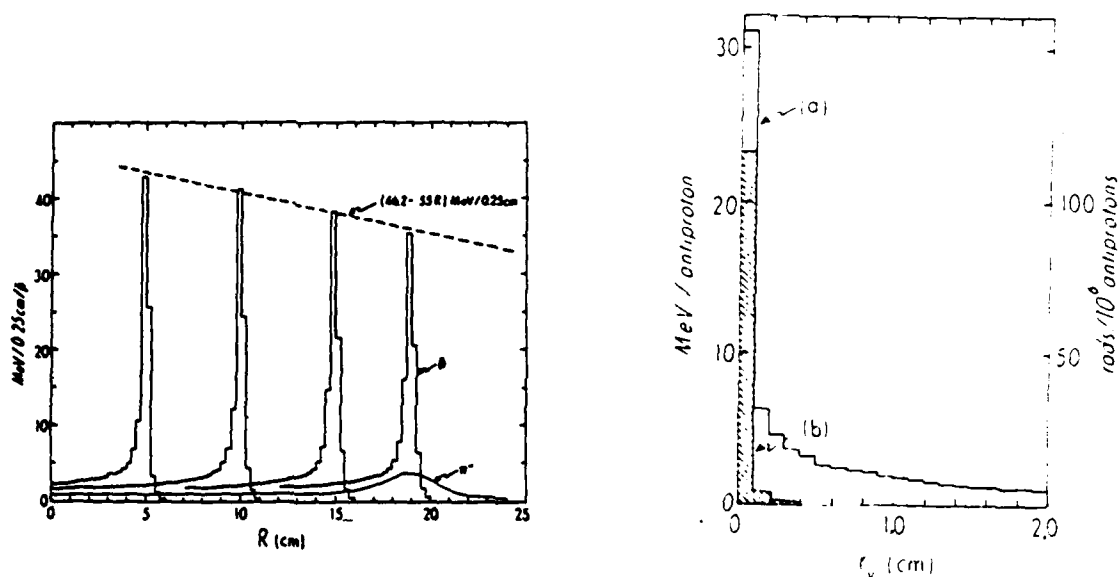


Fig. 19. Estimated energy released by antiprotons. (a) projected to the beam axis, and for four beams brought to rest at different water depths. (b) energy deposited in spherical shells from stopping antiprotons at the center of the sphere. Shaded histogram shows dose as a function of distance from the stopping point.

A radial profile from the annihilation point of the energy released is shown in Fig. 19b. The energy released within a sphere of 1 mm of radius is a factor of six larger than that in the spherical shell between $r = 1 \text{ mm}$ and $r = 2 \text{ mm}$. If the energy released in the shells is divided by their volume the absorbed dose is seen to be sharply limited to the region around the annihilation point.

Gray and Kalogeropoulos compared various charged particles for therapy purposes. In therapy one optimizes the ratio of the radiation delivered inside the tumor to that delivered outside, the relative dose or advantage factor. Fig. 20a gives the axial dose distributions achieved by different particle beams from uniformly irradiating tumors of various sizes located up to 12 cm of water equivalent depth. The antiproton is superior to all other particles. From these distributions the "advantage factor" (the ratio of the transversely to the beam integrated energy inside the tumor to that outside) as a function of tumor size has been obtained (Fig. 20b). For a tumor of 2 cm the advantage factor for antiprotons is a factor of about three larger than that for protons and deteriorates down to about

a factor of two for larger tumors. Sullivan³⁰, motivated by these simulations, measured with an ionization chamber the energy profile of antiprotons and protons using antiprotons from LEAR. His results are reproduced in Fig.21. These measurements are in reasonable agreement with the calculations.

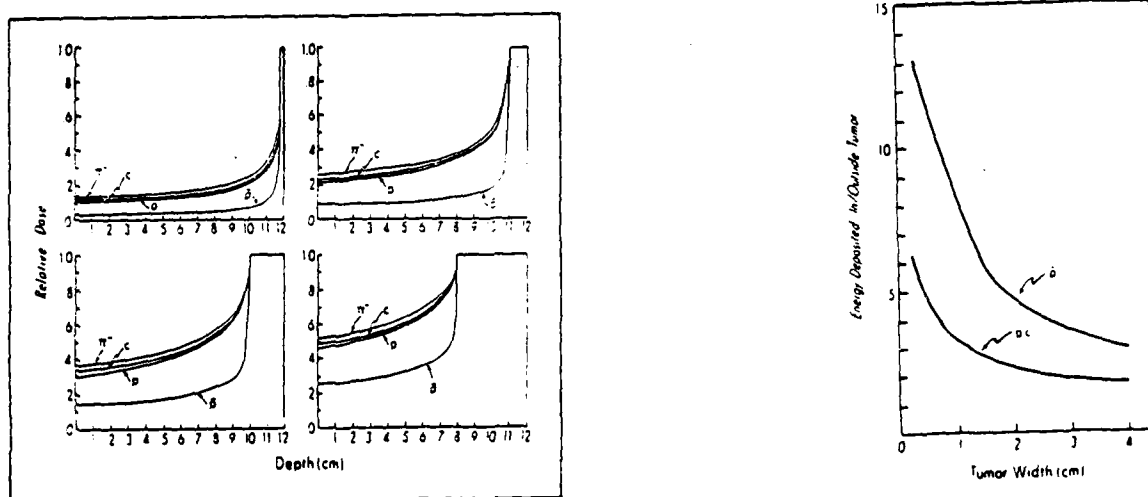


Fig. 20. Comparison of dose distributions with different charged particle beams. (a) computer simulations of the dose profile along the beam by delivering a uniform dose in a region of variable thickness located at 12 cm. The dose beyond 12 cm decreases rapidly and is not shown. (b) comparison of proton, antiproton delivery advantages using the distributions in (a).

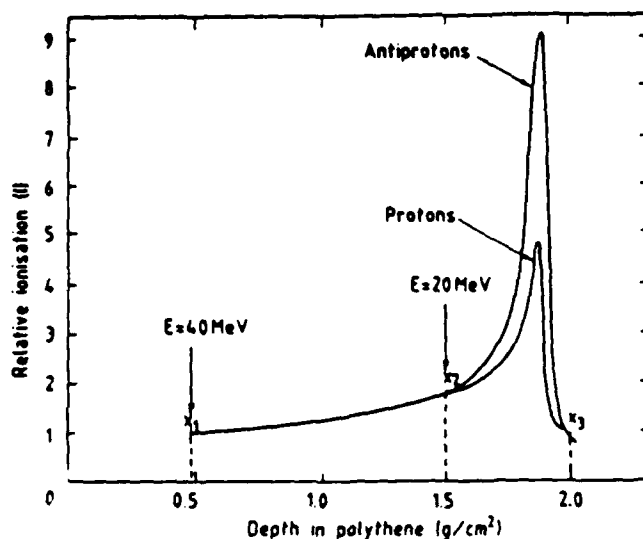


Fig. 21. Experimental measurements of the dose distribution with protons and antiprotons.

It has been estimated²³ that treatment of malignancies require 10^9 to 10^{10} antiprotons per 1 cm^3 depending on the biological factor (RBE). If LEAR were to be used exclusively for therapy, tissue volumes of about 100 cm^3 to 1000 cm^3 could be treated daily. Besides the dose advantage, the antiprotons are unique in regard to delivery. The availability of the coordinates of the stopping point gives the opportunity for feedback control of dose delivery. Various scenarios can be envisioned to take advantage of the knowledge of the stopping point. A most desirable one is to image the tumor via ASTER and then guide the delivery of either protons or antiprotons. This is simple, precise and can be totally under computer control. Because of the problem of antiproton availability, one may consider instead antiprotons as simulators³¹ of therapy with other charge particles. A few antiprotons would suffice to pin point the stopping position and define the energy required of the particle to be used for therapy.

In summary, the antiprotons have the best dose advantage among all charged particles and in addition, the delivery of radiation can be made easily and precisely under computer control. An improvement in antiproton collection of the order of 10 to 100 will make the antiproton the particle of choice for sensitive radiation treatments.

V. ANTIPROTONIC ATOMS

A. The Capture Process

When the antiprotons come to rest in matter they are attracted by the Coulomb field of the nuclei and form, like the μ^- , π^- , K^- , and Σ^- , "exotic" atoms. The mechanism of capture is complicated and poorly understood today. Fermi and Teller³² predicted that the capture probability (P) in a mixture of elements is proportional to the concentration (C) and atomic number (Z) of the element. Namely

$$P(Z) \propto C(Z) \cdot Z \quad (\text{Fermi - Teller Law}) \quad (12)$$

Experimentally, the law is poorly satisfied as the data³³ of Fig.22 show. Transfer mech-

anisms and molecular effects may produce as much as one to two orders of magnitude deviations³⁴. For example, the capture of π^- by hydrogen in a mechanical mixture of $N_2 + 2H_2$ is a factor of 30 larger than in hydrazine (N_2H_4). A complete theory of capture must include important modifications of the Fermi-Teller law and take into account chemical and transfer effects. Such modifications have been made for $H_n Z_m$ compounds (hydrides) assuming formation of macromolecules³⁴.

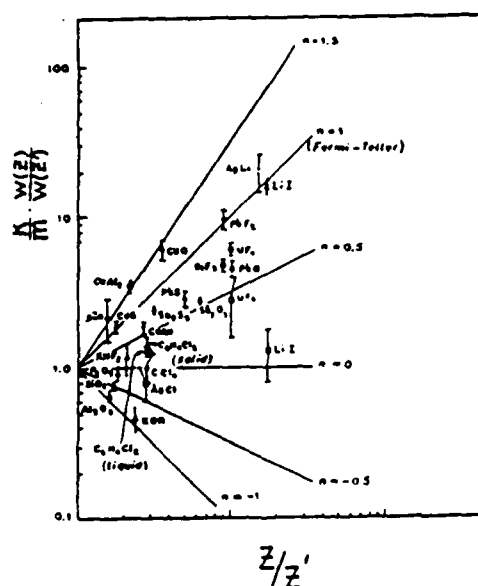


Fig. 22. Comparison of the Fermi-Teller law of capture for various compounds.

For our purposes, one should only remember that measurements of capture probabilities carry important elemental and chemical information which can be of great value to biomedical research and practical applications. What one needs, however, is the signature of the capture to a specific nucleus. Atomic x-rays produced by the cascade of the antiproton to lower atomic states are therefore of special interest.

B. Antiprotonic X-rays

Antiprotons reaching principal quantum numbers less than $\sqrt{m_p/m_e}$ ($= 43$) are unshielded by the electrons and can be treated like the hydrogen atom with nuclear charge $+Ze$. The dominant cascade transitions³⁵ are $n \rightarrow n-1$ and the corresponding x-ray energy

is:

$$E_n(\text{KeV}) \simeq 4.9 \cdot Z^2/n^3 \quad (13)$$

for $n \gg 1$. The antiproton as it cascades to the ground state gets absorbed by the nucleus and annihilates. From the data³⁵ shown in Fig. 23, the minimum n value (which corresponds to the maximum x-ray yield) as a function of Z has been estimated. From this, the following approximate relation is obtained for the "critical" energy (E_c) for which the yield is maximum:

$$E_c(\text{KeV}) \simeq 4 \cdot Z. \quad (14)$$

Thus for oxygen this line is expected at about 32 KeV and the spectrum shown in Fig.24a confirms it. For lead ($Z = 82$), this line is expected at about 338 KeV while the one observed (Fig.24b) is near 290 KeV. Except for the common light elements H, O, C, and N, most of the elements of biological interest have their dominant x-rays in the range of 90 to 200 KeV. Such energies are sufficient for a good fraction of the x-rays to exit the body and be easily detectable.

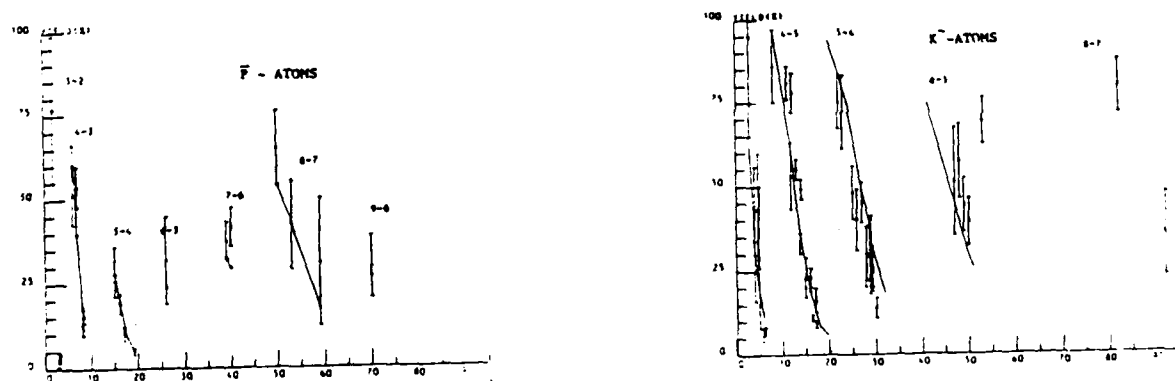


Fig. 23. Yields of $n \rightarrow n-1$ x-rays from K^- and \bar{p} exotic atoms as a function of Z . It indicates the lowest levels from which the nuclear absorption occurs.

$\pi^+\pi^-(K^+K^-)$ are not collinear. Fig.25a shows Monte Carlo generated distributions of these two body annihilations as a function of the collinearity angle in a mixture which results in 1% captures in hydrogen and 99% in carbon. The hydrogen signature is clear at small angles and can be substantially improved over the background with smaller angular errors. This signature has been used to make the only available measurement of antiproton capture rate. Fig.25b shows the scattergram of the momenta of the collinear events³⁶ and confirms the expectation that collinear events are due to hydrogen. The disadvantage of this signature is its low yield which is equal to the branching ratio for these collinear annihilations. Their combined branching ratio³⁷ in hydrogen is 4×10^{-3} . In principle, however, a magnetic detector can be used to find other hydrogen signatures such as $\bar{p}p \rightarrow 2\pi^-2\pi^+$ which might increase the efficiency to as much as 10%.

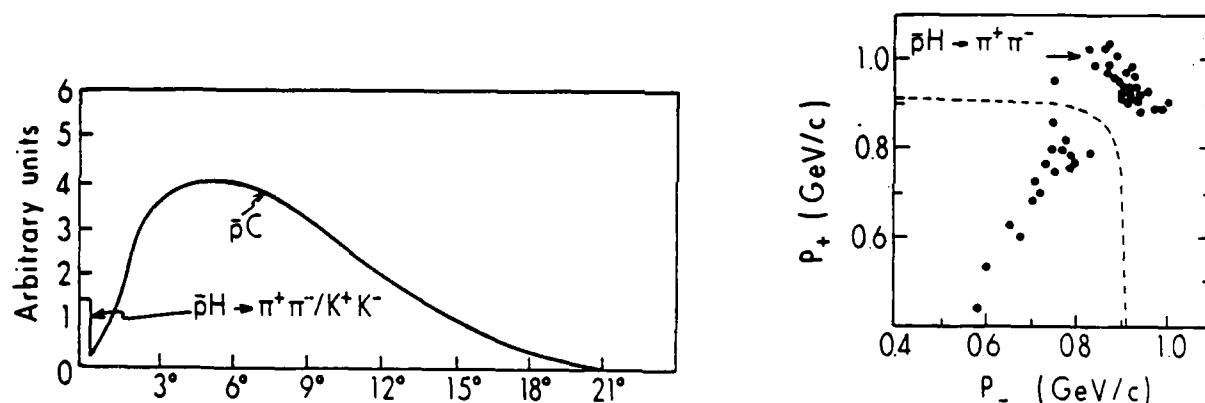


Fig. 25. Measurement of \bar{p} hydrogen capture rate in homogeneous targets via the collinearity of the two body $\pi^+\pi^-$ and K^+K^- final states. (a) expected angular distribution between two charged particles from a hydrogen - carbon target where only 1% of the antiprotons are captured by hydrogen. The peak at zero angle is the \bar{p} -hydrogen signal. (b) measurement of $\bar{p} - H$ in a propane bubble chamber showing the scattergram of the two track momenta for "almost" collinear two-prong events.

VI. IMAGING OF ELEMENTS

"Mesic Chemistry" of exotic atoms in vivo and in vitro has been recognized for some time as a potentially powerful tool^{34,35,38} for biomedical applications. The muon, because of its long (2 μ sec) lifetime and absence of strong interactions, almost always arrives to the ground state before decaying. Consequently, it emits x-rays of hundreds of KeV which

have good transmission. On the other hand, the muon has the following problems:

- ◆ Intense μ^- sources are difficult to get and in addition, they will always be associated with a high (500 to 1000 MeV) proton accelerator. Typical experiments measuring muonic atomic x-ray spectra are made with about 10^7 to $10^8 \mu^-$.
- ◆ Because of its low mass, the stopping region of muons is broad.
- ◆ The hydrogen x-ray energies are too small (2 KeV) to be useful for in vivo studies.

However, imaging of elements with antiprotons is very promising and may finally fulfil visions of "mesic chemistry". This optimism is justified because:

- ◆ The development of transportable antiproton sources will make antiprotons available to hospitals and research laboratories.
- ◆ The stopping region is small ($\sim 1 \text{ mm}^3$) and can be monitored via the pions.
- ◆ All elements provide signatures via their x-ray emissions or nuclear gammas. (Hydrogen also provides a signature via the kinematics of annihilations).
- ◆ A head dose of 1 rad ($\sim 10^9 \bar{p}$) is sufficient to image all elements at once.

Fig.26 shows the γ -ray mean free path in water as a function of γ -ray energy. The mean free path changes rapidly with energy. The "critical" x-ray energy in carbon is about 50 KeV and has a 4 cm mean free path. Thus, even at 10 cm of depth, 10% of these carbon x-rays will exit, while for phosphorus 20% of them survive. On the other hand, most nuclear γ -rays will exit the body. Taking concentrations of various elements from the "Standard Man"³⁹ and assuming the Fermi-Teller law of capture, the probability of forming various antiprotonic atoms has been calculated (Table I). If we assume that 10^3 x-rays of an element are sufficient to measure its rate, then with a 4π detector the sensitivity to detect an element is of the order of 10^{-6} which makes possible measurements of some trace elements.

Table I. Antiprotonic Atoms in "Standard Man"

Element	Formation ^(a) probability (%)	Captures detected ^(b) , millions per $10^9 \bar{p}$
Oxygen	56.0	56.0
Carbon	21.0	21.0
Hydrogen	18.0	1.0
Nitrogen	2.3	2.3
Calcium	1.3	1.3
Phosphorus	1.0	1.0
Sulfur	0.2	0.2
Potassium	0.2	0.2
Sodium	0.1	0.1
Chlorine	0.1	0.1
Magnesium	0.03	0.03
Silicon	0.03	0.03
Iron	0.005	0.005
Fluorine	0.004	0.004
Zinc	0.004	0.004
Rubidium	0.0004	0.0004

(a) The Fermi-Teller law was assumed and concentration given for "Standard Man".

(b) 10% characteristic x-rays detected per annihilation and from hydrogen the combined branching into $\pi^+\pi^-$, K^+K^- of 4×10^{-3} were assumed as detection efficiencies.

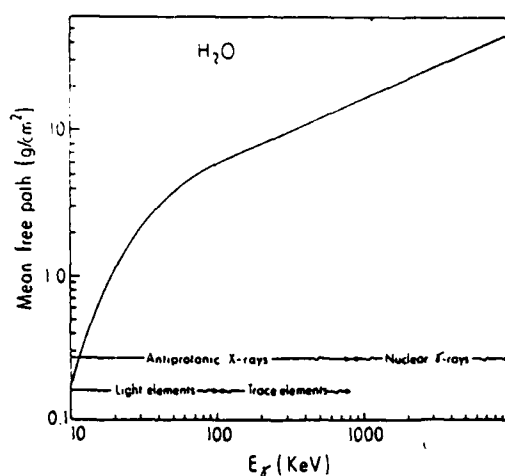


Fig. 26. Mean free path as a function of gamma energy in water and an overview of the applicability of antiprotonic x-rays and nuclear γ -rays.

If we were to image the head with 10^9 antiprotons (~ 1 rad) using 4π detectors and assuming 0.1 useful x-rays detected per atom then images of common constituents up to phosphorus can be made with millions of events. These are one to two orders of magnitude estimates. They will be affected by variations³⁹ of the concentration of elements in the body and will likely be strongly influenced by the chemical environment. For example, images of hydrogen and oxygen (mostly water) may be of special interest for tumor imaging. NMR (Fig.27) measurements⁴⁰ show that the relaxation time T_1 increases with the water content. Perhaps like T_1 , the capture rate may similarly be sensitive to the water content and, besides providing good tumor images, may perhaps be tumor specific.

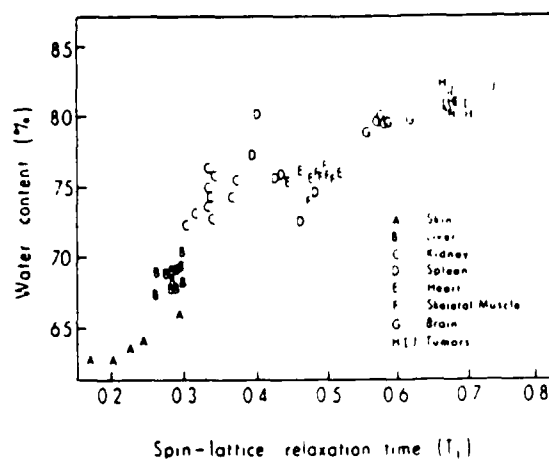


Fig. 27. Dependence of the relaxation time (T_1) on the water content of various human organs and malignancies.

VII. PROPOSED RESEARCH PROGRAM

While the development of antiproton sources is proceeding, an exploratory and development program should commence as soon as possible. This program can be carried out initially in an existing antiproton beam at the AGS where the beam may be available, for example, for about a month per year. LEAR is also a possibility.

A. Experimental Setup

1. Beam

The AGS low energy separated beam, LESBII, delivers about 10^7 stopping antiprotons per hour. Thus, in 100 hours, which is typically equivalent to one week of running, a "standard" measurement with 10^9 antiprotons can be made. The beam momentum varies up to 750 MeV/c and the momentum bite up to $\pm 2.5\%$. The momentum of each antiproton can be tagged easily with an accuracy of a few parts per thousand. The antiproton rate of about 10 KHz is at a level that makes the reconstruction of vertices on-line possible with a parallel configuration of micro-VAX's and thus considerably reduce the data transferred to tape.

2. Detector

The detector must have good coverage of the target, measure charged particle directions accurately, distinguish $\bar{p}p \rightarrow \pi^+\pi^-$ from K^+K^- and have a target area which can be easily adapted to different experimental needs. Fig.28 is a conceptual diagram of such a detector. The Inner (ICDC) and Outer (OCDC) cylindrical drift chambers measure directions of charged particles including the antiproton. The antiproton energy can be varied by adjusting the incident beam momentum and degrader thickness (D). The sixteen scintillation counters (S_i) measure time of flight (TOF) and resolve the $\pi^+\pi^-$, K^+K^- channels.

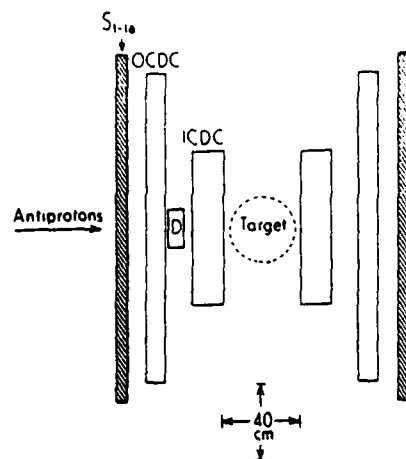


Fig. 28. A conceptual design of a detector to address biomedical applications. The two cylindrical drift chambers (ICDC, OCDC) measure the directions of the charged particles. The scintillators (S_i) measure the TOF.

Typical present detector performance for the various components is assumed. The detector must be adequately instrumented with equipment capable of handling the data rates for on-line analysis and storage for further off-line analysis.

3. Target

The target area consists of a three dimensional stage which is controlled by computer. This will allow the experimenter to send the antiproton beam in any direction through the irradiated object. In addition, x-ray and γ -ray detectors will be located within this area.

3. Data Handling

Wire chambers easily operate at 1 MHz. A cylindrical detector with tracking cylinders of 10^3 wires each provides the raw information for 10^9 charged particles per second. This information is used to reconstruct straight lines, vertices and stopping distributions. This calculational phase has to be ultimately addressed in a practical system. At the AGS, where the antiproton rate is ~ 10 KHz, off-the-shelf electronics and parallel microprocessors will be more than sufficient.

B. Research and Application Program

We envision a program which can be broken into the following phases:

1. Detector Construction and Installation

This is a two year program. It involves beam instrumentation, drift chambers, time-of-flight, target stage, an x-ray solid state detector, a nuclear γ -ray detector, data handling processors and software development. The cost estimate of the detector is \$600 K with details given in Table II.

Table II. Detector Cost Estimates

Drift Chambers (including electronics)	175 K
Gas System	10 K
TOF	70 K
Beam instrumentation	15 K
Vertex processors	80 K
Data acquisition	150 K
x- and γ -ray detectors	50 K
Miscellaneous (10%)	50 K
	<hr/> \$600K

2. Charged Particle Applications

The following three year program can be envisioned:

- ◆ Test and improve delivery systems used in present therapy with protons and heavy ions by measuring the stopping point.
- ◆ ASTER imaging of various organs and comparison with CT.

- ◆ Exploratory hydrogen imaging and search for specificity.
- ◆ In parallel with the charged particle work, x-ray and nuclear γ -ray spectra will be collected. The analysis of this information will be essential in evaluating "chemical imaging" and lead to the third phase. This phase will require beams like those available at LEAR and an x-ray or/and γ -ray large solid angle detector.

VIII. SUMMARY AND CONCLUSIONS

Antiproton production and accumulation in accelerator centers has been exponentially improving over the last 30 years. It has reached rates which are already sufficient for many biomedical applications and is at the threshold for using them for therapy. Moreover, efforts are currently in progress to make them available to anybody and everybody, by storing them in transportable rings.

The antiproton mass implies typical spatial definition of the stopping region of a beam of antiprotons entering water like targets of about 1 mm depending on depth. The annihilation products (charged pions and γ -rays) mostly exit the target and by using detectors external to the body the annihilation or stopping point of every antiproton can be measured with a typical precision of 1 mm. This feature is unique among all known stable particles and can be used for direct imaging and monitoring radiation treatments.

Imaging of the electronic density has been computer simulated and compared with CT x-ray imaging. ASTER (antiprotonic stereography) is superior to CT imaging. It is direct, images any volume without exposing other parts to radiation, is not limited in accuracy of the electronic density, is not limited in spatial resolution along the beam, there are no moving parts, and the radiation dose for the same quality imaging is better than an order of magnitude smaller than x-ray CT.

Due to the release of slow nuclear charged fragments from annihilations in complex nuclei, the radiation by antiprotons is better localized than protons or any other particles.

Computer simulations show that the advantage factor (dose in the tumor over that along the beam) is a factor of 2-3 larger than protons or heavy ions. One to two orders of magnitude improvement in production-collection of antiproton capabilities, which can easily be foreseen, will make precise computer controlled therapy treatment with antiprotons the modality of choice particularly for the smaller tumors or/and those near sensitive organs.

The antiprotons upon coming to rest are captured by nearby nuclei and form antiprotonic atoms before they annihilate on the nucleus with which they formed these 'exotic' atoms. It is known that the capture probability on a particular nucleus is proportional to its concentration and nuclear charge but orders of magnitude deviation have been observed. These deviations depend on the molecular structure or the local chemistry. Therefore measurements of capture rates to specific nuclei are of high promise to biomedical research and applications.

Signatures to measure the capture rates of stopping antiprotons to all nuclei are provided by characteristic x- and γ -rays or by annihilation reactions. It is estimated that concentrations in vivo as small as about one atom per million can be reached, thus making possible in vivo measurements of even some trace elements.

The high promise of antiprotons to biomedical research and practical applications and the possibility that antiprotons may become available everywhere in the next five years suggest that the time is ripe for initiating a research program in an accelerator center. This program should (a) explore the antiproton potential to biomedical science and technology, (b) provide basic measurements, and (c) develop appropriate instrumentation. Such a program is outlined.

Acknowledgments

We thank Michael Goitein for extensive discussions and suggestions. We also thank the Rand Corporation for making this report possible.

REFERENCES

1. O. Chamberlain, et al., Phys. Rev. 100; 947 (1955).
2. See D. Cline et al., Rand Second Antiproton Workshop, October 6-9, 1987.
3. See M. Hymes et al., *ibid.*
4. Y. Y. Lee has estimated that the power cost of producing antiprotons at the AGS is $\$2.5/10^9 \bar{p}$ (private communication).
5. D. C. Peaslee, Rand Second Antiproton Workshop, October 6-9, 1987.
6. L. H. Andersen et al., Phys. Rev. Lett. 51; 2147 (1986).
7. C. Tschalär and H. Bisel, Phys. Rev. 175; 476 (1968).
8. See e.g. J. O. Archambeau et al., Radiology 110; 445 (1974).
9. B. Rossi, High-Energy Particles, Prentice Hall, p.37, 1952.
10. P. H. Fowler and D.H. Perkins, Nature 189; 524 (1961).
11. K. Nakamura et al., Phys. Rev. Lett. 52; 731 (1981); V. Ashford et al., Phys. Rev. 31C; 663 (1985); D. Garreta et al., Phys. Lett. 149B; 64 (1984).
12. T. Kalogeropoulos and G.S. Tzanakos, Phys. Rev. 22D; 2585 (1980).
13. D. Bridges et al., Phys. Rev. Lett. 56; 211 (1986).
14. D.I. Lowenstein et al., Phys. Rev. D23; 2788 (1981).
15. T. E. Kalogeropoulos et al., Phys. Rev. Lett. 33; 1631 (1974).
16. *Ibid* page 1635.
17. S. Devons et al., Phys. Lett. 47B; 271 (1973).
18. L. Gray and T. E. Kalogeropoulos, IEEE Trans. on Nuclear Science, NS-29; 1051 (1982).
19. See e.g., E. C. McCullough et al., Radiology 111; 709 (1974).
20. K. Crowe et al., Nucl. Science, NS-22; 1752 (1975); S. Kramer, IEEE Trans. on Nucl. Science NS-8; 1910 (1981).
21. P. M. Joseph, Artifacts in computed tomography, (chapter 114 in Radiology of the Skull and Brain, T. H. Newton and D.G. Potts, eds., St. Louis: Mosley, 1981).
22. A. Deguzman, Ph D Dissertation, Syracuse University (1986).
23. L. Gray and T. E. Kalogeropoulos, Radiation Research 97; 246 (1984).
24. A.M. Koehler and K.N. Johnson, Harvard Cyclotron Report (unpublished). 24 June 1976.
25. B. P. Flannery et al., Science 237; 1439 (1987).
26. O. Chamberlain, et al., Phys. Rev. 113; 1615 (1959).
27. See e.g., T. von Egidy, Nature 328; 773 (1987).
28. N. Metropolis et al., Phys. Rev. 100; 204 (1958).
29. D. V. Ellis, J.S. Schweitzer, J. J. Ullo, Ann. Rev. Nucl. Sc., 37; 213 (1987).
30. A.H. Sullivan, Phys. Med. Biol. 30; 1297 (1985).
31. T. E. Kalogeropoulos, Paper presented at the Second Int. Charged Particle Therapy Workshop, Loma Linda Un. Medical Center, Oct. 12, (1987).
32. E. Fermi and E. Teller, Phys. Rev. 72; 399 947).
33. J.S. Baijal et al., Nuo. Cim., 30; 711 (1963).
34. L.I. Ponomarev, Ann. Rev. of Nuc. Sc. 23; 395 (1973).
35. C.J. Batty, Sov. J. of Part. and Nuclei, 13; 71 (1982).
36. C. T. Pawlewitz et al., Phys. Rev. D2; 2538 (1970).
37. C. Baltay et al., Phys. Rev. Lett. 15; 533 (1965).
38. E.M. Sapiro, Sov. J. Part. Nucl. 15; 69 (1984).
39. Report of The Task Group on Reference Man. ICRP number 23. Edited by W. Snyder et al. Pergamon Press, NY 1975.
40. L.A. Saryan et al., J. Nat'l. Cancer Inst., 52; 599 (1974).

POTENTIAL APPLICATIONS OF
ANTI-PROTONS FOR INSPECTION AND
PROCESSING OF COMPOSITES

L. B. Greszczuk
McDonnell Douglas Astronautics Co.
Huntington Beach, CA

There are a number of areas for potential applications of antiprotons for inspection and processing of advanced composite materials. These include:

- (1) Quantitative non-destructive evaluation (NDE) of materials through measurement of local densities and density gradients
- (2) New processing techniques for materials
- (3) Healing of defects in materials
- (4) Identification of material compositions (Stopping power is function of density and type of elemental composition).

By accurately measuring density variations in materials, fairly accurate estimates can be made of the various mechanical properties of composites (Figure 1) and potential sites of failure (Figure 2). Although Computed Tomography (CT), as described in Figure 3, can be used for measuring the density variations, neither the industrial nor medical CT systems have, at present time, the adequate accuracy or resolution to make them a quantitative inspection tool. Even if the resolution of existing CT systems were improved ($\ll 20$ mils), the scan time and thereby inspection cost would be prohibitive

(Table 1). The number of antiprotons required to accurately inspect the critical area of a carbon-carbon exit cone would be of the order of 10^{10} . An important advantage of using antiprotons for imaging, as pointed out by Kalogeropoulos, is that the pictures are direct images of measurements and thereby the problem of artifacts, as illustrated in Figure 4, which is quite common in CT, is eliminated.

Another potential application for antiprotons is in new processing techniques, especially for thick composite materials and porous solids. Using antiprotons, one may be able to cure composites from center outward, thus minimizing the internal entrapment of volatiles and other by-products of curing reactions. Antiprotons technology could also be used to improve uniformity of porous materials densified using chemical vapor deposition (CVD). Conventional CVD produces dense outer skins and less dense or porous inner material. By heating the interior of the material first using antiprotons, the densification could proceed from center out.

For metallic materials with internal damage in the form of flaws and microcracks, antiprotons could be used for healing these types of defects and/or blunting the growth and propagation of internal cracks. Finally, since the stopping power of antiprotons is a function of material density and elemental composition, antiprotons can be used for identifying the composition of material making up the component.

POTENTIAL APPLICATIONS OF ANTIPROTONS
FOR INSPECTION AND PROCESSING OF MATERIALS

L. B. GRESZCZUK



REDUCTION IN CROSS-PLY TENSILE STRENGTH DUE TO LOW DENSITY PLY/AREA.

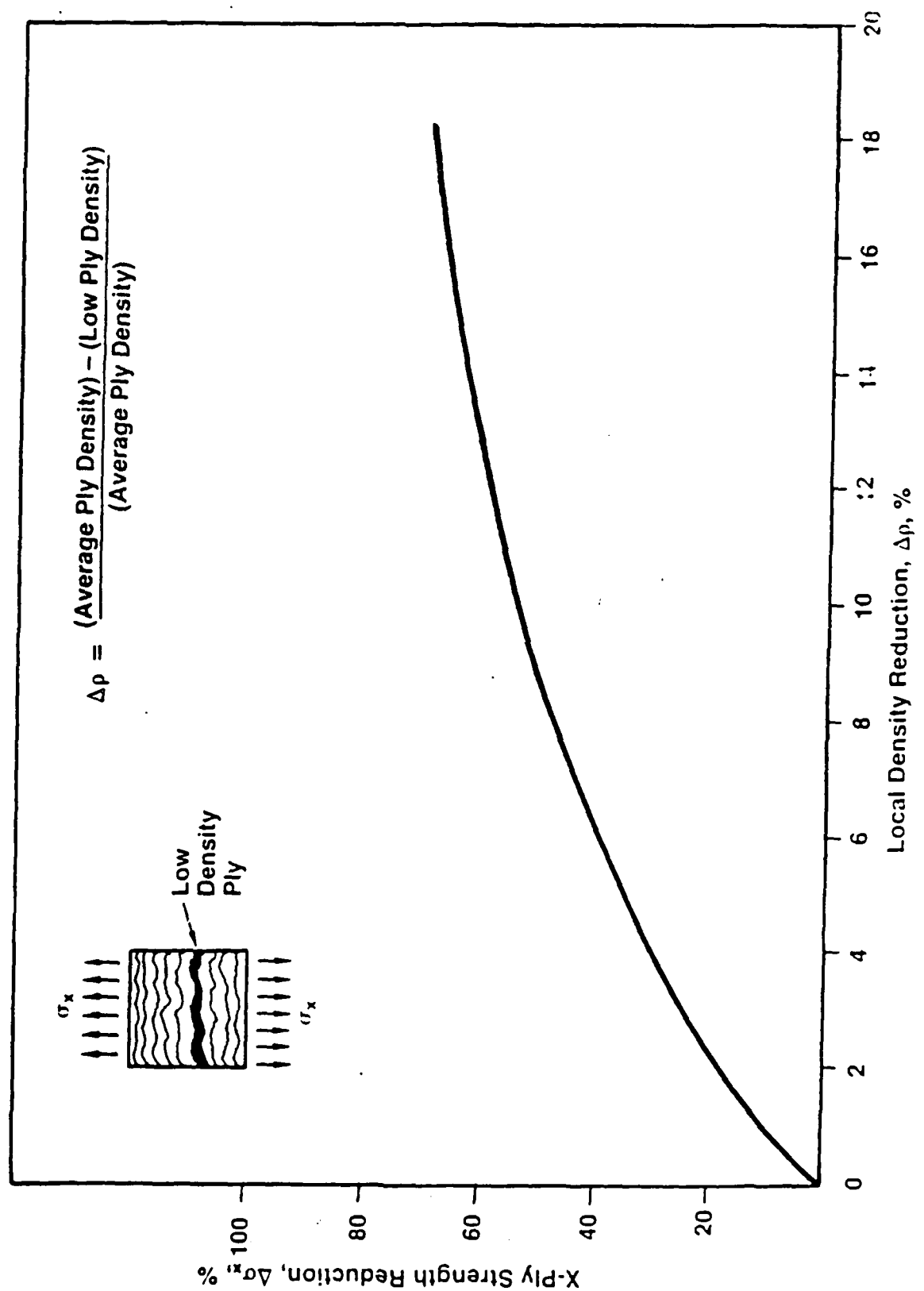
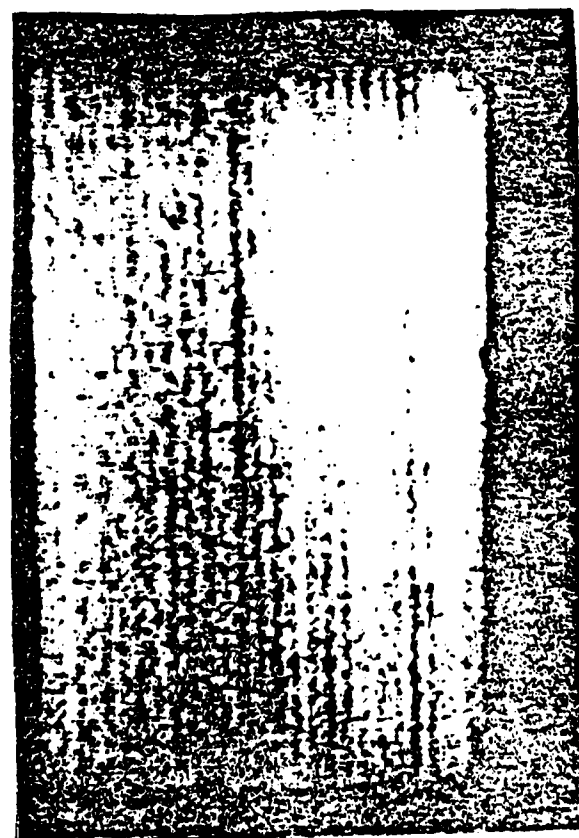
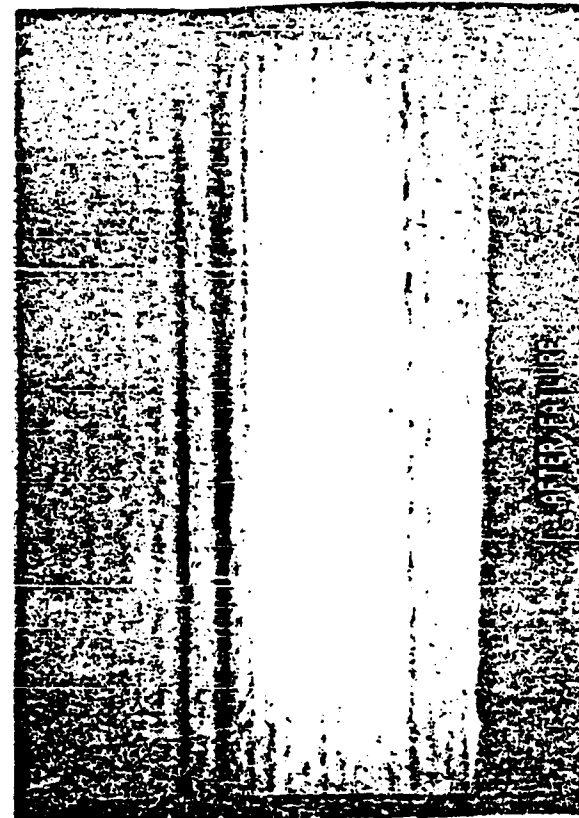


FIGURE 1.

ENHANCED X-RAY OF COMPOSITE CROSSPLY TENSILE SPECIMEN
SHOWING (A) LOCATION OF LOW DENSITY AREA AND
(B) X-RAY OF SPECIMEN AFTER FAILURE.



(A)



(B)

FIGURE 2.

INSPECTION BY COMPUTED TOMOGRAPHY (CT)

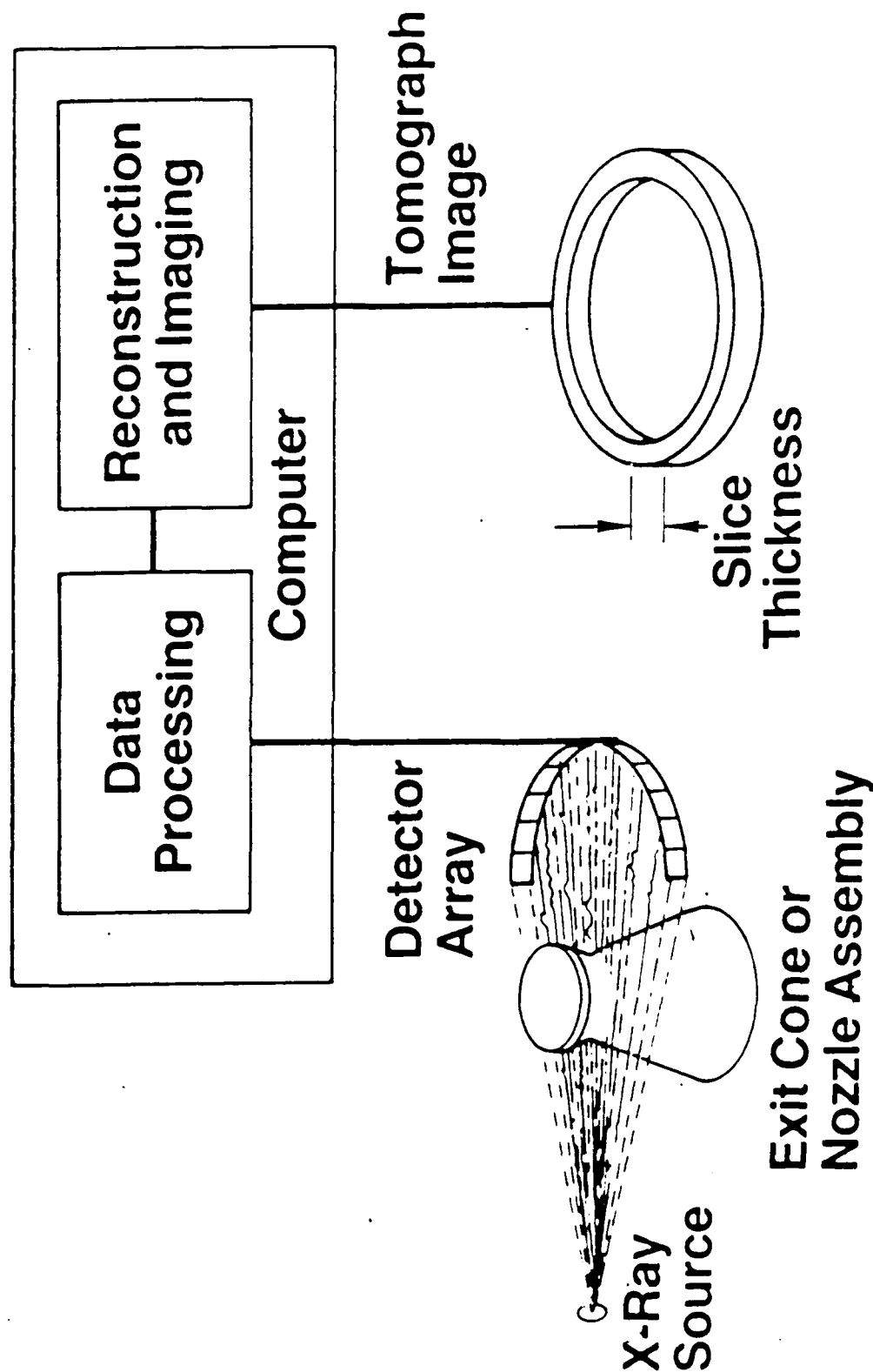


FIGURE 3.

TABLE 1
INSPECTION SPEED USING X-RAYS AND P

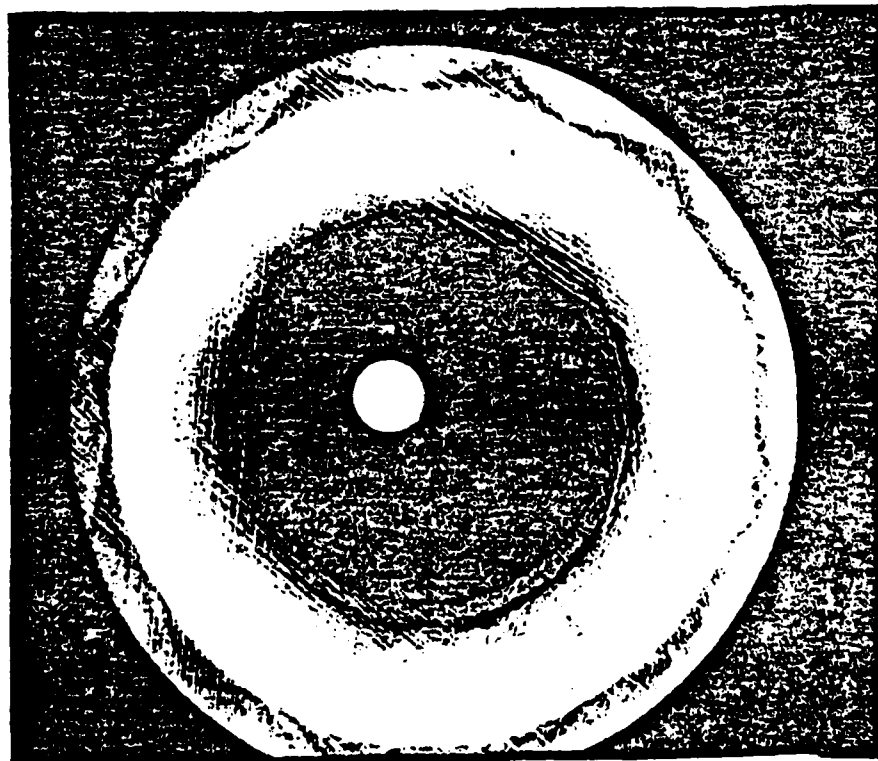
TECHNIQUE	PRESENT		REQUIRED (3)	
	RESOLUTION (MILS)	INSPECTION TIME (1)	RESOLUTION (MILS)	INSPECTION TIME
INDUSTRIAL CT	20 X 20 X 60	12 HRS. (1)	2 X 2 X 12	MONTHS
MEDICAL CT	20 X 20 X 60	15 MIN. (1)	2 X 2 X 12	DAYS
ANTIPROTON	20 X 20 X 60	<10 SEC. (2)	2 X 2 X 12	MINS

(1) ACTUAL INSPECTION TIME FOR A CARBON-CARBON EXIT CONE (CRITICAL AREA) IN 1985

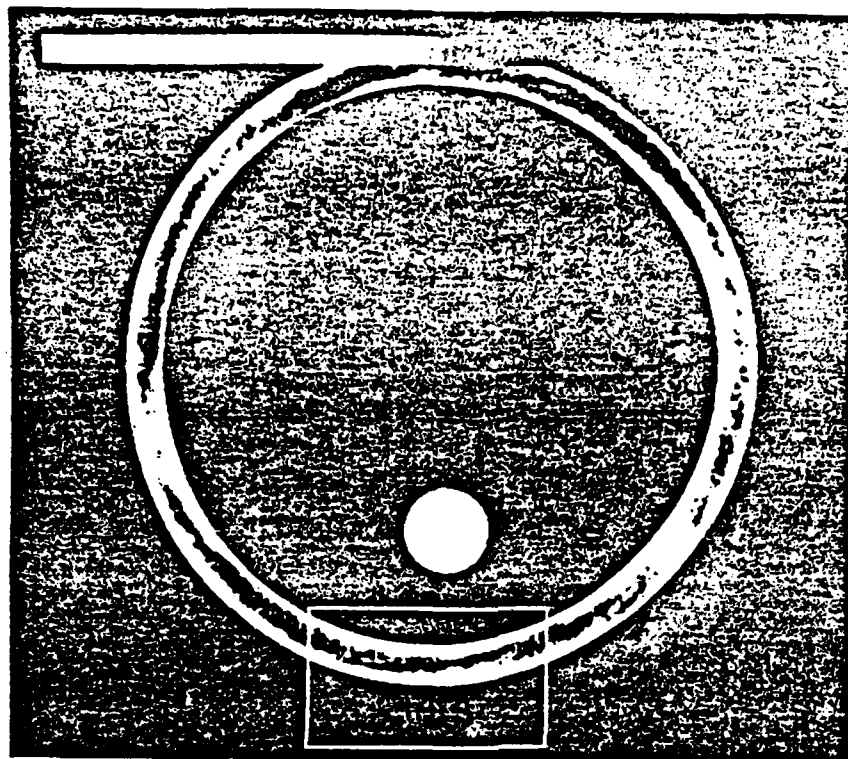
(2) ESTIMATED INSPECTION TIME; NUMBER OF ANTIPROTONS REQUIRED WOULD BE 10^7

(3) FOR QUANTITATIVE NDE

TYPICAL ARTIFACTS INHERENT TO CT



Artifacts Caused by Insufficient Photon Flow



Circular Artifacts Imaged in Normal Viewing Window

FIGURE 4.

ANTIMATTER SCIENCE AND TECHNOLOGY BIBLIOGRAPHY

Dr. Robert L. Forward
Senior Scientist
Hughes Research Laboratories
3011 Malibu Canyon Road
Malibu, CA 90265 USA

August 1987

1. PRODUCTION AND COLLECTION OF ANTIPROTONS
2. PRODUCTION OF HEAVY ANTINUCLEI
3. PRODUCTION OF LOW-ENERGY ANTIPROTONS
4. PRODUCTION OF ANTIHYDROGEN ATOMS, MOLECULES, AND CLUSTERS
5. SLOWING, COOLING, AND TRAPPING OF ATOMS, IONS, AND MOLECULES
6. LOW-ENERGY ANTIPROTON ANNIHILATION PROCESSES
7. NON-PROPULSION APPLICATIONS OF ANTIMATTER
8. ANTIMATTER PROPULSION
9. CONFERENCE PROCEEDINGS
10. ANTIMATTER NEWS AND POPULAR ARTICLES

1. PRODUCTION AND COLLECTION OF ANTIPROTONS

1973

T.A. Vsevolozhskaya and G.I. Sil'vestrov, "Optical properties of fast parabolic lenses," Zh. Tekh. Fiz. 43, 61-70 (1973) [English translation Sov. Phys. Tech. Phys. 18, 38-43 (1973)].

H. Hora, "Estimates for the efficient production of antihydrogen by lasers of very high intensities," Opto-Electronics 5, 491-501 (1973). [Ed: It is not clear how this technique avoids the production of lighter particle-antiparticle pairs that occurs during P+N production, in order to achieve the quoted high efficiency.]

M. Antinucci, A. Bertin, P. Capiluppi, M. D'Agostino-Bruno, A.M. Rossi, G. Vannini, G. Giacomelli, and A. Bussiere, "Multiplicities of charged particles up to ISR Energies," Lett. Nuovo Cimento 6, 121-127 (1973).

1974

D.C. Carey, et al., "Unified description of single-particle production in pp collisions," Phys. Rev. Lett. 33, 330-333 (1974).

1975

T.A. Vsevolozhskaya, M.A. Lyubimova, and G.I. Sil'vestrov, "Optical properties of cylindrical lenses," Zh. Tekh. Fiz. 45, 2494-2507 (1975) [English translation Sov. Phys. Tech. Phys. 20, 1556-1563 (1976)].

H. Hora, "Theory of relativistic self-focusing of laser radiation in plasmas," J. Opt. Soc. Am. 65, 882-886 (1975).

1976

F.E. Taylor, et al., "Analysis of radial scaling in single-particle inclusive reactions," Phys. Rev. D14, 1217-1242 (1976).

1977

H.J.C. Kouts, Chairman, Proceedings of an Information Meeting on Accelerator Breeding, Brookhaven National Laboratory, Upton, New York, 18-19 Jan. 1977.

E. Knapp, "Accelerator Costs and Efficiency," Proc. Information Meeting on Accelerator Breeding, Brookhaven, NY, p. 294, (Jan. 1977).

B.V. Chirikov, et al., "Optimization of antiproton fluxes from targets using hadron cascade calculations," Nuclear Instr. & Meth. 144, 129-139 (1977).

1978

G.S. Villeval'd, V.N. Karasyuk, and G.I. Sil'vestrov, "Magnetic field limited parabolic lens," Sov. Phys. Tech. Phys. 23, 332-336 (1978).

G.I. Budker and A.N. Skrinsky, "Electron cooling and new possibilities in elementary particle physics," Usp. Fiz. Nauk 124, 561-595 (1978) [English translation Sov. Phys. Usp. 21, 277-296 (1978)].

B.F. Bayanov and G.I. Sil'vestrov, "Use of lithium to produce a strong cylindrical magnetic lens," Zh. Tekh. Fiz. 48, 160-168 (1978) [English translation Sov. Phys. Tech. Phys. 23, 94-98 (1978)].

1979

R. Billinge and M.C. Crowley-Milling, "The CERN proton-antiproton colliding beam facilities," IEEE Trans. on Nuclear Sci., NS-26, 2974-2977 (1979).

D.B. Cline, et al., "Initial operation of the Fermilab antiproton cooling ring," IEEE Trans. Nuclear Sci. NS-26, 3158-3160 (1979).

1980

T.B.W. Kirk, "Antiproton production target studies - numerical calculations," Fermilab TM-1011 (14 Nov 1980).

D.E. Young, "Progress on beam cooling at Fermilab," pp. 800 ff, Proc. 11th Int. Conf. High Energy Accelerators, Geneva (1980).

F. Krienen, "Initial cooling experiments (ICE) at CERN," pp. 781 ff, Proc. 11th Int. Conf. High Energy Accelerators, Geneva (1980).

W. Kells, P. McIntyre, L. Oleksiuk, N. Dikansky, I. Meshkov, V. Parkhomchuk, and W. Herrmannsfeldt, "Studies of the electron beam for the Fermilab electron cooling experiment," pp. 814-818, Proc. 11th Int. Conf. on High Energy Accelerators, Geneva, Switzerland (1980).

H. Herr and C. Rubbia, "High energy cooling of protons and antiprotons for the SPS collider," pp. 825-829, Proc. 11th Int. Conf. on High Energy Accelerators, Geneva, Switzerland (1980).

J. Gareyte, "The CERN proton-antiproton complex," pp. 79-90, Proc. 11th Int. Conf. High Energy Accelerators, Geneva (1980).

B.F. Bayanov, A.D. Chernyakin, V.N. Karasyuc, G.I. Sil'vestrov, T.A. Vsevolozhskaya, V.G. Volohov, G.S. Willewald, "The antiproton target station on the basis of lithium lenses," pp. 362-368, Proc. 11th Int. Conf. High Energy Accelerators, Geneva (1980).

D.B. Cline, "The development of bright antiproton sources and high energy density targeting," pp. 345-361, Proc. 11th Int. Conf. High Energy Accelerators, Geneva (1980).

M.Q. Barton, et al., "Minimizing energy consumption of accelerators and storage ring facilities [panel discussion]," pp. 898-908, Proc. 11th Int. Conf. High Energy Accelerators, Geneva (1980).

V.V. Abramov, et al., "Production of hadrons with transverse momentum 0.5-2.5 GeV/c in 70-GeV proton-nucleus collisions," Sov. J. Nuclear Phys. 31, 343-346 (1980).

A.I. Ageyev, et al., "The IHEP accelerating and storage complex (UNK) status report," pp. 60-70, Proc. 11th Int. Conf. High Energy Accelerators, Geneva (1980).

1981

T. Vsevolozhskaya, B. Grishanov, Ya. Derbenev, N. Dikansky, I. Meshkov, V. Parkhomchuk, D. Pesrikov, G. Sil'vestrov, A. Skrinsky, "Antiproton source for the accelerator-storage complex, UNK-IHEP," Fermilab Report FN-353 8000.00 (June 1981), a translation of INP Preprint 80-182 (December 1980).

D.E. Young, "The Fermilab proton-antiproton collider," IEEE Trans. Nuclear Sci. NS-28, 2008-2012 (1981).

T.A. Vsevolozhskaya, "The optimization and efficiency of antiproton production within a fixed acceptance," Nuclear Instr. & Methods 190, 479-486 (1981).

S. van der Meer, "Stochastic cooling in the CERN antiproton accumulator," IEEE Trans. Nuclear Sci. NS-28, 1194-1998 (1981).

F. Krienen and J.A. MacLachlan, "Antiproton collection from a production target," IEEE Trans. Nuclear Sci. NS-28, 2711-2716 (1981).

W. Kells, F. Krienen, F. Mills, L. Oleksiuk, J. Peoples, and P.M. McIntyre, "Electron cooling for the Fermilab \bar{p} source," IEEE Trans. Nuclear Sci. NS-28, 2583-2584 (1981).

W. Kells, "Advanced stochastic cooling mechanisms," IEEE Trans. Nuclear Sci. NS-28, 2459-2461 (1981).

R. Forster, T. Hardek, D.E. Johnson, W. Kells, V. Kerner, H. Lai, A.J. Lennox, F. Mills, Y. Miyahara, L. Oleksiuk, T. Rhoades, D. Young, and P.M. McIntyre, "Electron cooling experiments at Fermilab," IEEE Trans. Nuclear Sci. NS-28, 2386-2388 (1981).

M. Bell, J. Chaney, H. Herr, F. Krienen, P. Møller-Petersen, and G. Petrucci, "Electron cooling in ICE at CERN," Nuclear Instr. & Methods 190, 237-255 (1981).

B.F. Bayanov, J.N. Petrov, G.I. Sil'vestrov, J.A. MacLachlan, and G.L. Nicholls, "A lithium lens for axially symmetric focusing of high energy particle beams," Nuclear Instr. & Methods, 190, 9-14 (1981).

1982

J.A. MacLachlan, "Current carrying targets and multitarget arrays for high luminosity secondary beams," FN-334, 8055.000, Fermi National Accelerator Lab, Batavia, Illinois (April 1982).

U. Bizzarri, M. Conte, C. Ronsivalle, R. Scrimaglio, L. Tecchio, and A. Viganti, "High-energy electron cooling at LEAR $p\bar{p}$ -collider," pp. 619-628, Physics at LEAR with Low-Energy Cooled Antiprotons, Workshop on Physics at LEAR with Low-Energy Cooled Antiprotons, Erice, Sicily, Italy, 9-16 May 1982; U. Gastaldi and R. Klapisch, ed., Plenum Press, NY (1984).

R.P. Johnson and J. Marriner, "Stochastic stacking without filters," Fermilab \bar{p} Note 226, Fermi National Accelerator Lab, Batavia, Illinois (17 August 1982).

R.P. Johnson and J. Marriner, "Stochastic stacking without filters," Fermilab \bar{p} Note 226, Fermi National Accelerator Lab, Batavia, Illinois (17 August 1982).

G. Chapline, "Antimatter Breeders?" J. British Interplanetary Soc., 35, 423-424 (1982).

H.-J. Möhring and J. Ranft, "Antiproton production from extended targets using a weighted Monte Carlo hadron cascade model," Nuclear Instr. & Methods 201, 323-327 (1982).

M. Bell and J.S. Bell, "Capture of cooling electrons by cool protons," Particle Accelerators, 12, 49-52 (1982).

1983

C. Hojvat, G. Biallas, R. Hanson, J. Heim, and F. Lange, "The Fermilab Tevatron I project target station for antiproton production," Fermilab TM-1174, 1983 Particle Accelerator Conf., Santa Fe, NM (21-24 March 1983).

S. van der Meer, "Practical and foreseeable limitations in usable luminosity for the collider," CERN Publication 83-04, Proc. Third Topical Workshop on Proton-Antiproton Collider Physics, Rome, 12-14 January 1983, pp. 555-561 (10 May 1983).

B. Autin, "Technical Developments for an Antiproton Collector at CERN," Proc. 12th Int. Conf. on High-Energy Accelerators, F.T. Cole and R. Donaldson (editors), 393-396 (11-16 August 1983). [Obtainable from Fermi National Accelerator Lab, Batavia, IL, USA.]

R.E. Shafer, "Overview of the Fermilab Antiproton Source," Proc. 12th Int. Conf. on High-Energy Accelerators, F.T. Cole and R. Donaldson (editors), 24-25 (11-16 August 1983). [Obtainable from Fermi National Accelerator Lab, Batavia, IL, USA.]

Ya.S. Derbenev, N.S. Dikansky, V.I. Kudelainen, V.A. Lebedev, I.N. Meshkov, B.B. Parkhomchuk, D.V. Pestrikov, A.N. Skrinsky, and B.N. Sukhina, "Status of Electron Cooling on NAP-M," Proc. 12th Int. Conf. on High-Energy Accelerators, 32-36 (11-16 August 1983). [Obtainable from Fermi National Accelerator Lab, Batavia, IL.]

E. Peschardt and M. Studer, "Stochastic cooling in the CERN ISR during pp colliding beam physics," IEEE Trans. Nuclear Sci. NS-30, 2584-2586 (August 1983).

C.D. Johnson, "Antiproton yield optimization in the CERN antiproton accumulator," IEEE Trans. Nuclear Sci. NS-30, 2821-2826 (August 1983).

G. Brianti, "Experience with the CERN pp complex," IEEE Trans. Nuclear Sci. NS-30, 1950-1956 (August 1983).

P.J. Bryant, "Antiprotons in the ISR," IEEE Trans. Nuclear Sci. NS-30, 2047-2049 (August 1983).

E. Jones, S. van der Meer, R. Rohner, J.C. Schnuriger, and T.R. Sherwood, "Antiproton production and collection for the CERN antiproton accumulator," IEEE Trans. Nuclear Sci. NS-30, 2778-2780 (August 1983).

H. Aihara and TPC Collaboration, "Charged hadron production in e^+e^- annihilation at 29 GeV," LBL-17142 preprint, Lawrence Berkeley Lab, Berkeley, California 94720 (December 1983)

Ya.S. Derbenev, N.S. Dikansky, V.I. Kudelainen, V.A. Lebedev, I.N. Meshkov, B.B. Parkhomchuk, D.V. Pestrikov, A.N. Skrinsky, and B.N. Sukhina, "Status of Electron Cooling at Novosibirsk (Theory and Experiment)," IEEE Trans. Nuclear Science, NS-30, 2672-2675 (1983).

G.S. Villeval'd (AKA Willewald), "High-Acceptance X-Lenses," Sov. Phys. Tech. Phys. 28, 801-805 (1983).

E.J.N. Wilson, "The CERN antiproton accumulator," pp. 567-571, Proc. Workshop on Proton-Antiproton Physics and the W discovery, La Plagne (1983).

J.P. Marriner, "The Fermilab $\bar{p}p$ collider," pp. 583-592, Proc. Workshop on Proton-Antiproton Physics and the W discovery, La Plagne, (1983).

J. Peoples, "The Fermilab antiproton source," IEEE Trans. Nuclear Sci. NS-30, 1970-1975 (1983).

R.E. Shafer, "The Fermilab antiproton debuncher betatron cooling system," pp. 581-583, Proc. 12th Int. Conf. High-Energy Accel., F.T. Cole and D. Donaldson, ed., Fermi National Accelerator Lab, Batavia, Illinois (1983).

C. Hojvat and A. Van Ginneken, "Calculation of antiproton yields for the Fermilab antiproton source," Nuclear Instr. & Methods 208, 67-83 (1983).

B. Autin, "The future of the antiproton accumulator," pp. 573-582, Proc. Workshop on Proton-Antiproton Physics and the W discovery, La Plagne (1983).

V.E. Balakin and A.N. Skrinsky, "Project VLEPP," Akademiya Nauk USSR, Vestnik, No. 3, 66-77 (1983).

B.R. Bayanov, T.A. Vsevolozhskaya, Yu. N. Petrov, and G.I. Sil'vestrov, "The investigation and design development of lithium lenses with large operating lithium volume," pp. 587-590, Proc. 12th Int. Conf. High-Energy Accel., F.T. Cole and D. Donaldson, ed., Fermi National Accelerator Lab, Batavia, Illinois (1983).

R. Billinge and E. Jones, "The CERN antiproton source," pp 14-16, Proc. 12th Int. Conf. High-Energy Accel., F.T. Cole and D. Donaldson, ed., Fermi National Accelerator Lab, Batavia, Illinois (1983).

G. Carron, R. Johnson, S. van der Meer, C. Taylor, and L. Thorndahl, "Recent experience with antiproton cooling," IEEE Trans. Nuclear Sci. NS-30, 2587-2589 (1983).

T. Ellison, W. Kells, V. Kerner, F. Mills, R. Peters, T. Rathbun, D. Young, P.M. McIntyre, "Electron cooling and accumulation of 200-MeV protons at Fermilab," IEEE Trans. Nuclear Sci. NS-30, 2636-2638 (1983).

L.R. Evans, "Intrabeam scattering in the SPS proton antiproton collider," pp. 229-231, Proc. 12th Int. Conf. High-Energy Accel., F.T. Cole and D. Donaldson, ed., Fermi National Accelerator Lab, Batavia, Illinois (1983).

1984

T. Kalogeropoulos (Spokesman), Physics Department, Syracuse University, Syracuse, NY 13244-1130, and 32 others (1 May 1984), "Development of a Time Purified/ Separated Antiproton Beam and High Precision Cross Section Measurements". [Proposal to BNL AGS.]

T.A. Vsevolozhskaya, "The Linear Approximation to the Hydrodynamic Consideration of Target Behaviour Under High Density Beam Exposure," INP Preprint 84-88 (17 May 1984), Institute of Nuclear Physics, 630090, Novosibirsk, USSR.

M. Harrison, "The Fermilab $\bar{p}p$ collider," pp. 368-378, CERN Pub. 84-09, Fourth Topical Workshop on Proton-Antiproton Collider Physics, Berne, 5-8 March 1984, (8 August 1984).

R. Billinge, "CERN's $p\bar{p}$ source," CERN Publication 84-09, Proc. Fourth Topical Workshop on Proton-Antiproton Collider Physics, Berne, 5-8 March 1984, pp. 357-364 (8 August 1984).

B. de Raad, "The SPS p - \bar{p} collider, present performance and future prospects," CERN Publication 84-09, Proc. Fourth Topical Workshop on Proton-Antiproton Collider Physics, Berne, 5-8 March 1984, pp. 344-356 (8 August 1984).

Fermilab staff, Design Report: Tevatron 1 Project, p. 4-13 to p. 4-16, Fermi National Accelerator Lab, Batavia, Illinois (September 1984).

V.V. Parkhomchuk, "Physics of Fast Electron Cooling," ECOOL 1984, Proc. Workshop on Electron Cooling and Related Applications, H. Poth (editor), 71-83 (24-26 Sept. 1984).

D. Young, F. Mills, and G. Michelassi, "Information relevant to the optimization of electric power versus equipment costs," Fermilab \bar{p} -Note 189 (1984?)

N.G. Jordan and P.V. Livdahl, "Costs to build Fermilab in 1984 dollars," Fermilab Technical Memo TM-1242, 0002.000 (1984).

1985

R. Billinge, "Introduction to CERN's Antiproton Facilities for the 1990s," pp. 13-24, Proc. Third LEAR Workshop, Tignes-Savoie-France (19-26 January 1985), U. Gastaldi, R. Klapisch, J.M. Richard, and J. Tran Thanh Van, Editors, Editions Frontieres, B.P. 44, 91190 GIF sur Yvette, France (1985).

U. Gastaldi, R. Klapisch, J.M. Richard, and J. Tran Thanh Van, Editors, Physics with Antiprotons at LEAR in the ACOL Era, Proc. Third LEAR Workshop, Tignes-Savoie-France (19-26 January 1985), Editions Frontieres, B.P. 44, 91190 GIF sur Yvette, France (1985). [Ed: Nearly 800 pages and 100 papers covering Machine Development, Nucleon-Antinucleon Interactions, Spectroscopy, Rare Decays, Antiproton-Nucleus Interactions, New Ideas, and New Detectors.]

J.L. Thron, T.R. Cardello, P.S. Cooper, L.J. Teig, Y.W. Wah, C. Ankenbrandt, J.P. Berge, A.E. Brenner, J. Butler, K. Doroba, J.E. Elias, J. Lach, P. Laurikainen, J. MacLachlan, J.P. Marriner, E.W. Anderson, A. Breakstone, and E. McCliment, "Search for Heavy Charged Particles and Light Nuclei and Antinuclei Produced by 400-GeV Protons," Physical Review D31, 451-463 (1 February 1985).

E. Malamud, "The Fermilab \bar{p} Collider: Machine and Detectors," Pbar Note 421 (1985), Pbar Source Department, Fermilab, P.O. Box 500, Batavia, Illinois 60510 USA. (Invited talk presented at the Fifth Topical Conf. on Proton-Antiproton Collisions, St. Vincent, Italy, 26 February 1985).

E. Malamud, "The Fermilab \bar{p} Collider: Machine and Detectors," Fermilab \bar{p} Note #421, Fifth Topical Conf. on Proton-Antiproton Collisions, St. Vincent, Italy (26 Feb 1985).

H. Poth, "A New Approach to a Pure Antiproton Beam at GeV Energies" [at the Brookhaven AGS machine], Preprint (May 1985), Kernforschungszentrum Karlsruhe, Institute fur Kernphysik, Postfach 3640, D-7500 Karlsruhe, West Germany.

Yu.M. Ado, E.A. Myae, A.A. Naumov, M.F. Ovchinnikov, O.N. Radin, V.A. Teplyskov, V.G. Tishin, E.F. Troyanov, "Initial operation of the IHEP proton synchrotron with a new ring injector," Paper H50, 1985 Particle Accelerator Conf., Vancouver, B.C., Canada (13-16 May 1985) [To be published in IEEE Trans. Nuclear Sci. (Oct 1985)].

T.W. Eaton, S. Hancock, C.D. Johnson, E. Jones, S. Maury, S. Milner, J.C. Schnuriger, and T.R. Sherwood, "Conducting targets for \bar{p} production of ACOL, past experience and prospects," Paper X40, 1985 Particle Accelerator Conf., Vancouver, B.C., Canada (13-16 May 1985) [To be published in IEEE Trans. Nuclear Sci. (Oct 1985)].

D.C. Fliander, C.D. Johnson, S. Maury, T.R. Sherwood, G. Dugan, C. Hojvat, and A. Lennox, "Beam tests of a 2 cm diameter lithium lens," Paper X39, 1985 Particle Accelerator Conf., Vancouver, B.C., Canada (13-16 May 1985) [To appear in IEEE Trans. Nuclear Sci. (Oct 1985)].

P. Sievers, R. Bellone, A. Ijspeert, P. Zanasco, "Development of lithium lenses at CERN," Paper X41, 1985 Particle Accelerator Conf., Vancouver, B.C., Canada (13-16 May 1985) [To be published in IEEE Trans. Nuclear Sci. (Oct 1985)].

David B. Cline, Ed., Low Energy Antimatter, World Scientific, Singapore (1986). Proceedings of the Workshop on the Design of a Low Energy Antimatter Facility, University of Wisconsin-Madison, Madison, Wisconsin, USA (October 1985).

Frank Krienen, "Progress in Hollow Cathode Electron Gun for Electron Cooling," p. 92.

D.J. Larson, et al., "Intermediate Energy Electron Cooling Applied to the Fermilab Antiproton Source," p. 167.

M. Sedlacek, "The Celsius-Ring in Uppsala: Electron Cooler Design," p. 196.

1986

Sekazi Mtingwa, "Stochastic Cooling of Antiprotons at the Tevatron," Pbar Note 445 (January 1986), Pbar Source Department, Fermilab, P.O. Box 500, Batavia, Illinois 60510 USA.

G. Dugan, "Antiproton Yield Calculations," Pbar Note 449 (20 January 1986), Pbar Source Department, Fermilab, P.O. Box 500, Batavia, Illinois 60510 USA. [Ed: Lengthy, detailed design calculations for the Fermilab Pbar Source. Order only if involved in target design.]

G. Dugan, "Comparisons of Yield Calculations with Data," Pbar Note 448 (1 February 1986), Pbar Source Department, Fermilab, P.O. Box 500, Batavia, Illinois 60510 USA.

Pisin Chen, "A Possible Final Focusing Mechanism for Linear Colliders," Preprint SLAC-PUB-3823 (Rev.) (February 1986), SLAC, Stanford University, Stanford, California 94305 USA. (Large transverse wake fields can be generated via the interaction between a relativistic electron or positron bunch and a plasma, and the bunch will therefore be self-pinched. A plasma lens based on the self-pinching effect is suggested with a conceptual design and a numerical example. Submitted to Particle Accelerators.)

G. Dugan, "Estimate of the Pbar Yields for the CERN ACOL Project," Pbar Note 461 (19 May 1986), Pbar Source Department, Fermilab, P.O. Box 500, Batavia, Illinois 60510 USA. (For a check of the yield estimate expected for the new ACOL target station, calculations have been performed for the CERN parameters using the relatively simple semi-analytical techniques outlined in Pbar Note 449.)

H. Poth, "Electron Cooling," Preprint CERN-EP/86-65 (June 1986), Inst. fur Kernphysik, Postfach 3640, D-7501 Leopoldshafen, Germany.

F.E. Mills, "Cooling of Stored Beams," Pbar Note 463 (10 June 1986), Pbar Source Department, Fermilab, P.O. Box 500, Batavia, Illinois 60510 USA. (The physics of beam cooling and the ranges of utility of stochastic and electron cooling are discussed in this paper.)

Eifionydd Jones, "ACOL: CERN's Upgrade of the Antiproton Accumulator Complex, $\bar{p}p$ Symposium, Aachen (July 1986).

G. Dugan, "Pbar Production and Collection at the FNAL Antiproton Source," Pbar Note 464 (July 1986), Pbar Source Department, Fermilab, P.O. Box 500, Batavia, Illinois 60510 USA. (Invited paper presented at the XIII International Conference on High Energy Accelerators, Novosibirsk, USSR, 7-11 August 1986.)

Pisin Chen and Robert J. Noble, "A Solid State Accelerator," Preprint SLAC-PUB-4042 (July 1986). [Ed: Obtainable from authors, SLAC, Stanford University, Stanford, CA 94305 USA.] (Particles are accelerated along crystal channels by longitudinal electron plasma waves in a metal. Acceleration gradients of 100 GV/cm are theoretically possible.) [Ed: Using this technique, a 100 GeV antiproton factory would shrink from a 40 km maze of copper microwave plumbing to a 0.00001 km (1 cm) block of tungsten crystal, saving considerably on real estate costs.]

Pisin Chen, J.J. Su, T. Katsouleas, S. Wilks, and J.M. Dawson, "Plasma Focusing for High Energy Beams," Preprint SLAC-PUB-4049 (August 1986), SLAC, Stanford University, Stanford, California 94305 USA. (We analyze the self-focusing effect of a relativistic electron or positron beam traversing through a thin slab of plasma in a linearized fluid theory, and show that the effect is very strong. The idea of employing this effect for a plasma lens suggested by Chen is then reviewed. Submitted to IEEE Plasma Science.)

John Marriner, "Stochastic Cooling at Fermilab," Preprint Fermilab-Conf-86/124 (August 1986), Fermilab, P.O. Box 500, Batavia, Illinois 60510 USA. (Presented at the XIII International Conference on High Energy Accelerators, Novosibirsk, USSR, 7-11 August 1986.)

H. Edwards, "The Fermilab Tevatron and Pbar Source Status Report," Preprint TM-1419 (August 1986), Fermilab, P.O. Box 500, Batavia, Illinois 60510 USA. (Submitted to the XIII International Conference on High Energy Accelerators, Novosibirsk, USSR, 7-11 August 1986.)

Y.Y. Lee, "A Thought on Very Low Energy Anti-Protons," BNL Accelerator Division Tech. Note 266 (17 October 1986), Accelerator Division, AGS Department, Brookhaven National Lab, Upton, New York 11973 USA. (The AGS extracts three rf buckets of protons to strike an anti-proton production target. The anti-protons will be collected by an appropriate lens system and injected into the booster. After deceleration to 200 MeV, they can be further decelerated through the linac and an RFQ preinjector. If one cools the anti-protons in the booster to 14.6 mm-mrad at 200 MeV energy, theoretically half of the 1.33×10^8 anti-protons collected at 3.5 GeV/c could be decelerated to 750 keV and then to 20 keV.)

P. Sievers, "Design Parameters for Long (Plasma?) Lenses," Pbar Note 437 (15 November 1986), Pbar Source Department, Fermilab, P.O. Box 500, Batavia, Illinois 60510 USA.

Heinrich Hora and Horst Löb, "Efficient Production of Antihydrogen by Laser for Space Propulsion," (in English), Zeitschrift für Flugwissenschaften und Weltraumforschung 10, 393-400 (November/December 1986). [Ed: I do not see how production of lighter mass particle-antiparticle pairs are avoided to achieve quoted efficiencies.]

Y.Y. Lee and D.I. Lowenstein, "A Conceptual Design for a Very Low Energy Antiproton Source," BNL AGS/AD/Tech. Note 269 (3 December 1986), Accelerator Division, AGS Department, Brookhaven National Lab, Upton, New York 11973 USA. [Ed: A more detailed engineering discussion and cost estimate for the Y.Y. Lee Tech. Note 266. The cost is estimated at \$8,620,000.]

M. Takasaki, S. Kurokawa, M. Kobayashi, M. Taino, Y. Suzuki, H. Ishii, Y. Kato, T. Fujitani, Y. Nagashima, T. Omori, S. Sugimoto, Y. Yamaguchi, J. Iwahori, H. Yoshida, F. Takeuchi, M. Chiba, M. Koike, "The Low-energy Antiproton Beam K4 at the KEK 12 GeV Proton Synchrotron," Nuclear Inst. and Methods A242, 210-207 (1986). (The beam K4 is designed to transport high-intensity, high-purity antiprotons in the momentum range between 0.4 and 0.8 GeV/c. The measured intensities of antiprotons at 650 MeV/c are 1.1×10^{15} ppp.)

T.A. Vsevolozhskaya and G.I. Silvestrov, "Conic Lithium Lenses," INP Preprint 85-67, Institute of Nuclear Physics, 630090, Novosibirsk, USSR. (Lithium lenses whose longitudinal profile is approached to the profile of a particle beam are considered. The calculation has been made for antiprotons with $p = 3.5$ GeV in the angle 0.13 mrad.)

Delbert John Larson, "Intermediate Energy Electron Cooling for Anti-Proton Sources" Preprint WISC-EX-86-271 (1986), University of Wisconsin/Madison, Madison, Wisconsin 53706 USA. (Ph.D. Thesis. 166 pages.)

2. PRODUCTION OF HEAVY ANTINUCLEI

1965

D.E. Dorfman, J. Eades, L.M. Lederman, W. Lee, and C.C. Ting, "Observation of Antideuterons," Physical Review Letters 14, 1003-1006 (14 June 1965). [Ed: Probably first observation of heavy antinuclei.]

T. Massam, Th. Muller, B. Righini, M. Schneegans, and A. Zichichi, "Experimental Observation of Antideuteron Production," Il Nuovo Cimento 39, 6574-6578 (1 September 1965).

1969

F. Binon, P. Duteil, V.A. Kachanov, V.P. Khromov, V.M. Kut'yin, V.G. Lapshin, J.P. Peigneux, Yu.D. Prokoshkin, E.A. Razuvaev, V.I. Rykalin, R.S. Shuvalov, V.I. Solianik, M. Spighel, J.P. Stroot, and N.K. Vishnevsky, "Production of Antideuterons by 43 GeV, 52 GeV, and 70 GeV Protons," Physics Letters 30B, 510-513 (24 November 1969).

1970

Yu.M. Antipov, N.K. Vishnevskii, Yu.P. Gorin, S.P. Denisov, S.V. Donskov, F.A. Ech, G.D. Zhilchenkova, A.M. Zaitsev, V.A. Kachanov, V.M. Kut'in, L.G. Landsberg, V.G. Lapshin, A.A. Lebedev, A.G. Morozov, A.I. Petrukhin, Yu.D. Prokoshkin, E.A. Razuvaev, V.I. Rykalin, V.I. Solyanik, D.A. Stoyanova, V.P. Khromov, and R.S. Shuvalov, "Observation of Antihelium 3," Yad. Fiz. 12, 311-322 (August 1970) [English translation: Soviet Journal of Nuclear Physics 12, 171-172 (February 1971)].

1971

Yu.M. Antipov, N.K. Vishnevskii, Yu.P. Gorin, S.P. Denisov, S.V. Donskov, F.A. Ech, A.M. Zaitsev, V.A. Kachanov, V.M. Kut'in, L.G. Landsberg, V.G. Lapshin, A.A. Lebedev, A.G. Morozov, A.I. Petrukhin, Yu.D. Prokoshkin, E.A. Razuvaev, V.I. Rykalin, V.I. Solyanik, D.A. Stoyanova, V.P. Khromov, and R.S. Shuvalov, "Production of Negative Particles with Low Momenta by 70-BeV Protons," Yad. Fiz. 13, 135-138 (January 1971). [English translation: Soviet Journal of Nuclear Physics 13, 78-79 (July 1971)]. The same material also appeared in: "Production of Low Momentum Negative Particles by 70-GeV Protons," Physics Letters 34B, 164-166 (1 February 1971).

1972

Yu.D. Prokoshkin, "Particles of Antimatter," *Die Naturwissenschaften* 59, 281-284 (1972).

1974

N.K. Vishnevskii, M.I. Grachev, B.I. Rykalin, V.G. Lapshin, V.I. Solyanik, Yu.S. Khodyrev, V.P. Khromov, B.Yu. Baldin, L.S. Vertogradov, Ya.V. Grishkevich, Z.V. Krumshtein, R. Leiste, Yu.P. Merekov, V.I. Petrukhin, D. Pose, A.I. Ronzhin, I.F. Samenkova, V.M. Suvorov, G. Chemnitz, N.N. Khovanskii, B.A. Khomenko, M. Szawlowski, G.A. Shelkov, and J. Schuler, "Observation of Antitritium Nuclei," *Yad. Fiz.* 20, 694-708 (October 1974) [English translation: *Soviet Journal of Nuclear Physics* 20, 371-378 (April 1975)].

J.A. Appel, M.H. Bourquin, I. Gaines, L.M. Lederman, H.P. Parr, J.-P. Repellin, D.H. Saxon, J.K. Yoh, B.C. Brown, and J.-M. Gaillard, "Heavy Particle Production in 300 GeV/c Proton/Tungsten Collisions," *Physical Review Letters* 32, 428-432 (25 February 1974).

1975

M.G. Albrow, D.P. Barber, P. Benz, B. Bosnjakovic, J.R. Brooks, C.Y. Chang, A.B. Clegg, F.C. Ern , P. Kooijman, F.K. Loebinger, N.A. McCubbin, P.G. Murphy, A. Rudge, J.C. Sens, A.L. Sessoms, J. Singh, and J. Timmer, "Search for Stable Particles of Charge >1 and Mass $>$ Deuteron Mass," *Nuclear Physics B97*, 189-200 (1975).

1978

W.M. Gibson, A. Duane, H. Newman, H. Ogren, S. Henning, G. Jarlskog, R. Little, T. Sanford, S.L. Wu, H. B ggild, B.G. Duff, K. Guettler, M.N. Prentice, and S.H. Sharrock, "Production of Deuterons and Antideuterons in Proton-Proton Collisions at the CERN ISR," *Lettere Al Nuovo Cimento* 21, 189-194 (11 February 1978).

W. Bozzoli, A. Bussiere, G. Giacomelli, E. Lesquoy, R. Meunier, L. Moscoso, A. Muller, R. Rimondi, and S. Zylberajch, "Production of d, t, ^3He , anti-d, anti-t, and anti- ^3He by 200 GeV Protons," *Nuclear Physics B144*, 317-328 (1978).

1979

W. Bozzoli, A. Bussiere, G. Giacomelli, E. Lesquoy, R. Meunier, L. Moscoso, A. Muller, D.E. Plane, R. Rimondi, and S. Zylberajch, "Search for Long-Lived Particles in 200 GeV/c Proton-Nucleon Collisions," *Nuclear Physics B159*, 363-382 (1979).

J.C.M. Armitage, P. Benz, G.J. Bobbink, F.C. Erne, P. Kooijman, F.K. Loebinger, A.A. Macbeth, H.E. Montgomery, P.G. Murphy, J.J.M. Poorthuis, L. Rabou, A. Rudge, J.C. Sens, D. Stork, and J. Timmer, "Search for new long-lived particles with masses in the range 1.4 to 3.0 GeV, at the CERN ISR," Nuclear Physics 150B, No. 1, 87-108 (2 April 1979). (Antideuterons were identified by annihilation in a scintillation calorimeter.)

1982

H. Koch, K. Kilian, D. Möhl, H. Pilkuhn, and H. Poth, "Antideuterons at LEAR," pp. 877-880, Proceedings Workshop on Physics at LEAR with Low-Energy Cooled Antiprotons, Erice, Italy (9-16 May 1982).

D. Möhl, K. Kilian, H. Pilkuhn, and H. Poth, "Production of Antideuterons in Antiproton Rings," Nuclear Instruments and Methods 202, 427-430 (1982).

1985

J.L. Thron, T.R. Cardello, P.S. Cooper, L.J. Teig, Y.W. Wah, C. Ankenbrandt, J.P. Berge, A.E. Brenner, J. Butler, K. Doroba, J.E. Elias, J. Lach, P. Laurikainen, J. MacLachlan, J.P. Marriner, E.W. Anderson, A. Breakstone, and E. McCliment, "Search for Heavy Charged Particles and Light Nuclei and Antinuclei Produced by 400-GeV Protons," Physical Review D31, 451-463 (1 February 1985).

ARGUS Collaboration, "Observation of Antideuteron Production in Electron-Positron Annihilation at 10 GeV Center of Mass Energy," Physics Lett. 157B, 326-332 (18 July 1985). [Ed: Despite the large "size" of the antideuteron compared to the "size" of the e^+e^- collision region, the ratio of production of antideuterons to antiprotons is the same in e^+e^- collisions as in $p\bar{p}$ collisions.]

1986

W.W. Buck, J.W. Norbury, L.W. Townsend, and J.W. Wilson, "Theoretical Antideuteron-Nucleus Absorptive Cross Sections," Phys. Rev. C33, 234-238 (1986).

1987

Robert L. Forward, "Production of Heavy Antinuclei: Review of Experimental Results," HRL Research Report 564 (May 1987). [Ed: Obtain from Hughes Research Labs, 3011 Malibu Canyon Rd., Malibu, California 90265 USA.] Presented at the Cooling, Condensation, and Storage of Hydrogen Cluster Ions Workshop, SRI International, Menlo Park, California USA (8-9 January 1987). (Small amounts of antideuterons, antitritons, and antihelium-3 have been observed during the production of antiprotons. The general experimental trend is that the ratio of production of antideuterons to antiprotons is 10^{-4} , and each added antibaryon lowers the production rate by another factor of 10^{-4} .)

3. PRODUCTION OF LOW-ENERGY ANTIPROTONS

1980

P. Lefèvre, D. Möhl, G. Plass, "The CERN low energy antiproton ring (LEAR) project," pp. 819-823, Proc. 11th Int. Conf. High Energy Accelerators, Geneva (1980).

J. Gareyte, "The CERN proton-antiproton complex," pp. 79-90, Proc. 11th Int. Conf. High Energy Accelerators, Geneva (1980).

1981

G. Lambertson, et al., "Experiments on stochastic cooling of 200 MeV protons," IEEE Trans. Nuclear Sci. NS-28, 2471-2473 (1981).

1982

U. Gastaldi and R. Klapish, Eds., Physics at LEAR with Low-Energy Cooled Antiprotons, Workshop on Physics at LEAR with Low-Energy Cooled Antiprotons, Erice, Sicily, Italy, 9-16 May 1982, Plenum Press, NY (1984); A.H. Sørensen, "Theory of electron cooling in a magnetic field," pp. 599-604; L. Hütten, H. Poth and A. Wolf, "The electron cooling device for LEAR," pp. 605-618; H. Herr, "A small deceleration ring for extra low energy antiprotons (ELENA)," pp. 633-642.

1983

T. Ellison, W. Kells, V. Kerner, F. Mills, R. Peters, T. Rathbun, D. Young, P.M. McIntyre, "Electron cooling and accumulation of 200-MeV protons at Fermilab," IEEE Trans. Nuclear Sci. NS-30, 2636-2638 (1983).

E. Asseo, M. Boutheon, R. Cappi, G. Carron, M. Chanel, D. Dumollard, R. Garoby, R. Giannini, W. Hardt, et al. "Low energy antiprotons at the CERN PS," pp 20-23 (in Russian), Proc. 12th Int. Conf. High-Energy Accel., F.T. Cole and D. Donaldson, ed., Fermi National Accelerator Lab, Batavia, Illinois (1983).

1984

K. Kilian, "Physics with antiprotons at LEAR," pp. 324-341, CERN Publication 84-09, Proc. Fourth Topical Workshop on Proton-Antiproton Collider Physics, Berne, 5-8 March 1984, (8 August 1984).

1985

U. Gastaldi, R. Klapisch, J.M. Richard, and J. Tran Thanh Van, Eds, *Physics with Antiprotons at LEAR in the ACOL Era*, Editions Frontieres, Gif-sur-Yvette, France (1985), \$100.00. Proceedings of the LEAR Workshop: Physics with Low Energy Cooled Antiprotons in the ACOL Era, Tignes (Savoie), France (19-26 January 1985).

R. Billinge, "Introduction to CERN's Antiproton Facilities for the 1990's," p. 13.

E. Jones, "Progress on ACOL," p. 25.

P. Lefevre, "LEAR Present Status and Future Developments," p. 33.

D.J. Simon, et al., "The LEAR Experimental Areas: Status Report and Possible Developments," p. 47.

D. Möhl, "Technical Implications of Possible Future Options for LEAR," p. 65.

D. Möhl, et al., "A Superconducting Low Energy Antiproton Ring (Super-LEAR)," p. 83.

J.H. Billen, et al., "An RFQ as a Particle Decelerator," p. 107.

C. Biscari and F. Iazzourene, "Post Deceleration of the LEAR Beam by a Radiofrequency Quadrupole," p. 115.

G. Carron, et al., "Status and Future Possibilities of the Stochastic Cooling System for LEAR," p. 121.

A. Wolf, et al., "Status and Perspectives of the Electron Cooling Device Under Construction at CERN," p. 129.

L. Tecchio, et al., "Possibilities for High Energy Electron Cooling in LEAR," p. 135.

D. Iaqu, "Possibilities of Cooling the Extracted Antiproton LEAR Beams," p. 143.

T. Katayama, et al., "Stochastic Momentum Cooling of Low Energy, 7 MeV Proton Beam," p. 151.

I. Hofmann, "Density Limitations in Cooled Beams," p. 159.

L. Tecchio, "Electron Cooling at Intermediate Energy," p. 167.

J.H. Billen, K.R. Crandall, T.P. Wangler, M. Weiss, "An RFQ as a particle decelerator," Los Alamos National Lab Preprint LA-UR-85-140, Third LEAR Workshop, Tignes-Savoie, France (19-26 Jan 1985).

A.M. Green and J.A. Niskanen, "Low-Energy Antiproton Physics in the Early LEAR Era," Preprint HU-TFT-85-60 (December 1985), Helsinki University, Siltavuorenpenger 20, SF-00170 Helsinki 17, Finland.

M.R. Pennington, Ed., *Antiproton 1984*, Hilger, Bristol, England (1985). Institute of Physics Conference Series, 73, 530p, \$76.00. Proceedings of 7th European Symposium on Antiproton Interactions: From LEAR to the Collider and Beyond, Durham, England (9-13 July 1984).

M. Chanel, et al., "LEAR: Machine and Experimental Areas: Experience and Future Plans After 1-Year of Operation," p. 119.

1986

B.E. Bonner and L.S. Pinsky, Proceedings of the First Workshop on Antimatter Physics at Low Energy, Fermilab, Batavia, Illinois (10-12 April 1986), U.S. Gov. Printing Office 1986-644-171.

Contains the following papers:

Rolf Landua, "The Future Physics at LEAR," pp. 35-68.

P. Lefevre, D. Mohl, D.J. Simon, "Future Machine Improvements in LEAR," pp. 69-82.

Petros A. Rapidis, "The Fermilab Antiproton Source: Prospects for $p\bar{p}$ Experiments," pp. 83-94.

Michael S. Chanowitz, "Physics Overview of the Fermilab Low Energy Antiproton Facility Workshop," pp. 393-418.

F.E. Mills, "Cooling of Stored Beams," Pbar Note 463 (10 June 1986), Pbar Source Department, Fermilab, P.O. Box 500, Batavia, Illinois 60510 USA. (The physics of beam cooling and the ranges of utility of stochastic and electron cooling are discussed in this paper.)

Y.Y. Lee, "A Thought on Very Low Energy Anti-Protons," BNL Accelerator Division Tech. Note 266 (17 October 1986), Accelerator Division, AGS Department, Brookhaven National Lab, Upton, New York 11973 USA. (The AGS extracts three rf buckets of protons to strike an anti-proton production target. The anti-protons will be collected by an appropriate lens system and injected into the booster. After deceleration to 200 MeV, they can be further decelerated through the linac and an RFQ preinjector. If one cools the anti-protons in the booster to 14.6 mm-mrad at 200 MeV energy, theoretically half of the 1.33×10^8 anti-protons collected at 3.5 GeV/c could be decelerated to 750 keV and then to 20 keV.)

Y.Y. Lee and D.I. Lowenstein, "A Conceptual Design for a Very Low Energy Antiproton Source," BNL AGS/AD/Tech. Note 269 (3 December 1986), Accelerator Division, AGS Department, Brookhaven National Lab, Upton, New York 11973 USA. [Ed: A more detailed engineering discussion and cost estimate for the Y.Y. Lee Tech. Note 266. The cost is estimated at \$8,620,000.]

Gerald A. Smith, "Is There a Need for a LEAR-like Facility in North America?," pp. 395-399, Proc. Conference on Intersections Between Particle and Nuclear Physics, Lake Louise, Canada (1986), Donald F. Geesaman, Ed., Am. Inst. Physics Conference Proceedings 150, AIP, New York (1986).

David B. Cline, Ed., Low Energy Antimatter, World Scientific, Singapore (1986). Proceedings of the Workshop on the Design of a Low Energy Antimatter Facility, University of Wisconsin-Madison, Madison, Wisconsin, USA (October 1985).

Frank Krienen, "Progress in Hollow Cathode Electron Gun for Electron Cooling," p. 92.

M. Sedlacek, "The Celsius-Ring in Uppsala: Electron Cooler Design," p. 196.

M. Takasaki, S. Kurokawa, M. Kobayashi, M. Taino, Y. Suzuki, H. Ishii, Y. Kato, T. Fujitani, Y. Nagashima, T. Omori, S. Sugimoto, Y. Yamaguchi, J. Iwahori, H. Yoshida, F. Takeutchi, M. Chiba, M. Koike, "The Low-energy Antiproton Beam K4 at the KEK 12 GeV Proton Synchrotron," Nuclear Inst. and Methods **A242**, 210-207 (1986). (The beam K4 is designed to transport high-intensity, high-purity antiprotons in the momentum range between 0.4 and 0.8 GeV/c. The measured intensities of antiprotons at 650 MeV/c are 1.1×10^{15} ppp.)

Delbert John Larson, "Intermediate Energy Electron Cooling for Anti-Proton Sources" Preprint WISC-EX-86-271 (1986), University of Wisconsin/Madison, Madison, Wisconsin 53706 USA. (Ph.D. Thesis. 166 pages.)

4. PRODUCTION OF ANTIHYDROGEN ATOMS, MOLECULES, AND CLUSTERS

1961

J.C. Mullins, W.T. Ziegler, and B.S. Kirk, "The thermodynamic properties of parahydrogen from 1 to 22 K," Tech. Report No. 1, Project No. A-593, Contract CST-7339, National Bureau of Standards, Boulder, Colorado (1 November 1961).

1973

H.M. Roder, G.E. Childs, R.D. McCarty and P.E. Angerhafer, "Survey of properties of H isotopes below their critical temperatures," TN 641, National Bureau of Standards, Boulder, Colorado (1973).

1974

F. Schmidt, "Diffusion and ortho-para conversion in solid hydrogen," Phys. Rev. D10, 4480-4484 (1974).

1975

R.D. McCarty, "Hydrogen technological survey," Thermophysical Properties," NASA SP-3089 [550 pages] (1975).

1980

I.F. Silvera, "The solid molecular hydrogens in the condensed phase: Fundamentals and static properties," Rev. Mod. Phys. 32, 393-452 (1980).

1981

R.D. McCarty, J. Hord, and H.M. Roder, Edited by J. Hord, "Selected properties of hydrogen (engineering design data)," Center for Chemical Engineering, National Engineering Lab, National Bureau of Standards, Boulder, Colorado (February 1981).

1982

M. Bell and J.S. Bell, "Capture of cooling electrons by cool protons," Particle Accelerators, 12, 49-52 (1982).

1983

H.J. Maris, G.M. Seidel, and T.E. Huber, "Supercooling of Liquid H_2 and the Possible Production of Superfluid H_2 ," J. Low Temp. Phys. 51, 471-487 (1983).

R. Neumann, H. Poth, A. Winnacker, and A. Wolf, "Laser-enhanced electron-ion capture and antihydrogen formation," *Z. Phys. A*, **313**, 253-262 (1983).

1984

I.Ya. Minchina, M.I. Bagatskii, V.G. Manzhelii, and A.I. Krivchikov, "Quantum Diffusion in Hydrogen, Studied by Calorimetric Methods," *Sov. J. Low Temp. Physics* **10**, 549-556 (1984). [English translation of *Fiz. Nizk. Temp.* **10**, 1051-1065 (1984).] [Dilute solid solutions of hydrogen were studied over the temperature range 0.4 to 3 K, with ortho concentrations of 0.10, 0.21, 0.50, and 1.10%.]

M.I. Bagatskii, I.Ya. Minchina, and V.G. Manzhelli, "Specific Heat of Solid Parahydrogen," *Sov. J. Low Temp. Physics* **10**, 542-548 (1984). [English translation of *Fiz. Nizk. Temp.* **10**, 1039-1051 (1984).] (We report the specific heat of hydrogen with an orthohydrogen concentration of 5×10^{-5} over the temperature range 0.5 to 8 K.)

H. Herr, D. Mohl, and A. Winnacker, "Production of and experimentation with antihydrogen at LEAR," pp. 659-676, *Physics at LEAR with Low-Energy Cooled Antiprotons*, Workshop on Physics at LEAR with Low-Energy Cooled Antiprotons, Erice, Sicily, Italy, 9-16 May 1982, U. Gastaldi and R. Klapisch, ed., Plenum Press, NY (1984).

1985

U. Gastaldi, R. Klapisch, J.M. Richard, and J. Tran Thanh Van, Eds, *Physics with Antiprotons at LEAR in the ACOL Era*, Editions Frontieres, Gif-sur-Yvette, France (1985), \$100.00. Proceedings of the LEAR Workshop: Physics with Low Energy Cooled Antiprotons in the ACOL Era, Tignes (Savoie), France (19-26 January 1985).

M. Conte, "Antihydrogen Storage Rings," p. 711.

1986

B.E. Bonner and L.S. Pinsky, *Proceedings of the First Workshop on Antimatter Physics at Low Energy*, Fermilab, Batavia, Illinois (10-12 April 1986), U.S. Gov. Printing Office 1986-644-171. Contains the following papers:

H. Poth, "Antiprotonic, Hyperonic, and Antihydrogen Atoms," pp. 325-345.

Giulio Casati, Boris V. Chirikov, Dima L. Shepelyansky, and Italo Guarneri, "New Photoelectric Ionization Peak in the Hydrogen Atom," *Phys. Rev. Lett.* **57**, 823-826 (18 Aug 1986).

A.P. Mills, Jr. and E.M. Gullikson, "Solid Neon Moderator for Producing Slow Positrons," Appl. Phys. Lett. **49**, 1121-1123 (27 October 1986). (Slow positrons can be obtained by moderating the energetic β^+ particles from a radioactive source. We find that solid Ne makes a more efficient moderator than any other material known to date. In a cylindrical geometry, the efficiency for production of slow (0.58 eV) positrons is 0.7%. Scaling to a neon coated 10^4 Ci ^{64}Cu source would produce 10^{11} slow positrons per second.)

David B. Cline, Ed., Low Energy Antimatter, World Scientific, Singapore (1986). Proceedings of the Workshop on the Design of a Low Energy Antimatter Facility, University of Wisconsin-Madison, Madison, Wisconsin, USA (October 1985).

Robert L. Forward, "Making and Storing Antihydrogen for Propulsion," p. 47.

A. Wolf, et al., "Electron Cooling of Low-Energy Antiprotons and Production of Fast Antihydrogen Atoms," p. 78.

R.S. Conti and A. Rich, "The Status of High Intensity, Low Energy Positron Sources for Anti-hydrogen Production," p. 105. Andreas Wolf, "Antihydrogen," Preprint CERN-EP/86-179 (12 November 1986), CERN, CH-1211 Geneva 23, Switzerland. (An overview is given of the possibilities of forming antihydrogen atoms in the laboratory. Presented at 8th European Symposium on Proton-Antiproton Interactions, Thessaloniki, Greece, 1-5 September 1986.)

G.M. Seidel, H.J. Maris, F.I.B. Williams, and J.G. Cardon, "Supercooling of Liquid Hydrogen," Phys. Rev. Lett. **56**, 2380 (1986).

A.Z. Tang and F.T. Chan, "Dynamic Multipole Polarizability of Atomic Hydrogen," Phys. Rev. **A33**, 3671 (1986).

William C. Stwalley and Marshall Lapp, Eds., Advances in Laser Science-I, American Institute of Physics Conference Proceedings No. **146**, New York (1986). Proceedings of First International Laser Science Conference (ILS-I), Dallas, Texas, USA (1985).

R.G. Beausoleil, B. Couillaud, C.J. Foot, T.W. Hänsch, E.A. Hildum, and D.H. McIntyre, "High Resolution Laser Spectroscopy of Atomic Hydrogen," p. 366.

C.W. Clark, "Autodetaching States of Negative Ions," p. 379.

G. Torelli and N. Beverini, "Antiproton Traps and Related Experiments," pp 111-115, Proc. Nuclear and Particle Physics at Intermediate Energies with Hadrons, T. Bressani and G. Pauli, Ed., Vol. 3, Societa Italiana di Fisica (1986). [Ed: Discusses feasibility of using Penning antiproton trap with a superposed rf field to trap positrons in order to form antihydrogen for a gravitational experiment. It is found to be difficult and further analysis is said to be needed.]

1987

H. Poth, "Anti-Hydrogen Formation Through Positron-Anti-Proton Radiative Combination," Preprint CERN-EP/87-75 (April 1987). [Ed: Obtain from Kernforschungszentrum Karlsruhe, Inst. fur Kernphysik, Postfach 3640, D-7501 Leopoldshafen, Germany.]

J.B.A. Mitchell, "The Role of Electron-Ion Recombination in Bulk Antimatter Production". Preprint (undated). [Ed: Obtain from Dept. Physics, Univ. Western Ontario, London, Ontario, Canada N6A 3K7.] (Discussion of how electron-ion recombination must be optimized in order to maximize the production of antimatter cluster ions.)

J.T. Bahns, "The Cluster Ion Approach to the Condensation and Storage of Antihydrogen," AFRPL preprint. Copies may be obtained from AFRPL/LKC, Edwards AFB, CA 93253-5000 USA. (The problem of concentrating antiprotons and positrons into a high energy density form is analyzed from the "containerless" condensation of cluster ions of (anti)hydrogen in ion traps using ion-neutral association. It is concluded that the condensation need only be done once in order to produce a multiply charged "mother" cluster that can be used to generate "seed" cluster ions suitable for growth of macroscopic crystals.)

5. SLOWING, COOLING, AND TRAPPING OF ATOMS, IONS, AND MOLECULES

1950

G. Herzberg, *Molecular Spectra and Molecular Structure - I. Spectra of Diatomic Molecules*, 2nd Ed., D. Van Nostrand, Princeton, NJ (1950).

1961

J.C. Mullins, W.T. Ziegler, and B.S. Kirk, "The thermodynamic properties of parahydrogen from 1 to 22 K," Tech. Report No. 1, Project No. A-593, Contract CST-7339, National Bureau of Standards, Boulder, Colorado (1 November 1961).

1966

R.D. Waldron, "Diamagnetic levitation using pyrolytic graphite," *Rev. Sci. Inst.* **37**, 29-34 (1966).

1968

I. Simon, et al., "Sensitive tiltmeter utilizing a diamagnetic suspension," *Rev. Sci. Inst.* **39**, 1666 (1968).

1969

R. Evrard and G.-A. Boutry, "An absolute micromanometer using diamagnetic levitation," *J. Vacuum Sci. and Tech.* **6**, 279 (1969).

1970

R. W. Waynant, J.D. Shipman, Jr., R.C. Elton, and A.W. Ali, "VUV laser emission from molecular hydrogen," *Appl. Phys. Lett.* **17**, 383 (1970).

A. Ashkin, "Acceleration and trapping of particles by radiation pressure," *Phys. Rev. Lett.* **24**, 156-159 (1970).

A. Ashkin, "Atomic-beam deflection by resonance-radiation pressure," *Phys. Rev. Lett.* **25**, 1321-1324 (1970).

R.T. Hodgson, "VUV laser action observed in the Lyman band of molecular hydrogen," *Phys. Rev. Lett.* **25**, 494 (1970).

1973

H.M. Roder, G.E. Childs, R.D. McCarty and P.E. Angerhafer, "Survey of properties of H isotopes below their critical temperatures," TN 641, National Bureau of Standards, Boulder, Colorado (1973).

1974

A.P. Kazantsev, "The acceleration of atoms by light," Sov. Phys. JETP, **39**, 784-790 (1974).

I. Nebenzahl and A. Szöke, "Deflection of atomic beams by resonance radiation using stimulated emission," Appl. Phys. Lett. **25**, 327-329 (1974).

R.W. Dreyfus, "Molecular hydrogen laser: 1098-1613 Angstrom," Phys. Rev. A9, 2635 (1974).

1975

R. D. McCarty, "Hydrogen technological survey," Thermophysical Properties," NASA SP-3089 [550 pages] (1975).

D.J. Wineland and H.G. Dehmelt, "Principles of the stored ion calorimeter," J. Appl. Phys. **46**, 919-930 (1975).

T.W. Hänsch and A.L. Schawlow, "Cooling of gases by laser radiation," Optics Comm. **13**, 68-69 (1975).

1976

R.S. Van Dyck, Jr., D.J. Wineland, P.A. Ekstrom, and H.G. Dehmelt, "High mass resolution with a new variable anharmonicity Penning trap," Appl. Phys. Lett. **28**, 446-448 (1976).

A. Ashkin and J.M. Dziedzic, "Optical levitation in high vacuum," Appl. Phys. Lett., **28**, 333-335 (1976).

H. Friedman and A.D. Wilson, "Isotope separation by radiation pressure of coherent pi pulses," Appl. Phys. Lett. **28**, 270 (1976).

1977

V.S. Letokhov, V.G. Minogin and B.D. Pavlik, "Cooling and capture of atoms and molecules by a resonant light field," Sov. Phys. JETP, **45**, 698-705 (1977).

W. Thompson and S. Hanrahan, "Characteristics of a cryogenic extreme high-vacuum chamber," J. Vac. Sci. Technol. **14**, 643-645 (1977).

1978

W. Neuhauser, M. Hohenstatt, P. Toschek, and H. Dehmelt, "Optical-sideband cooling of visible atom cloud confined in parabolic well," Phys. Rev. Lett. **41**, 233-236 (1978).

W. Neuhauser, M. Hohenstatt, P.E. Toschek, and H.G. Dehmelt, "Visual observation and optical cooling of electrostatically contained ions," Appl. Phys. 17, 121-129 (1978).

D.J. Wineland, R.E. Drullinger, and F.L. Walls, "Radiation-pressure cooling of bound resonant absorbers," Phys. Rev. Lett. 40, 1639-1642 (1978).

A. Ashkin, "Trapping of atoms by resonance radiation pressure," Phys. Rev. Lett. 40, 729-732 (1978).

J.E. Bjorkholm, R.R. Freeman, A. Ashkin, and D.B. Pearson, "Observation of focusing of neutral atoms by the dipole forces of resonance-radiation pressure," Phys. Rev. Lett. 41, 1361-1364 (1978).

1979

A. Ashkin and J.P. Gordon, "Cooling and trapping of atoms by resonance radiation pressure," Optics Lett. 4, 161-163 (1979).

V.I. Balykin, V.S. Letokhov, and V.I. Mishin, "Observation of the cooling of free sodium atoms in a resonance laser field with a scanning frequency," Pis'ma Zh. Exp. Teo. Fiz. 29, 614-618 (1979) [English translation JETP Lett. 29, 561-564 (1979)].

L.N. Breusova, I.N. Knyazev, V.G. Movshev, and T.B. Fogel'son, "Vacuum ultraviolet H₂ laser with a sealed gas-discharge cell," Kvant. Elektron. 6, 2458-2460 (1979) [English translation Sov. J. Quantum Elec. 9, 1452-1453 (1979)].

1980

P. Ekstrom and D. Wineland, "The isolated electron," Sci. Am. 243, 105-121 (August 1980).

V.S. Letokhov and V.G. Minogin, "Possibility of accumulation and storage of cold atoms in magnetic traps," Optics Comm., 35, 199-202 (1980).

J.P. Gordon and A. Ashkin, "Motion of atoms in a radiation trap," Phys. Rev. A21, 1606-1617 (1980).

W. Neuhauser, M. Hohenstatt, P.E. Toschek, and H. Dehmelt, "Localized visible Ba⁺ mono-ion oscillator," Phys. Rev. 22A, 1137-1140 (1980).

D.B. Pearson, R.R. Freeman, J.E. Bjorkholm, and A. Askin, "Focusing and defocusing of neutral atomic beams using resonance-radiation pressure," Appl. Phys. Lett. 36, 99-101 (1980).

W.H. Wing, "Electrostatic trapping of neutral atomic particles," Phys. Rev. Lett., **45**, 631-634 (1980).

V.I. Balykin, V.S. Letokhov, and V.I. Mishin, "Cooling of sodium atoms by resonant laser emission," Zh. Exp. Teo. Fiz. **78**, 1376-1385 (1980) [English translation Sov. Phys. JETP **51**, 692-696 (1980)].

V.I. Balykin, "Cyclic interaction of Na atoms with circularly polarized laser radiation," Optics Comm. **33**, 31-36 (1980).

R.W. Cline, et al., "Magnetic confinement of spin-polarized atomic hydrogen," Phys. Rev. Lett., **45**, 2117-2120 (1980).

1981

R.D. McCarty, J. Hord, and H.M. Roder, Edited by J. Hord, "Selected properties of hydrogen (engineering design data)," Center for Chemical Engineering, National Engineering Lab, National Bureau of Standards, Boulder, Colorado (February 1981).

V.S. Letokhov and V.G. Minogin, "Laser radiation pressure on free atoms," Phys. Reports **73**, 1-65 (1981) [review].

P.B. Schwinberg, R.S. Van Dyck, Jr., and H.G. Dehmelt, "New comparison of the positron and electron g factors," Phys. Rev. Lett. **47**, 1679-1682 (1981).

S.V. Adreev, V.I. Balykin, V.S. Letokhov, and V.G. Minogin, "Radiative slowing and reduction of the energy spread of a beam of sodium atoms to 1.5 K in an oppositely directed laser beam," Pis'ma Zh. Eksp. Teor. Fiz. **34**, 463-467 (1981) [English translation Sov. Phys. JETP Lett. **34**, 442-445 (1981)].

A.F. Bernhardt and B.W. Shore, "Coherent atomic deflection by resonant standing waves," Phys. Rev. **23A**, 1290-1301 (1981).

J.E. Bjorkholm, R.R. Freeman, and D.B. Pearson, "Efficient transverse deflection of neutral atomic beams using spontaneous resonance-radiation pressure," Phys. Rev. **23A**, 491-497 (1981).

T. Breeden and H. Metcalf, "Stark acceleration of Rydberg atoms in inhomogeneous electric fields," Phys. Rev. Lett. **47**, 1726-1729 (1981).

1982

R.J. Cook and R.K. Hill, "An electromagnetic mirror for neutral atoms," Optics Comm. **43**, 258-260 (1982).

S.V. Andreev, V.I. Balykin, V.S. Letokhov, and V.G. Minogin, "Radiative Slowing Down and Monochromatization of a Beam of Sodium Atoms in a Counter-propagating Laser Beam," Sov. Phys. JETP **55**, 828-834 (1982).

W.D. Phillips and H.J. Metcalf, "Laser deceleration of an atomic beam," Phys. Rev. Lett., 48, 596-599 (1982).

J.V. Prodan, W.D. Phillips, and H.J. Metcalf, "Laser production of a very slow monoenergetic atomic beam," Phys. Rev. Lett. 49, 1149-1153 (1982).

W-K Rhim, M.M. Saffren, and D.D. Elleman, "Development electrostatic levitator at JPL," pp. 115-119 of Materials Processing in the Reduced Gravity Environment of Space, G.E. Rindone, ed., Elsevier Science (1982).

I.F. Silvera and J. Walraven, "The stabilization of atomic hydrogen," Sci. Am. 246, 66-74 (January 1982).

R.R. Zito, "The cryogenic confinement of antiprotons for space propulsion systems," J. British Interplanetary Soc., 35, 414-421 (1982).

1983

W.D. Phillips, ed., Laser-cooled and trapped atoms, NBS Special Publication 653, Proc. Workshop on Spectroscopic Applications of Slow Atomic Beams, NBS Gaithersburg, MD (14-15 April 1983).

J. F. Lam, R.A. McFarlane, A.J. Palmer, and D.G. Steel, "Experimental and theoretical studies of laser cooling and emittance control of neutral beams," Hughes Research Laboratories, Malibu, California, Annual Report on AFOSR Contract F49620-82-C-0004, (September 1983).

D.G. Steel, J.F. Lam, R.A. McFarlane, "Studies of laser enhanced relativistic ion beam neutralization," White Paper, Hughes Research Laboratories, Malibu, California (October 1983).

A. Ashkin and J.P. Gordon, "Stability of radiation-pressure particle traps: an optical Earnshaw theorem," Optics Lett. 8, 511-513 (1983).

R. Blatt, W. Ertmer, and J.L. Hall, "Cooling of an atomic beam with frequency-sweep techniques," pp. 142-153, Laser-Cooled and Trapped Atoms, NBS SP-653, W.D. Phillips, ed. (1983).

J. Dalibard, S. Reynaud, and C. Cohen-Tannoudji, "Proposals of stable optical traps for neutral atoms," Optics Comm. 47, 395-399 (1983).

H.F. Hess, D.A. Bell, G.P. Kochanski, R.W. Cline, D. Kleppner, and T.J. Greytak, "Observation of three-body recombination in spin-polarized hydrogen," Phys. Rev. Lett. 51, 483-486 (1983).

M.S. Lubell and K. Rubin, "Velocity compression and cooling of a sodium atomic beam using a frequency modulated ring laser," pp. 125-136, *Laser-Cooled and Trapped Atoms*, NBS SP-653, W.D. Phillips, ed. (1983).

H.J. Metcalf, "Magnetic trapping of decelerated neutral atoms," *Laser-Cooled and Trapped Atoms*, NBS SP-653, W.D. Phillips, ed. (1983).

W.D. Phillips, J.V. Prodan, and H.J. Metcalf, "Neutral atomic beam cooling experiments at NBS," pp. 1-8, *Laser-Cooled and Trapped Atoms*, NBS SP-653, W.D. Phillips, ed. (1983).

J.V. Prodan and W.D. Phillips, "Chirping the light -- fantastic?," pp. 137-141, *Laser-Cooled and Trapped Atoms*, NBS SP-653, W.D. Phillips, ed. (1983).

R. Sprik, J.T.M. Walraven, and I.F. Silvera, "Compression of spin-polarized hydrogen to high density," *Phys. Rev. Lett.* 51, 479-482 (1983).

W.C. Stwalley, "A hybrid laser-magnet trap for spin-polarized atoms," pp. 95-102, *Laser-Cooled and Trapped Atoms*, NBS SP-653, W.D. Phillips, ed. (1983).

W.H. Wing, "Some problems and possibilities for quasistatic neutral particle trapping," pp. 74-93, *Laser-Cooled and Trapped Atoms*, NBS SP-653, W.D. Phillips, ed. (1983).

W.H. Wing, "Gravitational effects in particle traps," p. 94, *Laser-Cooled and Trapped Atoms*, NBS SP-653, W.D. Phillips (editor) (1983).

1984

W. Kells, G. Gabrielse, and K. Helmer, "On achieving cold antiprotons in a Penning trap," FERMILAB-Conf-84/68-E, Fermi National Accelerator Lab, Batavia, Illinois (August 1984). [Preprint submitted to the IX Int. Conf. on Atomic Physics, Seattle, Washington (23-27 July 1984).]

W. Kells, G. Gabrielse, and K. Helmer, "On achieving cold antiprotons in a Penning trap," FERMILAB-Conf-84/68-E, Fermi National Accelerator Lab, Batavia, Illinois (August 1984). [Preprint submitted to the IX Int. Conf. on Atomic Physics, Seattle, Washington (23-27 July 1984).]

Fermilab, Design Report: Tevatron 1 Project, pp. 4-13 to 1-16, Fermi National Accelerator Lab, Batavia, Illinois (September 1984).

R.A. McFarlane, D.G. Steel, R.S. Turley, J.F. Lam, and A.J. Palmer, "Experimental and theoretical studies of laser cooling and emittance control of neutral beams," Hughes Research Laboratories, Malibu, CA 90265, Annual report on contract F49620-82-C-0004, AFOSR, Bolling AFB, DC 20332 (Oct 1984).

A. Bernard, J.P. Canny, T. Juillerat, and P. Touboul, "Electrostatic suspension of samples in microgravity," Proc. 35th Congress of International Astronautical Federation, Lausanne, Switzerland (7-13 October 1984).

D.J. Wineland, "Trapped ions, laser cooling, and better clocks," Science 226, 395-400 (26 Oct 1984).

A.L. Welles, "Quantum Theory of Ion Motion and Laser Cooling in a Radio Frequency Quadrupole Trap," M.S. Thesis, AFIT/GEP/PH/84D-12, School of Engineering, Air Force Inst. of Tech., Wright-Patterson AFB, Ohio 45433, AD-A163838 (December 1984).

A.J. Palmer and J.F. Lam, "Radiation cooling with pi-pulses," Paper WG1, Annual Meeting Optical Soc. Am., San Diego (1984) [submitted to J. Opt. Soc. Am. (1985)].

N. Beverini, L. Bracci, V. Lagomarsino, G. Manuzio, R. Parodi, and G. Torelli, "A Penning trap to store antiprotons," pp. 771-778, Physics at LEAR with Low-Energy Cooled Antiprotons, Workshop on Physics at LEAR with Low-Energy Cooled Antiprotons, Erice, Sicily, Italy, 9-16 May 1982, U. Gastaldi and R. Klapisch, ed., Plenum Press, NY (1984).

L. Campbell, W.R. Gibbs, T. Goldman, D.B. Holtkamp, M.V. Hynes, N.S.P. King, M.M. Nieto, A. Picklesimer, and T.P. Wangler, "Basic research in atomic, nuclear and particle physics," LA-UR-84-3572, Los Alamos National Lab, Los Alamos, New Mexico (1984).

G. Gabrielse, "Detection, damping, and translating the center of the axial oscillation of a charged particle in a Penning trap with hyperbolic electrodes," Phys. Rev. 29A, 462-469 (1984).

V.I. Balykin, V.S. Letokhov, V.G. Minogin, and T.V. Zueva, "Collimation of Atomic Beams by Resonant Laser Radiation Pressure," Appl. Phys. B35, 149-153 (1984).

V.I. Balykin, V.S. Letokhov, and A.I. Sidorov, "Radiative Collimation of an Atomic Beam by Two-Dimensional Cooling by a Laser Beam," Pis'ma v Zh. Eksp. & Teor. Fiz. 40, 251-253 (1984). [English translation, JETP Lett. 40, 1026-1029 (1984)].

V.I. Balykin, V.S. Letokhov, and A.I. Sidorov, "Formation of an Intense Stationary Beam of Cold Atoms by Laser Deceleration of an Atomic Beam," Zh. Eksp. Teor. Fiz. 86, 2019-2029 (1984). [English translation, Sov. Phys. JETP 49, 1174-1179 (1984)].

F.J. Northrop, et al., "VUV laser-induced fluorescence of molecular hydrogen," Chem. Phys. Let. 105, 34-37 (1984).

1985

T. Goldman and M.M. Nieto, "Gravitational properties of antimatter," Los Alamos National Lab Preprint LA-UR-85-1092, Third LEAR Workshop, Tignes-Savoie, France (19-26 Jan 1985).

M.V. Hynes, "Physics with low temperature antiprotons," Los Alamos National Lab preprint LA-UR-85-1060, Third LEAR Workshop, Tignes, France (19-26 Jan 1985).

G. Gabrielse, et al., "Precision Comparison of Antiproton and Proton masses in a Penning Trap," pp. 665-674, Proc. Third LEAR Workshop, Tignes-Savoie-France (19-26 January 1985), U. Gastaldi, R. Klapisch, J.M. Richard, and J. Tran Thanh Van, Editors, Editions Frontieres, B.P. 44, 91190 GIF sur Yvette, France (1985).

M.V. Hynes, "Physics with Low Temperature Antiprotons," pp. 657-664, Proc. Third LEAR Workshop, Tignes-Savoie-France (19-26 January 1985), U. Gastaldi, R. Klapisch, J.M. Richard, and J. Tran Thanh Van, Editors, Editions Frontieres, B.P. 44, 91190 GIF sur Yvette, France (1985).

U. Gastaldi, R. Klapisch, J.M. Richard, and J. Tran Thanh Van, Eds, Physics with Antiprotons at LEAR in the ACOL Era, Editions Frontieres, Gif-sur-Yvette, France (1985), \$100.00. Proceedings of the LEAR Workshop: Physics with Low Energy Cooled Antiprotons in the ACOL Era, Tignes (Savoie), France (19-26 January 1985).

J.H. Billen, et al., "An RFQ as a Particle Decelerator," p. 107.

C. Biscari and F. Iazzourene, "Post Deceleration of the LEAR Beam by a Radiofrequency Quadrupole," p. 115.

M. Nieto, et al., "Gravitational Properties of Antimatter," p. 639.

G. Torelli, et al, "Gravitational Measurement on Antiprotons," p. 649.

M.V. Hynes, "Physics with Low Temperature Antiprotons," p. 657.

G. Gabrielse, et al., "Precision Comparison of Antiproton and Proton Masses in a Penning Trap," p. 665.

M. Conte, "Antihydrogen Storage Rings," p. 711.

M. Conte, "Antihydrogen Storage Rings," pp. 711-718, Proc. Third LEAR Workshop, Tignes-Savoie-France (19-26 January 1985), U. Gastaldi, R. Klapisch, J.M. Richard, and J. Tran Thanh Van, Editors, Editions Frontieres, B.P. 44, 91190 GIF sur Yvette, France (1985). (The existing magnetic bottles for ultra-cold polarized neutrons are reconsidered as possible containers for polarized antihydrogen atoms.)

J.H. Billen, K.R. Crandall, T.P. Wangler, M. Weiss, "An RFQ as a particle decelerator," Los Alamos National Lab Preprint LA-UR-85-140, Third LEAR Workshop, Tignes-Savoie, France (19-26 Jan 1985).

M. Nieto, et al., "Gravitational Properties of Antimatter," pp. 639-648, Proc. Third LEAR Workshop, Tignes-Savoie-France (19-26 January 1985), U. Gastaldi, R. Klapisch, J.M. Richard, and J. Tran Thanh Van, Editors, Editions Frontieres, B.P. 44, 91190 GIF sur Yvette, France (1985).

G. Gabrielse, H. Kalinowsky, W. Kells, and T.A. Trainor, "Precision Comparison of Antiproton and Proton Masses in a Penning Trap," Proposal P83 to the Proton Synchrotron Coordination Committee of CERN, Geneva, Switzerland (15 April 1985).

R.V.E. Lovelace, C. Mehanian, T.J. Tømmila, and D.M. Lee, "Magnetic Confinement of a Neutral Gas," Nature 318, No. 6041, 30-36 (7 November 1985). (A three-dimensional dynamic trap for confining a collisional neutral gas is described. The trap uses the interaction of the magnetic moments of the gas atoms with a time-dependent magnetic field.)

P. Meystre and S. Stenholm, The Mechanical Effects of Light. A special issue of J. Optical Soc. Am. B3, 1706-1860 (November 1985) containing the following papers relevant to the control, cooling, and trapping of ions and neutral atoms:

J. Dalibard and C. Cohen-Tannoudji, "Dressed-Atom Approach to Atomic Motion in Laser Light: The Dipole Force Revisited," 1707.

D.J. Wineland et al., "Angular Momentum of Trapped Atomic Particles," 1721.

A.P. Kazantsev et al., "Kinetic Phenomena of Atomic Motion in a Light Field," 1731.

S. Stenholm, "Dynamics of Trapped Particle Cooling in the Lamb-Dicke Limit," 1743.

W.D. Philips, J.V. Prodan, and H.J. Metcalf, "Laser Cooling and Electromagnetic Trapping of Neutral Atoms," 1751.

J. Javanainen, et al., "Laser Cooling of a Fast Ion Beam," 1768.

V.I. Balykin, et al., "Radiative Collimation of Atomic Beams Through Two-Dimensional Cooling of Atoms by Laser-Radiation Pressure," 1776.

P.E. Moskowitz, P.L. Gould, and D.E. Pritchard, "Deflection of Atoms by Standing-Wave Radiation," 1784.

V.P. Chebotayev, et al., "Interference of Atoms in Separated Optical Fields," 1791.

D.E. Pritchard and P.L. Gould, "Experimental Possibilities for Observation of Unidirectional Momentum Transfer to Atoms from Standing-Wave Light," 1799.

V.A. Grinchuk, et al., "Scattering of Atoms by Coherent Interaction with Light," 1805.

J.J. Bollinger, J.D. Prestage, W.N. Itano, and D.J. Wineland, "Laser-cooled atomic frequency standard," Phys. Rev. Lett. 54, 1000-1003 (1985).

W. Ertmer, R. Blatt, J.L. Hall, and M. Zhu, "Laser manipulation of atomic beam velocities: Demonstration of stopped atoms and velocity reversal," Phys. Rev. Lett. 54, 996-999 (1985).

S. Chu, L. Hollberg, J.E. Bjorkholm, A. Cable, and A. Ashkin, "Three-Dimensional Viscous Confinement and Cooling of Atoms by Resonance Radiation Pressure," Phys. Rev. Lett. 55, 48 (1985).

V.I. Balykin, V.S. Letokhov, and V.G. Minogin, "Cooling of Atoms by Laser Radiation Pressure," Usp. Fiz. Nauk. 147, 117-156 (1985). [A long review in Russian.]

V.I. Balykin, T.V. Zueva, V.S. Letokhov, and V.G. Minogin, "Collimation of Atom Beams by the Pressure of Resonant Laser Radiation," Sov. Phys. Tech. Phys. 30, 1027-1030 (1985).

V.I. Balykin, V.S. Letokhov, V.G. Minogin, Yu.V. Rozhdestvensky, and A.I. Sidorov, "Radiative Collimation of Atomic Beams Through Two-Dimensional Cooling of Atoms by Laser-Radiation Pressure," J. Opt. Soc. Am. B2, 1776-1783 (1985).

J. Prodan, A. Migdall, W.D. Phillips, I. So, H. Metcalf, and J. Dalibard, "Stopping atoms with laser light," Phys. Rev. Lett. 54, 992-995 (1985).

A. Ashkin and J.M. Dziedzic, "Observation of radiation-pressure trapping of particles by alternating light beams," Phys. Rev. Lett. 54, 1245-1248 (1985).

C.M. Surko, M. Leventhal, W.S. Crane, A.P. Mills, Jr., H. Kugel, J. Strachan, "The Positron Trap - A New Tool for Plasma Physics," pp. 221-232, Positron Studies of Solids, Surfaces, and Atoms, Allen P. Mills, Jr., William S. Crane, and Karl F. Canter, Eds., Proceedings Symposium to celebrate Stephan Berko's 60th Birthday, Brandeis Univ. (12 December 1985), World Scientific (1985).

G. Gabrielse, "Penning Traps, Masses and Antiprotons". Preprint (1985). [Ed: Obtain from Dept. Physics, University of Washington, Seattle, Washington 98195 USA.] Invited lecture at Int. School of Physics with Low Energy Antiprotons: Fundamental Symmetries, Erice, Italy (24 September-4 October 1986). [Ed: A tutorial review on accurate mass measurements of individual particles in Penning traps and trapping of antiprotons at CERN.]

A.P. Kazantsev, G.A. Ryabenko, G.I. Surdutovich, and V.P. Yakovlev, "Scattering of Atoms by Light," Phys. Rep. (Netherlands) 129, 75-144 (1985). [Long review paper in English.]

1986

L.S. Brown and G. Gabrielse, "Geonium Theory: Physics of a Single Electron or Ion in a Penning Trap," Rev. Modern Phys. 58, 233-311 (Jan 1986).

R.E. Brown, "Proposed Measurement of the Gravitational Acceleration of the Antiproton," LANL Preprint LA-UR-86-1806, presented at 2nd Conference on the Intersections Between Particle and Nuclear Physics, Lake Louise, Canada (26-31 May 1986). Copies may be obtained from Ronald E. Brown, LANL, Los Alamos, NM 87545 USA.

A.L. Robinson, "Sodium Atoms Trapped With Laser Light," Science 233, 623 (8 August 1986). (News item about Chu paper. Contains nice AT&T drawing of how the experiment works.)

A. L. Robinson, "Laser-Cooling Mercury Ions Via Beryllium," Science 233, 623-624 (8 August 1986). (News item about Larson paper.) [Finally, an intriguing application of sympathetic cooling may be the storage of antimatter, antiprotons in particular. It is difficult to cool antiprotons directly because there is no atomic structure. An alternative is to load electrons and antiprotons into the same trap. The electrons cool themselves by emitting radiation and the cold electrons could then sympathetically cool the antiprotons.]

A. Aspect, J. Dalibard, A. Heidmann, C. Salomon, and C. Cohen-Tannoudji, "Cooling Atoms with Stimulated Emission," Phys. Rev. Lett. 57, 1688-1691 (6 Oct 1986). (We have observed an efficient collimation of a cesium atomic beam crossing at right angles an intense laser standing wave. This new cooling scheme is mainly based on a stimulated redistribution of photons between the two counterpropagating waves by the moving atoms. By contrast with usual radiation pressure cooling, this "simulated molasses" works for blue detuning and does not saturate at high intensity.)

Y. Hakuraku and H. Ogata, "A Rotary Magnetic Refrigerator for Superfluid Helium Production," J. Appl. Phys. 60, 3266-3268 (1 November 1986). (A rotor containing 12 magnetic single crystals of $Gd_3Ga_5O_{12}$ is immersed in liquid helium at 4.2 K and rotated at 24 rpm in a steady magnetic field of 3 T. The maximum useful cooling power obtained at 1.8 K is 1.81 W which corresponds to a refrigeration efficiency of 34%.)

G. Gabrielse, X. Fei, K. Helmerson, S.L. Rolston, R. Tjoelker, T.A. Trainor, H. Kalinowsky, J. Haas, and W. Kells, "First Capture of Antiprotons in a Penning Trap: A Kiloelectronvolt Source," Phys. Rev. Lett. 57, 2504-2507 (17 November 1986). (Antiprotons from the Low Energy Antiproton Ring of CERN are slowed from 21 MeV to below 3 keV by being passed through 3 mm of

material, mostly Be. While still in flight, the kiloelectron-volt antiprotons are captured in a Penning trap created by the sudden application of a 3 kV potential. Antiprotons are held for 100 sec and more.)

William C. Stwalley and Marshall Lapp, Eds., *Advances in Laser Science-I*, American Institute of Physics Conference Proceedings No. 146, New York (1986). Proceedings of First International Laser Science Conference (ILS-I), Dallas, Texas, USA (1985).

W.D. Phillips, A.L. Migdall, and H.J. Metcalf, "Laser-Cooling and Electromagnetic Trapping of Neutral Atoms," p. 362.

W. Nagourney, H. Dehmelt, and G. Janik, "Optical Lamb-Dicke Confinement of a Ba^+ Mono-Ion Oscillator," p. 401.

S. Chu, J.E. Bjorkholm, A. Ashkin, and A. Cable, "Experimental Observation of Optically Trapped Atoms," *Phys. Rev. Lett.* 57, 314-317 (1986). [We report the first observation of optically trapped atoms. Sodium atoms cooled below 10^{-3} K in "optical molasses" are captured by a dipole-force optical trap created by a single, strongly focused, Gaussian laser beam tuned several hundred gigahertz below the D_1 resonance transition. We estimate that about 500 atoms are confined in a volume of about $1000 \mu\text{m}^3$ at a density of $10^{11}/\text{cm}^3$.]

N. Beverini, F. Scuri, and G. Torelli, "Antiprotons Trapping and Cooling," preprint (1986). (Copies obtainable from G. Torelli, INFN, Sezione di Pisa, Via Livornese, 582/a, 56010 S. Piero a Grado, Pisa, Italy.) [Ed: Seems to be a summary review of previous papers.]

N. Beverini, L. Bracci, F. Scuri, G. Torelli, V. Lagomarsino, and G. Manuzio, "Cryogenic Calorimetry in the Antiproton Gravitational Mass Measurement," preprint (1986). [Ed: Copies obtainable from G. Torelli, INFN, Sezione di Pisa, Via Livornese, 582/a, 56010 S. Piero a Grado, Pisa, Italy.] (It is proposed to replace the multichannel plate detector in the antiproton gravitational mass measurement apparatus with a doped silicon cryogenic calorimeter that can detect the deposition of 3 eV from a particle when at 0.1 K.)

D.J. Larson, J.C. Bergquist, J.J. Bollinger, W.M. Itano, and D.J. Wineland, "Sympathetic Cooling of Trapped Ions: A Laser-Cooled Two-Species Nonneutral Ion Plasma," *Phys. Rev. Lett.* 57, 70-73 (1986). (Sympathetic cooling of trapped ions has been demonstrated in an experiment where $^{198}\text{Hg}^+$ ions were confined in a Penning ion trap with laser-cooled $^9\text{Be}^+$ ions. Mercury ion temperatures below 1 K were achieved. The present results appear to have a direct bearing on proposed experiments to store and cool antiprotons at very low energies.)

G. Torelli and N. Beverini, "Antiproton Traps and Related Experiments," pp 111-115, Proc. Nuclear and Particle Physics at Intermediate Energies with Hadrons, T. Bressani and G. Pauli, Ed., Vol. 3, Societa Italiana di Fisica (1986). [Ed: Discusses feasibility of using Penning antiproton trap with a superposed rf field to trap positrons in order to form antihydrogen for a gravitational experiment. It is found to be difficult and further analysis is said to be needed.]

D.E. Pritchard, E.L. Raab, V. Bagnato, C.E. Wieman, and R.N. Watts, "Light Traps Using Spontaneous Forces," Phys. Rev. Lett. 57, 310-313 (1986). [We show that the optical Earnshaw theorem does not always apply to atoms and that it is possible to confine atoms by spontaneous light forces produced by static laser beams.]

A.J. Palmer and J.F. Lam, "Radiation Cooling with π Pulses," J. Optical Soc. of Am. B3, 719-723 (1986). [The concept of radiation cooling with π pulses is presented and quantified with a theoretical analysis. Numerical analysis of π pulse cooling on the hydrogen Lyman- α transition is presented as an example. The cooling rate ($<1 \mu s$) and limiting temperature (down to 10 mK) are compared with steady state radiation cooling.]

E.C. Beaty, "Calculated Electro-static Properties of Ion Traps," Phys. Rev. A33, 3645 (1986).

N. Beverini, L. Bracci, G. Torelli, V. Lagomarsino, and G. Manuzio, "Stochastic Cooling of Charged Particles in a Penning Trap," Europhysics Lett. 1, 435-439 (1986). (A method for cooling charged particles in a Penning trap is outlined. The method is analogous to the stochastic cooling of particles in storage rings. The cooling rates estimated in this way are encouraging.)

D. Thompson, R.V.E. Lovelace, and D.M. Lee, "Storage Rings for Spin-Polarized Hydrogen". Preprint (1986). [Ed: Obtain from Dept. Applied and Engineering Physics, Cornell Univ., Ithaca, New York 14853 USA.] (A strong-focusing storage ring is proposed for the long-term magnetic confinement of a collisional gas of neutral spin-polarized hydrogen atoms. The storage ring can be filled from a source at a few hundred mK and has an effective potential well depth of 1 mK.)

Richard J. Hughes, T. Goldman, and Michael Martin Nieto, "The Gravitational Properties of Antimatter," Preprint LA-UR-86-3882 (1986). [Ed: Obtain from LANL, P.O. Box 1633, Los Alamos, New Mexico 87545 USA.] Proc. Int. School on Low Energy Antiproton Physics, Ettore Majorana Center for Scientific Culture, Erice, Sicily, Italy (27 September-3 October 1986).

David B. Cline, Ed., Low Energy Antimatter, World Scientific, Singapore (1986). Proceedings of the Workshop on the Design of a Low Energy Antimatter Facility, University of Wisconsin-Madison, Madison, Wisconsin, USA (October 1985).

Ronald E. Brown, "An Experiment to Measure the Gravitational Force on the Antiproton," p. 105.

Michael H. Holzscheiter, "Trapping and Cooling of Externally injected antiprotons in a Penning Trap," p. 120.

C.F. Driscoll, "Containment of Single-Species Plasmas at Low Energies," p. 184.

V.G. Minogin, "Compression of Atomic Beams by Laser Radiation Pressure," Optical Spectroscopy (USSR) 60, 657-658 (May 1986). [English translation of Opt. Spektrosk. 60, 1061-1064 (May 1986).]

1987

J.E. Bjorkholm, "Experimental Observations of Laser Cooling and Trapping of Atoms," Physics Today, S47-S48 (January 1987). [Ed: Physics News in 1986-Optics summary of papers by Chu and Ashkin.]

T. Bergeman, Gidon Erez, and Harold J. Metcalf, "Magnetostatic Trapping Fields for Neutral Atoms," Physical Review 35A, 1535-1546 (15 February 1987).

William D. Phillips and Harold J. Metcalf, "Cooling and Trapping Atoms," Scientific American 256, No. 3, 50-56 (March 1987). [Ed: Some excellent color photographs of one laser beam slowing sodium atoms and six laser beams creating a region of 'optical molasses'.]

D.J. Wineland, "Ion Traps for Large Storage Capacity". Preprint (undated). [Ed: Obtain from Time and Frequency Division, National Bureau of Standards, Boulder, Colorado 80303 USA.] Presented at the Cooling, Condensation, and Storage of Hydrogen Cluster Ions Workshop, SRI International, Menlo Park, California USA (8-9 January 1987).

Peter J. Martin, Phillip L. Gould, Bruce G. Oldaker, Andrew H. Miklich, and David E. Pritchard, "Diffraction of Atoms Moving Through a Standing Light Wave". Preprint (undated). [Ed: Obtain from Dept. Physics, Massachusetts Institute of Technology, Cambridge, Massachusetts 02139 USA.]

V.S. Bagnato, G.P. Lafyatis, A.G. Martin, E.L. Raab, and D.E. Pritchard, "Continuous Stopping and Trapping of Neutral Atoms," Preprint (undated). [Ed: Obtain from Dept. Physics, Massachusetts Institute of Technology, Cambridge, Massachusetts 02139 USA.] (Neutral sodium atoms have been continuously loaded into a 0.1 K deep superconducting magnetic trap using laser light to slow and stop them. At least 1×10^9 atoms were trapped with a decay time of 2.5 minutes.)

N.S.P. King, Project Leader and 24 others, "Antiproton Technology: Status and Prospects," LA-UR-85-3687, Los Alamos National Lab, Los Alamos, NM 87545.

6. LOW-ENERGY ANTIPROTON ANNIHILATION PROCESSES

1960

L.E. Agnew, Jr., T. Elioff, W.B. Fowler, R.L. Lander, W.M. Powell, E. Sergé, H.M. Steiner, H.S. White, C. Wiegand, and T. Ypsilantis, "Antiproton interactions in hydrogen and carbon below 200 MeV," Phys. Rev., 118, 1371 (1960).

1964

H. Barkas and M.J. Berger, Tables of Energy Losses and Ranges of Heavy Charged Particles, NASA SP-3013, STI Division, NASA, Washington, DC (1964).

1970

D.L. Morgan and V.W. Hughes, "Atomic processes involved in matter-antimatter annihilation," Phys. Rev. D2, 1389-1399 (1970).

1973

D.L. Morgan and V.W. Hughes, "Atom-antiatom interactions," Phys. Rev. A7, 1811-1825 (1973).

1975

W. Kolos, D.L. Morgan, D.M. Schneider, and L. Wolniewicz, "Hydrogen-antihydrogen interactions," Phys. Rev. A11, 1792-1796 (1975).

1976

M. Wade and V.G. Lind, "Ratio of antiproton annihilations on neutrons and protons in carbon for low-energy and stopped antiprotons," Phys. Rev. D14, 1182-1187 (1976).

1982

M.R. Clover, R.M. DeVries, N.J. DiGiacomo, and Y. Yariv, "Low energy antiproton-nucleus interactions," Phys. Rev. C26, 2138-2151 (1982).

1983

R.R. Zito, "Chain reactions in a hydrogen-antiproton pile," J. British Interplanetary Soc., 36, 308-310 (1983).

1984

Physics at LEAR with Low-Energy Cooled Antiprotons, Workshop on Physics at LEAR with Low-Energy Cooled Antiprotons, Erice, Sicily, Italy, 9-16 May 1982, U. Gastaldi and R. Klapisch, ed., Plenum Press, NY (1984). G. Piragino, "Antiproton annihilation in nuclear matter: multipion-nucleus interactions and exotic phenomena," pp. 855-860; R.M. DeVries and N.J. DiGiacomo, "The annihilation of low-energy antiprotons in nuclei," pp. 543-560; G. Vulpetti, "A propulsion-oriented synthesis of the antiproton-nucleon annihilation experimental results," J. British Interplanetary Soc. 37, 124-134 (1984).

1985

George E. Walker, Charles D. Goodman, Catherine Olmer, Eds., Antinucleon and Nucleon-Nucleus Interactions, Plenum Press, New York, USA (1985), \$79.50. Proceedings of Conference on Antinucleon and Nucleon-Nucleus interactions, Telluride, Colorado, USA (18-21 March 1985).

F. Balestra, et al., "Low-Energy Anti-Proton Annihilation on Nuclei," p. 445.

H.V. von Geramb, Ed., Medium Energy Nucleon and Antinucleon Scattering, Lecture Notes in Physics, v. 243, Springer-Verlag, Berlin, Germany (1985), 576p., hardcopy \$70.90, paper \$36.50. Proceedings of international Symposium on Medium Energy Nucleon and Antinucleon Scattering, Bad Honnef, Germany (18-21 June 1985).

H. Poth, "Recent Results from Anti-Protonic Atoms at LEAR," p. 357.

J.A. Niskanen, "Antiproton-Proton Annihilation," p. 50.

M.R. Pennington, Ed., Antiproton 1984, Hilger, Bristol, England (1985). Institute of Physics Conference Series, 73, 530p, \$76.00. Proceedings of 7th European Symposium on Antiproton Interactions: From LEAR to the Collider and Beyond, Durham, England (9-13 July 1984).

S. Ahmad for ASTERIX Collaboration, " $\bar{p}p$ Annihilation at Rest from Atomic P States," p. 287.

S. Ahmad for ASTERIX Collaboration, "First Observation of K x-rays from $\bar{p}p$ Atoms," p. 131.

D. Gareta, et al., "PS-184: A Study of \bar{p} -Nucleus Interaction with a High Resolution Magnetic Spectrometer," p. 187.

M. Sakitt, et al., "Low-Energy Anti-Proton Interaction Studies at Brookhaven," p. 205.

S. Ahmad for ASTERIX Collaboration, "First Observation of K x-rays from $\bar{p}p$ Atoms," Physics Lett. 157B, 333 (1985).

F. Myhere, "Anti-Proton Annihilation and Quark Dynamic Selection Rules," Preprint SCY 86-1438 (April 1986), University of South Carolina, Physics and Astronomy Department, Columbia, South Carolina 29208 USA.

D.L. Morgan, "Annihilation of Antiprotons in Heavy Nuclei," AFRPL TR-86-011 (April 1986). Obtain from AFRPL/LKC, Edwards AFB, CA 93523-5000.

A.M. Green and J.A. Niskanen, "The Effect of Short Range Repulsions on NNbar Annihilations," Preprint HU-TFT-86-16 (April 1986), Helsinki University, Siltavuorenpenger 20, SF-00170 Helsinki 17, Finland.

C.B. Dover, "Antinucleon Physics," BNL preprint 38285, 2nd Conf. on Intersection between Particle and Nuclear Physics, Lake Louise, Canada (26-31 May 1986). [Ed: Obtainable from C.B. Dover, Physics Dept., Brookhaven National Lab, Upton, NY 11973 USA.] (We review and interpret some of the recent data from LEAR, BNL, and KEK on low and medium energy interactions of antinucleons with nucleons.)

F. Balestra, S. Bossolasco, M.P. Bussa, L. Busso, L. Ferrero, A. Grasso, D. Panzieri, G. Piragio, F. Tosello, G. Bendiscioli, V. Filippini, G. Fumagalli, C. Marciano, A. Rotondi, A. Zenoni, C. Guaraldo, A. Maggiora, Yu. A. Batusov, I.V. Falomkin, G.B. Pontecorvo, M.G. Sapozhnikov, M. Vascon, G. Zanella, E. Lodi Rizzini, "Low Energy Antiproton-Neon Interaction," Nuclear Physics A452, 573-590 (May 1986).

D.L. Morgan, Jr., "Antiproton-Hydrogen Atom Annihilation," AFRPL TR-86-019, Final Report on MIPR: RPL 59004 (May 1986). [Copies obtainable from AFRPL/LKC, Edwards AFB, CA 93523-5000.]

ASTERIX Collaboration, "Antiproton-Proton Annihilation into Collinear Charged Pions and Kaons," Preprint TRI-PP-86-45 (May 1986), TRIUMF, Canada, 2nd Conf. on Intersections Between Particles and Nuclear Physics, Lake Louise (26-31 May 1986). (An analysis is presented of two body final states of collinear charged pions or kaons from antiproton-proton annihilation at rest in the ASTERIX spectrometer at LEAR. The relative branching ratio of kaons to pions is shown to differ for P and S wave initial states.)

H. Koch, "Antiprotonic Atoms," Preprint CERN-EP/86-78 (25 June 1986), CERN, CH-1211 Geneva 23, Switzerland, presented at 2nd Conf. Intersections between Particle and Nuclear Physics, Lake Louise, Canada (26-31 May 1986). (The results of five LEAR experiments looking for \bar{p} -atomic X rays are reviewed.)

U. Gastaldi, R. Klapisch, J.M. Richard, and J. Tran Thanh Van, Eds, *Physics with Antiprotons at LEAR in the ACOL Era*, Editions Frontieres, Gif-sur-Yvette, France (1985), \$100.00. Proceedings of the LEAR Workshop: Physics with Low Energy Cooled Antiprotons in the ACOL Era, Tignes (Savoie), France (19-26 January 1985).

A.M. Green, et al., "N anti-N Annihilation Mechanisms," p. 185.

L. Linssen, " $\bar{p}p$ Total Cross Sections and $\bar{p}p$ Forward Elastic Scattering at Low Incoming \bar{p} Momenta, Results From PS172," p. 225.

T.A. Shibata, et al., " $\bar{p}p$ Cross Sections at Small Momenta," p. 231.

H. Poth, et al., "Anti-Protonic Atoms at LEAR: Achievements and Perspectives," p. 581.

W. Kanert, "Interaction of Stopped Antiprotons With Nuclei (PS186)," p. 593.

D. Garreta, "Elastic and Inelastic Scattering of Antiprotons From Nuclei (PS184)," p. 599.

U. Gastaldi, et al., "High Resolution Spectroscopy of $\bar{p}p$ Atoms Produced in Flight with \bar{p} and H^- Beams Co-rotating in LEAR," p. 681.

1986

D. Bridges and 13 others, "Evidence for a New State Produced in Antiproton Annihilations at Rest in Liquid Deuterium," *Phys. Rev. Lett.* **56**, 211-218 (20 Jan 1986).

W. Brückner, H. Döbbeling, F. Güttner, D. Von Harrach, H. Kneis, S. Majewski, M. Nomachi, S. Paul, B. Povh, R.D. Ransome, T.-A. Shibata, M. Treichel, and Th. Walcher, "Measurement of the $\bar{p}p \rightarrow \bar{n}n$ Cross Section at Low \bar{p} Momenta," *Physics Lett.* **169B**, 302-308 (27 March 1986). (First measurement of the differential cross section are presented for $\bar{p}p \rightarrow \bar{n}n$ at LEAR in the momentum range between 180 and 600 MeV/c. The differential cross sections show a forward peaking followed by a smooth drop-off.)

B.E. Bonner and L.S. Pinsky, *Proceedings of the First Workshop on Antimatter Physics at Low Energy*, Fermilab, Batavia, Illinois (10-12 April 1986), U.S. Gov. Printing Office 1986-644-171. Contains the following papers:

Stephen R. Sharpe, "Glueballs and Other Exotica in $\bar{p}p$ Annihilation," pp. 165-184.

F. Myhrer, "Antiproton Annihilation and Quark Dynamic Selection Rules," pp. 285-292.

Jean-Marc Richard, "Antiproton-Nucleus Interaction," pp. 309-324.

W.R. Gibbs, "Creating High Energy Density in Nuclei with Energetic Antiparticles," pp. 355-369.

B.I. Deutch, A.S. Jensen, A. Miranda, and G.C. Oades, " \bar{p} Capture in Neutral Beams," pp. 371-391.

Guido Piragino, "Antiproton-Nucleus Interaction: Review of the Experimental Situation," Preprint CERN-EP/86-75 (24 June 1986), CERN, CH-1211 Geneva 23, Switzerland, presented at Winter School on Hadronic Physics at Intermediate Energy, Folgaria (17-22 February 1986). [Ed: Detailed review paper with 37 references.]

Jan Fischer, "The pp and $p\bar{p}$ Difference and the Behavior of the Phase," Preprint BERN 86-1370 (July 1986), Physikalisches Inst., Univ. Bern, Sidlerstrasse 5, CH-3012 Bern, Switzerland.

L.A. Kondratyuk and M.G. Spozhnikov, "Interactions of Antiprotons with Neutrons and Nuclei at LEAR Energies," Preprint JINR-E4-86-487 (July 1986), Inst. Theoretical and Experimental Physics, B. Cheremushkinskaya ul. 89, 117259 Moscow V259, USSR.

B.Z. Kopeliovich, "Mechanisms of Anti- p p Interaction at Low and High Energies," Preprint JINR-E2-86-471 (July 1986), Joint Inst. of Nuclear Research, Head Post Office, P.O. Box 79, 101000 Moscow, USSR.

Yu. A. Batusov, S.A. Bunyatov, I.V. Falomkin, G.B. Pontecorvo, M.G. Sapozhnikov, F. Balestra, S. Bossolasco, M.P. Busa, L. Busso, L. Ferrero, D. Panzieri, G. Piragino, F. Tosello, C. Guaraldo, A. Maggiora, G. Bendiscioli, V. Filippini, A. Rotondi, A. Zenoni, and E. Lodi Rizzini, "Antiproton Annihilation on Ag/Br Nuclei," Europhysics Lett. 2, 115-122 (15 July 1986). (The charged-prong multiplicity distribution of (\bar{p} , Ag/Br) annihilation events has been measured in photographic emulsion at 300, 400, and 500 MeV/c, and at rest. The low multiplicity events are produced mainly by nuclear surface annihilations and the higher multiplicity events can be interpreted as annihilations occurring deep in nuclear matter.) [Ed: At rest, 93% of the annihilation events are low multiplicity with an average multiplicity of 4.5. Since the average number of pions is 3, there are only 1-2 heavy charged fragments produced.]

Yu.A. Batusov, S.A. Bunyatov, I.V. Falomkin, G.B. Pontecorvo, M.G. Sapozhnikov, F. Balestra, S. Bossolasco, M.P. Busa, L. Busso, L. Ferrero, D. Panzieri, G. Piragino, F. Tosello, C. Guaraldo, A. Maggiora, G. Bendiscioli, V. Filippini, A. Rotondi, A. Zenoni, and E. Lodi Rizzini, "Antiproton Annihilation on Ag/Br Nuclei," Europhysics Lett. 2, No. 2, 115-122 (15 July 1986). (The charged-prong multiplicity distribution of $\bar{p} \rightarrow \text{Ag/Br}$ annihilation events were measured at 500, 400, 300, and 0 MeV/c. The low-multiplicity events are produced mainly by nuclear surface annihilations and the higher multiplicity events can be interpreted as annihilations occurring deep in nuclear matter.)

Ron Ray, "A Search for Narrow Lines in γ Spectra from $p\bar{p}$ Annihilations at Rest," Preprint UCI 86-1018 (July 1986), University of California/Irvine, Irvine, California USA.

Th. Köler, P. Blüm, G. Büche, A.D. Hancock, H. Koch, A. Kreissl, H. Poth, U. Raich, D. Rohmann, G. Backenstoss, Ch. Findeisen, J. Repond, L. Tauscher, A. Nilsson, S. Carius, M. Suffert, S. Charalambus, M. Chardalas, S. Dedoussis, H. Daniel, T. von Egidy, F.H. Hartmann, W. Kanert, G. Schmidt, J.H. Reidy, M. Nicholas, and A. Wolf, "Precision Measurement of Strong Interaction Isotope Effects in Antiprotonic ^{16}O , ^{17}O , and ^{18}O Atoms," *Physics Lett.* 176B, 327-333 (28 August 1986).

L.H. Andersen, P. Hvelplund, H. Knudsen, S.P. Møller, K. Elsener, K.-G. Rensfelt, and E. Uggerhøj, "Single and Double Ionization of Helium by Fast Antiproton and Proton Impact," Preprint CERN-EP/86-107 (8 August 1986), CERN, CH-1211 Geneva 23, Switzerland. (We measured the single and double ionization cross section for 0.5-5 MeV antiprotons and protons colliding with helium. For ion energies above 2 MeV the single ionization cross section is the same. The double ionization cross section for antiprotons is a factor of two larger than that for protons. Submitted to *Phys. Rev. Lett.*)

Bernd Bassalleck, "AntiN-N Bound States," Preprint NM 86-1270 (August 1986), Physics and Astronomy, University of New Mexico, Albuquerque, New Mexico 87131 USA. (Presented at 1986 INS Symp. on Hypernuclear Physics, Tokyo, Japan, 20-23 August 1986).

Bernd Bassalleck, "AntiN-N Bound States". Preprint (undated). [Ed: Obtain from Dept. Physics and Astronomy, Univ. New Mexico, Albuquerque, New Mexico 87131 USA.] Invited talk at INS International Symposium on Hypernuclear Physics, Tokyo, Japan (20-23 August 1986).

F. Balestra, S. Bossolasco, M.P. Bussa, L. Busso, L. Ferrero, D. Panzieri, G. Piragio, F. Tosello, G. Bendiscioli, A. Rotondi, P. Salvini, A. Zenoni, C. Guaraldo, A. Maggiora, Yu. A. Batusov, I.V. Falomkin, F. Nichitui, G.B. Pontecorvo, M.G. Sapozhnikov, E. Lodi Rizzini, "Determination of the Ratio $\sigma(\bar{p}n)/\sigma(\bar{p}p)$ from $\bar{p}^4\text{He}$ Reaction Data," Preprint CERN-EP/86-104 (5 August 1986), CERN, CH-1211 Geneva 23, Switzerland.

A.M. Green, "The $\bar{p}p$ Interaction at Low Energies". Preprint HU-TFT-86-38 (1 September 1986). [Ed: Obtain from Research Inst. for Theoretical Physics, Univ. Helsinki, Siltavuorenpenger 20 C, SF-00170 Helsinki, Finland.]

Jayanti Mahalanabis, "Inelastic Scattering of Antiprotons by ^{12}C ," Preprint CERN-TH.4546/86 (September 1986), CERN, CH-1211 Geneva 23, Switzerland. (Inelastic scattering of antiprotons (600 MeV/c) by ^{12}C leading to the excitation of the three lowest normal parity T=0 levels is studied in the framework of the Glauber model.)

A.M. Green, "The $\bar{p}p$ Interaction at Low Energies," Preprint HU-TFT-86-38a (September 1986), Helsinki University, Siltavuorenpenger 20, SF-00170 Helsinki 17, Finland.

L. Adiels, G. Backenstoss, I. Bergström, S. Carius, S. Chjaralambous, M.D. Cooper, Ch. Findeisen, D. Hatzifotiadou, M. Hugi, A. Kerek, H.O. Meyer, P. Pavlopoulos, J. Repond, L. Tauscher, D. Tröster, M.C.S. Williams, and K. Zioutas, "Search for Narrow Signals in the γ -Spectrum from $\bar{p}p$ Annihilation at Rest," Preprint CERN-EP/86-155 (9 October 1986), CERN, CH-1211 Geneva 23, Switzerland. (No narrow peaks indicating exotic states such as baryonium were observed. Submitted to Physics Letters B.)

M.G. Sapozhnikov, "Investigations with Anti-Protons at LEAR Facility" [in Russian], preprint JINR-P4-86-695 (October 1986). [Ed: Obtain from Joint Inst. Nuclear Research, Head Post Office, P.O. Box 79, 101000 Moscow USSR.]

L. Adiels, G. Backenstoss, I. Bergström, S. Carius, S. Chjaralambous, M.D. Cooper, Ch. Findeisen, D. Hatzifotiadou, M. Hugi, A. Kerek, H.O. Meyer, P. Pavlopoulos, J. Repond, L. Tauscher, D. Tröster, M.C.S. Williams, and K. Zioutas, "Experimental Determination of the Branching Ratios $\bar{p}p \rightarrow 2\pi^0$, $\pi^0\gamma$, and 2γ at Rest," Preprint CERN-EP/86-154 (9 October 1986), CERN, CH-1211 Geneva 23, Switzerland. (Submitted to Physics Letters B.)

F. Balestra, S. Bossolasco, M.P. Bussa, L. Busso, L. Ferrero, D. Panzieri, G. Piragio, F. Tosello, G. Bendiscioli, G. Fumagalli, A. Rotondi, P. Salvini, A. Zenoni, C. Guaraldo, A. Maggiora, Yu. A. Batusov, I.V. Falomkin, G.B. Pontecorvo, M.G. Sapozhnikov, E. Lodi Rizzini, "Measurement of $\bar{p}^4\text{He}$ Annihilation Events Detected in a Self-Shunted Streamer Chamber," Preprint CERN-EP/86-163 (20 October 1986), CERN, CH-1211 Geneva 23, Switzerland. (The measurement of angles and momenta, as well as the identification of the masses of the products of $\bar{p}^4\text{He}$ annihilation events detected in a self-shunted streamer chamber are described. Submitted to Nuclear Instruments and Methods.)

L. Tauscher, "Antiproton-Nucleon and Antiproton-Nucleus Bound States," Preprint CERN-EP/86-200 (26 November 1986), CERN, CH-1211 Geneva 23, Switzerland. (Invited talk at 8th European Symposium on Nucleon-Antinucleon Interactions, Thessaloniki, Greece, 1-5 September 1986.)

C. Anslar, " $\bar{p}p$ Annihilation and Low Energy Spectroscopy," Preprint CERN-EP/86-178 (10 November 1986), CERN, CH-1211 Geneva 23, Switzerland. (Rapporteur's talk given at the 8th European Symposium on Nucleon-Antinucleon Interactions, Thessaloniki, Greece, 1-5 September 1986.)

D. Bridges, H. Brown, I. Daftari, R. Debye, A. Deguzman, W. Fickinger, T. Kalogeropoulos, R. Marino, D. Peaslee, Ch. Petridou, D.K. Robinson and G. Tzanakos, "Antiproton Annihilations in Deuterium at Rest into Two Pions: Evidence for \bar{p} N Bound States Near Threshold," Phys. Lett. B 180, 313-318 (13 November 1986). (The charged pion spectra in $\bar{p}d \rightarrow \pi^+ \pi^0 p$, and $\pi^- \pi^+ n$, have been measured. The Doppler broadening of the pion momentum due to the spectator neutron recoil is at least a factor of two larger than that due to the proton and in disagreement with that expected from the deuteron wave function.)

G. Bohnert, et al., "Magnetic Fine Structure of Anti-Protonic Atoms," Physics Lett. 174B, 15 (1986).

R.R. Zito, "Antimatter Reactor Dynamics," J. British Interplan. Soc. 39, 110-113 (1986).

P.L. McGaughey, K.D. Bol, M.R. Clover, R.M. DeVries, N.J. DiGiacomo, J.S. Kapustinsky, W.E. Sondheim, G.R. Smith, J.W. Sunier, Y. Yariv, M. Buenerd, J. Chauvin, D. Lebrun, P. Martin, and J.C. Dousse, "Dynamics of Low-energy Antiproton Annihilation in Nuclei as Inferred from Inclusive Proton and Pion Measurements," Phys. Rev. Lett. 58, 2156-2159 (1986). [The cross sections for the production of charged pions and protons from the annihilation of 608 MeV/c antiprotons on ^{12}C , ^{89}Y , and ^{238}U are presented. The results are in good agreement with intranuclear-cascade calculations.]

P.L. McGaughey, N.J. Digiacomo, W.E. Sondheim, J.W. Sunier, and Y. Yariv, "Low Energy Antiproton-Nucleus Annihilation Radius Selection Using an Active Silicon Detector/Target," LANL Preprint LA-UR-86-819 (1986). (Copies may be obtained from Physics Division, LANL, Los Alamos, NM 87545 USA.) [An intrinsic silicon transmission detector is used to experimentally select the annihilation radius of low energy antiprotons in silicon nuclei. By selecting events with sufficiently large energy deposition, annihilations occurring within the half-nuclear density radius are distinguished.]

B.O. Kerbikov and Yu.A. Simonov, "Parametrization and Analysis of Low-Energy Nucleon-Antinucleon Data," Preprint ITEP-38 (1986), Institute of Theoretical and Experimental Physics, Moscow, USSR. (Low energy (<200 MeV/c) $\bar{p}p$ scattering, charge exchange, and annihilation cross sections measured recently at LEAR are parametrized.)

M. Kohno and W. Weise, "Proton-Antiproton Scattering and Annihilation into Two Mesons," Nuclear Physics A454, 429-452 (1986). (A semiphenomenological analysis of the low-energy $\bar{p}p$ annihilation into two mesons.)

E.M. Henley, T. Oka, and J. Vergados, "Two-Meson Annihilation of a Nucleon and Antinucleon," Phys. Letters 166B, 274-278 (1986). [Low energy nucleon-antinucleon annihilation into two mesons is examined in a distorted wave, "effective" perturbative QCD approach. Interesting selection rules are predicted. Cross sections are evaluated.]

W.W. Buck, J.W. Norbury, L.W. Townsend, and J.W. Wilson, "Theoretical Antideuteron-Nucleus Absorptive Cross Sections," Phys. Rev. C33, 234-238 (1986).

Carl B. Dover, Paul M. Fishbane, and S. Furui, "Dynamical Selection Rules in $N\bar{N}$ Annihilation," Phys. Rev. Lett. 57, 1538-1540 (1986). (Observations of a strong dependence of nucleon-antinucleon annihilation modes on orbital angular momentum and spin-isospin are interpreted in a quark-gluon description of the reaction dynamics.)

S.M. Playfer, "AntiN-N Annihilation Experiments," pp. 412-417, Proc. Conference on Intersections Between Particle and Nuclear Physics, Lake Louise, Canada (1986), Donald F. Geesaman, Ed., Am. Inst. Physics Conference Proceedings 150, AIP, New York (1986). (General features of antiN-N annihilation at rest are discussed, with an emphasis on two meson annihilation channels. Data on P-wave annihilations at rest show surprising differences from S-wave annihilations.)

David B. Cline, Ed., Low Energy Antimatter, World Scientific, Singapore (1986). Proceedings of the Workshop on the Design of a Low Energy Antimatter Facility, University of Wisconsin-Madison, Madison, Wisconsin, USA (October 1985).

Carl B. Dover, "Low Energy $p\bar{p}$ Strong Interactions: Theoretical Perspective, p. 1.

1987

J.F. Reading and A.L. Ford, "Double Ionization of Helium by Protons and Antiprotons in the Energy Range 0.30 to 40 MeV," Physical Review Lett. 58, No. 6, 543-546 (9 February 1987).

F. Balestra, et al., "Annihilation of Anti-Protons at Rest in He-3 and He-4," Preprint CERN-EP/87-65 (April 1987). [Ed: Obtain from CERN, CH-1211, Geneva 23, Switzerland.]

7. NON-PROPULSION APPLICATIONS OF ANTIMATTER

1982

L. Gray and T.E. Kalogeropoulos, "Possible Bio-Medical Applications of Antiprotons-I. In-Vivo Direct Density Measurements: Radiography," IEEE Trans. Nuclear Sci. NS-29, 1051-1057 (April 1982). [We show that antiprotons can be used to extract density at any point within a biological medium by measuring the stopping power. The limit of density measurement is 1% when the measurements are taken within a volume of $\sim 10^{-2} \text{ cm}^3$.]

1984

K. Kilian, "Physics with antiprotons at LEAR," pp. 324-341, CERN Publication 84-09, Proc. Fourth Topical Workshop on Proton-Antiproton Collider Physics, Berne, 5-8 March 1984, (8 August 1984).

L. Gray and T.E. Kalogeropoulos, "Possible Biomedical Applications of Antiproton Beams: Focused Radiation Transfer," Radiation Research 97, 246-252 (1984). [A calculation of the energy lost by antiprotons stopping in water shows that the radiation transferred is localized within 1 mm of the stopping point. This "focusing" of the radiation is mainly due to heavily ionizing particles emitted from the nuclei on which the annihilation takes place.]

L. Campbell, W.R. Gibbs, T. Goldman, D.B. Holtkamp, M.V. Hynes, N.S.P. King, M.M. Nieto, A. Picklesimer, and T.P. Wangler, "Basic research in atomic, nuclear and particle physics," LA-UR-84-3572, Los Alamos National Lab, Los Alamos, New Mexico (1984).

S. Polikanov, "Could antiprotons be used to get a hot, dense plasma?," pp. 851-853, Physics at LEAR with Low-Energy Cooled Antiprotons, Workshop on Physics at LEAR with Low-Energy Cooled Antiprotons, Erice, Sicily, Italy, 9-16 May 1982, U. Gastaldi and R. Klapisch, ed., Plenum Press, NY (1984).

1985

U. Gastaldi, R. Klapisch, J.M. Richard, and J. Tran Thanh Van, Eds, Physics with Antiprotons at LEAR in the ACOL Era, Editions Frontieres, Gif-sur-Yvette, France (1985), \$100.00. Proceedings of the LEAR Workshop: Physics with Low Energy Cooled Antiprotons in the ACOL Era, Tignes (Savoie), France (19-26 January 1985).

D.J. Simon, et al., "The LEAR Experimental Areas: Status Report and Possible Developments," p. 47.

D. Möhl, "Technical Implications of Possible Future Options for LEAR," p. 65.

M. Nieto, et al., "Gravitational Properties of Antimatter," p. 639.

G. Torelli, et al, "Gravitational Measurement on Antiprotons," p. 649.

M.V. Hynes, "Physics with Low Temperature Antiprotons," p. 657.

G. Gabrielse, et al., "Precision Comparison of Antiproton and Proton Masses in a Penning Trap," p. 665.

M.V. Hynes, "Physics with low temperature antiprotons," Los Alamos National Lab preprint LA-UR-85-1060, Third LEAR Workshop, Tignes, France (19-26 Jan 1985).

T. Goldman and M.M. Nieto, "Gravitational properties of antimatter," Los Alamos National Lab Preprint LA-UR-85-1092, Third LEAR Workshop, Tignes-Savoie, France (19-26 Jan 1985).

A.D. Krisch, "Summary of Workshop on Polarized Antiproton Sources," Preprint UM-HE-85-23 (April 1985), Michican University. (Prepared after Workshop on Polarized Antiproton Sources, Bodega Bay, California, USA, 18-21 April 1985.)

G. Gabrielse, H. Kalinowsky, W. Kells, and T.A. Trainor, "Precision Comparison of Antiproton and Proton Masses in a Penning Trap," Proposal P83 to the Proton Synchrotron Coordination Committee of CERN, Geneva, Switzerland (15 April 1985).

B.W. Augenstein, "Concepts, problems, and opportunities for use of annihilation energy: an annotated briefing on near-term RDT&E to assess feasibility," Rand Note N-2302-AF/RC, Rand Corp., Santa Monica, CA 90406 (June 1985).

A.M. Green and J.A. Niskanen, "Low-Energy Antiproton Physics in the Early LEAR Era," Preprint HU-TFT-85-60 (December 1985), Helsinki University, Siltavuorenpenger 20, SF-00170 Helsinki 17, Finland.

G. Gabrielse, "Penning Traps, Masses and Antiprotons." Preprint (1985). [Ed: Obtain from Dept. Physics, University of Washington, Seattle, Washington 98195 USA.] Invited lecture at Int. School of Physics with Low Energy Antiprotons: Fundamental Symmetries, Erice, Italy (24 September-4 October 1986). [Ed: A tutorial review on accurate mass measurements of individual particles in Penning traps and trapping of antiprotons at CERN.]

M.R. Pennington, Ed., Antiproton 1984, Hilger, Bristol, England (1985). Institute of Physics Conference Series, 73, 530p, \$76.00. Proceedings of 7th European Symposium on Antiproton Interactions: From LEAR to the Collider and Beyond, Durham, England (9-13 July 1984).

M. Chanel, et al., "LEAR: Machine and Experimental Areas: Experience and Future Plans After 1-Year of Operation," p. 119.

D. Gareta, et al., "PS-184: A Study of \bar{p} -Nucleus Interaction with a High Resolution Magnetic Spectrometer," p. 187.

A.M. Green, "What Anti-Proton Physics Can Tell Us About Nuclear Physics," p. 213.

M. Sakitt, et al., "Low-Energy Anti-Proton Interaction Studies at Brookhaven," p. 205.

1986

T. Goldman, Richard J. Hughes, and Michael Martin Nieto, "Experimental Evidence for Quantum Gravity," Phys. Lett. B171, 217-222 (24 April 1986). (Geophysical and laboratory experimental data on anomalous gravitational effects are interpreted in terms of broken-super-symmetry quantum-gravity models. A measurement of the gravitational properties of antimatter would be of great value in distinguishing between the various theoretical possibilities.)

B.E. Bonner and L.S. Pinsky, Proceedings of the First Workshop on Antimatter Physics at Low Energy, Fermilab, Batavia, Illinois (10-12 April 1986), U.S. Gov. Printing Office 1986-644-171.

Contains the following papers:

R.L. Jaffe, " $\bar{p}p$ Physics in the Milli-TeV Region," pp. 1-34.

Rolf Landua, "The Future Physics at LEAR," pp. 35-68.

Petros A. Rapidis, "The Fermilab Antiproton Source: Prospects for $\bar{p}p$ Experiments," pp. 83-94.

Ezio A. Menichetti, "Charmonium $\bar{p}p$ Experiments," pp. 95-118.

M.G. Olsson, "Onia Spectroscopy by Direct Channel Production," pp. 119-130.

Stanley J. Brodsky, "Probing QCD in Low energy \bar{p} Collisions," pp. 131-164.

Stephen R. Sharpe, "Glueballs and Other Exotica in $\bar{p}p$ Annihilation," pp. 165-184.

T. Goldman, Richard J. Hughes, and Michael Martin Nieto. "Gravitational Properties of Antimatter: Experimental Evidence for Quantum Gravity?," pp. 185-200.

M.V. Hynes and L.C. Campbell, "Physics with Bottled Antiprotons," pp. 201-210.

G. Gabrielse, K. Helmersen, R. Tjoelker, X. Fei, T. Trainor, W. Kells, and H. Kalinowsky, "Prospects for Experiments with Trapped Antiprotons," pp. 211-226.

Lincoln Wolfenstein, "CP Violation and $\bar{p}p$ Experiments," pp. 227-241.

John F. Donoghue, "CP Violation Experiments Using Hyperons at a $p\bar{p}$ Machine," pp. 242-250.

Carl B. Dover, "Physics with Polarized \bar{p} 's," pp. 251-270.

E. Steffens, "Prospects for Producing Polarized Antiprotons," pp. 271-285.

F. Myhrer, "Antiproton Annihilation and Quark Dynamic Selection Rules," pp. 285-292.

Harry J. Lipkin, "Delta, Iota, and Other Meson Spectroscopies," pp. 293-308.

Nathan Isgur, Richard Kokosko, and Jack Paton, "Gluonic Excitations of Mesons: Why They are Missing and Where to Find Them," pp. 347-354.

W.R. Gibbs, "Creating High Energy Density in Nuclei with Energetic Antiparticles," pp. 355-369.

B.I. Deutch, A.S. Jensen, A. Miranda, and G.C. Oades, " \bar{p} Capture in Neutral Beams," pp. 371-391.

G. Bassompierre, R.K. Bock, A. Buzzo, M. Dameri, T. Fearnley, J. Franz, M. Gazzaly, N. Hamann, T. Johansson, E. Khan-Aronsen, K. Kilian, J. Kirkby, K. Kirsebom, K. Kuroda, A. Kylling, F. Levrero, A. Lundby, M. Macri, M. Marinelli, L. Mattera, B. Mouellic, B.A. Nielsen, W. Oelert, Y. Onel, B. Osculati, G. Pauletta, M.G. Pia, M. Poulet, E. Rössle, A. Santroni, H. Schmitt, B. Stugu, S. Terreni, F. Tommasini, "JETSET: Physics at LEAR with an Internal Gas Jet Target and an Advanced General Purpose Detector," pp. 419-442.

Y. Onel and A. Penzo, "Spin Studies with a Polarized Jet Target in LEAR," pp. 443-454.

Appendix I. B.E. Bonner and L.S. Pinsky, "A Summary of Topics Discussed at the First Fermilab Antimatter Physics at Low Energy Workshop," pp. 455-462.

C.B. Dover, "Antinucleon Physics," BNL preprint 38285, 2nd Conf. on Intersection between Particle and Nuclear Physics, Lake Louise, Canada (26-31 May 1986). [Ed: Obtainable from C.B. Dover, Physics Dept., Brookhaven National Lab, Upton, NY 11973 USA.] (We review and interpret some of the recent data from LEAR, BNL, and KEK on low and medium energy interactions of antinucleons with nucleons.)

R.E. Brown, "Proposed Measurement of the Gravitational Acceleration of the Antiproton," LANL Preprint LA-UR-86-1806, presented at 2nd Conference on the Intersections Between Particle and Nuclear Physics, Lake Louise, Canada (26-31 May 1986). Copies may be obtained from Ronald E. Brown, LANL, Los Alamos, NM 87545 USA.

J.W. Moffat, "Do Protons and Anti-Protons Fall at the Same Rate in a Gravitational Field?," Preprint UTPT-86-07 (May 1986), Department of Physics, University of Toronto, Toronto, Ontario M5S 1A7 Canada. (A proton falls faster than an antiproton in the gravitational field of the Earth as predicted by nonsymmetrical gravitational theory.)

A. Gsponer and J.-P. Hurni, "The Physics of Antimatter Induced Fusion and Thermonuclear Explosions," Proc. 4th Int. Conf. on Emerging Nuclear Energy Systems, Madrid, Spain (30 June-4 July 1986). Copies obtainable from A. Gsponer, ISRI, 15, Charles-Galland, CH-1206 Geneva, Switzerland. (The possibility of using antihydrogen for igniting inertial confinement fusion pellets or triggering thermonuclear explosions is investigated. The fusion fuel would be collapsed onto a tiny spherical pellet of solid antihydrogen by external chemical explosives. The levitation of a frozen antihydrogen pellet within a 1 mm diameter cryostat at the heart of a complex thermonuclear device is recognized as a tremendous challenge. The number of antiproton annihilations required is estimated to be $10^{21}/k^2$ where k is the compression factor of the fuel to be ignited.) [Ed: 10^{21} antihydrogen atoms mass about 2 milligrams.]

Richard J. Hughes, T. Goldman, and Michael Martin Nieto, "The Gravitational Properties of Antimatter," Proc. Int. School on Low Energy Antiproton Physics, Erice, Sicily, Italy (27 September-3 October 1986).

G. Gabrielse, X. Fei, K. Helmersen, S.L. Rolston, R. Tjoelker, T.A. Trainor, H. Kalinowsky, J. Haas, and W. Kells, "First Capture of Antiprotons in a Penning Trap: A Kilolectronvolt Source," Phys. Rev. Lett. 57, 2504-2507 (17 November 1986). (Antiprotons from the Low Energy Antiproton Ring of CERN are slowed from 21 MeV to below 3 keV by being passed through 3 mm of material, mostly Be. While still in flight, the kiloelectron-volt antiprotons are captured in a Penning trap created by the sudden application of a 3 kV potential. Antiprotons are held for 100 sec and more.)

Richard J. Hughes, T. Goldman, and Michael Martin Nieto, "The Gravitational Properties of Antimatter," Preprint LA-UR-86-3882 (1986). [Ed: Obtain from LANL, P.O. Box 1633, Los Alamos, New Mexico 87545 USA.] Proc. Int. School on Low Energy Antiproton Physics, Ettore Majorana Center for Scientific Culture, Erice, Sicily, Italy (27 September-3 October 1986).

David B. Cline, Ed., Low Energy Antimatter, World Scientific, Singapore (1986). Proceedings of the Workshop on the Design of a Low Energy Antimatter Facility, University of Wisconsin-Madison, Madison, Wisconsin, USA (October 1985).

Charles Goebel, "Antiparticles and Gravity: The Conventional View," p. 24.

M.G. Olsson, "Heavy Quark Spectroscopy and Anti-proton Collisions," p. 29.

Ronald E. Brown, "An Experiment to Measure the Gravitational Force on the Antiproton," p. 105.

T. Barnes, "Current Theoretical Expectations for Gluonic Hadrons," p. 134.

Theodore E. Kalogeropoulos, "Antiproton Neutron Annihilations at Rest: The $\zeta(1480)$," p. 138.

John Peoples, Jr., "Prospects for $\bar{p}p$ Experiments in the TEV I Accumulator," p. 144.

V. Bharadwaj, et al., "A Proposal to Investigate the Formation of Charmonium States Using the PBAR Accumulator Ring," p. 166.

J.W. Wilson, L.W. Townsend and W.W. Buck, "On the Biological Hazard of Galactic Antinuclei," Health Physics 50, 666-667 (1986).

G. Torelli and N. Beverini, "Antiproton Traps and Related Experiments," pp 111-115, Proc. Nuclear and Particle Physics at Intermediate Energies with Hadrons, T. Bressani and G. Pauli, Ed., Vol. 3, Societa Italiana di Fisica (1986). [Ed: Discusses feasibility of using Penning antiproton trap with a superposed rf field to trap positrons in order to form antihydrogen for a gravitational experiment. It is found to be difficult and further analysis is said to be needed.]

J. Rogers, "Measuring the Gravitational Properties of Antihydrogen," Preprint, Dept. of Physics and Astronomy, Univ. of Rochester, Rochester, NY 14627 (1986).

T. Goldman, M.V. Hynes, and M.M. Nieto, "The Gravitational Acceleration of Antiprotons," Gen. Rel. and Gravitation 18, 67-70 (1986). [Ed: The authors review the theoretical arguments and experimental evidence for the gravitational acceleration of antimatter being the same as antimatter. They conclude there is no compelling support for such a belief. Thus, they argue they should proceed with their experiment to measure the gravitational mass of the antiproton.]

N. Beverini, L. Bracci, F. Scuri, G. Torelli, V. Lagomarsino, and G. Manuzio, "Cryogenic Calorimetry in the Antiproton Gravitational Mass Measurement," preprint (1986). [Ed: Copies obtainable from G. Torelli, INFN, Sezione di Pisa, Via Livornese, 582/a, 56010 S. Piero a Grado, Pisa, Italy.] (It is proposed to replace the multichannel plate detector in the antiproton gravitational mass measurement apparatus with a doped silicon cryogenic calorimeter that can detect the deposition of 3 eV from a particle when at 0.1 K.)

N.S.P. King, Project Leader and 24 others, "Antiproton Technology: Status and Prospects," LA-UR-85-3687, Los Alamos National Lab, Los Alamos, NM 87545.

M.V. Hynes and 32 others, "A Measurement of the Gravitational Acceleration of the Antiproton," LA-UR-86-260, Los Alamos National Lab, Los Alamos, NM 87545.

T. Goldman, Richard J. Hughes, and Michael Martin Nieto, "The Gravitational Acceleration of Antiprotons and of Positrons," Preprint LA-UR-86-3617, LANL, Los Alamos, New Mexico 87545 USA.] (Theories of quantum gravity predict the existence of spin-1 graviphoton and spin-0 graviscalar partners of the graviton, which will yield non-Newtonian, non-Einsteinian effects. Since these new interactions couple to an unknown linear combination of baryon and lepton numbers, it is important to do both an antiproton and a positron [Ed: and/or antihydrogen] gravity experiment. Submitted to Phys. Rev. D.)

8. ANTIMATTER PROPULSION

1952

L.R. Shepherd, "Interstellar flight," J. British Interplanetary Soc. 11, 149-167 (1952).

1953

E. Sänger, "The theory of photon rockets," Ing. Arch. 21, 213 (1953) [in German].

1971

H. Löb, "Sinn oder Unsinn der Photonenrakete," Astronautik 8, 39-47 (1971).

1972

R. Hyde, L. Wood, and J. Nuckolls, "Prospects for rocket propulsion with laser induced fusion microexplosions," AIAA Paper 72-1063 (Dec 1972).

1975

D.F. Dipprey, "Matter-Antimatter Annihilation as an Energy Source in Propulsion," Appendix in "Frontiers in Propulsion Research," JPL TM-33-722, D.D. Papailiou, Editor, Jet Propulsion Lab, Pasadena, CA 91109 (15 March 1975).

D.L. Morgan, "Rocket thrust from antimatter annihilation," JPL Contract Report CC-571769, Jet Propulsion Lab, Pasadena, Calif. (1975).

1976

D.L. Morgan, "Coupling of annihilation energy to a high momentum exhaust in a matter-antimatter annihilation rocket," JPL Contract Report JS-651111, Jet Propulsion Lab, Pasadena, Calif. (1976)

1977

Ronald K. Goodman and Angus L. Hunt, "Ammonia-Pellet Generation System for the Baseball II-T Target Plasma Experiment," Rev. Sci. Instruments 48, 176 (1977). (A system for generating charged, uniformly sized, solid-ammonia 150 μm diameter spherical pellets having charge-to-mass ratio of 10^{-4} C/kg is described. These pellets are electrostatically guided at a speed of 32 m/s over a distance of several meters to a laser focal zone.) [Ed: The electrostatic acceleration, position sensing, and guidance systems would work equally well on antihydrogen ice pellets.]

1980

R.L. Forward, "Interstellar flight systems," AIAA Reprint 80-0823, AIAA Int. Meeting, Baltimore, MD (1980).

E. Mallove, R.L. Forward, Z. Paprotny, and J. Lehmann, "Interstellar travel and communication: a bibliography," J. British Interplanetary Soc., 33, 201-248 (1980) [entire issue].

1982

R.R. Zito, "The cryogenic confinement of antiprotons for space propulsion systems," J. British Interplanetary Soc., 35, 414-421 (1982).

D.L. Morgan, "Concepts for the design of an antimatter annihilation rocket," J. British Interplanetary Soc., 35, 405-412 (1982).

P.F. Massier, "The need for expanded exploration of matter-antimatter annihilation for propulsion application," J. British Interplanetary Soc., 35, 387-390 (1982).

R.L. Forward, "Antimatter propulsion," J. British Interplanetary Soc., 35, 391-395 (1982).

B.N. Cassenti, "Design considerations for relativistic antimatter rockets," J. British Interplanetary Soc., 35, 396-404 (1982).

1983

G. Vulpetti, "Relativistic astrodynamics: The problem of payload optimization in a two-star exploration flight with and intermediate powered swing-by," IAF Paper 83-327, 34th IAF Congress, Budapest, Hungary (Oct 1983).

G. Vulpetti, "A concept of low-thrust relativistic jet speed high efficiency matter-antimatter annihilation propulsion system," IAF Paper 83-397, 34th IAF Congress, Budapest, Hungary (Oct 1983).

F.R. Chang and J.L. Fisher, "The hybrid plume plasma rocket," Draper Lab preprint (1983).

R.L. Forward, Alternate Propulsion Energy Sources, AFRPL-TR-83-067, Final Report on Contract F04611-83-C-0013, Air Force Rocket Propulsion Lab, Edwards, CA 93523 (December 1983)

1984

B.N. Cassenti, "Antimatter propulsion for OTV applications," AIAA preprint 84-1485, AIAA/SAE/ASME 20th Joint Propulsion Conference, Cincinnati, Ohio (11-13 June 1984).

R.L. Forward, "Antiproton annihilation propulsion," AIAA preprint 84-1482, AIAA/SAE/ASME 20th Joint Propulsion Conference, Cincinnati, Ohio (11-13 June 1984).

B.N. Cassenti, "Optimization of relativistic antimatter rockets," J. British Interplanetary Soc., **37**, 483-490 (1984).

G. Vulpetti, "A propulsion-oriented synthesis of the antiproton-nucleon annihilation experimental results," J. British Interplanetary Soc. **37**, 124-134 (1984)

G. Vulpetti, "An approach to the modeling of matter-antimatter propulsion systems," J. British Interplanetary Soc., **37**, 403-409 (1984).

1985

S.D. Howe and Michael V. Hynes, "Anti-Matter Propulsion: Status and Prospects," Manned Mars Mission Workshop, Marshall Space Flight Center, Huntsville, AL, USA (10-14 June 1985). Preprint LA-UR-85-2443, LANL, Los Alamos, NM 87545 USA.

B.W. Augenstein, "Concepts, problems, and opportunities for use of annihilation energy: an annotated briefing on near-term RDT&E to assess feasibility," Rand Note N-2302-AF/RC, Rand Corp., Santa Monica, CA 90406 (June 1985).

B.W. Augenstein, "Some examples of propulsion applications using antimatter," Rand Paper 7113, Rand Corp., Santa Monica, CA 90406 (July 1985).

R.L. Forward, B.N. Cassenti, and D. Miller, "Cost Comparison of Chemical and Antihydrogen Propulsion Systems for High ΔV Missions," AIAA Paper 85-1455, 21st Joint Propulsion Conf., Monterey, CA (8-10 July 1985).

R.L. Forward, "Antiproton Annihilation Propulsion," AFRPL TR-85-034, Final Report on F04611-83-C-0046, Subcontract RI-32901 (Sept 1985). Obtain from AFRPL/LKC, Edwards AFB, CA 93523-5000.

R.L. Forward, "Antiproton Annihilation Propulsion," AFRPL TR-85-034, Final Report on F04611-83-C-0046, Subcontract RI-32901 (Sept 1985). Obtain from AFRPL/LKC, Edwards AFB, CA 93523-5000.

G. Vulpetti, "Antimatter Propulsion for Space Exploration," IAA Preprint 85-491, 36th Congress of the IAF, Stockholm, Sweden (7-12 Oct 1985).

R.L. Forward, "Antiproton Annihilation Propulsion," J. Propulsion and Power **1**, 370-374 (1985).

B.N. Cassenti, "Antimatter Propulsion for OTV Applications," J. Propulsion and Power **1**, 143-149 (1985).

Steven D. Howe and Michael V. Hynes, "Anti-Matter Propulsion: Status and Prospects," LA-UR-85-2443 (1985). [Ed: Obtain from LANL, P.O. Box 1663, Los Alamos, New Mexico 87545 USA.]
Proceedings Manned Mars Mission Workshop, NASA/Marshall Space Flight Center, Huntsville, Alabama (10-14 June 1985). [Ed: Precursor to paper given in Tokyo in 1986.]

1986

S.D. Howe, M.V. Hynes, R.E. Prael, J.D. Stewart, "Potential Applicability of the Los Alamos Antiproton Research Program to Advanced Propulsion," Preprint LA-UR-86-1689 for 15th Int. Symp. on Space Technology and Science, Tokyo, Japan (19-23 May 1986). [Ed: Obtainable from S.D. Howe, MS-F611, LANL, P.O. Box 1663, Los Alamos, NM 87545 USA.] [Ed: Although there are no detailed mission analyses in this review paper, it states that a round trip manned mission to Mars using antimatter for the energy source would take only 6 months and require only 400 tons in low Earth orbit, while chemically fueled missions would take 24 months and require 1800 tons. Figure 1 shows trend line for \bar{p} production predicting a gram/year by 2010. Figure 5 shows relative energy deposition of annihilation products as a function of radius in a solid core thermal rocket showing >95% of annihilation energy is absorbed in the first 40 cm of a homogenous mixture of tungsten and hydrogen in a heat exchanger.]

W.A. Sowell, "Antiproton Technology," Preprint of presentation at JANNAF Propulsion Meeting, New Orleans, LA (26-28 August 1986). Copies obtainable from AFRPL/CX, Edwards AFB, CA 93523-5000. [Through Project Forecast II, the Air Force has selected antiprotons, a form of antimatter, as a highly promising research area to advance space propulsion.]

G.D. Nordley, "Basic Considerations for Energy Limited Rockets," Preprint of presentation at JANNAF Propulsion Meeting, New Orleans, LA (26-28 August 1986). [Copies obtainable from AFRPL/CX, Edwards AFB, CA 93523-5000.]

Franklin B. Mead, Jr., "Future Possibilities for Nonconventional Propulsion Developments at the Air Force Rocket Propulsion Laboratory," Proc. 1986 JANNAF Prop. Meet., New Orleans, LA (26-29 Aug 1986). [Ed: Reprints obtainable from F.B. Mead, AFRPL/LKC, Edwards AFB, CA 93523-5000 USA.]

Giovanni Vulpetti and Enrico Pieragostini, "Matter-Antimatter Annihilation Engine Design Concept for Earth-Space Missions," Preprint IAF-86-178, Proc. 37th Congress of the IAF, Innsbruck, Austria (4-11 Oct 1986). (Paper presents design considerations for an antiproton-nucleon annihilation-at-rest engine in the energy-limited mode appropriate for high-energy mission in Earth-space. Engine performances are detailed.)

H.D. Froning, Jr., "Investigation of Very High energy Rockets for Future SSTO Vehicles," MDC-H1589, 37th IAF Congress, Innsbruck, Austria (4-12 October 1986). [Ed: Obtainable from H.D. Froning, McDonnell Douglas Astronautics, Huntington Beach, CA 92647 USA.]

9. CONFERENCE PROCEEDINGS

1984

U. Gastaldi and R. Klapish, Eds., *Physics at LEAR with Low-Energy Cooled Antiprotons*, Workshop on Physics at LEAR with Low-Energy Cooled Antiprotons, Erice, Sicily, Italy, 9-16 May 1982, Plenum Press, NY (1984).

A.H. Sørensen, "Theory of electron cooling in a magnetic field," 599.

L. Hütten, H. Poth, and A. Wolf, "The electron cooling device for LEAR," 605.

H. Herr, "A small deceleration ring for extra low energy antiprotons (ELENA)," 633.

H. Herr, D. Mohl, and A. Winnacker, "Production of and experimentation with antihydrogen at LEAR," 659.

G. Piragino, "Antiproton annihilation in nuclear matter: multiplication-nucleus interactions and exotic phenomena," 855.

R.M. DeVries and N.J. DiGiacomo, "The annihilation of low energy antiprotons in nuclei," 543.

S. Polikanov, "Could antiprotons be used to get a hot, dense plasma?" 851.

1985

P. Meystre and S. Stenholm, *The Mechanical Effects of Light*. A special issue of *J. Optical Soc. Am. B3*, 1706-1860 (November 1985) containing the following papers relevant to the control, cooling, and trapping of ions and neutral atoms:

J. Dalibard and C. Cohen-Tannoudji, "Dressed-Atom Approach to Atomic Motion in Laser Light: The Dipole Force Revisited," 1707.

D.J. Wineland et al., "Angular Momentum of Trapped Atomic Particles," 1721.

A.P. Kazantsev et al., "Kinetic Phenomena of Atomic Motion in a Light Field," 1731.

S. Stenholm, "Dynamics of Trapped Particle Cooling in the Lamb-Dicke Limit," 1743.

W.D. Philips, J.V. Prodan, and H.J. Metcalf, "Laser Cooling and Electromagnetic Trapping of Neutral Atoms," 1751.

J. Javanainen, et al., "Laser Cooling of a Fast Ion Beam," 1768.

V.I. Balykin, et al., "Radiative Collimation of Atomic Beams Through Two-Dimensional Cooling of Atoms by Laser-Radiation Pressure," 1776.

P.E. Moskowitz, P.L. Gould, and D.E. Pritchard, "Deflection of Atoms by Standing-Wave Radiation," 1784.

V.P. Chebotayev, et al., "Interference of Atoms in Separated Optical Fields," 1791.

D.E. Pritchard and P.L. Gould, "Experimental Possibilities for Observation of Unidirectional Momentum Transfer to Atoms from Standing-Wave Light," 1799.

David B. Cline, Ed., Low Energy Antimatter, World Scientific, Singapore (1986). Proceedings of the Workshop on the Design of a Low Energy Antimatter Facility, University of Wisconsin-Madison, Madison, Wisconsin, USA (October 1985).

Robert L. Forward, "Making and Storing Antihydrogen for Propulsion," p. 47.

R.R. Zito, "Antimatter Reactor Dynamics," J. British Interplan. Soc. 39, 110-113 (1986).

Giovanni Vulpetti, "Antimatter Propulsion for Space Exploration," J. British Interplanetary Soc., 39, 391-409 (1986). [Ed: Chiefly a review paper.]

M.J. Harris, "On the Detectability of Antimatter Propulsion Spacecraft," Astrophysics and Space Sci. 123, 297-303 (1986). (It is shown that the NASA Gamma-Ray Observatory will be able to detect large interstellar spacecraft at distance up to 300 parsecs by the gamma ray emission from the propulsion system.) [Ed: These are BIG spacecraft, the amount of antimatter fuel is in gigatons!]

1987

Robert L. Forward, "Prospects for Antiproton Production and Propulsion," HRL Research Report 563 (February 1987). [Ed: Obtain from Hughes Research Labs, 3011 Malibu Canyon Rd., Malibu, California 90265 USA.] Presented at the Cooling, Condensation, and Storage of Hydrogen Cluster Ions Workshop, SRI International, Menlo Park, California USA (8-9 January 1987). [Ed: A condensed version of prior work presented as introductory background material to attendees at the workshop.]

B.N. Cassenti, "Radiation Shield Analyses for Antimatter Rockets," AIAA Paper 87-1813, [Ed: Obtain from UTRC, Silver Lane, East Hartford, Connecticut 06108 USA.] To be presented at 23rd Joint Propulsion Conference, San Diego, California, 29 June-2 July 1987. [Ed: Assumes antimatter engine is 2 m dia. and therefore shield must be too, resulting in 3.5 tonnes mass. Annihilation region needing shielding will probably be much smaller and shield proportionately less massive.]

Giovanni Vulpetti, "A Further Analysis About the Liquid-Propellant Thermal Antimatter Engine Design Concept," Preprint AA-87. [Ed: Copies obtainable from G. Vulpetti, Telespazio, SpA per le Comunicazioni Spaziali, Via A. Bergamini 50, 00159 Rome, Italy.] (The heat converter-transmitter system mass is 476 kg, hydrogen flow rate is 10 kg/s, mixing zone pressure is 150 atm, thrust to mass ratio 80 to 140 m/s², exhaust power 130 to 357 MW, specific impulse 862 sec, efficiency 65%.)

V.A. Grinchuk, et al., "Scattering of Atoms by Coherent Interaction with Light," 1805.

U. Gastaldi, R. Klapisch, J.M. Richard, and J. Tran Thanh Van, Eds, *Physics with Antiprotons at LEAR in the ACOL Era*, Editions Frontieres, Gif-sur-Yvette, France (1985), \$100.00. Proceedings of the LEAR Workshop: Physics with Low Energy Cooled Antiprotons in the ACOL Era, Tignes (Savoie), France (19-26 January 1985).

R. Billinge, "Introduction to CERN's Antiproton Facilities for the 1990's," p. 13.

E. Jones, "Progress on ACOL," p. 25.

P. Lefevre, "LEAR Present Status and Future Developments," p. 33.

D.J. Simon, et al., "The LEAR Experimental Areas: Status Report and Possible Developments," p. 47.

D. Möhl, "Technical Implications of Possible Future Options for LEAR," p. 65.

D. Möhl, et al., "A Superconducting Low Energy Antiproton Ring (Super-LEAR)," p. 83.

J.H. Billen, et al., "An RFQ as a Particle Decelerator," p. 107.

C. Biscari and F. Iazzourene, "Post Deceleration of the LEAR Beam by a Radiofrequency Quadrupole," p. 115.

G. Carron, et al., "Status and Future Possibilities of the Stochastic Cooling System for LEAR," p. 121.

A. Wolf, et al., "Status and Perspectives of the Electron Cooling Device Under Construction at CERN," p. 129.

L. Tecchio, et al., "Possibilities for High Energy Electron Cooling in LEAR," p. 135.

D. Taqq, "Possibilities of Cooling the Extracted Antiproton LEAR Beams," p. 143.

T. Katayama, et al., "Stochastic Momentum Cooling of Low Energy, 7 MeV Proton Beam," p. 151.

I. Hofmann, "Density Limitations in Cooled Beams," p. 159.

L. Tecchio, "Electron Cooling at Intermediate Energy," p. 167.

A.M. Green, et al., "N anti-N Annihilation Mechanisms," p. 185.

L. Linssen, " $\bar{p}p$ Total Cross Sections and $\bar{p}p$ Forward Elastic Scattering at Low Incoming \bar{p} Momenta, Results From PS172," p. 225.

T.A. Shibata, et al., " $\bar{p}p$ Cross Sections at Small Momenta," p. 231.

H. Poth, et al., "Anti-Protonic Atoms at LEAR: Achievements and Perspectives," p. 581.

W. Kanert, "Interaction of Stopped Antiprotons With Nuclei (PS186)," p. 593.

D. Garreta, "Elastic and Inelastic Scattering of Antiprotons From Nuclei (PS184)," p. 599.

U. Gastaldi, et al., "High Resolution Spectroscopy of $p\bar{p}$ Atoms Produced in Flight with \bar{p} and H^- Beams Co-rotating in LEAR," p. 681.

- M. Nieto, et al., "Gravitational Properties of Antimatter," p. 639.
 G. Torelli, et al., "Gravitational Measurement on Antiprotons," p. 649.
 M.V. Hynes, "Physics with Low Temperature Antiprotons," p. 657.
 G. Gabrielse, et al., "Precision Comparison of Antiproton and Proton Masses in a Penning Trap," p. 665.
 M. Conte, "Antihydrogen Storage Rings," p. 711.

George E. Walker, Charles D. Goodman, Catherine Olmer, Eds., *Antinucleon and Nucleon-Nucleus Interactions*, Plenum Press, New York, USA (1985), \$79.50. Proceedings of Conference on Antinucleon and Nucleon-Nucleus interactions, Telluride, Colorado, USA (18-21 March 1985).

F. Balestra, et al., "Low-Energy Anti-Proton Annihilation on Nuclei," p. 445.

H.V. von Geramb, Ed., *Medium Energy Nucleon and Antinucleon Scattering*, Lecture Notes in Physics, v. 243, Springer-Verlag, Berlin, Germany (1985), 576p., hardcopy \$70.90, paper \$36.50. Proceedings of international Symposium on Medium Energy Nucleon and Antinucleon Scattering, Bad Honnef, Germany (18-21 June 1985).

H. Poth, "Recent Results from Anti-Protonic Atoms at LEAR," p. 357.

J.A. Niskanen, "Antiproton-Proton Annihilation," p. 50.

M.R. Pennington, Ed., *Antiproton 1984*, Hilger, Bristol, England (1985). Institute of Physics Conference Series, 73, 530p, \$76.00. Proceedings of 7th European Symposium on Antiproton Interactions: From LEAR to the Collider and Beyond, Durham, England (9-13 July 1984).

M. Chanel, et al., "LEAR: Machine and Experimental Areas: Experience and Future Plans After 1-Year of Operation," p. 119.

A.M. Green, "What Anti-Proton Physics Can Tell Us About Nuclear Physics," p. 213.

S. Ahmad for ASTERIX Collaboration, " $\bar{p}p$ Annihilation at Rest from Atomic P States," p. 287.

S. Ahmad for ASTERIX Collaboration, "First Observation of K x-rays from $\bar{p}p$ Atoms," p. 131.

D. Gareta, et al., "PS-184: A Study of \bar{p} -Nucleus Interaction with a High Resolution Magnetic Spectrometer," p. 187.

M. Sakitt, et al., "Low-Energy Anti-Proton Interaction Studies at Brookhaven," p. 205.

1986

B.E. Bonner and L.S. Pinsky, *Proceedings of the First Workshop on Antimatter Physics at Low Energy*, Fermilab, Batavia, Illinois (10-12 April 1986), U.S. Gov. Printing Office 1986-644-171. Contains the following papers:

- B.I. Deutch, A.S. Jensen, A. Miranda, and G.C. Oades, "p Capture in Neutral Beams," pp. 371-391.
- H. Poth, "Antiprotonic, Hyperonic, and Antihydrogen Atoms," pp. 325-345.
- Jean-Marc Richard, "Antiproton-Nucleus Interaction," pp. 309-324.
- R.L. Jaffe, "pp Physics in the Milli-TeV Region," pp. 1-34.
- Rolf Landua, "The Future Physics at LEAR," pp. 35-68.
- Petros A. Rapidis, "The Fermilab Antiproton Source: Prospects for pp Experiments," pp. 83-94.
- Ezio A. Menichetti, "Charmonium pp Experiments," pp. 95-118.
- M.G. Olsson, "Onia Spectroscopy by Direct Channel Production," pp. 119-130.
- Stanley J. Brodsky, "Probing QCD in Low energy p Collisions," pp. 131-164.
- Stephen R. Sharpe, "Glueballs and Other Exotica in pp Annihilation," pp. 165-184.
- T. Goldman, Richard J. Hughes, and Michael Martin Nieto, "Gravitational Properties of Antimatter: Experimental Evidence for Quantum Gravity?," pp. 185-200.
- M.V. Hynes and L.C. Campbell, "Physics with Bottled Antiprotons," pp. 201-210.
- G. Gabrielse, K. Helmersen, R. Tjoelker, X. Fei, T. Trainor, W. Kells, and H. Kalinowsky, "Prospects for Experiments with Trapped Antiprotons," pp. 211-226.
- Lincoln Wolfenstein, "CP Violation and pp Experiments," pp. 227-241.
- John F. Donoghue, "CP Violation Experiments Using Hyperons at a pp Machine," pp. 242-250.
- Carl B. Dover, "Physics with Polarized p's," pp. 251-270.
- E. Steffens, "Prospects for Producing Polarized Antiprotons," pp. 271-285.
- F. Myhrer, "Antiproton Annihilation and Quark Dynamic Selection Rules," pp. 285-292.
- Harry J. Lipkin, "Delta, Iota, and Other Meson Spectroscopies," pp. 293-308.
- Nathan Isgur, Richard Kokosko, and Jack Paton, "Gluonic Excitations of Mesons: Why They are Missing and Where to Find Them," pp. 347-354.
- W.R. Gibbs, "Creating High Energy Density in Nuclei with Energetic Antiparticles," pp. 355-369.
- B.I. Deutch, A.S. Jensen, A. Miranda, and G.C. Oades, "p Capture in Neutral Beams," pp. 371-391.
- G. Bassompierre, R.K. Bock, A. Buzzo, M. Dameri, T. Fearnley, J. Franz, M. Gazzaly, N. Hamann, T. Johansson, E. Khan-Aronsen, K. Kilian, J. Kirkby, K. Kirsebom, K. Kuroda, A. Kylling, F. Levrero, A. Lundby, M. Macri, M. Marinelli, L. Mattera, B. Mouellic, B.A. Nielsen, W. Oelert, Y. Onel, B. Osculati, G. Pauletta, M.G. Pia, M. Poulet, E. Rössle, A. Santroni, H. Schmitt, B. Stugu, S. Terreni, F. Tommasini, "JETSET: Physics at LEAR with an Internal Gas Jet Target and an Advanced General Purpose Detector," pp. 419-442.

Y. Onel and A. Penzo, "Spin Studies with a Polarized Jet Target in LEAR," pp. 443-454.

P. Lefevre, D. Mohl, D.J. Simon, "Future Machine Improvements in LEAR," pp. 69-82.

Michael S. Chanowitz, "Physics Overview of the Fermilab Low Energy Antiproton Facility Workshop," pp. 393-418.

Appendix I. B.E. Bonner and L.S. Pinsky, "A Summary of Topics Discussed at the First Fermilab Antimatter Physics at Low Energy Workshop," pp. 455-462.

William C. Stwalley and Marshall Lapp, Eds., *Advances in Laser Science-I*, American Institute of Physics Conference Proceedings No. 146, New York (1986). Proceedings of First International Laser Science Conference (ILS-I), Dallas, Texas, USA (1985).

R.G. Beausoleil, B. Couillaud, C.J. Foot, T.W. Hänsch, E.A. Hildum, and D.H. McIntyre, "High Resolution Laser Spectroscopy of Atomic Hydrogen," p. 366.

C.W. Clark, "Autodetaching States of Negative Ions," p. 379.

W.D. Phillips, A.L. Migdall, and H.J. Metcalf, "Laser-Cooling and Electromagnetic Trapping of Neutral Atoms," p. 362.

W. Nagourney, H. Dehmelt, and G. Janik, "Optical Lamb-Dicke Confinement of a Ba⁺ Mono-Ion Oscillator," p. 401.

David B. Cline, Ed., *Low Energy Antimatter*, World Scientific, Singapore (1986). Proceedings of the Workshop on the Design of a Low Energy Antimatter Facility, University of Wisconsin-Madison, Madison, Wisconsin, USA (October 1985).

Charles Goebel, "Antiparticles and Gravity: The Conventional View," p. 24.

M.G. Olsson, "Heavy Quark Spectroscopy and Anti-proton Collisions," p. 29.

T. Barnes, "Current Theoretical Expectations for Gluonic Hadrons," p. 134.

Theodore E. Kalogeropoulos, "Antiproton Neutron Annihilations at Rest: The $\zeta(1480)$," p. 138.

John Peoples, Jr., "Prospects for $\bar{p}p$ Experiments in the TEV I Accumulator," p. 144.

V. Bharadwaj, et al., "A Proposal to Investigate the Formation of Charmonium States Using the PBAR Accumulator Ring," p. 166.

Carl B. Dover, "Low Energy $\bar{p}p$ Strong Interactions: Theoretical Perspective," p. 1.

Ronald E. Brown, "An Experiment to Measure the Gravitational Force on the Antiproton," p. 105.

Michael H. Holzscheiter, "Trapping and Cooling of Externally injected antiprotons in a Penning Trap," p. 120.

C.F. Driscoll, "Containment of Single-Species Plasmas at Low Energies," p. 184.

Robert L. Forward, "Making and Storing Antihydrogen for Propulsion," p. 47.

A. Wolf, et al., "Electron Cooling of Low-Energy Antiprotons and Production of Fast Antihydrogen Atoms," p. 78.

R.S. Conti and A. Rich, "The Status of High Intensity, Low Energy Positron Sources for Anti-hydrogen Production," p. 105.

Frank Krienen, "Progress in Hollow Cathode Electron Gun for Electron Cooling," p. 92.

D.J. Larson, et al., "Intermediate Energy Electron Cooling Applied to the Fermilab Antiproton Source," p. 167.

M. Sedlacek, "The Celsius-Ring in Uppsala: Electron Cooler Design," p. 196.

10. ANTIMATTER NEWS AND POPULAR ARTICLES

1972

Yu.D. Prokoshkin, "Particles of Antimatter," Die Naturwissenschaften 59, 281-284 (1972).

1977

H.J.C. Kouts, Chairman, Proceedings of an Information Meeting on Accelerator Breeding, Brookhaven National Laboratory, Upton, New York, 18-19 Jan 1977.

1979

Physics Today editors, "CERN builds proton-antiproton ring; Fermilab plans one," Search and Discovery Section, Physics Today, 32, No. 3, 17-19 (March 1979).

1981

A.L. Robinson, "CERN sets intermediate vector boson hunt," Science 213, 191-194 (10 July 1981).

1982

Physics Today editors, "CERN SPS now running as 540-GeV $\bar{p}p$ collider," Search and Discovery Section, Physics Today, 35, No. 2, 17-20 (February 1982).

D.B. Cline, C. Rubbia, and S. van der Meer, "The search for intermediate vector bosons," Scientific American 247, No. 3, 48-59 (March 1982).

Physics Today editors, " $\bar{p}p$ collisions yield intermediate boson at 80 GeV, as predicted," Search and Discovery Section, Physics Today, 35, No. 4, 17-20 (April 1982).

1983

CERN Courier editors, "When antimatter mattered," CERN Courier, 23, 6-7 (January/February 1983).

CERN Courier editors, "LEAR arrives," CERN Courier, 23, 314 (October 1983).

CERN Courier editors, "From AA to Z," CERN Courier, 23, 365-369 (November 1983).

CERN Courier editors, "Going for antiprotons," CERN Courier, 23, 380-383 (November 1983).

CERN Courier editors, "First results from LEAR," CERN Courier, 23, 416-417 (December 1983).

CERN Proton Synchrotron Staff, "The CERN PS complex as an antiproton source," IEEE Trans. Nuclear Sci. NS-30, 2039-2041 (1983).

1984

Physics Today editors, "Fermilab's superconducting synchrotron strives for 1 TeV," Search and Discovery Section, Physics Today, 37, No. 3, 17-20 (March 1984).

CERN Courier editors, "Antiprotons in orbit," CERN Courier, 24, 53-55 (March 1984).

Richard Wohl, "New Propulsion Systems for the Next Frontier," Defense Science 2002+, pp. 54-57 (April 1984). [Ed: Makes some highly speculative estimates for future antiproton production rates.]

1985

Robert L. Forward, "Antimatter Propulsion," pp. 1-18, Proceedings Fermilab Industrial Affiliates Fifth Annual Meeting (21-22 May 1985). [Ed: Popular lecture on one possible future application of particle physics. Other talks were on applications of muons, quarks, neutrinos, and magnetic monopoles. Copies of the proceedings obtainable from Dr. Richard A. Carrigan, Jr., Fermilab, P.O. Box 500, Batavia, Illinois 60510 USA.]

Laser Focus Staff, "Lasers Make Cold Atomic Gases," pp. 32-38, Laser Focus/Electro-optics (Dec 1985).

1986

CERN Courier Staff, "CERN Antiprotons 1985," CERN Courier 26, No. 2, 1 (March 1986). (Although the new Fermilab Tevatron took the world collision energy record, 1985 was still a vintage year for CERN antiprotons. The accumulated luminosity in 1985 reached a record figure of 655 inverse nanobarns, surpassing the total number of collisions from all previous runs.)

David Cline, "Low Energy US Antiprotons," CERN Courier 26, No. 3, 3 (March 1986). [Ed: News item about University of Wisconsin, Madison Workshop on the Design of a Low Energy Antiproton Facility in the USA.]

J. Maddox, "Catching Atoms in Beams of Light," Nature 322, 403 (31 July 1986).

D.E. Thomsen, "Stopping an Atom in its Tracks," Science News 129, 388 (?? July 1986). [Optical molasses produces what amounts to a new state of matter--an ultracooled gas. These atoms are cooled to 1 mK, which is well below the solidification temperature for any substance, yet they remain physically a gas.]

Robert Walgate, "Defence Lobby Eyes Antimatter," Nature 322, 678 (21 Aug 1986). [Ed: News item about Rand report by B.W. Augenstein, Rand Note N-2302-AF/RC, Rand Corp., Santa Monica, CA 90406 USA (June 1985). Bruno Augenstein reports that the cost quoted for antimatter in the Walgate article of 133 M\$/mg was based on the wrong \bar{p}/p ratio; it should be 15 M\$/mg.]

B. Schwarzschild, "Laser Beam Focus Forms Optical Trap for Neutral Atoms," Physics Today, 17-19 (Sept 1986). (Summarizing 16 years of work on optical trapping, Ashkin points out that "we can now make simple single-beam traps that work over a size range of 10^5 --from atoms, to submicron Rayleigh particles, up through 10-micron Mie-size particles.")

B. Schwarzschild, "Now They're Even Trapping Antiprotons," Physics Today 39, No. 9, 19 (Sept 1986).

Arthur L. Robinson, "Antiprotons Captured at CERN," Science 233, 1383-1384 (26 Sept 1986).

D.E. Thomsen, "Trapping Antimatter: Antiprotons on Hold," Science News 130, 340-341 (29 November 1986).

John Maddox, "How to Make Antimatter Last," News and Views, Nature 324, 299 (27 November 1986). (An experiment at CERN has shown that antiprotons can be kept for several minutes in an electromagnetic trap. But the prospect of making reality of the science fiction of using antimatter for military operations remains remote.)

CERN Courier Staff, "Ionization Surprise," CERN Courier 26, No. 9, 18 (November 1986). (At CERN's LEAR, a pocket-sized experiment by an Aarhus/CERN team has found that 100 MeV/c antiprotons are much more effective than protons in ripping out both electrons from the atoms of helium gas.)

CERN Courier Staff, "Stopping Antiprotons," CERN Courier 26, No. 9, 25 (November 1986). (On 23 August, the healthy stack of antimatter in CERN's Antiproton Accumulator AA was ceremonially destroyed, making the end of an era for the AA. Now begins a one-year antiproton pause to construct the new ACOL Antiproton Collector.)

LIST OF WORKSHOP ATTENDEES

Dr. John Archambeau
Loma Linda University Medical Center
Department of Radiation Sciences
P.O. Box 2000
11234 Anderson Street
Loma Linda, CA 92354

Professor James R. Arnold
California Space Institute, A021
University of California
at San Diego
La Jolla, CA 92093

Dr. John Bahns
AFAL/DYCRL
Edwards AFB, CA 93523-5000

Gerald W. Bennett
AGS Dept./911B
Brookhaven National Laboratory
Upton, NY 11973

C. Bilby
Large Scale Programs Institute
2815 San Gabriel
Austin, TX 78705

Dr. E. Blackmore
TRIUMF
4004 Wesbrook Mall
Vancouver, B.C.
Canada, V6T2A3

Professor B.E. Bonner
Rice University
Department of Physics
P.O. Box 1892
Houston, TX 77251-1892

Dietrich W. Brunner
Boeing Aerospace
P.O. Box 3999
M/S 82-23
Seattle, WA 98124

Dr. John Callas
Jet Propulsion Laboratory
Advanced Systems Analysis
Propulsion Systems Section
4800 Oak Grove Avenue
Pasadena, CA 91109

Dr. L. Campbell
Theoretical Division
Los Alamos National Laboratory
Los Alamos, NM 87545

Brice N. Cassenti
United Technologies Research Center
MS - 18
Silver Lane
East Hartford, CT 06084

Professor D.B. Cline
University of California
at Los Angeles
Department of Physics
405 Hilgard Avenue
Los Angeles, CA 90024

Dr. Robert C. Corley
Air Force Astronautics Laboratory
AFAL/CX
Edwards Air Force Base, CA 93523-5000

C. Fred Driscoll
University of California/San Diego
Physics Department
La Jolla, CA 92093

Mr. Robert A. Duffy
Charles Stark Draper Lab., Inc.
555 Technology Square
Cambridge, MA 02138

Walt Dyer
General Dynamics Space Systems Division
P.O. Box 85990
Mail Zone C-1-8270
San Diego, CA 92138

Dr. Robert L. Forward
Forward Unlimited
P.O. Box 2783
Malibu, CA 90265

Mr. Dave Froning
McDonnell Douglas
5301 Bolsa Avenue
Huntington Beach, CA 92647

John P. Gille
Martin Marietta Astronautics Group
P.O. Box 179
M/S B0441
Denver, CO 80201

Dr. T. Goldman
Los Alamos National Laboratory
T-5 MSB283
Los Alamos, NM 87545

Dave Goodwin
U.S. Department of Energy
ER-20.1/GTN
Washington, DC 20545

Longin Greszczuk
McDonnell Douglas
5301 Bolsa Avenue
MS/13-3
Huntington Beach, CA 92647

Dr. V. Haloulakos
McDonnell Douglas Astronautics Co.
5301 Bolsa Avenue
Huntington Beach, CA 92647

John R. Henley
Theoretical Physics Group, ORG. 91-10
Applied Physics Laboratory
Lockheed R&D Division
3251 Hanover Street
Palo Alto, CA 94304-1191

Dr. Steve Howe
S-4, F607
Los Alamos National Laboratory
Los Alamos, NM 87545

Dr. Michael Hynes
P-15, MS-D406
Los Alamos National Laboratory
Los Alamos, NM 87545

Professor Theodore Kalogeropoulos
Syracuse University
Department of Physics
Syracuse, NY 13244-1130

Professor Andreas M. Koehler
Harvard Cyclotron Laboratory
Harvard University
44 Oxford Street
Cambridge, MA 02138

Delbert Larson
University of California
at Los Angeles
Department of Physics
405 Hilgard Avenue
Los Angeles, CA 90024

Dr. Y.Y. Lee
Brookhaven National Laboratory
Building 911B
Upton, NY 11973

Dr. Richard G. Madonna
Grumman Corporate Research Center
MS A01-26
Bethpage, NY 11714

Dr. Bogdan C. Maglich
AELABS, Inc.
20 Nassau Street
Princeton, NJ 08542

James Miller
Boston University
Department of Physics
590 Commonwealth Avenue
Boston, MA 02215

Dr. Fred Mills
Fermi National Accelerator Laboratory
P.O. Box 500
Batavia, IL 60510

Professor J. Brian A. Mitchell
The University of Western Ontario
Department of Physics
London, Ontario,
Canada N6A3K7

Dr David L. Morgan, Jr.
Lawrence Livermore National Laboratory
L-35
P.O. Box 808
Livermore, CA 94550
or
728 Polaris Way
Livermore, CA 94550

Dr. Michael M. Nieto
Los Alamos National Laboratory
Theoretical Division
T-8, MS-B285
Los Alamos, NM 87545

Major Gerald B. Nordley
AFAL/CX
Edwards Air Force Base, CA 93523

Eric H. Ottewitte
Idaho National Engineering Lab
P.O. Box 1625
Idaho Falls, ID 83415

D.C. Peaslee
University of Maryland
Department of Physics & Astronomy
College Park, MD 20742

J.R. Perrin
Litton Industries
360 N. Crescent Drive
Beverly Hills, CA 90210

D. Preston
LANL
X-4, MS-F664
Los Alamos, NM 87545

Major John Prince
AFOSR/NP
Building 410
Bolling Air Force Base
Washington, DC 20332

Dr. Johann Rafelski
University of Arizona
Department of Physics
Tucson, AZ 85721

Professor Charles K. Rhodes
University of Illinois at Chicago
Physics Department M/C 273
P.O. Box 4348
Chicago, IL 60680

Wayne E. Roe
AF Astronautics LAB
XRX
Edwards AFB, CA 93523

Major W. Seward
AFWAL/POOC-3
Aero Propulsion Laboratory
Wright Patterson AFB, OH 45433

Stephen Sharpe
Stanford Linear Accelerator Center
Stanford University
P.O. Box 4349, Bin 81
Stanford, CA 94305

James N. Shoji
Rockwell International
Rocketdyne Division
6633 Canoga Avenue
Canoga Park, CA 91303

Professor Gerald A. Smith
Pennsylvania State University
104 Davey Lab
University Park, PA 16802

Dr. Johndale C. Solem
University of Illinois at Chicago
Physics Department
P.O. Box 4348
M/C 273
Chicago, IL 60680

Captain William A. Sowell
Air Force Astronautics Laboratory
Edwards Air Force Base, CA 93523

Professor W.C. Stwalley
Iowa Laser Facility
University of Iowa
Iowa City, IA 52242-1294

Dr. H. Takahashi
Brookhaven National Laboratory
Building 130
Upton, NY 11973

Dr. Marcia Urie
Department of Radiation Medicine
Mass. General Hospital
Boston, MA 02114

Major Dennis Vincent
HQ AFSC/DLWS
Andrews AFB
Washington DC 20334-5000

John Warren
TRIUMF
4004 Wesbrook Mall
Vancouver, B.C.
Canada, V6T2A3

Dr. R. Weiss
AFAL-CA
Edward AFB, CA 93523-5000